# GENESIS AND DIAGENESIS OF SANTONIAN TO EARLY CAMPANIAN (CRETACEOUS) PHOSPHATIC CHALKS OF THE ANGLO-PARIS BASIN

## VOLUME 2 : SEDIMENTOLOGY, GEOCHEMISTRY, BELEMNITE PALAEOBIOLOGY and CONCLUSIONS

I. Jarvis BSc FGS

Wolfson College

and

Department of Geology and Mineralogy

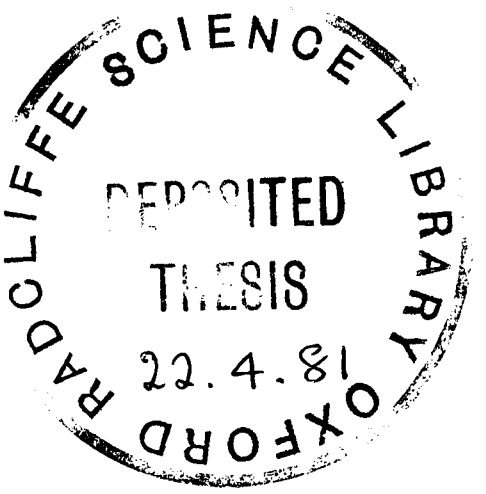


D.Phil Thesis

October 1980

# Chapter 3 : Sedimentology


| | | |
|---|---|---|
| 3.1 | Introduction | 229 |
| 3.2 | White chalk | 230 |
| | 3.2.1 Petrography | 230 |
| | 3.2.2 Depositional environment | 236 |
| | a. Substrates | 236 |
| | b. Sedimentation rates | 237 |
| | c. Depth | 238 |
| | d. Temperature and salinity | 239 |
| | 3.2.3 Early diagenesis | 240 |
| 3.3 | Hardgrounds | 241 |
| | 3.3.1 Morphology | 242 |
| | 3.3.2 Biological processes | 245 |
| | 3.3.3 Petrography | 251 |
| | a. Glauconitization | 253 |
| | b. Phosphatization | 255 |
| | c. Phosphatic skins | 257 |
| | d. Ferruginization | 263 |
| | e. Manganese oxides | 265 |
| | f. Silicification | 266 |
| | 3.3.4 Early diagenesis and depositional environment | 266 |
| 3.4 | Phosphatic chalks | 272 |
| | 3.4.1 Sedimentary structures | 273 |
| | a. Burrowed junctions | 273 |
| | b. Burrowed-out white chalks | 275 |
| | c. Pseudoconglomerates | 275 |
| | d. Planar structures | 278 |
| | e. Cross-bedding | 280 |
| | 3.4.2 Phosphatic chalk microfacies | 280 |
| | a. Basal lags | 281 |
| | b. Phosphatic chalks | 284 |
| | 3.4.3 Phosphatic chalk components | 296 |
| | a. Intraclasts | 296 |
| | b. Coprolites and pellets | 301 |
| | c. Ooliths | 303 |
| | d. Foraminiferans | 307 |
| | e. Inoceramid prisms | 307 |
| | f. Echinoderm debris | 309 |
| | g. Bone fragments | 310 |
| | h. Other skeletal grains | 311 |
| | 3.4.4 Early diagenesis and depositional environment | 313 |
| 3.5 | Calcarenites | 318 |
| 3.6 | Cuvettes | 327 |
| | 3.6.1 Morphology | 327 |
| | 3.6.2 Environment | 328 |
| | 3.6.3 Genesis | 329 |

| | | | |
|---|---|---|---|
| 3.7 | Synsedimentary folding | | 331 |
| | 3.7.1 | Morphology | 332 |
| | 3.7.2 | Comparisons and origin | 334 |
| 3.8 | Late diagenesis | | 336 |
| | 3.8.1 | Silicification | 339 |
| | | a. Bioclasts | 339 |
| | | b. Nodular flints | 340 |
| | | c. Tabular flints | 345 |
| | | d. Flint genesis | 345 |
| | 3.8.2 | Pressure solution | 348 |
| | | a. Flaser structures | 348 |
| | | b. Stylolites | 349 |
| | 3.8.3 | Pyrite | 350 |
| | 3.8.4 | Cementation | 350 |
| 3.9 | Conclusions | | 352 |

## 3.1 Introduction

Chalk is usually defined as a white, soft, fine-grained carbonate rock. Research into the composition of the 'type' chalks of the Upper Cretaceous (Latin: creta = chalk) and the English Chalk in particular, has led to more precise definitions depending on the bias of the author (see Håkansson et al., 1974; Hancock, 1975a; Kennedy and Garrison, 1975b; Scholle, 1974, 1977a for recent work and reviews). In general it has been demonstrated that the majority of chalks were originally relatively-pure coccolith (a nannofossil group of golden-brown algae) biomicrites. The friability of the sediment may be a measure of synsedimentary lithification (3.3.4) or may result from burial and other late diagenetic effects. Therefore, it cannot be regarded as being implicit to a definition of the rock type. Consequently, I have adopted Scholle's (1977a p.2) definition of chalks as being:

> "fine-grained carbonate sediments composed primarily of calcareous nannofossils (especially coccoliths) and calcareous macrofossils (such as Foraminifera and calcispheres). No limitation is placed on the degree of induration".

In the context of this study the general term 'chalk' has been further subdivided into three broad categories:

(a) White chalk, refering to the predominantly-soft, white lithology that forms the bulk of English and European successions (3.2.1).

(b) Hardground chalk, for indurated varieties where lithification was demonstrably a synsedimentary process (3.3.4) and

(c) Phosphatic chalk, where the sediment contains $\geq 5\%$ $P_2O_5$ due to the presence of appreciable amounts of pelletal phosphate (3.4.3).

Boundaries between the rock types are necessarily somewhat arbitrary since white chalks may pass almost imperceptibly vertically and/or laterally into a hardground facies. Similarly, gradational transitions and sediment inhomogeneities mean that even with the more precise definition of phosphatic chalk, the boundary with other varieties is not always easily distinguished. In practise, however, the terms may be readily applied by anyone familiar with the lithologies.

## 3.2 White chalk

### 3.2.1 Petrography

White chalks consist predominantly of planktonic components - scattered foraminiferans and calcispheres surrounded by a micritic coccolith-rich matrix (Fig. 3.1A). Coccoliths generally account for >60% of the <20 μm fraction (Håkansson et al., 1974). In addition they contain varying proportions of fragmented skeletal material of benthonic origin (Fig. 3.2), chiefly inoceramid, benthonic foraminiferan and echinoderm but including articulate brachiopod, bryozoan, oyster and other bivalves, ostracode, serpulid and scleractinian coral debris. Comminuted inoceramid is the dominant non-planktonic component of the white chalks considered here and it is that element that becomes most prominent where finer elements have been removed by winnowing (Fig. 3.1B). Broken and crushed grains are common and fragmentation may be attributed to a combination of biodegredation (Kennedy and Garrison, 1975b) and compaction (Scholle, 1974). Elongate grains may be aligned within prominent borrow systems or by severe compaction but are generally randomly oriented. Calcisphere and foraminiferan chambers are usually filled with micrite or more rarely calcite spar (Fig. 3.1).

In addition to coccoliths and skeletal calcite, four other components are important:

(1) Clay minerals. Predominantly illite and mixed-layer clays (± small amounts of montmorillonite and kaolinite) in varying proportions but usually in amounts of <1%. They are probably both neoformed and of terrigenous origin (see e.g. Millot, 1964; Weir and Catt, 1965; Jeans, 1968, 1978; Morgan-Jones, 1977).

(2) Coarse detrital minerals. Mainly silt to fine-sand grade quartz and heavy minerals, they generally only account for a fraction of a percent of the total sediment.

(3) 'Authigenic' minerals. Glauconite and silica occur as minor constituents throughout the whole Chalk but are of relatively little importance in the white chalks considered here. Scattered pelletal phosphate occurs in

Fig. 3.1 White and hardground chalk microfacies.
A. Soft white chalk from 1.20 m below the surface of the basal hardground, Beauval quarry. General view of the typical lithology at this level. Note the dominance of comminuted inoceramid amongst the coarser component. PPL.
B. As (A) but showing the coarser winnowed facies that occurs in small (~1 cm) patches throughout the bed. In addition to the higher percentage of inoceramid debris, calcispheres and small planktonic foraminiferans are also important. PPL.
C. Coarse hardground chalk of the Beauval Basal Hardground. The sediment contains a considerably higher proportion of large planktonic foraminiferans and calcispheres than the underlying chalks (A,B). Note the completeness of the majority of tests. Boundaries of small white chalk intraclasts that are clearly visible in hand specimen (e.g. Fig. 2.14) are rarely discernible in thin section, indicating that their sediment is identical to the matrix. PPL.
D. Summit of the intermediate white chalk, Taplow. This unlithified white chalk is closely comparable to the sediment of the basal hardground at Beauval. PPL.


A
0·5mm


B
0·5mm


C
0·5mm

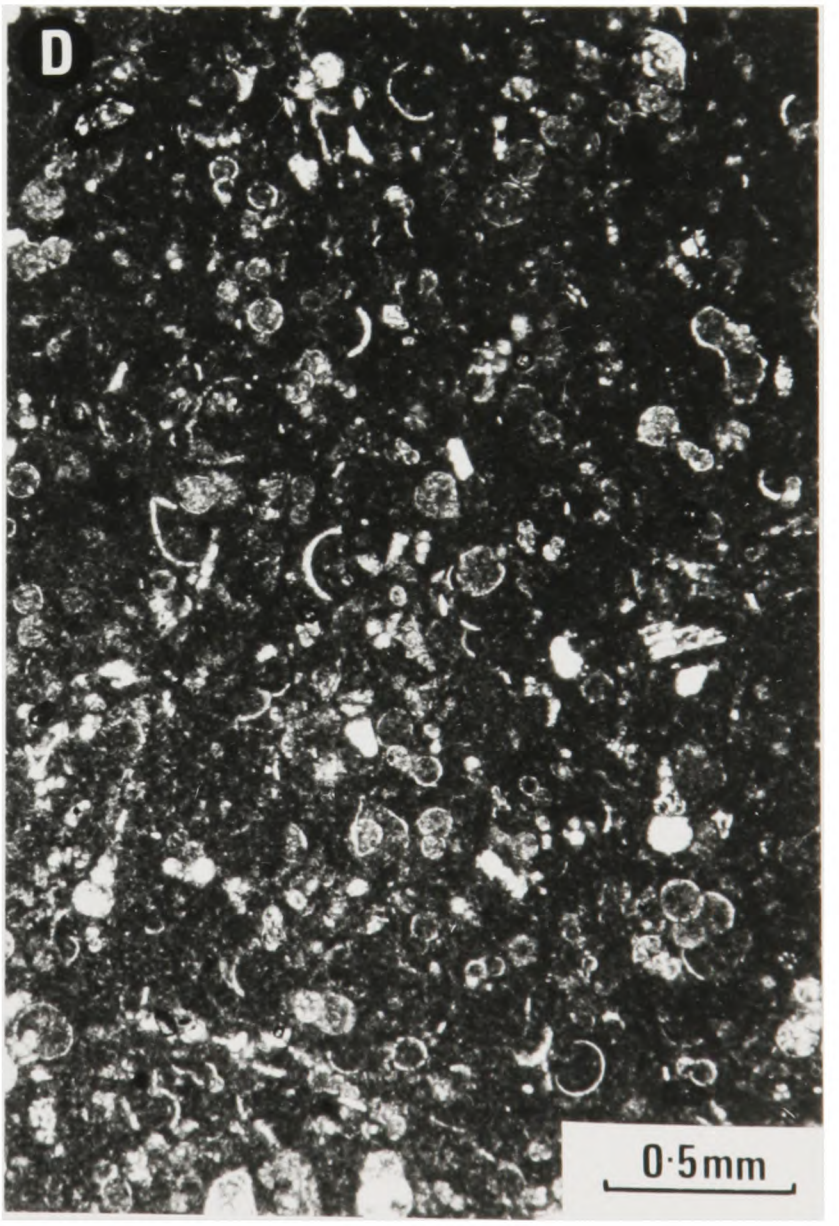
D
0·5mm

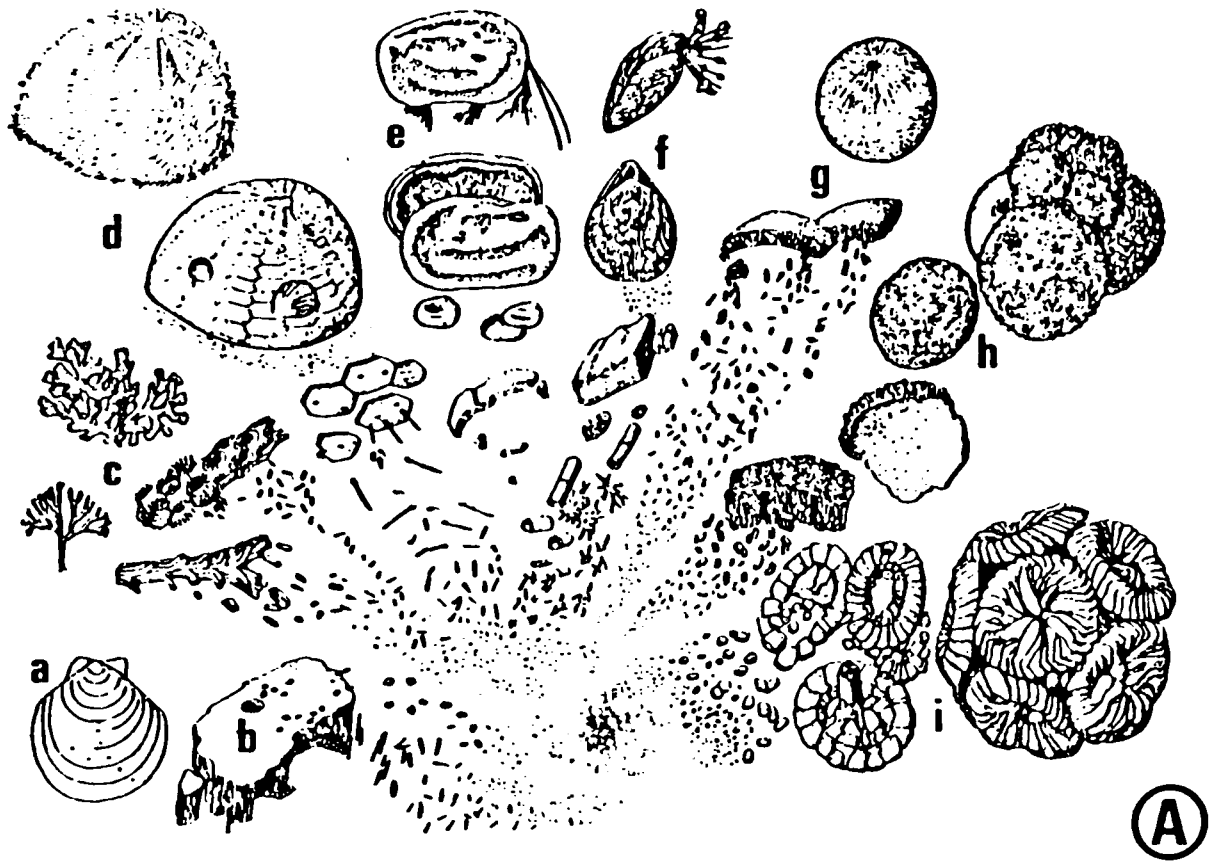


Fig. 3.2 Graphic representation of the biogenic constituents of white chalk.

A. Diagram of the main constituents. All stages of breakdown of skeletons occur in the final rock but the proportion of breakdown stages and organism groups vary considerably laterally and stratigraphically. No indication of proportions is given here. (a) bivalves, (b) bivalves and sponge borings, (c) cyclostome and cheilostome bryozoans, (d) echinoids, (e) ostracodes, (f) brachiopods, (g) calcispheres, (h) foraminiferans. (i) coccolithophores. Groups omitted include coelenterates, serpulid worms, asteroids and organisms having siliceous, purely aragonitic or organic skeletons. Scale is variable, increasing and then decreasing again centripetally. (After Bromley, 1979).

B. Representation of the grain-size variation of chalk components. Vertical columns represent four size fractions (sieve sizes indicated at bottom) viewed at four different magnifications (top right). Note the extreme range of grain size. It should be noted that the >500 µm fraction ranges up to whole skeletons several centimetres in size. (for further discussion see Bromley, 1979 fig. 1).

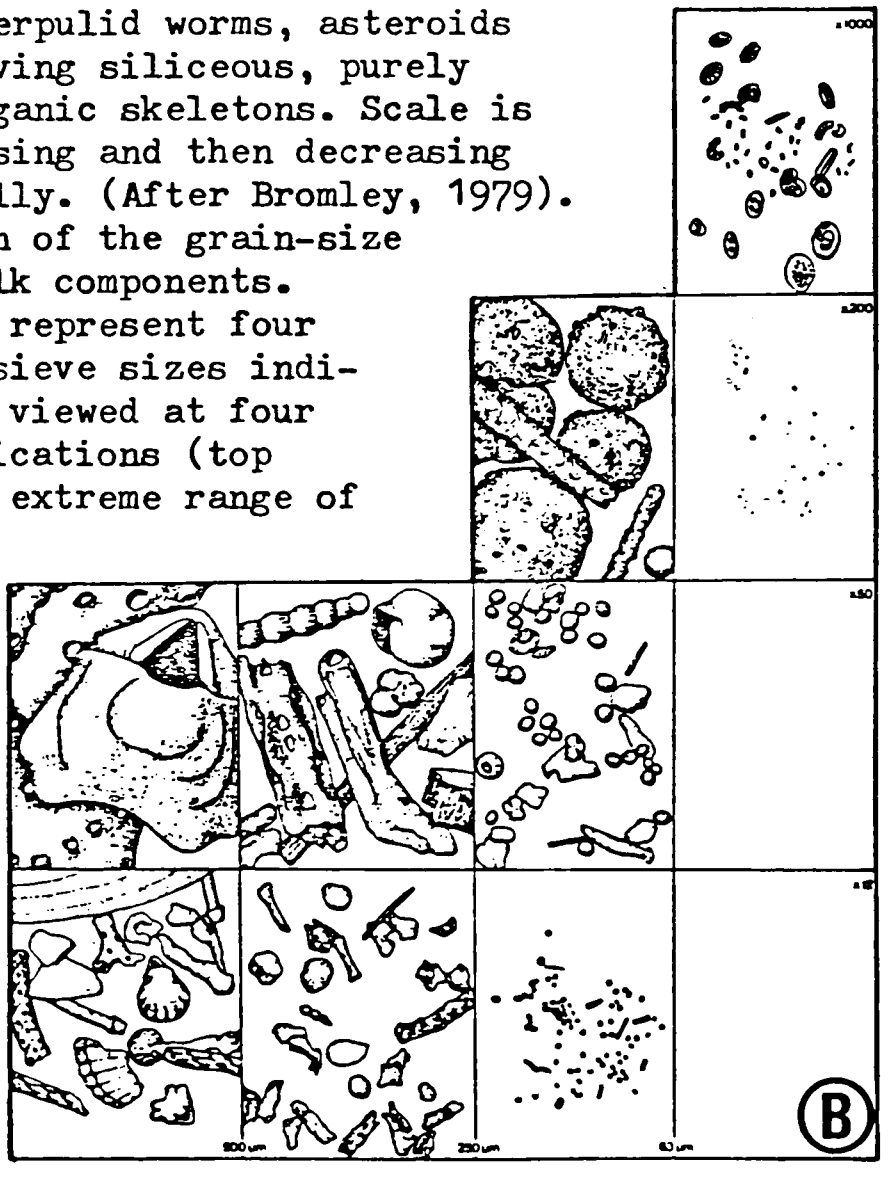

white chalks intercalated within phosphatic chalk successions but is less significant elsewhere.

(4) Siliceous skeletal material. Silicisponge spicules and rare radiolaria, now usually calcitized, glauconitized or limonitized. The former are an important constituent at some levels.

In addition to the four components listed above, it may be infered that skeletal aragonite was once present on the seafloor. The majority of white chalks are rich in inoceramid debris, and inoceramid bivalves typically have a shell consisting of a thick outer layer of prismatic calcite and two thinner inner aragonitic layers (Kennedy and Garrison, 1975b). It is possible, therefore that chalk rich in comminuted inoceramid once contained several percent aragonite. The length of time this survived on the seafloor is difficult to determine but there is strong evidence for pre-burial seafloor dissolution of aragonite (Jefferies, 1962, 1963; Hudson, 1967; Kennedy, 1969; Bathurst, 1975). Whether the sediment ever contained other aragonitic elements (ammonites, gastropods, bivalves etc.) is even more difficult to confirm; certainly no aragonite remains in the sediment.

It was noted at Beauval that even where other aragonitic fauna is preserved as composite internal/external moulds in the cemented, phosphatized lag on top of the basal hardground, evidence of inoceramid aragonite was absent. This may indicate that the inoceramid component had been reworked prior to its inclusion in the basal lag or alternatively may result from the aragonitic layers of these bivalves being especially susceptible to seafloor dissolution. In contrast at least some of the coral aragonite was unusually stable and is now preserved as its inversion product - calcite. No other originally aragonitic skeleton is known to preserve in this way. An aragonitic fauna is commonly preserved in hardground chalks (Bromley, 1965; Kennedy and Garrison, 1975b) and those associated with phosphatic chalks are no exception but here even more factors must be considered before a preservational model can be proposed (3.3.4).

Thin beds of grey to greenish marl a few centimetres thick occur within white chalk successions (e.g. the Beauval Intermediate White Chalk Marl). These

differ petrographically chiefly in having a higher clay (and to a lesser extent other non-carbonate) content and also tend to contain a marginally higher percentage of skeletal carbonate. In addition all types of coarser organic-calcite are better preserved at these horizons (cf. Jørgensen, 1975), possibly because the reduced porosity and permeability resulting from the elevated clay content hinders syntaxial overgrowth of the calcite. In detail the seams have a finely-laminated appearance that may in part reflect primary bedding but has been considerably modified by dissolution of some of the enclosed micrite to produce a flaser structure (Garrison and Kennedy, 1977). The late diagenetic nature of the flasering is demonstrated (3.8.2a) by the way in which the secondary lamination pinches and swells around burrows that penetrate the seams, leaving the more calcareous chalk of the fill relatively unaffected. The marl seams commonly contain white-chalk filled Chondrites burrow mottling, made prominent by the contrast in sediment types. It is probable that the seams, like many others in the Chalk (Jefferies, 1963; Hancock, 1975a; P. Woodroof pers. comm.), rest on top of erosion surfaces, but in the white chalks considered here the lack of any lateral control and the absence of a precise biozonation make the hiatus difficult to prove.

In addition to the bedding indicated by marl seams, many white chalks (and upper white chalks in particular) contain prominent levels of nodular flint. These are a late diagenetic feature (3.8.1) but are nevertheless excellent bedding indicators (Håkansson et al., 1974; Hancock, 1975a) and continue to act as such even when the deposit has been contorted by slumping (Kennedy and Juignet, 1974; Gale, 1980). Their origin will be considered later (3.8.1). Further indicators of bedding include laterally discontinuous winnow patches of calcarenite rich in inoceramid and other skeletal carbonate, and minor erosion surfaces that are picked out by their limonite-stained surfaces (probably after glauconite) and occasional overlying mineralized and/or unmineralized white chalk intraclasts.

In general the bedding indicators demonstrate that the lower, intermediate and upper white chalks are horizontally bedded with only very low angle tectonic dips (Winterbourne and Boxford, 2.11.2, 2.11.3 are important exceptions). This

contrasts strongly with the high angle depositional dips associated with basal hardgrounds and their associated phosphatic chalks.

### 3.2.2 Depositional environment

Evidence concerning the depositional environment of chalks comes from a variety of sources but is rarely unequivocal. Some of the data will be examined in the subsequent sections.

#### 3.2.2a Substrates

The majority of white chalk components are of pelagic origin and were produced in the water column above the seafloor. To this were added subordinate quantities of skeletal material produced by the benthos. Coccoliths are proportionally the major constituent of the sediment and these, being of floral origin, are restricted to the photic zone. The chief level of coccolith production in modern tropical seas is at ~50 m below the surface (Black, 1965) but is shallower in temperate waters. It has been observed in the modern oceans that coccolith sedimentation rates are too high and their distribution too restricted to be accounted for by Stokesian settling. It has been suggested (Roth et al., 1975; Hattin, 1975) that ingestion by zooplankton (mainly copepods) and subsequent production of coccolith-bearing faecal pellets with much higher settling velocities explain these apparent anomalies. On reaching the bottom the pellets may be expected to go through further cycles of ingestion and excretion by the deposit-feeding benthos.

A pelletal substrate is indicated by a number of indirect lines of evidence although the rocks do not exhibit a general pelletal texture. Sparse, mineralized faecal pellets occur throughout the Chalk (Strahan, 1891, 1896; Hume, 1893; Jukes-Browne and Hill, 1903, 1904; Willcox, 1953a, b; Kennedy, 1970b). Examples are known (e.g. Kennedy, 1970b pl.4 fig.6) where fossils are filled with a pelletal sediment and it has been suggested that this may represent the original composition of the chalk substrate prior to compaction (Kennedy, 1970b; Kennedy and Garrison, 1975b). Studies on recent mud bottoms (Rhoads, 1967, 1973; Rhoads and Young, 1970) demonstrate that intense bioturb-

ation of the type present in the Chalk generates a thixotropic pelletal substrate.

Some of the best evidence for unstable substrates is provided by an examination of Chalk faunas. Fluid bottoms support a benthos that has developed a number of adaptions (Rhoads op cit.), all of which are represented in white chalk associations (Carter, 1968, 1972; Kauffman, 1965, 1966; Surlyk, 1972), particularly amongst the bivalves. Examples include Spondylus which has a cemented juvenile stage but becomes free-living and developes large supporting spines during ontogeny, and Lopha which develops large marginal spines at some levels (but the same species shows no such adaption in other facies). Plicatula has specialised supporting flanges and a gryphaete form develops in some groups. The root-like pedicle of the common Chalk brachiopod Terebratulina is regarded as an adaption to an unstable substrate. Finally, a prolific epifauna develops on any large skeletal elements (ammonites, Platyceramus) occurring at some levels.

At other horizons, however, the occurrence of endobyssate bivalves (Stanley, 1972) and a relatively unspecialised epifauna indicates firm bottoms, while the prolific boring and encrustation associated with many hardground horizons is clear evidence of true rocky substrates.

Clearly the Chalk seafloor cannot be regarded as being permanently thixotropic, but the evidence suggests that this was the dominant nature of the sediment/water interface. At depth, however, the preservation of clear outlines of Thalassinoides, Chondrites and Zoophycus burrows demonstrates that below ~50 cm the sediment was firm (Håkansson et al., 1974), but not necessarily non-thixotropic. At these shallow depths of burial by a sediment having such a high water content (probably $\geqslant 50\%$; Rhoads op cit.), firming of the substrate cannot be attributed to overburden pressure but was probably due to dewatering caused by bioturbation (Håkansson et al., 1974).

### 3.2.2b Sedimentation rates

Even with the relatively stable environment of the Chalk, sedimentation rates must have varied greatly both laterally and through time. Attempts have

been made to calculate rates of deposition by measuring the thickness of particular successions or stages, recalculating for compaction (generally estimated as ~10%) and dividing by the calculated length of time (based on radiometric data) that unit represents (see Håkansson et al., 1974; Hancock, 1975a; Kennedy and Garrison, 1975b). These are necessarily only rough order-of-magnitude estimates. Errors are introduced by the presence of numerous breaks in sedimentation (omission), erosion surfaces and early-cemented horizons which have not undergone compaction. Another potential source of error lies in the interpretation of marl seams (Bromley, 1979). In addition to the erosional hiatus beneath the clay seam the high clay content of the overlying sediment may result from seafloor dissolution of calcite due to reduced carbonate sedimentation (Worsley, 1971; Hansen, 1977; Ernst, 1978). Alternatively, it may represent a rapid influx of fine terrigenous detritus into the basin (Troelsen, 1955; Jefferies, 1963). These diametrically-opposed hypotheses have a considerable effect on estimates of sedimentation rates in successions containing an appreciable number of marls.

Overall, therefore, we may assume that estimates of $2 - 4 \times 10^{-3}$ cm y (Black, 1953; Hancock, 1975a) for the bulk of the Chalk and $13 \times 10^{-3}$ cm y for the Maastrichtian of the Danish Basin (Håkansson et al., 1974; Hancock, 1975a) are considerable underestimates of the actual rate of accumulation of sediment in the white chalk during periods of deposition. All estimates indicate, however, that rates of chalk deposition were considerably higher in the Cretaceous than for similar modern sediments.

### 3.2.2c Depth

Modern coccolith-rich sediments occur in shallow-water areas where other carbonate and clastic terrigenous inputs are low (Scholle and Kling, 1972) but in general modern chalks are found in water depths of 100 - 4000 m (Scholle, 1977a). However, the stable tectonic setting of the Anglo-Paris Basin during the Cretaceous and the infered outer-shelf environment for the Gault, Upper Greensand and Chalk means that water depths much in excess of 300 m are inconsistent with the facies analysis (Hancock, 1975b).

Actual estimates of the depth of the Chalk sea have been based on lithological, faunal and floral characteristics (see reviews in Håkansson et al., 1974; Scholle, 1974; Kennedy and Garrison, 1975b; Hancock, 1975a). In white chalks the fine-grained nature of the sediment indicates deposition below wave-base ( ~20 m) while the general absence of bioherms, algal grains and algal borings suggests that the seafloor was aphotic ( >150 m). Quantitative analysis of hexactinellid sponge assemblages (Reid, 1962a, b, 1968, 1973; Bignot and Defretin, 1967) indicates depths in the range of 100 - 600 m and probably <300 m. Foraminiferal studies (Barr, 1962; Jefferies, 1962; Burnaby, 1962; Hart, 1970) are generally consistent with these data and seafloor-spreading models (Hayes and Pitman, 1973) also indicate a maximum Upper Cretaceous eustatic rise in sea-level of this order of magnitude.

It may be concluded that the general depth of white chalk sedimentation was between 150 and 300 m but some hardground horizons yield evidence of enterolithic algae and possible algal crusts, indicating deposition within the euphotic zone (3.3.4) and therefore water depths of <150 m.

### 3.2.2d Temperature and salinity

Palaeomagnetic evidence (Smith and Briden, 1977) places the centre of the Anglo-Paris Basin at ~35°N during the Santonian. This corresponds with the present subtropical belt. During the late Cretaceous, however, the absence of ice caps and the non-seasonal climate (Hancock, 1975a) would have resulted in much lower climatic gradients and annual temperature ranges so the climate was probably more tropical in aspect.

Attempts at determining absolute water temperatures (Urey et al., 1951; Lowenstam and Epstein, 1954; Bowen, 1966) using oxygen isotopes, have suggested water temperatures of ~18°C for the Santonian to early Campanian. It is recognised, however, that results obtained by these methods are based on a number of doubtful suppositions including the absence of isotopic fractionation, original mineralogy and lack of diagenetic alteration. Furthermore, the trend revealed by these methods of a temperature 'high' during the Coniacian to early Campanian is not supported by the faunal evidence (Voigt, 1964).

This indicates a restricted distribution of 'warm' water groups such as hermatypic corals, rudistid bivalves and the larger foraminiferans during the Coniacian to Campanian and therefore relatively lower temperature at this time.

Coccoliths have wide salinity tolerances (Bukry, 1974) and are known to survive salinities as low as 11 parts per thousand in the Sea of Azov, so chalk deposition does not necessarily imply fully marine conditions. The abundance and diversity of stenohaline groups such as echinoderms, sponges, brachiopods and planktonic foraminiferans in all chalk lithologies in the Anglo-Paris Basin, however, indicate deposition in normal marine salinities (~36 ppt).

### 3.2.3 Early diagenesis

The primary low-Mg calcite composition of both coccoliths and the bulk of other components, makes chalk sediments abnormally stable mineralogically and therefore much less prone to early diagenetic alteration than most other carbonate sediments. For white chalks early diagenesis is essentially restricted to compactional dewatering and the loss of unstable organic matter. Initially burrowing and later overburden pressure lead the sediment to expel water until a grain-supported framework is formed (Scholle, 1974, 1977a). It is probable that any aragonite was removed during or prior to this stage (3.2.1). Continued burial resulted in the loss of Mg from the small proportion of high-Mg calcite (e.g. echinoderm) to produce the homogenous low-Mg calcite mineralogy of the final rock.

Modern coccolith oozes have porosities of 70 - 80% but these are reduced during dewatering to 50 - 60% within the first few tens to hundreds of metres burial (Schlanger and Douglas, 1974). Beyond this point, considerable burial is required to significantly further reduce porosities and most white chalks have values of 35 - 50% (Scholle, 1974, 1977a). Additional stability at this stage is contributed by the extremely low permeability of the rock (1 - 8 md; Scholle, op cit.) which prevents further movement of porewaters and thereby

effectively seals-off the sediment geochemically.

## 3.3 Hardgrounds

Hardground is applied to units of sediment that have undergone synsedimentary lithification to produce hard seafloors. My definition is not restricted to the surface of the lithified unit (Voigt, 1959; Bromley, 1965, 1967b, 1968, 1975a, 1978) because I regard the total thickness of synsedimentarily lithified sediment as being the result of an abnormal depositional environment (see below) and not just the consequence of a break in sedimentation within a normal soft white chalk substrate (e.g. Kennedy and Garrison, 1975b). The majority of hardgrounds (and all those considered in detail here) are of local or extremely local extent, only covering a few $km^2$ or even hundreds of $m^2$. A few prominent hardgrounds (e.g. Chalk Rock), however, cover thousands of $km^2$ and are demonstrably diachronous (Bromley, op cit.).

Hardgrounds are particularly prominent in Chalk successions because their intense lithification and prominent jointing contrasts strongly with white chalks which are soft and unjointed. Differences are made even more obvious by the different weathering styles of the two sediments. The synsedimentary nature of the lithification may be demonstrated (Bromley, 1978) by:

(1) An overhanging surface sculpture that could not support itself unlithified,

(2) Overlying angular intraclasts,

(3) An encrusting epifauna,

(4) Boring,

(5) Mineral skins that are mutually intergrown with the encrusting fauna or cut by borings,

(6) A petrographic fabric and burrow systems that show zero compaction.

All of these features are exhibited by phosphatic chalk basal hardgrounds (see below), and to a lesser extent by other hardgrounds in the successions considered here.

Basal hardgrounds are the generally strongly-lithified and mineralized hardgrounds that underlie most (and all well-developed) phosphatic chalks. Where two distinct beds of phosphorite underlain by hardgrounds are present in the same succession the upper of the two hardgrounds is designated as the upper basal hardground. The best current exposure of a basal hardground is at Beauval quarry (2.3.2) where recent excavations have revealed considerable lateral variation (Fig. 2.15). Poorer exposures are also seen at most other extant exposures (Chapter 2). The following descriptions are primarily based on careful examination of these basal hardgrounds although other hardgrounds display the same features to greater or lesser degrees.

### 3.3.1 Morphology

Detailed morphology of the basal hardground varies from exposure to exposure and between cuvettes (3.6.1) but all show a majority of features in common. These are:

(1) A strongly-lithified top up to 30 cm thick, passing down into -

(2) Less indurated lower levels with lithification becoming poor or absent 60 cm below the surface of the hardground.

(3) Vertical penetration of the hardground by numerous Thalassinoides burrow systems which were open at the time of lithification and were subsequently filled with the richly phosphatic basal lag that rests on top of the hardground surface. The burrow systems penetrate beneath the lithified portions of the hardground and may commonly be traced 3 m and sometimes as much as 5 m below the hardground surface.

(4) Mineralization is concentrated in the upper portions of the hardground and is typified by phosphatization and glauconitization of lithified chalk, downwards from the surface and outwards from burrow walls. The top of the hardground is invariably coated by a thin (generally $\leq 1$ mm) shiny phosphate skin that extends down into the upper portions of the burrow system, and may be encrusted by an unphosphatized epifauna.

(5) The hardground surface is commonly extensively bored. Borings are

of a variety of types and may be attributed to sponges, sipunculid and polychaete worms and pholadid bivalves. The walls of the borings are invariably extensively phosphatized. The borings have usually been infilled by an intraclastic phosphorite and their tops sealed-off by an overlying shiny phosphate veneer complex.

(6) The hardground sediment itself contains both mineralized and unmineralized intraclasts and shell debris, which have been incorporated into the main body of the hardground and plastered on top during the later stages of accretionary lithification.

(7) During the later stages of hardground formation, the incorporation of intraclastic material into the hardground top has commonly led to the sealing-off of the upper passages of the Thalassinoides systems and the stenomorphism (Bromley, 1975a) or restriction of others. The lag, where it has been lithified during early diagenesis, is frequently overlain by 'Terebella' phosphatica patch reefs and phosphate skin complexes.

(8) The final stage of hardground formation was followed oy mantling with a coarse intraclastic lag containing bored and otherwise bioeroded fragments of hardground, all coated with the same ubiquitous shiny phosphate patina that coats the hardground top. Other components of the lag include phosphatized faecal pellets, ooliths, shell fragments and bone debris (all similarly coated) floating in an unmineralized, unlithified micrite.

(9) Coral patch reefs were formed prior to the deposition of the phosphatic chalk, since the coral beds are only poorly phosphatic, although they are commonly reworked into basal lags.

Where the basal hardground is extensively exposed i.e. Beauval and Nurlu quarries, the nature of the hardground can be seen to vary greatly laterally. At Beauval quarry it is composed of a series of converging and diverging hardground surfaces (Fig. 2.15) superimposed one on top of the other. Nevertheless, present-day exposure and lateral control are insufficient to trace a basal hardground from a cuvette axial to a cuvette marginal (3.6.1) facies. However, the lateral changes in both phosphatic chalk and basal hardground recorded

during the exploitation of Flour's quarry at Fresnoy-le-Grand (2.6.2) provide valuable data. The descriptions demonstrate that as the phosphate content of the basal phosphatic chalk decreases, lithification of the basal hardground becomes less pronounced (Fig. 2.59). This is interpreted as representing the transition from an axial to a marginal facies and as such suggests a positive correlation between the amount of white chalk eroded and the degree of lithification of the basal hardground. This relationship is also well-demonstrated by the Hardivillers Upper Hardground (Fig. 2.182).

The morphology of hardground surfaces in particular vary greatly laterally. In general it is the product of a number of distinct processes:

(1) Pre-lithification scour, producing essentially planar surfaces,

(2) Scour and bioerosion during induration which pick out inhomogeneities in the surface of the lithifying unit (e.g. burrows) and produces a convolute surface and lag intraclasts.

(3) Post-lithification erosion may result in a variety of surface morphologies depending on whether the agent is dominantly physical (planar) or biological (convolute).

(4) Accretion of successive generations of later (commonly intraclastic) sediment. This initially smooths out irregularities in the pre-existing surface but later modifications may result in a variety of distinct new topographies.

(5) Mineralization. Predominantly a passive process except phosphate skins (3.3.3c) which fill minor surface irregularities (including the entrances to borings and burrows) to produce a smooth topography.

The gross morphology of the hardground is controlled by two distinct and opposed processes. Physical scour and abrasion planes-off the hardground surface and produces rounded, well-sorted intraclasts, while, conversely, bioerosion leads to a convolute or even filigree morphology and angular, concave-surfaced intraclasts. Even when the small-scale features of a hardground have been modified by biological activity, the large scale morphology ( >1 m) is dependent on physical rather than organic processes. The relative importance of these factors in the genesis of a particular surface is not always readily

discernible. Early stages during the evolution of the hardground will be considerably modified or destroyed by later erosion. Such erosion is clearly demonstrated by the truncation of both borings (Fig. 2.14) and Thalassinoides burrows (c.f. Bromley, 1975a fig. 18.7) and in some cases this erosion postdates mineralization since glauconitization zones are also truncated.

### 3.3.2 Biological processes

Basal hardgrounds are characterised by a number of trace-fossil assemblages which are absent in both phosphatic and white chalks. These associations are the result of the profound changes which synsedimentary lithification had on the sedimentology and ecology of the seafloor. In all cases two distinct suites of trace (cf. Bromley, 1975a) may be defined:

(1) Pre-lithification burrows

(2) Post-lithification burrows and borings.

Pre-lithification burrows are characterised by large and extensive networks of broad, idiomorphic Thalassinoides. The soft-sediment fill of these burrows testify that they remain open and more or less empty during cementation of the hardground. Their hardened walls have been strongly mineralized; glauconitization being concentrated in the gallery roofs and phosphatization in the floors. Most are also lined with phosphate skin complexes that penetrate tens of centimetres below the hardground surface. Thus an extensive open gallery system must have existed below the hardground surface at least during the early stages of its evolution. It is noteworthy, therefore, that both borings and crevice faunas are rare within the galleries although both are well-developed in other deposits (e.g. Palmer and Fürsich, 1974; Bromley, 1975a). This may indicate a lack of aeration of abandoned tunnel systems or alternatively may be the result of phosphate skins or their precursors (3.3.3c) preventing the settlement of 'spat'.

Chondrites are also present in the pre-lithification assemblage (along with Planolites and Zoophycus) but are less noticeable because they generally contain a hard white chalk fill that shows little contrast with the surround-

ing sediment (indicating that they were abandoned during lithification). In some cases, however, a contrasting fill makes the burrows more prominent. At Nurlu quarry (2.5.2) a green glauconitized chalk infilling the Chondrites suggests that the system remained open during cementation and the fill was subsequently mineralized.

Although burrowing is essentially restricted to soft sediment it must not be supposed that burrowing ceased during or after lithification. The complex interaction between burrowing and cementation is indicated by the changing morphology of the Thalassinoides burrows during cementation. The idiomorphic Thalassinoides present in the hardground are identical to those occurring in white chalks but in the same hardgrounds are narrower, constricted networks of burrows (stenomorphic Thalassinoides; Bromley, 1975a). These interconnect with the larger idiomorphic systems, commonly reexcavate their fill and were clearly constructed at a later stage during cementation of the hardground and accretionary lithification of earlier burrow fills. These stenomorphic systems (Fig. 2.94) have been refered to Thalassinoides paradoxicus by Kennedy (in Bromley, 1967b p.181; 1970) and are characteristic of the final stages of hardground development.

The idiomorphic system remained open during lithification but rarely continued to be void of sediment. More often sediment falling down from the hardground surface was plastered onto burrow walls where it becomes cemented in place. More extreme infilling events require complete reexcavation, but again some material remained within the system cemented to burrow walls. These processes have two important implications. Firstly, sediment preserved in the burrows may date from the hiatus when no sediment was being deposited on the surface of the hardground. Secondly, the plating process resulted in the gradual restriction of idiomorphic burrows and converted them to a stenomorphic system similar to that seen elsewhere in the hardground. It has also been noted (Voigt, 1959; Bromley, 1967b, 1975a) that the protected microenvironment of hardground burrows provides unusually favourable conditions for fossilization and may preserve extremely delicate forms (e.g. bryozoans) unknown elsewhere in the succession. Certainly some of the best preserved moulds of

gastropods and aragonitic bivalves are found within the phosphorite filled burrows of basal hardgrounds. A final point is that the last burrow infill will represent the turnover stage between non-deposition and sedimentation. It is not unexpected therefore that the fill commonly consists of a coarse intraclastic basal lag, which is not always represented on top of the hardground where later deposition under decreasing current conditions has produced a finer sediment. Thus the highest grade phosphorite is commonly found within burrows in the basal hardground (cf. Cayeux, 1941 p.395).

In some cases extensive horizontal idiomorphic and stenomorphic Thalassinoides galleries (particularly the former), just below the surface, undermine large blocks of hardground. Subsequent boring, synsedimentary fracturing and undercutting by currents have resulted in the complete isolation and displacement of the blocks (Fig. 2.93). Further erosion and reworking has degraded many of these fragments which are now a major component of basal lags.

The post-lithification trace-fossil assemblage is dominated by borings, which in basal hardgrounds are essentially restricted to the hardground surface. These may be distinguished from burrows by their sharp outlines that cut into the fabric of the hardground and truncate both grains and cement (although the latter is rarely visible). Their walls are invariably strongly-mineralized and the bores are made further conspicuous by their phosphatized intraclastic lag fill.

A number of borers may be present in the general endolithic community in the hardground, but individuals tend to form clusters of the same taxa. Thus pholadid bivalves (Fig. 2.14) are the dominant borer in the uppermost surface of the basal hardground at the centre of Beauval quarry (Fig. 2.15) while (?)spionid polychaetes are abundant in other portions of the same basal hardground and at Nurlu (Figs. 2.48, 2.53a,b, 3.3C,D), Hallencourt quarry (Fig. 2.66B) and elsewhere. Sponge and sipunculid worm borings are also prominent in some areas. This clustering is probably the result of preferential 'spat' settlement in areas already colonised by that group rather than a measure of 'spat' availability. Discontinuous and probably intermittent exposure is indicated by the concentration of borings and epizoans (particularly Pycnodonte, Spondylus,

Fig. 3.3 Boring in basal lags and hardgrounds.
A,B. Straight polychaete boring in a phosphatized basal lag intraclast, Hardivillers. A phosphatized plug of sediment (light-coloured upper half) contrasts with the unmineralized micrite filling the lower portion of the boring. A complex of laminated veneers and phosphatized sediment has sealed-off the entrance to the bore. (A) PPL, (B) XN.
C. Negative print of typical figure-of-eight(?)spionid-worm borings in a basal lag intraclast, Hardivillers. The rectangle marks the position of (D).
D. Phosphatized micrite infilling the margins of a(?)spionid boring. Thin phosphate veneers (arrowed) occur on the inner walls. The strong phosphatization of the plastered sediment contrasts with the indurated but poorly-mineralized surrounding and enclosed micrite. PPL.
E. Small basal lag intraclasts, Beauval. The intense boring displayed by the majority of mineralized intraclasts within and directly above the basal hardground contrasts with those present within the bulk of the phosphatic chalk, which are commonly unbored. PPL.


A
0·5mm

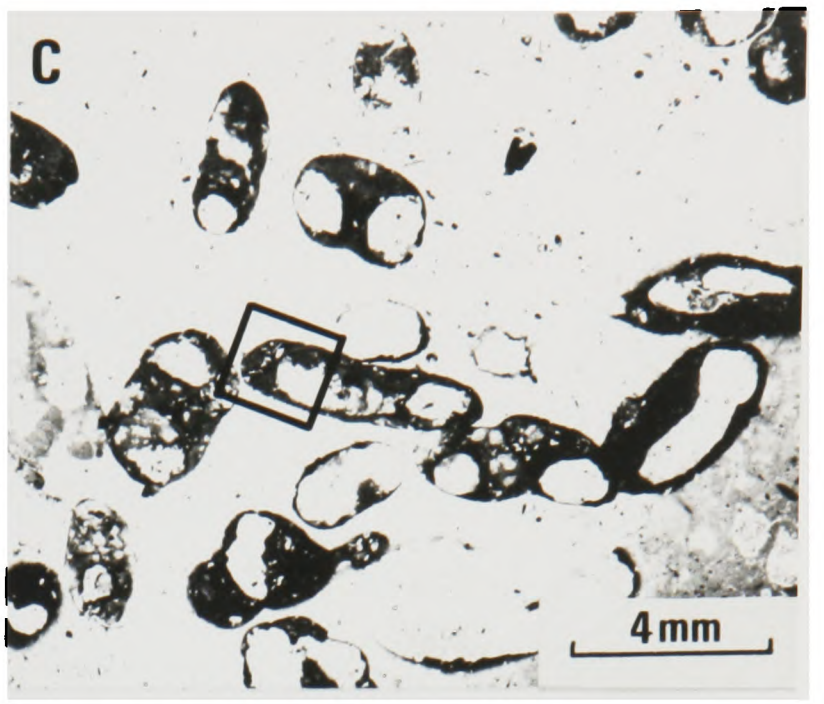
C
4mm

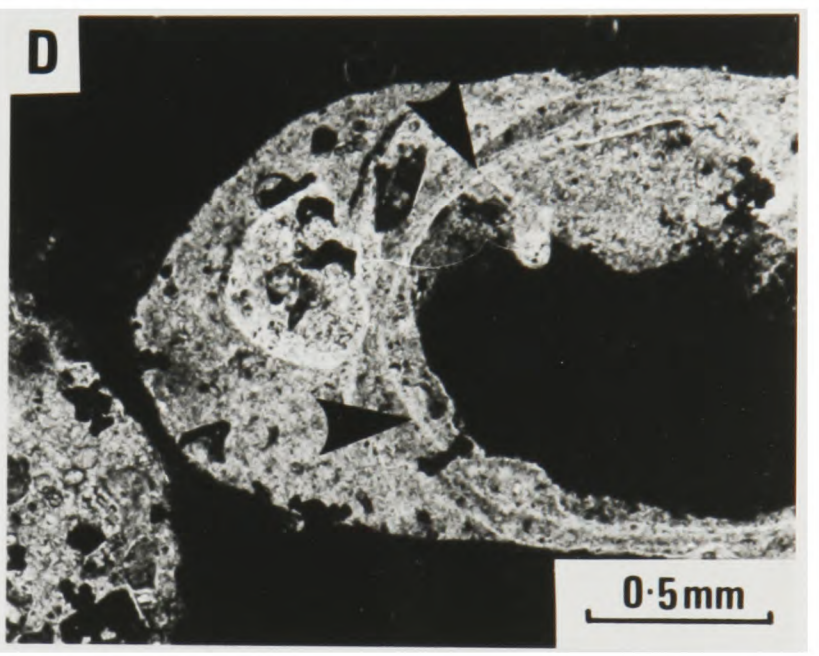
D
0·5mm


B
0·5mm

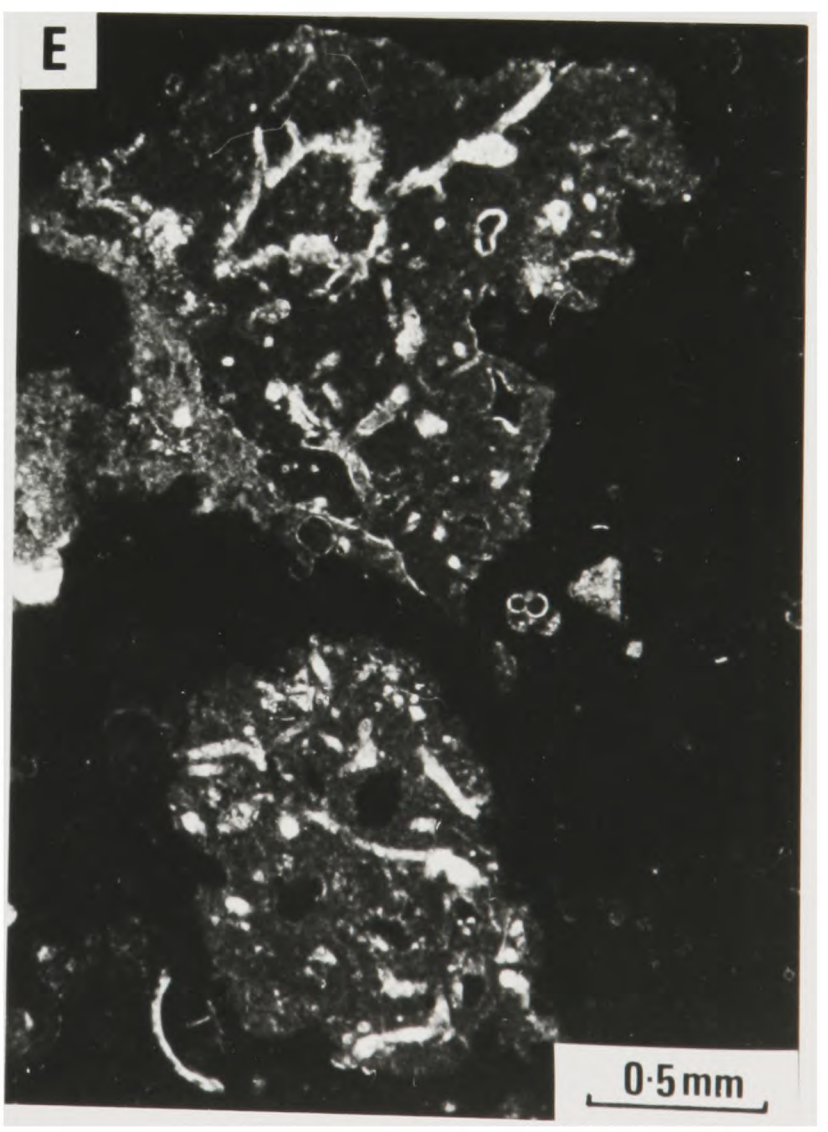
E
0·5mm

'Terebella' phosphatica, serpulids, octocorals and ectoproct bryozoans) to bosses on the hardground surface (Fig. 2.48). This suggests that these hummocks stood as islands surrounded by soft sediment which prevented the establishment of borers and epizoans.

A close interaction between boring and cementation can be seen in many basal hardgrounds. Patches of intraclastic sediment moving across the hardground surface have infilled whole generations of borings (and may have been responsible for the death of the occupants). The coarse sediment trapped within the borings was protected from agitation and became cemented (3.3.4) into the surface of the hardground. Subsequent reexposure led to the establishment of a second endolithic community which cuts both the walls and hardened fill of the earlier borings. This cycle is commonly repeated so that generations of boring become superimposed one on top of the other, and may reach a point where the hardground surface is completely destroyed and replaced by a fill of superimposed suites of boring. This latter stage is particularly common in areas that have been intensely bored by (?)spionid polychaetes (Fig. 2.53a,b).

It has been mentioned that the truncation of borings is indicative of post-lithification erosion of the hardground. However, the endolithic assemblage rarely consists of a single 'population' of truncated bores but contains a whole variety of borings in all stages of erosion. This may result from phases of mechanical erosion alternating with quieter periods when the abraded surface was recolonised by boring organisms, but the borers themselves also provide an important potential mechanism for degrading the hardground. Neumann (1966) quotes erosional rates of 1 m per 70 years by clionid sponges in the limestone coasts of Bermuda. Warme has illustrated (Warme and Marshall, 1969; Warme, 1970, 1975; Warme et al., 1971, 1978) that similar rates can be achieved by whole communities of borers down to depths of 1000 m. In addition to the endolithic community, additional bioerosion may be attributed to surface rasping by echinoids, crustaceans and fish, while nestlers (including bivalves and sponges) may further enlarge vacated borings. Clearly bioerosion is potentially the dominant post-lithification erosional process although such erosion must be considerably enhanced by additional physical abrasion.

Despite the abundant evidence of bioerosion it is uncertain whether the quantity of borings in a hardground provides an indication of the length of the hiatus represented by its surface. On many modern hardgrounds migrating waves of sediment periodically bury and then uncover the surface and thereby prevent the establishment of an endolithic community, or elsewhere impenetrable layers of unpreserved benthos (e.g. algae or sponges) may prevent settlement. In addition mineralization, and phosphatization in particular, may inhibit the penetration of boring organisms that depend on carbonate substrates. The occurrence of bored 'islands' particularly favours a soft sediment control.

The effect of a hardground on burrowing does not cease when the hardground surface becomes buried by sediment. The hardground subsequently acts as a baselevel to organisms burrowing-down through the overlying sediment and causes them to deflect their burrows and concentrate them along its surface. This 'imposed horizontality' (Bromley, 1967b) is well-displayed in many basal hardgrounds where phosphatic-chalk filled Thalassinoides spread along and then penetrate the uppermost surface of the hardground by reexcavating a pre-existing system, but are then again blocked and spread horizontally along an older underlying surface. This is best seen at Beauval quarry where the basal lag is carried down below the poorly phosphatic chalk of the Coral Bed and concentrated along the surface of the basal hardground sensu stricto. The process may be repeated a number of times where several closely-spaced hardground surfaces overlie one another, resulting in secondary concentrations of phosphatic chalk on top of hardgrounds that were not primarily phosphatic. The final burrow system presents the anomaly that it crosses several hardground surfaces without apparent interruption (cf. Bromley, 1967b p.162, 1975).

### 3.3.3 Petrography

Study of polished surfaces reveals that basal hardground and many other hardground sediments contain a high proportion of sand to pebble-grade, mineralized and unmineralized intraclasts and shell debris (Figs. 2.14, 2.17A, 2.66A). Commonly unmineralized white chalk intraclasts are the dominant component

which, although clearly visible on wet polished-surfaces, are difficult if not impossible to detect on fractured blocks or in thin section. This is because the intraclasts lack sharp margins and are compositionally identical to their enclosing matrix.

Hardground chalks show a considerable amount of petrographic variation. The intensely-lithified basal hardgrounds at Beauval and Hallencourt quarries are composed of coarse planktonic foraminiferal biomicrites (Fig. 3.1C) while the Nurlu and Hardivillers Basal Hardgrounds are finer-grained and petrographically similar to white chalks (Fig. 3.1A). In addition coarse but unlithified sediment similar to the Beauval Basal Hardground microfacies (Fig. 3.1D) occurs below the upper phosphatic chalk at Taplow. The indurated sediments differ, however, in having a lower incidence of broken or crushed microfossil tests (compare Figs. 3.1C and D) and a higher proportion of empty or spar-filled tests. The general lack of orientation of elongate grains is even more pronounced than in white chalks since early cementation has prevented compactional reorientation of grains during burial.

The fact that hardground chalks do not invariably contain a higher proportion of non-intraclastic coarse material (e.g. inoceramid debris) suggests that although current activity was obviously important in their formation, it did not always predate the initiation of lithification. In addition the poorly-defined nature of the unmineralized intraclasts suggests that in its initial stages, cementation was sufficient to produce only relatively soft patches of sediment. A further complication is that the hardground sediment may no longer represent the sedimentology of the hardground during its initial stages of development. It has been demonstrated (3.3.1b) that a considerable thickness of indurated chalk may be removed by erosion during the evolution of the hardground. Thus if initial cementation was restricted to a surface layer of coarse sediment, but then extended down into the underlying white chalk, it is unlikely that the upper coarse division would be preserved. The evidence of current activity prior to lithification contrasts with the observations of Kennedy and Garrison (1975b p.352) based on other Chalk hardgrounds.

A further difference in petrography displayed by hardground chalks is

the relative abundance of borings in both skeletal debris and intraclasts (Fig. 3.3E). The smaller of these borings have been attributed to algae (Bromley, 1965, 1970; Kennedy, 1970b; Kennedy and Garrison, 1975b) and if this is correct, indicates deposition within the photic zone (i.e. < 150 m even in extremely clear water).

Unlike many other hardgrounds in the geological record, sparry calcite is volumetrically unimportant in Chalk hardgrounds, despite the intense lithification. Void filling spar is restricted to microfossil tests, vugs left by the dissolution of silicisponge spicules, rare geopetals and late diagenetic fractures (Fig. 3.4). Borings are invariably filled with sediment rather than spar, and voids left following the dissolution of aragonitic fauna cemented into the hardground surface have remained empty. Voids remaining in the hardground following its burial must have been filled by sediment filtering down from above the surface and thereby precluded the precipitation of coarse void-filling spar. The most prominent sparry calcite occurs in fractures (Fig. 3.4) probably formed by overburden pressure late in the history of the hardgrounds, indicating that spar development was a late diagenetic rather than synsedimentary process.

The complex cementation/mineralization events revealed by field studies and examination of hand specimens and polished surfaces may be refined by the study of thin sections. Six dominant types of mineralization are present in phosphatic chalk hardgrounds:

(1) Glauconitization of the hardground surface and the walls of burrows and borings,

(2) Subsequent phosphatization of the above,

(3) Deposition of carbonate-fluorapatite skins,

(4) Ferruginization by goethite, lepidocrocite and limonite,

(5) Emplacement of manganese oxides,

(6) Silicification of bioclastic material.

### 3.3.3a Glauconitization

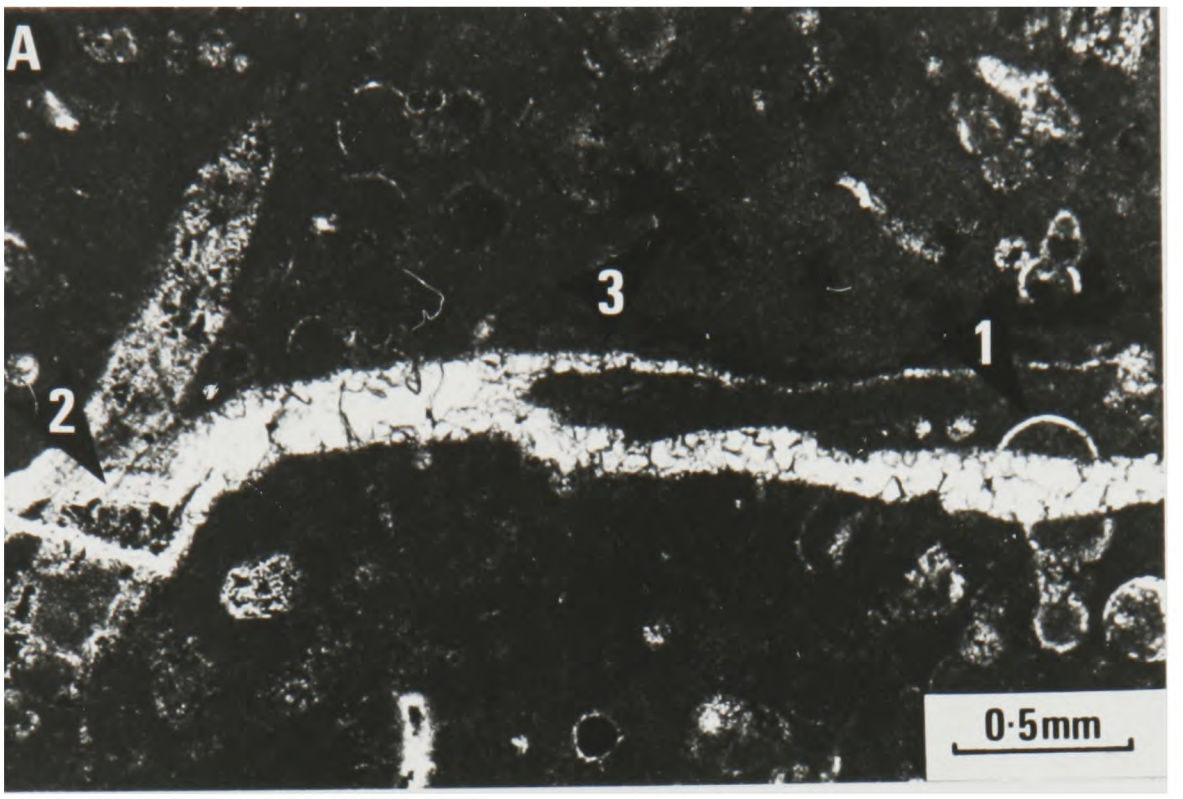


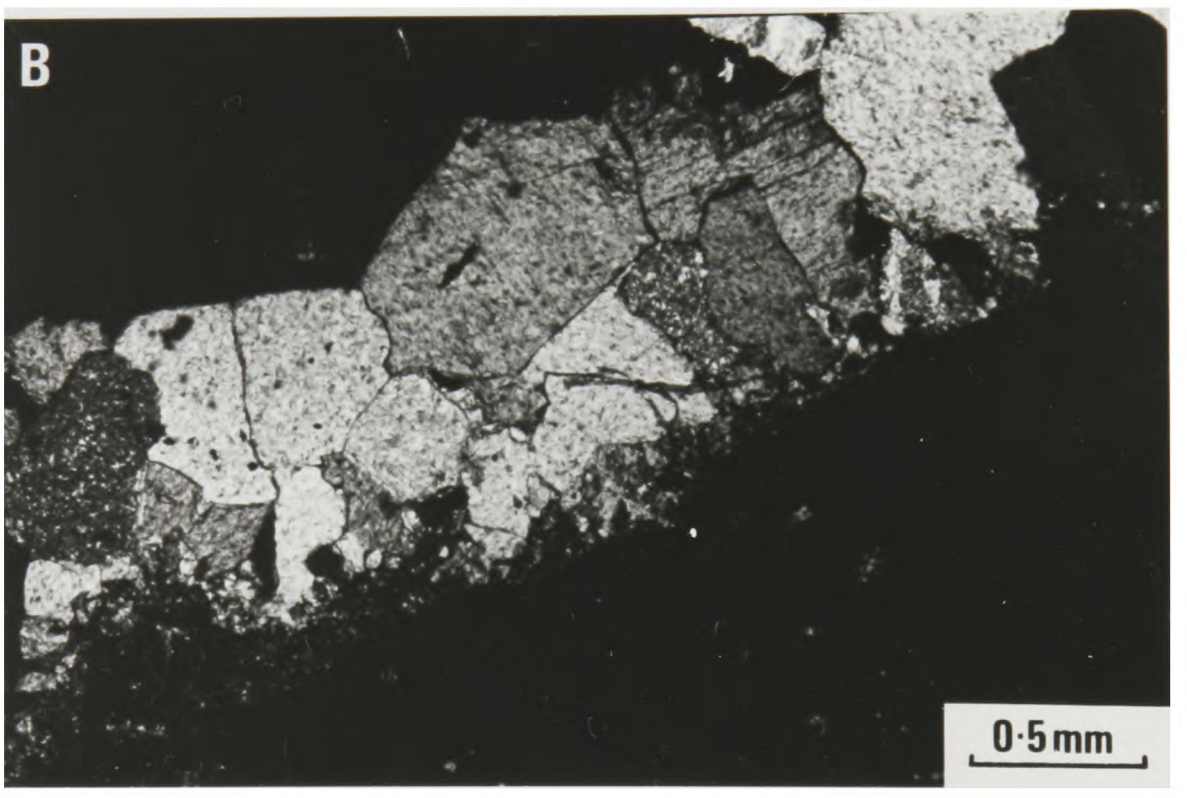


Fig. 3.4 Late diagenetic spar in basal hardgrounds.
A. Bisected microfossils (1) and bone fragments (2) exhibit no lateral displacement on either side of the spar-filled fracture. Dendritic manganese oxides (3) are also clearly visible. Beauval Basal Hardground. PPL.
B. Coarse calcite spar in a large open fracture in the Beauval Basal Hardground. XN.

Thin ( <5 mm) replacive zones of glauconite occur in the hardground surface and extend outwards from the walls of burrows and borings. The bright-green colour of the glauconitized sediment makes the mineralization particularly prominent on wet polished-surfaces where the zones display sharp upper or outer margins but fade out rapidly towards the interior of the hardground.

In thin section, however, the replacement zones are irregular and nebulous in appearance. The pale greenish-yellow of the mineral under plain polarised light is generally only seen as a weak discolouration within the sediment and is clearly only a minor constituent. Where glauconitization occurs alongside phosphate the textural evidence suggests that it predates phosphatization, while truncation of glauconitized zones by boring also indicates that the process was probably authigenic. Where glauconitization and phosphatization are present in the same burrow wall the former tends to concentrate in the roof and the latter in the floor.

Other types of glauconite are also common within basal hardgrounds and these are generally more distinctive in thin section. The first category are the glauconitized infillings of microfossil (especially foraminiferan) chambers occurring in intact, usually unmineralized tests. These are distributed throughout the hardground but are concentrated in burrow-fills with other glauconitic material and within the glauconitization zones associated with the hardground surface and trace fossils. The second group consists of ovoid sand-grade material composed of bright-green cryptocrystalline glauconite. These are apparently glauconitized faecal pellets similar to those seen in most greensands (McRae, 1972). The final variety consists of coarse sand to pebble-grade, angular to subrounded, glauconitized and commonly intensely-bored intraclasts. These are volumetrically the most important (Fig. 2.66A) and may constitute up to 10% of the hardground sediment, although more commonly they only account for 2 or 3%. The occurrence of prolific glauconitized intraclasts within basal hardgrounds and their heavily bored morphology (indicating prolonged exposure on the seafloor) are further evidence of the authigenic nature of the process. This will be considered in more detail later (Chapter 4).

### 3.3.3b Phosphatization

Phosphate shows the same range of replacive mineralization within hardgrounds as glauconite, including replacive zones, mineralized faecal pellets, intraclasts, steinkerns and rare replaced skeletal carbonate. In addition a small proportion of primary skeletal phosphate (particularly mineralized

elasmobranch teeth and teleost bones and scales) is also present.

Pale brown replacement zones are the most prominent type of phosphatization seen in phosphatic chalk hardgrounds. They are generally thicker ($\leqslant 1$ cm) but less obvious than the glauconitized portions of the hardground and similarly have well-defined, dark coloured strongly-mineralized outer margins and gradually fade into unmineralized chalk. The darkest portions of the zones are the most phosphatic but even here the replacement process is rarely complete and individual grains and patches of unmineralized micrite and cement remain. Petrographic studies indicate that mineralization preferentially replaces lithified micrite and rarely effects coarse skeletal carbonate although some foraminiferan tests are replaced by cryptocrystalline carbonate-fluorapatite in the most intensely mineralized regions.

There is commonly evidence for a number of distinct phosphatization episodes within the hardground. Earlier zones may be truncated by borings and both the truncation surface and the fillings usually display later phases of mineralization. Infilling and cementation followed by reboring is likewise a common phenomenon (3.3.1b) and again each phase of boring is accompanied by a period of phosphatization. This highlights the close interaction between biological activity and mineralization that is seen in most hardgrounds. Phosphatized sediment filling the meshwork of replaced silicisponges is prominent (as in most other phosphatized hardgrounds; Bromley, 1965) but the most intensely phosphatized sediment is invariably that which occurs within borings, closely followed by that in the walls of borings and burrows. This is exemplified by an examination of portions of hardground top that have been intensely bored by(?)spionid polychaetes. Spionids, (and some other polychaetes) adopt a U-shaped posture within their borings (see review in Bromley, 1970) and plaster sediment on the walls of the boring and in the core of the U, resulting in a characteristic figure-of-eight cross-section (Fig. 3.3C, D). The borings are similar to but more sinuous than traces assigned to the ichnogenus Polydorites in Jurassic hardgrounds (Holder and Hollmann, 1969). In basal hardgrounds and their overlying intraclasts the micrite plastered within the borings has been intensely phosphatized, the walls weakly mineralized and the boring subsequently infilled with soft

sediment although later boring and mineralization may result in lithification of the fill.

Intense phosphatization of infills is common in other types of boring (Fig. 3.3A,B) and the association between phosphatization and organic activity is also seen in some epizoans. The tubes of 'Terebella' phosphatica (Fig. 3.5B,C) are invariably intensely phosphatic with both the agglutinated material and the original organic(?) cement being replaced by phosphate. It is probable in this case, however, that the material cemented into the tube had already been mineralized prior to its inclusion by the worm. Composite moulds of spiral serpulid tubes overlying the spionid-bored top of the basal hardground at Hallencourt quarry are similarly also strongly phosphatized (Fig. 3.5A,B).

### 3.3.3c Phosphate skins

Shiny phosphate skin complexes are ubiquitous to all basal hardgrounds and have also been observed (albeit less well-developed) on other Chalk hardgrounds, including the Cenomanian Limestone and Chalk Basement Bed of SW England, the Chalk Rock of southern England and the Tun of northern France.

The skin complexes are generally light buff in colour and exhibit a strongly-iridescent glaze on their surface. Where the hardground has been iron stained during weathering the skins become a dark chocolate-brown e.g. the Nurlu and Marcheville Basal Hardgrounds. The skins are predominantly $\leqslant 0.5$ mm thick but thicken ( $\leqslant 5$ mm) where they infill depressions in the hardground surface and the floors of Thalassinoides burrows in the upper portion of the hardground. Thus the skins are not restricted to the hardground surface. They extend down into the upper portions of burrows and borings and also coat the majority of basal lag intraclasts and phosphatic material in the phosphatic chalk; they characterise both phosphatic and hardground chalk lithofacies.

The complexes have two discrete constituents. The first are ultra-fine (20 - 200 $\mu$m) laminated veneers of pure carbonate-fluorapatite (Fig. 3.6) that occur at the base and summit of the complexes and intermittently throughout. Individual laminations are difficult to differentiate because of refraction between successive layers, but are certainly $<10$ $\mu$m thick. The lamellae are

Fig. 3.5 Phosphatized epizoans
A. General view of composite moulds of spiral serpulid worm tubes encrusting the basal hardground at Hallencourt quarry. Large phosphatized faecal pellets and ooliths (indicated) and phosphate veneered echinoderm fragments are commonly cemented into the complex. The calcitic tubes have been dissolved during weathering but are preserved in sections through the complex (B).
B. Cross-section through a number of serpulid tubes as seen in (A). The broadly-laminated structure (indicated) of the tubes is clearly visible. The tubes are filled with phosphatized micrite containing scattered intraclasts (i), ooliths (o) and echinoderm fragments (e) and are surrounded by an unmineralized white chalk. PPL.
C. General view of a 'Terebella' phosphatica worm tube encrusting the Beauval Basal Hardground (see Fig. 2.24 for gross morphology). The tube is composed almost entirely of ovoid faecal pellets cemented with their long axes normal to the direction of accretion.
D. Cross-section through a 'T'. phosphatica worm tube from the phosphatic chalk lens in the intermediate white chalk of Beauval quarry. In the absence of faecal pellets the worm has encorporated phosphatized intraclasts into its tube. The structure is closely comparable to that seen in sabellariid worm tubes (e.g. Scholle, 1978 p.42). PPL.

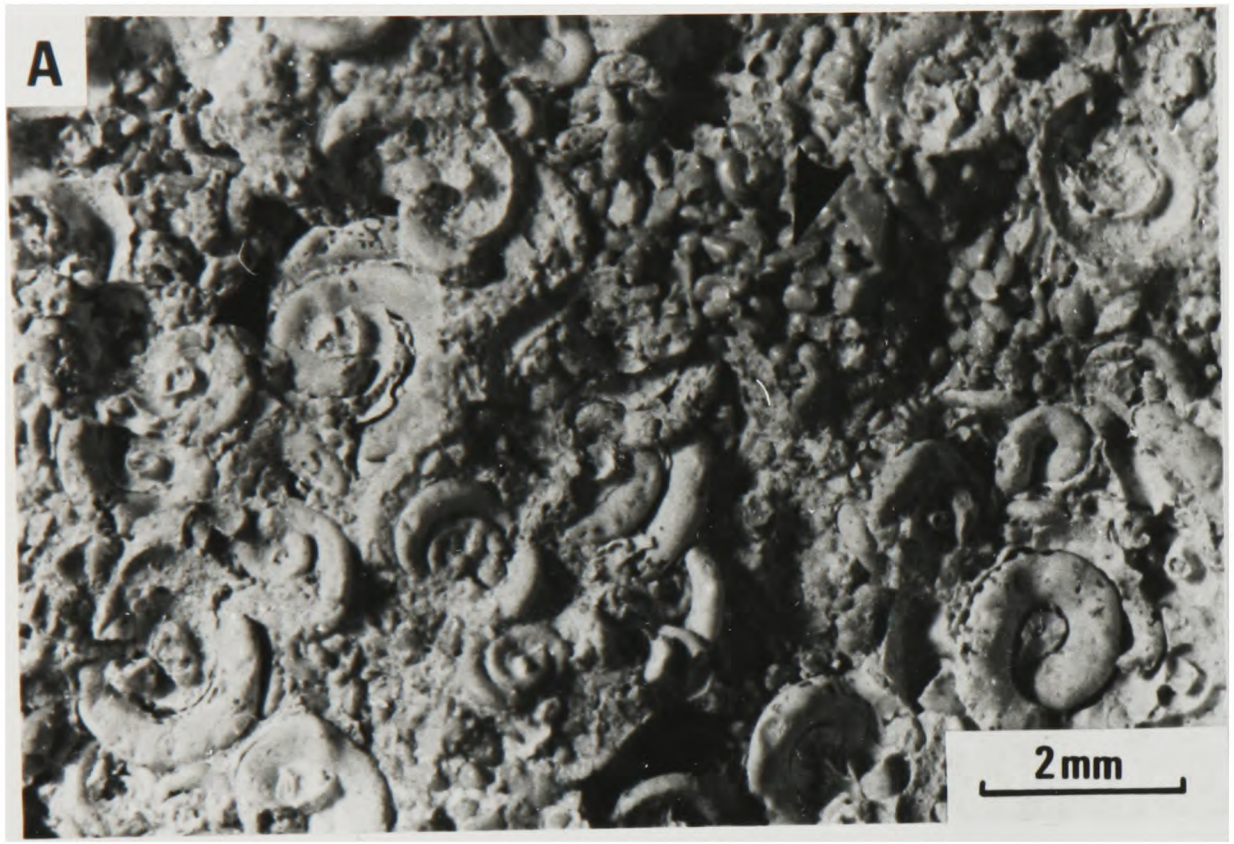
A
2mm


B
i
i
o
e
e
0·5mm

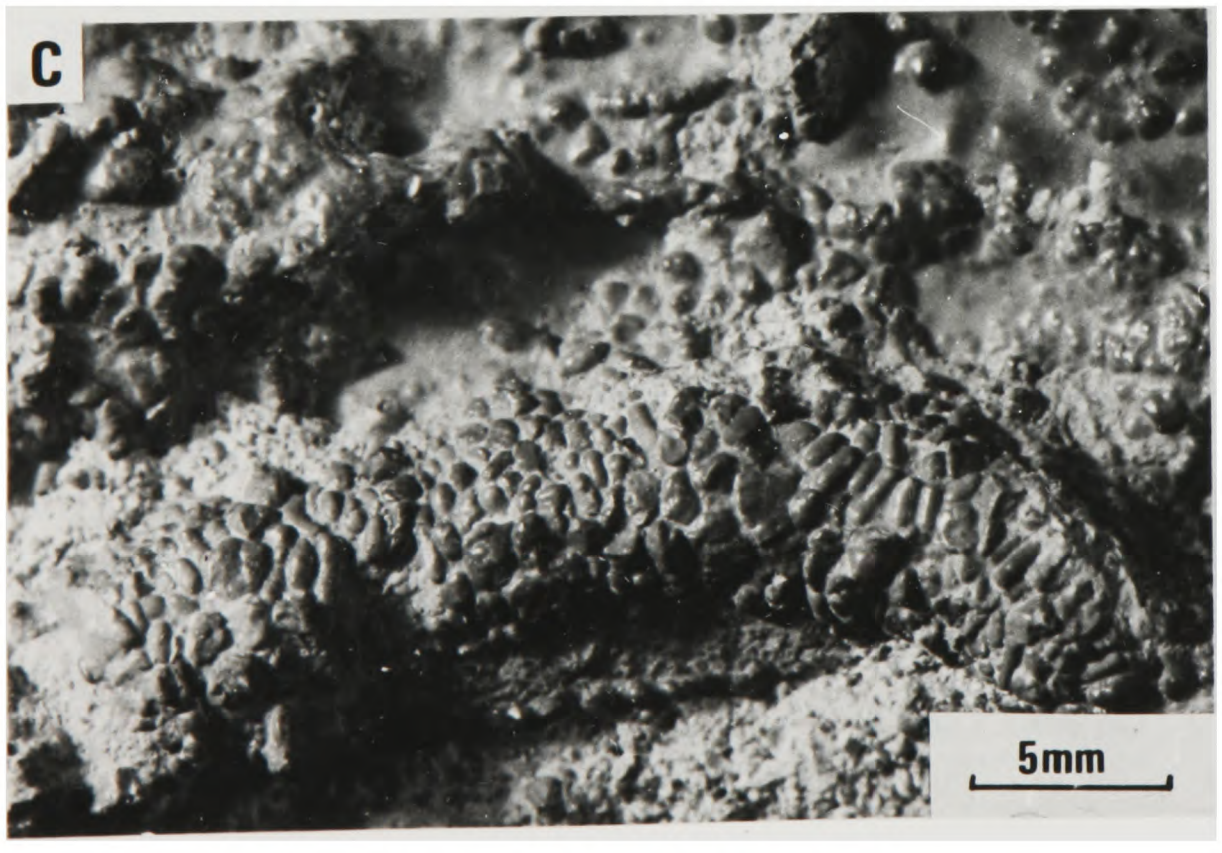
C
5mm

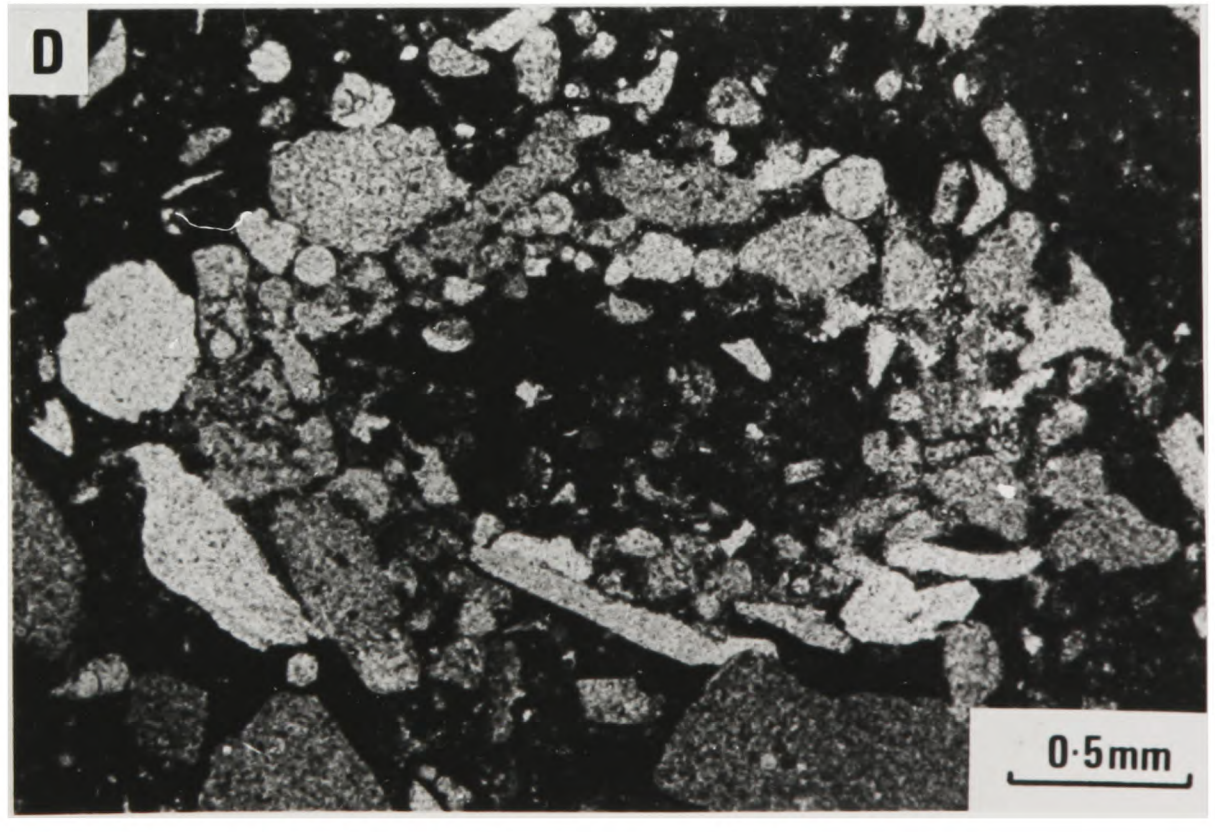
D
0·5mm

Fig. 3.6 Phosphate skin complexes
A. Negative print of a thick complex filling a depression in the Hardivillers Basal Hardground.
B. Section through the main body of the same skin complex. The phosphatized sediment of the hardground is visible bottom left. This is immediately overlain by an abnormally thick (0.2 mm) laminated veneer of pure carbonate-fluorapatite (D,E) followed by alternations of thinner veneers and dark phosphatized micrite. The rectangle marks the location of (C). PPL.
C. Closeup of veneer/phosphatized alternations. The dark colour of the latter appears to be due to the inclusion of blebs of organic matter. PPL.
D.E. Closeup of the pure apatite veneer that occurs at the base of the skin complex. In detail it consists of numerous thin (~10 µm) laminations of iridescent anisotropic phosphate. (D) PPL, (E) XN.
F. Skin complex filling a depression in the Nurlu Basal Hardground. Here laminated phosphate veneers alternate with phosphatized sediment including a high percentage of phosphatic ooliths and phosphate veneered intraclasts, bioclasts and faecal pellets. Hardground chalk bottom right. PPL.

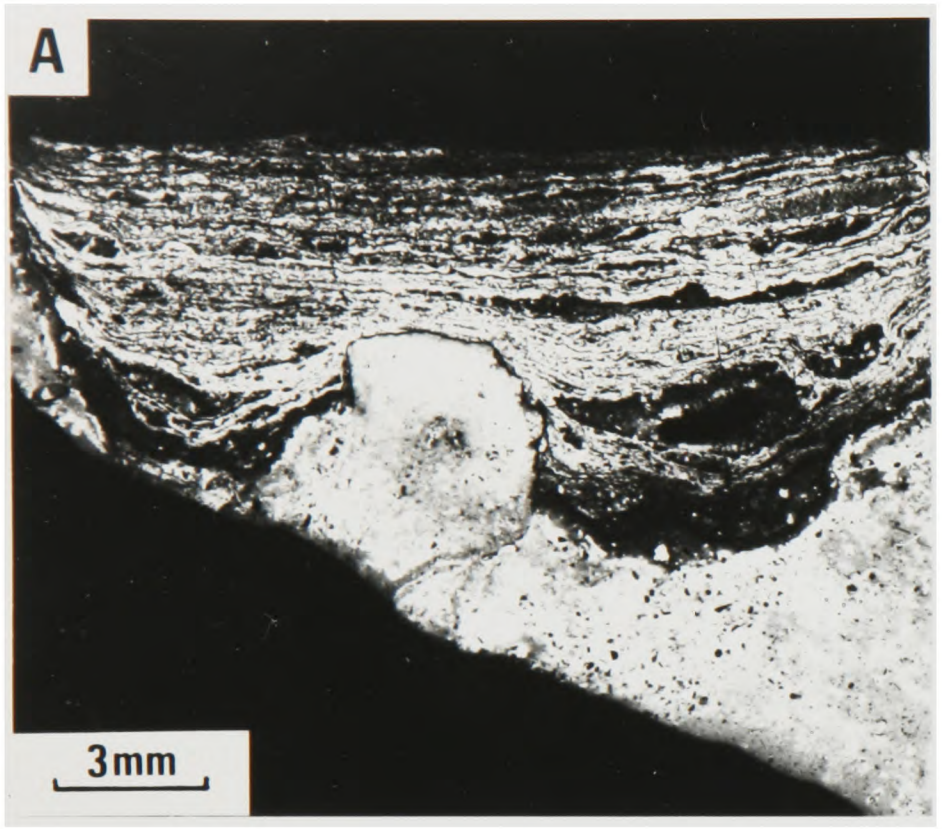
A
3mm


B
0·5mm

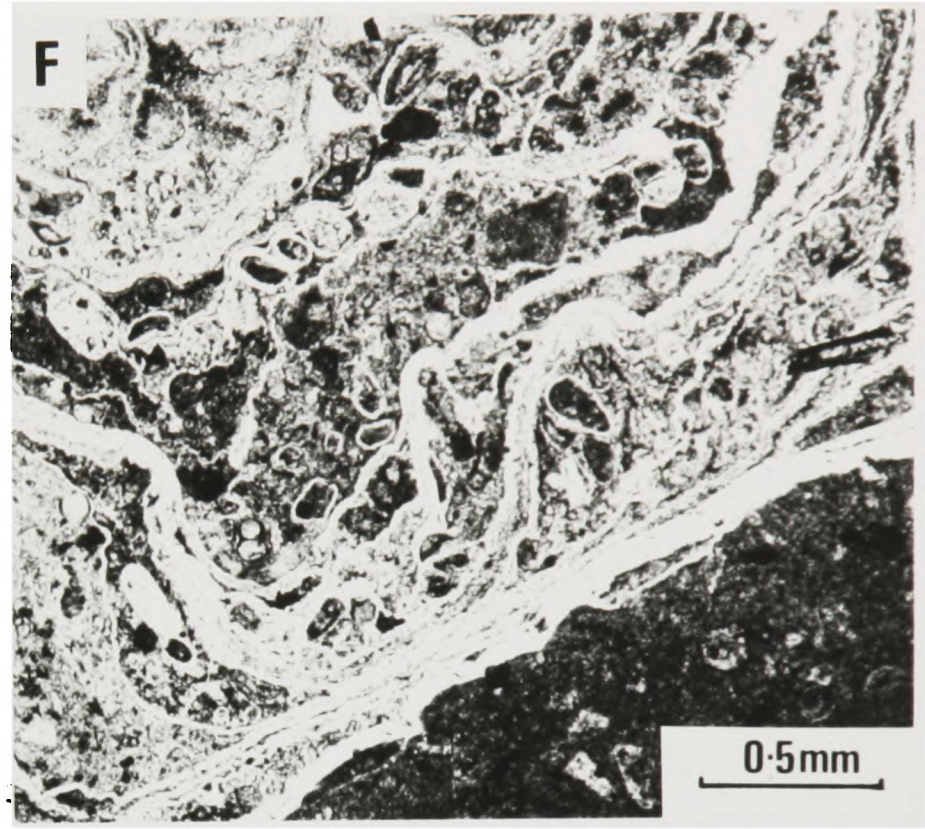
F
0·5mm

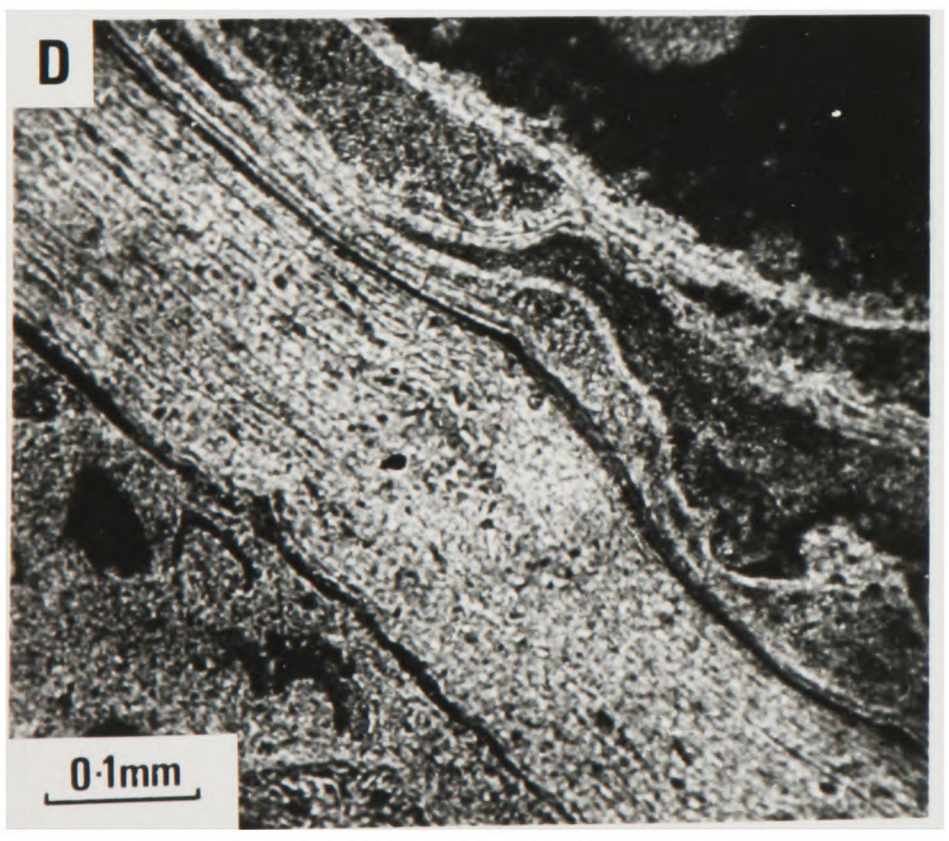
D
0·1mm

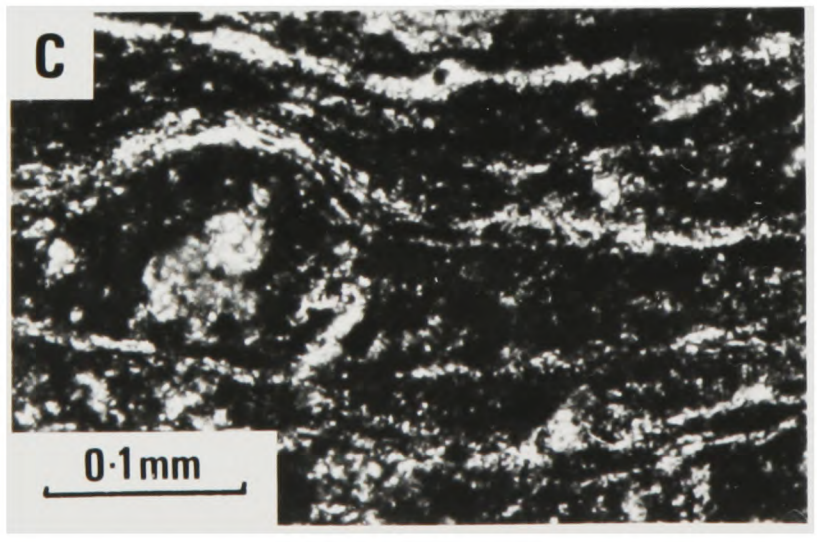
C
0·1mm

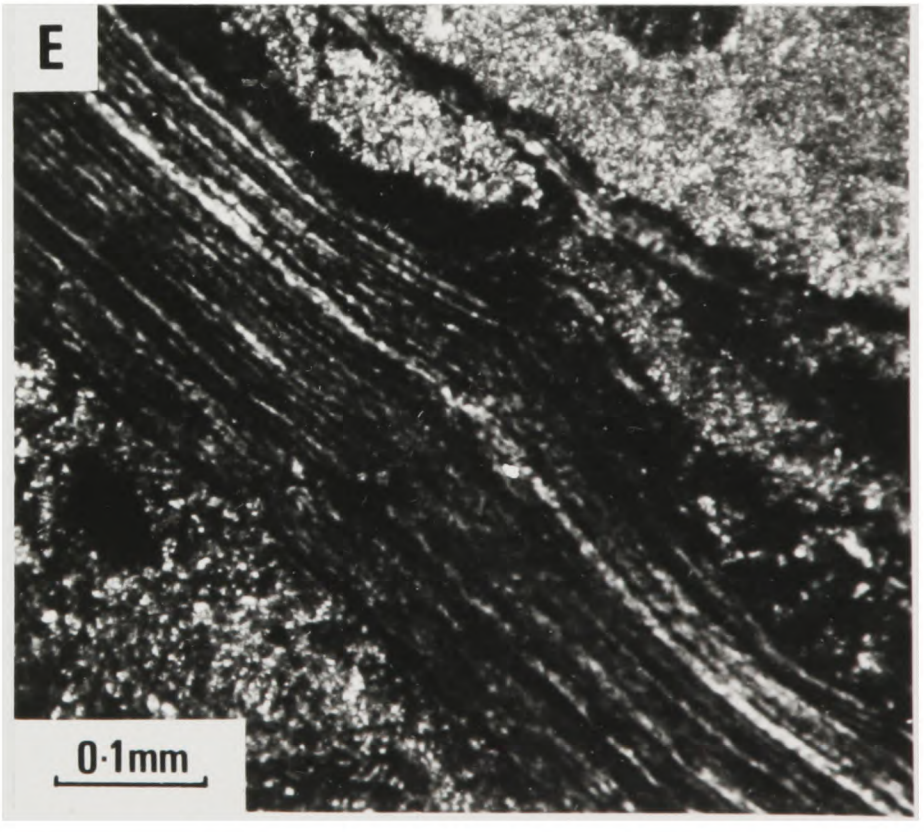
E
0·1mm

in optical continuity (Fig. 3.6) suggesting that they are composed of elongate apatite crystallites aligned with their c-axes normal to the surface of growth. Unfortunately individual crystallites have not yet been resolved under the SEM. The first veneers drape the hardground and mimic its topography in fine detail, but above this micrite trapped in surface irregularities produces a smoother morphology that is also draped by veneers.

Phosphatized micrite is the second constituent of the skin complex and is volumetrically its dominant component. The micrite is characteristically much darker than hardground chalk due to the inclusion of disseminated blebs of organic matter (Fig. 3.6B,C) which give it a filamentous nannostructure (Tabatabai", 1977). In all cases the alternations of sediment and veneer record an intricate series of infill events that act to smooth out the small scale topography of the basal hardground surface.

Similar skin complexes on Chalk hardgrounds have been ascribed to direct precipitation of phosphate (Bromley, 1965 p.85) or replacement of algal lamellae (Kennedy, 1970a; Kennedy and Garrison, 1975b). In addition subaerial void-filling cementation of calcarenites by phosphate from leached guano deposits produces comparable structures (Braithwaite, 1968). In the case of phosphatic chalk hardgrounds the textural evidence mediates against a void-filling origin and seafloor precipitation of carbonate-fluorapatite is inconsistent with the faunal data which clearly indicates a well-oxygenated seafloor; precipitation of phosphate requires reducing conditions of high pH and high alkalinity (Senin, 1970; Cook, 1976). Suitable physico-chemical conditions for precipitation might be found below the sediment/water interface subsequent to the hardground being mantled in sediment but the total absence of diluents within the laminated zones indicates precipitation or replacement in a medium other than micrite.

The similarity of these laminated structures to algal mats is striking (e.g. Bathurst, 1975 fig.208) and the binary structure of such mats is well-documented (Black, 1933; Monty, 1965, 1967), sediment being interlayered with organic veneers. Phosphatized stromatolites are known from the Proterozoic of India, USSR and China (Bushinskii, 1964; Banerjee, 1971; Sant, 1979) and

have recently been reported overlying middle Cambrian hardgrounds in the Georgina Basin of northern Australia (Southgate, 1980). Intense phosphatization is restricted to algal-bound sediment and is absent in the intercolumn areas.

Occasional skeletal material (particularly oyster debris) within hardground chalks has been bored by thallophytes but the rarity of such borings suggests that, even if they are of algal rather than fungal origin, the depth of the seafloor must have been near the limit of light penetration ( ~150 m). It is unlikely therefore that phosphatic chalk skin complexes are true replaced stromatolites.

Algae are not always the dominant organism within subtidal mats. In addition to fungi and bacteria Bathurst (1975) has noted a proliferation of micromolluscs, foraminiferans, polychaetes, arthropods, nematodes, ostracodes, diatoms and many other organisms within these mats. It is noteworthy that '<u>Terebella' phosphatica</u> and serpulid worm tubes are commonly intimately associated with basal hardground phosphate skin complexes.

It is suggested that the phosphate skins are replacements of a subtidal organic mat, dominantly of fungal or bacterial origin. The breakdown of such an organic substrate would also provide a local concentration of orthophosphate for the mineralization of micrite trapped by the mat, and might lead to precipitation or direct replacement by carbonate-fluorapatite of the organic layers. It accounts for both the high organic content of the associated sediment, its filamentous nannostructure and its abnormally intense phosphatization, and is consistent with the close connection seen between phosphatization and organic activity elsewhere in the hardgrounds.

### 3.3.3d Ferruginization

Apart from glauconite, iron mineralizations occur in basal and other hardgrounds in three main forms:

(1) Pale-brown limonitic impregnations of the hardground chalk and included glauconitized intraclasts,

(2) Goethitic crusts up to 2 mm thick that line the roofs of <u>Thalassinoides</u> burrows in the upper part of the hardground, and

(3) Goethitic replacements of pyrite nodules and cubes immediately below the surface of the hardground.

In addition a pale-yellow, evenly-distributed limonitic stain is present in many weathered exposures, being best developed in examples displaying Liesegang rings and secondary goethitic crusts.

Iron oxide 'fronts' commonly occur at a constant distance of a few millimetres from the walls of Thalassinoides burrows (cf. Bromley, 1965 p.108) where they are intimately admixed with similar glauconitization 'fronts'. Limonitic 'fronts' also occur in the absence of glauconite, picking out omission surfaces and burrow infilling events within hardgrounds. The original state in which this disseminated iron was incorporated into the hardground is uncertain. The present brown, oxidised state conforms with the aerobic environment indicated by the benthos but does not preclude the possibility that ferrous iron was incorporated during periods of subsurface or microenvironmental anoxia as suggested for phosphatization (3.4.4). The only hardgrounds examined in detail here that contained blue, reduced iron, were those of the 'flintless unit' at Whitecliff Ledge on the Isle of Wight (2.11.5). Sedimentologically these are similar to many other weakly-developed hardgrounds and it is uncertain whether they are rare examples of iron preserved in its original ferrous state, or are the result of late stage reduction.

Goethitic crusts essentially occur on the roofs of burrows and on the hardground surface where they have been strongly glauconitized. The goethite/ledipocrocite crust passes down into a goethitic impregnation that penetrates up to 0.5 cm into the lithified chalk. Superficially-similar crusts are seen in strongly-weathered hardgrounds such as the Marcheville Basal Hardground and the Boxford Paired Hardgrounds. Here they are associated with prominent Liesegang rings and are the result of iron migration and reprecipitation from overlying Tertiary sediments combined with the breakdown of primary iron minerals within the hardgrounds. These weathering products are clearly distinct from the crusts seen in most basal hardgrounds.

The crusts commonly show an indistinct banding indicating the addition of successive generations of iron. In all cases the mineralization appears to

be replacive. The strong association with glauconite suggests that goethite may be an alteration product of that mineral, mobilized iron replacing sediment at hardground/white chalk interfaces. The mechanism of breakdown and replacement remains unclear and it should be noted that it is only in severely weathered hardgrounds that all glauconite has been destroyed.

The occurrence of goethitic pseudomorphs of pyrite within the upper portion of many hardgrounds clearly indicates that glauconite was not the only primary iron mineral. Pyrite formation is a result of anaerobic sulphidic diagenesis which, in modern sediments, generally occurs in the uppermost 10 cm of the sediment column (Berner, 1970; Goldhaber and Kaplan, 1974). It is limited by the amount of organic matter available to be metabolised by sulphate reducing bacteria that produce the $H_2S$ necessary for pyrite formation. In clastic sediments the iron content is rarely a limiting factor since iron absorpted onto grains is available in excess of that required for pyrite genesis. In pure carbonates, however, this major source of iron is absent and organic matter becomes the major source of iron within the sediment. Clearly then the original presence of pyrite within a hardground indicates a primary high organic matter content and subsurface anoxia, both of which are consistent with the environmental interpretation derived from other lines of evidence. It should be noted, however, that pseudomorphed pyrite also occurs as foraminiferal infillings and linings in the closed valves of brachiopods. In both cases an organic-rich anoxic microenvironment may have existed within an otherwise oxygenating sediment and widespread reducing conditions are unnecessary.

In addition to the smaller (0.5 - 5.0 mm) pyrite cubes within the hardgrounds, larger nodules are also commonly present. These exhibit a radiating internal structure and cube-encrusted surfaces but are also commonly totally replaced by goethitic minerals. These nodules are never found reworked in basal lags and are considered to be products of late diagenesis caused by dissolution and reprecipitation (commonly in burrows) of early diagenetic pyrite and/or other iron sulphides.

### 3.3.3e Manganese oxides

Concentrations of manganese oxides ('pyrolusite') are characteristic of all well-developed Chalk hardgrounds. These oxides have been preferentially precipitated within the late-stage fracture systems that are a prominent feature of all intensely-lithified chalks. The discordant nature of the 'pyrolusite' (Fig. 3.4A) clearly demonstrates its late (probably post-regional uplift since 'pyrolusite' does not occur in offshore chalks; Kennedy and Garrison, 1975b; W.J. Kennedy pers. comm.) nature but the origin of the manganese is less certain and may reflect primary high Mn contents in the hardground cement (Chapter 4).

### 3.3.3f Silicification

The final prominent mineralization seen in phosphatic chalk hardgrounds is the silicification of bioclastic material, predominantly inoceramid shell but including oyster, brachiopod and coral debris. The silica is in the form of isolated and interlocking spherules of chalcedonic $\alpha$-quartz (see Section 3.8.1a for details). In the case of inoceramid shells, silica is at first restricted to prism boundaries but further silicification results in the overgrowth of the initial silica and replacement of prism calcite (Fig. 3.7).

## 3.3.4 Early diagenesis and depositional environment

The preceding discussion demonstrates that considerable environmental changes occurred during the transition from white to hardground chalk deposition. The intraclastic nature of hardground sediments indicate that, in many cases, these changes began prior to lithification, but the synsedimentary timing of cementation means that (unlike white chalks) early diagenetic effects and other modifications of the depositional regime are not easily separated. Consequently the two aspects will be considered together in the following discussions.

The high percentage of both mineralized and unmineralized intraclastic and bioclastic material in most basal hardground sediment must have had a considerable effect on the nature of the substrate even before the initiation

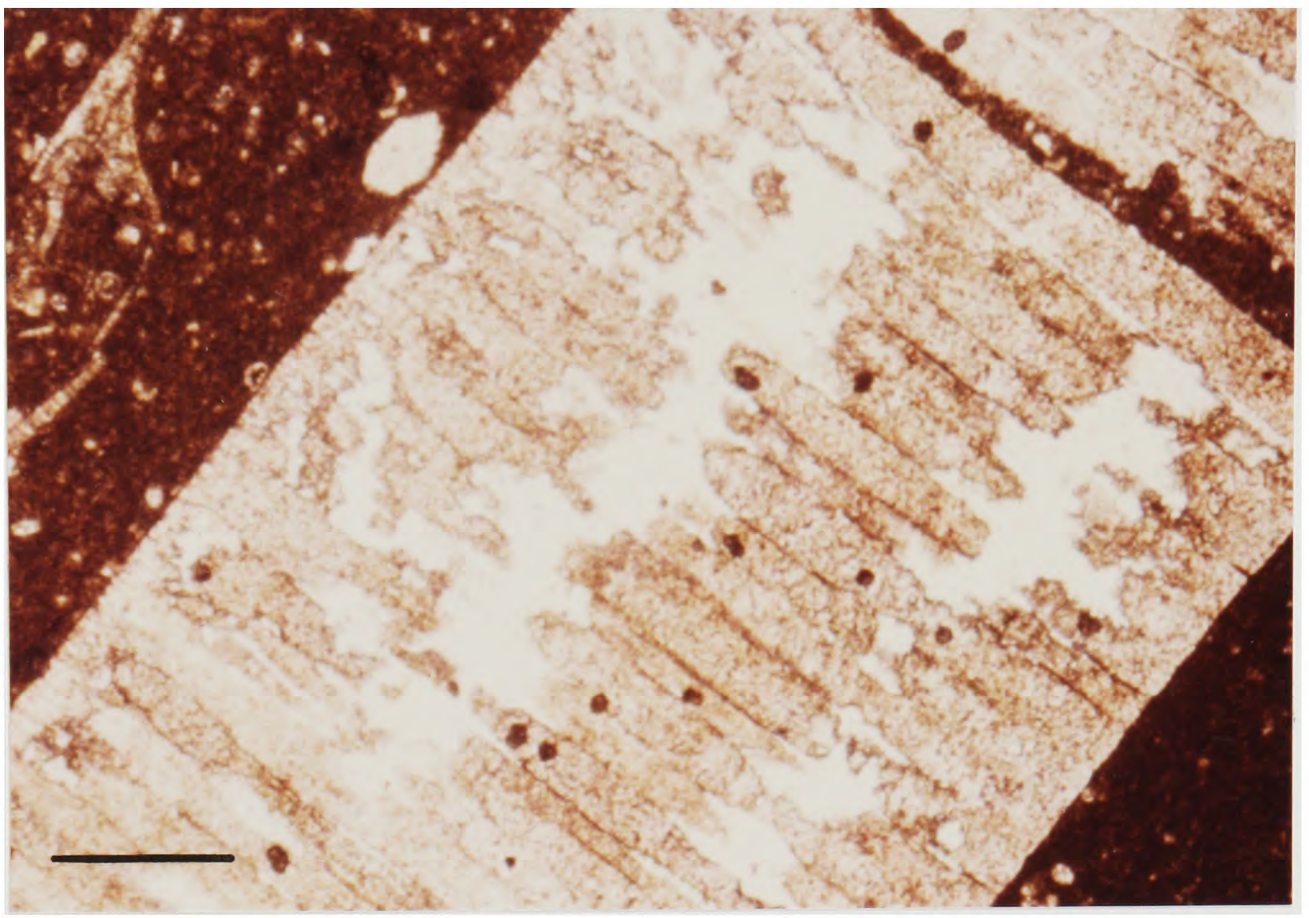

Fig. 3.7 Silicified inoceramid shell.
Silica occurs as coalescing spherules of ∝-quartz, concentrated along prism boundaries and in a replacive zone ~0.5 mm below the surface of the shell fragment. Silicified areas are colourless in plain polarised light (top); the first-order grey birefringence under crossed nicols (bottom) contrasts strongly with the bright fourth and fifth order colours of the prismatic calcite. The micritic matrix is typically brown. The fragment is from the lower white chalk of Beauval quarry. Scale bars = 0.5 mm.

of widespread lithification. The soft pelletal bottom inferred for white chalks (3.2.2a) was replaced by firmer calcarenitic substrates and it is to be expected that these would favour the establishment of a more diverse benthos (e.g. including endobyssate bivalves). This may in part explain the occurrence of an abundant aragonitic fauna in some hardground chalks, although preservational effects must also be considered.

Aragonite is preserved in hardground chalks as empty moulds produced by cementation of the surrounding sediment before dissolution of the aragonitic skeleton. In a soft sediment these moulds are destroyed during compaction. Similarly silicisponges occur as uncompacted phosphatized 'steinkerns' in hardground preservation. Aragonite may also be preserved by superficial phosphatization but this is a subordinate process in hardground chalks and will be considered separately (3.4.4) during the examination of the phosphorite.

It cannot be assumed, however, that the lack of an aragonitic fauna at a particular horizon is purely preservational. Not all hardgrounds contain such a fauna and even those which do (e.g. the Beauval Basal Hardground) generally only contain sparse, laterally discontinuous patches of material. The number of aragonite moulds preserved has no direct relationship with the degree of hardground development beyond the fact that some initial lithification is necessary (Bromley, 1965, 1979). Thus a thin, poorly-developed hardground in the upper phosphatic chalk at Orville (2.3.3) contains numerous moulds of aragonitic bivalves, while many intensely-indurated and mineralized basal hardgrounds contain none. The preservation of an aragonitic fauna, therefore, is dependent on both its original abundance and the existence of a suitable preservational environment, in chalks it is rarely possible to determine which is the dominant factor.

The increase in grain-size associated with many hardgrounds is clearly of significance to the lithification process. Ordinary white chalks have high porosities of 35 - 50% (Scholle and Kennedy, 1974; Scholle, 1977a) but a low permeability - 1 - 8 md (Scholle, 1974), hardground chalks on the other hand have a much reduced porosity, 10 - 20% or less (Scholle and Kennedy, 1974). This large reduction in porosity is due to the introduction of cement, a

process which is difficult to envisage in a sediment with such a low permeability. However, the permeability will be considerably enhanced if the finer fraction of the sediment is removed by winnowing and the mean grain-size increased. It is suggested that such an increase in permeability acts as a substantial aid to lithification (cf. Mullins et al., 1980). Increased grain-size is not the only requirement, however, since not all coarse-grained chalks become hardened. Similarly, elsewhere, not all hardened chalks are coarse grained.

Nevertheless, in a continually winnowed environment, the top few centimetres of sediment would be too mobile to allow cementation, while at depth interaction with fresh seawater is lacking and the pore-water reaches equilibrium with the surrounding grains. Between these two extremes, there must lie a zone where particle movement is sufficiently slight to allow cementation and there is enough replacement of pore-water to provide the necessary amount of calcium carbonate. It is by such a flushing action by currents and possibly burrowing organisms, as suggested by Bromley (1967, 1975a) that sufficient cement could be introduced into a sediment with such a high initial porosity.

It is suggested therefore, that cementation occurred a few centimetres below the sediment/water interface in a winnowed sediment of increased permeability. Cementation probably occurred by the overgrowth of calcitic particles but was prevented in areas of Thalassinoides burrows which remained open, and in the top few centimetres of sediment, which were in motion. The mineralogy of the cement will be considered later (Chapter 4).

The generally accepted model of hardground formation (Bromley, 1975a; Kennedy and Garrison, 1975b fig.6) involves an initial stage of early diagenesis associated with a pause in sedimentation causing the growth of calcareous nodules below the sediment/water interface (nodular chalks). Further prolonged diagenesis may lead to the coalescing of individual nodules to produce a continuous lithified subsurface layer (an incipient hardground). If subsequent erosion of the overlying soft sediment exposes this layer at the seafloor a true hardground will develop. This sequence of events can be convincingly demonstrated in Turonian to mid Coniacian chalks throughout the Anglo-Paris Basin.

It is occasionally possible to trace a hardground laterally into a nodular chalk facies, a transition which has also been observed on the Bahamian slopes (Mullins et al., 1980) at the present day. Here contour-following bottom-currents control the permeability of the near-surface sediment and thus the degree of interstitial circulation and subsequent cementation. Well-lithified hardgrounds form at depths of <375 m, nodules from 375 - 500 m and soft oozes are deposited at greater depths, although clearly it is current velocity and not absolute depth that controls the distribution.

However, whereas nodular chalks are a dominant lithology in Turonian to mid Coniacian chalks, both they and hardgrounds are infrequent in chalks younger than the late Coniacian. Furthermore when basal hardgrounds are traced laterally they do not go through an obvious nodular stage of lithification but grade imperceptibly into uncemented burrowed junctions (cf. Bromley, 1975a fig.18.3A). Masses of chalk isolated by intense burrowing are common but unlithified and do not display the hard porcelaneous characteristics of true nodular chalks.

The absence of nodularity may be attributed to a number of factors. Calcisphere-rich chalks which characterise the Turonian are replaced by foraminiferal biomicrites with high coccolith contents during the Coniacian (Aubry, 1974). It may be suggested that compositional changes altered the properties of the sediment during early diagenesis (calcispheres may have been originally composed of high-Mg calcite) and prevented the development of an intermediate nodular stage, cementation being more evenly distributed through the sediment. In addition the progressive eustatic rise in sealevel during the period (Hancock, 1975a; Cooper, 1977; Hancock and Kauffman, 1979) must have resulted in considerable palaeo-oceanographic changes. Massifs and 'swells' which appear to control the distribution of nodular chalks and hardgrounds during the early part of the late Cretaceous (Kennedy and Garrison, 1975b) were buried and exerted less influence on sedimentation patterns. Hardground development became less extensive and dependent on local erosion by major currents (3.6.3) and synsedimentary tectonism (2.11.3) rather than being evenly distibuted over regional 'highs'. It is not surprising, therefore, that these changes are reflected in

the early-diagenetic history of the sediment. However, more physico-chemical data are required on the processes of nodule and hardground cementation before the precise nature of the controls can be determined, certainly lithology, palaeogeographical setting and sedimentation rates must all have played a part.

Whatever the exact nature of the lithification process the winnowed aspect of the hardground sediment is clear evidence of the existence of a stronger current regime than that which characterised white chalk deposition. The occurrence of hardground-associated faunas including corals and sabellariid-(?) ('Terebella' phosphatica) worms which are favoured by high current activity corroborate the evidence provided by the hardground sediment itself.

It is well established that hardground surfaces commonly (but not invariably) correspond to major hiatuses in a succession. It must be stated, however, that the degree of hardground development (lithification, mineralization, boring etc.) is not necessarily an indication of the duration of the hiatus. In the present oceans hardground cementation may occur in a matter of decades (Shinn, 1969) while elsewhere areas of unlithified seafloor may receive no net sediment input for millenia. Cementation depends on sediment permeability, current activity, seawater and pore-water geochemistry etc. and not on the period of exposure alone. Thus an uncemented and inconspicuous omission surface may represent a more extreme hiatus than an intensely-indurated hardground in the same succession (Bromley, 1979). Similarly, mineralization and boring also depend on favourable seafloor environments. Thus although a hardground represents a distinct change in sedimentation, the lithology of the hardground gives little evidence of the duration of the hiatus.

Each hardground is the result of a unique series of conditions. The nature of the stratigraphical condensation associated with the hardground surface is particularly important. It may be due to non-deposition prior to, during or after lithification (primary omission of Bromley, 1975a, 1979) and/or erosion at any time during the evolution of the hardground (secondary omission). Clearly most hardgrounds are the result of a combination of these two processes and have a complex history of burial-reexhumation events. In addition they show varying degrees of lateral variation and in some cases evidence of

diachroneity. Thus not only may the length of the hiatus vary along the surface of a single hardground but the timing of the hiatus may also change.

In basal hardgrounds the discordance between the hardground surface and the near-horizontal bedding of the underlying white chalks (Figs. 2.42, 2.64, 2.83) clearly indicates that erosion has removed several metres of sediment prior to or concurrent with lithification. The erosional origin of basal hardgrounds provides further evidence of increased current activity at that time.

The absence of algal structures in white chalks indicates depths of >150 m but two lines of evidence suggest that many hardgrounds were deposited in shallower water. Skeletal material associated with basal hardgrounds commonly contains an intricate system of fine borings which may be attributed to thallophytes. If as suggested by several authors (Bromley, 1965, 1970; Kennedy, 1970a; Kennedy and Garrison, 1975b) some of these are of algal origin, they indicate deposition within the photic zone and therefore water depths of 150 m or less. The phosphate skin complexes associated with all basal hardgrounds (3.3.3c) are also of potential algal origin and indicate a similar depth although the absence of a more widespread and varied flora suggests that even here depths were towards the limit of light penetration.

## 3.4 Phosphatic chalks

A phosphatic chalk is a chalk containing $\geqslant 5\%$ $P_2O_5$ due to the presence of appreciable amounts of pelletal phosphate (faecal pellets, ooliths, phosphatized intraclasts and bioclasts, bone fragments etc.). They are readily distinguished from white chalks by their deep chocolate-brown colour when wet (Fig. 2.49). Phosphorite has been defined by Bushinskii (1966) as a sedimentary deposit that contains more than 18% $P_2O_5$, approximating to 50% apatite. In general, however, phosphorite is used more loosely by workers in the field (few commercial 'phosphorites' have untreated whole-rock $P_2O_5$ values of $>18\%$) and I have followed the general useage and applied the term to all sediments or rocks containing $\geqslant 5\%$ $P_2O_5$ (this approximates to 10% phosphate grains).

Phosphatic chalks are therefore a subdivision of phosphorites which also include strongly-mineralized hardground top and intraclastic basal lag conglomerates. Where a chalk contains 0.5 - 5% $P_2O_5$ (1 - 10% phosphate grains) it is termed a poor phosphatic chalk. Phosphate is a more general term that applies to a class of chemical compounds, a group of minerals, individual sedimentary grains or particles or a mineral deposit.

### 3.4.1 Sedimentary structures

In a similar way to that in which the gross morphology of hardgrounds is controlled by biological processes and current action, so the majority of structures seen in phosphatic chalks can also be explained by the interaction of these two processes

#### 3.4.1a Burrowed junctions

The oldest phosphatic chalk in a succession may overlie a well-developed hardground, a soft white chalk, or a sediment exhibiting any degree of lithification between these two extremes (3.4.6). In all cases, however, the junction between the two lithologies is characterised by a phosphatic-chalk filled Thalassinoides burrow system that penetrates up to 5 m below the junction. A distinction between erosional and non-erosional junctions (erosion and omission surfaces) has been made by some authors (Bromley, 1975a; Kennedy and Garrison, 1975b) but in phosphatic chalks it is rarely possible to differentiate the two (even omission surfaces require some initial scour) so both are referred to as 'burrowed junctions'.

The contrast in sediment types at these junctions and the weak ferruginization of the white chalk immediately below the interface enable three categories of trace-fossil assemblage to be distinguished (Bromley, 1975a). The pre-omission suite represents bioturbation of the white chalk prior to erosion (or non-deposition). The suite is typified by Thalassinoides, Chondrites, Planolites and Zoophycus but the burrows are generally poorly differentiated because of the lack of contrast between burrow matrix and fills. Some fills show a feint

blue colouration, possibly due to the presence of disseminated pyrite. The most prominent burrows are those which form during the hiatus. This omission suite consists exclusively of Thalassinoides, made conspicuous by their contrasting fill, density and cross-cutting relations. As deposition resumed the surface and fills of the omission suite were modified by a post-omission suite consisting of Thalassinoides, Chondrites, Planolites and Zoophycus but including a typical phosphatic chalk suite - Trichichnus, white-chalk rind burrows, Muensteria-like and other meniscus-fill varieties. In general the post-omission burrows do not cut the surface of the junction but only penetrate it by re-excavating the fill of the Thalassinoides of the omission suite - perhaps because of the high organic content of the latter (Bromley, 1975a). In some examples, however, the post-omission suite is abnormally active and may destroy the continuity of the junction (see below).

The conspicuous nature of the omission-suite Thalassinoides indicates a number of characteristics of the sediment. Where the phosphorite overlies a basal hardground it may be suggested that lithification of the white chalk prevented mixing of the two sediment types, but this cannot be argued for the soft chalks below the upper indurated horizons or in cases where the junction is unlithified. In all cases the outline of the burrows and the surface of the junction are well defined. This indicates that the substrate was competent enough to support an open burrow system. The contrast between the two lithologies demonstrates that the burrows must have remained open during the duration of the hiatus.

The phosphatic chalk that fills the omission-suite Thalassinoides is commonly coarser grained and has a higher phosphate content than that which overlies the junction. This is because this sediment represents the turnover stage between non-deposition and sedimentation and therefore reflects the highest current regime under which deposition could occur for that particular lithology. Thus, subsequent deposition generally took place under waning current conditions and produced less phosphatic chalks. Other aspects of these changes will be discussed later (3.4.4).

3.4.1b Burrowed-out white chalks

Most burrowed junctions have a well-defined surface from which distinct omission-suite Thalassinoides penetrates the underlying sediment but some junctions are more complex. Where the post-omission suite of burrows is restricted to reexcavating pre-existing fills they do not fundamentally alter the morphology of the underlying chalks. In some cases, however, the post-omission Thalassinoides cross-cut an underlying burrowed junction, break-up the continuity of its surface and the underlying white chalk (Fig. 3.8). This is termed a burrowed-out structure and is commonly seen in phosphatic chalks (Fig. 2.19A; Bromley, 1975a fig.18.3A). It occurs both in the (unlithified) burrowed junctions at the base of the successions and more commonly where a thin bed of white chalk is intercalated within the phosphatic chalk succession. In the latter case bioturbation may entirely destroy the integrity of the bed and leave only a line of isolated pseudonodules (e.g. Beauval Fig. 2.8). These pseudonodules are unlithifed and show no evidence of exposure but are commonly iron stained a deep yellow.

3.4.1c Pseudoconglomerates

The isolation of fragments of white chalk by post-omission Thalassinoides burrows is commonly followed by further bioturbation by deposit-feeding infauna after the infilling of the Thalassinoides system. These later burrows further disrupt the white chalk by displacing and rotating the original masses until they adopt the nodular morphology of a pseudoconglomerate (Fig. 3.8). This process of in-situ displacement is clearly seen at the base of the second phosphatic chalk at Ribemont quarry (Fig. 2.86). The absence of boring and/or encrustation demonstrates that the rounding is a subsurface phenomenon although more rounded examples may be superficially phosphatized or iron stained. More extreme mineralization combined with boring and encustation occurs if the overlying chalk is eroded and the summit of the unit is exposed on the seafloor to produce an intraclastic pseudoconglomerate (the majority of pseudonodules remain unexposed).

The initial stages of isolation and rounding are not accompanied by

Fig. 3.8 Generalized model to illustrate the genesis of bioturbation-controlled structures in phosphatic chalks.
1. Normal white chalk deposition with a pre-omission suite of trace-fossils is followed by scour and non-deposition which produces 2. an omission suite of Thalassinoides. 3. If the burrows are filled with phosphatic chalk a simple burrowed junction (omission or erosion surface) results. 4. Where the omission suite of trace-fossils is followed by a strong phase of post-omission burrowing the junction is destroyed. 5. Renewed deposition of phosphorite forms a structure where fragments of white chalk 'float' in a matrix of phosphatic chalk - a burrowed-out white chalk. This structure is most prominent where a bed of white chalk is intercalated within a phosphatic chalk succession and the continuity of that bed is subsequently destroyed by bioturbation. 6. The deposit-feeding infauna causes the rounding and superficial mineralization of the fragments of white chalk producing a pseudoconglomerate. 7. Compaction may cause brecciation and high-angle microfaulting of the pseudoconglomerate. 8. Where prolonged scouring results in a winnow-coarsened sediment, seawater moving through the porespaces may precipitate carbonate and form a lithified subsurface layer or incipient hardground. 9. Further scour will erode the superficial layer of soft sediment and expose the hard layer at the seafloor. Such a simple hardground may be encrusted, bored and mineralized. 10. Intense post-omission burrowing will concentrate along the surface of the hardground (imposed horizontality of Bromley, 1965), penetrate it by reexcavating preexisting burrow-fills and then spread horizontally in the soft sediment below the lithified layer. 11. Infilling of the post-omission suite by phosphatic chalk results in the lithified equivalent of a burrowed-out white chalk - an undermined hardground. 12. Where the formation of a phosphatic-chalk filled burrowed junction is followed by renewed white chalk deposition the continuity of the original junction may be destroyed by the post-omission suite of trace-fossils. 13. The phosphorite is then restricted to burrow fills as a burrowed-in phosphatic chalk in an otherwise homogenous white chalk succession. 14. Erosion of a pseudoconglomerate exposes 'nodules' of white chalk on the seafloor where they are liable to be encrusted, bored and mineralized. Subsequent burial of the unit forms an intraclastic pseudoconglomerate, or if more than the surface of the bed is exposed, an intraformational conglomerate. 15. Compactional fracturing may also occur in these types of junction.

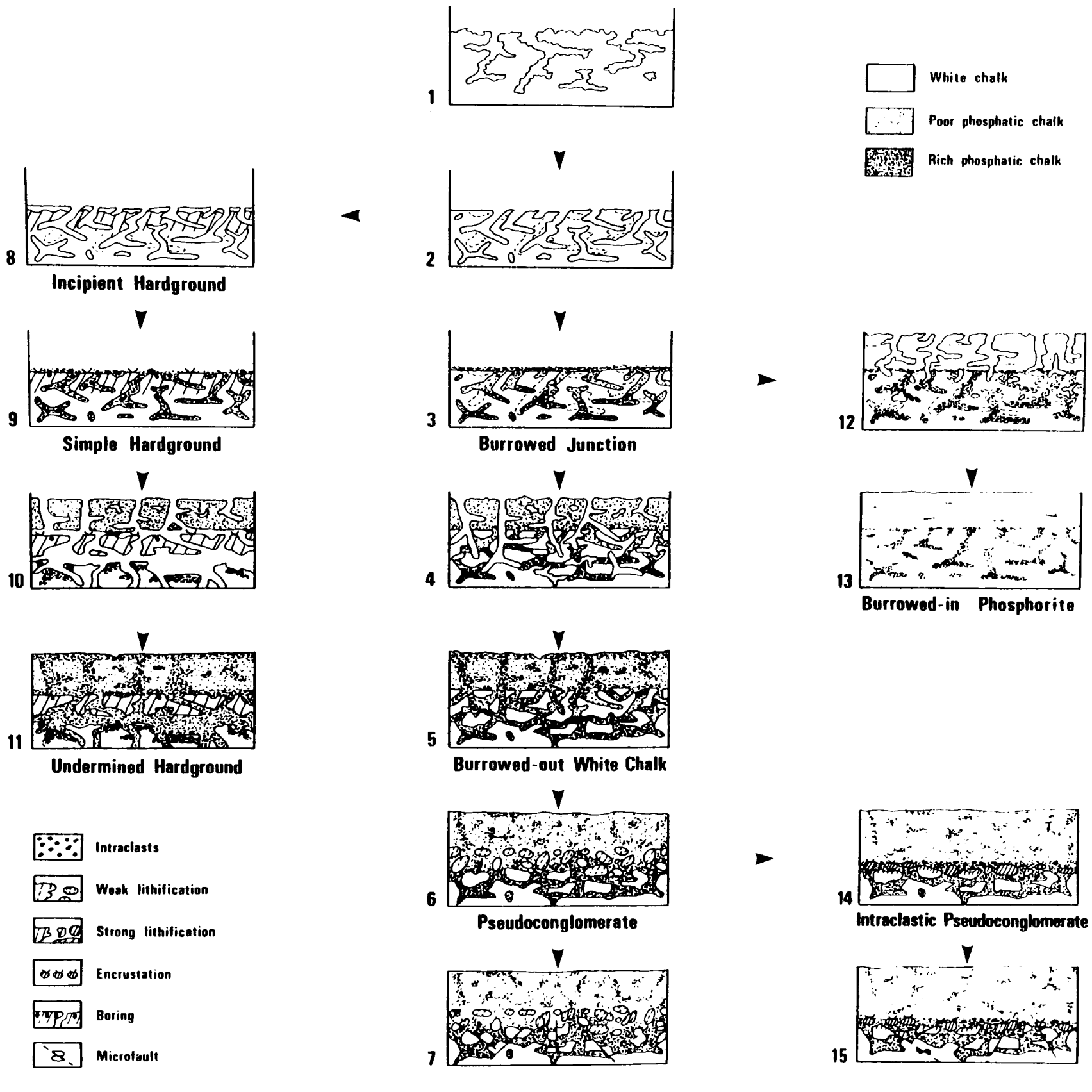
White chalk
Poor phosphatic chalk
Rich phosphatic chalk
1
2
3
4
5
6
7
8
Incipient Hardground
9
Simple Hardground
10
11
Undermined Hardground
12
13
Burrowed-in Phosphorite
14
Intraclastic Pseudoconglomerate
15
Burrowed Junction
Burrowed-out White Chalk
Pseudoconglomerate
Intraclasts
Weak lithification
Strong lithification
Encrustation
Boring
Microfault

discernible lithification and although weak cementation pre-dates or accompanies phosphatization it is only reworked and subsequently mineralized material that is strongly indurated. The weakly-lithified nodules are highly susceptible to fracturing and brecciation during burial and in some cases small high-angle compactional microfaulting occurs (Fig. 2.105B). Similar fractures are recorded from white chalks (Håkansson et al., 1974 fig.6) but are undoubtedly accentuated by the contrasting sediment types.

3.4.1d Planar structures

In general the intense bioturbation displayed by phosphatic chalks has destroyed all but the largest scale bedding features. In rare cases (e.g. the summit of the upper phosphatic chalk at Beauval), however, a primary planar bedding is preserved (Tabatabai", 1977 fig.32d) as thin (millimetres to a few centimetres) alternations of white and phosphatic chalk. The phosphorite in these alternations is characteristically well-sorted, intraclastic and shows primary orientation of elongate grains parallel to bedding. The phosphatic chalk is coarser and more phosphatic at the base of each lamination which apparently represent minor erosion surfaces produced by local scour. The absence of an infauna must be attributed to unsuitable (anoxic?) bottom conditions perhaps combined with higher rates of deposition. The laminar structure is accentuated by the development of late-diagenetic flasering (3.8.2a).

The summit of most phosphatic chalks is characterised by a gradual return to white chalk deposition via a strongly-bioturbated transitional junction a few tens of centimetres thick. An extreme type of planar bedding occurs, however, at the top of some phosphatic chalk successions e.g. Faucouzy and Bouchavesnes-Bergen. Here the junction between the phosphatic chalk and overlying white chalk is sharp and planar and exhibits no bioturbation of the interface (Figs. 2.90, 3.9). The contrast between the two sediments is so extreme that the junction must represent a considerable change in depositional regime.

The phosphatic chalk that occurs immediately below the junction is coarser-grained, better-sorted, contains more ooliths and is more phosphatic than that lower in the succession. At Bouchavesnes-Bergen it contains a high

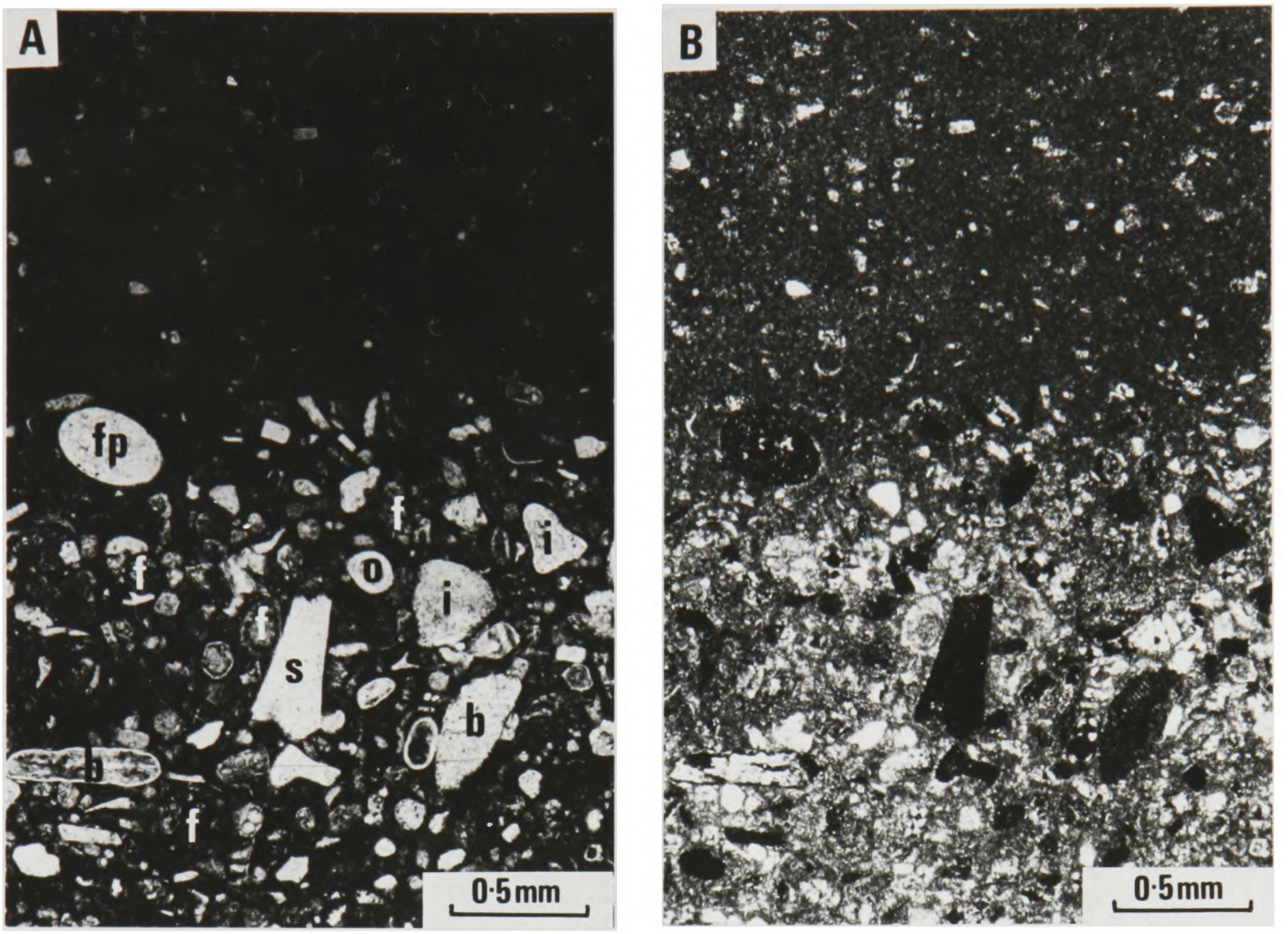


Fig. 3.9 Sharp contact between the phosphatic chalk and overlying white chalk at Faucouzy quarry. A coarse phosphorite (bottom) containing a diverse association of phosphatized components including faecal pellets (fp), ooliths (o), intraclasts (i), bone fragments (b), foraminiferans (f) and steinkerns (s) is immediately overlain by a soft white chalk (top). The finely-intraclastic nature of the white chalk, although visible in hand specimen, is invisible in thin section. (see Fig. 2.90 for macroscopic features of the junction). (A) PPL, (B) XN.

proportion of very coarse skeletal debris, particularly comminuted Platyceramus. This coarse facies is burrowed down into the more typical underlying phosphatic chalk by a prominent omission suite of Thalassinoides (Fig. 2.90A). Clearly this phosphorite was deposited under stronger current conditions than the bulk of the phosphatic chalk.

The white chalk that overlies the junction is also abnormal since it contains a high proportion of small (0.5 - 5.0 cm) rounded to subangular white chalk intraclasts but no pelletal phosphate. Rare Thalassinoides burrows do penetrate the junction but these originate from a considerable distance (perhaps several metres) above the interface. Any model for the development of these planar junctions must explain all these features.

One possible explanation is that the scouring which produced the coarsened

sediment at the summit of the phosphorite also undercut an area of laterally equivalent white chalk upslope of the area of phosphatic chalk deposition. Failure of this unstable mass of sediment caused it to move downslope and be deposited on top of the phosphorite. Rapid deposition of several tens of centimetres of white chalk explains why the junction is planar and unbioturbated and accounts for the intraclastic nature of the sediment. The requirement of a laterally equivalent white chalk at a relatively higher elevation on the seafloor is consistent with the facies interpretation derived from other lines of evidence (3.6.1).

### 3.4.1e Cross-bedding

Large-scale (0.5 - 2 m) cross-beds are clearly seen infilling minor erosional troughs at the base of the phosphatic chalks at Hallencourt quarry (Fig. 2.64) and Templeux-la-Fosse (Fig. 2.42) and may also be present in the oldest phosphatic chalk at Hardivillers quarry (Fig. 2.69). Bioturbation has considerably modified even these large-scale features and has totally destroyed most smaller-scale bedding structures. The indistinct nature of the features and the lack of any lateral control means that it is uncertain whether they should be interpreted as migrating bedforms or as channel-fill structures, although their low-angle unidirectional orientation suggests that the latter is the more likely.

## 3.4.2 Phosphatic chalk microfacies

Phosphatic chalks contain a diverse assemblage of phosphatized material including intraclasts, ooliths, faecal pellets and bioclastic debris (principally benthonic and planktonic foraminiferans, comminuted inoceramid, echinodern and bryozoan debris, sponge spicules, bone fragments, elasmobranch teeth, teleost otoliths and scales and ostracodes). The sand grade of most of the material contrasts strongly with the micritic matrix and results in a strongly bimodal grain-size distribution. The micrite consists primarily of an abundant and diverse flora of complete and dissociated coccoliths, rare Nannoconus

(only common in Micraster coranguinum Zone phosphorites) and accessory clay minerals. The phosphorites can be divided into two broad groups of microfacies: (a) basal lags and (b) phosphatic chalks.

3.4.2a Basal lags

Basal lags are phosphatized intraclastic conglomerates that occur at the base of most phosphatic chalk successions. They are best developed where they rest on a strongly mineralized and lithified basal hardground but may also be present where the hardground is weakly developed or absent. In addition to the phosphatized sand-grade component, bioclastic debris and a micritic matrix, basal lags also contain numerous partly-phosphatized intraclasts of pebble and cobble grade. These large intraclasts are commonly bored and encrusted and are of five distinct types:

(1) Lithified, poor phosphatic chalk intraclasts. Many may be identified as phosphatized steinkerns of e.g. ventriculitid sponges, Micraster, Echinocorys, bivalves, gastropods. The phosphatic chalk infill of most identifiable steinkerns demonstrates that the fauna post-dates the development of the basal hardground and has not been reworked from the underlying white chalk.

(2) Subangular to rounded, phosphatic-skin coated, encrusted (particularly by 'Terebella' phosphatica, Pycnodonte, Spondylus) and polychaete bored intraclasts. These have strongly-mineralized margins with phosphatization decreasing inwards. They commonly have goethitic cores.

(3) Undermined and isolated blocks of hardground, bored, encrusted and mineralized in the same style as equivalent areas of laterally-continuous hardground top.

(4) Superficially ($\leqslant 5$ mm below the surface) glauconitized and phosphatized irregular intraclasts of hardground chalk occurring at the base of depressions. Glauconitization dominates at the base and sides and phosphatization the top. These intraclasts are essentially in situ and commonly have goethitic cores.

(5) Softer, light-brown, dull-surfaced phosphatized intraclasts, occasion-

ally having Thalassinoides ornatus-like scratch marks on their surface.

The phosphatic chalk infilling of the first category indicates that they contain the youngest sediment but does not necessarily imply that they are the youngest intraclasts. Recognizable steinkerns range from infillings of individual foraminiferan chambers to whole Echinocorys and are characteristically abundant in all basal lags. They consist of undeformed phosphatized internal moulds of both calcitic and aragonitic fauna. The former commonly retains adhering fragments of unmineralized shell while in the latter the original external morphology may be preserved by a fine coating of iridescent phosphate. Fossil preservation will be discussed in more detail below (3.4.3). Intact shells with phosphatized infillings grade down through recognizable but heavily bored (particularly by clionid and other sponges, spionid polychaete and sipunculid worms and more rarely pholadid bivalves) steinkerns to unidentifiable 'inorganic' intraclasts. This sequence of steinkern destruction is seen in many other phosphate deposits (e.g. Kennedy and Garrison, 1975a fig.12). The restriction of phosphatic chalk intraclasts to steinkern preservation indicates the importance of pre-fossilization processes (Seilacher, 1971, 1973) in the production of mineralized intraclasts from a soft sediment. The microenvironments afforded by fossil skeletons enabled the cementation of the fill, probably in part because the grains were protected from agitation by currents and burrowers, and partly because organic decay provided suitable geochemical conditions. Subsequent reworking of these cemented internal moulds led to their mineralization and biodegredation. In basal lags the fine detail preserved on most steinkerns suggests that they underwent only a single or a small number of burial/reexhumation events and that their destruction was primarily the result of bioerosion rather than physical processes.

The remaining four categories of intraclast clearly result from the breakdown of the basal hardground. The nature of the intraclasts depends on two factors - the original composition of the included sediment and the degree to which it has been subsequently abraded, mineralized etc. The largest proportion of intraclasts originate from the physical and biological breakdown of the hardground surface (Types 2 and 3). Again it is possible to trace a continuum

from dislocated blocks of hardground surface with mineralization, encrustation and boring restricted to their upper surfaces through progressively degraded material to well-rounded, phosphate-skin coated, strongly-mineralized and intensely-bored pebbles exhibiting a number of phases of boring etc.

The two superficially mineralized categories (Types 4 and 5) originate from lower in the hardground, below the intensely-phosphatized surface and in an area where glauconitization of burrow walls and dull phosphatization of roofs results in contrasting mineralization styles. Large glauconitized intraclasts are essentially in-situ areas of hardground that have been isolated by burrowing and only occur in well-developed hardgrounds. Heavily-bored and strongly-glauconitized intraclasts may also be produced during bioerosion of lithified sediment but the small angular nature of these clearly differentiates them from type 4 intraclasts. Soft, superficially-phosphatized, dull-surfaced intraclasts may similarly originate from low in the hardground but are also common where a well-developed hardground is absent (e.g. Villers-devant-le-Thour). Here the weakly-lithified burrowed junction is broken up by bioturbation and currents leaving isolated blocks of sediment to be subsequently reworked, mineralized, encrusted and bored.

The proportions of the five types of intraclast vary considerably both laterally at a single exposure and between outcrops. In general, however, rounded fragments of reworked hardground top (Type 2) predominate where there is a strongly-developed basal hardground, although locally steinkerns (Type 1) may be the dominant element. Poorly-lithified intraclasts (Type 5) are the commonest form overlying burrowed junctions but are a minority element on top of well-lithified hardgrounds.

Examination of the surface morphology of basal lag intraclasts indicates that a number of processes were active during the genesis of the deposit. The occurrence of concave surfaces including recognizable pholadid bivalve crypts, clionid bores and Thalassinoides ornatus tunnels demonstrate that both boring and burrowing were in part responsible. The presence of planar structures that truncate enclosed grain boundaries indicates early-diagenetic fracturing of the lithified sediment, while the dominance of convex, smoothly rounded morph-

ologies suggests that mechanical abrasion was also important.

In addition to the abundance of steinkerns, basal lags are typified by the occurrence of two other faunal elements - 'Terebella' phosphatica tubes and fragments of Diblasus arborescens. Where 'T'. phosphatica is found in situ the tubes are invariably cemented on an early-diagenetically lithified portion of the basal lag that passes upwards into an uncemented phosphatized calcarenite substrate. Comparable tubes have been described from the present day and are attributed to sabellariid worms (Kirtley and Tanner, 1968). D. arborescens is found in the poor phosphatic chalk that occurs on top of the basal hardground but beneath the basal lag. Beauval quarry is the only site where a patch reef is exposed in situ but the coral is ubiquitous to all basal lags into which it is reworked. Calcitic fossils, particularly the thick-shelled oyster Lopha semiplana, comminuted prismatic layers of Platyceramus, belemnites and echinoderms - asteroid ossicles, cidarid spines and fragments of Micraster test (Fig. 3.10), are also common.

The composition of the pelletal phosphate associated with basal lags is as characteristic as are the larger intraclasts and bioclastic material. Phosphate is more abundant and coarser grained than in phosphatic chalks higher in the succession. Benthonic foraminiferans dominate over planktonic and faecal pellets, ooliths, bone fragments and echinoid debris are all common (Fig. 3.11). Phosphatized intraclasts are phosphate-veneered, larger, more rounded and more intensely mineralized, and compound intraclasts consisting of cemented aggregates of ooliths, faecal pellets, intraclasts etc. are also present. An oolitic microfacies may directly overlie the hardground surface.

### 3.4.2b Phosphatic chalks

Tabatabai"s (1977) quantitative work on the phosphatic chalks of Hardivillers, Nurlu and Beauval quarries has demonstrated that significant compositional changes occur within the phosphatic chalk succession. Near the basal hardground and in the basal lag phosphatized faecal pellets comprise a large proportion of the recognizable elements of the sediment and may in extreme cases form a coprolitic microfacies (Figs. 3.10D, 3.13). Laterally, an oolitic

Fig. 3.10 Phosphatic chalk sediments
A. Coarse fraction of the Beauval Basal Lag. Mineralized and unmineralized bioclastic debris (particularly Lopha semiplana) predominates and includes oyster (o), coral (c), inoceramid (i), echinoid (e) and asteroid (a) derived components. Corals (Diblasus arborescens) occur both as calcitized and/or silicified replacements of the epitheca (and more rarely the entire corallum), as phosphatized internal moulds of the thecarium (bottom left) or are preserved by a combination of these processes (top centre).
B. Medium fraction of the Beauval Basal Lag. Bored and phosphatized intraclasts are dominant but bioclastic debris remains an important constituent. Fragments of 'Terebella' phosphatica tube are common.
C. Fine fraction of the Beauval Basal Lag after removal of the micritic matrix. Components include bored and phosphatized intraclasts, phosphatized faecal pellets and ooliths and mineralized and unmineralized bioclastic debris (particularly benthonic foraminiferans, bone fragments, sponge, echinoid, oyster and comminuted inoceramid).
D. A naturally washed and partly decalcified residue of a phosphatic chalk from Hallencourt quarry. The sediment is composed almost entirely of ovoid faecal pellets (Willcox's, 1953a type D).


A
e
o
o
c
o
a
i
o
o
a
o
o
o
c
2cm


B
1cm


C
4mm


D
4mm

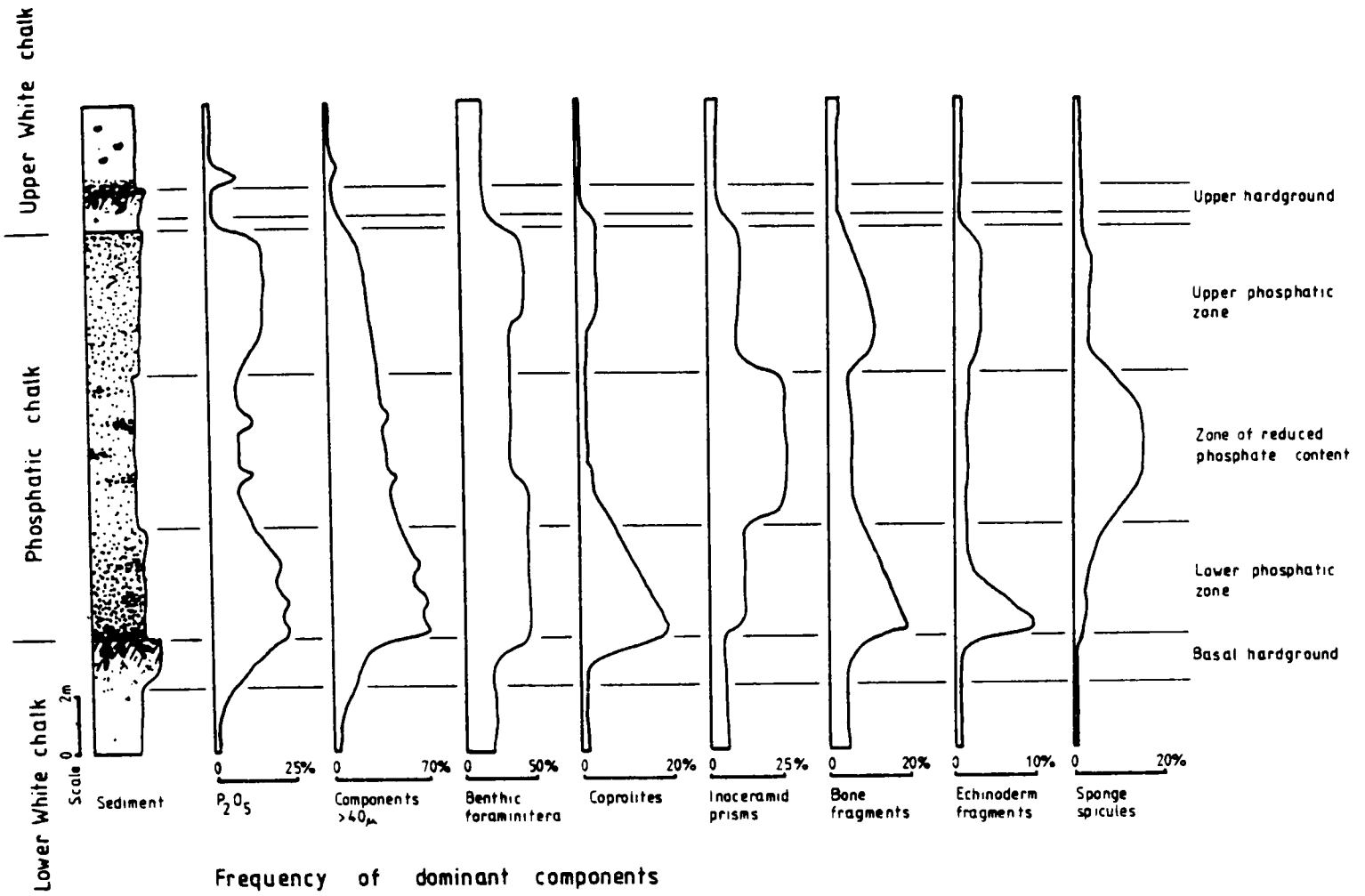


Fig. 3.11 Component analysis of an idealized phosphatic chalk. The tailing-off of components below the basal hardground, rather than a sharp cut-off, is due to bioturbation. The sediment log has a weathering profile. Based on Tabatabaï (1977) and personal observation.

phosphorite may overlie the basal hardground (Fig. 3.14). As further sediment is deposited the percentage of coprolites, ooliths, echinoderm, bone fragments and benthonic foraminiferans decline and the percentage of sponge spicules and inoceramid prisms increases, although all fragments return to a low level on the resumption of white chalk deposition. The most phosphatic sediments are generally the coarsest but the phosphatic chalk directly above the hard-ground is coarser than equally phosphatic sediment higher in the sequence.

Where the phosphatic chalk overlies a well-developed basal hardground the phosphatic component is strongly mineralized and phosphate-veneered (Fig. 3.15A,B), but in some marginal deposits such as those at Ribemont, Villers-devant-le-Thour and in the upper part of the succession at Orville and Faucouzy, phosphatization is less pronounced. In these examples the coarse calcarenitic texture of the bed is produced by the abundance of dissociated inoceramid prisms (Fig. 3.16A,B) or a high proportion of foraminiferans (Fig. 3.15C,D). The phosphatic component is generally restricted to incompletely-phosphatized, unveneered, subangular white chalk intraclasts (Fig. 3.16C,D) and phosphatized

Fig. 3.12 Phosphatic chalk microfacies I: Basal lags.
A,B. Medium to coarse sand grade phosphatized and unmineralized grains with a micritic matrix. The intensely-mineralized, pseudo-isotropic nature of the faecal pellets (fp) contrasts to the patchy partly-birefringent phosphatization displayed by most intraclasts (i). The walls of foraminiferans (f) and echinoderm calcite (e) are generally unmineralized. Intraclasts include both simple (i) and compound (ci) varieties. Nurlu Basal Lag. (A) PPL, (B) XN.
C,D. A grain-supported phosphorite consisting essentially of foraminiferans with phosphatized fills. Faecal pellets within compound intraclasts (ci) are more strongly mineralized than those outside (fp). Beauval Basal Lag. (C) PPL, (D) XN.

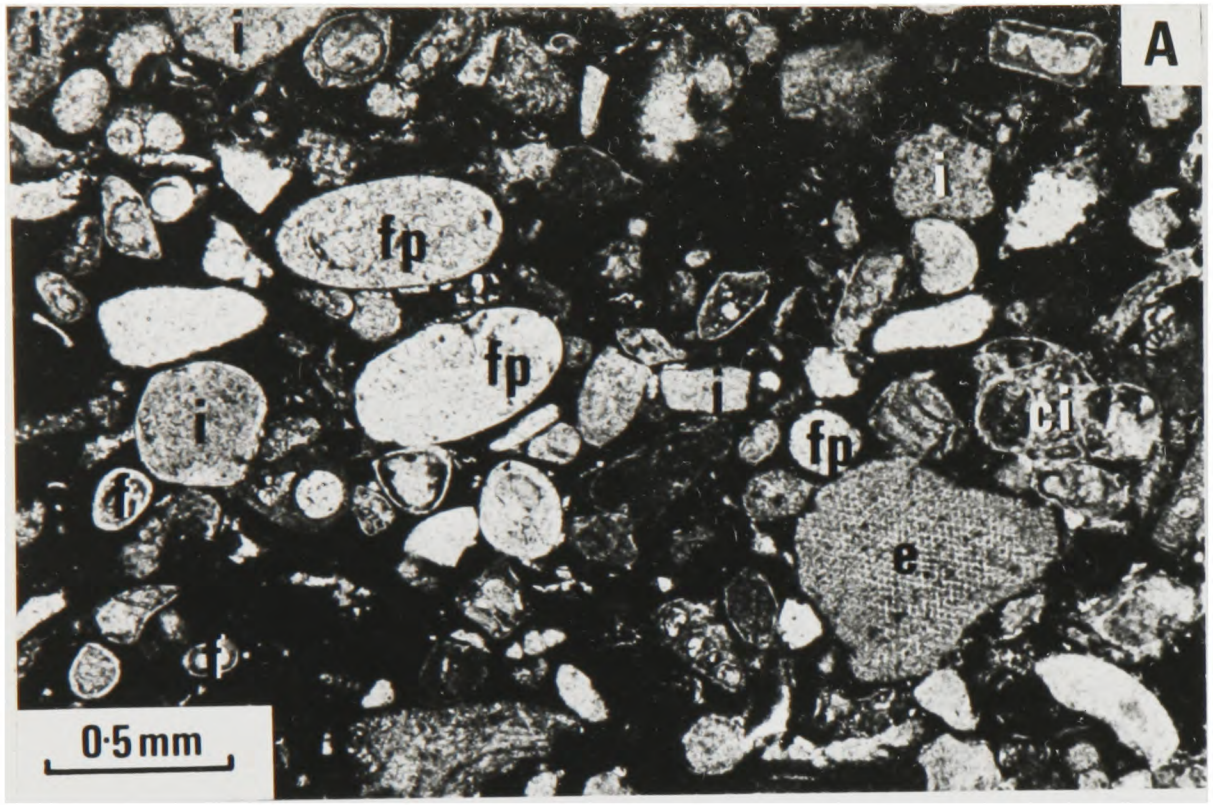
A
i
fp
fp
i
f
cf
i
fp
e
ci
0·5 mm

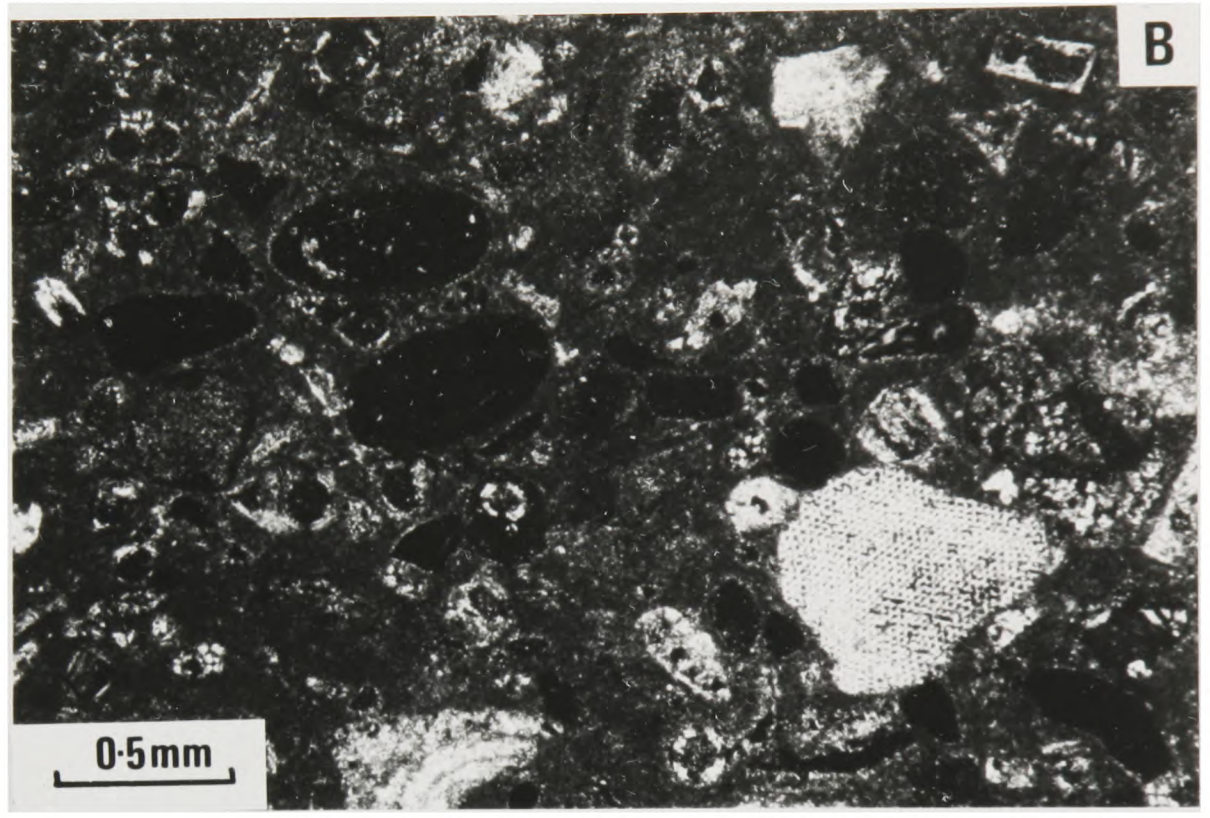
B
0·5 mm

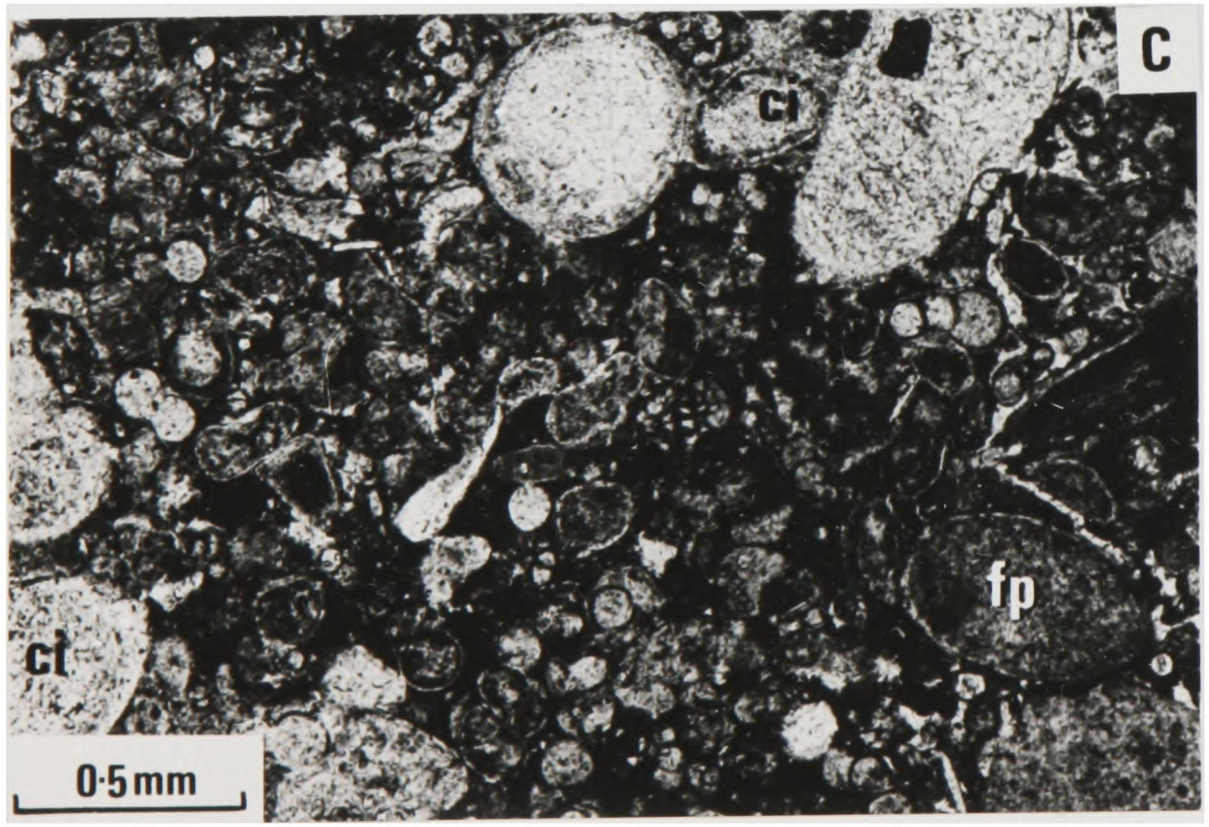
C
ci
ci
fp
0·5 mm

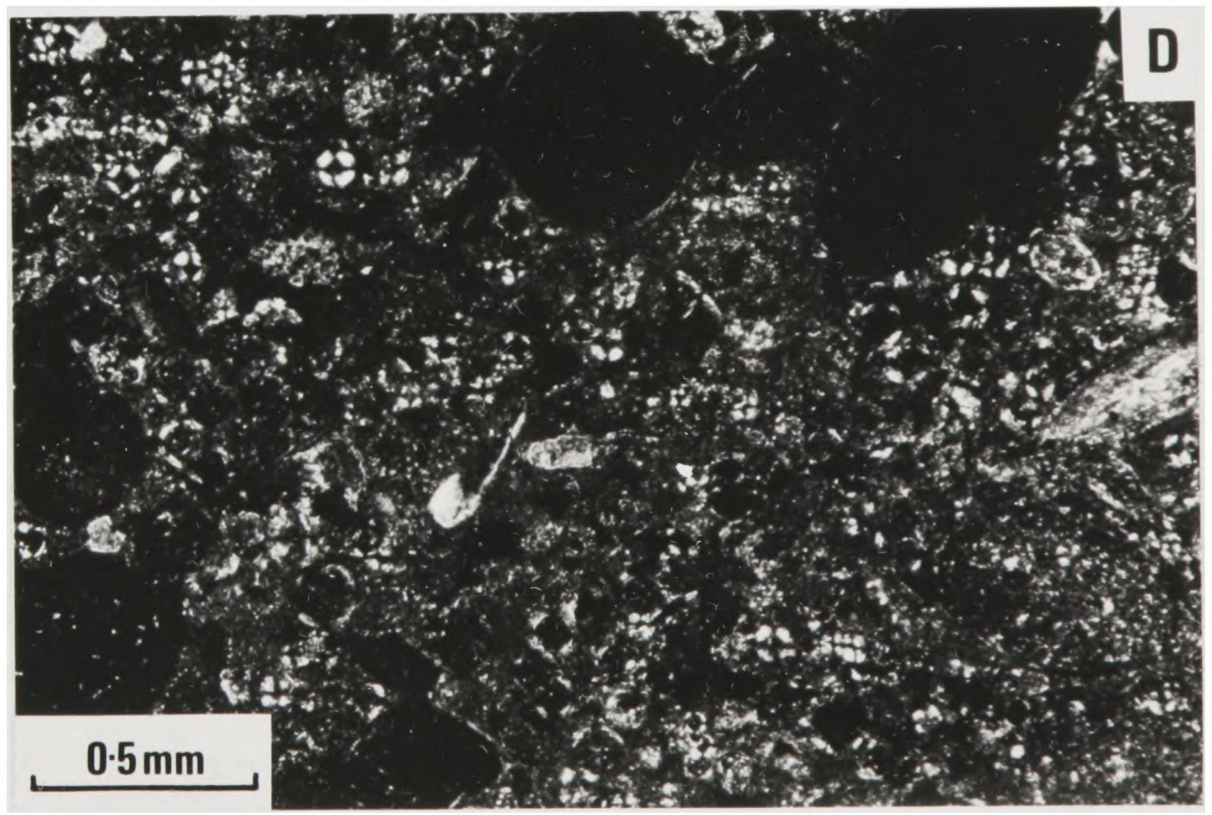
D
0·5 mm

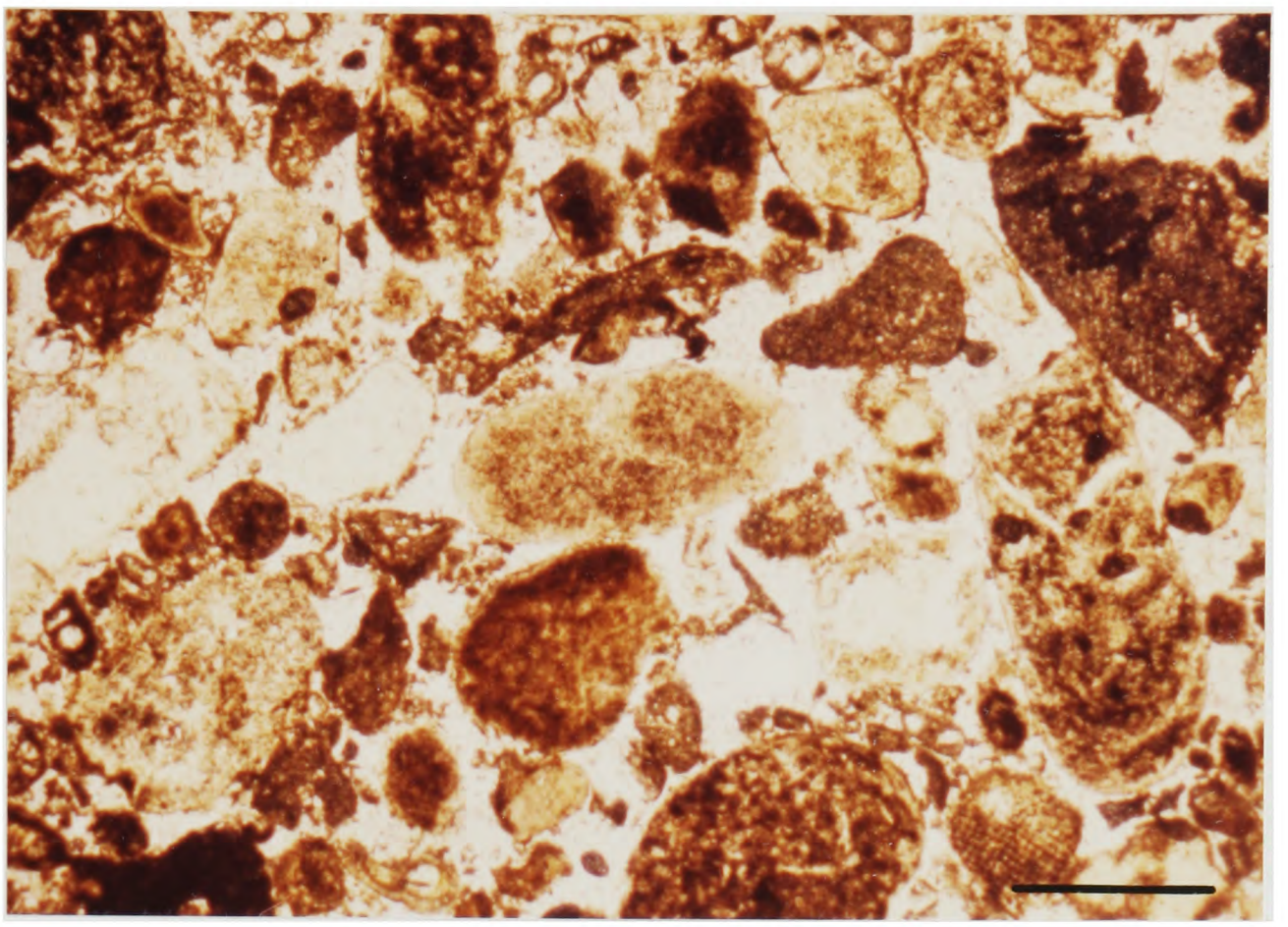

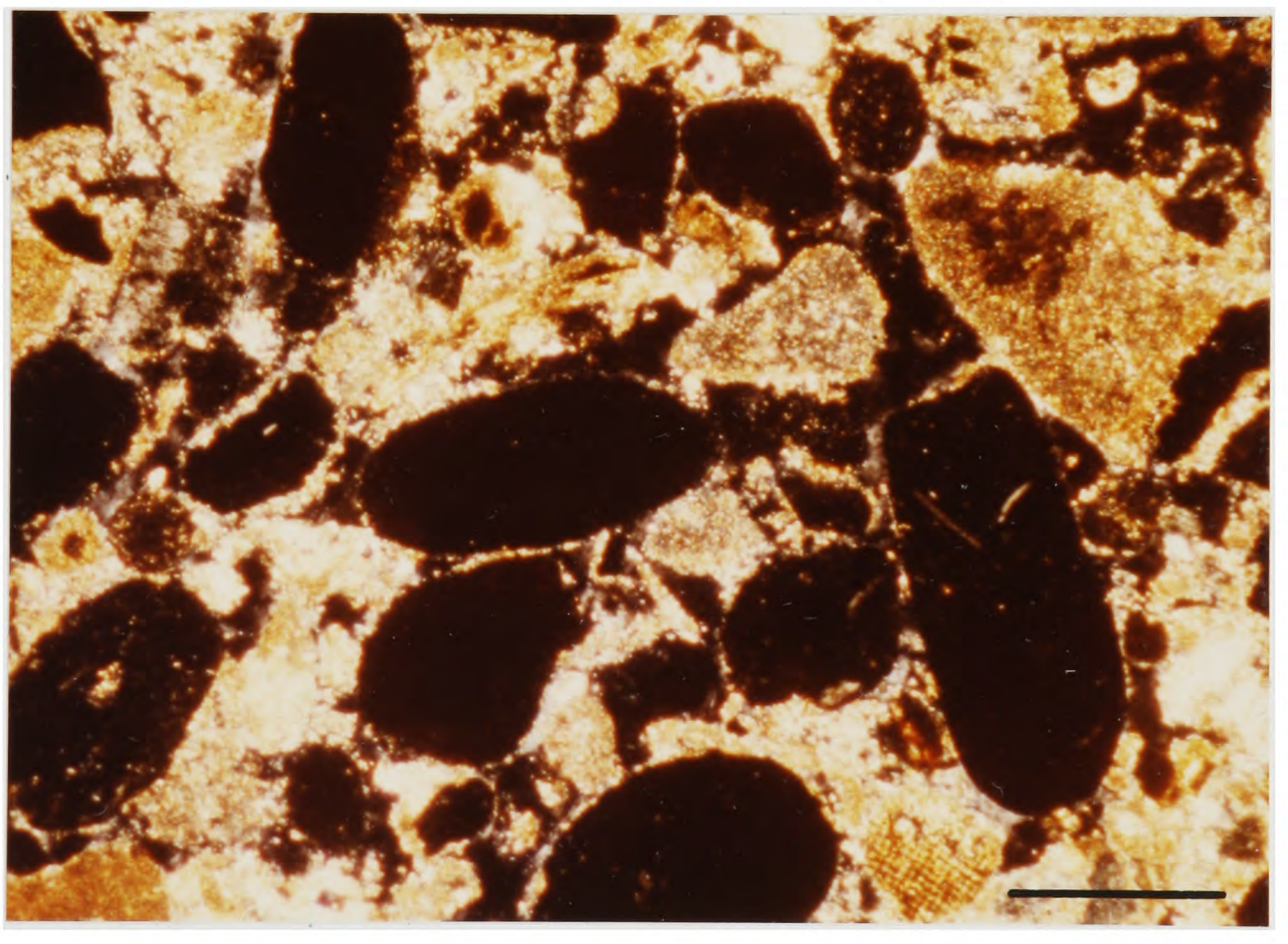

Fig. 3.13 Phosphatic chalk microfacies II: Coprolitic phosphorite.
Intensely-phosphatized ovoid faecal pellets are the main constituent of this sediment. Pellets are dark brown in plain polarised light (top) but pseudo-isotropic under crossed nicols (bottom). The bright birefrigence of the micritic matrix indicates that the section is <30 µm thick. Incompletely-mineralized intraclasts are dark brown in plain polarised light but retain a (albeit reduced) bright birefringence. A phosphatized echinoderm fragment is visible bottom right. Phosphatic chalk from Hallencourt quarry.
Scale bars = 0.5 mm.

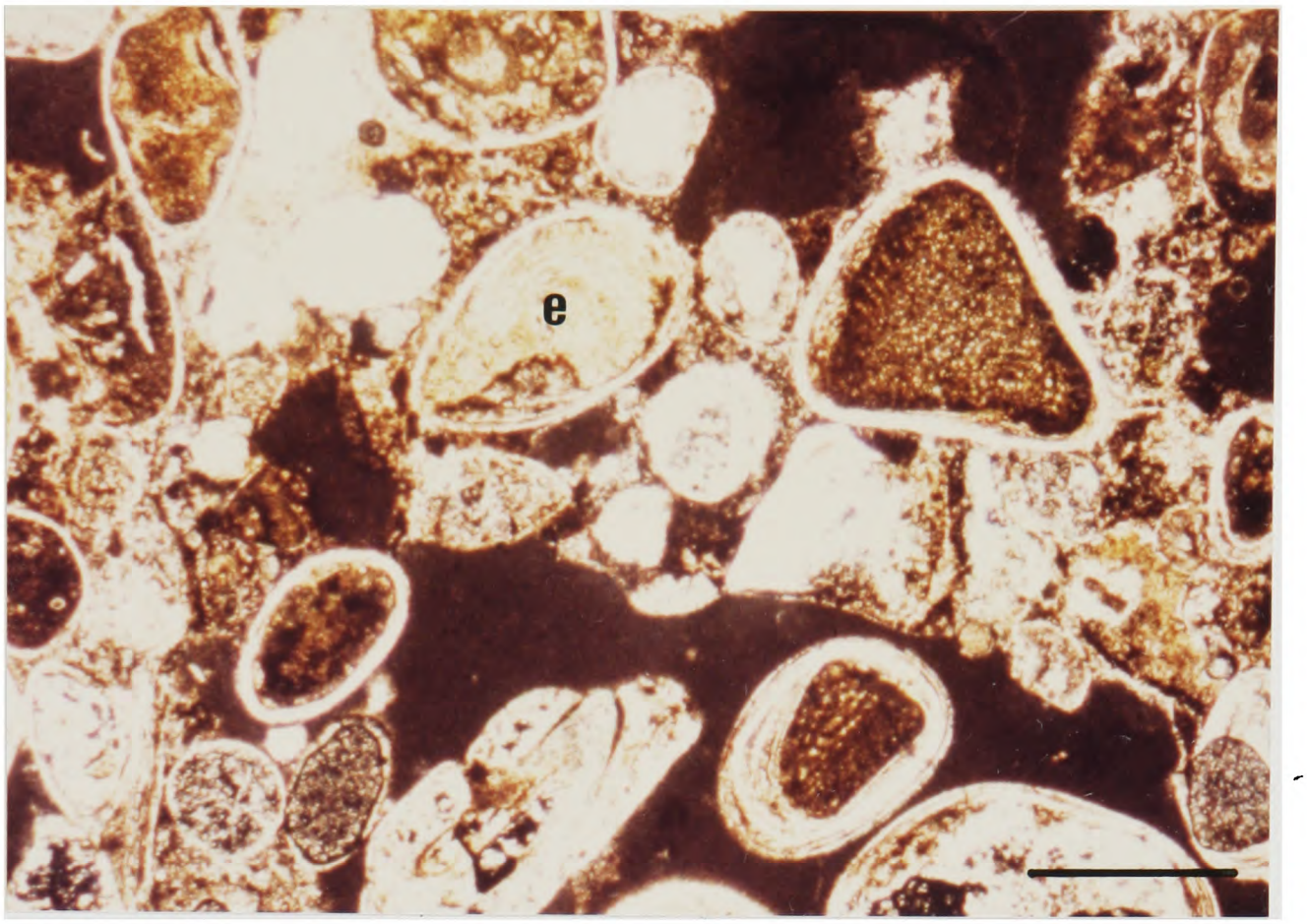


Fig. 3.14 Phosphatic chalk microfacies III: Oolitic phosphorite.
The phosphorite is cemented onto the surface of the basal hardground at Hallencourt quarry. The nuclei of ooliths include echinoderm calcite (e) and phosphatized faecal pellets (fp) and intraclasts. In most cases the phosphate veneers that produce the oolitic structure on the grains are relatively thin. Note the thickened coating in embayed areas; this is typical of oolitic growth. Much of the material is cemented with a phosphatized micrite which is light brown in plain polarised light (top) but dark under crossed nicols (bottom). Thin phosphate veneers coat the phosphatized portions of the matrix. Note the typical first-order grey birefringence and pseudo-unixial interference figures of the phosphate veneers. Scale bars = 0.5 mm.

Fig. 3.15 Phosphatic chalk microfacies IV: Mixed and foraminiferal phosphorites.
A,B. Mixed phosphorite from 1 m below the top of the phosphatic chalk (bed N1/2), Nurlu quarry. Intraclasts show varying degrees of mineralization, the most strongly phosphatized (pseudo-isotropic) being coated by phosphate veneers. Foraminiferans with phosphatized infills, and mineralized and unmineralized inoceramid prisms are all abundant. (A) PPL, (B) XN.
C,D. Foraminiferal phosphorite (bed O1/2) from 'les Champs d'Argent' quarry, Orville. Phosphatized micrite within foraminiferal tests (f) is commonly more intensely mineralized than the phosphatized intraclasts (i) occurring in the same bed. The foraminiferan tests retain their calcite mineralogy. Note the absence of phosphate veneers. (C) PPL, (D) XN.


A
0·5mm


B
0·5mm

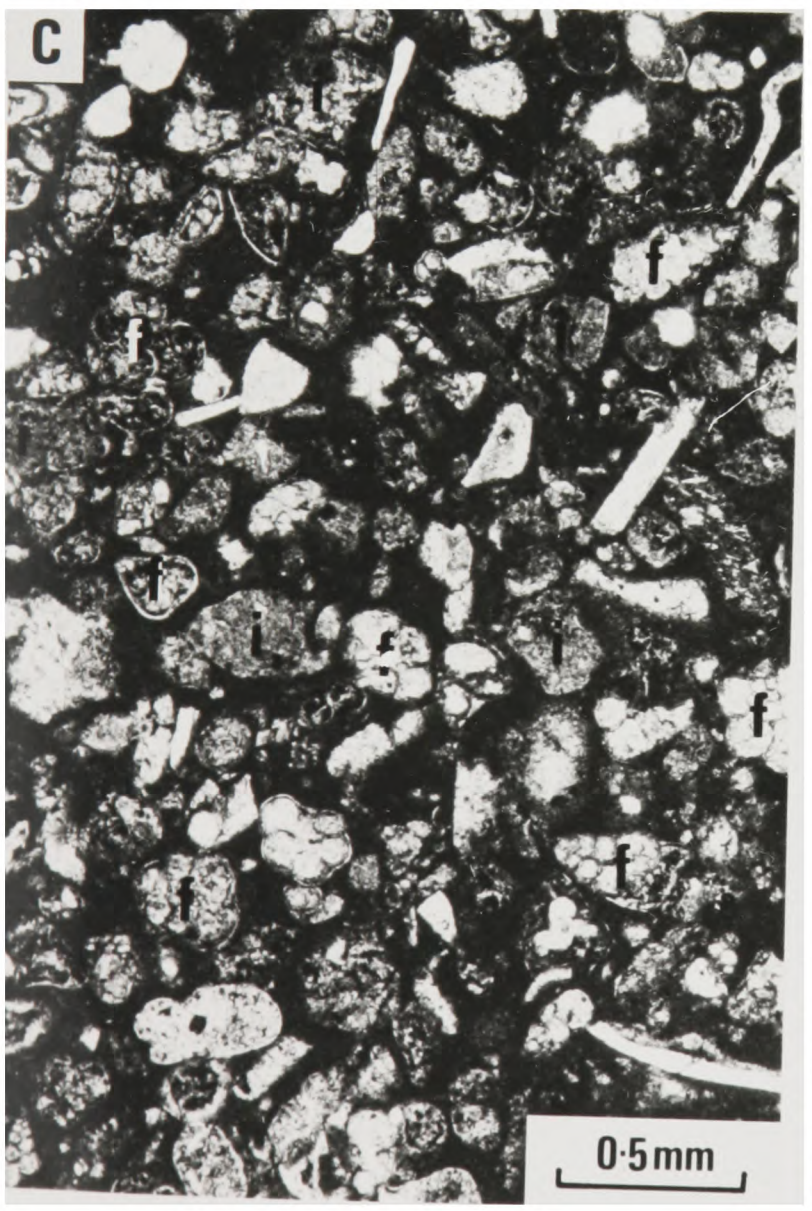
C
f
f
f
f
f
f
f
f
0·5mm


D
0·5mm

Fig. 3.16 Phosphatic chalk microfacies V: Phosphatic inoceramite and intraclastic phosphorite.
A,B. Phosphatic inoceramite from the second phosphatic chalk (bed R1/4), Ribemont quarry. The calcarenitic nature of the bed is provided by the high concentration of inoceramid prisms and small phosphatized intraclasts. The bulk of the bed is matrix supported (left) but burrow fills are commonly grain supported and have a higher phosphate content due to the inclusion of phosphatized-micrite infilled foraminiferans (right). (A) PPL, (B) XN.
C,D. Intraclastic phosphorite from the phosphatic chalk overlying the Ribemont Gonioteuthis Hardground. Incomplete phosphatization of the intraclasts is shown by their partly birefringent properties under crossed nicols. Note the absence of phosphate veneers. The bed passes laterally into similar chalks with an even lower phosphate content. (C) PPL, (D) XN.

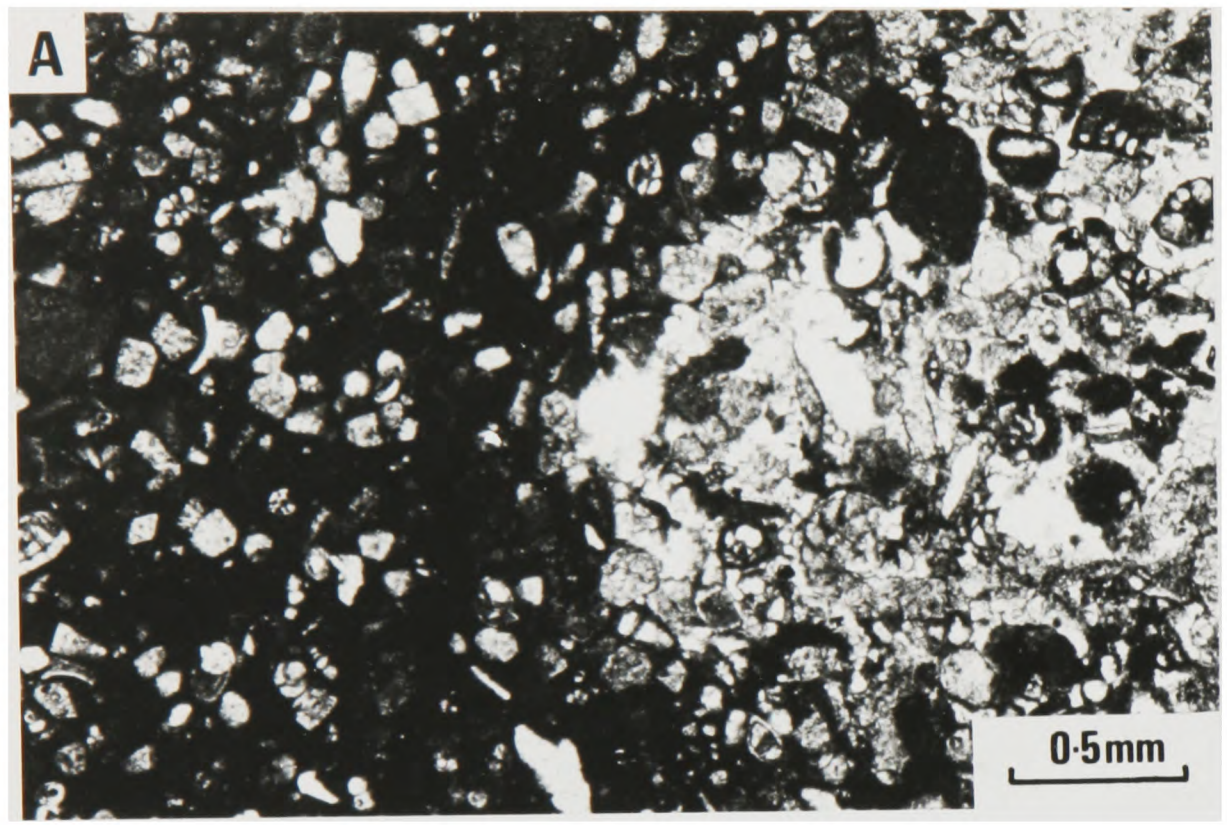
A
0·5mm

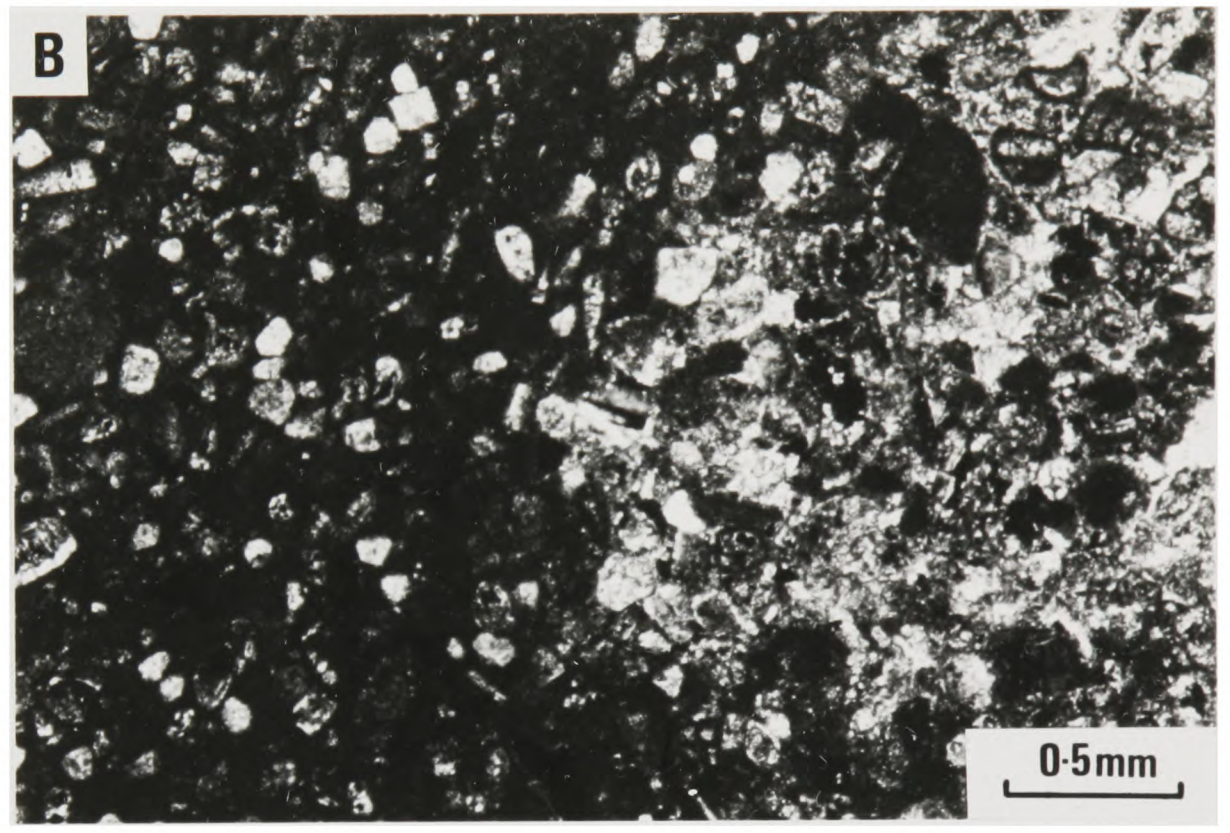
B
0·5mm

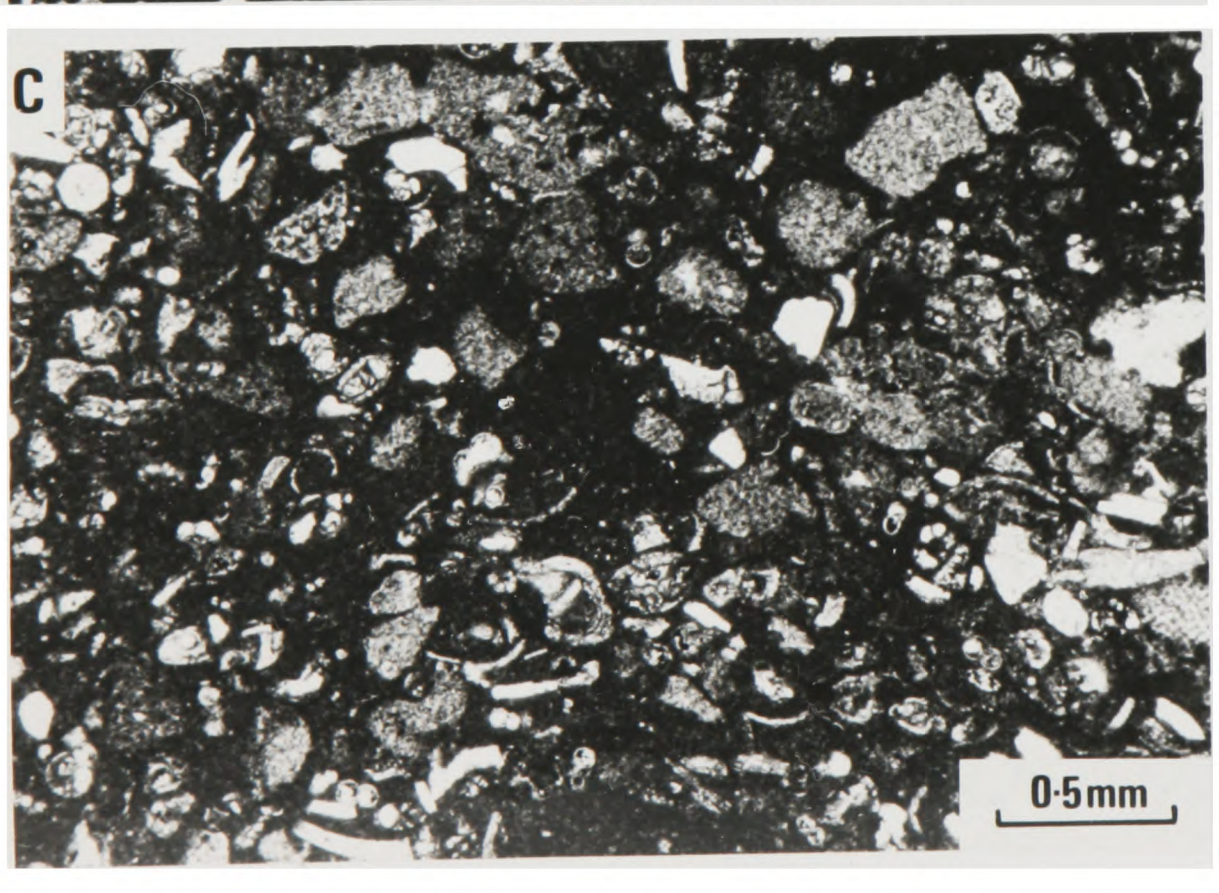
C
0·5mm

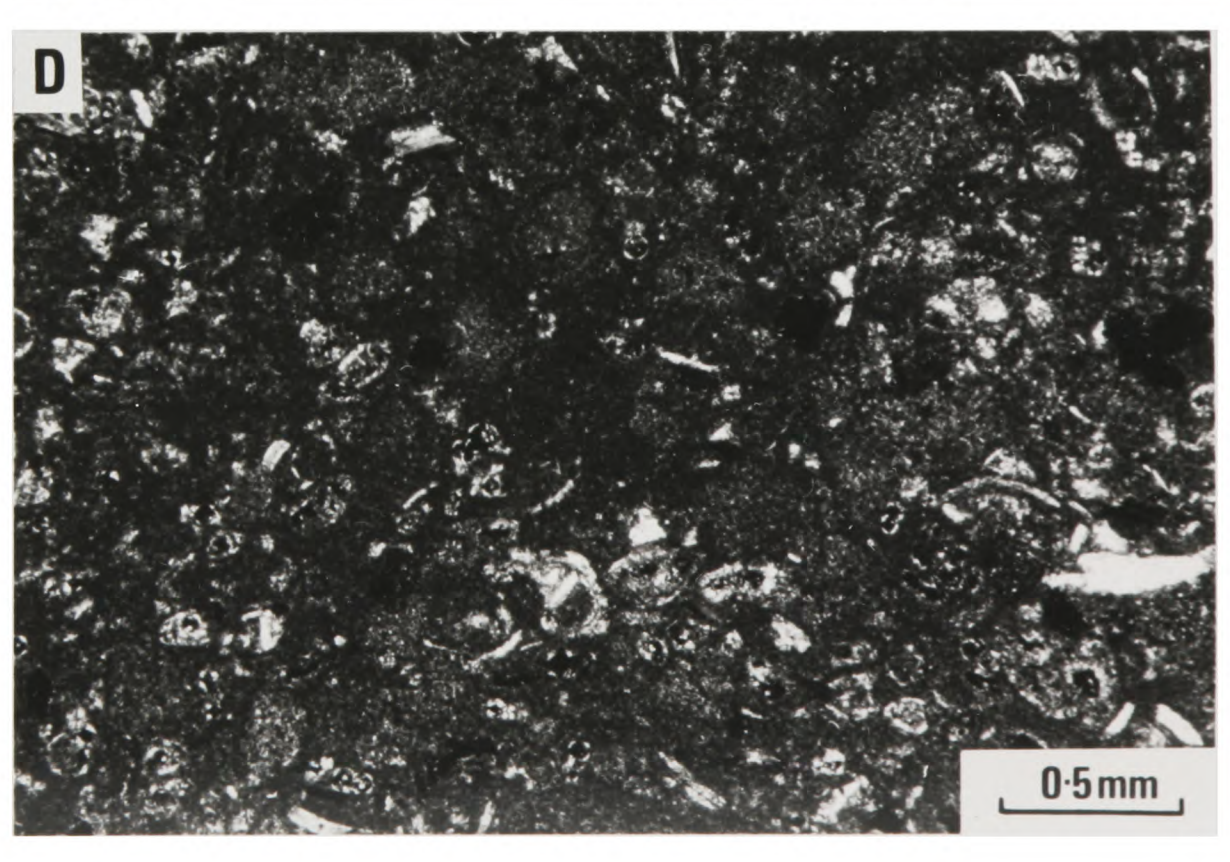
D
0·5mm

internal moulds of foraminiferans (Fig. 3.15C,D). The dominance of coarse skeletal carbonate indicates that although current conditions were sufficient to produce a winnow-coarsened sediment the environment was unsuitable for wholesale replacement of carbonate by phosphate (see below). Like most winnowed chalks, burrow-fills are generally coarser-grained than their enclosing sediment. In these phosphatic calcarenites the grain-supported burrow fills contrast with the matrix-supported textures of the bed as a whole (Fig. 3.16 A,B). The teleost fish debris and fragmented thin-shelled oyster which are prominent in hand specimens of the microfacies are seen to be volumetrically minor elements when examined in thin section.

### 3.4.3 Phosphatic chalk components

The pelletal material in phosphatic chalks may be conveniently divided into non-skeletal and skeletal categories. The former group includes intraclasts, pellets, coprolites and ooliths and the latter encompasses all bioclastic debris, dominantly foraminiferans, inoceramid prisms and bone fragments.

#### 3.4.3a Intraclasts

The origin of large basal lag intraclasts has been discussed in detail (see above) but intraclastic debris is also important in the sand-grade component. Where a phosphatic chalk overlies a well-developed basal hardground the included intraclasts invariably exhibit diverse origins. They vary in size from the finest sand to gravel (0.0625 - $\geqslant$2.00 mm), are light to dark brown in colour and have highly-polished phosphate veneered exteriors. All are well-indurated and strongly phosphatized. Many (particularly at the base of the succession) are heavily bored and mineralized bioeroded fragments of hardground chalk and exhibit all the textural variation shown by that lithology (Fig. 3.3E). Some are aggregates of non-skeletal grains having a grapestone texture (Fig. 3.17A,B) - apparently fragments of a high to moderate energy deposit that have been incorporated (either by reworking from below or lateral

Fig. 3.17 Intraclasts from phosphatic chalks.
A,B. A strongly-phosphatized compound (grapestone) intraclast from the phosphatic chalk (bed F1/1) of Faucouzy quarry. Primary components include foraminiferal (f) and micritic (m) chalks which have been reworked, mineralized and coated with phosphate veneers. These first-stage intraclasts (1) have been subsequently reworked and show second-stage addition of sediment (2) - bottom left, and fragmentation (3) - top left. A third stage of cementation mineralization and veneering has led to the final intraclast being embedded in an intraclastic phosphorite. (A) PPL, (B) XN.
C,D. A weakly-phosphatized phosphatic chalk intraclast from the phosphorite (bed F1/1) of Faucouzy quarry. A fragment of phosphatic chalk has been reworked into a sediment of closely comparable composition. The lithified sediment is differentiated by the smaller number of infilled foraminiferan tests (due to the introduction of cement) and its generally lower microfossil content. Both sediments contain phosphatic ooliths (o). (C) PPL, (D) XN.
E,F. Weakly-lithified white chalk intraclasts in the phosphatic chalk (bed N1/2) of Nurlu quarry. The micritic intraclasts contrast strongly with the inoceramid prism and foraminiferan-rich sand-grade phosphorite. (E) PPL, (F) XN.

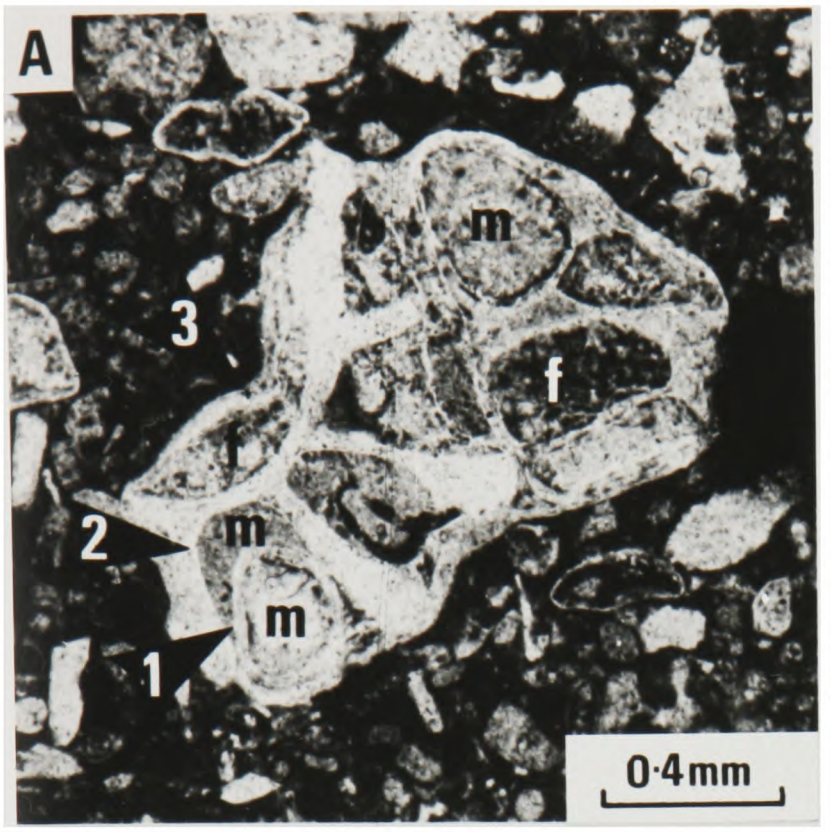
A
m
3
f
2
m
m
1
0·4mm

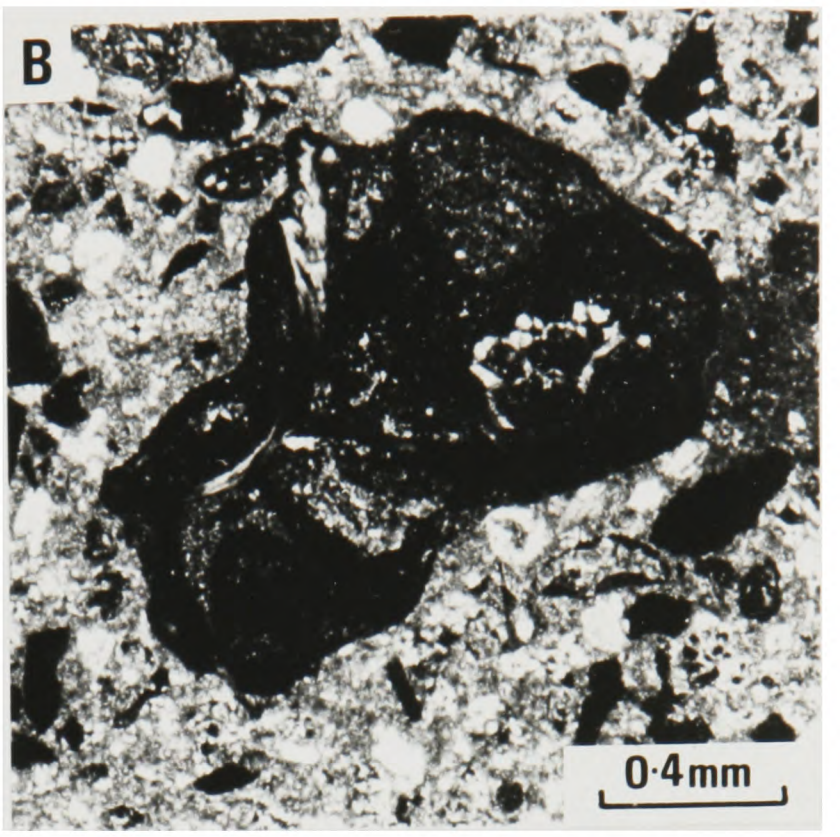
B
0·4mm

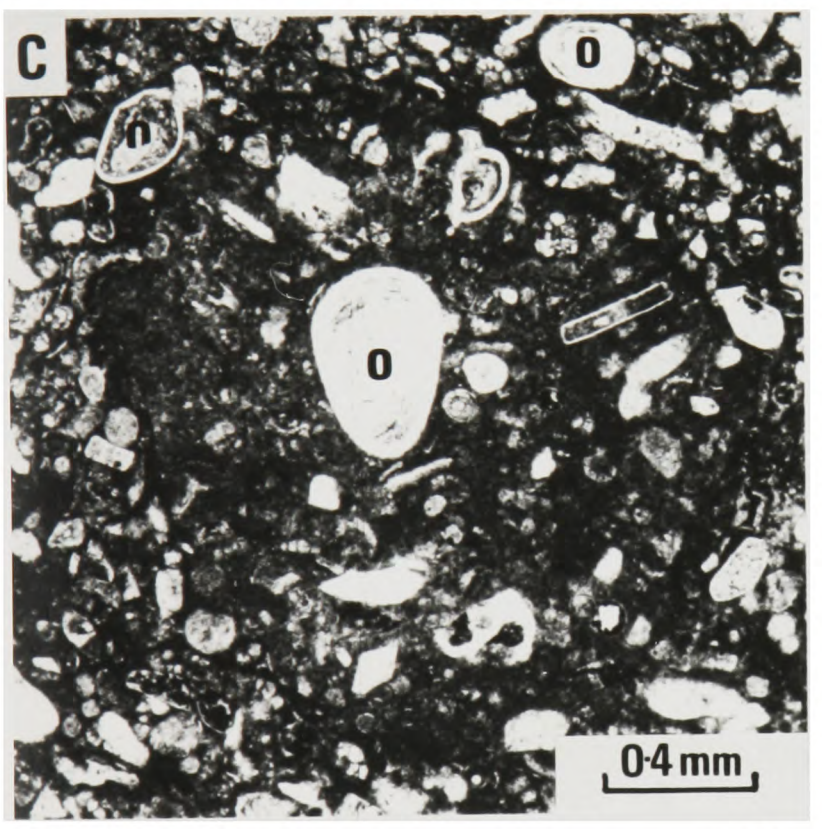
C
o
n
o
0·4 mm

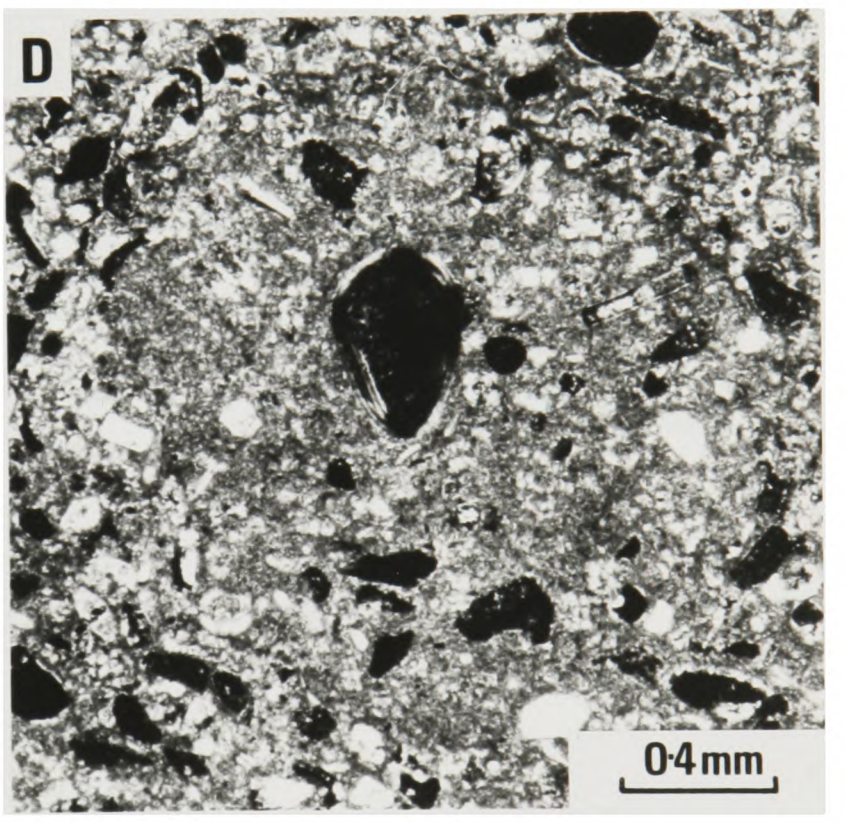
D
0·4 mm

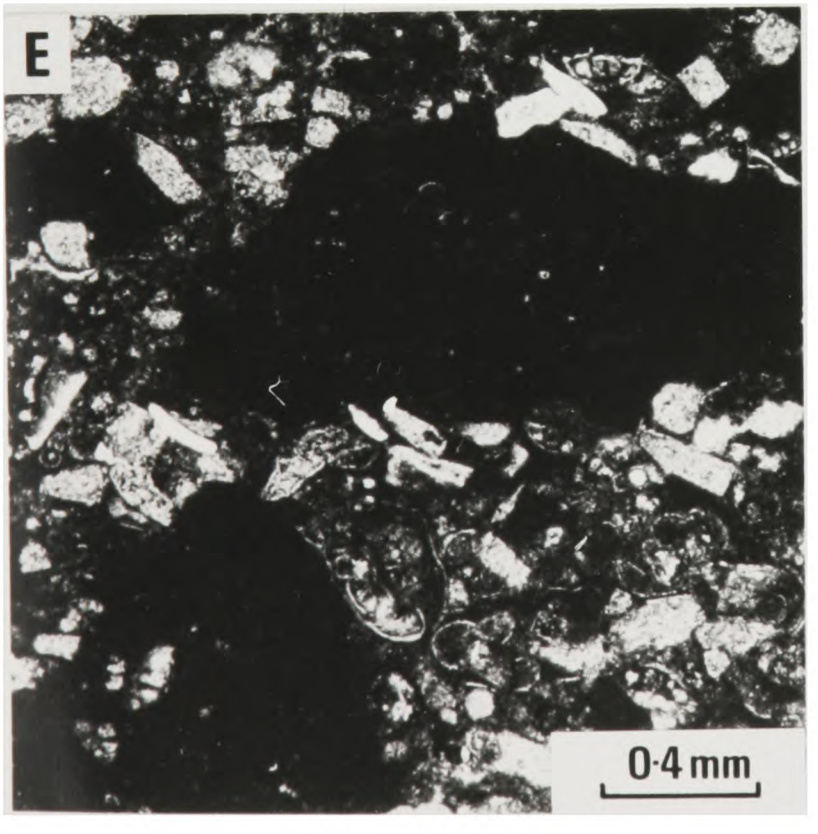
E
0·4 mm

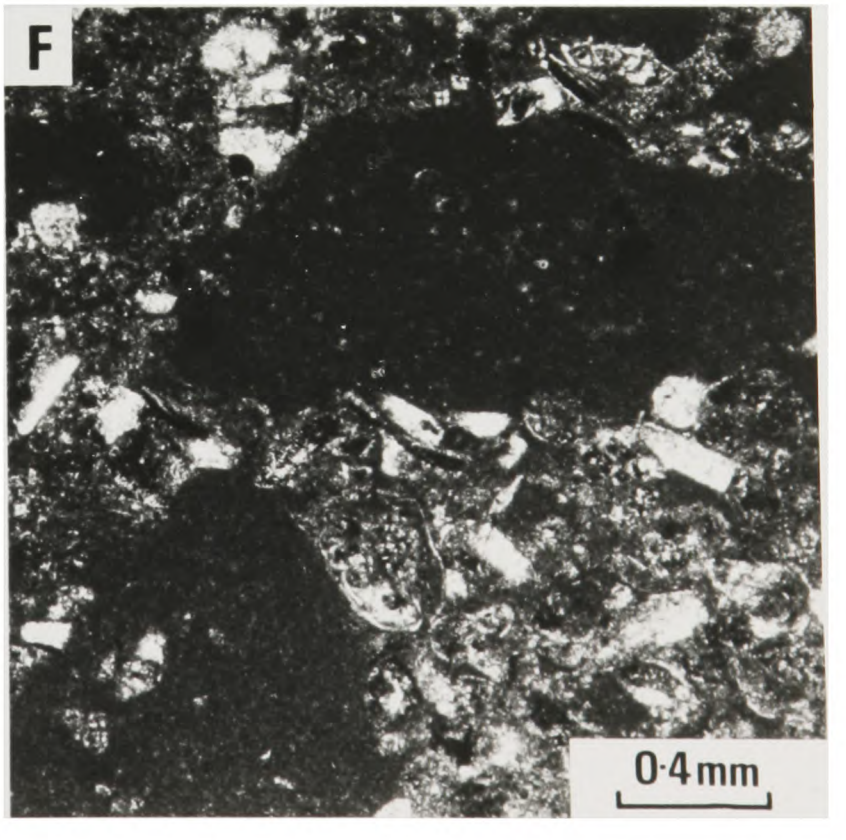
F
0·4 mm

derivation) into a lower energy phosphorite. Other intraclasts composed of phosphatic chalk contain more micrite than the enclosing matrix (Fig. 3.17C,D). With decreasing grain-size all three types become more rounded and difficult to differentiate from pelletal material of other origins (see below). The diversity of phosphatized intraclasts in the phosphorite illustrates the complex diagenetic history and numerous phases of reworking that the sediment must have undergone.

In contrast, intraclasts from thin, poor phosphatic chalks that do not overlie strongly-developed basal hardgrounds (e.g. the intraclastic phosphorites of the phosphatic chalk lens in the intermediate white chalk at Beauval quarry and those at Ribemont quarry) are poorly-indurated, lighter in colour, more angular and have dull exteriors (Fig. 3.18). These intraclasts are essentially incompletely-phosphatized fragments of white chalk that have been derived locally and not been sujected to repeated reworking. They are occasionally accompanied by unmineralized, weakly-indurated, white-chalk intraclasts that are probably precursors of the mineralized varieties. Similar subangular 0.5 - 5.0 mm white chalk intraclasts occur in patches at the summit of the phosphatic chalk at Nurlu quarry. This indicates that even in well-developed 'mature' phosphorites, deposition and reworking of white chalk was taking place right up until the final burial of the sediment.

In most cases, phosphate is replacing previously lithified carbonate such as hardground chalk and grapestone aggregates, but whether phosphatization is entirely restricted to cemented material is less easily demonstrated. Certainly weakly-lithified sediment may be replaced. In all examples, however, phosphatization is an external process that decreases progressively from the outside of the intraclasts inwards. Intraclasts commonly have non-phosphatic or only weakly-mineralized cores. This indicates that in intraclasts at least, phosphate was not the primary cement (which would be disseminated throughout the intraclast) but is replacing a preexisting carbonate. As in all phosphatized carbonates, cemented micrite is more readily mineralized than the enclosed bioclasts, while foraminiferal infillings are commonly more intensely phosphatized than their surrounding mineralized matrix.

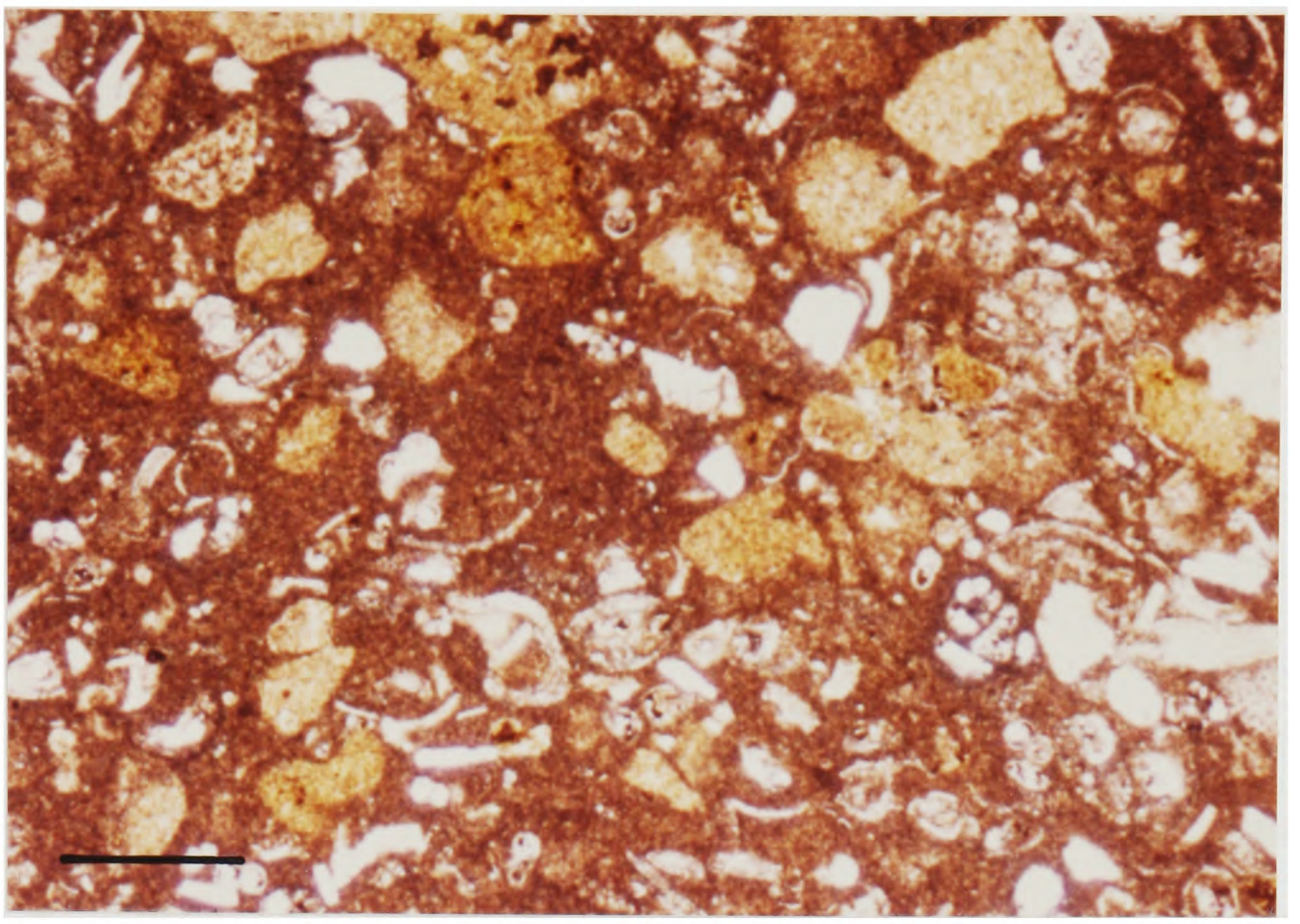

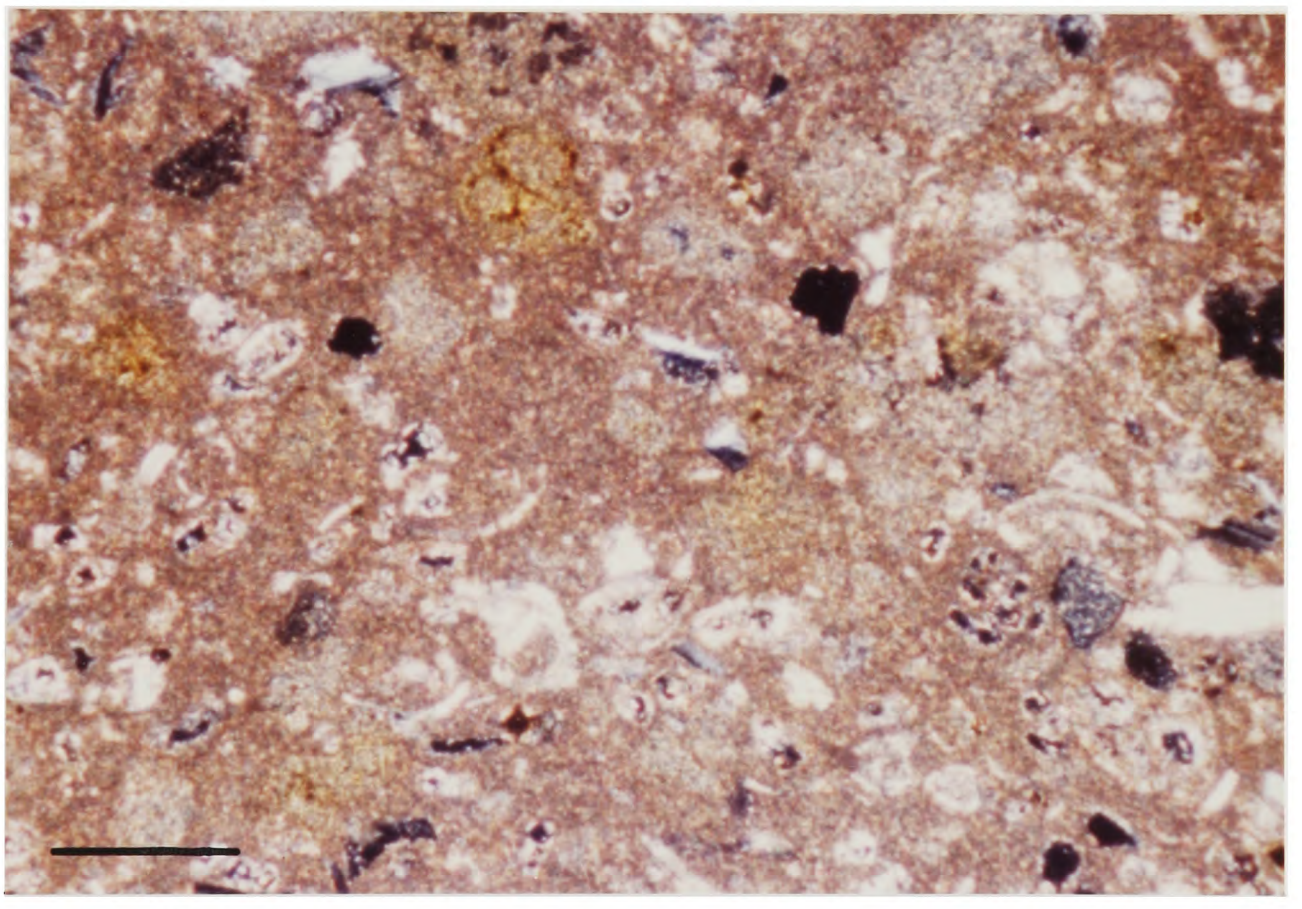

Fig. 3.18 Phosphatic chalk microfacies VI: Intraclastic phosphorite.
Incompletely-mineralized angular micrite intraclasts may be distinguished by a lighter brown colour in plain polarised light (top). A mixture of birefringent carbonate, pseudo-isotropic phosphate and green glauconite produces light blue-green tints under crossed nicols (bottom). The dark-brown limonitic stain is a weathering product of glauconite. Phosphatic chalk from above the Ribemont Gonioteuthis Hard-ground. Scale bars = 0.5 mm.

3.4.3b Coprolites and pellets

Pellets are spherical, ovoid or cylindrical carbonate grains that have a disordered internal structure. The enclosed carbonate is generally micrite but may contain larger bioclastic grains such as foraminiferans and inoceramid prisms. Pellets from phosphatic chalks are light-brown in colour with a highly polished exterior, are invariably intensely-phosphatized and contain a high proportion of enclosed organic matter. They fall into two size groupings, the first and dominant group consists of small (40 - 200 μm long) regular and irregular spherules, ovoids and rare rods; the second of larger (0.2 - 2.0 mm) regular ovoid and cylindrical grains. Members of the latter group occasionally display grooves and canals similar to those described from Recent (Moore, 1939) and Cretaceous (Willcox, 1953a) coprolites indicating that these are indeed of faecal origin, although the origin of the smaller grain-size is less certain. Faecal pellets may be most readily recognised where they form clusters or aggregates of uniform size and geometry infilling burrows, internal moulds of fossils or cemented onto the surface of the basal hardground. In most cases, however, the pellets are unclustered and generally slightly deformed suggesting that the excreted pellets remained soft during the initial stages of transport and were only later indurated prior to burial.

In modern environments pellets are produced by a number of mechanisms other than excretion. Some originate from the micritization of skeletal particles, coralgal fragments and ooliths by processes associated with endolithic algae and fungi (Bathurst, 1966, 1975) and others are simply well-rounded intraclasts modified by long-term abrasion. Primary phosphatic pellets are produced as kidney stones by bivalves in high-stress environments (Doyle et al., 1978) and phosphate precipitated in cavities of vertebrate skeletons may be liberated as pelletal material subsequent to the dissolution of the enclosing bone (P. Cros in Tabatabai", 1977). The general absence of any internal structure (such as the concentric layering that is typical of bivalve kidney stones) and the inclusion of both carbonate and non-carbonate diluents (bioclastic debris, clays etc.) in most pellets make such sources unlikely for the bulk of the pelletal material, although an intraclastic origin appears most likely for

more irregular grains.

The similarity of the sediment enclosed in and that surrounding the pellets suggests that they were produced by fine-grained deposit feeders. The abundant evidence of an active infauna incluing worms, crustaceans, bivalves and echinoderms provides an ample source of faecal material but because of the large number of animals that produce faecal pellets and because most pellets are unsculptured ovoids (Moore, 1939) it is impossible to identify the pellet producing organism.

Faecal pellets are produced in all environments but they are only rarely preserved for although carbonate muds are readily aggregated into pellets, these pellets are generally only loosely bonded and easily disintegrate (e.g. Shinn et al., 1969). Modern coprolites are preserved by intragranular lithification of the individual pellets by a process that is initiated in the gut of the excreting organism (Moore and Kruse, 1956) but requires rapid subsequent cementation. This occurs in the shallow, warm, relatively low-energy, supersaturated (with respect to $CaCO_3$) waters of the Bahama Banks at the present day.

It is uncertain whether faecal pellets in phosphatic chalks ever had carbonate-cemented precursors since no unphosphatized examples have been observed. Nevertheless, faecal pellets possess a number of properties that must aid in their mineralization. All faecal pellets contain a large proportion of organic matter (between 50 and 90 percent of the solid material in faecal pellets of the gastropod Batillaria minima at Alacran Reef is organic matter; Folk and Robles, 1964) and it has been suggested (Purdy, 1963) that cementation is related to decomposition of the organic mucus within the pellets by bacteria. Bacterial decay of organic matter provides a major source of orthophosphate and may produce a favourable geochemical microenvironment for the phosphatization of the enclosed micrite. This mechanism can only explain the initial stages in the mineralization of the coprolite since the high porosity of the initial pellet requires more apatite than could be provided by 'autophosphatization'. Further mineralization requires an external source of phosphate and/or carbonate, the addition of which is favoured by the high initial porosity of the pellet.

Similar processes may occur where the pellet is the product of micritization by thallophytes. Like coprolites, these pellets contain a high proportion of organic inclusions, and where the margins of the pellet exhibit prominent microboring they also display higher concentrations of organic matter. The original structure of these grains has been totally destroyed by a tightly interlocking complex of algal and fungal borings and this organic tissue provided an appropriate medium for bacterial growth. This microenvironment may provide suitable physico-chemical conditions for carbonate precipitation and/or phosphatization, but again an external source of phosphate is required to produce the final strongly-mineralized grain.

A number of part-phosphatized pellets are also present, including examples with intensely phosphatized nuclei but micritic envelopes, those with phosphatized margins but unmineralized cores and others with unmineralized cores and cortexes. These variations reflect the instability of the depositional environment with both carbonate and phosphatic material being continually reworked and bored, buried and mineralized to produce inumerable combinations of phosphatized and unphosphatized components.

### 3.4.3c Ooliths

Where phosphatic chalks overlie well-developed basal hardgrounds, the majority of components throughout the succession are coated by a thin (5 - 10 µm) patina of pure phosphate (Fig. 3.15A,B) identical to that seen in the phosphate skin complexes that overlie the basal hardground (3.3.3c). It is generally only a few grains, however, where the phosphate veneers are thick enough to produce a well-developed oolith, although all grains fall within the general definition of the term:

> "a grain which displays one or more regular lamellae found as successive coatings around a nucleus" and in which "the constituent crystals of the lamellae show a systematic crystallographic orientation with respect to the grain surface" (Newell et al., 1960).

Ooliths are clearly differentiated in thin section by their lamellae and pseudo-uniaxial interference figure under crossed nicols (Figs. 3.14, 3.19A,B).

In phosphatic-chalk ooliths individual lamellae are generally 5 - 10 µm

Fig. 3.19 Phosphatic chalk components.
A,B. An oolith from the phosphatic chalk (bed F1/1) of Faucouzy quarry. An incompletely-phosphatized intraclast acts as a nucleus to a series of phosphate veneers. (A) PPL, (B) XN.
C,D. An echinoid spine from the phosphatic chalk (bed F1/1) of Faucouzy quarry. Essentially unmineralized skeletal calcite with a strongly-phosphatized stereome infilling is the nucleus for a series of phosphate veneers (C) PPL, (D) XN.
E,F. Bone fragments (teleost fish?) in a phosphatic inoceramite microfacies from the second phosphatic chalk (bed R1/4), Ribemont quarry. Note the undulose extinction typical of all bone material (E) PPL, (F) XN.

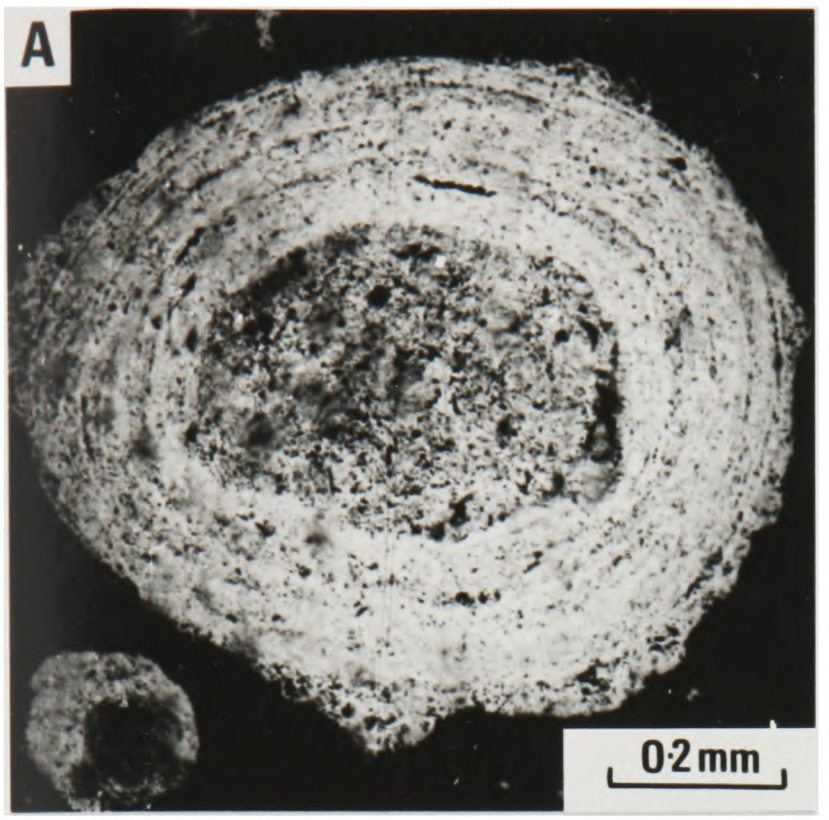
A
0·2 mm

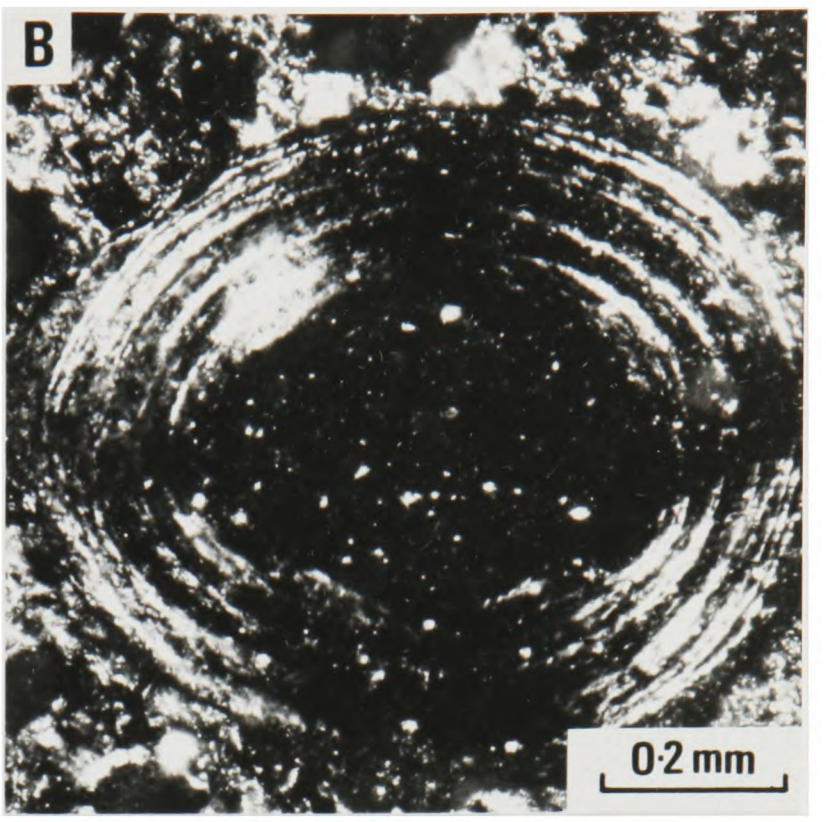
B
0·2 mm

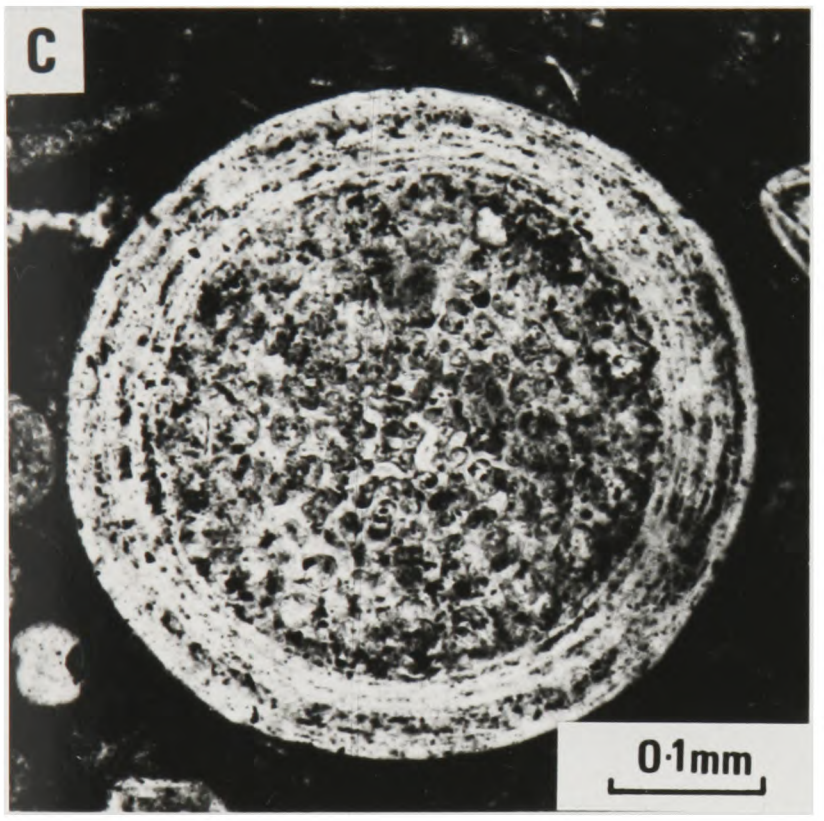
C
0·1mm

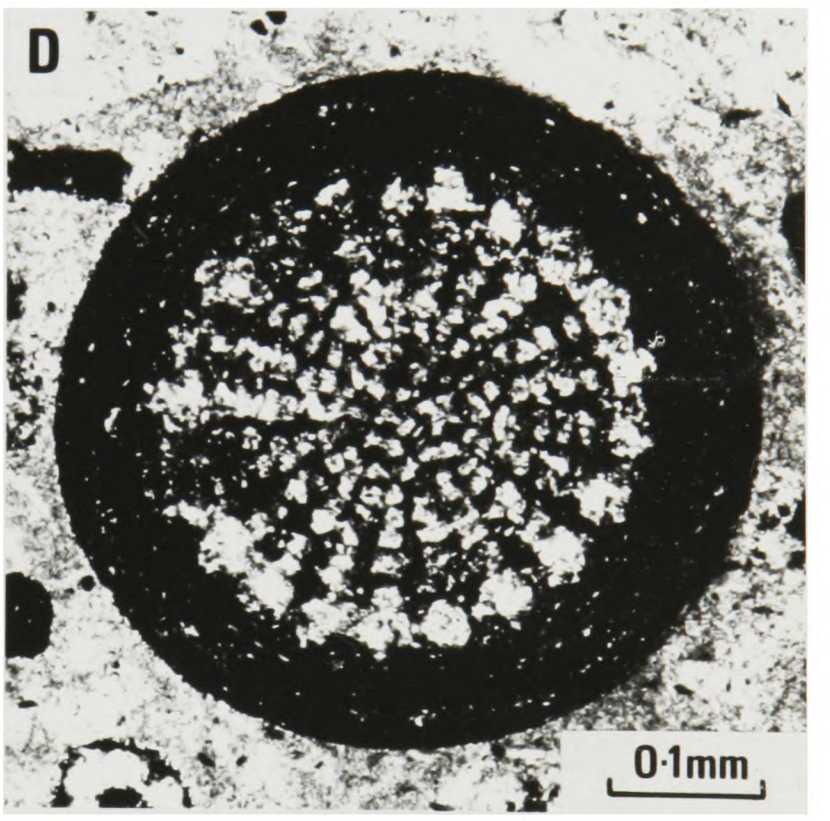
D
0·1mm

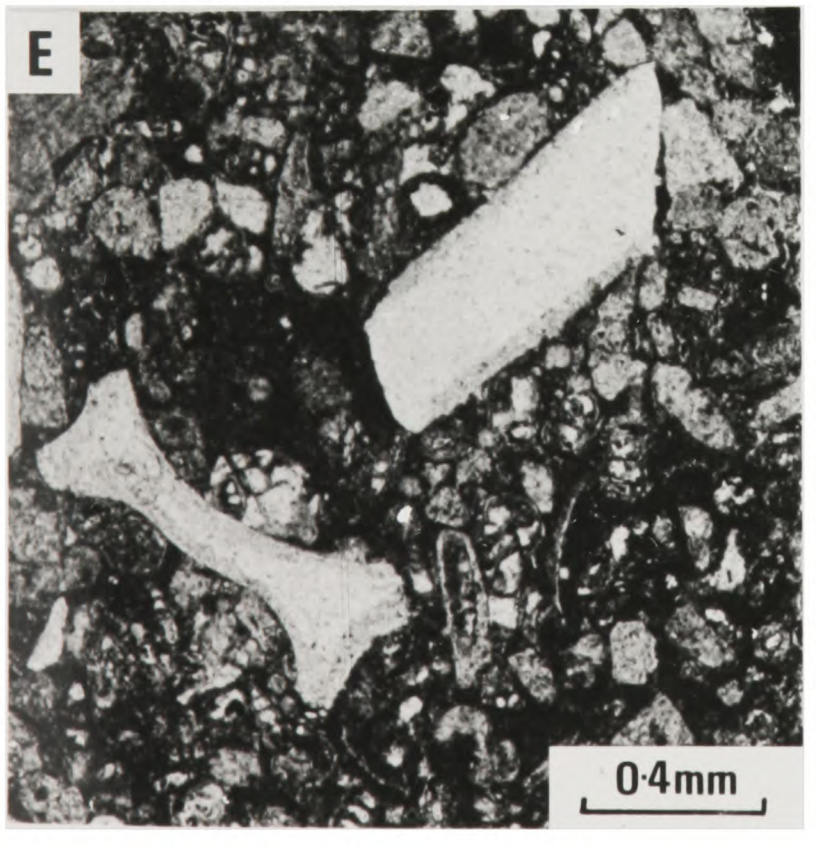
E
0·4mm

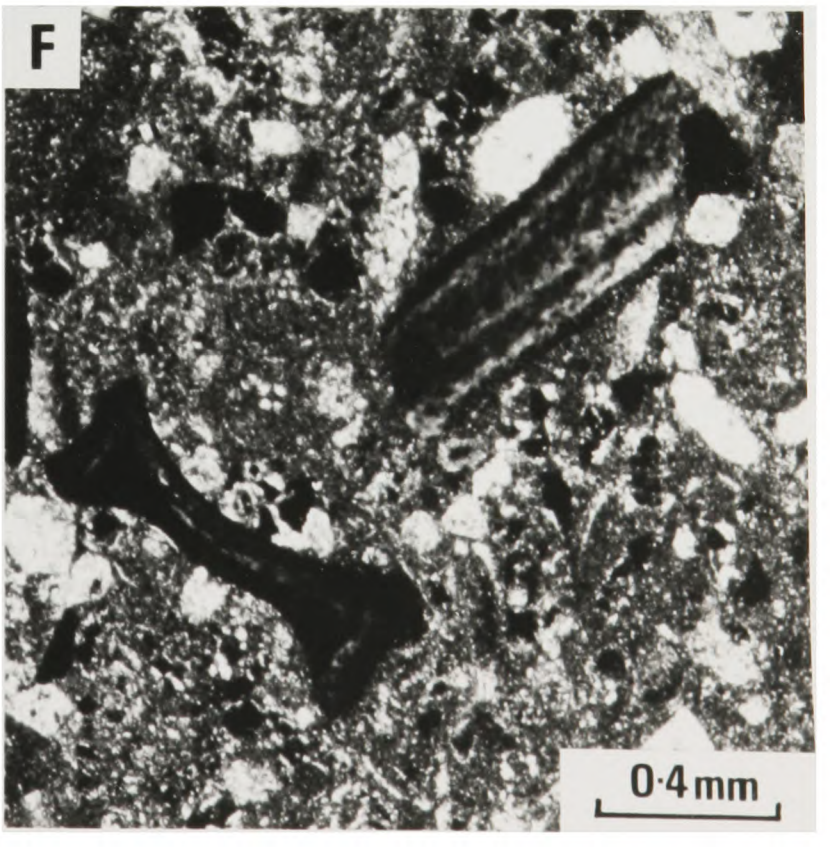
F
0·4mm

thick and some ooliths contain up to 40 lamellae. The c-axes of the individual crystallites are arranged radially as in most calcitic ooliths. Many of the ooliths contain layers and inclusions of disoriented phosphatized organic matter-rich micrite. The majority of ooliths range in size from 0.2 - 0.6 mm and are characteristically spherical although their shape ultimately depends upon the shape of the grain around which the oolith has nucleated (Figs. 3.14, 3.19A,B). In basal lags occasional larger grains ( $\geqslant$ 2 mm) displaying the same characteristics as ooliths are also present. These are more properly termed 'pisoliths' (Teichert, 1970). Similarly, larger intraclasts may be enclosed by thick phosphate skin complexes giving them an oncolite-like (Fig. 2.23) morphology. The nature of the nuclei varys considerably but fragments of echinoderm, faecal pellets and phosphatized intraclasts are all common. Rare empty ooliths may have originally had organic or aragonitic nuclei that have been subsequently destroyed. Although ooliths occur as accessory grains in most phosphatic chalk successions they only rarely occur in sufficient numbers to form a true oolitic phosphorite (e.g. cemented on top of the basal hardground at Hallencourt quarry).

The literature on the origin of ooliths is one of the oldest and largest in carbonate petrology (see Milliman, 1974; Bathurst, 1975 for reviews). It is generally agreed that ooliths require a high-energy environment to provide the agitation necessary for the addition of evenly-coated lamellae and to prevent individual ooliths becoming cemented together. Pellets, on the other hand, are characteristically deposited in low-energy environments so their close association with ooliths in phosphatic chalks requires either alternating current conditions or lateral derivation of different sediment types. The origin of ooliths remains unresolved although biological processes seem to be important. Like coprolites and micritized pellets, ooliths are closely linked with organic processes. Modern ooliths are invariably infested by a diverse assemblage of algae, fungi and bacteria and the laminae are commonly coated with mucilagenous sheaths. The effects this biota has on precipitation/replacement processes is uncertain but the compositional similarity to other non-skeletal carbonate and phosphate grains and skins cannot be overlooked. The

similarities suggest a common origin with petrographic differences depending on environmental controls. As with faecal pellets, the absence of unreplaced carbonate ooliths indicates that in phosphatic chalks, phosphate was the primary mineralization and does not necessarily require a carbonate precursor. This suggests an additional overall environmental control on phosphatization that cannot be accounted for by microenvironmental processes. This is discussed later (Chapter 7).

### 3.4.3d Foraminiferans

Both planktonic and benthonic foraminiferans are subject to varying degrees of mineralization although the latter are more susceptible to replacement than the former. Some foraminiferan tests are empty (commonly calcite-spar lined and more rarely spar-filled), phosphate veneered and have unreplaced walls (Fig. 3.20). Unaltered tests commonly form nuclei to phosphatic ooliths. Phosphatization of tests is rare and restricted to those having an intensely-mineralized sediment infill. This sediment is usually a micrite similar to that enclosing the test (Fig. 3.20). It commonly contains a high proportion of dark, organic inclusions and may be clearly differentiated by its strong, but generally incomplete phosphatization (with or without glauconitization). Even where the enclosed sediment is heavily mineralized, the test walls are generally only partly replaced, having unmineralized but phosphate-coated exteriors and weakly-phosphatized interior walls. Clearly phosphatization is a microenvironmental process that only occurs in sediment-filled tests, the coarsely-crystalline structure of which makes them highly resistant to replacement. The high proportion of foraminiferans in most phosphatic chalks may be partly due to the protection from dissolution afforded by their phosphate veneers. Preferential dissolution of foraminiferans is believed to be an important process in white chalks (D. Curry in Hancock, 1975a).

### 3.4.3e Inoceramid prisms

Isolated inoceramid prisms are an important constituent of all phosphatic chalks and fragments of inoceramid shell are common in most basal lags. Both

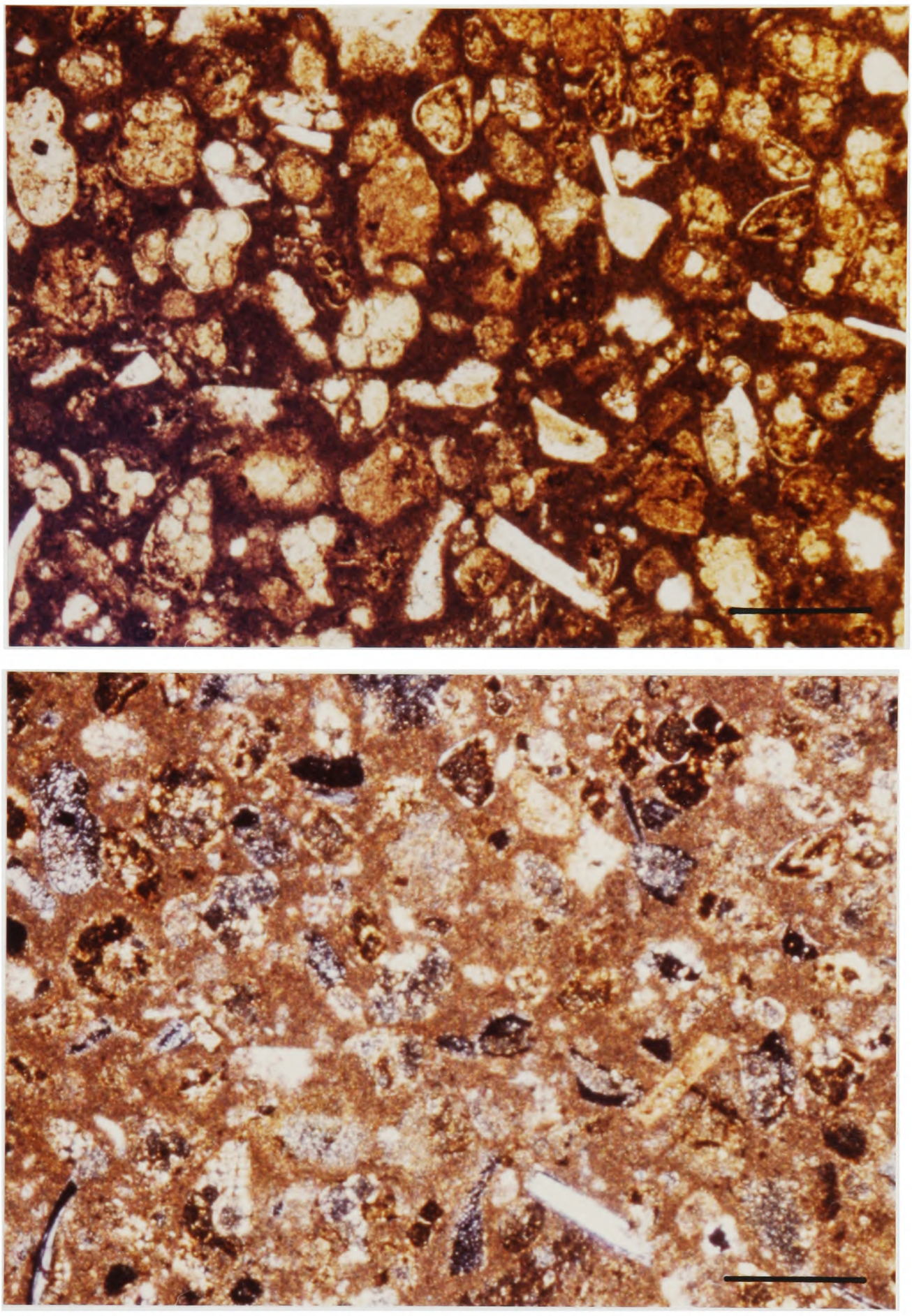

Fig. 3.20 Phosphatic chalk microfacies VII: Foraminiferal phosphorite.
Empty tests have colourless fills under plain polarised light (top) but may exhibit an anomalous mottled first-order grey birefringence under crossed nicols (bottom) due to strain patterns in the araldite mounting medium. Many tests are filled with phosphatized micrite but nevertheless rarely exhibit replacement of the shell walls. Strongly-mineralized fills are pseudo-isotropic under crossed polars. Incompletely-phosphatized intraclasts (blue-green under crossed nicols) are also common. Phosphatic chalk (bed 01/2) from 'Les Champs d'Argent' quarry, Orville. Scale bars = 0.5 mm.

are usually coated by shiny phosphate. Larger fragments of shell generally only show superficial mineralization and the phosphate patina may rest on unphosphatized calcite. Phosphatization concentrates along prism boundaries and the margins of the fragment and is visible as a yellow-brown discolouration of the calcite but is much less prominent than the wholesale silicification that the fragments also usually exhibit (3.8.1a; Fig. 3.7). Isolated prisms are generally better mineralized than more articulated material but the degree of phosphatization is difficult to assess. Certainly in thin section these prisms are discoloured and contain dark organic inclusions which may be related to microboring. The macrostructure of the grains, however, remains unaltered and the prisms maintain a single optical orientation and largely display a calcitic birefringence. Further work is required to determine the nature of the replacement.

### 3.4.3f Echinoderm debris

Most echinoderm debris in phosphatic chalks is either unmineralized, or phosphatization is restricted to sediment infilling the stereome, leaving the skeletal calcite unaffected. Other fragments, however, demonstrate a continuous series of progressive phosphatization and alteration.

The best preservation occurs where the stereome is filled with white chalk and has subsequently remained unaltered. Where the stereome has remained empty the structure may be partly obscured by syntaxial overgrowths of calcite. The initial stages of phosphatization occur in a similar way to the mineralization of the internal moulds of foraminiferans. Phosphatization is essentially restricted to the micritic infill of the stereome, canal systems and microborings, and sediment adhered to the surface of the grains. The skeletal calcite remains unaffected (Fig. 3.19C,D). The next stage involves the replacement of calcite outwards from the sediment infilling. On a larger scale mineralization proceeds from the outside of the grain inwards, indicating an external source of phosphate.

In some fragments the entire skeleton and stereome infilling have been replaced by phosphate and this stage is followed by complete recrystallization

to a uniform light-brown, homogenous crystal of apatite. This crystal maintains the optical continuity of the original calcite, indicating that it is the result of syntaxial processes similar to those which occur on echinoderm calcite in white chalk.

3.4.3g Bone fragments

This category includes all material with a skeletal microstructure, including teleost bones and scales, elasmobranch teeth, skeletal elements of marine reptiles (particularly Mosasaurs) and other vertebrate remains. It is colourless to light-brown in thin section and is distinguished by very low first-order grey to white birefringence and wavy extinction under crossed nicols (Fig. 3.19E,F).

The majority of fragments are elongate grains up to 3 mm in length exhibiting a vesicular microstructure produced by the complex of Haversian canals and finer tubular passages or vascular canals (Bloom and Fawcett, 1968 p.224 - 227) that occur in all bone. Other fragments have a denser compact microstructure; these are pieces of the massive wall that surrounds the vesicular interior of the complete bone. Flat, plate-like grains composed of fine laminae are teleost fish scales. Teeth also exhibit a combination of vesicular and massive microstructure (Peyer, 1968). In most cases the finer, vascular canals are obscured by a phosphate infilling; in more intensely-altered examples the entire fragment has recrystallized to a homogenous crystalline phosphate. Larger vesicles and the main central canals of teleost bones may be filled by phosphatized micrite or remain open. Grains are commonly coated with phosphate veneers. In some examples a dense system of microboring occurs just below the phosphate patina and produces an opaque micritized fabric similar to that seen in some pellets. This micritization is most pronounced in bone fragments from basal lags and other hardground-associated phosphorites. The micritized layer is invariably strongly phosphatized.

The degree of phosphatization exhibited by a grain partly depends on its primary microstructure. The purest phosphate (other than that of the phosphate veneers) is tooth dentine which originally has a highly crystalline prismatic

structure (Peyer, 1968 p.204). The infill of the canal systems is also highly phosphatized but contains impurities (organic matter, carbonate, clay minerals) that are not present in the dentine. Least mineralized is the vesicular bone. These distinctions are clearly displayed by elasmobranch teeth. Here, the soft friable roots have a vesicular structure and are commonly destroyed by reworking while the denser, massive exterior of the crowns remain highly resistant to degredation. In addition to the differences in mineralization styles afforded by the primary microstructure, the majority of grains also show preferential mineralization of the external surface inwards. Phosphate-veneered grains are generally better phosphatized than unveneered examples.

Bone fragments are essentially the only component in phosphatic chalks that has a primary phosphate mineralogy. The initial structure, however, is a hydroxyapatite (Newman and Newman, 1953; Glimcher and Krane, 1968; McConnell, 1973) and the transition to carbonate-fluorapatite must occur during diagenesis, probably by a combination of dissolution-reprecipitation (dissolution structures are visible under SEM; Tabatabai", 1977) and micritization-phosphatization processes associated with algae, fungi and bacteria.

Bone displays contrasting diagenetic histories in phosphatic chalks and white chalks. In the former it becomes phosphatized, canal systems are filled with organic-rich phosphatized micrite and the exterior is enveloped by phosphate veneers. Finally, the entire fragment is recrystallized to homogenous carbonate-fluorapatite. In white chalks, however, fragments are subject to dissolution and enlargement of the canals which may become filled with calcite spar. Clearly the major source of phosphate must be the surrounding sediment or pore-water and cannot be entirely derived from the decay of enclosed organic matter.

### 3.4.3h Other skeletal grains

Important biogenic material not already dealt with include bivalve (other than inoceramid) and brachiopod shell, coral debris, belemnite guards, worm tubes, cirriped plates, bryozoans, ostracodes and sponge spicules. In addition the phosphatization of coccoliths has also been briefly examined.

Although inoceramid debris is the dominant bivalve-derived element in phosphatic chalks, other bivalves (Spondylus, Lopha, Pycnodonte, Gryphaeostrea) provide calcitic material; phosphatized internal moulds of small aragonitic bivalves (and gastropods) are important in basal lags. Prismatic calcite is altered in the same way as in inoceramids but foliated and cross-lamellar structures are highly resistant to mineralization and most oyster shell is unaltered - even in basal lags, where it is coated with a phosphate veneer. Brachiopod calcite is also resistant to early diagenesis. No examples of phosphatized brachiopod shell have been observed although punctae may contain phosphatized sediment and the entire shell may be coated by a phosphate skin. Silicification of bivalve and brachiopod shell is common, particularly in basal lags.

Coral fragments exhibit a number of preservations including calcitization, phosphatization and silicification. Diblasus arborescens is the main coral preserved in these ways although calcitized Synhelia has also been recovered. Most of the recognizable coral in phosphatic chalks consists of phosphatized internal moulds of individual corallites, although fragments and complete calcitized and/or silicified epitheca also occur. The Beauval Coral Bed (Fig. 2.17) exhibits all these preservations. Phosphatized coral aragonite has not been observed. Contrary to the opinion of Tabatabai" (1977 p.212), belemnite guards are generally unaltered (Chapter 5) although specimens recovered from basal lags may bear phosphate skins and exhibit superficial phosphatization of the calcite. This may be infilling or replacing an infill of the original void space within the guard (Veizer, 1974).

Calcareous worm tubes may be composed of calcite, aragonite or a combination of the two minerals. Consequently they show a variety of preservations from apparently unaltered calcitic serpulids to composite moulds of some aragonitic genera. Some serpulid tubes also exhibit silicification. The organic tubes of 'Terebella' phosphatica are invariably preserved as strongly-phosphatized micritic replacements of the organic cement surrounding equally mineralized faecal pellets, intraclasts etc. (Fig. 3.5C,D). Bryozoans also have a variety of primary mineralogies but in general cheilostome bryozoans

are preserved as phosphatized internal moulds and cyclostomes as phosphatized or unmineralized skeletal carbonate. This reflects their primary mineralogy - aragonite and calcite respectively. Unmineralized cyclostomes are commonly found encrusting skeletal debris. Cirriped plates are commonest in basal lags where they are phosphate-veneered and superficially phosphatized. Ostracodes are rarely veneered and generally unmineralized.

Silicisponges are preserved as moulds of the original spicule material. The best preservation occurs at horizons that have undergone synsedimentary lithification and the delicate morphology is preserved in indurated chalk. Sponges are also common in basal lags where they occur as phosphatized micrite infills of the spicule mesh. Typically the siliceous lattice has been dissolved, the resulting void having been filled by calcite spar. Small, compact sponges such as ventriculitids are commoner and better preserved than those with more open networks, presumably because they acted as better sediment traps and were therefore more susceptible to 'steinkern' preservation. Many sponges exhibit pre-burial breakage but the detail preserved in phosphatized steinkerns is indicated by the conservation of the axial canals - as internal moulds of phosphatized micrite or glauconite. Most sponges have become dissociated from their roots, which are preserved separately. The occurrence of spar-filled spicule moulds in poorly-indurated chalks demonstrates that silica dissolution was a late-diagenetic process. Some calcisponges are apparently preserved in a similar manner to silicisponges but those with larger, more resistant spicules may remain as primary calcite and these form the dominant component of the spiculite microfacies (3.5). Calcareous spicules are essentially unmineralized.

Nannopetrographical studies utilising SEM and microanalytical techniques (Tabatabai", 1977 p.213) indicate that in general phosphatization of micrite is restricted to the precipitation or replacement of cement and does not initially effect the enclosed nannofossils. It is only at advanced stages of recrystallization that coccoliths are replaced by phosphate.

### 3.4.4 Early diagenesis and depositional environment

The nature and degree of mineralization shown by skeletal grains depends

partly on their primary mineralogy and ultrastructure, but the diagenetic environment is equally important in their final composition. Invariably it has been shown (3.4.3) that phosphatization is in part a microenvironmental process, aided by the decay of organic matter. However, it is only when there is an ample external supply of orthophosphate that a grain may become strongly mineralized (see below).

Once the basal hardgrounds had formed they provided a special environment within the Chalk sea. The number of potential ecological niches was considerably increased by the formation of mixed hard and soft substrates. Thus the hard surfaces were colonised by a community that included corals, tube-worms and oysters, and an infaunal community, including bivalves and echinoderms, inhabited the mobile calcarenite that locally covered the hardground. This fauna, its associated flora, and the pelagic biota, concentrated phosphorus from seawater and, on death, produced an organic-rich substrate. Decomposition of organic matter released $PO_4$ into the surrounding pore-water and overlying bottom water, thereby providing a local concentration of dissolved phosphorus. There followed the selective mineralization of material of an initially high phosphate content, such as bone fragments, faecal pellets and bioclasts, and of lithified carbonate, including the hardground surface and its associated intraclasts.

The occurrence of phosphatized faecal pellets and ooliths in the absence of unmineralized examples, suggests that the phosphatization process was intrinsic to their preservation. Under normal marine conditions faecal pellets are destroyed rapidly (3.4.3b), their conservation therefore indicates that mineralization was relatively fast. Furthermore, if the pellets did not have carbonate cemented precursors, they must have resulted from a combination of replacement of the enclosed micrite and cementation by phosphate, probably by syntaxial overgrowth on existing grains. Since calcite may act as a surface for the nucleation of apatite (Stumm amd Morgan, 1970), cementation may pre-, postdate, or be concurrent with replacive phosphatization.

The preferential phosphatization of lithified carbonate has been discussed by Kennedy and Garrison (1975b) who suggest that if the hardground cement was

high-Mg calcite or aragonite, it would dissolve more easily and therefore be more liable to mineralization than the surrounding and enclosed low-Mg calcite. In skeletal grains, however, the metastable carbonates show no greater susceptibility to phosphatization than calcite and it is suggested that the primary cement may equally have been low-Mg calcite (see Chapter 4 for discussion). The presence of superficially phosphatized, originally aragonitic shells of gastropods and bivalves demonstrates that phosphatization preceded aragonite dissolution, a seafloor or early post-burial phenomenon (Jefferies, 1962; Bromley, 1965; Kennedy and Garrison, 1975b). Aragonite replacement, therefore, provides evidence of the early diagenetic nature of the phosphatization process. Records of the phosphatized soft parts of gastropods (Casey, 1960) and ostracodes (Bate, 1972) support this conclusion. If it is accepted that phosphate skins are a product of the phosphatization of algal mucilage and other organic matter (3.3.3c) then such a flourishing algal growth would act as a major concentrator of phosphorus on the seafloor (Charles, 1953). Decay of such a coating might induce the precipitation of phosphate within the microenvironment formed by the mat or, alternatively, result in the phosphatization of the organic material itself, or the enclosed and underlying micrite.

Interpretation of the trends observed within phosphatic chalks (Fig. 3.11) is not as clear cut as it might be for a clastic sediment. It would appear that a progressively waning current regime is the logical mechanism to produce this type of sequence. However, other factors must also be considered. Faecal pellets are an important factor in the observed sediment coarsening near the hardground surface. The majority of pellets are of the simple ovoid variety (3.4.3b), Willcox's (1953a) type D. Willcox (op cit.) suggests that this type of faecal pellet could be attributed to either detritus or the boring worms that penetrate the hardground surface. If the latter is the case, the pellets are primarily the result of a hardground-tied fauna and such pellets would have to be derived laterally after occlusion of a significant area of hardground surface by phosphatic chalk. Much of the intraclastic debris which rests on top of the hardground is eroded hardground sediment; its abundance markedly increases the grain size of the sediment, yet its origin was probably primarily due to bio-

erosion and does not necessarily reflect any hydrodynamic effects.

If the processes of early diagenetic phosphatization was solely related to the prolific biota that developed on the hardground, than as the hardground became mantled in sediment, fewer and fewer pellets would be produced and therefore preserved, but in addition the amount of organic matter being supplied to the sediment would be greatly reduced. All of the above factors; energy levels, the supply of material suitable for phosphatization and the concentration of dissolved phosphate, are all closely related and interdependant. Undoubtedly all three contributed to the final composition of the lithofacies.

It is suggested that phosphatization was directly linked to the proliferation of organic debris which must have accompanied the formation of these sediments. Cornet (1905) has shown that the brown colouration of the Ciply phosphatic chalk (Maastrichtian, Belgium) a deposit sedimentologically nearly identical to, but younger than, the phosphorites considered here, is a weathering phenomenon. Examination of phosphatic chalks from boreholes and in deep quarry sections, demonstrates (Cornet, 1905) that the brown colour is due to the oxidised state of the enclosed iron minerals, and that fresh, unoxidised rock collected from below the water-table is blue-grey in colour and contains abundant disseminated pyrite. This occurrence of pyrite, reduced iron and the ubiquitous occurrence of organic matter in all phosphate grains are clear indications of anaerobic conditions within phosphatic chalk sediments. Tabatabai" (1977) records up to 0.3% organic carbon in Anglo-Paris Basin phosphatic chalk, although values of 4.5% were obtained from the acid-insoluble fractions of the same rocks. Tabatabai" (1977) considers that the clay minerals associated with this organic matter aid in its preservation. It is proposed that the organic content of the clay fraction may be applicable to the whole rock in its unoxidised form, and that subsurface weathering of phosphorite above the water-table has subsequently reduced the organic-carbon content.

In modern environments, decaying organic matter may raise the pH within the sediment (Berner, 1969) because of the formation of $NH_4$ and other nitrogenous bases. This environment of high pH and high alkalinity is required for

phosphate replacement and precipitation (Senin, 1970; Cook, 1976) at the present day. Evidence from Recent sediments further suggests that phosphatization occurs in diatomaceous muds a few centimetres below the sediment/water interface. It is suggested that a similar subsurface environment might also provide suitable geochemical conditions in the carbonate muds of the phosphatic chalk lithofacies, and explains the occurrence of poorly-indurated and unexposed phosphatized clasts in many pseudoconglomerates.

The rich fauna which is associated with the basal hardgrounds clearly indicates that the bottom water and sediment were oxygenating for most of the period of hardground formation, but above this, macrofauna is rare except for pelagic elements such as belemnites. Benthonic foraminiferans, an important component in all phosphatic chalks, flourish in, and adjacent to, the oxygen minimum layer (the layer in the oceans' vertical profile in which dissolved oxygen is at its minimum) off the Peru coast at the present day (Frankenberg and Menzies, 1968; Bandy and Rodolfo, 1964), indicating that they are facultative anaerobes; similarly some species of worm can also tolerate intermittent anoxia. The occurrence of less versatile fauna, including octocorals and echinoderms, and the presence of a varied infauna (as evidenced by the trace-fossil assemblage), however, demonstrate that the seafloor and probably surface sediment were aerobic for much of the time. These two trends are not necessarily mutually exclusive, for it is possible to envisage a seafloor where aerobic and anaerobic conditions alternate beneath the sediment surface but where previous anaerobic phases are destroyed by the bioturbation of the next aerobic phase. The occasional preservation of laminated bedding supports this conclusion. Another possibility is that anaerobia was largely restricted to the microenvironments provided by faecal pellets, beneath algal and other organic coatings and within shells, sites known to be favourable for mineralization.

Evidence of intermittent anoxia is accompanied by similar support for discontinuous rather than persistent current activity. The sediment consists of two distinct grain sizes - phosphate sand and carbonate mud, which have very different hydrodynamic properties. In addition the current conditions indicated by the different phosphate components are highly varied. Ooliths

and possibly intraclasts indicate a high-energy environment undergoing continual agitation; grapestones suggest pauses in current activity and pelletal substrates indicate low current regimes. The occurrence of angular soft white chalk intraclasts at some levels suggest that more prolonged phases of white chalk sedimentation also occurred. The degree to which the final composition of the sediment is the result of lateral derivation is impossible to determine without considerably more lateral control than is currently available. Certainly the geometry of phosphatic chalk cuvettes (3.6.1) favours at least limited downslope movement and mixing of sediment types. However, the juxtaposition of phosphate sand and carbonate mud, and the general rarity of clean-washed sands (see below) both indicate that intermittent winnowing was an important mechanism in determining the final composition of the sediment.

The abundance of algal and fungal microborings in phosphate grains indicates the inferred shallowing that accompanied hardground formation was maintained throughout the period of phosphorite deposition. The decline of thallophytic structures at the summit of phosphatic chalks and the concurrent return to white chalk deposition may indicate that water depth increased at that time.

## 3.5 Calcarenites

In addition to the three main lithologies (white, hardground and phosphatic chalks) a fourth minor sediment type occurs in association with Chalk phosphorites. This calcarenitic facies is essentially restricted to the early Campanian and is best developed at Lavant and in the upper part of the successions at 'les Champs d'Argent' quarry Orville and Hallencourt quarry. A trend towards calcarenitic sediments was also noted in phosphorites of early Campanian age elsewhere, noteably the Beauval Offaster Bed and the poor phosphatic chalks of Downend quarry (Gale, 1980 p.148). In all cases the lithologies are bioclastic carbonate sands and gravels with accessory pelletal phosphate. They may be grain or mud supported.

These calcarenites are characterised by a profusion of two elements - calcisponge spicules and echinoderm debris. Micrite supported gravels (Fig. 3.21)

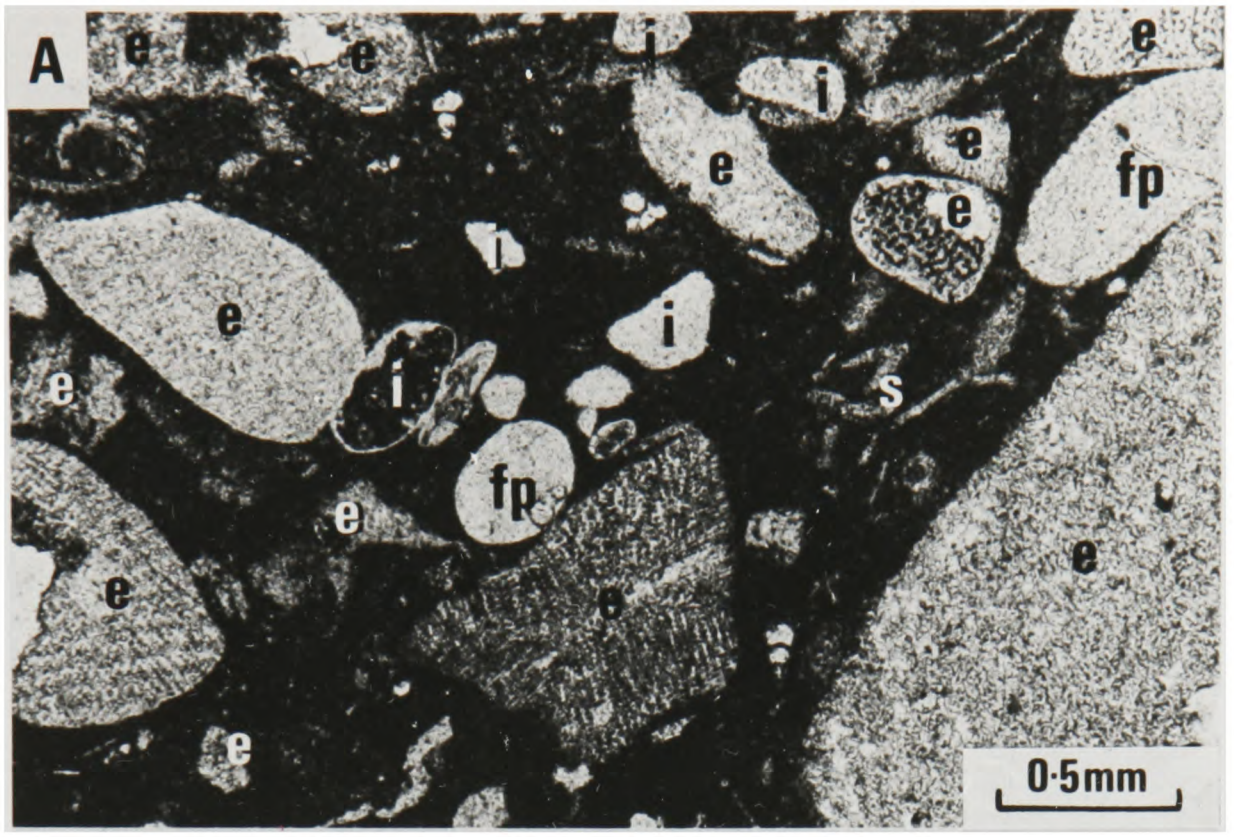


Fig. 3.21 **Phosphatic chalk microfacies VIII: Phosphatic echinodermite.**
Phosphatic **echinoderm gravels** occur within the phosphatic chalk succession at Hallencourt quarry. The coarse-grained component is dominated by fragments of echinoderm (e) - asteroid, echinoid and crinoid, but also includes phosphatized faecal pellets (fp) and intraclasts (i), scattered calcisponge spicules (s) and other bioclasts. The phosphatization exhibited by all intraclasts and faecal pellets contrasts with the infrequency of mineralized echinoderm fragments (where present, phosphatization is essentially restricted to the stereome infilling). (A) PPL, (B) XN.

occur in the absence of calcisponge material at Hallencourt quarry but elsewhere calcisponges are the dominant source (Fig. 3.22) of sediment and echinoderm debris, although abundant and abnormally diverse, is subordinate. The richest spiculites originate from the field rubble at Lavant (2.11.4) where

Fig. 3.22 Spiculites
A. General view of a weakly-indurated coarse-grained calcisponge spiculite from Lavant. Scattered phosphatized intraclasts (i) and ooliths (o), and unmineralized echinoid shell fragments (s) occur as minor accessories.
B. Negative print from a thin section of the Orville Offaster Bed. A typical spiculite microfacies, the bed contains a higher percentage of phosphatic material than the Lavant example.
C. Orville Offaster Bed. Bifurcating paddle-shaped terminations of the spicules are clearly visible. PPL.
D. Biosparite texture of a Lavant spiculite. Dusty organic inclusions preserve the outline of the individual spicules despite extreme syntaxial calcite overgrowths. Note the saw-tooth margin (bottom left). PPL.

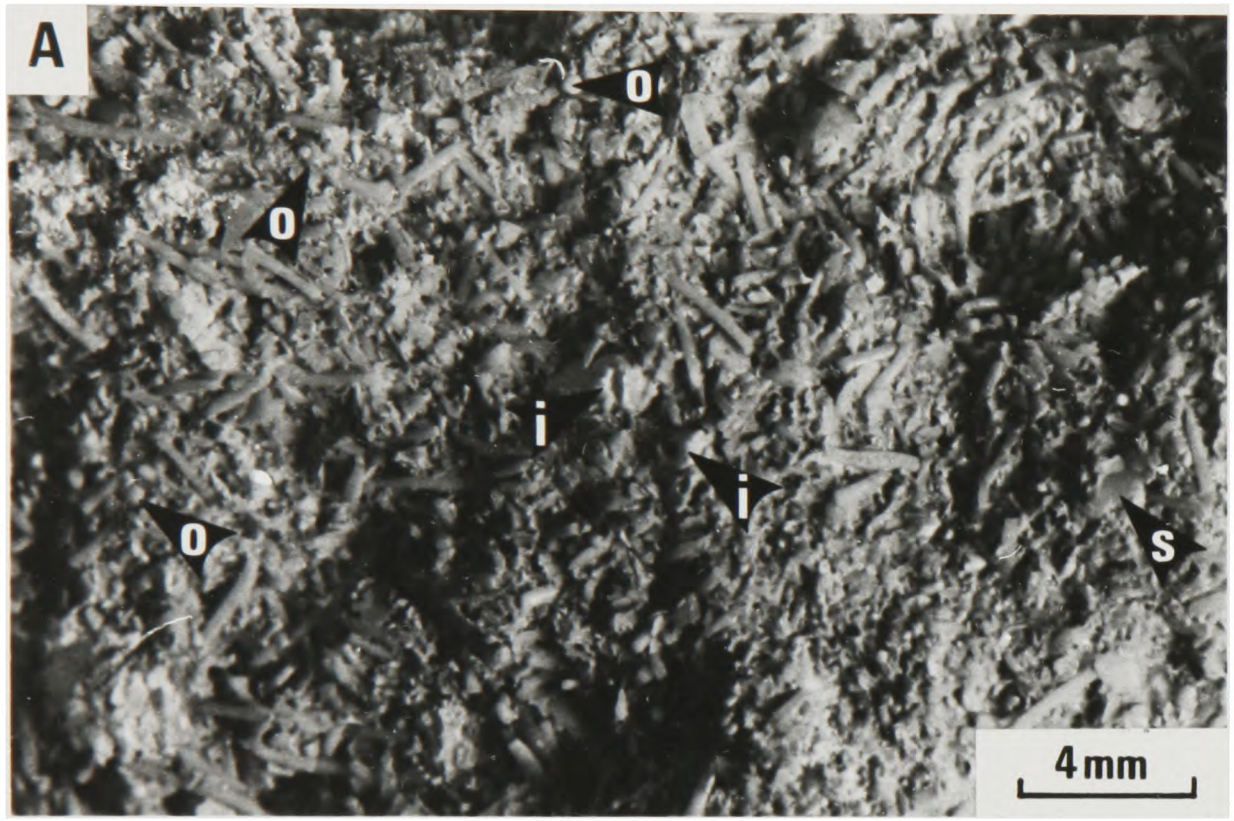
A
o
o
i
i
o
s
4mm

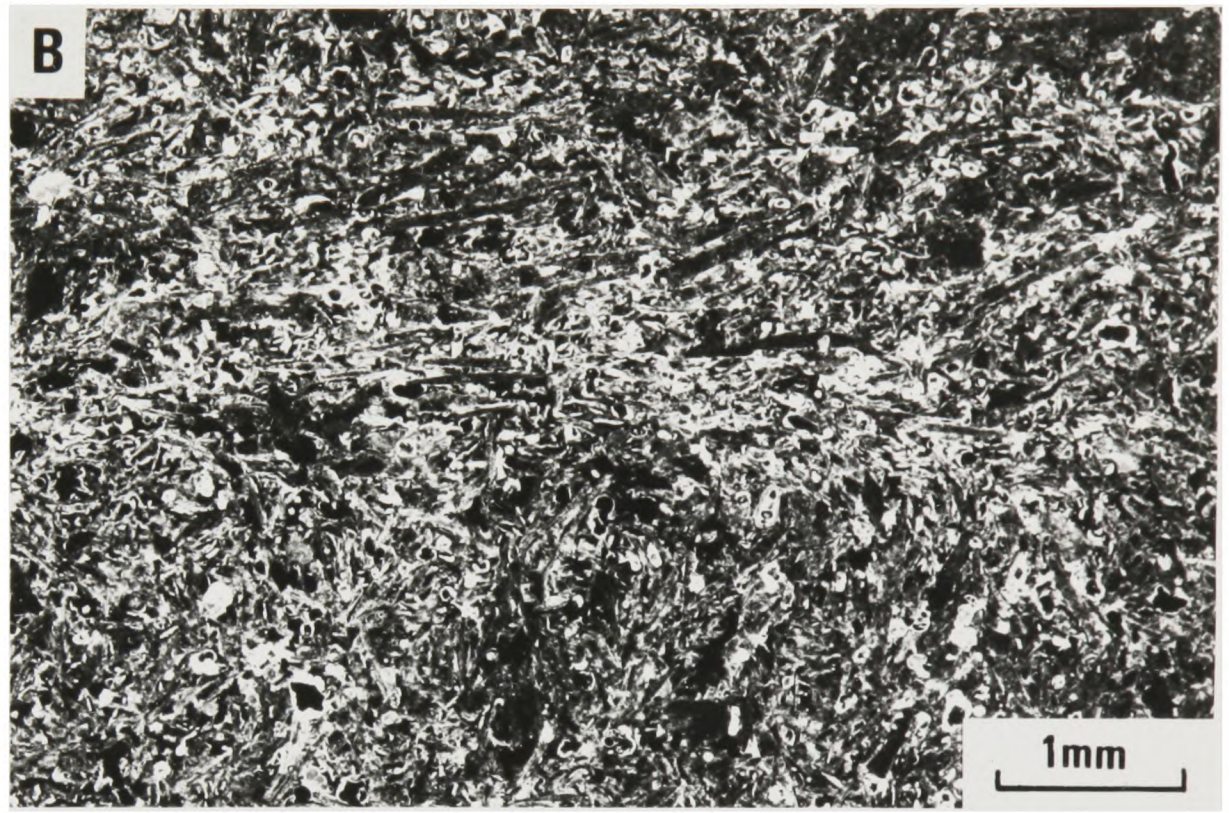
B
1mm


C
0·5mm

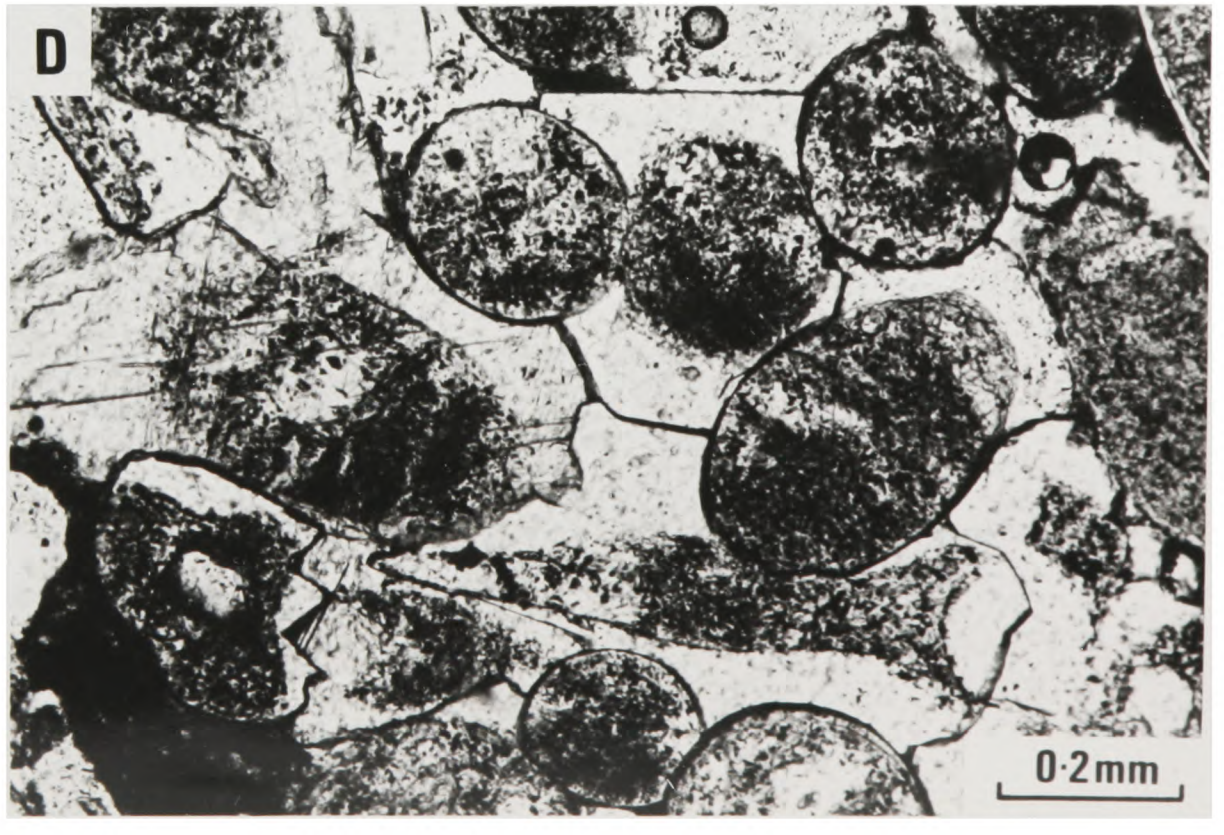
D
0·2mm

unhappily the lateral relationships of the facies cannot be ascertained. The spicules are smooth rod-like megascleres composed of single biocrystals of impure low-Mg calcite, although the original mineralogy was probably high-Mg calcite (Jones and Jenkins, 1970). Axial canals have not been differentiated, each spicule being composed of a homogenous organic-matter rich calcite. Coarse grain-supported spiculites consist almost entirely of giant monact (uniradiate) sclerites syntaxially cemented by calcite (Fig. 3.23A,B). As the percentage of micrite increases (indicating a decrease in current activity) and the sediment becomes matrix-supported, other smaller, more complex spicules (Figs. 3.23C,D, 3.24) become commoner - the diact (biradiate), triact (triradiate) and tetract (quadraradiate) varieties (Jones, 1970). The introduction of a carbonate mud prevents syntaxial overgrowth of the sclerites during weathering and results in less indurated sediments. The more ornate spicules are probably from the same group(s) of sponges as the larger monacts, their appearance merely reflecting the reduction in current activity indicated by the introduction of fine-grained carbonate. Although rarely spicules may be coated with phosphate veneers and form the cores to ooliths (Fig. 3.25), not even superficial mineralization was observed, presumably because of the large crystal size, low porosity and relative stability of the calcite.

Most modern calcisponges live in water depths of <100 m and are particularly abundant on hard bottoms with swift currents (Hartman and Goreau, 1970). Additional fauna associated with the spicules includes elements that only occur in white chalks as extreme rareities (e.g. Synhelia) and others that are restricted to the calcarenites (e.g. a spinose species of the asteroid Metopaster and an undescribed arthrasterid starfish). Offaster, Stereocidaris and Echinocorys are also common and occur with pycnodonteine oysters, elasmobranch teeth, Porosphaera, serpulids and bone fragments. The echinodermite facies at Hallencourt quarry similarly contains an abnormal benthonic fauna including comatulid crinoids that are unrecorded elsewhere from the Cretaceous (A.S. Gale pers. comm.). Clearly the abnormal environment led to the development of highly specialised faunas adapted to current-swept substrates. Thus the palaeoecological data agree with the sedimentology in indicating a shallow, high-

Fig. 3.23 Phosphatic chalk microfacies IX: Phosphatic spiculites. A,B. A biosparite from Lavant, composed almost entirely of giant monact calcisponge spicules. The sclerites consist of single biocrystals of impure calcite and are syntaxially overgrown by calcite spar. The addition of spar is a weathering phenomenon commonly exhibited by calcarenites. The packestone texture passes laterally (or vertically?) into similar wackestones (see below) that do not contain any significant proportion of spar. A phosphate veneered echinoderm fragment is visible at the right of the photograph. (A) PPL, (B) XN.
C,D. Spiculite-biomicrite from Lavant. Although finer grained, calcisponge spicules are again the dominant component. Note the diact and triact morphology of many of the spicules. Phosphatic grains are commonly only an accessory in the microfacies. (C) PPL, (D) XN.


A
0·5mm


B
0·5mm

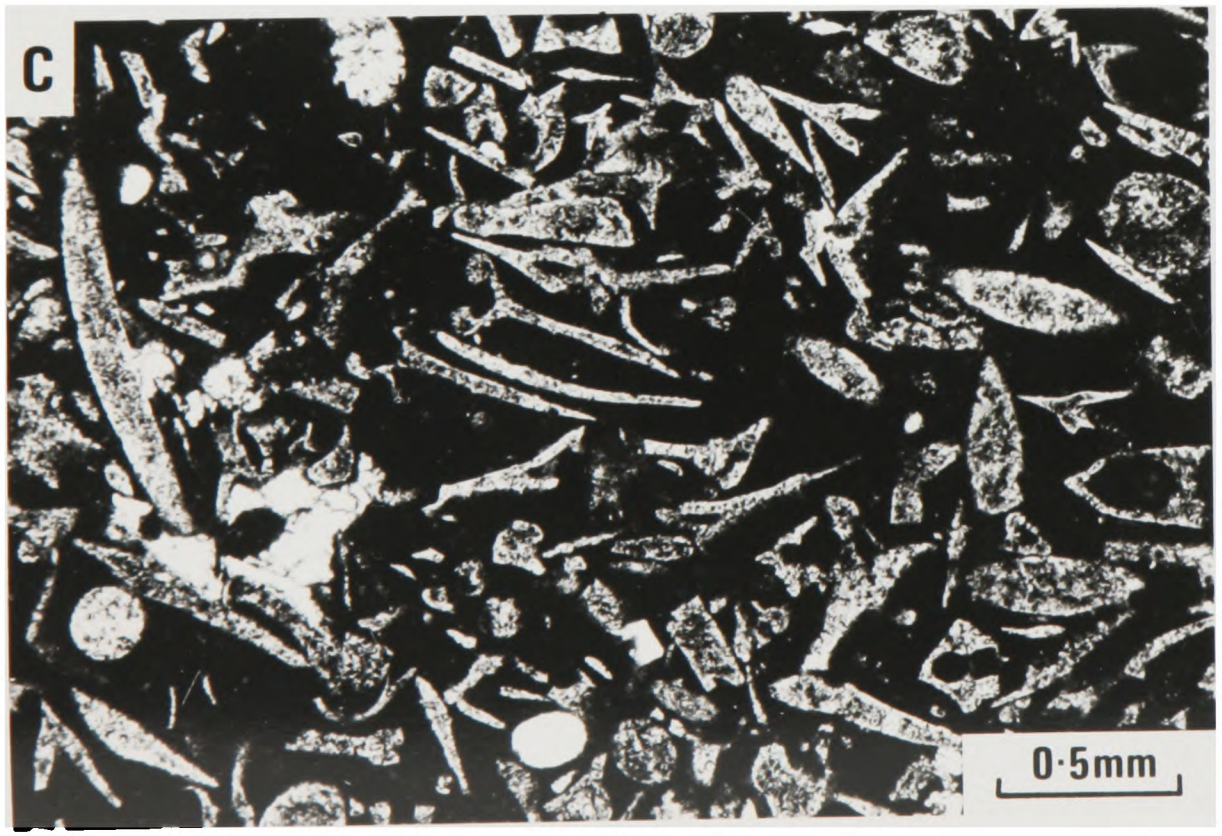
C
0·5mm


D
0·5mm

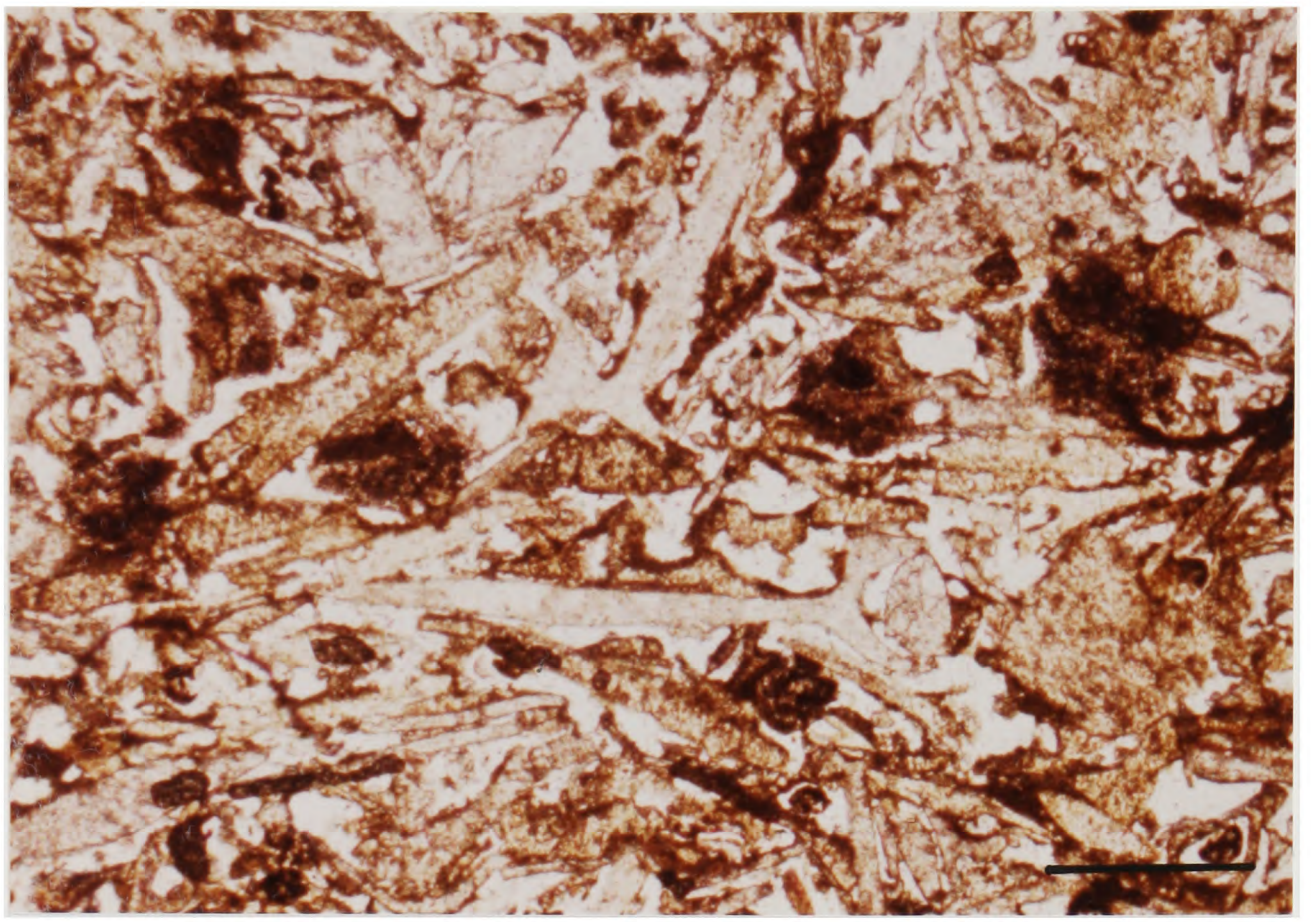

Fig. 3.24 Calcisponge spicules
Monact and triact calcisponge spicules in a micritic matrix. Spicules are colourless in plain polarised light (top) but contain dark dusty inclusions of organic matter. The single crystal composition is illustrated by the optical continuity of the sclerites under crossed polars (bottom). Orville Offaster Bed. Scale bars = 0.5 mm.

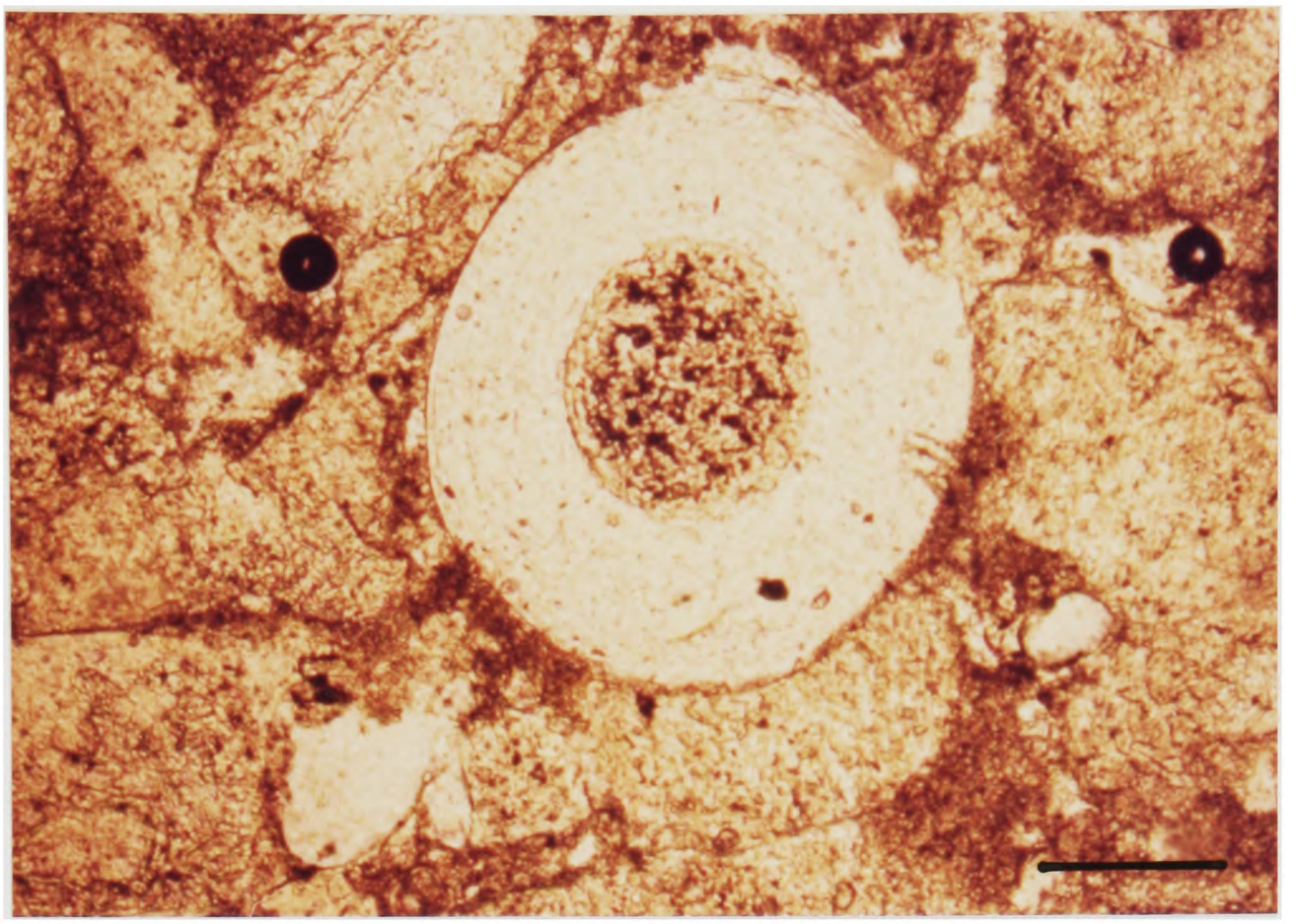

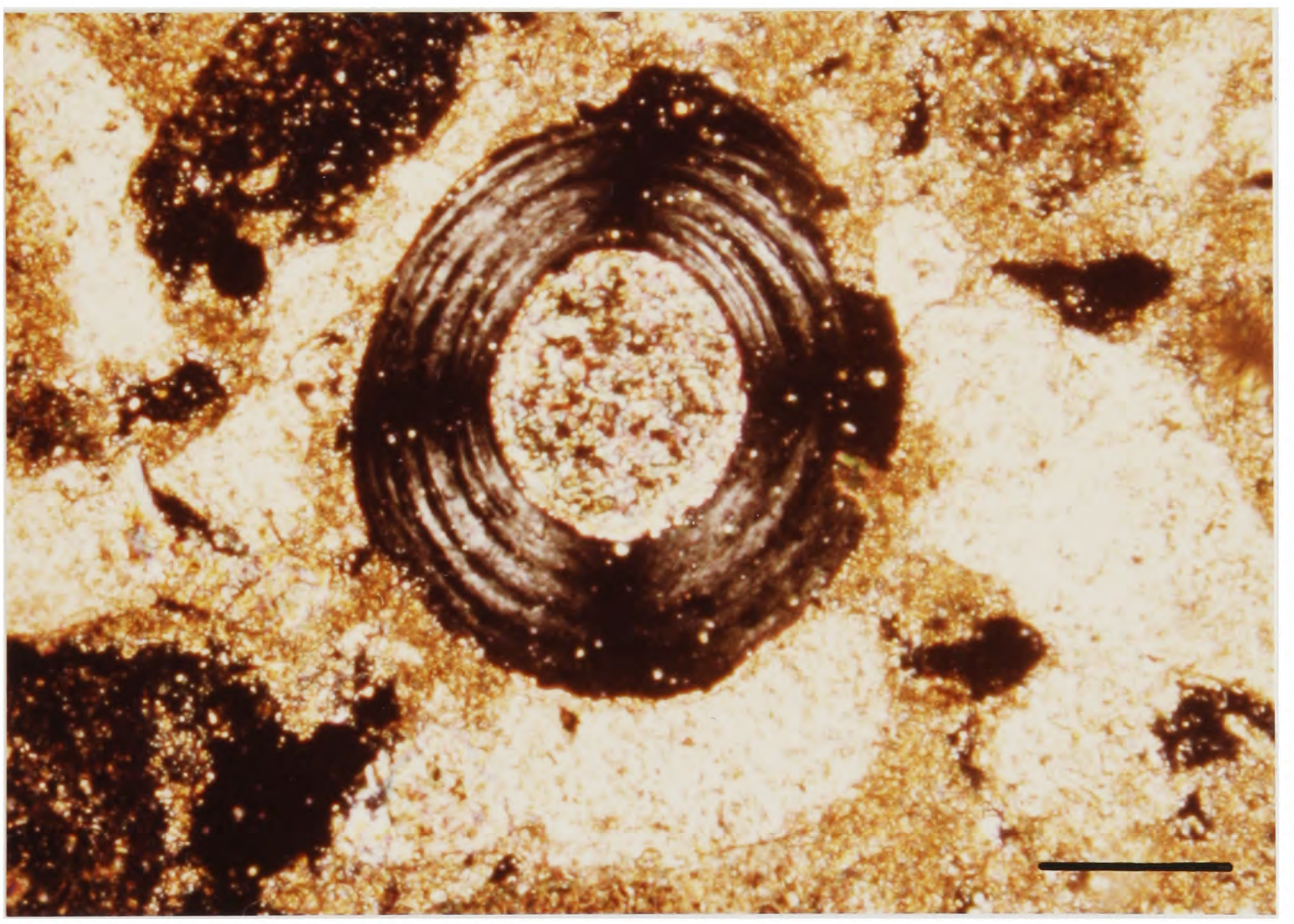

Fig. 3.25 Phosphatic oolith with a calcisponge spicule core. The calcite of the enclosed spicule is entirely unaffected by its veneer of pure phosphate. Organic inclusions within the calcite are clearly visible in plain polarised light (top). The pseudo-uniaxial interference figure of the phosphate veneers is well-displayed under crossed nicols (bottom). Note the finely laminated appearance of the phosphate. Spicule calcarenite from Lavant. Scale bars = 0.1 mm.

energy environment associated with hardgrounds.

Calcarenites developed towards the end of the period of phosphatic chalk deposition. Their low pelletal phosphate content indicates that high current-activity, shallowing and an abundant benthos are not the only requirements for phosphorite deposition and suggest that other major environmental changes terminated phosphatization (Chapter 7).

## 3.6 Cuvettes

Phosphatic chalks occur in isolated or small groups of troughs (cuvettes) up to 1 km in length, 250 m in width and 30 m deep in the white chalks of the late Coniacian to early Campanian. The original distribution and extent of these cuvettes is uncertain because the majority occur as erosional outliers of late Santonian to early Campanian age (Chapter 2), while much of the outcrop in the southern and central area of the Paris Basin has a thick Tertiary cover. Nevertheless most have a very restricted distribution (Fig. 2.2; Map 1) and were probably never common outside Picardy.

### 3.6.1 Morphology

All cuvettes have an erosional origin and truncate the bedding of the underlying white chalk. The erosional relationship can best be seen at Hallencourt quarry and has been noted elsewhere (Lasne, 1892; de Grossouvre, 1901; Raguin, 1926; Broquet, 1973). The base of all cuvettes is marked by a strongly-developed basal hardground which has formed in a winnow coarsened sediment of late Coniacian to early Santonian (e.g. Beauval quarry, Hallencourt pit) or late Santonian (e.g. Hallencourt quarry) age. Only very limited information is available on the gross morphology of phosphatic chalk cuvettes, and at the present time (1980) exposure is too poor to add anything to the descriptions in the literature. Cuvette cross-sections have been drawn by several authors (Fig. 2.62), but only Broquet (1973) considers the three-dimensional characteristics of a cuvette (2.7.1). To reiterate, the deposits at Hallencourt pit

consist of three cuvettes trending north-south and display the following features:-

(1) The oldest cuvette contains sediment of mid to late Santonian age but rests on chalk of the earliest late Coniacian. The phosphatic chalk is 4 - 4½ m thick and contains 6 - 13% $P_2O_5$.

(2) The unit is truncated by a second smaller cuvette of similar age which contains 3 m of phosphatic chalk with 10 - 19% $P_2O_5$.

(3) The third cuvette, the one now being exploited, lies slightly to the north and has 12 m of phosphatic chalk with 8 - 18% $P_2O_5$. It contains sediment dated as early Campanian and rests on low Santonian at its centre.

These three cuvettes, which vary in age from mid Santonian to early Campanian, all have the same axial trend and are all developed in the same area.

Facies variations have not been studied in detail but Broquet (1973) confirms the data from Fresnoy-le-Grand (2.6.2; Fig. 2.59) indicating that strongly-developed basal hardgrounds are characteristic of the axial regions of cuvettes and grade into weakly-lithified burrowed junctions in a marginal facies. Where small locally-developed cuvettes are seen in cross-section (i.e. at Hallencourt quarry, Templeux-la-Fosse and Templeux-le-Guérard) the phosphorite commonly exhibits a channel-fill structure (3.4.1e) which is rarely seen in larger cuvettes. The relationship between these minor 'channels' and larger cuvettes is unknown.

### 3.6.2 Environment

The positive correlation between regions of maximum erosion and strong hardground development suggests a causative relationship. The regions that have undergone the greatest amount of erosion (i.e. the axial facies) must also have been subject to the strongest current action. They would therefore contain the coarsest sediment and have the most rapid movement of pore-water, both factors which are believed to aid lithification (3.3.4). The model implies that strong current activity pre-dated and accompanied the formation of the

basal hardgrounds. This is supported by the coarseness of hardground chalks and the erosion of appreciable thicknesses of white chalk prior to hardground formation. The coarse nature of the overlying sediment indicates that current activity continued during the subsequent stages of phosphorite deposition. This is confirmed by the establishment of current requiring faunas of sabellariid worms and scleractinian corals, and the deposition of oolitic sediments.

Thus winnowing, mechanical and biological erosion, together with a continuing process of mineralization and degredation, resulted in the concentration of the most phosphatic material on the hardground surface. As the process continued the coarsest and densest sediment (the phosphatized component) was transported into the axial region of the cuvette by downslope movement, thus amassing the richest and coarsest phosphorite in this area. As the cuvette evolved, production of material suitable for phosphatization was able to continue both in the newly formed phosphorite and on the basal hardground of the still uncovered sides. In the deeper parts of the cuvette, the biological communities gradually became limited to calcarenite-associated faunas such as certain asteroids and echinoids, but some other material was derived laterally. Intense bioturbation throughout the entire sequence destroyed almost all original bedding lamination.

### 3.6.3 Genesis

Undoubtedly current action was an important factor in the production of the phosphatic chalk lithofacies. Ocean currents, apart from those related to breaking waves in the surf zone, may be divided (Shepard, 1973; Johnson, 1978) into those produced by:-

(1) Wind stress on the surface of the ocean,

(2) Tidal forces,

(3) Differences of water density.

Wind induced currents are of two types. The first, related to local climatic conditions, reaches depths of only up to 50 m from the water surface. A depth of 50 m is the absolute minimum estimated for phosphatic chalks and it seems

unlikely that, even with depths of 50 m, this type of current would be sufficient to erode such large-scale features just within the limit of its depth range. A second form of wind induced currents are permanent surface currents, maintained by the Earths' prevailing wind systems. These currents, and the underlying bottom current systems which are directly related to them, can move at considerable velocities and be erosive to depths in excess of 1000 m (Heezen and Hollister, 1971). This type of current is therefore a clear candidate for the mechanism of erosive scour that produced phosphatic chalk cuvettes.

Tidal currents have a larger effect on the shallow seafloor than permanent currents, but depend on restriction of flow within straits to achieve their erosional potential. Such currents are unlikely to have been pronounced in the broad, generally unrestricted, epicontinental sea inferred for northwest Europe during Santonian to Campanian times (see Hancock, 1975 fig.2). The possible range of shelf depths involved, however, means that they cannot be entirely discounted.

The most significant form of erosive density currents are turbidity currents, which are well-known contributors to many clastic sequences. Such flows require potential energy for their initiation and it seems unlikely that the necessary slopes would be present on the continental shelf prior to cuvette formation. Furthermore, none of the basal sediments exhibit characteristics one would normally expect of a turbidite.

The Hallencourt pit cuvettes may provide some clue to the type, since currents which produced them must have been operating in the same position for over 4 million years (mid Santonian to early Campanian) and yet maintain the same trend. Of the three current types considered, only a permanent current would be expected to produce such a constant orientation. Newton et al. (1973), in their study of the continental shelf off the Spanish Sahara, report what they consider to be longitudinal erosional 'windows' of over 200 m in width and 1 km in length for the larger forms. These 'windows', which are up to 20 m deep, have their long axes parallel to the isobaths and occur in water depths between 50 and 80 m. The authors consider that these structures were produced by erosion by the Canary current. Clearly, these features might be considered

comparable to phosphatic chalk cuvettes.

Erosion by a permanent current does not explain why phosphatic chalk cuvettes only formed during a relatively short period of geological time - mid Santonian to early Campanian. One possible mechanism for this temporal control involves a eustatic change of sealevel. It has been suggested (e.g. Cooper, 1977) that during a regressive period in basinal areas away from a sediment source, lowering of sealevel may result in submarine erosion of topographic highs and the development of hardgrounds. Such a link between regression and the development of hardgrounds has been proposed by Bromley (1965, 1967a). Indications of marine transgression during the early and mid Santonian come from such widely spaced areas as Ireland, Sweden, Madagascar and Australia (Cooper, 1977). The late Santonian to early Campanian, on the other hand, appears to have been a period of lowering of sealevel (Hancock, 1975; Cooper, 1977; Hancock and Kauffman, 1979) which resulted in widespread disconformity in the North Sea (Ziegler, 1978). The next transgressive episode has been dated in southern Sweden as uppermost Lower Campanian (Christensen, 1975). The phosphatic chalk lithofacies itself provides ample evidence of shallower water environments (3.4.4).

Thus erosion by a permanent ocean current provides the mechanism for cuvette formation, while regression may be necessary for it to achieve significant erosional effects (thereby providing a temporal control), but neither mechanism explains why deposition of phosphatic chalk took place on such a wide scale in the Anglo-Paris Basin (including Belgium; Leriche, 1935) during the mid Santonian to early Campanian. The reasons for the abnormal concentration of phosphate in these sediments are discussed later (Chapter 7).

## 3.7 Synsedimentary folding

White chalks have long been regarded as monotonous, near-horizontally bedded, massive sediments containing few bedding indicators or sedimentological structures. The recognition of hardgrounds (3.3.1) and the importance of flint bands as indicators of bedding (3.8.1b) have fundamentally changed these views

and a range of disorganised bedding, slumping and folding has now been recognised in chalks from northern France (Kennedy and Juignet, 1974; Juignet and Kennedy, 1974; Curry and Smith, 1975) and southern England (Gale, 1980; Jarvis and Woodroof, 1981). Nevertheless such structures are uncommon in the Chalk and any occurrence requires special attention and explanation.

Folding in phosphatic chalks was recognised (Cayeux, 1939 p.247) long before the present resurgence in Chalk research because the contrasting lithologies made the structures easily visible and because of the special problems it introduced to the exploitation of these deposits. However, only the gross morphology of these features was described in the literature and no satisfactory explanation has been forwarded concerning their origin. The purpose of this section is to examine the charcteristics of the folding and to propose a model for its genesis.

The only current exposure of folded phosphorite occurs at Beauval quarry, although dislocated blocks of hardground are visible at Hem-Monacu and Hardivillers quarries. Folds described in the literature are those at Marcheville, Vaux, Hargicourt and Etaves-et-Bocquiaux. Each of these structures is described in detail in Chapter 2 and only those features relevent to their origin will be discussed here. The hardground mélange at Boxford is stratigraphically, geographically and genetically distinct from these folds and its formation is discussed elsewhere (2.11.3; Jarvis and Woodroof, 1981).

### 3.7.1 Morphology

Folding deforms the basal hardground and overlying phosphorite in many phosphatic chalk cuvettes. A pair of folds described from Etaves-et-Bocquiaux (2.6.1; Fig. 2.58) have wavelengths of 50 m and amplitudes of 15 m, a scale that is closely comparable with all other known phosphatic chalk folding, and also that in the Upper Turonian to Santonian chalks of Haute Normandie (Juignet and Kennedy, 1974). Folding exhibits a number of styles including broadly asymmetric forms at Etaves-et-Bocquiaux, recumbent folding at Beauval (2.3.2; Figs. 2.9, 2.21, 2.22) and isoclinal structures with vertical (Société de St Gobains'

quarry Vaux 2.4.3; Fig. 2.43) or horizontal (Mommert's quarry Hargicourt 2.5.4; Fig. 2.57) axes, elsewhere.

In general the folding affects only the basal hardground (and presumably the underlying white chalk) - phosphatic chalk couplet at each locality. Intraformational erosion and truncation of the folds prior to the return of white chalk deposition demonstrates that they are contemporaneous with deposition. Deformation of the basal hardgrounds was accomplished by a combination of plastic and brittle deformation; the latter clearly shows that folding and slumping post-dates early carbonate diagenesis. Much of the deformation must have been accomplished by plastic flow since even in the tight closures of recumbent (Fig. 2.22) and isoclinal folds, the hardground maintains its integrity and displays only superficial fracturing.

Plastic deformation of the hardground occurs on two scales. The larger is accomplished by movement being taken up in the soft sediment filled Thalassinoides system within the hardground. Many basal hardgrounds have their strongly-indurated summit broken up, undermined and isolated by burrowing (3.3.2; Fig. 3.8). This enables the hard sediment to be reoriented within the surrounding soft sediment with only minor fracturing. In the most deformed parts of the fold, however, not all deformation can be explained by this mechanism and smaller-scale flow must have occurred within the indurated unit. In this case a solution-reprecipitation process (probably at grain contacts) must have been responsible since there is no obvious change in texture (e.g. brecciation) with increasing deformation. Examination of the ultrastructure of these highly-deformed chalks may help illuminate these processes.

In contrast to the relatively minor displacements associated with plastic deformation the amount of movement displayed by fractured blocks is commonly considerable. At the summit of the Beauval overfold, sheets of hardground top have been dislocated by low-angle shearing and stacked one on top of the other (Fig. 2.20). In this area the strongly-lithified surface of the basal hardground has been completely dissociated from its less indurated lower levels. The imbricate structure is associated with smaller blocks of hardground that have mineralized sides and bottoms, rounded pebbles with oncolite-like coatings

(Fig. 2.23) and an abnormally coarse basal lag containing large Lopha semiplana and Actinocamax verus. These characteristics suggest that at least some of the dislocated hardground was exposed on the seafloor and that the mélange was formed before the hardground surface was buried by a significant thickness of sediment. This conclusion is supported by larger dissociated blocks of basal hardground that occur elsewhere in the quarries. One large ( ~3 m) block at Beauval quarry (Fig. 2.24) is entirely surrounded by phosphatic chalk and is capped by a portion of basal lag that has been cemented onto its surface by synsedimentary lithification. Angular fragments of this cemented lag float in the surrounding phosphorite. The block is encrusted by a 'Terebella' phosphatica patch reef that passes up into the unlithified overlying sediment, indicating that it was colonised after its emplacement and that the block was therefore exposed on the seafloor after being dissociated from the main basal hardground. The fact that these allochthonous blocks are completely surrounded by phosphorite means that they must have been rafted into the centre of the cuvettes, probably by mass flow from the nose of the fold where extensional fracturing caused the basal hardground to break up.

Small-scale faults with displacements ranging from a few tens of centimetres to several metres are commonly associated with the folds. Many of these are clearly post-Cretaceous in age but others die out upwards, and are overlain by undisturbed strata. These small-scale brittle fractures are penecontemporaneous with the folding and in some cases provided a seafloor topography that influenced sedimentation (e.g. Hem-Monacu quarry 2.4.1a; Fig. 2.40A).

### 3.7.2 Comparisons and origin

The best documented penecontemporaneously deformed chalks in northern France are those from the Upper Turonian to Santonian Chalk in the Bec de Caux and Pays de Caux, north and northeast of Le Havre. Here sedimentary features including erosional channels floored by hardgrounds, slumped beds, intraformational breccias and winnowed bioclastic gravels have been described (Juignet and Kennedy, 1974; Kennedy and Juignet, 1974). These occur in association with

'carbonate banks' up to 50 m high and 1500 m across, the internal structure of which is picked out by hardgrounds, nodular chalks and flint lines. Individual beds tend to thicken over the summit of the 'banks' and this has led Juignet and Kennedy (op cit.) to interpret the larger mounds as accretionary bioherms, despite the absence of a binding organism (algae or marine grasses are suggested). A more plausible explanation, however, is that the mounds are the result of differential erosion by submarine channels (Gale, 1980). An erosional origin is well illustrated by the Banc à Cuves north of Etretat (Juignet and Kennedy, 1974 fig.5a) where a hardground cross-cuts horizontally bedded chalks at an angle of 20° and cuts out some 50 m of sediment. If an erosional origin is accepted for these structure, then they resemble phosphatic chalk folds and cuvettes genetically as well as morphologically.

Whatever the origin of the topography, the folding associated with the Normandy structures is clearly the result of slumping off the flanks of mounds into the surrounding troughs or channels, and does not require tectonic activity as suggested by some authors (Lombard, 1956; Boltenhagen et al., 1968; Ternet, 1969). Similarly I believe the folding in phosphatic chalk cuvettes to be slump structures, probably initiated by erosional oversteepening on the sides of the cuvettes. Certainly no deformation has been observed in other chalks in the Picardy region, nor is there any correlation with the structure of the underlying Turonian marls (D'Arcy and Roux, 1971); both would be expected if the folding had a tectonic origin. The angle of slope that caused the slump folding is difficult to assess since primary erosional slopes and slump-fold modified dips cannot easily be distinguished. Nevertheless, movement on slopes of a few degrees seems likely and is compatible with observations from other sediments (e.g. Bradley, 1931; Rigby, 1958).

Folding and dislocation of hardgrounds has been recorded in southern England at Downend near Portsmouth (Gale, 1980) and at Boxford near Newbury (Jarvis and Woodroof, 1981). At Downend an anticlinal structure produces very high dips, extensive fracturing and exhibits at least two phases of movement. The folding has a very localised effect on sedimentation and Gale (1980) suggests that these properties, together with the small scale and tightness of the

structure, indicate a diapiric origin. There is, however, no direct evidence here or elsewhere in onshore Britain of diapiric activity affecting late Cretaceous sedimentation, and slumping on a regional slope remains a feasible mechanism for this structure.

Small-scale slump folding and mass movement of hardgrounds occurs at Boxford quarry but the concordance between the surface of the major hardgrounds (Boxford Paired Hardgrounds) and the underlying soft white chalks indicates that slumping was triggered by tectonism rather than erosion (see 2.11.3 and Jarvis and Woodroof, 1981 for discussion). The exposure nevertheless substantiates the feasibility of folding of hardgrounds during mass movement.

It may be concluded that phosphatic chalks are slump structures that occur on the sides of cuvettes during the initial stage of formation where erosional oversteepening has caused the slopes to become unstable (Fig. 3.26). Slump folding has resulted in dislocation of the basal hardground on the nose of some structures. Later mass-movement has rafted these blocks into the centre of the cuvettes where they were reexposed on the seafloor. The allochthonous blocks provided islands of hard substrate surrounded by soft mobile phosphorites, and were consequently sites of tube-worm patch-reef formation. The structures were subsequently buried but are commonly truncated by later phases of erosion within the cuvette. The planed-off sequences are generally overlain unconformably by an upper (or intermediate) white chalk which rarely (Marcheville may be an exception) exhibits any indications of later movement.

## 3.8 Late diagenesis

Late diagenesis or burial diagenesis is the changes that a sediment undergoes after it has been deeply buried ( $\geqslant$100 m) by subsequent deposition. At this depth interaction with fresh seawater is lacking and reactions take place between pore fluids and the enclosed grains and between adjacent grains. There are two main mechanisms which may operate during burial diagenesis (Scholle, 1974, 1977a): mechanical compaction and chemical compaction (also called solution-reprecipitation or solution transfer). External introduction of cement is

Fig. 3.26 Generalized block diagram illustrating the development of of phosphatic chalk slump folds.
A. Erosion of the cuvette incises a sequence of parallel bedded white chalks and weakly-indurated hardgrounds, resulting in the formation of a basal hardground.
B. Further erosion causes an oversteepening of the cuvette sides. Primary irregularities in the cuvette floor are accentuated by down-slope movement of the basal hardground and deformation of the under-lying chalks. Phosphatic chalk is concentrated in the axial region where it is continually upgraded by winnowing.
C. Deformation results in the shearing and imbrication of the basal hardground in the extensional regions of the fold. Slumping carries phosphorite and blocks of hardground en mass into the centre of the cuvette. Some blocks within the debris flows are reexposed by currents and colonised by tube-worm patch reefs.
D. Infilling of the cuvette with phosphatic chalk stabilises the slopes and folding ceases. Declining and intermittent current conditions result in the deposition of white chalk intercalations within the phos-phorite. A final phase of planar erosion, apparently unaccompanied by hardground formation, truncates the phosphorite and surrounding chalk prior to the return of white chalk deposition. The cuvette axis may shift laterally before the initiation of a second cuvette. The second cuvette has cut down from the surface of a second white chalk which is not shown.
The illustrations are not to scale and represent only the central por-tion of a cuvette disected along the final planar erosion surface. Laterally the slope and induration of the basal hardground decline and the hardground is replaced by a burrowed junction before passing into homogenous white chalk. The phosphorite also thins and decreases in grade towards the margins of the cuvette where it too passes into white chalks. Slump folding is only recorded from the oldest (mid to late Santonian) phosphorite in each region.

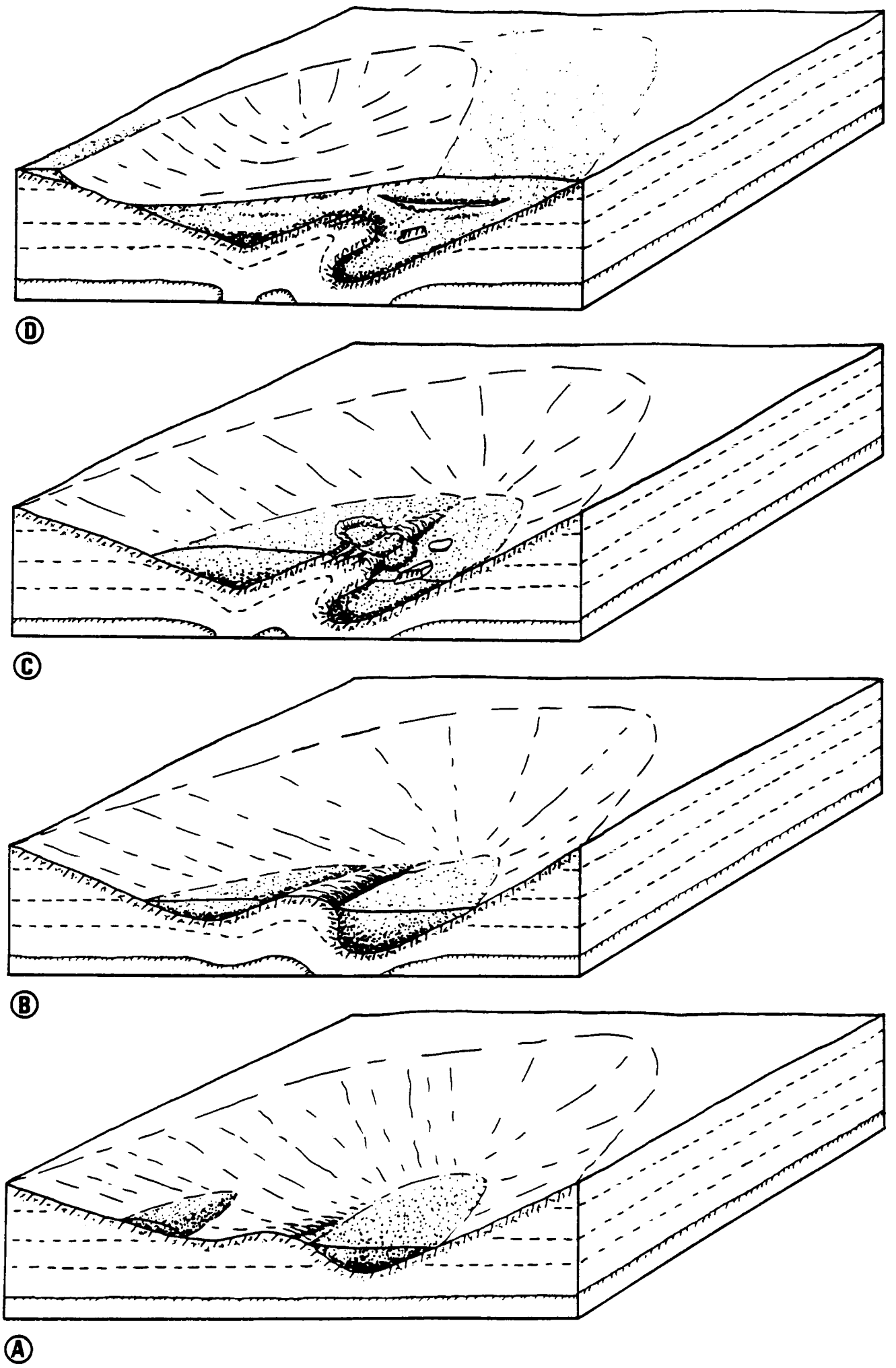
D
C
B
A

another possibility but involves movement of large volumes of pore water and is relatively insignificant in a sediment of such a low permeability as the chalk. The process is, however, important during the tectonic deformation of chalks (Mimran, 1975, 1977, 1978). Detailed petrophysical examination of the changes that a chalk undergoes during burial is outside the scope of this study and has been examined recently by Scholle (op cit.). Late diagenetic processes may, however, accentuate or modify bedding, produce new sedimentological structures or cause major mineralogical transformations in the sediment, and it is some of these aspects that will be considered here.

### 3.8.1 Silicification

Silicification is commonly the most conspicuous form of late diagenesis in white and phosphatic chalks. With the exception of rare grains of detrital quartz, silica occurs in two main forms: as a replacement of biogenic calcite in bioclasts, and as nodules or sheets of black chert, called flint. At least two generations of flint formation may be distinguished and these will be considered separately under the general headings of 'nodular' and 'tabular' flint.

#### 3.8.1a Bioclasts

Silicification of bioclastic material is common in most chalks (Bromley, 1965; Brown et al., 1969; Håkansson et al., 1974). It is commonest and most conspicuous in fragments of inoceramid shell (3.3.3f; Fig. 3.7) but is also seen in other bivalves, echinoids, brachiopods, corals and belemnites. Silicification in inoceramid shell is in the form of coalescing spherulitic masses of chalcedonic $\alpha$-quartz ~10 $\mu$m across. Silica concentrates along prism boundaries and is particularly well-developed at triple junctions where it forms 'rods' that extend inwards from the outer surface, demonstrating that silica was derived from outside the shell. Silica is initially restricted to the interprism area, the site of the organic conchiolin wall, but then extends outwards and replaces the surrounding calcite. Even in completely silicified examples

the prism boundaries remain visible in thin section due to the different optical properties of adjacent replaced prisms. Additional silicification commonly occurs in a zone just below the surface of the shell fragment (Fig. 3.7) perhaps concentrating along prominent growth lines in the prismatic calcite. Development of a spherulitic morphology in the silica may have been aided by the diverging elements of the calcite ultrastructure (Taylor et al., 1969). Such preferential silicification is rarely seen in other types of shell. Here coalescing spherules form botryoidal aggregates that are dispersed as 'clots' throughout the shell, although such 'clots' may be commonest in the umbonal regions of terebratulids, for instance.

Håkansson et al. (1974) have recorded rare ammonite and gastropod shell preserved as delicate silica replacements. Here silica is replacing aragonitic skeletons that show no evidence of compaction. This clearly demonstrates that mineralization was initiated, if not completed, during early diagenesis, since aragonite dissolution and compaction of aragonite moulds are both early diagenetic events (3.3.4). It has been demonstrated that flints preferentially form at sites of organic matter (see below). This may in part explain the silicification of bioclastic material in general and the site of the conchiolin wall of inoceramids in particular. These were undoubtedly areas with high organic-matter contents during early diagenesis. Silicification was not completed at this stage since reworked examples never show any evidence of preferential resistance to abrasion, biodegredation etc. of now silicified areas. It is likely, therefore, that silicification of bioclasts was a multistage process similar to that envisaged for flint formation (see below).

### 3.8.1b Nodular flints

Nodular flints occur as rhythmic layers and scattered nodules in the upper white chalk at many localities and in the uppermost phosphatic chalk at Hallencourt quarry. Both layered and scattered nodules show a close association with trace fossils (Voigt and Häntzschel, 1956; Bromley, 1965, 1967b; Kennedy, 1970b, 1975; Rasmussen, 1971; Håkansson et al., 1974; Kennedy and Juignet, 1974; Kennedy and Garrison, 1975; Hancock, 1975a) and the majority can be shown to

have originated within the fill of Thalassinoides systems. In most cases, however, silicification has extended beyond the walls of the original burrow and produced a nodular or semitabular morphology. Scattered nodules may be connected with other sites of organic remains and may incorporate silicisponges (Fig. 2.67B), fill echinoid tests or occur between the valves of brachiopods or bivalves (Håkansson et al., 1974).

Most nodular flints are 5 - 10 cm across and display a binary structure having a dark grey or black core of massive chalcedonic quartz surrounded by a 1 - 10 mm thick white cortex of incompletely-silicified chalk (Fig. 2.67B). The only flints studied in detail here are those from the phosphatic chalk of Hallencourt quarry, since they illustrate the characteristics of silica diagenesis in a chalk phosphorite. These flints contain pelletal phosphate, and 'ghosts' of calcitic bioclasts and bioturbation structures that are now completely replaced by silica (Figs. 3.27, 3.28). The micritic matrix has been entirely replaced by chalcedonic $\alpha$-quartz and the pore space filled with the same mineral. In contrast, the phosphate enclosed within the flints remains unaffected. Where a phosphate grain has a micritic envelope or contains some unmineralized micrite, the carbonate admixed with the apatite has been silicified and a quartz-apatite pellet (Fig. 3.17C,D) results. Clearly silicification post-dates phosphatization but the latter does not prevent the subsequent replacement of admixed carbonate.

The silicification process can be best examined within the cortex of the flints. Here the silicification 'front' consists of a coalescing complex of $\sim$10 $\mu$m $\alpha$-quartz spherules (Figs. 3.27A,B, 3.28C,D), similar to those seen in silicified bioclastic debris. The spherules are dispersed throughout the sediment and initially only replace fine-grained carbonate. With continued growth they expel impurities (primarily organic matter) originally enclosed within the carbonate, and coalesce until they enclose both phosphate and skeletal calcite. The latter is gradually replaced from the outside (Fig. 3.28C,D) but maintains its gross morphology even when entirely silicified (Fig. 3.28A,B). The organic material expelled during silicification is concentrated in a dark 'front' at the core/cortex boundary. Under SEM the spherules do not generally have a well-

Fig. 3.27 Phosphatic chalk microfacies X: Phosphatic chalk flints
A,B. Silicification front of a flint from the uppermost phosphatic chalk at Hallencourt quarry. The light-coloured cortex of the flint consist of ~10 μm α-quartz spherules mixed with phosphatic chalk. Many of the spherules have black organic matter-rich cores and margins. The core/cortex boundary is marked by a dark 'expulsion' zone also rich in organic material. Carbonate within the core has been entirely replaced by a mass of tightly interlocking α-quartz spherules but the phosphatic component remains unaltered. (A) PPL, (B) XN.
C,D. Core of a phosphatic flint from Hallencourt quarry. Phosphatized intraclasts and faecal pellets remain unaltered while the surrounding micrite and skeletal carbonate is totally replaced by quartz. (C) PPL, (D) XN.


A
0·5mm

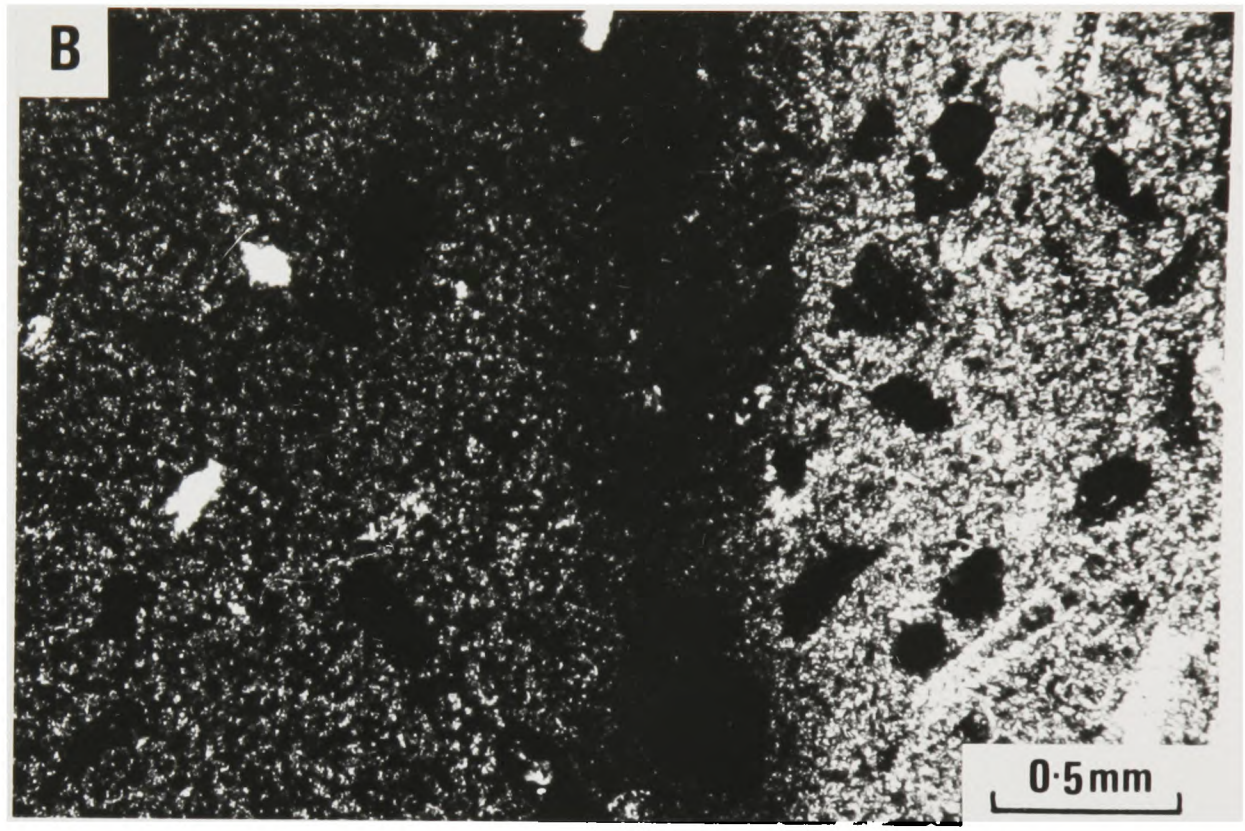
B
0·5mm

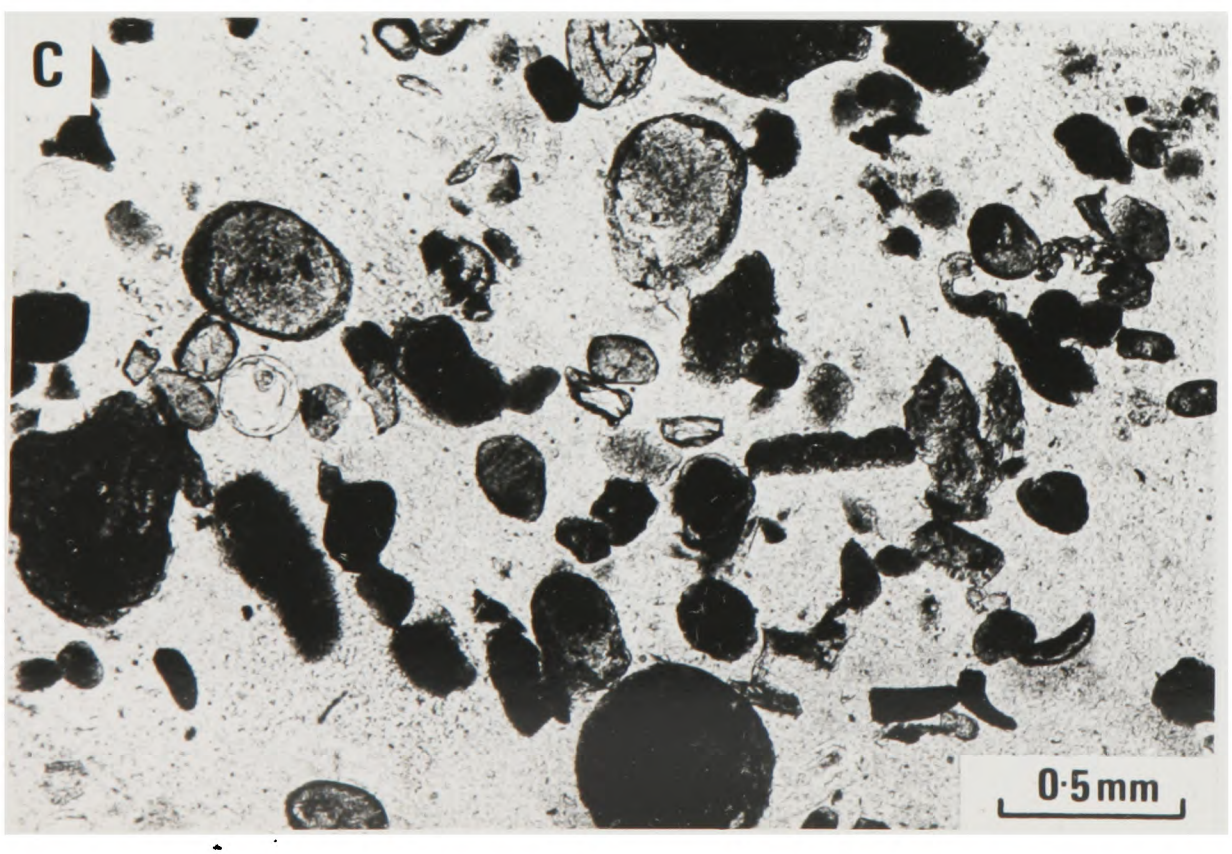
C
0·5mm

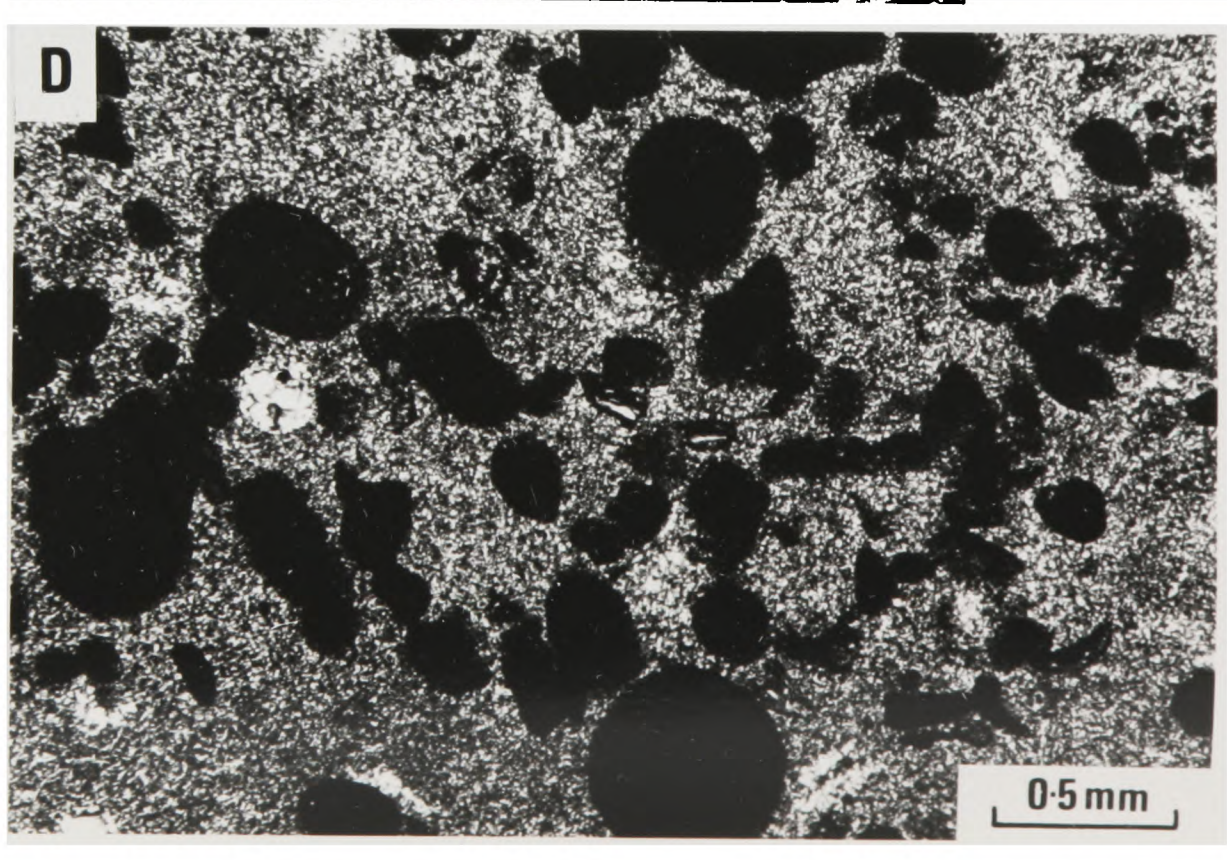
D
0·5mm

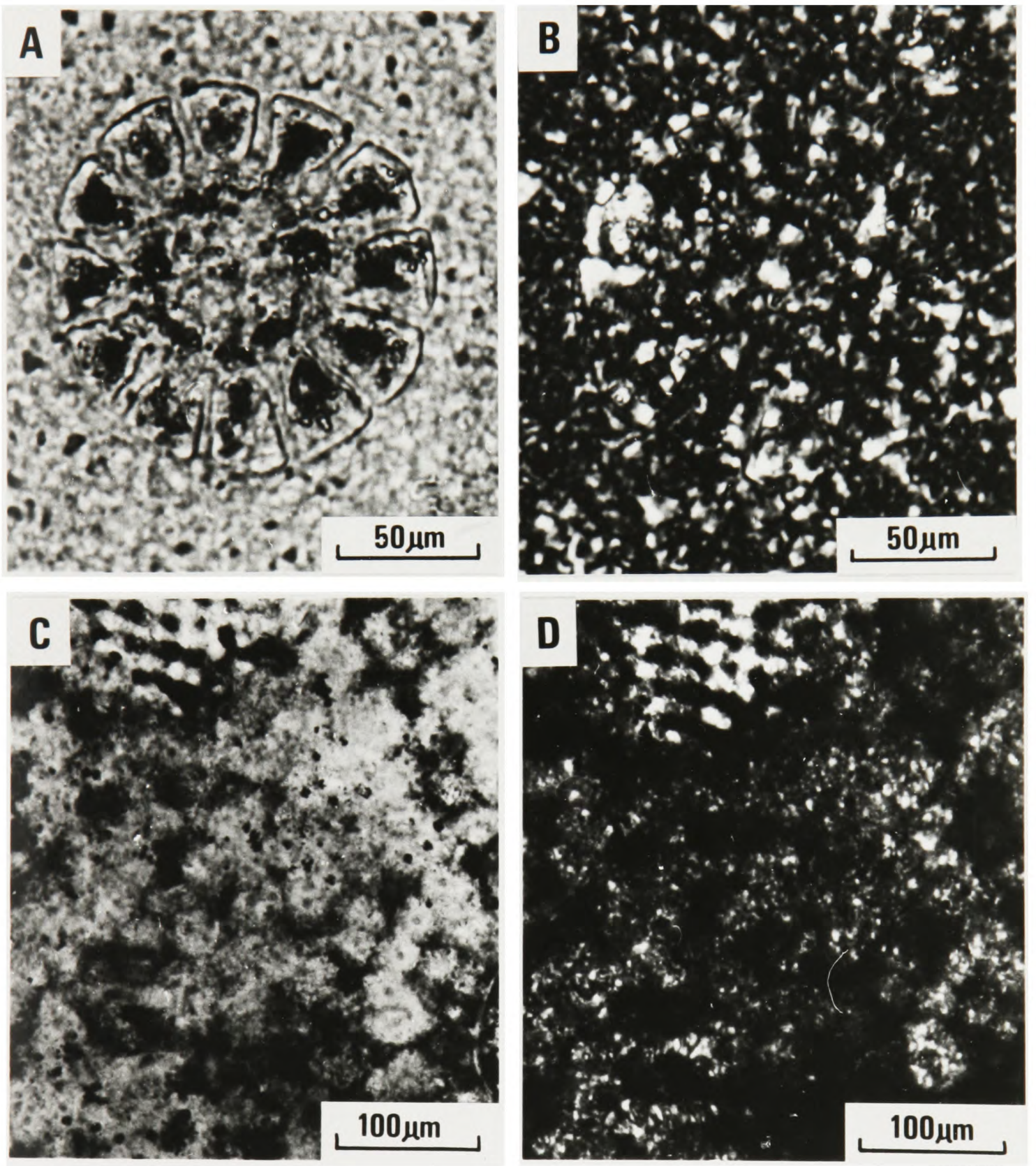


Fig. 3.28 Silicification structures.
A,B. A small fragment of skeletal carbonate within the core of a flint from the phosphatic chalk of Hallencourt quarry. The grain retains its original outline and contains relic blebs of organic matter, but has been completely replaced by an interlocking complex of ∝-quartz spherules. (A) PPL, (B) XN.
C,D. Quartz spherules in the cortex of a flint from the phosphatic chalk of Hallencourt quarry. The coalescing process can be seen as 'clots' of pure silica. An echinoderm grain (top left) is more resistant to replacement than the surrounding micrite but is nevertheless being engulfed. (C) PPL, (D) XN.

developed lamellate structure typical of opal-CT lepispheres (Wise et al., 1972; Scholle, 1974 fig.16; Jeans, 1978 figs.6,11; Riech and von Rad, 1979 fig.4) but are composed of minute (~0.1μm) irregular platelets.

### 3.8.1c Tabular flints

Thin (2 - 10 cm) sheets of flint have developed along joints, fault planes, shears and other fractures in the upper white chalk of many localities, particularly at Hardivillers and Nurlu quarries. These tabular flints are uniformly dark and vitreous and rarely have a distinct cortex. They vary greatly in thickness and are in many cases subparallel to bedding. When tabular flints are traced laterally they commonly alter level or disappear and are therefore poor lithostratigraphical markers. Their association with post-Cretaceous faulting demonstrates that at least some are post-Cretaceous in age.

### 3.8.1d Flint genesis

Field observations of flint from all chalk facies demonstrates a number of limitations concerning flint formation. Even where deep channelling incises a sequence of flinty chalks (e.g. Juignet and Kennedy, 1974 fig.5A), flint nodules are never found reworked into intraformational conglomerates. They never show signs of brecciation or recementation (except where associated with post-Cretaceous faulting), even where the enclosing bed has undergone considerable slumping and dislocation (e.g. the Normandy slumps, Boxford quarry mélange). The rarity with which aragonitic fauna is preserved in flint suggests that silicification post-dated most aragonite dissolution. Fossils preserved in flint are sometimes crushed, suggesting a post-compactional date, but they predate the development of at least parts of flaser seams and stylolites (3.8.2). Derived flints are abundant in basal Tertiary conglomerates (e.g. the Palaeocene Bullhead Bed in Kent) and second generation flints are often related to post-Cretaceous faulting and fracturing.

This evidence of a late date for flint formation is apparently contradicted by the fact that flint formed preferentially at sites of organic matter, for example the area of the adductor muscles of brachiopods (Steinich, 1965) and

oysters (Müller, 1956). The correlation with Thalassinoides burrow fills and bioclasts has been discussed already. In addition many flints follow bedding even where it has been severely disturbed by slumping (Kennedy and Juignet, 1974; Gale, 1980).

Recent observations made on DSDP core material have provided data for a model of silica diagenesis that may explain these apparent anomalies. It is now generally agreed that the silica in cherts is of biogenic origin (Cayeux, 1929; Buurman and van der Plas, 1971; Wise and Weaver, 1974; Kastner and Keene, 1975; von Rad et al., 1978; Riech and von Rad, 1979); a volcanic source (Gibson and Towe, 1971; Mattson and Pessagno, 1971; Pomerol and Aubry, 1977) is rejected because although volcanogenic sediments are abundant in DSDP cores they are only occasionally associated with porcellanites or chert, both commonly occur where there is no association with volcanicity. Clay mineral diagenesis may provide an additional minor source of silica (Siever, 1962). The silica is believed to originate from the dissolution of the opaline (opal-A) skeletons of radiolaria, diatoms and silicisponges which are occasionally preserved as 'ghosts' in flints (Wetzel, 1971), suggesting that they were also once present in the surrounding sediment. Desilicified or quartz-replaced sponge spicules are common in most chalk facies.

Chert formation is not a single stage process. It is the end product of a series of mineral growths and neoformations, and it is these transformations that may explain the apparent anomalies observed in the development of chalk flints. Dissolution or in situ replacement of biogenic opal-A occurs during early diagenesis (von Rad et al., 1978; Riech and von Rad, 1979), predating the precipitation of smectite-mica clay assemblages but post-dating the authigenic formation of glauconite (Jeans, 1978). The resulting $Si(OH)_4$-rich pore fluids precipitate opal-CT at favourable (see below) nucleation sites. It is only during subsequent late diagenesis that the opal-CT is transformed by solution-reprecipitation processes to $\alpha$-quartz (Keene, 1975; Robertson, 1977). The opal-CT to quartz transition is dependant on time, depth of burial (temperature) and the lithology of the enclosing sediment (Ernst and Calvert, 1969; Heath and Moberly, 1971; Murata and Nakata, 1974; Murata and Larsen, 1975;

Riech and von Rad, 1979) but is a slow process requiring something in excess of 30 million years.

Precipitation of opal-CT during early diagenesis may explain the correlation with sites of high organic matter content (Hâkansson et al., 1974; Jeans, 1978). Opal-CT is initially deposited as a syntaxial overgrowth on carbonate particles, and then subsequently replaces the enclosed calcite. Organic decay may lower the pH enough to cause the migration of $HCO_3^-$ and $Ca^{2+}$ ions away into the surrounding area but also reduces the $SiO_2$ solubility of the site (Emery and Rittenberg, 1952; Siever, 1962). These processes may set up a chemical gradient that causes further $Si(OH)_4$ to migrate into the area and complex with organic matter. If sufficient silica-enriched organic matter survives the initial oxidation stages of burial, it then produces a local source of silica which during the subsequent decay of the organic material leads to the precipitation of opal-CT lepispheres and the replacement of carbonate. Reworking during these initial stages would merely disseminate the opal-CT and leave no evidence of the proto-flint. Slumping of the sediment, however, would not have a pronounced effect on the location of the silicification sites. During late diagenesis the proto-nodules are converted to flint by the transformation of opal-CT to quartz and the addition of further silica from the surrounding sediment. Once formed, the flints act as nuclei for further precipitation of silica from migrating pore-fluids which result in the over-silicification of the original burrow or bioclast. Similarly these migrating fluids precipitated silica in the void space produced by late stage fracturing.

The general absence of flints in phosphatic chalks requires some consideration. Phosphatic material is extremely resistant to silicification but nevertheless cherts are common in most phosphorite deposits, including the sedimentologically similar phosphatic chalks in the Maastrichtian of the Mons Basin (F.L. Cornet and Briart, 1878; F.L. Cornet, 1886; Renard and F.L. Cornet, 1891a, b; J. Cornet, 1905, 1922). A lithological control is therefore unlikely. It is noteworthy that flint is absent in white chalks underlying and intercalated within the phosphatic chalk successions, but appears in the overlying low Campanian white chalks at several localities. Clearly a stratigraphical (palaeo-

geographical?) factor must be responsible but its elucidation requires further research.

### 3.8.2 Pressure solution

It has been demonstrated that the major sedimentological features of chalks - hardgrounds, nodules, burrowed-out horizons etc., are produced by synsedimentary processes. These structures are modified during burial. In white chalks flowage and microfaulting takes place and poorly-indurated nodules may be fractured (3.4.1c). Hardgrounds, however, maintain a rigid framework that protects the enclosed burrow fills from compaction. Nevertheless, both indurated and soft chalks are effected by late diagenetic dissolution caused by load and tectonic pressure. Soft chalks exhibit anastomosing complexes of residual clay seams that may develop a flaser structure (Garrison and Kennedy, 1977), while indurated chalks develop stylolites. Where hard nodules are surrounded by soft sediment, flaser seams may pass laterally into stylolites but the two structures are rarely seen in the same sediment.

#### 3.8.2a Flaser structures

Solution seams and flaser structures occur in soft, uncemented chalks and are particularly prominent in sediment with a high primary clay content. Thin (generally only a few millimetres) anastomosing clay-rich partings divide the chalk into discrete lenses a few millimetres or centimetres across. This 'flaserkalk' structure is closely comparable to the griotte texture of the limestones of the Montagne-Noir Devonian (Tucker, 1974) and the knollenkalke of the Ammonitico Rosso facies of the Tethyan Jurassic (Jenkyns, 1974). Flasering is well developed in the clay-rich Cenomanian and Turonian chalks of the Anglo-Paris Basin but is less common in younger chalks. In the sediments considered here flaser structures are only prominent as secondary modifications of primary marl seams (e.g. The Beauval Intermediate White Chalk Marl) although residual clay seams commonly overlie hardgrounds and are associated with other sharp lithological boundaries.

Solution seams cut across primary depositional features such as bedding planes and omission surfaces, and they cut and truncate burrows. The seams are never in turn cut by burrows, truncated by erosion surfaces or effected by slumping. They are clearly, therefore, of post-depositional origin. In thin section the flaser chalk is similar to the surrounding white or phosphatic chalk but contains a higher proportion of skeletal grains, phosphate, glauconite, clay minerals and other insolubles - indicating removal of fine-grained carbonate in solution. The flaser chalk also displays preferential orientation of elongate grains either subparallel to bedding or in flow structures around lithified nodules. Skeletal grains are commonly crushed or broken in flaser chalks but never show clear evidence of solution.

It is apparent that solution seams and flaser structures were produced during deep burial diagenesis by a combination of dissolutional and compactional processes. Theoretical considerations (Neugebauer, 1974) indicate that pressure solution in chalks is insignificant at burial depths of $<300$ m but should result in substantial lithification at depths of $\geqslant 1000 - 2000$ m (Schlanger and Douglas, 1974). Certainly similar structures occur in DSDP cores between these depths and have been produced in the laboratory by compaction of modern carbonate sediment (Shinn et al., 1977). Solution is most marked within beds that have high primary clay contents, so flasering tends to accentuate original clay seams. This may be because clay films between grains increase diffusion rates (Weyl, 1959). The concentration of solution seams along the surface of hardgrounds may be due to the amplification of compactional effects at the hard/soft sediment interface, a process that is seen in many other hardground horizons elsewhere (Purser, 1978; Sarkar et al., 1980). Evidence of mechanical deformation during compaction indicates that the chalk remained unconsolidated and plastic into the late stages of burial diagenesis. Grain alignment and fracturing demonstrates that flaser chalks have undergone more pronounced compaction than other types of chalk. This is further evidence of the causative relationship between compaction and the genesis of solution seams.

3.8.2b Stylolites

The intensely-indurated chalk of some basal hardgrounds and basal lag nodules (e.g. those at Nurlu quarry) are traversed by stylolites that show a variety of orientations but are commonly subparallel to bedding. Stylolites are totally absent from associated white chalks, demonstrating that lithification is a necessary prerequisite for stylolite formation in chalks. It is generally agreed (Bathurst, 1975 p.468; Hancock, 1975a) that stylolites are a late diagenetic pressure-solution phenomenon. They form as clay partings along inhomogeneities such as bedding planes, and then become progressively contorted with increased compaction. They are thus the lithified sediment equivalent of flaser seams and have a similar origin.

### 3.8.3 Pyrite

Large (up to 10 cm) goethitic nodules pseudomorphing late diagenetic pyrite are common in hardground and phosphatic chalks. The nodules are subspherical and have a radiating internal structure. Cubic crystal faces on their surface reveal an original pyritic composition. Texturally, ferruginization effects phosphatic chalks in a similar way to silicification (Fig. 3.29), replacing carbonate but leaving enclosed phosphate essentially unaffected. These nodules show several other similarities to flints. They are never found reworked into intraformational conglomerates but are commonly associated with sites of organic matter, such as burrow fills and the closed valves of bivalves and brachiopods. Although they may originally have had a fossil or burrow as a nucleus they have usually overgrown the original site to produce a subspherical morphology. Thus again a multi-stage process appears likely, early diagentic pyrite acting as nuclei to further precipitation of iron from migrating pore fluids during late stage anaerobic burial diagenesis. The transition to goethite is a weathering phenomenon.

### 3.8.4 Cementation

Late-diagenetic cementation of chalks has been discussed by Neugebauer

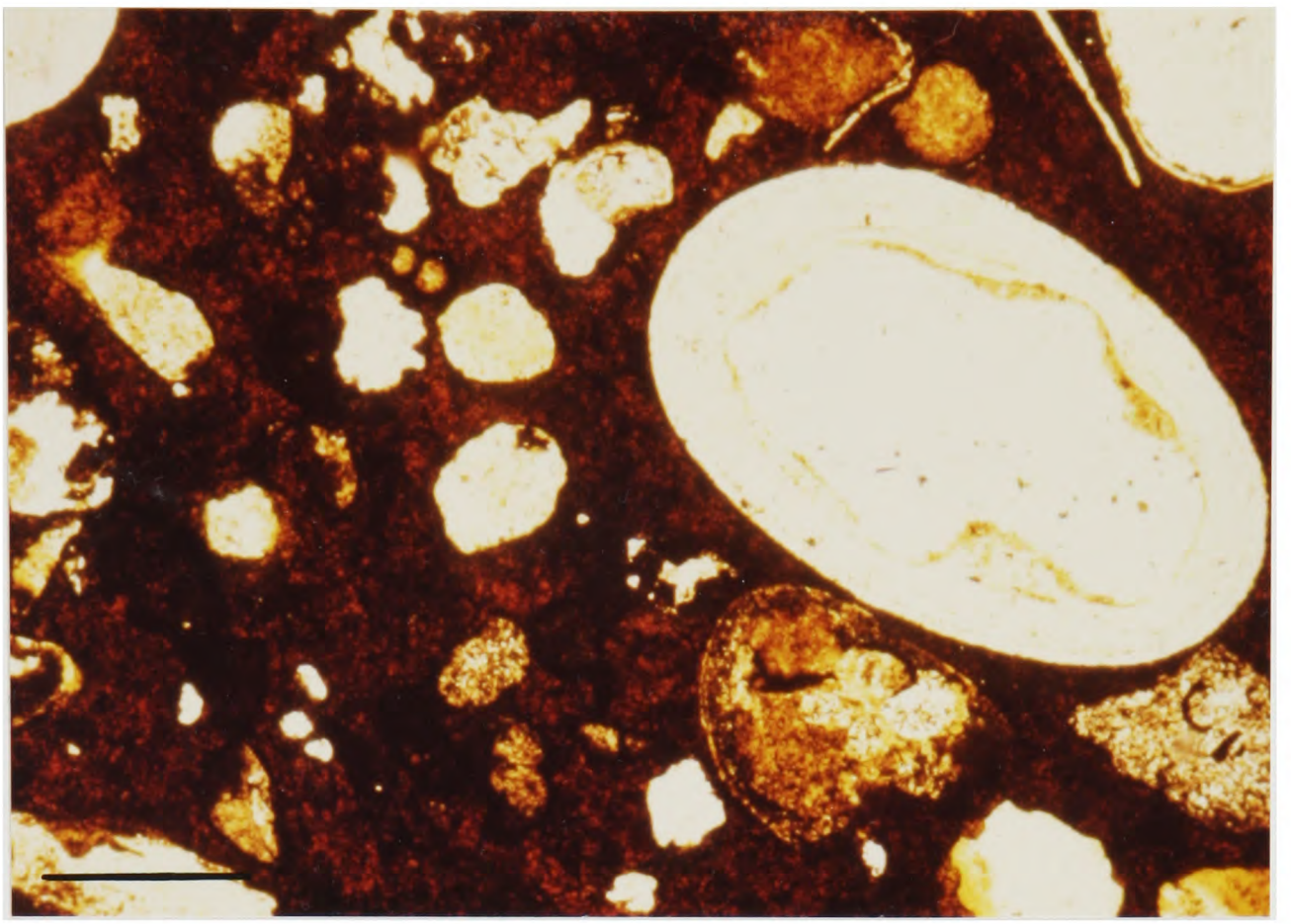

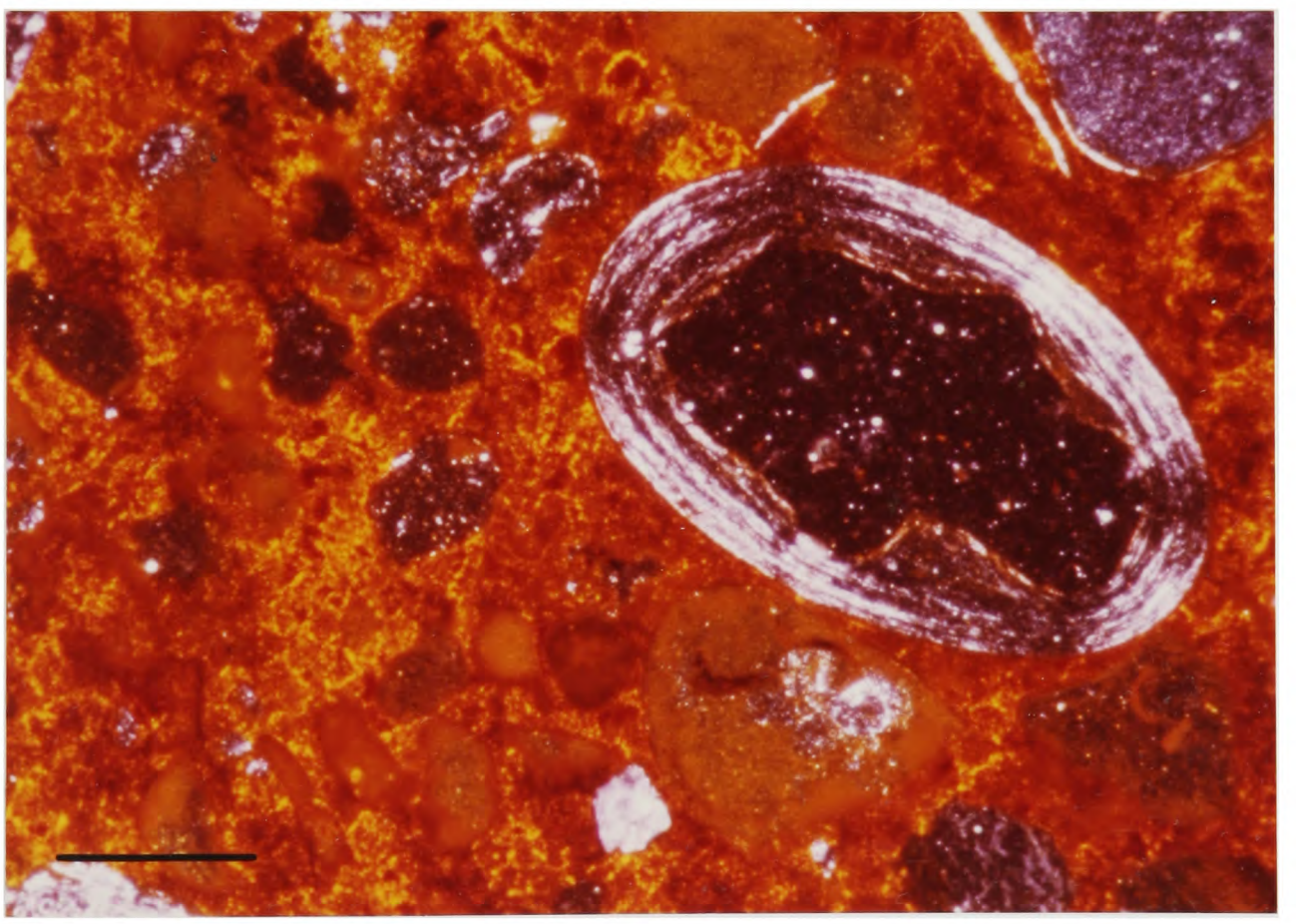

Fig. 3.29 Ferruginization of phosphatic chalk.
A late diagenetic pyrite nodule (now replaced by goethite) from a burrow in the phosphatic chalk of Faucouzy quarry (bed F1/1). The micritic matrix has been completely replaced by dark red-brown goethitic iron minerals which are nearly opaque in plain polarised light (top). The replaced matrix has a microbrecciated texture under crossed polars (bottom), probably the result of volume changes that accompanied the pyrite to goethite transition. White chalk intraclasts and the carbonate of mixed phosphate-carbonate pellets are also replaced but their original distribution may still be discerned under crossed nicols because of the different optical properties of the replacive goethite. Strongly-phosphatized material (e.g. the phosphatic oolith, right) remains essentially unaltered but displays minor iron staining along its margins. Scale bars = 0.2 mm.

(1973, 1974), Scholle and Kinsman (1973), Scholle (1974, 1977a,b), Hancock and Scholle (1975) and Mimran (1975, 1977, 1978) and will not be reexamined in detail here. An association between lithification and minor tectonic deformation was noted at Hem-Monacu quarry (2.4.1a). Such local lithification associated with faulting cannot be explained by an internal source of carbonate during burial diagenesis, as suggested for most late diagenetic induration of chalks by Scholle (op cit.). It requires migration of calcium carbonate along fractures as indicated by Mimran (op cit.) who argues for Tertiary hardening in a fresh-water environment by the introduction of $CaCO_3$ (derived from an external source) into the pore spaces. Such local, tectonically controlled late-stage induration is supported by local Tertiary lithification of white chalks elsewhere in the Anglo-Paris Basin.

## 3.9 Conclusions

The dominant lithology in the Anglo-Paris Basin during the late Cretaceous consists of white, coccolith biomicrites containing accessory skeletal carbonate (especially foraminiferans and inoceramid prisms) and traces of terrigenous and 'authigenic' minerals. These white chalks are essentially parallel-bedded and subhorizontal, bedding being picked out by marl seams, nodular-flint lines and erosion surfaces.

The main constituent of these chalks, the coccoliths, were deposited within zooplankton faecal pellets which settled on the seafloor and produced thixotropic substrates. Occasional changes in the seafloor environment, however, produced firm or hard substrates at some levels. Sedimentation rates were considerably higher than for similar modern sediments and probably in excess of $4 \times 10^{-3}$ cm y for most of the Chalk. Deposition occurred at depths of 150 - 300 m in a tropical or subtropical sea of normal salinity.

The carbonate is now exclusively low-Mg calcite although skeletal aragonite and high-Mg calcite were once present in small quantities. Aragonite was dissolved during early diagenesis, either on the seafloor or after shallow burial. Magnesium was probably mobilized during subsequent burial. The high porosity

(35 - 50%) and low permeability (1 - 8 md) of white chalks reflect the absence of substantial modifications of the sediment during diagenesis.

The homogeneity of the lithology is broken by the occurrence of hard bands of synsedimentarily lithified chalk, termed hardgrounds. The most prominent hardgrounds in the Santonian to low Campanian chalks of northern France and southern England are those that occur at the base of phosphatic chalk successions. These basal hardgrounds are strongly lithified and mineralized, and are penetrated by numerous phosphatic-chalk filled Thalassinoides burrow systems. They display complex morphologies due to the interaction of physical and biological processes. Physical scour and abrasion has resulted in planed-off hardground surfaces and well-rounded intraclasts while, conversely, bioerosion has led to convolute or filigree morphologies and angular, concave-surfaced intraclasts. Distinct pre- and post-lithification suites of trace-fossils may be differentiated. The former consists entirely of burrows - large and extensive networks of broad idiomorphic Thalassinoides with occasional Chondrites, Planolites and Zoophycus. The latter includes both burrows and borings but is dominated by borings. Burrows are confined to restricted stenomorphic-Thalassinoides but borings include those produced by clionid sponges, pholadid bivalves, polychaete and sipunculid worms.

Hardground chalks show a considerable amount of petrographical variation but commonly contain a high proportion of sand and pebble-grade mineralized and unmineralized intraclasts and shell debris. Cementation occurs on an intergranular scale and sparry calcite is volumetrically unimportant. Light-green replacive zones of glauconite occur in the hardground surface and extend up to 5 mm outwards from the walls of burrows and borings. In addition, glauconitized foraminiferal infills, faecal pellets and intraclasts are present in the hardground sediment. Glauconitization only replaces a small percentage of the affected sediment and predates phosphatization. Light-brown phosphatization zones show similar characteristics but may be up to 1 cm thick. Phosphate preferentially replaces lithified micrite and is intimately related to biological activity, particularly boring and encrustation of the hardground surface. Basal hardgrounds are invariably coated with ~0.5 mm thick phosphate skins. These

have a binary structure consisting of alternations of thin laminated-veneers of pure carbonate-fluorapatite and thicker layers of phosphatized organic-rich micrite. The skins are believed to be replaced organic mats. 'Ferruginization' by goethitic minerals is a weathering phenomenon produced by the breakdown of glauconite and pyrite within hardgrounds. The occurrence of pseudomorphed pyrite is indicative of high organic-matter contents and subsurface anoxia within the hardground sediment during early diagenesis. Dendritic manganese oxides which are ubiquitous to all hardgrounds are also a weathering product.

Lithification occurred a few centimetres below the sediment/water interface in a winnow-coarsened sediment of increased permeability. Cement was introduced from seawater, flushed through the sediment by currents and bioturbation. Unlike older chalks, these post-Coniacian hardgrounds have not passed through an obvious nodular stage, probably because compositional changes in the bioclastic component altered the response of the sediment to early diagenesis. The winnowed nature of the hardground sediment confirms the stronger current regime indicated by hardground-associated faunas including corals and tube worms that are favoured by high current activity. The discordance between the surface of the hardgrounds and the horizontal bedding of the underlying white chalks illustrates that erosion has removed several metres of sediment prior to, or concurrent with, lithification. Elevated current conditions and erosion may be related to shallowing since algal borings and mats(?) indicate deposition at the limits of the photic zone i.e. at depths of <150 m.

Basal hardgrounds are overlain by phosphatic chalks containing in excess of 5% $P_2O_5$. The occurrence of channel-fill cross-beds at the base of some phosphorites indicates that strong current conditions continued into the phase of phosphatic chalk deposition. White chalks intercalated within tne phosphorite are commonly broken up by bioturbation to produce a pseudonodular or burrowed-out structure. Rounding and mineralization of these nodules during subsequent burrowing forms unexposed pseudoconglomerates. Bioturbation has destroyed most bedding lamination but the rare occurrence of laminated planar beds indicates phases when the benthos was inactive. Planar unbioturbated junctions at the top of some phosphatic chalks may be related to scouring followed by the deposit-

ion of a mass flow of white chalk on top of the erosion surface.

The pelletal component of phosphatic chalks consists of phosphatized sediment - intraclasts, ooliths, faecal pellets; and bioclasts - foraminiferans, comminuted inoceramid, echinoderm and bryozoan debris, sponge spicules, bone fragments, elasmobranch teeth, teleost otoliths and ostracodes. The matrix is an unmineralized friable biomicrite. A coarse intraclastic basal lag occurs at the base of most phosphatic chalk successions. The phosphatized intraclasts were produced by both biological and physical processes and include fragments of white, hardground and phosphatic chalk. Mineralized steinkerns are common and all clasts display boring, encrustation and mineralization similar to that seen in basal hardgrounds. 'Terebella' phosphatica and Diblasus arborescens are commonly found reworked into basal lags along with other hardground-associated fauna. Phosphatic chalks show varying degrees of compositional variation through the succession. The proportion of faecal pellets, ooliths, echinoderm, bone fragments and benthonic foraminiferans decline as the phosphate becomes finer-grained and less phosphatic. Coprolitic and oolitic microfacies are characteristic of basal beds while inoceramid prisms or pelagic foraminiferans are the dominant components of poor phosphatic chalk facies. During the early Campanian calcisponge and echinoderm biocalcarenites were deposited in phosphatic chalk successions and elsewhere. These indicate shallow, high-energy conditions at a time when phosphatization was declining in importance due to palaeoceanographical changes.

The petrography of the pelletal phosphate indicates that phosphatization is partly dependent on the structure and mineralogy of the grain. The cement of lithified micrite is more prone to replacement than skeletal material; foram tests and echinoderm etc. are only phosphatized in the most extremely-mineralized sediment. Phosphatization is related to high organic-matter contents (both primary and linked to microboring) in the original grains although a dominantly external source of phosphate is indicated by decreasing phosphatization from the margins inwards.

Phosphate was concentrated by the prolific biota that was associated with basal hardgrounds. The reduced state of unweathered phosphatic chalks indicate

that, as with modern phosphorites, phosphate was incorporated into the sediment during anaerobic diagenesis. Phosphatization was a rapid early-diagenetic, subsurface and microenvironmental process. Intermittent seafloor anoxia is suggested by the sedimentology and fauna of the phosphorite. Similarly, the mixture of ooliths and faecal pellets, and the strongly bimodal grain-size distribution of the sediment suggest variable current activity. Oxic phases of colonization, bioturbation and winnowing alternating with quiescent anoxic phases of mineralization.

Phosphorite deposition occurred in troughs up to 1 km in length, 250 m wide and 30 m deep. These cuvettes are of erosional origin. Current activity was strongest in their axial regions and produced a strongly-indurated basal hardground associated with a pronounced hiatus and overlain by a coarse, rich phosphorite. Laterally, declining current regimes resulted in less erosion, weaker lithification and finer, less phosphatic sediments. Nevertheless, during the later stages of cuvette evolution the margins were an important source of fresh sediment by lateral derivation. The constancy of orientation displayed by cuvettes demonstrates that erosion by a permanent ocean current was responsible for their formation. Regression was necessary for the current to achieve its erosional potential, thereby effectively limiting the period of phosphorite formation. During their early history, erosional oversteepening of the sides of some cuvettes produced large intraformational slump-folds in the basal hardground and overlying phosphatic chalk. Folding was accompanied by dislocation and rafting of hardground blocks into the axial region and produced local mélanges in the phosphorite.

Late diagenesis is characterised by silicification of bioclasts and the formation of flint nodules. Silicification was a multi-stage process involving the liberation of silica from biogenic opal-A and the early-diagenetic formation of opal-CT lepispheres at the sites of organic matter. Migration of silica during late diagenesis and the transformation of opal-CT to chalcedonic $\alpha$-quartz produced the present structures. Other late-diagenetic products are pressure-solution structures such as flaser seams that modify primary marls, and stylolites which form in some hardgrounds. Pyrite-nodule formation and

fracture- and fault-associated induration and flints also formed at this time.

Chapter 4 : Geochemistry


| | | | |
|---|---|---|---|
| 4.1 | Introduction | | 359 |
| 4.2 | Analytical methods | | 360 |
| 4.3 | Mineralogy | | 361 |
| 4.4 | Geochemistry | | 364 |
| | 4.4.1 | Lithostratigraphical variation | 364 |
| | 4.4.2 | Statistical analysis | 370 |
| | | a. Factor 1 - carbonate-fluorapatite | 370 |
| | | b. Factor 2 - clay minerals | 374 |
| | | c. Factor 3 - lithification | 377 |
| | | d. Factor 4 - iron minerals | 377 |
| | | e. Factor 5 - weathering | 378 |
| | | f. Factor 6 - analytical error | 379 |
| 4.5 | Discussion | | 379 |
| | 4.5.1 | Hardground lithification | 379 |
| | 4.5.2 | Mineralization | 381 |
| 4.6 | Conclusions | | 384 |

## 4.1 Introduction

Sedimentological and petrographical examination of chalks provides important information concerning the origin of the lithofacies. Supplementary data may be obtained by the study of the mineralogical and chemical changes that occur during lithification and mineralization of basal hardgrounds and their overlying phosphatic chalks. These data clarify or explain many of the observations made by other methods and provide further parameters for the formulation of a general genetic model.

Basal hardgrounds are particularly well suited for a geochemical study of hardground lithification since they are the products of one or a small number of distinct lithification events and consist of ~45 cm of indurated chalk (3.3.1). Furthermore, both the hardgrounds and the overlying phosphatic chalks contain only a small percentage of the diluents (e.g. quartz, glauconite, clay minerals, feldspar, pyrite, dolomite) that hinder the geochemical interpretation of many other phosphorite deposits (e.g. Price and Calvert, 1978; Cheney et al., 1979; Birch, 1979b).

Weathering may substantially alter the chemistry of phosphates (Cook, 1972; McArthur, 1978; Howard and Hough, 1979) so wherever possible samples were collected from sites currently (1978) undergoing excavation. Despite this precaution, oxidation is indicated by the characteristic brown colour of these sediments which is considered (3.4.4) a product of the breakdown of reduced iron compounds within the phosphate component. Thirty-five samples were analysed from the two main localities of Beauval quarry (2.3.2) and Nurlu quarry (2.5.2). Specimens were collected from sampling traverses that originated in the soft white chalk below the basal hardground, continued up into the progressively-indurated sediment of the hardground and hardground surface and terminated in the overlying phosphatic chalk (Fig. 4.1). The scheme was designed to display the major changes that occur during the transition from soft white chalk to hardground and phosphatic chalk without the necessity of analysing large numbers of near-identical sediments. In addition samples were analysed from the basal lag at Villers-devant-le-Thour (2.10.1), a cemented

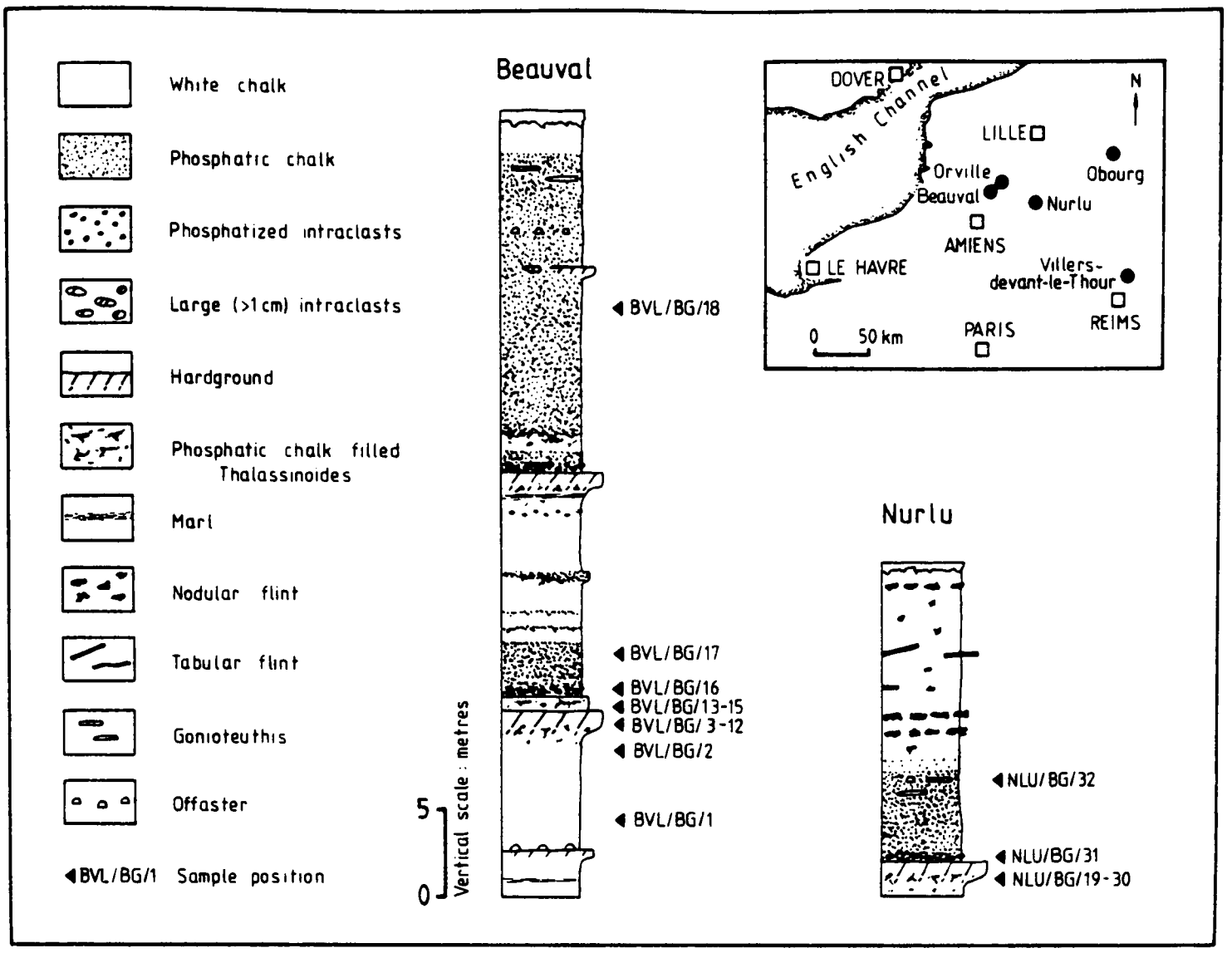


Fig. 4.1 Lithostratigraphical location of geochemical samples from Beauval and Nurlu quarries. Inset shows the location of sites chosen for geochemical sampling.

basal lag from the 'Champs d'Argent' quarry, Orville (2.3.3) and two comparative samples of early Campanian phosphatic chalk from the Craie de Trivières of the Ciment d'Obourg quarry near Mons in Belgium.

## 4.2 Analytical methods

X-ray diffraction analyses of desalinated whole-rock powders (Appendix 1) were made to identify the major mineral phases. High calcite contents precluded a detailed study of the phosphate mineralogy in many samples but calcite-free powders were produced by digestion in 0.5M acetic acid; these were used in the subsequent detailed mineralogical analysis. Interplanar spacings and lattice constants of the apatite phase were determined on samples with negligible clay and quartz content. The $CO_2$ content of the apatite was calculated from the position of the (004) and (410) peaks (Gulbrandsen, 1970) and the lattice constants from the position of the (300) and (002) reflections (McClellan and Lehr, 1969 eq.2). The clay component of a small number of samples

was separated by preferential settling and oriented specimens prepared on glass slides. These were analysed in plain and glycolated form to determine the dominant clay mineralogy.

Major and minor elements were determined by Atomic Absorption Spectrophotometry except for P and Si which were analysed by Colourimetry and X-ray Fluorescence respectively. Three separate solutions were prepared for each sample in an attempt to isolate the different phases present (cf. Barber, 1974; Froelich et al., 1977): (a) a whole-rock solution obtained by HF-$HClO_4$ digestion, (b) an HCL-soluble solution and (c) an acetic acid soluble solution obtained by dissolution with acetic acid buffered to pH 5 by sodium acetate. Whole-rock and HCl-soluble solutions were analysed for Al, Fe, Mn, Mg, Ca, Na, K, P and Sr. The sodium acetate buffer prevented the measurement of Na and K on the acetic solutions while their Al contents were found to be below the detection limit for the technique; samples with Fe contents below the detection limit (50 ppm) were given default values of 50 ppm. Reproducibility was generally within $\pm$3% of the amount reported but a lower precision ($\pm$10%) was obtained for those elements at low levels in the acetic solutions. Full details of the analytical techniques and precision are given in Appendix 1. Statistical analysis showed that the whole-rock and HCl-soluble solutions were the same for P, Na, Mn and Sr. Averaged values of these elements were then utilised in all further calculations.

## 4.3 Mineralogy

The dominant minerals present are calcite, carbonate-fluorapatite and quartz with accessory clay minerals. The X-ray pattern of the phosphate mineral exhibits well-defined diffraction lines at d-spacings similar to those reported by Rooney and Kerr (1967) for carbonate-fluorapatite and also a number of additional peaks (Table 4.1). No significant differences were found between the phosphate mineral present in any of the samples. The average $CO_2$ content of the carbonate-fluorapatite is 6.2% (range 6.0 - 6.4%) which compares to that in phosphorites formed by the replacement of carbonate sediments off N.

(McArthur, 1978) and SW Africa (Birch, 1979b). Petrographical and microprobe examination indicates that within the phosphate, carbonate-fluorapatite is invariably admixed with clay- and silt-grade impurities, principally calcite and clay minerals.

| | North Carolina pellets | Santonian-Campanian phosphates | Intensity |
|---|---|---|---|
| hkl | d(Å) | d(Å) | $I/I_o$ |
| 100 | 8.12 | 8.08 | 6 |
| 200 | | 4.04 | 6 |
| 111 | | 3.87 | 6 |
| 002 | 3.45 | 3.45 | 45 |
| 102 | 3.16 | 3.17 | 16 |
| 120,210 | 3.06 | 3.05 | 18 |
| 121,211 | 2.79 | 2.79 | 100 |
| 112 | 2.78 | 2.77 | 55 |
| 300 | 2.70 | 2.69 | 50 |
| 202 | 2.62 | 2.62 | 30 |
| 301 | | 2.51 | 4 |
| 122,212 | 2.29 | 2.28 | 8 |
| 130,310 | 2.24 | 2.24 | 20 |
| 131,311 | 2.13 | 2.13 | 6 |
| 113 | 2.06 | 2.06 | 6 |
| 123$\beta$ | | 2.02 | 2 |
| 203 | 1.996 | 1.998 | 4 |
| 222 | 1.932 | 1.931 | 25 |
| 132,312 | 1.875 | 1.878 | 12 |
| 123,213 | 1.835 | 1.836 | 30 |
| 231,321 | 1.789 | 1.789 | 12 |
| 140,410 | 1.763 | 1.762 | 10 |
| 402 | 1.738 | 1.742 | 10 |
| 004 | 1.724 | 1.724 | 16 |
| 232,322 | | 1.632 | 4 |
| 133,313 | | 1.604 | 2 |
| a | 9.34 | 9.322 | |
| c | 6.39 | 6.898 | |
| c/a | 0.738 | 0.740 | |

North Carolina data from Rooney and Kerr (1967). Other data obtained using Cu K$\alpha$ radiation at 40kV/20mA scanned at $\frac{1}{2}°$ 2$\theta$ $min^{-1}$ with a chart speed of 120 cm $hr^{-1}$ and calibrated against an $\alpha$-quartz standard (average of 12 analyses)

TABLE 4.1 Carbonate-fluorapatite X-ray diffraction data.

The high calcite content of the white and hardground chalks masks reflections produced by other minerals but when removed by acetic acid it was found that carbonate-fluorapatite was always the next most abundant mineral (Fig. 4.2). Clay minerals consist of poorly-crystalline illite and some mixed-layer

clay. Silica occurs as fine ( <10 μm) microspherules, some of which are similar to Opal-CT lepispheres (3.8.1) although only α-quartz was detected by X-ray diffraction (Fig. 4.2). Most microspherules occur as a replacement of calcite in bioclasts, particularly along prism boundaries within comminuted inoceramid-bivalve shell.

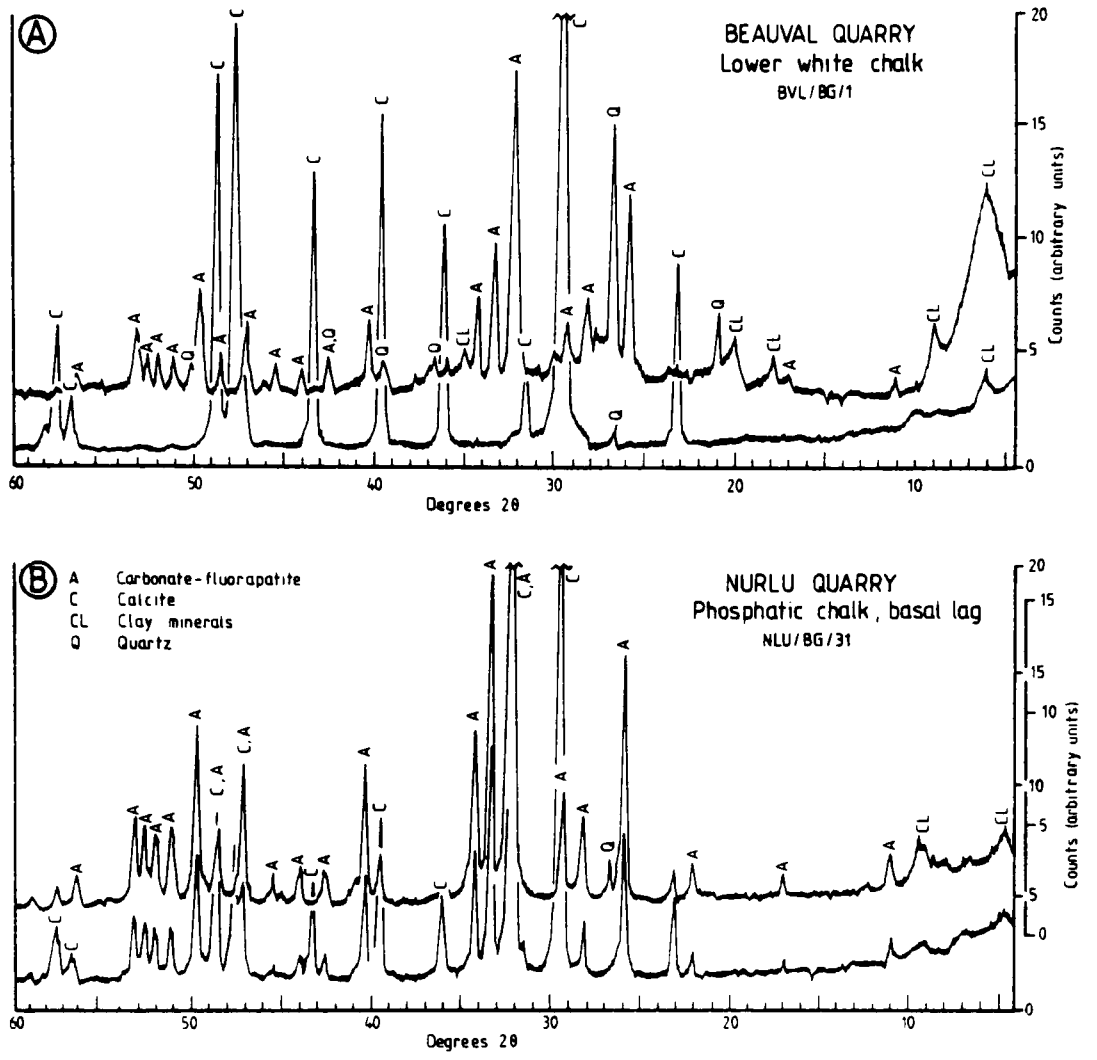


Fig. 4.2 X-ray diffractograms of representative rock types. A. white chalk, B. phosphatic chalk. Whole-rock (lower) and acetic-insoluble (upper) diffractograms are shown for each sample. The base line is the same for both traces in (A) but has been raised for the acetic-insoluble example (right-hand scale) in (B) to facilitate separation. (Cu Kα radiation at 40 kV/20 mA scanned at $2^{o}$ 2θ $min^{-1}$ with a chart speed of 120 cm $hr^{-1}$).

Glauconite was identified petrographically both in mineralized intraclasts and as a replacement in the upper portion of the burrow walls of the Thalassinoides systems that penetrate the basal hardgrounds (3.3.3a). Dendritic manganese oxides are common on fracture surfaces within the hardgrounds and occur to a lesser extent within white and phosphatic chalks (3.3.3e). They are commonest in indurated chalks. Blebs of goethite and lepidocrocite occur within the basal hardgrounds and, particularly at Nurlu, form cores to some of the phosphatized intraclasts of the basal lags; a limonitic stain is ubiquitous

to the phosphorite (3.3.3d). None of these last five minerals are present in sufficient quantity to be identified on the X-ray traces.

## 4.4 Geochemistry

The geochemical data were examined from two standpoints. Firstly, the nature of the sampling scheme enables much of the data to be plotted against the lithostratigraphy of the two main localities. Element/lithology diagrams provide valuable information concerning the lithological controls that produce particular element trends but they only enable a quantitive judgement to be made concerning inter-element relationships and their possible mineralogical controls. Furthermore, samples that are unsuited to this type of analysis may be included in more sophisticated methods. Consequently the data were analysed statistically utilising an SPSS (Statistical Package for the Social Sciences) version 7.0 package on ICL2980 and ICL2976 computers.

### 4.4.1 Lithostratigraphical variation

The element distributions (Figs. 4.3 - 4.6) clearly illustrate the major control that lithology exerts on geochemistry. Samples from Beauval extend ~8 m below the basal hardground but limited exposure at Nurlu only enables sampling to be carried out in the uppermost 110 cm of the underlying chalk.

The whole-rock and HCl-soluble data (Figs. 4.3, 4.4) display a number of trends. The transition from white to hardground chalk is accompanied by large increases in Mn, Mg, P and (particularly at Nurlu) Fe (Table 4.2), and to a lesser extent Na. Lithification results in a reduction in the percentage of Si, Al and K but, especially in the uppermost 10 cm of the hardgrounds, an increase in the HCl-soluble portion of the latter two elements. The amount of Sr is also reduced by cementation. The percentage of Ca and the proportion of Fe which is HCl soluble remain relatively constant.

The hardground surfaces and the overlying mineralized intraclasts within the basal lags (Fig. 4.4 NLU/BG/31) have closely-comparable element

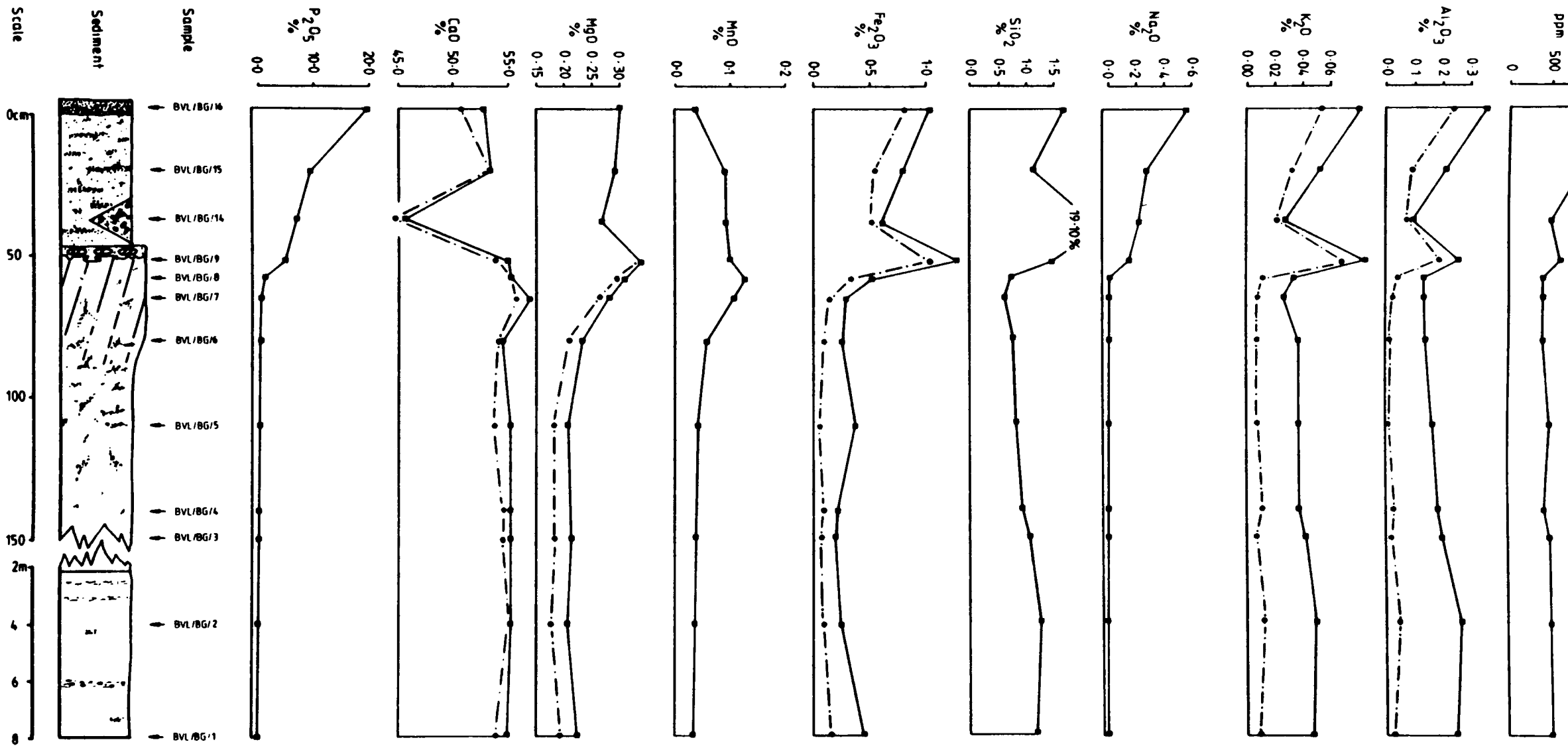


Fig. 4.3 Element distributions plotted against lithostratigraphy for the lower part of the succession at Beauval quarry, illustrating the transition from white chalk to basal hardground and overlying phosphatic chalk. Burrow fills were excluded from all samples of the hardground. The sediment log has a weathering profile and utilises the same symbols as Fig. 4.1. Solid line = whole rock; Broken line = HCl soluble values.

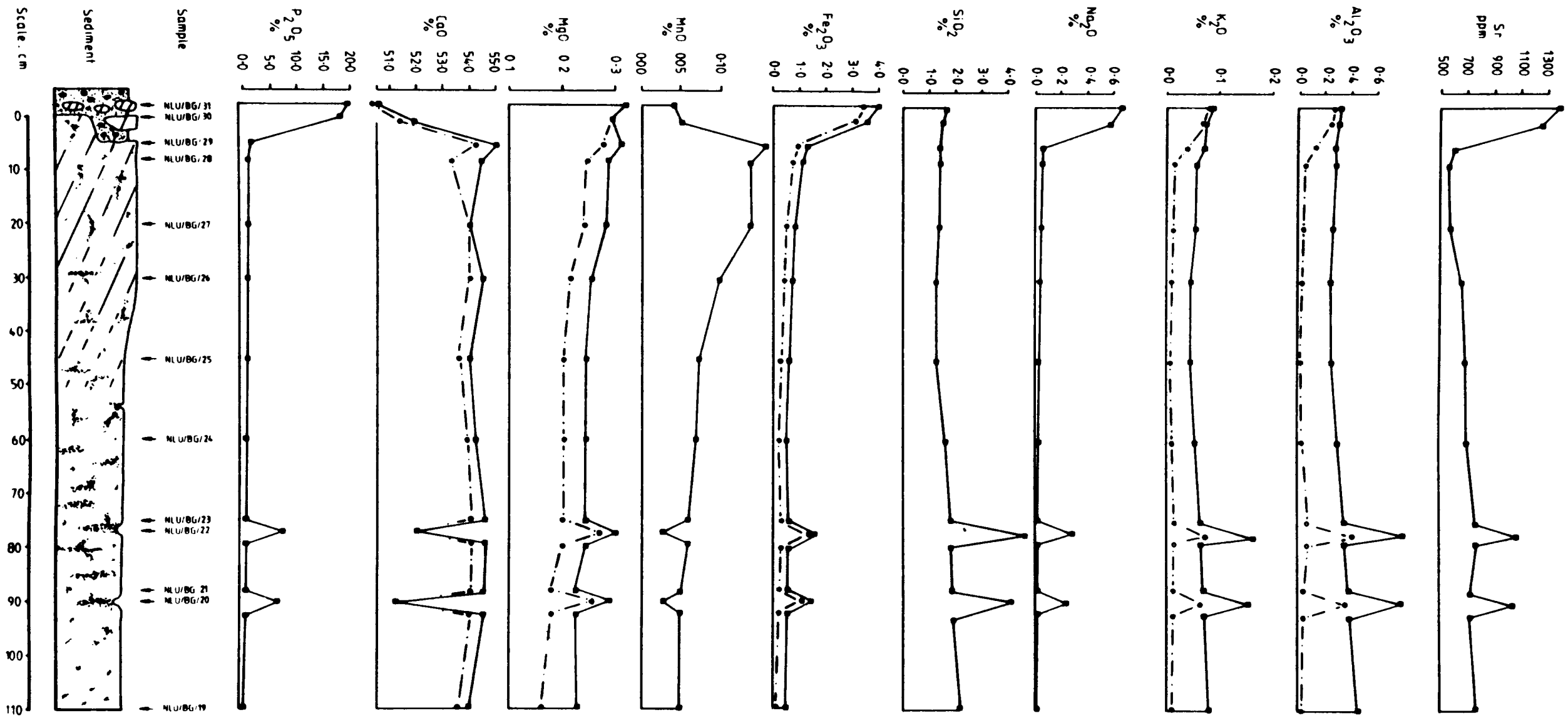


Fig. 4.4 Element distributions plotted against lithostratigraphy for the lower part of the succession at Nurlu quarry, illustrating changes within the basal hardground and overlying mineralized intraclasts in the basal lag. Samples NLU/BG/20 and NLU/BG/22 are phosphatic chalk (basal lag) infillings of Thalassinoides burrows; all other burrow fills excluded. The sediment log has a weathering profile and utilises the same symbol as Fig. 4.1. Solid line = whole rock; Broken line = HCl soluble values.

| Element | Beauval quarry | | | | | | | | | | | | | | |
|---|---|---|---|---|---|---|---|---|---|---|---|---|---|---|---|
| | Soft white chalk BVL/BG/1 | | | Hardground chalk BVL/BG/8 | | | Hardground surface BVL/BG/10 | | | Basal lag BVL/BG/16 | | | Phosphatic chalk BVL/BG/18 | | |
| $SiO_2$ | 1.200 | | | 0.740 | | | 2.220 | | | 1.700 | | | 0.740 | | |
| $Al_2O_3$ | 0.249 | 0.024 | | 0.134 | 0.043 | | 0.385 | 0.352 | | 0.342 | 0.242 | | 0.174 | 0.118 | |
| $Fe_2O_3$ | 0.370 | 0.170 | 0.014 | 0.510 | 0.301 | 0.019 | 3.500 | 3.250 | 0.007 | 1.060 | 0.829 | <0.005 | 0.413 | 0.320 | <0.005 |
| MnO | 0.035 | 0.035 | 0.035 | 0.127 | 0.127 | 0.121 | 0.051 | 0.051 | 0.030 | 0.037 | 0.037 | 0.016 | 0.029 | 0.029 | 0.021 |
| MgO | 0.233 | 0.195 | 0.167 | 0.310 | 0.291 | 0.253 | 0.363 | 0.358 | 0.081 | 0.298 | 0.298 | 0.085 | 0.255 | 0.253 | 0.154 |
| CaO | 54.900 | 53.900 | 53.900 | 55.300 | 55.000 | 51.900 | 53.500 | 51.800 | 21.300 | 53.000 | 50.700 | 22.800 | 53.700 | 52.600 | 38.600 |
| $Na_2O$ | 0.031 | 0.031 | | 0.039 | 0.039 | | 0.560 | 0.560 | | 0.546 | 0.546 | | 0.306 | 0.306 | |
| $K_2O$ | 0.047 | 0.009 | | 0.035 | 0.012 | | 0.175 | 0.164 | | 0.079 | 0.054 | | 0.045 | 0.035 | |
| $P_2O_5$ | 0.300 | 0.300 | 0.017 | 1.140 | 1.140 | 0.028 | 19.900 | 19.900 | 0.265 | 19.500 | 19.500 | 0.227 | 10.100 | 10.100 | 0.121 |
| Sr | 0.059 | 0.059 | 0.058 | 0.046 | 0.046 | 0.042 | 0.135 | 0.135 | 0.024 | 0.152 | 0.152 | 0.027 | 0.113 | 0.113 | 0.044 |

| Element | Nurlu quarry | | | | | | | | | | | | | | |
|---|---|---|---|---|---|---|---|---|---|---|---|---|---|---|---|
| | Soft white chalk NLU/BG/19 | | | Hardground chalk NLU/BG/28 | | | Hardground surface NLU/BG/30 | | | Basal lag (burrow-fill) NLU/BG/22 | | | Phosphatic chalk NLU/BG/32 | | |
| $SiO_2$ | 2.140 | | | 1.430 | | | 1.520 | | | 4.640 | | | 1.000 | | |
| $Al_2O_3$ | 0.484 | 0.028 | | 0.300 | 0.052 | | 0.317 | 0.255 | | 0.817 | 0.406 | | 0.219 | 0.180 | |
| $Fe_2O_3$ | 0.422 | 0.115 | 0.028 | 1.090 | 0.689 | 0.057 | 3.570 | 3.150 | <0.005 | 1.540 | 1.290 | <0.005 | 1.040 | 0.925 | <0.005 |
| MnO | 0.048 | 0.048 | 0.047 | 0.137 | 0.137 | 0.135 | 0.052 | 0.052 | 0.036 | 0.033 | 0.033 | 0.025 | 0.034 | 0.034 | 0.026 |
| MgO | 0.234 | 0.165 | 0.148 | 0.288 | 0.245 | 0.204 | 0.295 | 0.286 | 0.086 | 0.306 | 0.271 | 0.110 | 0.271 | 0.269 | 0.148 |
| CaO | 54.000 | 53.600 | 52.200 | 54.500 | 54.300 | 52.100 | 51.900 | 51.400 | 23.600 | 52.100 | 52.100 | 38.900 | 53.300 | 52.200 | 35.200 |
| $Na_2O$ | 0.026 | 0.026 | | 0.041 | 0.041 | | 0.600 | 0.600 | | 0.306 | 0.306 | | 0.406 | 0.406 | |
| $K_2O$ | 0.086 | 0.012 | | 0.059 | 0.015 | | 0.076 | 0.068 | | 0.170 | 0.070 | | 0.048 | 0.042 | |
| $P_2O_5$ | 0.150 | 0.150 | 0.016 | 0.680 | 0.680 | 0.022 | 18.200 | 18.200 | 0.215 | 7.830 | 7.830 | 0.082 | 10.900 | 10.900 | 0.205 |
| Sr | 0.086 | 0.086 | 0.082 | 0.063 | 0.063 | 0.059 | 0.136 | 0.136 | 0.029 | 0.116 | 0.116 | 0.056 | 0.126 | 0.126 | 0.050 |

TABLE 4.2 Representative analyses of major rock types.
Analyses of (left to right) whole-rock, HCl-soluble and buffered acetic acid solutions.
Total iron expressed as $Fe_2O_3$.

distributions. Both display continued increases in Mg, Na and P but decreases in Mn and Ca (Table 4.2). Many other elements are enriched in this portion of the hardground, notably Si, Al, Fe, K and Sr. The high proportion of Al, Fe, Mg and K that are HCl soluble indicates that the mineralogical controls on these elements are different from those influencing their distribution in white chalks. The silicified fauna of the Beauval Coral Bed (Fig. 4.3 BVL/BG/14; 2.3.2) has a predictably high percentage of Si and less Ca but the sample also has a high proportion of HCl-soluble Al, Fe and K.

Basal lags (including samples of burrow fills within the basal hardground at Nurlu - Fig. 4.4 NLU/BG/20, NLU/BG/22) contain considerably more Si, Al, Fe, Mg, Na, K, P and Sr than either white or hardground chalks (excluding their mineralized surfaces), but are relatively depleted in Mn and Ca (Table 4.2). The proportion of Al and K that are HCl soluble is usually high within the lithology. More generally, phosphatic chalks contain large amounts of Na, P and Sr but less Ca than white and hardground chalks. Other elements are variable but phosphatic chalks commonly contain less Si, Al and K than other lithologies.

Carbonate-associated elements are revealed by the analyses of the acetic-soluble solutions (Table 4.2). The low P content of these solutions demonstrates that the amount of carbonate-fluorapatite being dissolved by the method is negligible. Therefore, when normalised relative to their respective Ca contents these solutions should provide accurate measures of the minor-element geochemistry of the calcite within the different lithologies. Plotted lithostratigraphically (Figs. 4.5, 4.6) the data confirm that cementation of the basal hardgrounds is accompanied by a calcite-associated enrichment in Fe, Mn and Mg but depletion in Sr. The micritic component of the overlying phosphorite has, however, a similar element distribution to white chalks from below the basal hardground.

It is noticable that the geochemical changes that accompany lithification are clearly discerible $>90$ cm below the hardground surface and reach a peak in the most indurated portion of the hardground immediately below its mineralized surface.

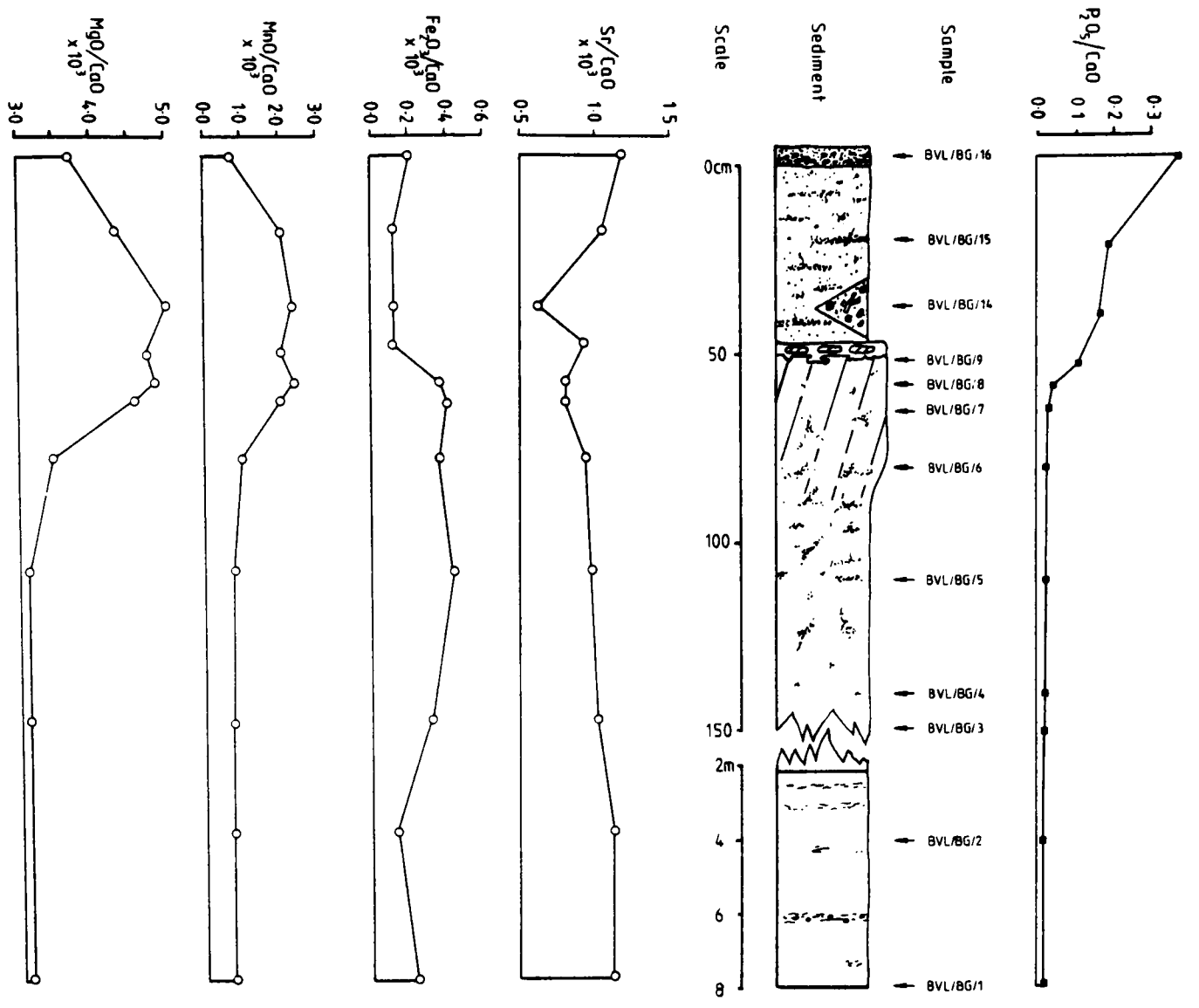


Fig. 4.5 Variation in calcite-associated elements plotted against lithostratigraphy at Beauval quarry. Distributions on the left of the sediment log are normalized acetic-soluble values, that on the right is derived from the whole-rock data and illustrates that the calcite-associated trends are independant of phosphate content. Symbols as Fig. 4.1 (Samples with < 50 ppm acetic-soluble $Fe_2O_3$ given default values of 50 ppm).

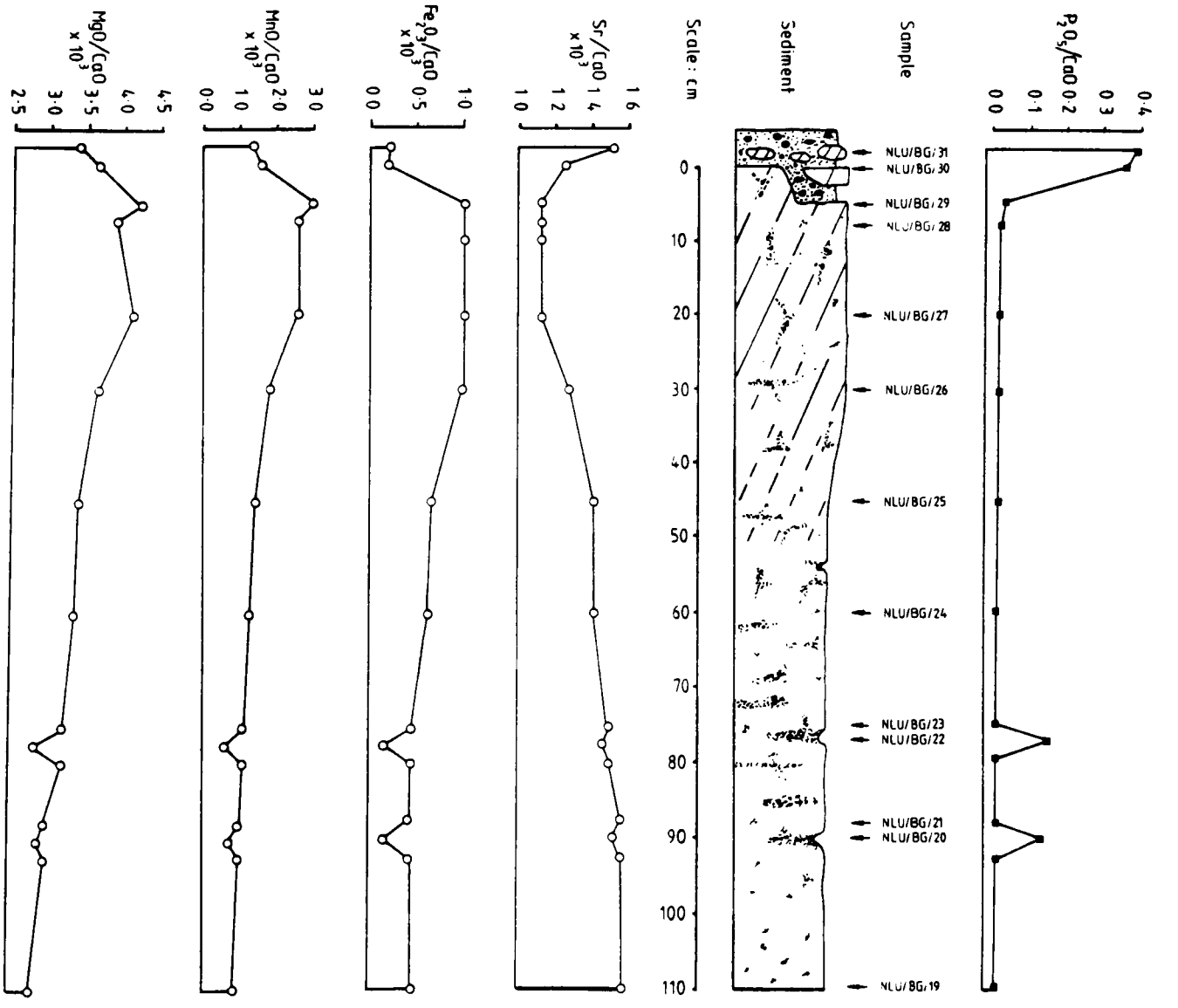


Fig. 4.6 Variation in calcite-associated elements plotted against

### 4.4.2 Statistical analysis

A number of univariate, bivariate and multivariate techniques were used, but factor analysis, a method which has been used in previous studies of phosphorite geochemistry (Reeves and Saadi, 1971; Summerhayes, 1972), was found to be most significant in terms of data reduction. Essentially, factor analysis reduces complex relationships between large numbers of variables to a small number of simple relationships which explain most of the variance in the original data. Variables are grouped on the basis of their intercorrelation into factors which are associations of highly-correlated variables. These factors, which are statistically the dominant features of the data variation, are derived from a Pearson correlation matrix. In this study the principal factor matrix was rotated to produce a varimax orthogonal solution in which each factor represents a single dimension in the data. Factor analysis does not replace interpretation but merely assembles the data in a more readily interpretable form. The most significant results were obtained when principal component factor analysis was applied to whole-rock, insoluble residue (whole rock - HCl-soluble values), carbonate-fluorapatite associated (HCl - acetic soluble) and normalised calcite-associated data sets. The results are summarised in Tables 4.3 and 4.4.

#### 4.4.2a Factor 1 - carbonate-fluorapatite

Statistically the dominant factor, accounting for >40% of the variation, this comprises a very strong association of whole-rock Na, P and Sr and carbonate-fluorapatite associated Mn, Mg, Ca, P and Sr. The factor also exhibits moderate positive loadings for whole-rock and carbonate-fluorapatite associated Fe and negative loadings for whole-rock Ca and insoluble-residue Mg. Mineralogically it must be attributed to the only phosphorus-bearing mineral identified - carbonate fluorapatite.

The low loadings of many elements in the whole-rock data are clearly due to the effects of other mineralogical controls which are removed in the carbonate-fluorapatite associated data set. Although more than 25 minor

| | | A - whole rock | | | | | | | | | B - insoluble residue | | | | | C - carbonate-fluorapatite associated | | | | | | D - calcite associated | | | |
|---|---|---|---|---|---|---|---|---|---|---|---|---|---|---|---|---|---|---|---|---|---|---|---|---|---|
| | | $SiO_2$ | $Al_2O_3$ | $Fe_2O_3$ | MnO | MgO | CaO | $Na_2O$ | $K_2O$ | $P_2O_5$ | Sr | $Al_2O_3$ | $Fe_2O_3$ | MgO | CaO | $K_2O$ | $Fe_2O_3$ | MnO | MgO | CaO | $P_2O_5$ | Sr | $Fe_2O_3$ | MnO | MgO | Sr |
| A | $SiO_2$ | 1.000 | | | | | | | | | | | | | | | | | | | | | | | | |
| | $Al_2O_3$ | [illegible] | 1.000 | | | | | | | | | | | | | | | | | | | | | | | |
| | $Fe_2O_3$ | 0.341 | 0.357 | 1.000 | | | | | | | | | | | | | | | | | | | | | | |
| | MnO | -0.397 | -0.423 | -0.223 | 1.000 | | | | | | | | | | | | | | | | | | | | | |
| | MgO | 0.180 | 0.065 | 0.541 | 0.358 | 1.000 | | | | | | | | | | | | | | | | | | | | |
| | CaO | -0.613 | -0.677 | -0.656 | 0.512 | -0.124 | 1.000 | | | | | | | | | | | | | | | | | | | |
| | $Na_2O$ | 0.113 | 0.199 | 0.696 | -0.433 | 0.378 | -0.576 | 1.000 | | | | | | | | | | | | | | | | | | |
| | $K_2O$ | [illegible] | [illegible] | 0.588 | -0.382 | 0.372 | -0.641 | 0.351 | 1.000 | | | | | | | | | | | | | | | | | |
| | $P_2O_5$ | 0.047 | 0.127 | 0.641 | -0.390 | 0.395 | -0.486 | [illegible] | 0.302 | 1.000 | | | | | | | | | | | | | | | | |
| | Sr | 0.301 | 0.404 | 0.613 | -0.585 | 0.189 | -0.682 | [illegible] | 0.463 | [illegible] | 1.000 | | | | | | | | | | | | | | | |
| B | $Al_2O_3$ | 0.675 | 0.701 | -0.218 | -0.174 | -0.398 | -0.236 | -0.460 | 0.416 | -0.511 | -0.180 | 1.000 | | | | | | | | | | | | | | |
| | $Fe_2O_3$ | 0.431 | 0.406 | 0.596 | -0.030 | 0.184 | -0.497 | 0.080 | 0.387 | 0.010 | 0.129 | 0.328 | 1.000 | | | | | | | | | | | | | |
| | MgO | 0.340 | 0.327 | -0.375 | 0.067 | -0.486 | 0.077 | -0.658 | 0.080 | -0.679 | -0.433 | [illegible] | 0.256 | 1.000 | | | | | | | | | | | | |
| | CaO | -0.316 | -0.327 | 0.045 | -0.037 | 0.226 | 0.360 | 0.420 | -0.201 | 0.508 | 0.300 | -0.546 | -0.264 | -0.480 | 1.000 | | | | | | | | | | | |
| | $K_2O$ | [illegible] | [illegible] | -0.160 | -0.217 | -0.265 | -0.287 | -0.391 | 0.532 | -0.445 | -0.132 | [illegible] | 0.319 | [illegible] | -0.533 | 1.000 | | | | | | | | | | |
| C | $Fe_2O_3$ | 0.308 | 0.329 | [illegible] | -0.245 | 0.558 | -0.640 | 0.743 | 0.580 | 0.694 | 0.646 | -0.283 | 0.498 | -0.448 | 0.089 | -0.219 | 1.000 | | | | | | | | | |
| | MnO | -0.029 | 0.005 | 0.582 | -0.005 | 0.607 | -0.323 | [illegible] | 0.209 | [illegible] | 0.665 | -0.549 | 0.047 | -0.662 | 0.561 | -0.498 | 0.623 | 1.000 | | | | | | | | |
| | MgO | 0.240 | 0.303 | [illegible] | -0.333 | 0.558 | -0.579 | [illegible] | 0.531 | [illegible] | [illegible] | -0.404 | 0.119 | -0.632 | 0.370 | -0.309 | [illegible] | [illegible] | 1.000 | | | | | | | |
| | CaO | 0.082 | 0.163 | 0.672 | -0.384 | 0.419 | -0.512 | [illegible] | 0.343 | [illegible] | [illegible] | -0.488 | 0.035 | -0.666 | 0.465 | -0.420 | 0.723 | [illegible] | [illegible] | 1.000 | | | | | | |
| | $P_2O_5$ | 0.048 | 0.128 | 0.643 | -0.390 | 0.396 | -0.488 | [illegible] | 0.304 | [illegible] | [illegible] | -0.511 | 0.012 | -0.680 | 0.502 | -0.445 | 0.696 | [illegible] | [illegible] | [illegible] | 1.000 | | | | | |
| | Sr | 0.111 | 0.198 | 0.635 | -0.438 | 0.361 | -0.548 | [illegible] | 0.343 | [illegible] | [illegible] | -0.447 | 0.024 | -0.651 | 0.460 | -0.377 | 0.686 | [illegible] | [illegible] | [illegible] | [illegible] | 1.000 | | | | |
| D | $Fe_2O_3$ | -0.116 | -0.132 | -0.250 | 0.533 | -0.199 | 0.280 | -0.443 | -0.221 | -0.426 | -0.345 | 0.290 | 0.176 | 0.580 | -0.172 | 0.202 | -0.309 | -0.317 | -0.451 | -0.416 | -0.428 | -0.431 | 1.000 | | | |
| | MnO | -0.378 | -0.391 | -0.042 | [illegible] | 0.440 | 0.401 | -0.310 | -0.304 | -0.275 | -0.487 | -0.235 | 0.064 | -0.011 | -0.028 | -0.285 | -0.063 | 0.107 | -0.197 | -0.264 | -0.273 | -0.328 | 0.459 | 1.000 | | |
| | MgO | -0.405 | -0.567 | -0.057 | 0.533 | 0.601 | 0.441 | -0.048 | -0.385 | 0.006 | -0.260 | -0.605 | -0.168 | -0.488 | 0.321 | -0.538 | -0.037 | 0.237 | -0.047 | -0.007 | 0.005 | -0.053 | -0.054 | 0.502 | 1.000 | |
| | Sr | 0.541 | 0.631 | 0.273 | -0.609 | -0.270 | -0.612 | 0.380 | 0.465 | 0.317 | 0.655 | 0.456 | 0.290 | 0.255 | -0.183 | 0.443 | 0.252 | -0.030 | 0.284 | 0.341 | 0.315 | 0.375 | 0.051 | -0.598 | -0.559 | 1.000 |

TABLE 4.3 Pearson correlation matrix.
Data are grouped into (A) whole rock, (B) insoluble residue, (C) carbonate-fluorapatite associated and (D) normalised calcite-associated data sets. Red = major positive correlation, Green = major negative correlation. Solid colour = correlation $\geq 0.750$, coloured underline = correlation 0.500 - 0.749.

TABLE 4.4 Varimax-rotated principal component factor matrix

| | Element | Factor 1 | 2 | 3 | 4 | 5 | 6 | Mean | Standard deviation |
|---|---|---|---|---|---|---|---|---|---|
| A | $SiO_2$ | 0.064 | [redacted] | -0.092 | 0.195 | -0.114 | -0.029 | 1.56 | 0.95 |
| | $Al_2O_3$ | 0.161 | [redacted] | -0.194 | 0.134 | -0.031 | -0.135 | 0.30 | 0.16 |
| | $Fe_2O_3$ | 0.629 | 0.172 | 0.119 | 0.698 | -0.121 | -0.137 | 1.07 | 0.93 |
| | MnO | -0.280 | -0.249 | [redacted] | -0.066 | 0.466 | -0.072 | 0.07 | 0.04 |
| | MgO | 0.427 | 0.169 | [redacted] | 0.213 | -0.176 | 0.090 | 0.28 | 0.04 |
| | CaO | -0.503 | -0.462 | 0.274 | -0.361 | 0.109 | 0.478 | 54.20 | 1.40 |
| | $Na_2O$ | [redacted] | -0.003 | -0.113 | 0.125 | -0.145 | 0.012 | 0.20 | 0.23 |
| | $K_2O$ | 0.327 | [redacted] | 0.027 | 0.240 | -0.170 | -0.092 | 0.07 | 0.04 |
| | $P_2O_5$ | [redacted] | -0.046 | -0.075 | 0.061 | -0.125 | 0.089 | 5.99 | 7.75 |
| | Sr | [redacted] | 0.198 | -0.331 | 0.081 | -0.037 | 0.003 | 0.09 | 0.04 |
| B | $Al_2O_3$ | -0.475 | [redacted] | -0.322 | 0.022 | 0.251 | -0.097 | 0.17 | 0.12 |
| | $Fe_2O_3$ | -0.012 | 0.299 | -0.012 | [redacted] | 0.190 | -0.042 | 0.26 | 0.12 |
| | MgO | -0.642 | 0.439 | -0.276 | 0.044 | 0.485 | -0.019 | 0.02 | 0.02 |
| | CaO | 0.448 | -0.298 | 0.081 | -0.142 | -0.028 | [redacted] | 1.09 | 0.91 |
| | $K_2O$ | -0.417 | [redacted] | -0.245 | 0.007 | 0.129 | -0.075 | 0.03 | 0.02 |
| C | $Fe_2O_3$ | 0.683 | 0.144 | 0.127 | 0.623 | -0.170 | -0.140 | 0.80 | 0.87 |
| | MnO | [redacted] | -0.067 | 0.313 | 0.065 | -0.032 | 0.149 | 0.01 | 0.01 |
| | MgO | [redacted] | 0.157 | 0.081 | 0.135 | -0.179 | -0.008 | 0.08 | 0.08 |
| | CaO | [redacted] | -0.012 | -0.059 | 0.081 | -0.117 | 0.054 | 9.15 | 11.10 |
| | $P_2O_5$ | [redacted] | -0.046 | -0.073 | 0.064 | -0.127 | 0.088 | 5.90 | 7.63 |
| | Sr | [redacted] | 0.014 | -0.122 | 0.048 | -0.128 | 0.054 | 0.04 | 0.05 |
| D | $Fe_2O_3$ | -0.318 | -0.025 | 0.075 | 0.061 | [redacted] | 0.015 | 0.39 | 0.29 |
| | MnO | -0.167 | -0.258 | [redacted] | 0.058 | 0.435 | -0.127 | 1.39 | 0.76 |
| | MgO | -0.012 | -0.409 | 0.697 | -0.011 | -0.188 | 0.256 | 3.88 | 0.70 |
| | Sr | 0.333 | 0.469 | -0.645 | 0.121 | 0.225 | -0.094 | 1.19 | 0.29 |
| Eigenvalues | | 10.985 | 6.669 | 2.826 | 1.340 | 1.092 | 0.653 | | |
| Percent variance | | 43.9 | 26.7 | 11.3 | 5.4 | 4.4 | 2.6 | | |
| Cumulative variance | | 43.9 | 70.6 | 81.9 | 87.3 | 91.6 | 94.3 | | |

Factor models containing more than six factors were rejected on geochemical grounds. The data are grouped into A. Whole rock, B. Insoluble residue, C. Carbonate-fluorapatite associated and D. Normalized calcite-associated data sets. Red = major positive correlation, Green = major negative correlation. Solid colour = correlation $\geq 0.750$, underline = correlation 0.500 - 0.749.

elements have been reported to occur in carbonate-fluorapatite, it has been shown (Lehr et al., 1967; McClellan and Lehr, 1969) that the mineral may be adequately described by its Mg, Ca, Na, P, F and $CO_2$ content. Regression analyses of Mn, Mg, Ca, P and Sr in the carbonate-fluorapatite data set and Na and P in the whole-rock data demonstrate that not only do these elements have very high correlation coefficients (Table 4.3) but also that the regression lines pass through the origins of the graphs (Fig. 4.7). It is possible, therefore, to determine the

composition of the carbonate-fluorapatite by utilising the regression lines to recalculate element abundances based on the Ca content of a highly substituted carbonate-fluorapatite (Lehr et al., 1967; McClellan and Lehr, 1969). In addition the $CO_2$ content has already been determined by X-ray methods (see above) and semiquantitive microprobe analysis indicates F contents of 2 - 3% which are consistent with previously published analyses (Cayeux, 1939). The values obtained by these methods are: 0.03% MnO, 0.36% MgO, 55.1% CaO, 1.12% $Na_2O$, 38.5% $P_2O_5$, 0.23% Sr, 2 - 3% F and 6.2% $CO_2$. The calculated $P_2O_5$ value lies between the fluorapatite and francolite end members of the carbonate-fluorapatite system which contain 42.2 and 34.0% $P_2O_5$ respectively (Lehr and McClellan, 1973; Cheney et al., 1979). It is noteworthy that the $Na_2O$ and Sr values are close to those (1.4 and 0.24% respectively) predicted by McArthur (1978) as being typical of unweathered phosphorites, although the $CO_2$ content is somewhat lower than the predicted value (8.4%).

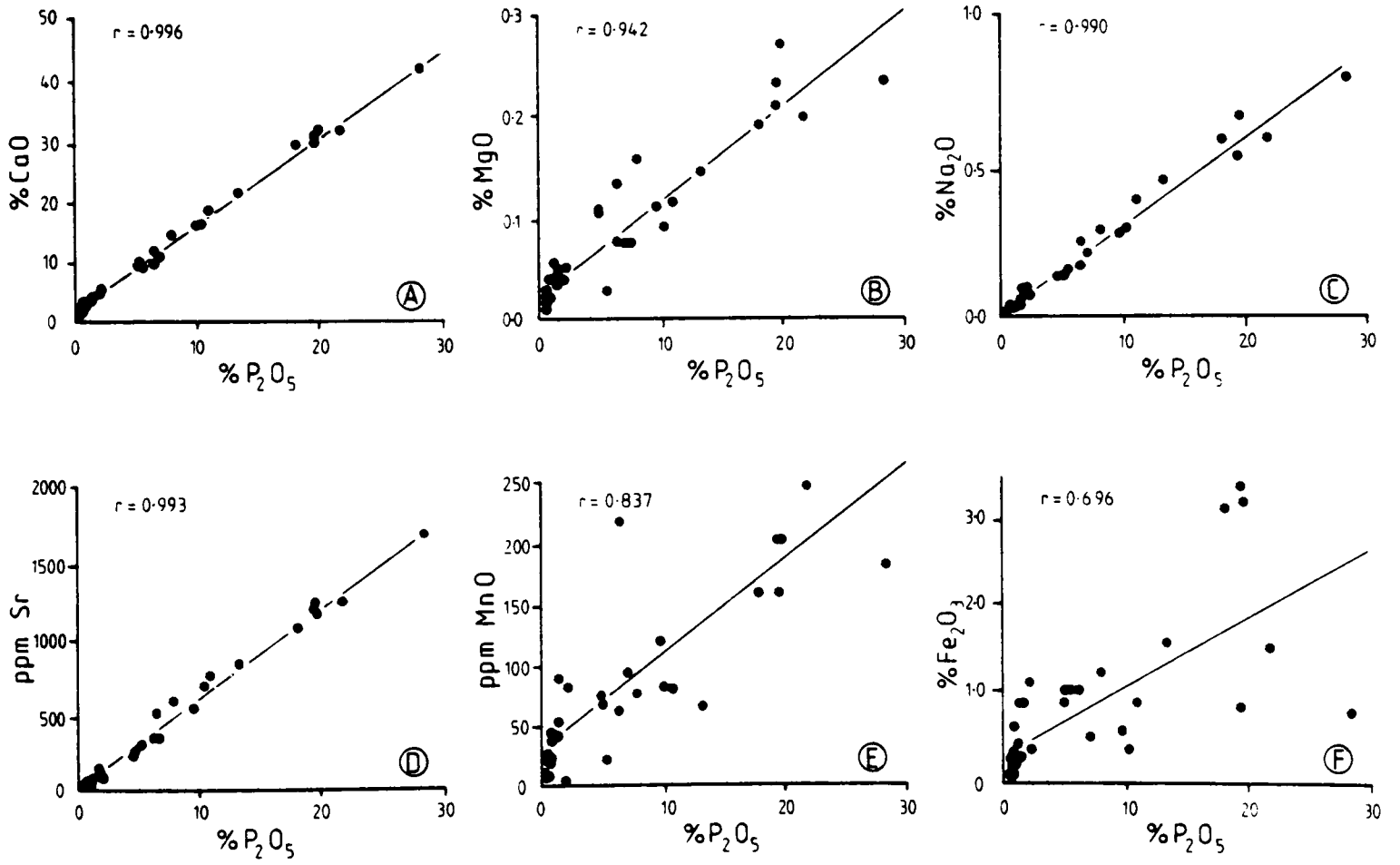


Fig. 4.7 Carbonate-fluorapatite associated elements as a function of $P_2O_5$.
A,B,D,E,F.- derived by subtracting acetic from HCl-soluble values.
C.- unadjusted HCl-soluble $Na_2O$. Regression lines determined by the least-squares method.

Iron is the main element to show divergence from the general trend in the carbonate-fluorapatite associated data set. It shows a greater scatter of values

that Fe and probably some Mg in the association are not contained within the apatite structure but are probably related to glauconite (see below).

These inter-element relationships explain the high positive loadings of the carbonate-fluorapatite factor, while the negative loading for total Ca is to be expected since apatite contains less Ca than calcite. However, the factor is also negatively loaded for insoluble-residue Mg, and to a lesser extent Al and K. These three elements are highly correlated within the insoluble residue (Table 4.3 Group B), so their negative loading with respect to apatite may be regarded as a decline in the weight per cent clay (see below) in phosphatized sediments, due to either mineralization of clays or simply because carbonate-fluorapatite has a higher density than calcite.

4.4.2b Factor 2 - clay minerals

The second principal factor shows high positive loadings for whole-rock Si, Al and K and insoluble residue Al and K; it is negatively loaded for total Ca. This close relationship between Si, Al and K has been recognised in many sediments including chalks (Spears, 1979) and phosphorites (Gulbrandsen, 1966) and has been interpreted as a clay mineral factor.

Regression analysis indicates that the interelement correlation is generally excellent ($r \geqslant 0.97$) but two groups of analyses reduce the overall coefficients (Table 4.3) by falling outside the general trends (Fig. 4.8). The first group consists of the Beauval Coral Bed (which was deleted from the factor analysis because of its disruptive influence on the correlation coefficients) and the two phosphatic chalks from Belgium. It is distinguished by abnormally-high $SiO_2$ values (Fig. 4.8). The second group comprises three samples of strongly-mineralized hardground surface from Beauval. The most strongly mineralized sample (Table 4.2 BVL/BG/10) lying furthest from the regression lines of the $K_2O$ plots (Fig. 4.8A,C) and the general trend on the triangular diagram (Fig. 4.8D).

The $SiO_2/K_2O$ and $SiO_2/Al_2O_3$ ratios of the northern French samples are ~25 and 5 respectively compared with ~35 and 7 for the Belgian material. Few clay minerals contain such a high proportion of Si (Deer et al., 1962a; Weaver and Pollard, 1973) so the ratios probably result from a combination of clays and

the winnowing and erosion that produced these hiatuses may be invoked as potential methods of concentrating these two components. Late diagenetic processes provide a further mechanism since pressure solution may cause migration of carbonate within the sediment (3.8.2) and produce flaser seams with elevated insoluble-residue contents.

The isolation of the hardground top group, particularly on the triangular diagram (Fig. 4.8D) demonstrates that the dominant mineralogical control is different for these samples. It has been noted that hardground surfaces are characterised by a high proportion of HCl-soluble K and Al and to a lesser extent Fe and Mg (Figs. 4.3, 4.4). If the HCl-soluble and insoluble-residue values are plotted (Fig. 4.9) the data confirm the high solubility of this mineral compared to clay minerals and silica. A mineral which is common in samples of the hardground

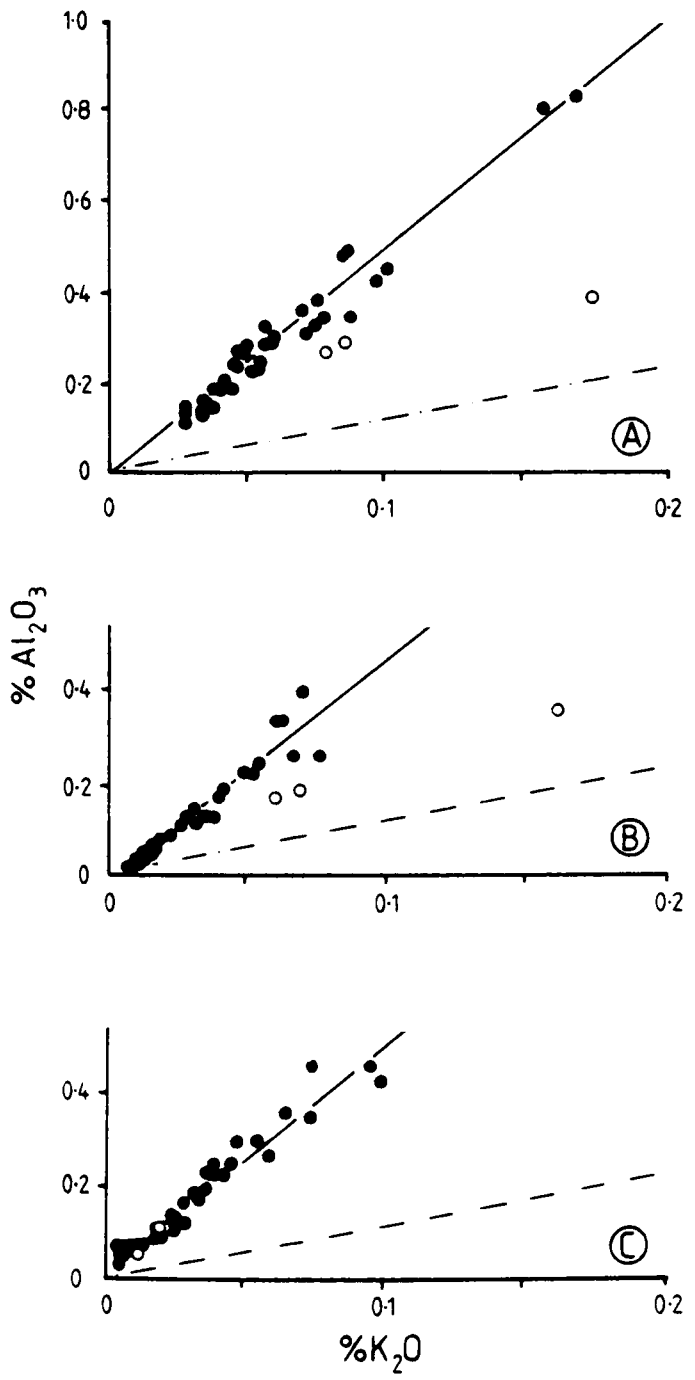


Fig. 4.9 Relative solubilities within the $Al_2O_3/K_2O$ system. A. whole rock, B. HCl soluble, C. insoluble residue. Samples of the hardground surface from Beauval (circles) are clearly differentiated. Regression lines determined by the least-squares method and excluding the hardground-surface samples. Discontinuous line = regression line for pure glauconite (calculated from Table 4.3).

surface from Beauval is glauconite. Microprobe analysis (Table 4.5) indicates that this mineral could cause the observed divergences from the whole-rock $SiO_2/K_2O$ and $Al_2O_3/K_2O$ regression lines. The correlation with Fe and Mg which

must also be associated with this mineral becomes apparent in Factor 4 and also accounts for the high correlation of Fe and Mg within the carbonate-fluorapatite associated data set.

Clearly the second factor is predominantly a clay mineral - silica factor that provides a measure of the biogenic(?) silica and clastic content of the sediment. The presence of glauconite, however, results in a minor reduction of the loadings associated with Si, Al and K.

| Oxide | % |
|---|---|
| $SiO_2$ | 51.09 |
| $Al_2O_3$ | 8.14 |
| $Fe_2O_3$ | 23.22 |
| MgO | 4.05 |
| CaO | 1.20 |
| $Na_2O$ | 0.06 |
| $K_2O$ | 6.91 |
| $P_2O_5$ | 0.29 |

Total iron expressed as $Fe_2O_3$.

TABLE 4.5 Average composition of glauconite mineral as determined by microprobe analysis. Average of nine analyses of glauconite-filled microborings within mineralized intraclasts from the Beauval Basal Hardground.

4.4.2c Factor 3 - lithification

The third factor has a high positive loading for whole-rock and calcite-associated Mn and Mg and a negative loading for calcite-associated Sr. The relationship to these elements suggests that it may be considered as a lithification factor that reflects the enrichment in Mn and Mg but depletion in Sr exhibited by indurated chalks (Figs. 4.3, 4.4). The lack of a significant loading for Fe is explained by its occurrence as a separate factor (see below). The high positive loadings for whole-rock Mn and Mg indicates that the degree of cementation is the dominant control on these elements.

4.4.2d Factor 4 - iron minerals

This factor has a high positive loading for one element alone - Fe. The strongest loading is associated with the insoluble residue, but high loadings also occur for whole-rock and carbonate-fluorapatite associated iron. Iron is

the major constituent of goethite, lepidocrocite, limonite and glauconite and must also be present in the montmorillonitic portion of the mixed-layer clays. This multiplicity of forms leads to the element being moderately positively correlated with a number of elements in the whole-rock data set (Table 4.3) but hinders an interpretation of the factor. Low positive loadings for Si, Al, K and Mg (Table 4.4) indicate that glauconite is one control but the correspondingly higher loadings for Fe clearly demonstrates that various forms of iron oxide are the dominant contributors to the factor. Certainly a pervasive light-brown iron stain is typical of all phosphatic chalks.

4.4.2e Factor 5 - weathering

The only major positive loading shown by this factor is for calcite-associated Fe. The isolation of this element as a separate factor explains its absence from the factor loadings of the lithification factor (Factor 3). Minor positive loadings are also indicated for whole-rock and calcite-associated Mn and insoluble Mg.

The main property that isolates Fe from other calcite-associated elements is its large variation between localities. At Beauval the white chalk has ~50 ppm and the hardground chalk ~150 ppm Fe, but comparable figures from Nurlu are ~150 and 400 ppm respectively. Thus although the trends are the same, the actual amount of calcite-associated Fe cannot be regarded as a good indicator of the degree of lithification. Both the white and hardground chalks at Nurlu have a pervasive limonitic stain that is absent at Beauval. This stain becomes pronounced in strongly-weathered exposures, where it develops a Liesegang-rings structure - it is clearly a secondary alteration product that indicates weathering of the Nurlu samples. Similarly Mn commonly becomes concentrated during the weathering of chalks.

This factor can therefore be interpreted as a measure of the degree of weathering shown by the samples. The minor positive loading for insoluble Mg is less certain. It may reflect Mg enrichment of clay minerals during weathering, but may equally be the result of analytical error. It cannot be entirely discounted that the whole factor is the result of the arbitrary Fe values

assigned to those rocks with <50 ppm acetic-soluble Fe. This would explain the isolation of calcite-associated Fe but would not account for its correlation with Mn.

4.4.2f Factor 6 - analytical error

This factor only has a significant positive loading for calcium, particularly insoluble but also whole-rock Ca. The high percentage of Ca in both the whole-rock and HCl-soluble portions of the rocks may lead to large absolute errors in the determination of insoluble Ca by subtraction, despite low standard deviations in the original data. This factor is therefore considered to be 'analytical error' and confirms that such errors are minimal in the bulk of the data.

4.5 Discussion

The analytical results demonstrate that cementation and mineralization are distinct but interrelated processes. The data provide the first comprehensive study of the chemical changes that accompany synsedimentary lithification in chalks and thereby provides tighter parameters for any model of hardground genesis.

4.5.1 Hardground lithification

Basal hardground formation is the first stage in the formation of phosphatic chalks. It is now generally accepted that Chalk hardgrounds are the result of synsedimentary seafloor cementation (3.3.4). Indications that lithification occurred at or near the sediment/water interface include boring and encrustation of the hardground surface, and the indurated intraclasts that overlie it. Furthermore, the lithified sediment of phosphatic chalk basal hardgrounds itself contains both mineralized and unmineralized intraclasts and bioclastic debris which have been incorporated into the main body of the hardground and plastered on top during the later stages of accretionary lithification. It has been

suggested (Kennedy and Garrison, 1975b; Scholle, 1977a) that extended periods of non-deposition are sufficient to initiate cementation. The coarse nature of basal hardground sediments, however, indicates that it was in part the increased permeability of the sediment that enabled the introduction of cement and not merely a decline in sedimentation rates.

In recent sediments, chalks have the same or similar trace-element compositions as the coccoliths and planktonic foraminiferans that are their dominant components (Scholle, 1977a). Cretaceous chalks are compositionally very similar (3.2.1), so it is reasonable to assume that their initial trace-element distribution was also comparable to these biogenic calcites. Modern coccolith oozes (Thompson and Bowen, 1969; Milliman, 1974) have total Fe and Mn contents of ~1000 and 265 ppm and acetic-soluble Mg and Sr values of 1100 and 1500 ppm. Calcite-associated Fe and Mn would certainly be lower as indicated by analyses of planktonic foraminiferans (Milliman, 1974) which give Fe and Mn values of only 150 and 10 ppm respectively. Clearly, soft white chalks (Table 4.2; Figs. 4.3 - 4.6) have Fe, Mn and Mg contents comparable to their modern counterparts but contain less Sr.

Lithification results in further Sr depletion and enrichment in Fe, Mn and Mg. Manganese enrichment and Sr depletion of this order are the normal processes that accompany the dissolution and reprecipitation of pelagic carbonate during burial diagenesis (Matter et al., 1975; Sayles and Manheim, 1975) and similar trends accompany the seafloor cementation of micrites by primary low-Mg calcite (Schlager and James, 1978). It has been suggested (Kennedy and Garrison, 1975b) that high-Mg calcite was the most likely cement for Chalk hardgrounds. However, this does not conform with the interpretation (Scholle and Kennedy, 1974) that the isotopic composition of hardgrounds is a relic of seafloor diagenesis. This implies that the original cement must have been low-Mg calcite or high-Mg calcite that rapidly converted while still exposed on the seafloor. All other cements would have lost their original isotopic composition through conversion during subsequent burial diagenesis (Schlager and James, 1978). A similar conclusion has been reached from studies of the Lower Ordovician hardgrounds of Sweden (Lindström, 1979).

It must be concluded that the most likely original cement in Chalk hardgrounds was low-Mg calcite. In basal hardgrounds this cement was introduced by precipitation from seawater passing through a coarser sediment of higher permeability than normal chalk oozes. It is only by the passage of considerable quantities of seawater through the sediment that sufficient cement could be introduced into a sediment with such a high initial porosity ( ~45% for white chalks compared with ~10% for hardground chalks). This was accomplished by enhanced current activity which caused the original coarsening and/or by the flushing action of burrowing organisms (3.3.4). Cementation probably occurred by the overgrowth of calcitic particles and was aided by the increased grain size since the small size of coccolith plates is one of the main factors that prevents their syntaxial overgrowth in normal oozes (Neugebauer, 1974). In addition to overgrowth, dissolution/reprecipitation processes are indicated by the presence of corroded coccoliths in some hardgrounds (Hancock and Kennedy, 1967).

Little is known concerning the behaviour of Fe and Mn during lithification of recent coccolith oozes although both elements commonly substitute in the calcite structure (Deer et al., 1962b). In basal hardgrounds these elements are apparently introduced with Mg during cementation, however, calcite-associated Fe in particular may be further enhanced by the breakdown of iron minerals during weathering. The concentration of manganese oxides on fracture surfaces within the hardgrounds is clearly a late diagenetic effect but may reflect a primary enrichment of Mn in lithified chalks.

### 4.5.2 Mineralization

Lithification of basal hardgrounds is accompanied and closely followed by mineralization. The petrography of the glauconitization and phosphatization of Chalk hardgrounds has been discussed in detail in Chapter 3 (3.3.3a, b).

In general where replacive glauconite and phosphate occur together the textural evidence suggests that glauconitization consistently occurred prior to phosphatization. The glauconite in basal hardgrounds occurs as mineralized

intraclasts, faecal pellets and foraminiferal chamber infillings cemented within the hardground sediment and as thin <5 mm replacement zones outwards from burrow walls and downwards from the hardground surface. Where phosphate and glauconite occur within the same burrow, glauconite is preferentially concentrated in the roof which also commonly has a goethitic crust up to 3 mm thick. In all its occurrences glauconitization is intimately associated with microborings and is most prominent where boring is greatest. The hardground surface and the roofs of burrows would remain exposed to seawater after the floor had become buried by sediment, while boring greatly increased the surface-area of the sediment/water interface - both of these factors suggest that glauconitization occurs where lithified chalk is in prolonged contact with seawater but ceases on burial. In contrast, phosphatization appears to occur in areas that have been mantled by sediment, which is consistent with the replacement process being a sub-sediment/water interface phenomenon (3.4.4).

Although the green pigment of glauconite makes it more prominent than phosphate, the whole-rock analyses indicate that it is volumetrically minor within the hardground (it was not even detected by X-ray diffraction). Microprobe examination demonstrates that even in the most strongly-glauconitized micrite, when averaged over an area of 10 μm, glauconite sensu stricto is usually subordinate to carbonate-fluorapatite and/or calcite. Pure glauconite was only found filling microborings within the most intensely-mineralized intraclasts.

It has been observed that the amount of glauconite increases at the hardground surface and that this is indicated geochemically by the high percentage of HCl-soluble K. However, this dramatic increase in soluble K also implies a lower clay content for although the amount of clay (as indicated by total $SiO_2$-$Al_2O_3$-$K_2O$) declines with the introduction of cement, in the bulk of the hardground this is accompanied by a synchronous reduction in HCl-soluble K and Al. It is generally considered (Burst, 1958a, b; Hower, 1961; McRae, 1972) that the diagenetic replacement of degraded layer silicates (particularly clay minerals) is the major process of glauconite formation. The virtual absence of clay minerals in strongly-glauconitized samples indicates that this is also the

the nature of the source material are therefore the major factors that separate the two processes. This explains why glauconitization will proceed only in the early stages of development when the hardground is continually, or at least intermittently exposed on the seafloor, whereas phosphatization will predominate during the burial phase.

However, a continual anoxic environment cannot be envisaged either for the basal hardground or the overlying phosphorite since both contain ample evidence of an oxygen-dependent benthos. Suitable conditions might occur, however, within the microenvironments afforded by faecal pellets, foraminiferal shells and other bioclastic debris, and beneath organic coatings within burrows, on the hardground surface and on mineral grains within the overlying sediment. Furthermore, large-scale but intermittent anoxia probably occurred in the phosphorite just below the sediment/water interface but with individual events being destroyed by bioturbation during subsequent oxic phases (3.4.4). Long-term but not necessarily continual exposure of the hardgrounds and the attenuated nature of the overlying phosphorite provides a further factor - time - during which these processes could operate and produce recognisable lithological changes. Thus it is not cementation itself that leads to mineralization but the environment that accompanies and post-dates its initiation.

## 4.6 Conclusions

(1) Chalks are dominantly composed of low-Mg calcite, carbonate-fluorapatite, $\alpha$-quartz, glauconite, goethitic-iron and clay minerals. Proportions vary considerably with lithofacies; even in phosphatic chalks, apatite is usually subordinate to calcite, but the former is at least the second most abundant mineral in all facies.

(2) Lithification is geochemically discernible ~90 cm below the surface of basal hardgrounds. The calcite cement of the hardgrounds shows slight enrichment in Fe, Mn and Mg but is depleted in Sr compared to white chalks.

(3) Factor analysis demonstrates that four main factors control element distributions in white, hardground and phosphatic chalks :

(a) carbonate-fluorapatite,

(b) clay minerals and silica,

(c) lithification,

(d) iron minerals (dominantly goethite).

(4) White chalks are geochemically similar to modern coccolith oozes but hardgrounds have been synsedimentarily lithified by the addition of a primary low-Mg calcite cement.

(5) Glauconitization was generally restricted to replacement of clay minerals during the early stages of hardground development while lithified carbonate remained in contact with seawater.

(6) Phosphatization occurred by the replacement of low-Mg calcite during burial of the hardground by an organic-rich sediment. Mineralization was intimately related to organic decay which produced suitable geochemical conditions for replacement and precipitation.

# Chapter 5 : Belemnite palaeobiology


| | | |
|---|---|---|
| 5.1 | Introduction | 387 |
| 5.2 | Stratigraphy | 387 |
| | 5.2.1 Sample location | 387 |
| | 5.2.2 Belemnite biostratigraphy | 388 |
| 5.3 | Biometry of Gonioteuthis from phosphatic chalks | 390 |
| | 5.3.1 Statistical methods | 390 |
| | a. Guard morphology | 393 |
| | b. Univariate analysis | 393 |
| | c. Ratios | 394 |
| | d. Bivariate analysis | 395 |
| | 5.3.2 Results | 395 |
| | a. Ratios | 401 |
| | b. Regression analysis | 401 |
| | c. Length of guard (x) versus depth of pseudoalveolus (y) | 403 |
| | d. Analytical summary and comparisons | 407 |
| | e. Factor analysis | 410 |
| 5.4 | Taphonomy and depositional environment | 411 |
| 5.5 | Facies and ecology | 414 |
| 5.6 | Stratigraphical and environmental controls | 416 |
| 5.7 | Conclusions | 418 |

## 5.1 Introduction

Belemnites occur throughout the Santonian to early Campanian sequences of the Anglo-Paris Basin, their rarity may be measured, however, by the observations of Rowe (1908 p.311) who obtained only 10 specimens of Gonioteuthis from the entire Campanian section on the Isle of Wight during more than two months intensive collecting. Similarly, Brydone (1914) states that only 13 accurately located and identifiable specimens of Gonioteuthis had hitherto been recorded from the Chalk of Hampshire and Sussex. The infrequency of belemnites in soft white chalks of this age has been noted by other authors in successions outside the Anglo-Paris Basin (e.g. Ernst, 1964; Christensen, 1976b). Belemnites, in particular Gonioteuthis and Actinocamax verus Miller are, however, frequent and at some levels extremely abundant in the phosphatic chalk lithofacies (Chapter 2). Consequently, while the sporadic occurrence of belemnites in soft white chalks has led to the inapplicability of population analysis, material from phosphatic chalks provides a unique opportunity to examine accurately located 'populations', rather than isolated specimens.

## 5.2 Stratigraphy

### 5.2.1 Sample location

Despite the relative abundance of fauna at certain levels within phosphatic chalks, little information has been published on their macrofauna, although short faunal lists and descriptions are provided by Leriche (1908, 1911). The common occurrence of G. ex gr. quadrata in the upper portion of phosphatic chalks has been noted previously by several authors (Lasne, 1902; Gosselet, 1901b; de Grossouvre, 1894a, 1899, 1901, 1907; Leriche, 1908, 1911).

A large 'population' of over 200 guards was collected by me in 1977 - 78 from Hardivillers quarry (2.8.1). This material, which forms the bulk of the guards examined in this section, originated from the Hardivillers Gonioteuthis Bed in the NE quarry (bed H5/2). This bed yielded 270 specimens (CUM KZ6001 - KZ6270) of which 136 were complete guards. All of the material utilised in the

present study has been deposited in the Oxford University Museum (OUM). A second 'population' was collected from Ribemont quarry (2.9.1). Here the uppermost phosphatic chalk (bed R1/6) yielded 174 specimens (OUM KZ6281 - KZ6455) of which 73 are near-complete guards. The phosphorite overlies the Ribemont Gonioteuthis Hardground which has a bow-shaped cross-section in the central upper portion of the quarry face. This is interpreted as a synsedimentary depression in the surface of the hardground, which has important consequences when considering the stratinomy of the belemnites (5.3.2). A final 'population' was collected from Villers-devant-le-Thour (2.10.1). At the eastern side of Le Tremblot quarry the phosphatic chalk contains a basal unit of large (up to 10 cm) phosphatized intraclasts (bed V2/2) and abundant G. ex gr. quadrata. This was the source of the 69 guards (OUM KZ6480 - KZ6549), including 24 near-complete examples, analysed here. Additional comparative material was collected from throughout the succession at Beauval (2.3.2 - several specimens), Faucouzy (2.9.2 - KZ6601 from a minor phosphatic chalk intercalacted within the upper white chalk; no bed number) and Nurlu (2.5.2 - KZ6788, KZ6801 from the phosphatic chalk of the basal lag, bed N3/1) quarries.

### 5.2.2 Belemnite biostratigraphy

Four genera of belemnite occur in the Santonian to early Campanian deposits of the Anglo-Paris Basin. These are Actinocamax Miller 1829, Belemnellocamax Naidin 1964, Gonioteuthis Bayle 1879 and Belemnitella d'Orbigny 1840. Of the four genera, Belemnitella is restricted to one species - B. praecursor Stolley, Belemnellocamax to one group, B. ex gr. grossouvrei (Janet) and Actinocamax also to one species - A. verus Miller. The genus Gonioteuthis, on the other hand, is represented by an evolutionary lineage of six species and is consequently the most stratigraphically useful of the four genera.

The genus Gonioteuthis has been studied in detail by Stolley (1897, 1916, 1930), Ernst (1963a, b, 1964, 1966, 1968), Ernst and Schultz (1974) and Christensen (1971, 1973, 1975a, b). The genus consists of the evolutionary lineage - Gonioteuthis westfalica (Schlüter) (oldest), G. westfalicagranulata

(Stolley), G. granulata (Blainville), G. granulataquadrata (Stolley), G. quadrata quadrata (Blainville) and G. quadrata gracilis (Stolley) (youngest) and is an outstanding example of phyletic gradualism (Christensen, 1976b). The Gonioteuthis stock extended from the middle Coniacian to the summit of the early Campanian, a period of 10 million years (Van Hinte, 1976). The genus shows three main trends during its evolution:

(1) Progressive calcification of the anterior portion of the guard which evolves from a convexly conical, flat or shallow alveolus in G. westfalica to a deep pseudoalveolus constituting up to one-third of the length of the guard in specimens of G. q. quadrata.

(2) The development of granulation, which is non-existent or poorly developed in specimens of G. westfalica but is pronounced in G. granulata and stratigraphically younger species.

(3) Increasing size and stoutness of the guard which reaches a maximum with G. granulataquadrata and early forms of G. q. quadrata.

G. westfalica is further isolated from the other species by its greater variation in guard shape and oval to pointed anterior cross-section as compared to subrectangular to subquadrate in later species. The evolution of G. q. gracilis during the latest early Campanian marks a reversal of some of the general trends with the return of slimmer, shorter guards and shallower pseudoalveoli. The species does, however, remain distinct by the continued prominence of granulation and the presence of a notched pseudoalveolus (Ernst in Christensen, 1975a p.37).

De Grossouvre (1894a, 1899, 1901, 1907) suggested a three-fold division of French phosphatic chalks based on his observations at Hardivillers. He dates the lowest phosphatic chalk at that locality as early Santonian Micraster coranguinum Zone , a conclusion that is consistent with the foraminiferal evidence (Biozone e, Tabatabai", 1977). His lower unit was typified by M. coranguinum Leske and A. verus, the middle unit by G. ex gr. quadrata and Offaster pilula and the upper unit by G. ex gr. quadrata and Belemnitella 'mucronata'. The overlying upper white chalk also contains the latter two species together with M. pseudoglyphus de Grossouvre (de Grossouvre op cit.).

This general classification has been confirmed, with some additional details. G. granulata has previously been identified from a small number of localities (Leriche, 1908) and certainly this belemnite is present in the lowest phosphatic chalk at Beauval and Nurlu, furthermore, fragments of Gonioteuthis have been collected from a similar level at Hardivillers. De Grossouvre's (op cit.) record of B. mucronata (Schlottheim) is regarded as a misidentification of B. praecursor (Fig. 5.1, nos. 1 - 3, 9), which forms a minor element of the belemnite fauna in the Hardivillers Gonioteuthis Bed (3%) and in the uppermost phosphatic chalk at Ribemont (4%).

A. verus (Fig. 5.1, nos. 10 - 13) is the commonest belemnite in the lowest phosphatic chalk at Beauval, Hardivillers and Nurlu but proportions and relative abundances vary. At Nurlu fifty fragments and seven complete A. verus (KZ6733 - KZ6738, KZ6763; Fig. 5.1, nos. 10, 11), and a well-preserved guard of G. granulata (KZ6788; Fig. 5.1, num. 7) were collected from the lag on top of the basal hardground, yet at Beauval despite the larger fauna collected, no belemnites were found in the basal lag on the floor of the quarry. In the lowest phosphatic chalk at the top of the Beauval overfold (bed B3/4), however, five specimens of A. verus (KZ6552 - KZ6556; Fig. 5.1, nos. 12, 13) and one G. granulata (KZ6551; Fig. 5.1, nos. 4 - 6, 8) were recovered. Belemnellocamax ex gr. grossouvrei has been described from phosphatic chalks (de Grossouvre, 1894a, 1899, 1901, 1907; Leriche, 1908, 1911) but despite the collection of several hundred belemnites, no examples of this species were recovered by me. De Grossouvre (op cit.) suggests that this belemnite is typical of the lower portions of phosphatic chalks.

## 5.3 Biometry of Gonioteuthis from phosphatic chalks

### 5.3.1 Statistical methods

The variation within belemnite 'populations' and their identification has been based on a series of univariate and bivariate statistics, histograms and scattergrams similar to those applied by Christensen (1970, 1971, 1973, 1974, 1975a, 1976a) and Christensen et al. (1975). Most statistical parameters were

Fig. 5.1 Phosphatic chalk belemnites I.
Nos. 1 - 3. Belemnitella praecursor Stolley, from the Hardivillers Gonioteuthis Bed, low Campanian Offaster pilula Zone. The anterior portion of the guard KZ6272 is missing. 1. dorsal, 2. left lateral, 3. ventral views, all x 1.
Nos. 4 - 6. Gonioteuthis granulata (Blainville). Lower phosphatic chalk, Beauval, low - mid Santonian Micraster coranguinum Zone. The specimen is coated in a thin shiny phosphate patina, typical of basal lag preservation. Granulation is minimal. KZ6551. 4. dorsal, 5. left lateral, 6. ventral views, all x 1.
Num. 7. Gonioteuthis granulata (Blainville). Base of phosphatic chalk, Nurlu, low - mid Santonian M. coranguinum Zone. Anterior end of specimen KZ6788 with a pronounced rhombohedral anterior cross-section. Note the concentric growth rings, x 1.5.
Num. 8. Gonioteuthis granulata (Blainville). Anterior view of KZ6551 (nos. 4 - 6). The guard has a circular cross-section. Note the shallow pseudoalveolus, x 1.5.
Num. 9. Belemnitella preaecursor Stolley. Uncoated right lateral view of KZ6272 (nos. 1 - 3). The specimen is honeycombed by Entobia cretacea Portlock, a clionid sponge boring. The fine (0.15 - 0.50 mm) surface pores can be seen in nos. 1 - 3, x 1.
Nos. 10 - 13. Actinocamax verus Miller. Base of phosphatic chalk, Nurlu (nos. 10, 11) and lower phosphatic chalk, Beauval (nos. 12, 13). Low - mid Santonian M. coranguinum Zone. 10. KZ6738, left lateral view of a juvenile guard, x 2. 11. KZ6736, left lateral view of an adult guard, x 2. 12. left lateral and 13. ventral views of a large specimen, KZ6556. Note surface wrinkling and tapering, pyramidal anterior termination to the guard, x 2.

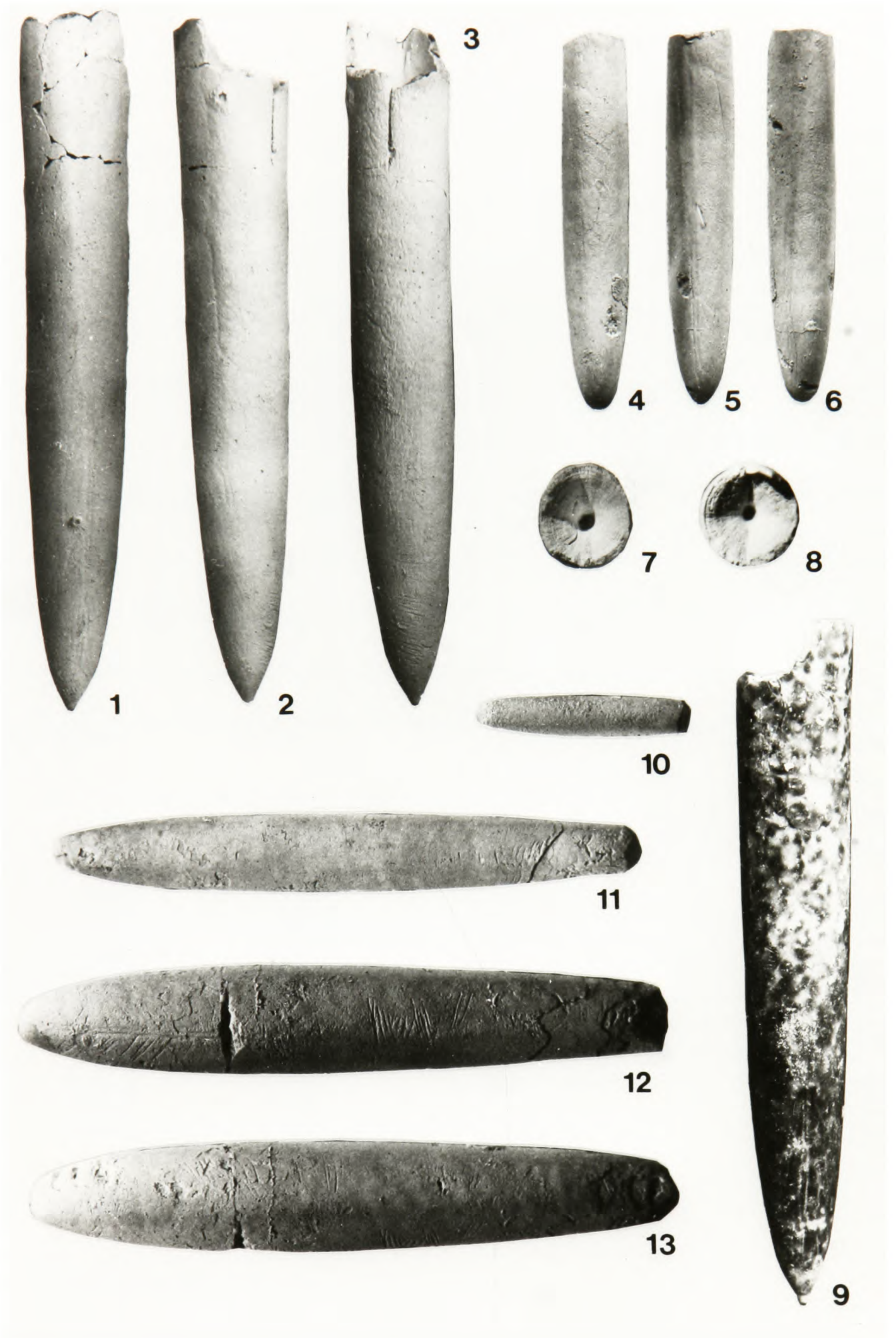
1
2
3
4
5
6
7
8
9
10
11
12
13

calculated utilising an SPSS (Statistical Package for the Social Sciences) version 7.0 package on an ICL 2980 computer. Statistical formulae are presented in Appendix 2.

5.3.1a Guard morphology

The following characters (Fig. 5.2) were measured: total length of guard (L), depth of the pseudoalveolus (D), dorso-ventral diameter at the alveolar end (DVDAE), lateral diameter at the alveolar end (LDAE) and maximum lateral diameter (MLD). Measurements were made with a vernier caliper to an accuracy of 0.1 mm. A number of other parameters e.g. length of ventral fissure, have been measured by previous authors, but these have been found to be of little taxonomic value and have therefore been ommited. A small number of specimens were split to study the internal characteristics of the guard (method in Christensen, 1971 p.370) but since internal characters are of limited diagnostic use in the genus Gonioteuthis, no measurements were made on split material.

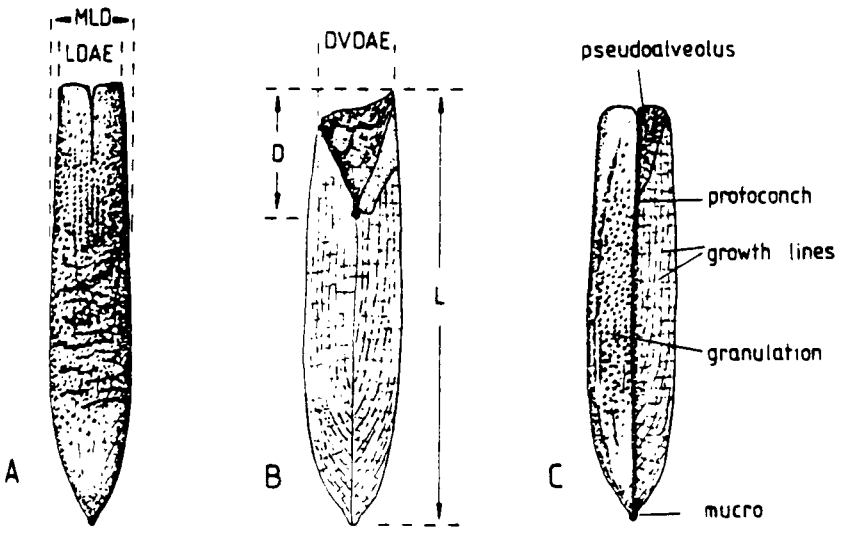


Fig. 5.2 Diagram showing the morphological elements of the Gonioteuthis guard.
A. Ventral view, B. Left lateral view of a ground guard. C. Cut-away dorsal view. MLD = maximum lateral diameter; LDAE = lateral diameter at the alveolar end; D = depth of pseudoalveolus; L = length of guard; DVDAE = dorso-ventral diameter at the alveolar end.

5.3.1b Univariate analysis

The following statistics were estimated: the arithmetic mean ($\bar{X}$), standard deviation (SD) and coefficient of variation (CV). Histograms of two of the five characters (L , D) are shown in Fig. 5.3. The frequency distributions were tested for normality using the Kolmogorov-Smirnov one sample test for goodness of fit. Clearly the univariate statistics of 'size' parameters can be effected by a large number of factors including sampling bias and post-mortem sorting, furthermore a sample commonly contains an indeterminate number of juveniles

(cf. Kermack, 1954 p.391) and in belemnites, as in Recent coleoids (Cousteau and Diolé, 1973 p.93), there are no criteria for determining the ontogenetic stage of an individual (Christensen, 1975a). Nevertheless, the values may be of interpretive value, although bivariate statistics are regarded as being of greater taxonomic significance.

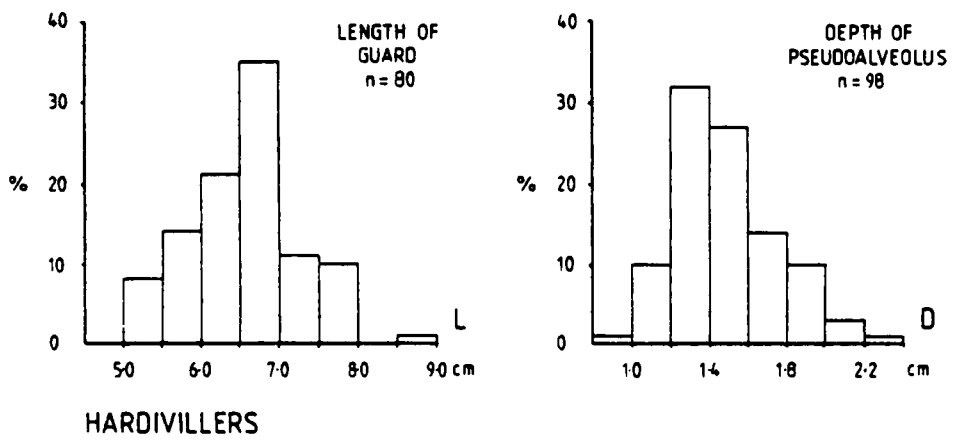


Fig. 5.3 Histograms of length of guard (L) and depth of pseudoalveolus (D) of Gonioteuthis from the Hardivillers Gonioteuthis Bed.

5.3.1c Ratios

Ratios of 'size' parameters have been widely used in the study of belemnites. Ernst (1963a, b, 1964, 1966, 1968), in particular, characterised his samples of Gonioteuthis by mean values of various ratios, the most diagnostic of which were the Riedel-Quotient (ratio of length of guard to depth of the pseudoalveolus) and the Schlanksheits-Quotient (ratio of length of guard to dorso-ventral diameter at the alveolar end). Numerous authors (e.g. Shaw, 1956; Simpson et al., 1960; Sokal, 1965; Sokal and Rohlf, 1969) have criticised the use of ratios. The main objections are that a ratio is a secondary statistic with greater variance than either of its components, that ratios may not be normally distributed and lastly that if the relationship between the characters is allometric, the ratio will change during growth. Despite these mathematical limitations, Ernst's Gonioteuthis stratigraphy based on mean Riedel-Quotient is generally valid, since the relationship between length of guard and depth of pseudoalveolus is isometric in nearly all samples of Gonioteuthis (Christensen, 1975a, b) and furthermore the ratio has been found to be approximately normally distributed in the present study. Consequently, Riedel-Quotients (RQ) are reported for each sample.

5.3.1d Bivariate analysis

The five 'size' parameters and the Riedel-Quotients were correlated utilising Pearson correlation matrices. Regression analysis was used to study the relationship between variable pairs during growth. Regression lines were fitted by the least-squares method primarily because of the ability to compare the slope and intercept of different samples (see Christensen, 1973 p.115 - 116 for discussion). The regression line is written $y = a + bx$ and the original measurements were used because of their rectilinear trend on arithmetically-scaled scatterplots. The following statistical parameters were calculated (see Appendix 2 for details): the percentage of the variance explained by the linear relationship ($r^2$), the standard error of the y-intercept ($SE_a$), the standard error of the slope ($SE_b$), the standard error of the regression line ($SE_{yx}$), and the value of t ($t_a$) and the associated probability calculated by t-testing the intercept on the y-axis to test whether the intercept differed significantly from zero (Hald, 1957). This final test has important biological implications since only a regression line passing through the origin represents isometric growth (ie. $y = bx$). Other possible equations ($y = a + bx$; $y = bx^a$) represent allometric growth (the latter equation is often refered to as simple allometry e.g. Christensen, 1975a). The regression lines were compared with each other, and with comparable 'populations' from Germany, by the methods described by Hald (1957 p.571 - 579).

5.3.2 Results

The results of the univariate statistical analyses of the three 'populations' are given in Table 5.1. Although histograms of the various 'size' parameters show a slight asymmetry (Fig. 5.3), statistical analysis utilising the Kolmogorov-Smirnov one sample test (Table 5.2) shows that all characters in all three 'populations' correspond well to a normal distribution. It was noted, however, that the probability associated with the length of guard for the Ribemont 'population' was considerably lower than that for the other two samples. Although no further specimens were available for detailed measurement, two

HARDIVILLERS

| Character | N | $\bar{X}$ | $\sigma$ | CV | OR |
|---|---|---|---|---|---|
| L | 80 | 6.537 | 0.701 | 10.72 | 5.00-8.67 |
| D | 98 | 1.475 | 0.257 | 17.42 | 0.93-2.26 |
| DVDAE | 94 | 1.032 | 0.158 | 15.31 | 0.71-1.45 |
| LDAE | 94 | 0.955 | 0.148 | 15.50 | 0.63-1.37 |
| MLD | 86 | 1.099 | 0.168 | 15.29 | 0.74-1.61 |
| RQ | 79 | 4.437 | 0.531 | 11.97 | 3.38-6.08 |

RIBEMONT

| Character | N | $\bar{X}$ | $\sigma$ | CV | OR |
|---|---|---|---|---|---|
| L | 12 | 6.303 | 0.678 | 10.76 | 5.43-7.21 |
| D | 10 | 1.608 | 0.322 | 20.02 | 1.15-2.11 |
| DVDAE | 5 | 1.162 | 0.134 | 11.53 | 1.05-1.38 |
| LDAE | 9 | 1.091 | 0.140 | 12.83 | 0.87-1.29 |
| MLD | 12 | 1.148 | 0.159 | 13.85 | 0.90-1.40 |
| RQ | 10 | 4.038 | 0.539 | 13.35 | 3.33-4.92 |

VILLERS-DEVANT-LE-THOUR

| Character | N | $\bar{X}$ | $\sigma$ | CV | OR |
|---|---|---|---|---|---|
| L | 8 | 6.749 | 0.603 | 8.93 | 5.94-7.62 |
| D | 10 | 1.649 | 0.300 | 18.19 | 1.23-2.05 |
| DVDAE | 9 | 1.256 | 0.196 | 15.61 | 0.91-1.52 |
| LDAE | 10 | 1.134 | 0.164 | 14.46 | 0.83-1.35 |
| MLD | 9 | 1.194 | 0.155 | 12.98 | 0.97-1.39 |
| RQ | 8 | 4.074 | 0.445 | 10.92 | 3.59-4.88 |

TABLE 5.1 Univariate analyses of the 'size' parameters of three 'populations' of Gonioteuthis from phosphatic chalks.

HARDIVILLERS

| Character | N | D | Probability |
|---|---|---|---|
| L | 80 | 0.0620 | 0.92 |
| D | 98 | 0.0783 | 0.59 |
| DVDAE | 94 | 0.0777 | 0.62 |
| LDAE | 94 | 0.0863 | 0.49 |
| MLD | 86 | 0.0559 | 0.95 |
| RQ | 79 | 0.1033 | 0.37 |

RIBEMONT

| Character | N | D | Probability |
|---|---|---|---|
| L | 12 | 0.2480 | 0.45 |
| D | 10 | 0.1384 | 0.99 |
| DVDAE | 5 | 0.2175 | 0.97 |
| LDAE | 9 | 0.1984 | 0.87 |
| MLD | 12 | 0.1075 | 1.00 |
| RQ | 10 | 0.1701 | 0.94 |

VILLERS-DEVANT-LE-THOUR

| Character | N | D | Probability |
|---|---|---|---|
| L | 8 | 0.1964 | 0.92 |
| D | 10 | 0.1324 | 1.00 |
| DVDAE | 9 | 0.1075 | 1.00 |
| LDAE | 10 | 0.0933 | 1.00 |
| MLD | 9 | 0.1395 | 1.00 |
| RQ | 8 | 0.2534 | 0.68 |

TABLE 5.2 Results of the Kolmogorov-Smirnov one sample test for goodness of fit to a normal distribution for three 'populations' of Gonioteuthis from phosphatic chalks.

parameters, length of guard and maximum lateral diameter, could be measured to a lower precision (± 0.25 and ± 0.05 cm respectively) on a further forty-three guards. The resulting histograms (Fig. 5.4) are strongly bimodal, a K-S test giving D statistics of 0.1958 (P = 0.03) and 0.1891 (P = 0.04) respectively, both of which are significant at the 0.05 level. The mean length of the guards studied in detail from Ribemont is 6.30 cm, a value that lies in the trough between the two modes of the larger sample, indicating that the 'population' studied in detail is a mixture of two distinct components.

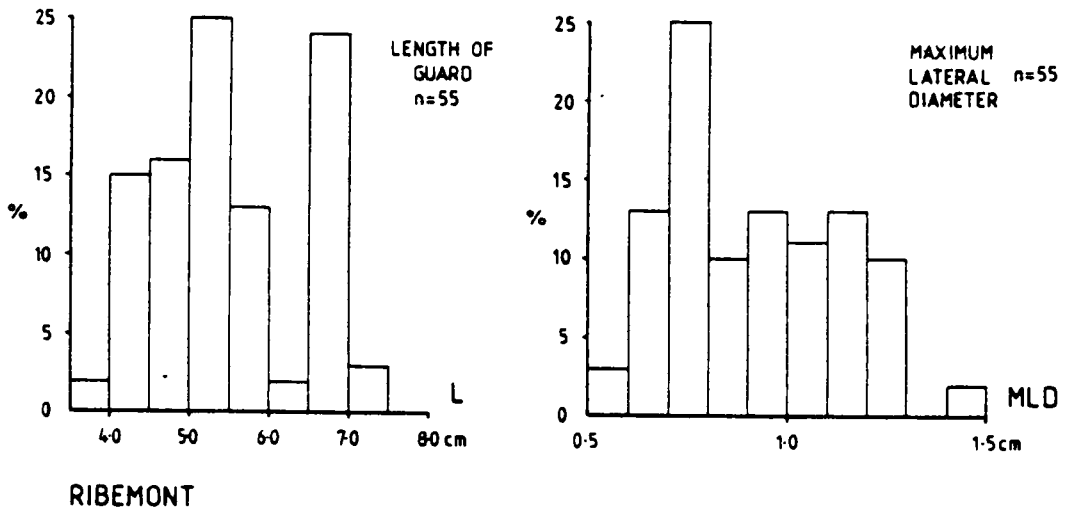


Fig. 5.4 Histograms of length of guard (L) and maximum lateral diameter (MLD) of Gonioteuthis from the phosphatic chalk overlying the Ribemont Gonioteuthis Hardground.

All three samples, like Gonioteuthis 'populations' collected from other facies (e.g. Christensen, 1974 p.5, 1975 p.32), are presumable an accumulation of several generations and consist of a growth series which contains both juveniles and adults (Fig. 5.5 nos. 1 - 15). The approximation of the length of guard size-distributions to normality results in mean length roughly corresponding to the size which most specimens had reached when they died. This is not true of the Ribemont sample which shows two mortality peaks - around 5.0 and 6.8 cm. The second of these two maxima approximating to the mortality peaks of the 'populations' from Hardivillers and Villers-devant-le-Thour (Table 5.1) and from the low Campanian O. pilula Zone of SW Münsterland (Ernst, 1964 p.126); material from Hover in Lower Saxony (Ernst, 1964 p.132) has a lower mean length, approximately 6.0 cm, at this level. Comparisons with Ernst's results must be treated with caution, however, since he has sorted out specimens of less than 4.0 cm length.

The smallest guard for which detailed measurements were obtained comes

Fig. 5.5 Phosphatic chalk belemnites II.
Nos. 1 - 15 Gonioteuthis quadrata quadrata (Blainville) from the Hardivillers Gonioteuthis Bed, low Campanian Offaster pilula Zone. 1 - 3. a medium-sized guard of average shape, KZ6040, dorsal, left lateral and ventral views x 1. 4. split anterior end of KZ6099 showing conellae x 1. 5 - 7. an adolescent guard, KZ6033, the smallest complete specimen recovered from the bed, dorsal left lateral and ventral views x 1. 8. anterior end of KZ6066 (nos. 13 - 15) showing the depth of the pseudoalveolus x 1.5. 9. anterior end of KZ6040 (nos. 1 - 3) x 1.5. 10 - 12. the largest specimen collected, KZ6039, dorsal, left lateral, and ventral views x 1. 13 - 15. the stoutest individual in the 'population', KZ6066, dorsal, left lateral and ventral views x 1.


1


2


3


4


5


6


7

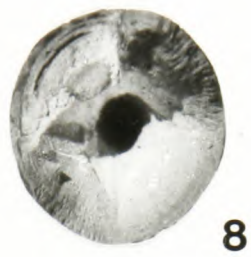
8


9


10


11


12


13


14


15

from Hardivillers and has an overall length of 5.00 cm (Fig. 5.5 nos. 5 - 7); the smallest specimens from Ribemont lie within the range 3.5 - 4.0 cm. A number of guards with damaged pseudoalveoli and lengths of <5.00 cm were also collected from Hardivillers but the proportion of individuals within this size range is small. The rarity of small guards in most samples and the total absence of guards of less than 3.5 cm in length may be attributed to the interaction of low juvenile mortality rate and high initial growth rate. Such an interaction will also control the shape of the size frequency distributions (Craig, 1967; Surlyk, 1972). The means of 'size' parameters of samples of Gonioteuthis have been used successfully for the analysis of time trends in evolutionary lineages (Ernst, 1964) and similar studies have been applied to A. verus (Reyment and Naidin, 1962) but such studies are only viable with normally distributed characters. Since the mortality peak for early Campanian Gonioteuthis is apparently between 6.5 and 6.8 cm in length, the lower mortality peak of the Ribemont sample requires explanation. There are several possible interpretations which include:

(1) the peaks represent different species,

(2) 'size' parameter distributions are normally bimodal for 'populations' of Gonioteuthis,

(3) the 'population' has been current sorted or

(4) bimodality is the result of a catastrophic event.

There is no morphological evidence to support the occurrence of more than one species of Gonioteuthis within the Ribemont 'population', however, stratigraphically close but specifically distinct Gonioteuthis 'populations' would, once mixed, be impossible to separate on morphological criteria alone. No Gonioteuthis 'population' has been described with a mean length as low as 5.0 cm and with appropriate mean Riedel-Quotient, but it should be noted that the value for G. q. gracilis from Misburg (Ernst, 1964) does approach this value. Thus the possibility of specific mixing in the Ribemont phosphatic chalk cannot be totally dismissed although it is, in my opinion, unlikely.

Bimodality of 'size' parameters may result from annual or biannual mortality peaks of a species but since no other 'population' exhibits a bimodal

distribution it must be concluded that such an explanation is invalid. Current sorting may lead to a reduction rather than an enhancement of the proportion of juveniles within a population but transport of smaller individuals into the area of deposition remains a possibility. Bimodal distributions of this type frequently result from catastrophic events which cause the death of abnormally young 'populations' which are overprinted on the normal mortality curves. A storm deposit is the commonest example although Red Tides provide a further possibility. The concentration of fauna into what is apparently a depression in the hardground accords most favourably with the storm-event hypothesis.

On the basis of univariate analysis the samples of Gonioteuthis from Hardivillers and Villers-devant-le-Thour may be considered homogenous while the 'population' from Ribemont is heterogenous. Consequently, interpretations made from the bivariate analysis of the small number of complete specimens available from this latter locality can only be regarded as tentative.

5.3.2a Ratios

In general ratios have not been utilised in the present study but the validity of the Riedel-Quotient is recognised (see above) as a method of speciation of specimens of Gonioteuthis. Mean values of the Quotient for all three 'populations' (Table 5.1) lie within the range of values for G. q. quadrata (Ernst, 1964, 1968) but individual specimens from Hardivillers (Fig. 5.5, nos. 1 - 15) may be refered to G. granulata (one specimen only), G. granulataquadrata, G. q. quadrata or G. q. gracilis. Specimens from the other two localities may all be identified as either G. granulataquadrata or G. q. (or possibly G. q. gracilis). This range of possible 'species' within a single bed illustrates the importance of the study of 'populations' rather than individuals for the reliable identification of Gonioteuthis species.

5.3.2b Regression analysis

All five 'size' parameters and the Riedel-Quotient were compared by means of Pearson correlation matrices (Table 5.3). The correlation coefficients

HARDIVILLERS

| | L | D | DVDAE | LDAE | MLD | RQ |
|---|---|---|---|---|---|---|
| L | 1.000 | | | | | |
| D | 0.763 | 1.000 | | | | |
| DVDAE | 0.839 | 0.808 | 1.000 | | | |
| LDAE | 0.825 | 0.810 | 0.980 | 1.000 | | |
| MLD | 0.814 | 0.711 | 0.955 | 0.940 | 1.000 | |
| RQ | -0.219 | -0.786 | -0.434 | -0.426 | -0.334 | 1.000 |

RIBEMONT

| | L | D | DVDAE | LDAE | MLD | RQ |
|---|---|---|---|---|---|---|
| L | 1.000 | | | | | |
| D | 0.773 | 1.000 | | | | |
| DVDAE | 0.870 | 0.923 | 1.000 | | | |
| LDAE | 0.817 | 0.785 | 0.985 | 1.000 | | |
| MLD | 0.800 | 0.631 | 0.992 | 0.952 | 1.000 | |
| RQ | -0.344 | -0.850 | -0.877 | -0.530 | -0.287 | 1.000 |

VILLERS-DEVANT-LE-THOUR

| | L | D | DVDAE | LDAE | MLD | RQ |
|---|---|---|---|---|---|---|
| L | 1.000 | | | | | |
| D | 0.916 | 1.000 | | | | |
| DVDAE | 0.720 | 0.854 | 1.000 | | | |
| LDAE | 0.794 | 0.900 | 0.970 | 1.000 | | |
| MLD | 0.916 | 0.900 | 0.946 | 0.959 | 1.000 | |
| RQ | -0.717 | -0.931 | -0.853 | -0.943 | -0.906 | 1.000 |

TABLE 5.3 Pearson correlation matrices of the 'size' parameters of three 'populations' of Gonioteuthis from phosphatic chalks

for the Hardivillers 'population' were all highly significant ($P < 0.001$) except for the correlation between L and RQ which were less significant ($P < 0.03$). Probabilities associated with matrices from other localities were generally higher although all correlations remained significant at the 0.05 level in the Villers-devant-le-Thour sample and only probabilities associated with RQ were not significant at this level for the Ribemont sample.

Since all five 'size' parameters are very closely related, four regression analyses were made for each 'population'. The plots chosen follow the useage of Christensen (1975a):

(1) length of guard (x) versus depth of pseudoalveolus (y),

(2) length of guard (x) versus dorso-ventral diameter at the alveolar end (y),

(3) dorso-ventral diameter at the alveolar end (x) versus lateral diameter at the alveolar end (y),

(4) maximum lateral diameter (x) versus lateral diameter at the alveolar end (y).

With three exceptions (Table 5.5) the relationships of the characters in the twelve analyses were isometric.

5.3.2c Length of guard (x) versus depth of pseudoalveolus (y)

A regression analysis of these two characters provides an analogous but more comprehensive quantity than Ernst's Riedel-Quotient and is specifically the most diagnostic of the four regression analyses, partly because of the greater number of comparative analyses in the literature (e.g. Christensen, 1971, 1973, 1975a). Christensen (1975a) has published regression analyses of Ernst's (1964, 1968) original measurements of six species of Gonioteuthis. The statistical parameters for these six 'populations' are given in Table 5.4 and the regression lines plotted on the relevant scattergrams (Figs. 5.6 - 5.8).

Hardivillers. The statistical parameters are given in Table 5.5 and the values plotted on Fig. 5.6A. The 'population' was compared to G. granulataquadrata and was found to differ significantly in slope ($0.01>P>0.001$). A comparison with G. q. quadrata from the low Campanian Inoceramus ex gr. lingua - G. ex gr. quadrata Zone of Hover" gave a significant correlation between slopes ($0.70>P>0.60$) but the position of the lines are different ($P<0.001$). However, when compared with a stratigraphically younger 'population' of the same species (from the Echinocorys conica - Galeola papillosa Zone), the variances, slopes ($P>0.90$) and positions ($0.40>P>0.30$) of the lines were found to be the same. Similar results were obtained from a comparison with a 'population' of G. q. quadrata from the 'Smectite' of Hallembaye quarry in eastern Belgium (W.K. Christensen pers. comm.) where G. q. quadrata also occurs with B. praecursor. When compared to G. q. gracilis, the variances were found to differ significantly ($F = 2.2422$ with 77 and 45 degrees of freedom; $P = <0.01$), so the test for non-equal variances was used (Hald, 1957). The correspondence between the slopes of the two lines was found to be just significant ($0.10>P>0.05$ with 106 degrees of freedom) so the positions of the lines were also tested. The test gave a probability of $0.05>P>0.02$ with 122 degrees of freedom, which is not

G. westfalica westfalica from the lower 'westfalica beds', Essen-Vogelheim (Ernst, 1964a p.118; Christensen, 1975a p.38)
D = 0.1150 + 0.0597 L; N = 196; r = 0.2826; $r^2$ = 7.99%; $SE_a$ = 0.0828; $SE_b$ = 0.0145; $SE_{yx}$ = 0.1089; $t_a$ = 1.3882 (0.20>P>0.10)

G. westfalicagranulata from Bülten (Ernst, 1968 p.278; Christensen, 1975a p.38)
D = 0.0102 + 0.1106 L; N = 51; r = 0.4809; $r^2$ = 23.13%; $SE_a$ = 0.1611; $SE_b$ = 0.0279; $SE_{yx}$ = 0.1146; $t_a$ = 0.0633 (P>0.90)

G. granulata from Gleidingen (Ernst, 1968 p.278; Christensen, 1975a p.38)
D = 0.0701 + 0.1299 L; N = 45; r = 0.7311; $r^2$ = 53.45%; $SE_a$ = 0.0920; $SE_b$ = 0.0185; $SE_{yx}$ = 0.1083; $t_a$ = 0.7620 (0.50>P>0.40)

G. granulataquadrata from Weinberg (Ernst, 1968 p.278; Christensen, 1975a p.38)
D = 0.1030 + 0.1760 L; N = 45; r = 0.7404; $r^2$ = 54.82%; $SE_a$ = 0.1623; $SE_b$ = 0.0244; $SE_{yx}$ = 0.1370; $t_a$ = 0.6342 (0.60>P>0.50)

G. quadrata quadrata from the I. ex gr. lingua - G. ex gr. quadrata Zone of Hover (Ernst, 1964a p.119; Christensen, 1975a p.39)
D = -0.0888 + 0.2685 L; N = 24; r = 0.7982; $r^2$ = 63.71%; $SE_a$ = 0.2640; $SE_b$ = 0.0432; $SE_{yx}$ = 0.2166; $t_a$ = 0.3364 (0.80>P>0.70)

G. quadrata quadrata from the E. conica - G. papillosa Zone of Hover (measurements by Ernst, statistics after W.K. Christensen, pers. comm.)
D = -0.3776 + 0.2917 L; N = 65; r = 0.7649; $r^2$ = 58.51%; $SE_a$ = 0.1772; $SE_b$ = 0.0309; $SE_{yx}$ = 0.1711; $t_a$ = 2.0977 (0.05>P>0.02)

G. quadrata gracilis from the Germania IV quarry (north Germany) (Christensen, 1975a p.42)
D = -0.7641 + 0.3620 L; N = 47; r = - ; $r^2$ = - ; $SE_a$ = 0.1820; $SE_b$ = -0.0318; $SE_{yx}$ = 0.1152; $t_a$ = 4.1975 (P<0.001)

TABLE 5.4 Statistical relationship between depth of pseudoalveolus and length of guard for six species of Gonioteuthis from Germany. y = a + bx (modified from Christensen, 1975a).

HARDIVILLERS GONIOTEUTHIS BED

| y = a + bx | N | $r^2$ | $SE_a$ | $SE_b$ | $SE_{yx}$ | $t_a$ | Probability |
|---|---|---|---|---|---|---|---|
| D = -0.3784 + 0.2870 L | 79 | 58.20% | 0.1821 | 0.0277 | 0.1725 | 2.0775 | 0.05>P>0.02 |
| DVDAE = -0.1974 + 0.1933 L | 75 | 70.32% | 0.0961 | 0.0147 | 0.0882 | 2.0538 | 0.05>P>0.02 |
| LDAE = 0.0188 + 0.8978 DVDAE | 90 | 96.11% | 0.0202 | 0.0193 | 0.0290 | 0.9331 | 0.40>P>0.30 |
| LDAE = 0.0614 + 0.8264 MLD | 81 | 88.35% | 0.0377 | 0.0338 | 0.0510 | 1.6316 | 0.20>P>0.10 |

PHOSPHATIC CHALK ABOVE THE RIBEMONT GONIOTEUTHIS HARDGROUND

| y = a + bx | N | $r^2$ | $SE_a$ | $SE_b$ | $SE_{yx}$ | $t_a$ | Probability |
|---|---|---|---|---|---|---|---|
| D = -0.5653 + 0.3417 L | 10 | 59.76% | 0.6343 | 0.0991 | 0.2166 | 0.8913 | 0.40>P>0.30 |
| DVDAE = 0.1310 + 0.1604 L | 5 | 75.54% | 0.3404 | 0.0527 | 0.0768 | 0.3849 | 0.80>P>0.70 |
| LDAE = 0.1894 + 0.7665 DVDAE | 5 | 96.95% | 0.0918 | 0.0786 | 0.0211 | 2.0629 | 0.20>P>0.10 |
| LDAE = 0.0908 + 0.8526 MLD | 9 | 90.55% | 0.1231 | 0.1041 | 0.0459 | 0.7376 | 0.50>P>0.40 |

PHOSPHATIC CHALK, VILLERS-DEVANT-LE-THOUR

| y = a + bx | N | $r^2$ | $SE_a$ | $SE_b$ | $SE_{yx}$ | $t_a$ | Probability |
|---|---|---|---|---|---|---|---|
| D = -1.3240 + 0.4455 L | 8 | 83.90% | 0.5396 | 0.0797 | 0.1271 | 2.4536 | 0.05>P>0.02 |
| DVDAE = -0.4975 + 0.2556 L | 7 | 51.88% | 0.7578 | 0.1101 | 0.1476 | 0.6565 | 0.60>P>0.50 |
| LDAE = 0.1007 + 0.8331 DVDAE | 9 | 94.01% | 0.1009 | 0.0795 | 0.0440 | 0.9985 | 0.40>P>0.30 |
| LDAE = -0.0287 + 0.9533 MLD | 9 | 92.05% | 0.1167 | 0.1059 | 0.0463 | 0.2459 | 0.90>P>0.80 |

G. q. gracilis, GERMANIA IV QUARRY, NORTHERN GERMANY (CHRISTENSEN, 1975a)

| y = a + bx | N | $r^2$ | $SE_a$ | $SE_b$ | $SE_{yx}$ | $t_a$ | Probability |
|---|---|---|---|---|---|---|---|
| D = -0.7641 + 0.3620 L | 47 | - | 0.1820 | 0.0318 | 0.1152 | 4.1975 | P<0.001 |
| DVDAE = -0.2428 + 0.2003 L | 47 | - | 0.0693 | 0.0121 | 0.0583 | 3.5054 | 0.01>P>0.001 |
| LDAE = 0.0250 + 0.9064 DVDAE | 47 | - | 0.0253 | 0.0278 | 0.0290 | 0.9885 | 0.40>P>0.30 |
| LDAE = 0.0506 + 0.9055 MLD | 47 | - | 0.0299 | 0.0339 | 0.0351 | 1.6910 | 0.10>P>0.05 |

TABLE 5.5 Statistical results of regression analyses of four 'populations' of Gonioteuthis.

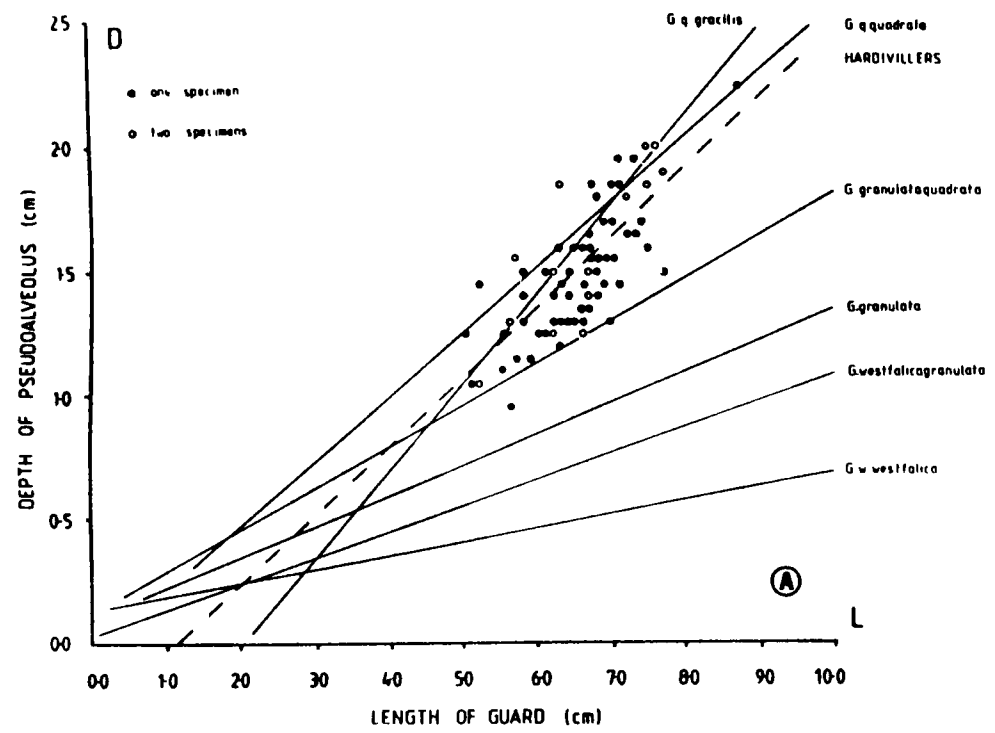


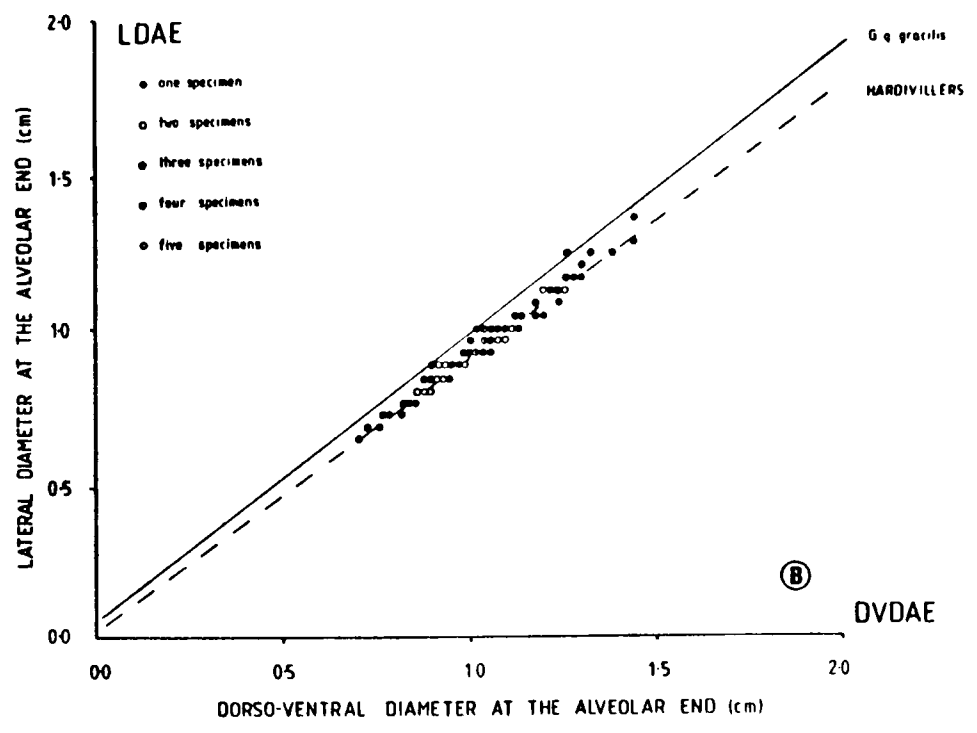


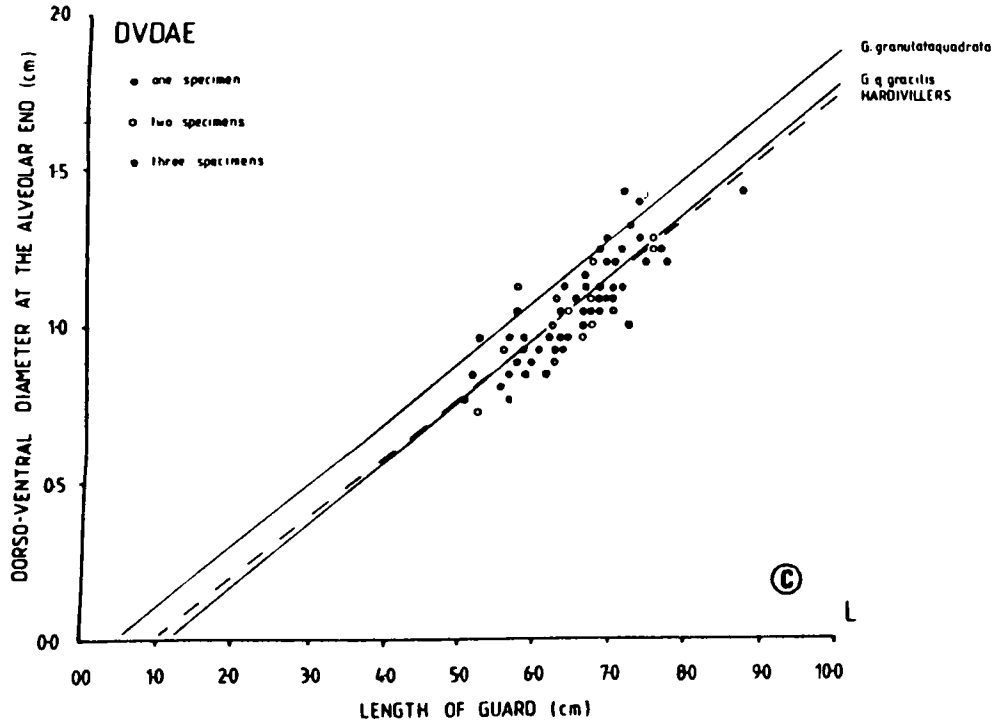


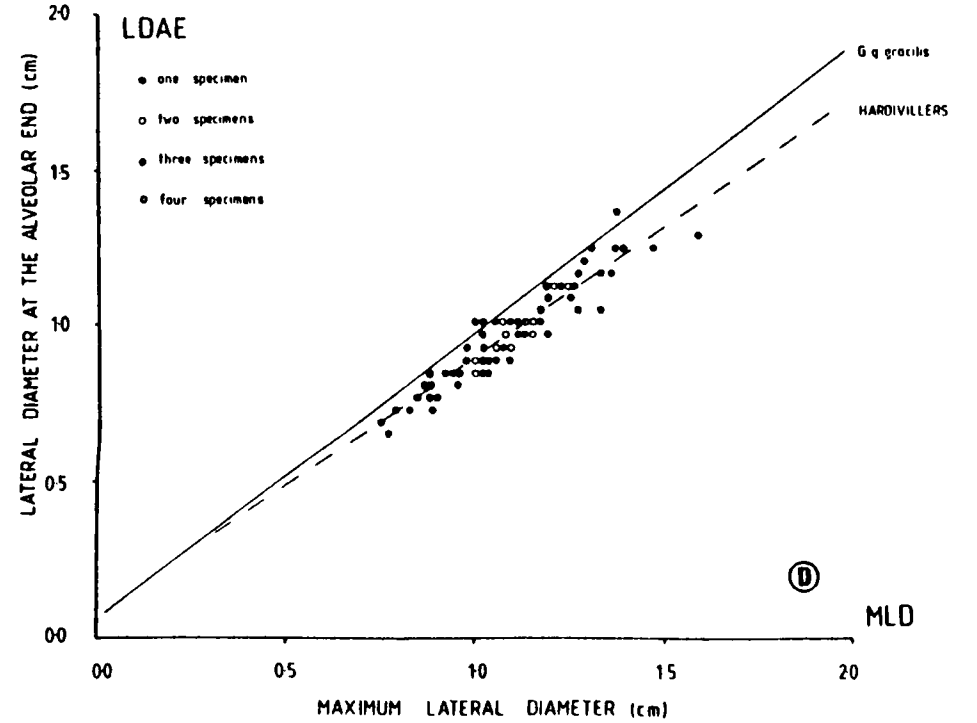


Fig. 5.6 Scatter diagrams and regression lines for G. q. quadrata from the Hardivillers Gonioteuthis Bed. A. length of guard (L) versus depth of pseudoalveolus (D); the regression lines of six control 'populations' from Germany (Christensen, 1975a) are plotted for comparison (the G. q. quadrata line is from the older Höver 'population'). B. dorso-ventral diameter at the alveolar end (DVDAE) versus lateral diameter at the alveolar end (LDAE); the regression line for G. q. gracilis is plotted for comparison. C. length of guard (L) versus dorso-ventral diameter at the alveolar end (DVDAE); the regression lines of G. granulataquadrata and G. q. gracilis are plotted for comparison. D. maximum lateral diameter (MLD) versus lateral diameter at the alveolar end (LDAE); the regression line of G. q. gracilis is plotted for comparison.

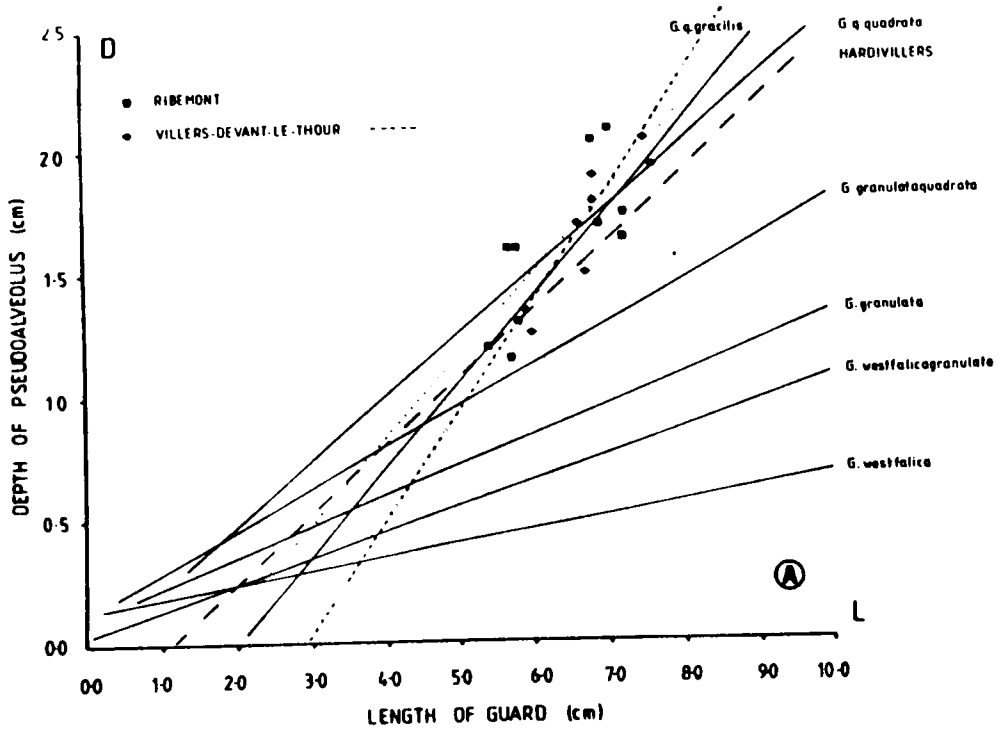


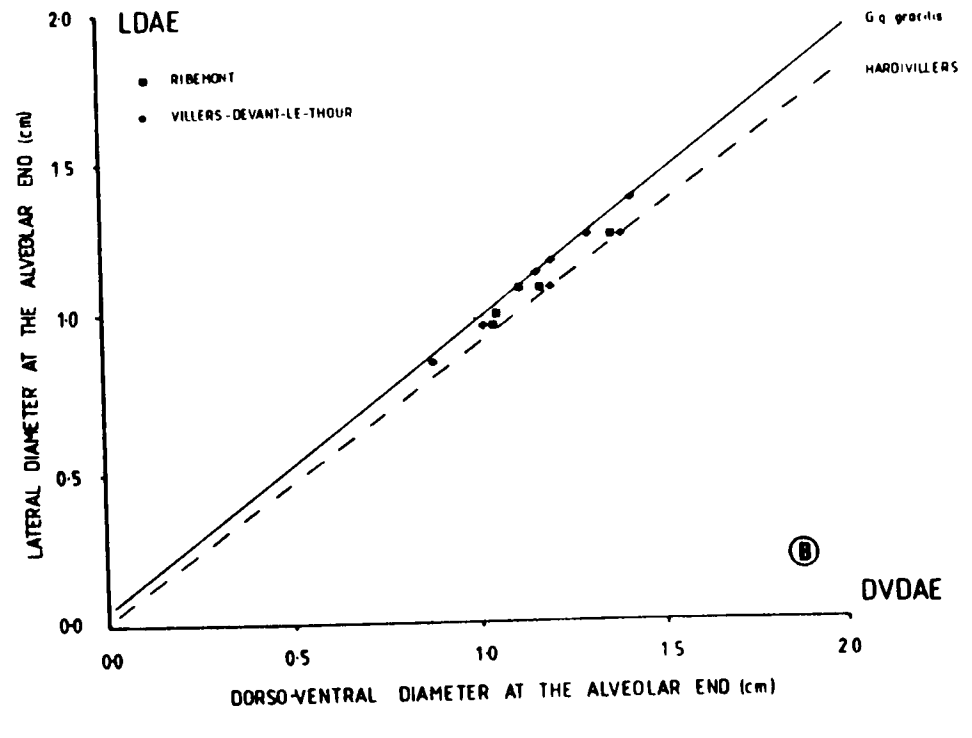


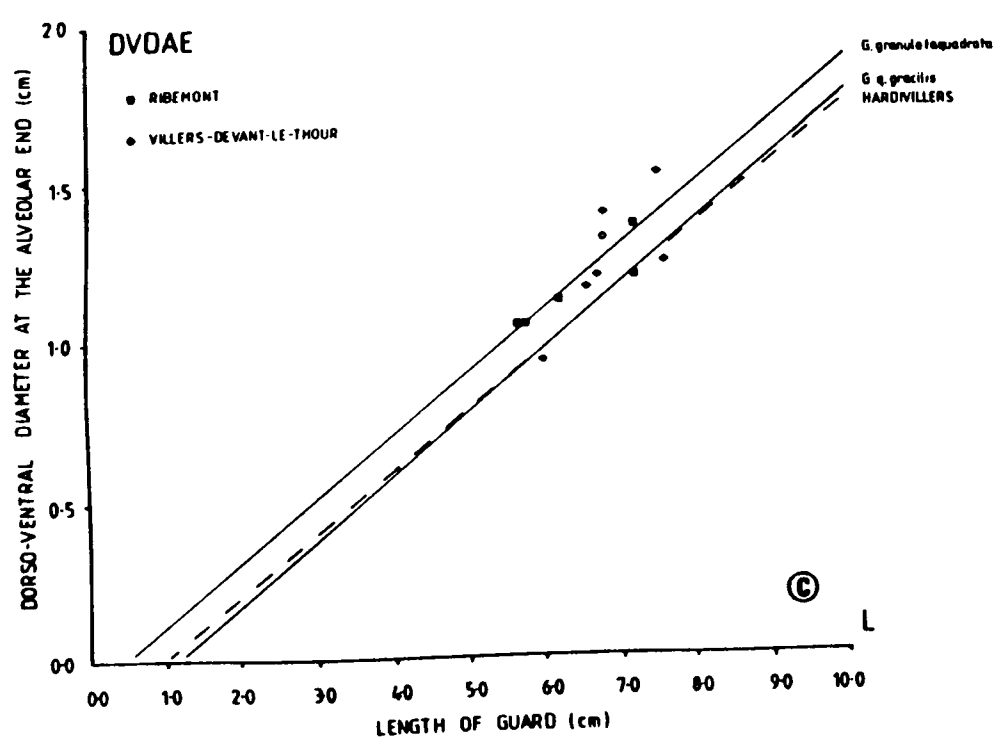


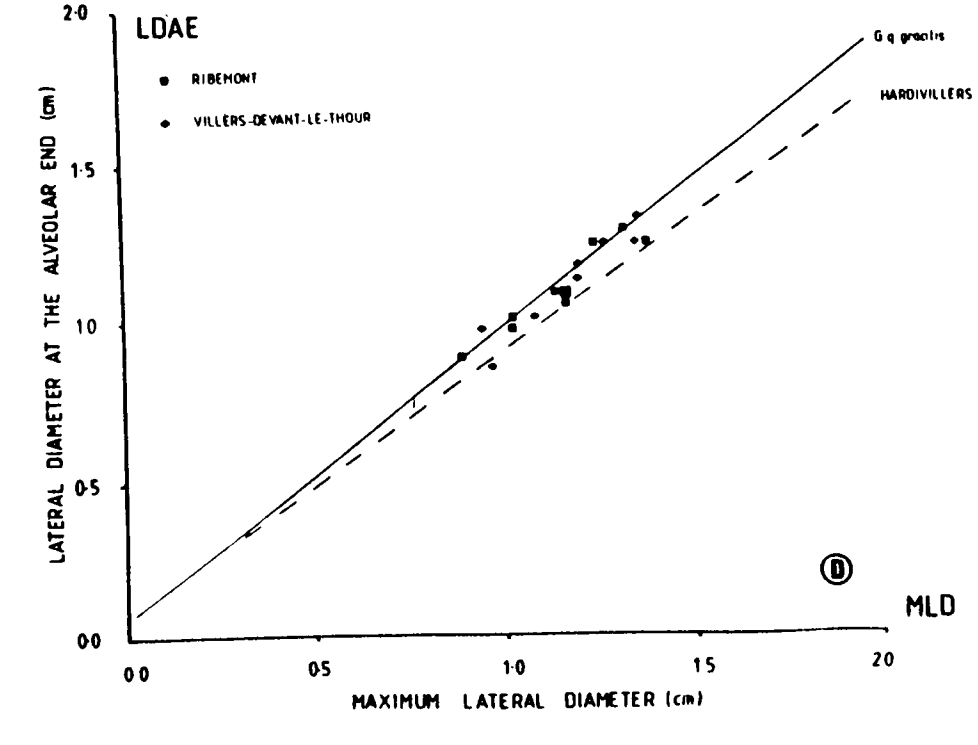


Fig. 5.7 Scatter diagrams and regression lines for G. ex gr. quadrata from Ribemont and Villers-devant-le-Thour. The plots follow the same format as Fig. 5.6.

significant. Clearly the regression line compares most closely with that for G. q. quadrata from the Hallembaye 'Smectite' and the German E. conica - G. papillosa Zone. It is noteworthy that a t-test on the y-intercept for the younger G. q. quadrata 'population' from Germany, G. q. quadrata from Belgium and the Hardivillers 'population' gives significant values (0.05>P>0.02), indicating an allometric relationship between the characters as seen in G. q. gracilis (Christensen, 1975a).

Ribemont and Villers-devant-le-Thour. A comparison between the slopes and positions of the regression lines of the two 'populations' showed that they do not differ significantly (P>0.40). A comparison between the slopes of the two lines and the slope of the Hardivillers 'population' also revealed no significant differences (0.60>P>0.50; 0.20>P>0.10), but a comparison between the positions of the lines indicated that although the Ribemont belemnites differed significantly from those from Hardivillers (0.01>P>0.001); the Villers-devant-le-Thour and Hardivillers 'populations' are apparently the same (0.10>P>0.05). The two samples were compared to three species of Gonioteuthis from Germany (Fig. 5.7A) and were found to differ significantly from G. granulataquadrata but could correspond with either G. q. quadrata or G. q. gracilis both in slope and position. The small number of specimens available from these two localities makes the statistical data inconclusive. Certainly the 'population' can be assigned to G. ex gr. quadrata but subspecific identification remains uncertain. Intuitively the 'populations' correspond more closely to stratigraphically younger 'populations' of Gonioteuthis (Fig. 5.7A) than that from Hardivillers (Fig. 5.6A).

5.3.2d Analytical summary and comparisons

Individual specimens from all three localities have Riedel-Quotients within the range of values typical of G. granulataquadrata and G. q. quadrata but the mean value for all three 'populations' is within the range of G. q. quadrata. The high degree of scatter of values of length of guard versus depth of pseudoalveolus has led to occasionally ambiguous results, nevertheless,

the Hardivillers sample shows the greatest similarity to 'populations' of G. q. quadrata from the Hallembaye 'Smectite' and the E. conica - G. papillosa Zone of Germany. Unfortunately, no further 'size' parameter regression analyses have been published for 'populations' of G. q. quadrata, so it has been impossible to statistically compare other parameters with control 'populations'. However, unpublished data (W.K. Christensen pers. comm.) indicates that the Hardivillers sample may be distinguished from E. conica - G. papillosa Zone 'populations' on plots of L v DVDAE. When this additional parameter is considered the Hardivillers sample is seen to be similar to a 'population' of G. q. quadrata from the I. ex gr. lingua - G. ex gr. quadrata Zone of Ziegelei Bremer, Bottrop-Fuhlenbrock (S. Münsterland) (Ernst, 1964). Unfortunately no regression data are available for this 'population' so a more precise comparison is impossible.

G. q. quadrata from Hardivillers may be distinguished from German 'populations' of G. granulataquadrata on L v D and L v DVDAE (Fig. 5.6C) and from G. q. gracilis on L v D and MLD v LDAE (Fig. 5.6D). It is noteworthy that the relationship between L v D, L v DVDAE and MLD v LDAE must be considered allometric in the sample. The Ribemont and Villers-devant-le-Thour 'populations' cannot be distinguished from one another on any character or combination of characters. Generally the values lie closer to those of G. q. gracilis than those of G. q. quadrata from Hardivillers. This is apparent in the plots of L v D, DVDAE v LDAE (Fig. 5.7B) and MLD v LDAE (Fig. 5.7D), while in the plot of L v DVDAE the values are closer to those of G. granulataquadrata. These observations demonstrate that the G. ex gr. quadrata from these two localities have a guard morphology similar to G. q. gracilis but are stouter than either German G. q. gracilis or G. q. quadrata from Hardivillers. It is suggested, therefore, that these 'populations' are stratigraphically younger than those from Hardivillers, but are still G. q. quadrata albeit more evolved forms.

Remaining complete specimens of Gonioteuthis which have been collected from phosphatic chalks are plotted in Fig. 5.8. In the plot of D v L (Fig. 5.8A) three specimens clearly lie outside the scatter of values of the three 'populations' of Gonioteuthis from the facies (Figs. 5.6A, 5.7A). All three

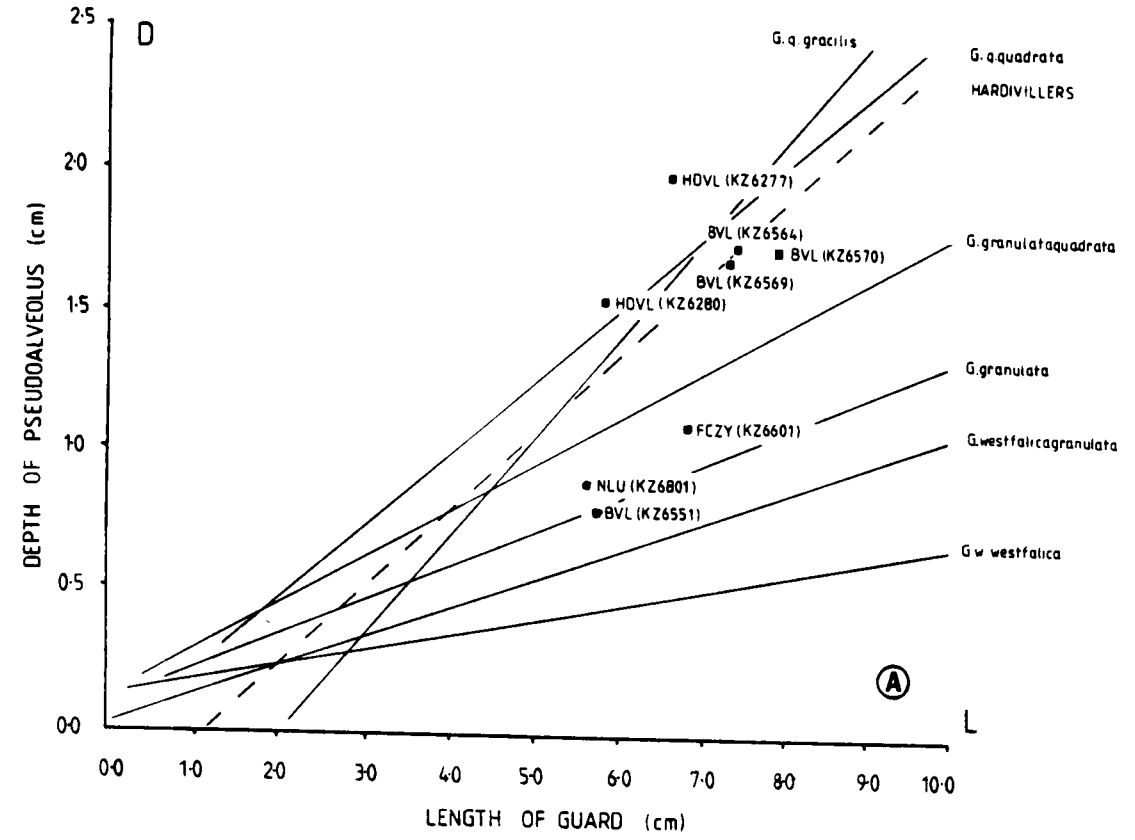


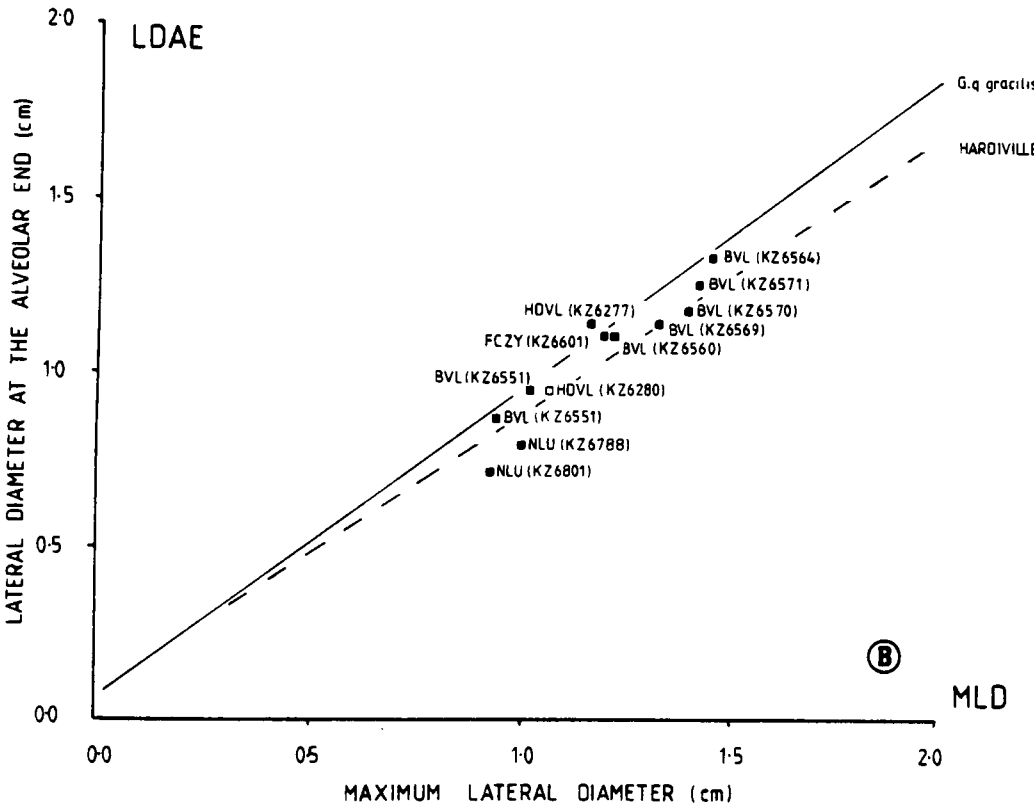


Fig. 5.8 Scatter diagrams of isolated specimens of Gonioteuthis collected from phosphatic chalks. A. length of guard (L) versus depth of pseudo-alveolus (D); the regression lines of the six German control 'populations' (excluding G. q. quadrata from the E. conica - G. papillosa Zone) and G. q. quadrata from Hardivillers are plotted for comparison. B. maximum lateral diameter (MLD) versus lateral diameter at the alveolar end (LDAE); the regression lines for G. q. gracilis from Germany and G. q. quadrata from Hardivillers are plotted for comparison.

specimens are identified as G. granulata on their Riedel-Quotients. Two of the three (KZ6551, Fig. 5.1 nos. 4 - 6, 8; KZ6801) come from the base of phosphatic chalk sequences while the other (KZ6601) originates from above the main phosphatic chalk at Faucouzy. Additional material from Beauval (BVL) on the plot of D v L comes from the upper portion of the upper phosphatic chalk and it all lies very close to the regression line for the Hardivillers 'population'. The additional examples from Hardivillers (HDVL) originate from the upper white

chalk. It is noteworthy that both lie in the same region of the plot as the material from Ribemont and Villers-devant-le-Thour.

The plot of LDAE v MLD (Fig. 5.8B) shows a high degree of scatter between the two reference regression lines. All of the material from Beauval was collected from the upper phosphatic chalk except KZ6551 (Fig. 5.1 nos. 4 - 6, 8) which is from the base of the lower phosphatic chalk. The Hardivillers examples are from the upper white chalk. It is clear that the specimens from Nurlu (KZ6788, Fig. 5.1 num. 7; KZ6801), which are both from the base of the phosphatic chalk, lie outside the scatter of values for the three 'populations'.

Scatterplots of DVDAE v L and LDAE v DVDAE do not have sufficient resolution to differentiate species of Gonioteuthis on the small amount of comparative material available. These comparisons highlight the necessity for large collections in the identification of Gonioteuthis species but they also show that material from the base of phosphatic chalks may be attributed to G. granulata and that this species is readily distinguished on plots of LDAE v MLD as well as Riedel-Quotient and D v L plots.

### 5.3.2e Factor analysis

Since factor analysis requires listwise deletion of missing values, only the 'population' from Hardivillers was regarded as being of sufficient size to enable a statistically valid application of factor analysis. A total of sixty-nine guards were utilised in the analysis, results of which are given in Table 5.6.

The first principal component accounts for 87.2% of the variation and possesses a strong positive correlation with all of the 'size' parameters. It is interpreted as representing guard size, which is consistent with similar results from biological studies (Blackith and Reyment, 1971 p.147 - 150) and for a 'population' of Actinocamax plenus from England (Christensen, 1974). Clearly size is intimately related to age in marine invertebrates such as belemnites although food availability may become an overiding factor in Recent coleoids (Mangold-Wirz, 1963).

The second principal component accounts for 6.8% of the total variance.

| Eigenvector: | 1 | 2 | 3 |
|---|---|---|---|
| Eigenvalue: | 4.361 | 0.342 | 0.228 |
| Variance: | | | |
| % total | 87.2 | 6.8 | 4.6 |
| cumulative | 87.2 | 94.0 | 98.6 |
| Character | | | |
| L | 0.902 | 0.043 | 0.429 |
| D | 0.860 | 0.492 | -0.125 |
| DVDAE | 0.984 | -0.099 | -0.097 |
| LDAE | 0.974 | -0.104 | -0.116 |
| MLD | 0.943 | -0.279 | -0.077 |

Calculated from a 'population' of 69 guards.

TABLE 5.6 Eigenvalue and Eigenvector matrix from a principal component factor analysis of G. g. quadrata from the Hardivillers Gonioteuthis Bed.

It shows a strong positive correlation with D, a moderate negative relationship with MLD and negative correlations of approximately equal magnitude with DVDAE and LDAE. The factor is consequently interpreted as representing the evolutionary stage reached by each individual within the total 'population'. It reflects the increasing depth of the pseudoalveolus combined with a progressive increase in the slenderness of the guard from the maximum robustness reached in G. granulataquadrata.

The third principal component only allows for 4.6% of the observed variation. It shows a strong positive correlation with L and a weak negative interrelationship of approximately equal magnitude with the remaining characters. The factor may be interpreted as a shape effect which results in the production of elongate guards. Alternatively, it may be due to an indeterminate taphonomic control, perhaps sorting of material prior to deposition.

## 5.4 Taphonomy and depositional environment

Some degree of taphonomic bias will inevitably be present in any fossil assemblage. Consequently it is necessary to examine and if possible remove or 'allow for' any bias before zoological or stratigraphical conclusions can be reached. Furthermore, an assemblages' taphonomy, together with its associated sedimentology, may provide valuable insights into the depositional environment of that assemblage.

Most guards from the Hardivillers Gonioteuthis Bed are in excellent preservation and complete. A summary of the encrustation is given in Table 5.7.

| Locality | Number of guards | Number encrusted (%) | | | | |
|---|---|---|---|---|---|---|
| | | Total | Oyster | Octocoral | Serpulid | >1 species |
| Hardivillers | 136 | 53 | 32 | 31 | 10 | 20 |
| Ribemont | 73 | 40 | 30 | 3 | 6 | 6 |
| Villers-devant-le-Thour | 24 | 6 | 6 | 0 | 0 | 0 |

TABLE 5.7 Summary of encrustation exhibited by three 'populations' of Gonioteuthis from phosphatic chalks

Although pycnodonteine oysters, octocorals and serpulids are the major encrusters, a small number of cemented foraminiferans were present on some guards. Clionid sponge borings are present in many specimens (Fig. 5.1 nos. 1 - 3, 9) but they rarely form extensive networks. A second common form of boring consists of a radiating pattern of small ( <0.1 mm) ramifying bores which occur just below the surface of the guards. These may be attributed to thallophytes. Oysters are the dominant encruster (Fig. 5.5 num. 13) but only 5% of specimens bear more than two individuals and where larger numbers are present they are generally small and have identical orientations of their hinge-lines. Only four specimens exhibit more than a single generation of encrustation, octocorals and serpulids following the pattern displayed by the oysters. The small size of the majority of the epifauna (oysters only reaching a few millimetres across) suggests that it is mostly juvenile. Examination of all specimens, including fragmentary guards, demonstrates that few, if any, show signs of mechanical abrasion, the poor preservation of the small number of broken guards being predominantly due to the activities of boring sponges. Many belemnites display fine subparallel scratch marks (Fig. 5.1 nos. 12, 13; Fig. 5.5 num. 13), generally oriented in a dorso-ventral direction and probably produced by the rasping action of a marine organism grazing the surface of the guards. Several guards show late-stage compactional effects including partial crushing of their pseudoalveoli and in situ fracturing, occasionally accompanied by recementation of the dislocated fragments. Recent solution and partial decalcification,

but in general the guards are complete.

Specimens from the other localities display similar features to those seen in the Hardivillers sample. Most guards from Ribemont and Villers-devant-le-Thour are severely etched and corroded by weathering due to the proximity of the phosphatic chalk to the soil. Consequently, the data on the encrustation (Table 5.7) are less reliable for these sites. The guard from the basal lag at Nurlu (KZ6788) and hardground-associated guards from Faucouzy and Hallencourt pit (2.7.1) display thin shiny-phosphate surface veneers (Fig. 5.1 nos. 4 - 6, 8) underlain by a portion of phosphatized calcite. In contrast to the opinion expressed by Tabatabai" (1977 p.212) extensive phosphatization of belemnite guards was found to be uncommon.

The different proportions of encrusters and encrustation are not necessarily of environmental significance since they are too readily affected by the proximity of a 'spat' source. The well-preserved nature of the guards, the juvenile stage of the majority of the epifauna and the lack of extensive boring suggest that burial was rapid. Furthermore, the general lack of more than one generation of encrustation indicates that reexhumation was rare. These observations have important implications concerning the environment of deposition. The sedimentology indicates that the phosphatic chalk lithofacies was a relatively high-energy environment, within which sediment was being winnowed by current action (3.4.4). Yet the taphonomy of the belemnites suggests rapid burial and lack of reexhumation. Clearly this removes the possibility of a low sedimentation rate due to continual winnowing as this would result in the belemnites being exposed on the seafloor for extended periods. Intermittent current action with rapid winnowing events followed by periods of quiescence and burial, therefore, seems a more likely mechanism. Such a cyclic process may also explain the apparent paradox between oxic bottom waters and sediment as demonstrated by the epi- and infauna and the subsurface anoxia associated with contemporary phosphorites (Chapter 6; Baturin and Bezrukov, 1979). It may be postulated that phosphatization took place during quiescent periods and colonisation and bioturbation during times of stronger current activity (cf. 4.5.2).

## 5.5 Facies and ecology

The abundance of belemnites within the phosphatic chalk lithofacies vis-à-vis soft white chalks requires some explanation. Both Gonioteuthis and A. verus occur very commonly in shallow-water deposits situated close to ancient massifs, such as the biocalcarenites and glauconitic sands of the Balto-Scandian area (Christensen, 1976). Furthermore, Gonioteuthis from near-shore facies are characterised by the presence of all ontogenetic stages, while 'populations' from offshore chalks only contain adult specimens (Ernst, 1964). This general trend also applies to other genera of belemnite e.g. Belemnella and Belemnitella. It must be concluded that the occurrence of juveniles in phosphatic chalk 'populations' is indicative of a near-shore and therefore shallow-water environment for the facies. This is consistent with the sedimentology (3.4.4).

In both facies belemnites are common just below, and particularly above, hardgrounds. The formation of Chalk hardgrounds is commonly accompanied by evidence of shallow water conditions (3.3.4). This explains the occurrence of hardground associated belemnites in offshore chalks but it does not explain their concentration in the phosphatic chalk environment which was initially also shallow water (3.4.4).

It has been suggested (Surlyk and Birkelund, 1977) that belemnites found in offshore chalks may be considered as straying adult individuals buried outside their normal habitat. Christensen (1976) has postulated that this apparent facies control may be causally related through the food-chain. Belemnites probably preyed on small fish, crustaceans and cephalopods, as do their Recent relatives (Naef, 1922) and such prey would be more readily available in a shallow water environment.

The association with hardgrounds results from the interaction of two independent factors. Firstly, hardgrounds are generally regarded as representing levels of faunal condensation whether due to omission, active erosion coupled with winnowing or a combination of these processes. Either mechanism would be expected to result in above average concentrations of belemnites but the taphonomy of the material indicates that the guards were not exposed on

the seafloor for extended periods. The Ribemont sample, which originates from above a hardground, does have a greater proportion of bored fragments, but the proportion is considered insufficient to confirm the condensation hypothesis. Furthermore, the bimodality of the 'population' suggests deposition following a catastrophic event rather than long-term addition of material.

The second factor is the change in ecology which would be expected after seafloor lithification. The new environment would embrace a mixed hard/soft substrate ecosystem which might be expected to lead to an increase in diversity, and probably increased abundance of organisms. The increase in the seafloor dependent biota would provide a food source for animals higher in the food chain including the fish and crustaceans which are assumed to have been the main prey of belemnites. The two factors are not mutually exclusive and undoubtedly acted in concert in the majority of cases but it is considered, on taphonomic grounds, that the second of the two factors predominates in phosphatic chalks.

The Recent coleoid, Loligo opalescens generally inhabits water depths of 120 - 330 m but enters shallower water for mating and at night to feed. L. opalescens congregates in vast numbers to mate and reproduce, after which the majority of individuals die. An estimated 20 million dead have been observed in a small area off Baja California after such an event (Cousteau and Diolé, 1973). Clearly this feature of the life cycle of a modern coleoid, similar in size and morphology to belemnites, provides one mechanism for the formation of the so-called "Belemnitenschlachtfeld" (belemnite battlefield) of the literature (e.g. Naef, 1922).

The Gonioteuthis beds are around 1 m thick and contain belemnites scattered throughout, although patches of larger numbers of individuals occur. The higher concentrations are not at a particular level within the beds nor are they on top of recognisable omission or erosion surfaces. It may be postulated, therefore, that these beds are the result of a series of mass mortalities following reproduction. The reproductive cycle of L. opalescens has another important aspect, after mating the squids attach their eggs to epibenthic organisms and other suitable anchorage points on the seafloor (Cousteau and Diolé, 1973; Recksiek, 1978). It is suggested that hardgrounds would provide a greater

number of potential attachment sites than a soft substrate and therefore be prefered as breeding areas.

It is not necessary to assume that the 'populations' of the Gonioteuthis beds were buried in the immediate area of their death. During the later stages of cuvette evolution, hardgrounds would be concentrated at the cuvette margins, where areas of lithified chalk remained uncovered. These areas would provide prefered living/breeding sites for belemnites but, on death, individuals would be swept into the central portions of the cuvette and deposited. Subsequent bioturbation would remove the identity of individual mortality events and tend to disseminate guards throughout an interval of sediment. A further factor to be considered is the suggestion (Chapter 7) that phosphatic chalk formation was in part the result of upwelling of deep ocean water in the Anglo-Paris Basin which provided the quantities of phosphate necessary for the deposition of such extensive phosphorites. Such an increase in orthophosphate would undoubtedly lead to higher plankton abundancies which, as the base of the marine food-chain would result in increased numbers of higher animals including belemnites.

The Gonioteuthis beds occur at the summit of the phosphatic chalks and perhaps represent an acme prior to the change in environment that resulted in the cessation of phosphatic chalk deposition. Such an acme might result from any of the factors discussed when considering the range of A. verus in phosphatic chalks (see below).

## 5.6 Stratigraphical and environmental controls

The facies model does not explain all aspects of the occurrence of belemnites in phosphatic chalks. The best-developed hardgrounds are at the base of phosphatic chalks, yet no basal hardground shows the concentration of Gonioteuthis guards typical of hardgrounds higher in the sequences. A. verus ranges from the Santonian to early Campanian in Yorkshire (Jukes-Browne and Hill, 1904; Wright and Wright, 1942), Norfolk (Peake and Hancock, 1961) and Germany (Schmid, 1956; Ernst, 1963a) but in southern England (Rowe, 1901; Jukes-Browne and Hill, 1904; Griffith and Brydone, 1911) and northern France (de Grossouvre, 1899) the

species is apparently restricted to the Santonian being particularly characteristic of the Uintacrinus socialis Zone. Gonioteuthis, on the other hand, appears infrequently in the Coniacian (as G. westfalica) chalks of northern France (de Grossouvre, 1899, 1901, 1907) and southern England (Rowe, 1901; de Grossouvre in Rowe, 1901). Rare G. westfalicagranulata and G. granulata occur with A. verus in the mid to high Santonian of both areas (de Grossouvre, 1899; Jukes-Browne and Hill, 1904; Rowe, 1904; Peake and Hancock, 1961) but G. granulata is most abundant in the late Santonian Marsupites testudinarius Zone where A. verus is uncommon. The base of the low Campanian Echinocorys depressula Subzone of the Offaster pilula Zone is typified by forms intermediate between G. granulata and G. q. quadrata i.e. G. granulataquadrata (Jukes-Browne and Hill, 1904; Griffith and Brydone, 1911) and Belemnitella (probably B. praecursor) makes its first appearance at this level (Jukes-Browne and Hill, 1904). G. q. quadrata appears above the base of the Campanian in the 'abundant O. pilula' Subzone of the O. pilula Zone and continues into the overlying G. quadrata Zone, where it becomes the index fossil (e.g. Griffith and Brydone, 1911). Thus throughout the Anglo-Paris Basin Gonioteuthis is only relatively common in chalks where A. verus is rare or absent. This relationship is clearly shown by phosphatic chalks where the occurrence of the two genera is almost antipathetic. Explanations for this phenomenon must be sought from environmental, evolutionary or provincialistic controls since it is not due to the relative ranges of the two fossils.

Firstly, the current regime that originally produced the cuvettes must have been of a higher order than that which accompanied their infill. This is demonstrated by the transition from erosion to deposition and is reflected in the coarser and generally higher phosphate content of the lowest phosphatic chalks. In turn, changes in regime be reflected in substrate and biota both within the cuvettes and elsewhere in the basin. Secondly, the major increase in the abundance of Gonioteuthis coincides with the evolution of G. q. quadrata. It might be suggested therefore that evolutionary changes in the Gonioteuthis stock may have enabled the genus to diversify and occupy previously unfavourable niches. Broader environmental tolerances or changes in food requirements, for example, would provide a mechanism. Lastly, it will be suggested (Chapter 7)

that the initiation of phosphatic chalk sedimentation was in part due to major changes in oceanic circulation during the Santonian, which accompanied the opening of the proto-Atlantic Ocean. Later changes in the distribution of water masses during the period of phosphatic chalk sedimentation may have enabled populations of Gonioteuthis to enter into an area which, because of oceanographical conditions, was previously dominated by A. verus and B. ex gr. grossouvrei, similarly, A. verus might have been excluded from that area. Any one, or a combination of these factors can be invoked to explain the observed changes in belemnite distribution during the evolution of the lithofacies.

## 5.7 Conclusions

(1) The phosphatic chalks of northern France provide rare examples of Santonian to early Campanian 'populations' of Gonioteuthis. This enables the application of statistical analysis for the identification of species.

(2) These phosphatic chalks can be divided into three biostratigraphical subdivisions on their belemnite assemblages:

(a) A lower unit characterised by A. verus with M. coranguinum, occasional G. granulata and rare B. ex gr. grossouvrei.

(b) An intermediate division typified by G. q. quadrata with O. pilula.

(c) An upper unit with G. q. quadrata with occasional B. praecursor.

(3) A combination of univariate and bivariate statistics has demonstrated that the 'populations' from the Hardivillers Gonioteuthis Bed and the phosphatic chalk at Villers-devant-le-Thour are homogenous, whereas the 'population' from above the Ribemont Gonioteuthis Hardground is inhomogenous. Inhomogeneity in the latter sample is the result of a catastrophic event, probably a storm, which resulted in the concentration of a mixed 'population' of young and old individuals.

(4) Mean Riedel-Quotients for all three 'populations' fall within the range of G. ex gr. quadrata but subspecies cannot be identified of Riedel-Quotient alone.

(5) G. q. quadrata has been identified as the subspecies present in the

Hardivillers Gonioteuthis Bed. This 'population' of the subspecies shows an allometric relationship of L v D, L v DVDAE and MLD v LDAE.

(6) The Ribemont and Villers-devant-le-Thour 'populations' cannot be distinguished from each other but are distinct from that studied from Hardivillers. The subspecies at the former localities shows affinities to both G. q. quadrata and G. q. gracilis.

(7) Principal component factor analysis illustrates that the major controls on Gonioteuthis guard morphology are:

(a) the size of the guard, which accounts for 87.2% of the observed variation,

(b) the evolutionary stage of the individual within the Gonioteuthis gradualistic series, 6.8% of the variation, and

(c) a shape factor which produces elongate guards (or perhaps a taphonomic factor), 4.6%.

(8) The well-preserved nature of the guards, the juvenile nature of the epifauna and the absence of extensive boring suggest relatively rapid burial, while the general lack of more than one generation of epifauna implys that re-exhumation was rare.

(9) Guard taphonomy suggests that the environment of deposition was one of intermittent current activity with rapid winnowing followed by periods of quiescence and burial.

(10) The occurrence of juveniles in the 'populations' indicates a shallow-water environment which was the belemnites normal habitat because of the greater availability of food.

(11) Belemnites are concentrated at hardground levels because of:

(a) a concentration of potential prey associated with hardgrounds,

(b) they may be prefered breeding sites and would therefore be the recipients of the large number of cadavers following the mass mortalities that accompany reproduction.

(12) The virtual mutually exclusive relationship between A. verus and Gonioteuthis in phosphatic chalks may be controlled by:

(a) the decline in the current regime during cuvette evolution

favouring Gonioteuthis,

(b) evolutionary changes in Gonioteuthis allowing the genera to occupy a previously unfavourable niche and to oust A. verus or

(c) changes in provincial boundaries which accompanied alterations in oceanic circulation.

# Chapter 6 : Phosphate and seafloor phosphorites


| | | | |
|---|---|---|---|
| 6.1 | Introduction | | 422 |
| 6.2 | Marine chemistry | | 422 |
| | 6.2.1 | Classification of elements in seawater | 422 |
| | 6.2.2 | Phosphorus in seawater | 425 |
| | | a. Dissolved inorganic phosphate | 425 |
| | | b. Dissolved organic phosphate | 426 |
| | | c. Particulate phosphate | 427 |
| | 6.2.3 | Variations in phosphate distribution | 428 |
| | 6.2.4 | The phosphorus cycle | 430 |
| | 6.2.5 | Geochemical modelling | 432 |
| 6.3 | Seafloor phosphorites | | 437 |
| | 6.3.1 | California Shelf, USA | 439 |
| | 6.3.2 | Baja California Shelf, Mexico | 440 |
| | 6.3.3 | Blake Plateau, Florida USA | 441 |
| | 6.3.4 | Straits of Florida, USA | 441 |
| | 6.3.5 | Georgia and North Carolina Shelf, USA | 443 |
| | 6.3.6 | Peru-Chile Shelf | 444 |
| | 6.3.7 | Walvis Bay, Namibia SW Africa | 445 |
| | 6.3.8 | North-west African Shelf | 447 |
| | 6.3.9 | Agulhas Bank, South Africa | 448 |
| | 6.3.10 | Gulf of Aden, Somalia East Africa | 450 |
| | 6.3.11 | Northern New South Wales, Australia | 450 |
| | 6.3.12 | Chatham Rise, New Zealand | 451 |
| | 6.3.13 | Other localities | 451 |
| | 6.3.14 | Classification | 452 |
| 6.4 | Genesis of seafloor phosphorites | | 454 |
| | 6.4.1 | Source of the phosphate | 454 |
| | 6.4.2 | Phosphatization mechanisms | 456 |
| | | a. Precipitation | 456 |
| | | b. Replacement | 459 |
| | | c. Reworking | 461 |
| | 6.4.3 | Global factors | 461 |
| 6.5 | Conclusions | | 463 |

## 6.1 Introduction

A basic tenet of geology is the Lyellian doctrine that the "present is the key to the past". It follows that an appreciation of the distribution of phosphate in the present-day oceans and the depositional environment of Recent phosphorites is fundamental to our understanding of ancient deposits. The chapter has been divided into three sections; the first two are predominantly descriptive resumes of current knowledge concerning the nature and distribution of phosphates and phosphorites in the world's oceans; the third section discusses the consequences of these observations and the limitations that they impose on the processes of phosphate transfer and phosphorite genesis. By its nature, the review has drawn from a broad range of source material, much of which lies outside the field of classical geology, but, as such, provides large amounts of pertinent information which might otherwise be overlooked.

## 6.2 Marine chemistry

Palaeontological, sedimentological and geochemical associations demonstrate that the majority of the world's phosphorites are undoubtedly of marine origin. Their formation, therefore, must be intrinsically related to the movement of phosphorus in seawater.

### 6.2.1 Classification of elements in seawater

The elements which occur in seawater may be conveniently divided into three categories (Broecker, 1974):

(a) biolimiting elements,

(b) biointermediate elements,

(c) biounlimiting elements.

The biolimiting elements, sometimes also called the nutrient or micronutrient elements, are those which are totally depleted in the surface waters of the oceans. Biointermediate elements display some depletion while those which

are biounlimiting show no significant differentiation between shallow and deep water masses.

The three biolimiting elements are nitrogen, phosphorus and silicon. Plant activity (and in the case of silicon, animal activity), which is essentially restricted to the photic zone, is efficient enough to totally extract these elements from surface waters (Fig. 6.1). The unicellular algae of the phytoplankton are the main agencies of removal although in shallow water benthonic algae are important. At P concentrations of >0.3 µg atom P $l^{-1}$ the growth rates of most species of phytoplankton are independent of the phosphate concentration; below this cell division becomes increasingly inhibited, phosphorus deficient cells are produced (Ketcham, 1939) and photosynthesis eventually ceases. Phosphorus is not normally the growth limiting factor, however, since nitrate is

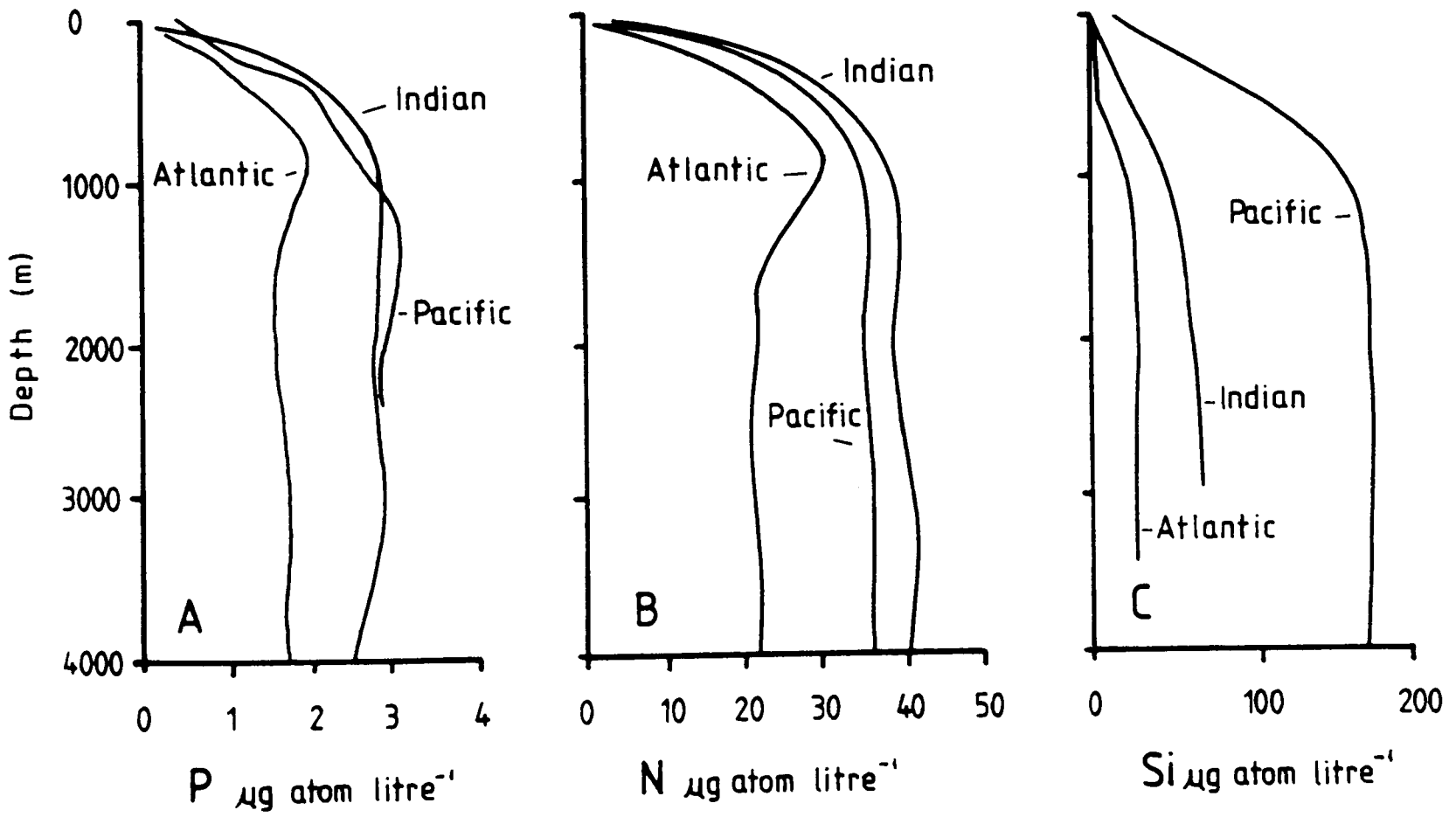


Fig. 6.1 Vertical distribution of phosphate (A), nitrate (B) and silicate (C) in the Atlantic, Pacific and Indian Oceans (after Sverdrup et al., 1942).

usually exhausted before phosphate falls to its critical level (Riley, 1971). Silicon is commonly exhausted in surface waters during the growth of siliceous phytoplankton, but the element is probably not important for the growth of non-siliceous marine algae. Thus productivity in the surface waters must ultimately be limited by the availability of the biolimiting elements. Deep water is greatly enriched in these elements relative to surface water, demonstrating the

fundamental importance of photosynthetic organisms in determining the chemical makeup of the oceans. Many other elements and classes of organic compound have been proposed as biolimiting but regions where neither nitrate nor phosphate is the limiting nutrient, are probably small.

Those elements which cannot be shown to differ significantly in shallow and deep water are Na, K, Rb, Ce, Mg, Sr, B, S, F, Cl and Br, while Ca, C, Ba and Ra show significant depletion and are therefore classified as biointermediate.

The chemical composition of organic tissue of both plants and animals is relatively constant with phosphorus, nitrogen and carbon combining in the atom ratios of 1P:15N:80C. The atom ratios of these three elements in deep sea water is 1P:15N:800C. Clearly, available and required P:N ratios are identical while carbon is present as a ten times excess over that required for the production of new organic tissue. The fact that nitrate and phosphate are removed from seawater in constant proportions (Fig. 6.2) as a result of phytoplankton growth, has been known (Harvey, 1926) for some time. Consequently, parcels of seawater differ in their P : N : C content to the extent to which organisms have removed or added elements in the fixed organic ratio. Whether life evolved to utilise a preexisting P:N ratio or has modified that ratio through geological time, remains unresolved.

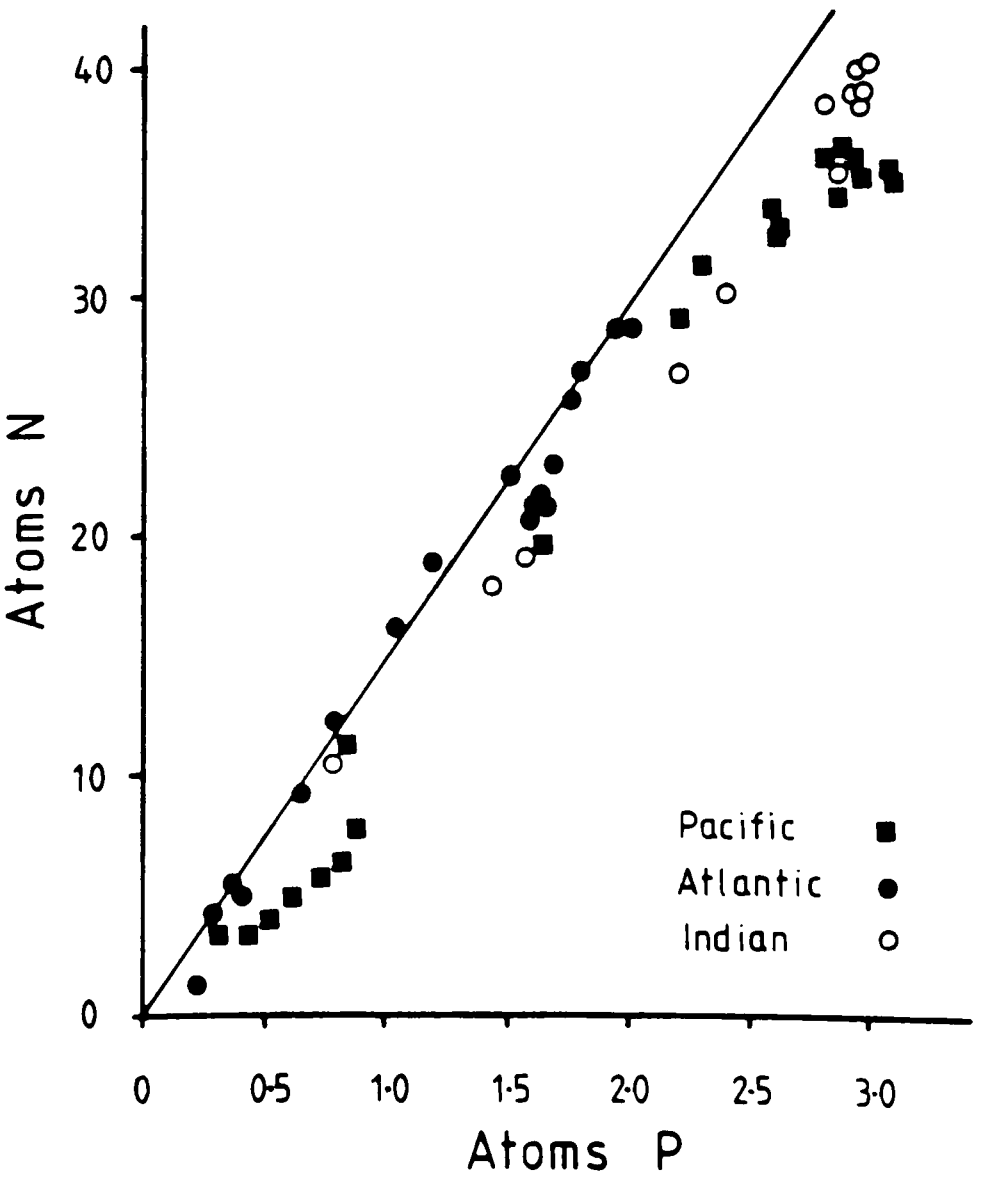


Fig. 6.2 Relation between phosphate and nitrate in the oceans.
The points represent averages for individual depths used in the construction of Fig. 6.1. The straight line represents the 'normal' P:N ration of 1: 15. (After Sverdrup et al., 1942).

Silicon occurs in deep water in the atom ratio of 1P:50Si, and since the element is biolimiting, all of this is used in the secretion of hardparts by organisms in surface waters. Calcium, on the other hand, is available in large excess, organisms utilising only 1% of that available. Since calcium is predominantly used in the formation of skeletal material in the form of $CaCO_3$, a small percentage of the excess carbon is utilised at the same time.

The major sources of the biolimiting elements are the products of rock weathering and decay of terrestrial organic matter which are transported to the sea by land runoff, predominantly by rivers. Further contributions come from submarine weathering, glacial action, volcanic activity and other geothermal sources. Atmospheric contributions include gaseous uptake by the sea, addition of rainwater and deposition of wind-transported solids. The chemical processes that control the removal of the elements from seawater are essentially the formation of solid material and sedimentation. For the biolimiting elements, these processes are predominantly organic but also include the formation of authigenic minerals and sorption reactions on suspended material.

## 6.2.2 Phosphorus in seawater

Phosphorus occurs in seawater in three forms: dissolved inorganic phosphate, dissolved organic phosphate, and particulate phosphate.

### 6.2.2a Dissolved inorganic phosphate

The nature of orthophosphate species in seawater is extremely complex, primarily because phosphoric acid dissociates in three steps:

$$H_3PO_4 \rightleftharpoons H^+ + H_2PO_4^- \quad (6.1)$$

$$H_2PO_4^- \rightleftharpoons H^+ + HPO_4^{2-} \quad (6.2)$$

$$HPO_4^{2-} \rightleftharpoons H^+ + PO_4^{2-} \quad (6.3)$$

Sillén (1961) considers that the dominant species in seawater is $HPO_4^{2-}$. This conclusion is consistent with the experimental data (Kester and Pytkowicz, 1967) which demonstrates that in artificial seawater at pH 8.0, about 1% of the orthophosphate is present as $H_2PO_4^-$, 87% as $HPO_4^{2-}$ and 12% as $PO_4^{3-}$

(Fig. 6.3); 96% of the $PO_4^{3-}$ and 44% of the $HPO_4^{2-}$, however, are present as as complexes of $Na^+$, $Mg^{2+}$ and $Ca^{2+}$. The most common complex is $MgHPO_4^o$ at normal pH but at higher pH $CaHPO_4^o$ becomes more important. At normal seawater pH (~8) $MgHPO_4^o$ will comprise 41.4% of the complex Mg. Free $PO_4^{3-}$ makes up only 0.01% of the phosphate species in seawater (Atlas, 1979). Consequently, calcium phosphate is more soluble in seawater than in distilled water and its solubility product has been estimated in seawater as $K_s = 4.0 \times 10^{-20}$ at 20°C (Pytkowicz and Kester, 1967); three orders of magnitude higher than earlier estimates.

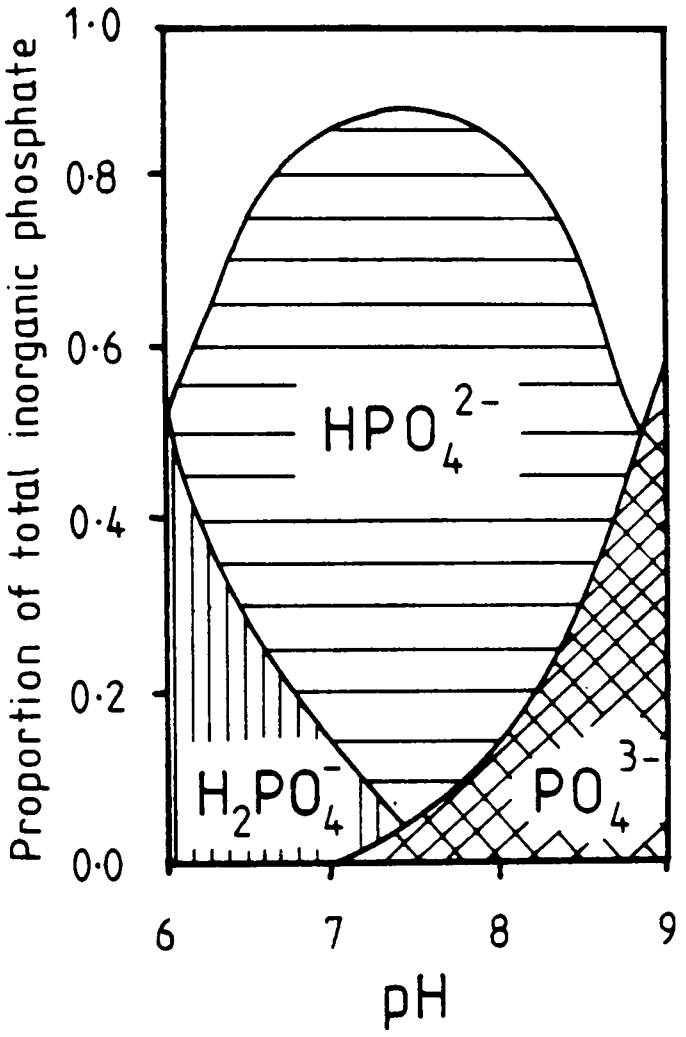


Fig. 6.3 Variation with pH of the relative proportions of orthophosphoric acid at 20°C in artificial seawater; salinity 33‰. (After Kester and Pytkowicz, 1969).

Higher degrees of saturation, therefore, are probably due to an increase in pH causing an enhanced activity of the triply charged orthophosphate ion, rather than higher absolute concentrations of orthophosphate. The effects of temperature and pressure on the solubility of calcium phosphate are unknown but the solubility of apatite decreases with temperature rise (Kramer, 1964; Valyashko et al., 1968; Atlas, 1979).

### 6.2.2b Dissolved organic phosphate

Phosphorus compounds such as adenosine triphosphate and nucleotide coenzymes, play a key role in photosynthesis and other processes in plants. Phytoplankton normally satisfy their requirements by direct assimilation of

orthophosphate which they convert to organic compounds. On death, this solid organic material is rapidly converted to soluble organic phosphates through the agency of the phosphatases in their cells. In the sea, however, most of the phytoplankton is consumed by animals, mainly zooplankton which obtain their own phosphorus requirement in that way. Some of the total phosphorus is assimilated but the remainder is ejected in urine and faecal material which contain appreciable amounts of both organic and inorganic phosphate (Butler et al., 1969). The organic phosphorus is rapidly hydrolysed to soluble organic phosphate which, in turn, is quickly converted to orthophosphate, bacterially or enzymatically. Nevertheless, undecomposed organic phosphate may constitute up to 75% of the total phosphate content of seawater (Riley, 1971).

The detailed nature of the organically combined phosphorus in seawater is unknown. Watt and Hayes (1963) have demonstrated the occurrence of monophosphate esters, although Strickland and Solórzano (1966) suggest that such esters may only account for a small proportion of dissolved phosphate in seawater. Aminophosphoric acids occur in many marine organisms and it is likely that these, together with phosphonucleotides, also occur in seawater (Spencer, 1975).

6.2.2c Particulate phosphate

Both inorganic and organic phosphates occur in the particulate matter suspended in the sea although little is known about the constitution of this material. Inorganic phosphorus is associated with suspended clay minerals which adsorb phosphorus (as do ferric oxides), while solid calcium and ferric phosphate may also be present (Cooper, 1948). The phosphate associated with clay minerals may go back into solution and enrich estuaries (Rochford, 1951) and inner continental shelf waters (Cooper, 1951), thus suspended clays may exert a controlling influence on the concentration of dissolved phosphate in seawater (Spencer, 1975).

Phosphate is also likely to be adsorbed onto organic matter, which itself contains a wide range of phosphorus compounds. Work on the particulate matter from the surface of the Antarctic Ocean (Correll, 1965) provides some insight into the composition of the phosphate fraction; 30 - 60% of the phosphorus was

present as orthophosphate while 2 - 10% occurred in the form of oligopolyanions. The organic phosphorus fraction was 25 - 57% of the total and consisted of RNA-polyphosphates, DNA and some phosphoproteins; 2 - 15% was acid insoluble phosphorus and 4 - 7% occurred as lipid phosphorus.

### 6.2.3 Variations in phosphate distribution

Phosphate was one of the first elements for which rapid and simple analytical techniques were developed, consequently a large amount of data is available concerning the distribution of the element in surface waters. The maximum concentration in most areas ranges from 0.5 - 1.0 $\mu$g-atom P $l^{-1}$ but in the tropics maximum values drop to 0.1 - 0.2 $\mu$g-atom P $l^{-1}$ (Spencer, 1975). Higher values occur in the North Pacific, in the Antarctic, in areas of upwelling and in coastal waters as a consequence of the influx of river water. The resulting increase in phosphate in the last case, however, is predominantly due to an increase in particulate varieties and is accompanied by a corresponding decrease in salinity. Armstrong (1965) has given an extensive account of the global distribution of phosphate in the oceans, while Riley (1971) has noted the correlation between phosphate concentrations in the upper layers of the oceans and their zooplankton (and therefore their phytoplankton) content.

In temperate latitudes the phosphate concentration in surface waters shows considerable seasonal variation (e.g. Armstrong and Harvey, 1950). During winter (Fig. 6.4B) phosphate is almost entirely present as orthophosphate but during spring the inorganic phosphate is utilised by phytoplankton and therefore decreases in abundance so that by early summer most of the phosphate is present as organic matter (Fig. 6.4A). It is noteworthy that although peak phytoplankton productivity occurs in mid spring, zooplankton and fish abundancies tend to show a time lag, reaching their peak during the late spring (Harvey, 1955), when orthophosphate concentrations are less than 0.05 $\mu$g-atom P $l^{-1}$ within the photic zone. Following this seasonal bloom, the phosphate distribution gradually returns to its winter form although a minor bloom may also occur in the autumn. Tropical seas exhibit less variation than temperate areas, but algal

blooms do occur in association with the monsoons (Riley, 1971). In the tropics organic phosphate may reach appreciable quantities in areas where inorganic phosphate is undetectable (Kuenzler et al., 1963).

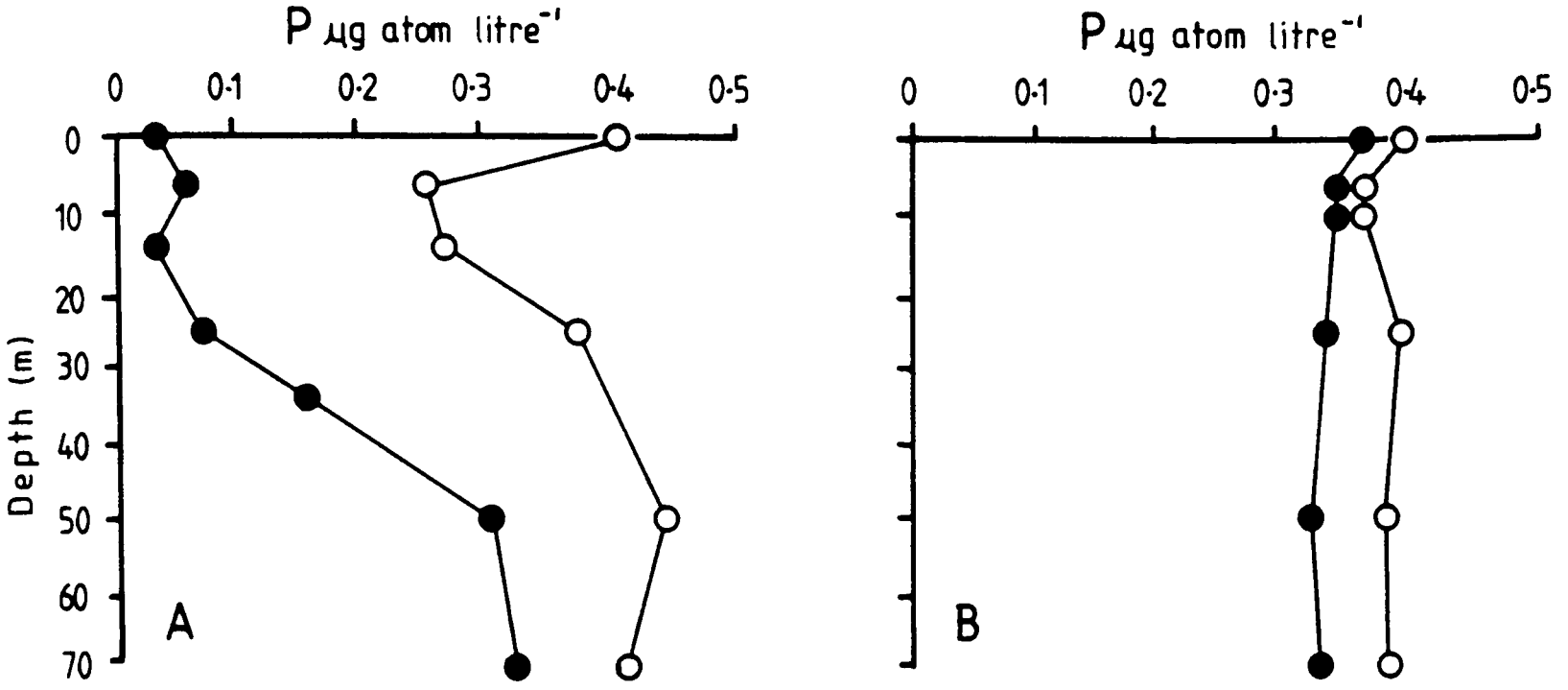


Fig. 6.4 Vertical profiles of orthophosphate (filled circles) and total phosphorus (open circles) in the English Channel in August (A) and January (B) (After Armstrong and Harvey, 1950).

As with the other biolimiting elements (Fig. 6.1), the concentration of inorganic phosphate increases with depth and reaches a maximum between 500 and 2000 m depth. The phosphate maximum layer is most pronounced in the Atlantic Ocean, where it contains $>3.0$ µg-atom P $l^{-1}$ (Seiwell, 1935). Here the phosphate maximum (Fig. 6.5) lies close to, or just below, the oxygen minimum layer.

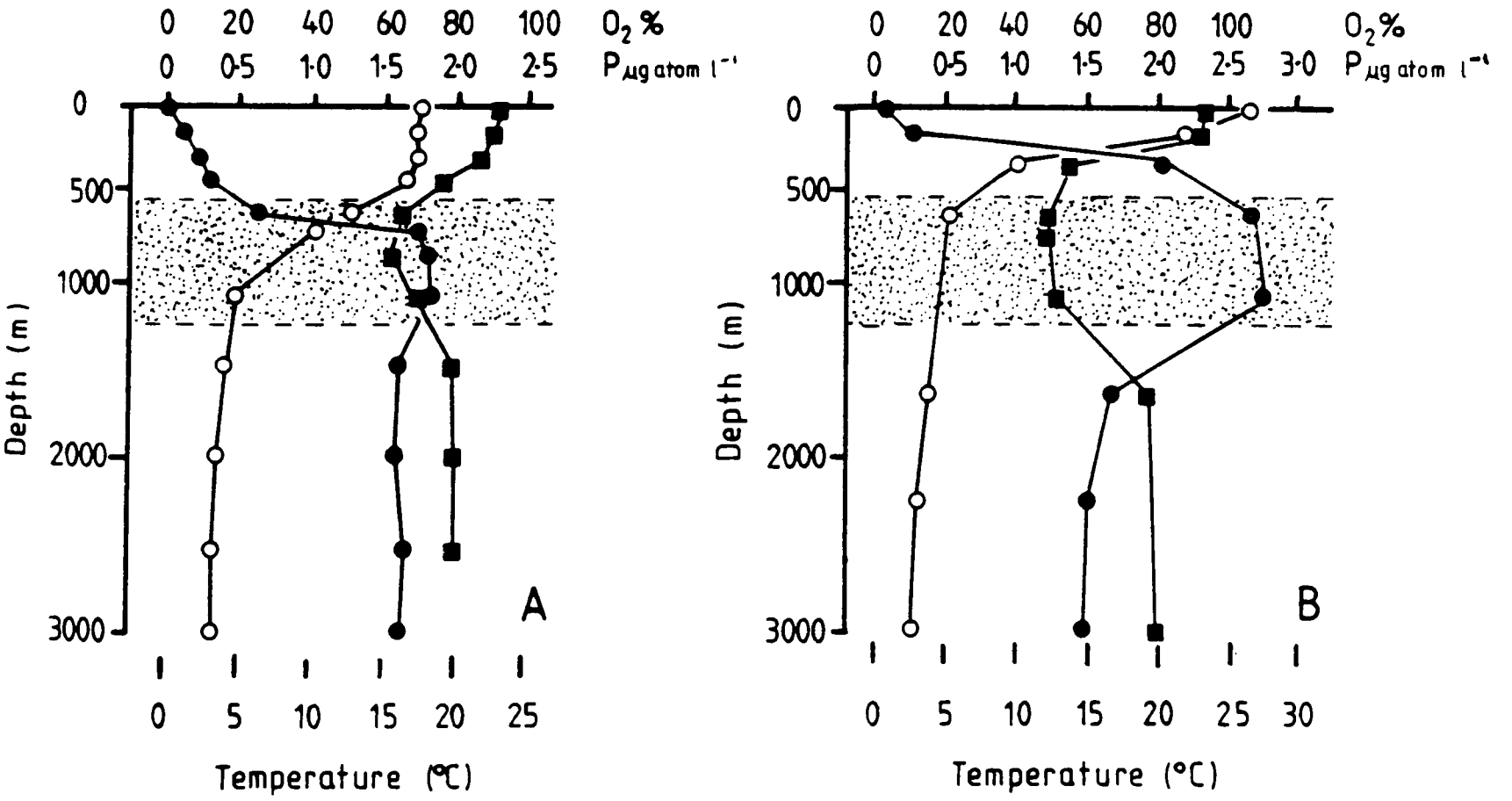


Fig. 6.5 Vertical distribution of phosphate (filled circles), oxygen (squares) as percent saturation and temperature (open circles) in the NE Sargasso Sea (A) and equatorial Atlantic (B). Stippled region represents the oxygen minimum/phosphate maximum layer. (Modified from Seiwell, 1935).

The rapid increase with depth in the neighbourhood of the permanent thermocline (the depth at which the rate of decrease in temperature with increasing depth is at a maximum) is the result of the oxidation of detritus falling from the surface. This oxidation, which may be partially due to the activities of zooplankton, results in the evolution of appreciable quantities of $CO_2$, thereby producing a $CO_2$ maximum layer at that level. The reaction may be represented by the equation (Riley, 1971):

$$(CH_2O)_{106}(NH_3)_{16}H_3PO_4 + 138O_2 \longrightarrow 106CO_2 + 122H_2O + 16NO_3^- + PO_4^{3-} + 19H^+ \quad (6.4)$$

Higher concentrations than those typical of deep ocean water are found in anoxic basins and trenches (Richards and Vaccaro, 1956; Richards, 1960). The increased percentage of inorganic phosphate in deep water makes low concentrations of organic phosphate difficult to detect. However, the equatorial Atlantic, for example, generally shows significant decreases in organic phosphate with depth (Ketcham et al., 1955) such as to be undetectable at depths of $>1000$ m.

### 6.2.4 The phosphorus cycle

The principal method of removal of inorganic phosphate from seawater is assimilation by marine algae (particularly phytoplankton). These plants transform orthophosphate to organic phosphorus compounds and also regenerate some organic phosphate during photosynthesis as extracellular metabolites (Kuenzler and Ketchum, 1962; Watt and Hayes, 1963; Johannes, 1964; Kuenzler, 1970). On death, solid organic phosphate is rapidly regenerated by microbial action while senescent or damaged cells release orthophosphate as a result of autolysis (Vaccarro, 1963). Protozoa may be an important regenerator of phosphate from detritus (Johannes, 1965), both as a primary agent and by the enhancement of bacterial activity.

Although animals obtain their phosphate from plants they only utilise a very small proportion of their total phosphate uptake. Zooplankton may excrete between 10 and 40% of their body phosphate per day (Corner and Davies, 1971; Spencer, 1975). Thus since phytoplankton are generally ingested rather than allowed to decay, regeneration of phosphate by animals is an important mechanism in the

sea. When the zooplankton population is low and the biomass of higher animals, such as fish, is high, excretion by larger fauna may be important A proportion of this phosphate will be in solid form.

It is probable that both phytoplankton and animals are equally important in the production of dissolved and particulate organic phosphate. Bacteria play an important role in the regeneration of phosphate from the solid calcium phosphate of bone (Spencer, 1975) and also concentrate phosphate from sediment, dissolved organic and inorganic phosphate, and particulate matter. During autolysis, however, they provide an important regeneration mechanism for although their biomass is small, their high metabolic rate offsets their volumetric insignificance in the sea.

This general cycle is represented in Fig. 6.6. Phosphorus may only leave the system by sedimentation of particulate material and its permanent consignment to the sediment column. This process may involve the formation of new minerals in the sediment and the absorption of phosphate onto preexisting grains (6.4.2). Ultimately, uplift and erosion will return this phosphate to the system by means of a terrestrially derived input.

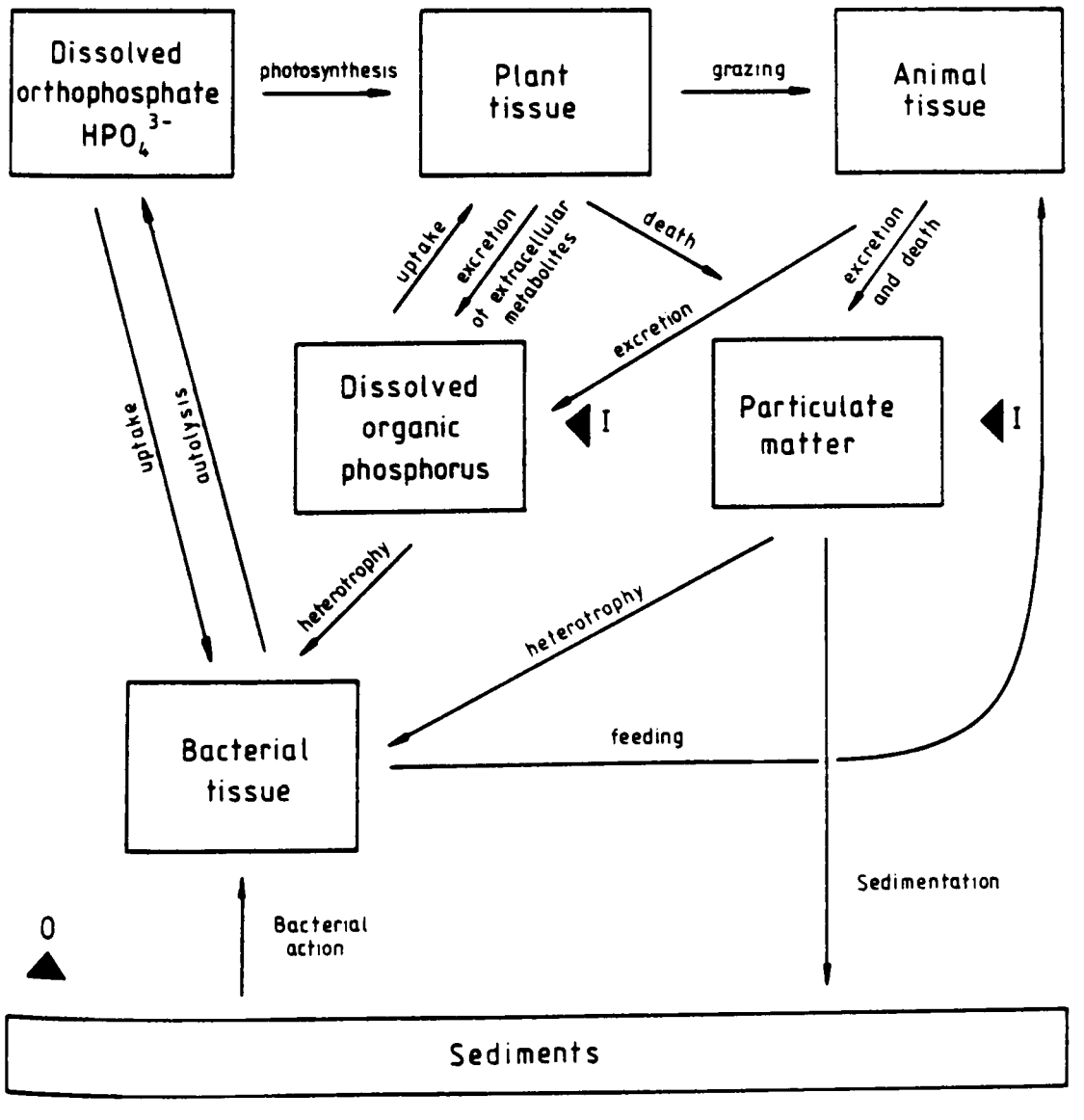


Fig. 6.6 Schematic diagram of the biogeochemical cycle of phosphorus in the oceans.
O = major output,
I = major input to system.

## 6.2.5 Geochemical modelling

The nature of any model is partly dependent on previous knowledge of the way in which a substance is distributed on the Earth's surface. This a priori information is necessary in order to gauge the validity of the assumptions and generalizations which will be ultimately utilised in the construction of the model. Despite these limitiations, geochemical modelling is becoming an increasingly important part of marine chemistry and has been successfully applied to a number of elements (e.g. papers in Goldberg et al., 1977). Phosphorus models have been proposed by Broecker (1971, 1974), Lerman et al. (1975) and Holland (1978). The model considered here is based on that of Broecker (op cit.).

An idealized model of an ocean may be constructed by dividing ocean water into two components, warm water and cold water. The former consists of the thin upper layer of surface water within the photic zone of tropical and temperate regions; the latter consists of the deep oceans and polar waters. The two masses remain distinct because of density differences, and are separated by a permanent thermocline which is generally between 100 and 1000 m depth, but rises to the surface as polar regions are approached. The bulk of the oceans' plant life is concentrated in the warm surface layer.

Movement of an element in this simple two-box system (Fig. 6.7) can be determined if three further assumptions are made:

(a) the element can only be added by river input,

(b) the only way by which dissolved salts may be removed is by sedimentation of particulate matter, some of which escapes biological and physical destruction and is locked up in the sediment,

(c) the model is assumed to be equilibrium, therefore any output from the system is balanced by a corresponding input.

These three assumptions approximate to the real ocean to varying degrees. River transport accounts for 90% of the total material entering the oceans, while transport related to water (streams, icebergs, groundwater) represent 98% of the total (Mackenzie and Wollant, 1977). The remainder consists of wind-blown dust and land-generated volatiles such as the gases released during the

decomposition of organic matter. In absolute terms it has been estimated (Kazakov, 1950; Holland, 1978) that the annual total phosphorus input from rivers is in the order of $2 \times 10^{12}$g. The pre-agricultural input was undoubtedy lower, somewhere between 4 and $8 \times 10^{11}$ g P $y^{-1}$ being estimated by most authors (Veeh, 1979).

The degree to which particulate matter is the only means of phosphorus removal is less certain. Recent studies (Veeh, 1979) indicate the following phosphate sinks: fish debris ($< 2.3 \times 10^{11}$g P $y^{-1}$), metalliferous sediments ($1.4 \times 10^{11}$g P $y^{-1}$), organic matter ($1 \times 10^{11}$g P $y^{-1}$), biogenic carbonates ($< 1 \times 10^{11}$g P $y^{-1}$), phosphorites ($< 1 \times 10^{11}$g P $y^{-1}$), manganese nodules ($< 0.4 \times 10^{11}$ g P $y^{-1}$) and guano ($0.1 \times 10^{11}$g P $y^{-1}$). Thus the total phosphorus removed by these sinks is less than $7.2 \times 10^{11}$g P $y^{-1}$, which compares closely with the estimated pre-agricultural input. There is ample evidence for seafloor precipitation/replacement processes (6.4.2) as well as sorption reactions although these are only the fixing processes that occur once the phosphorus has been incorporated into the sediment. They do not fundamentally affect the validity of the assumption that particulate matter is ultimately the major mechanism of incorporation.

Although a steady state must be assumed in the initial construction of the model, rates may be altered subsequently and their effects on the model determined. Certainly the oceans are nearly in a steady state within the time scales covering the oceanic residence time of phosphorus.

The warm water mass, therefore, receives its phosphate from two sources - river input and recirculation of deep water. If the system is in equilibrium, these two inputs must be matched by an equal loss due to downwelling and particulate settling. However, since phosphorus is totally depleted in surface waters, it may only be lost to the surface layer by the second of these processes. The total mass balance for the idealized ocean must therefore be:

$$C_S V_S = C_R V_R + C_L V_M - C_U V_M \qquad (6.5)$$

where movements within the system have two properties: a phosphate concentration, C and a flux, V; S = particulate matter, R = river influx, M = mixing of layers, L = lower layer and U = upper layer (Fig. 6.7).

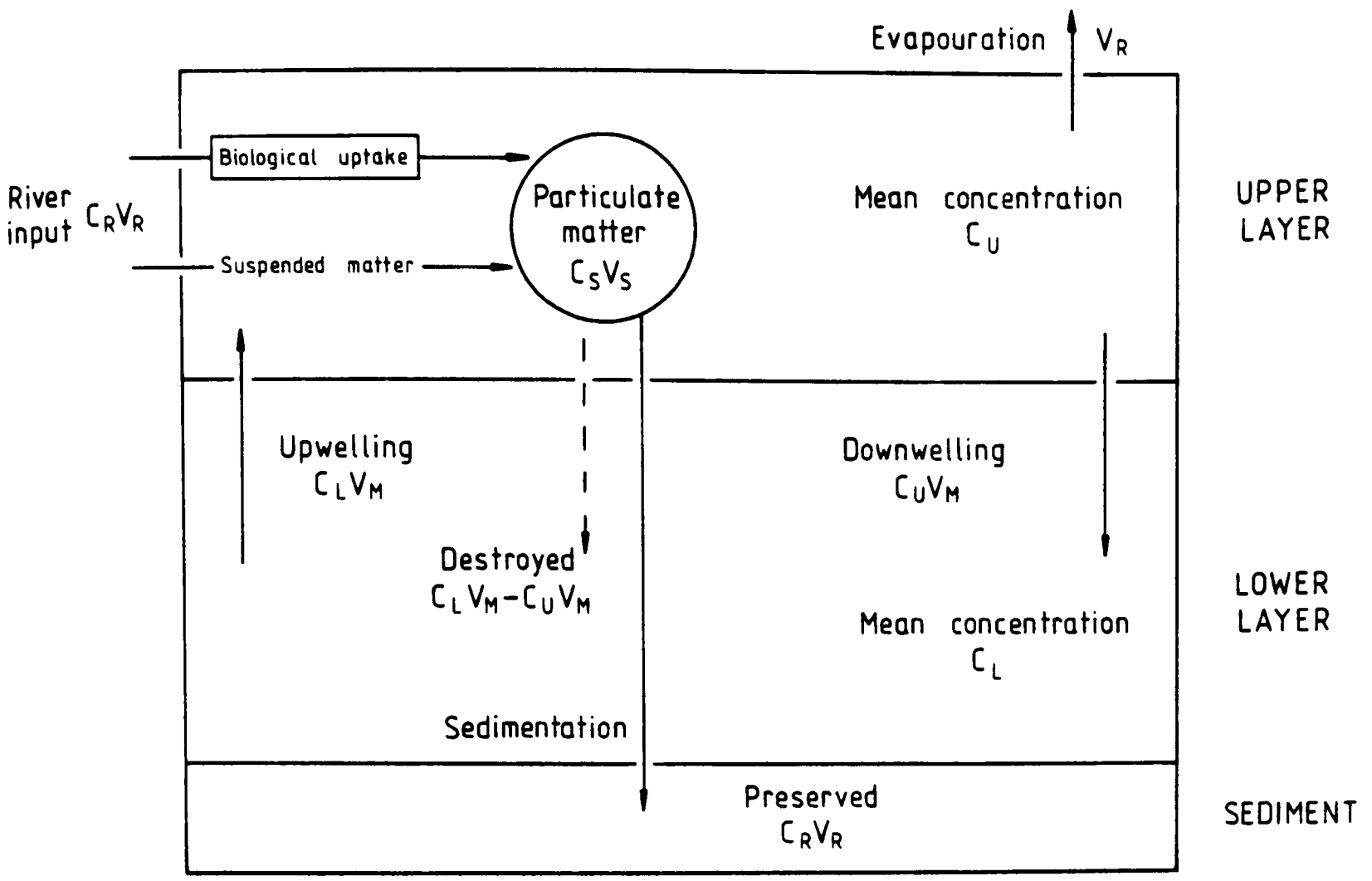


Fig. 6.7 Simple two-box model of the ocean showing the major phosphate fluxes. Fluxes are labelled with the parameters utilised in the text.

If removal from the system is accomplished by burial of particles which escape destruction, then the fraction f of the particle flux $C_SV_S$ surviving destruction must be equal to the river input $C_RV_R$, if the system is to remain in equilibrium. This relationship may be represented by the equation:

$$fC_SV_S = C_RV_R \tag{6.6}$$

substituting for $C_SV_S$:

$$f(C_RV_R + C_LV_M - C_UV_M) = C_RV_R \tag{6.7}$$

solving for f:

$$f = \frac{C_RV_R}{C_RV_R + C_LV_M - C_UV_M} \tag{6.8}$$

or:

$$f = \frac{1}{1 + \frac{V_M}{V_R}\left(\frac{C_L}{C_R} - \frac{C_U}{C_R}\right)} \tag{6.9}$$

In the present oceans the ratio of $V_M$ to $V_R$ is about 20 (Broecker, 1974). In other words, upwelling provides twenty times the volume of water to the

upper layer compared to that provided by runoff. Furthermore, river water contains five times less phosphate per litre than deep water but four times more than the water of the surface layer, thus $C_L/C_R = 5$ and $C_U/C_R = 0.25$. If these values are inserted in Eq. 6.9, f = 0.01. That is only 1% of particulate matter escapes destruction and is therefore removed from the system.

It is also possible to estimate the fraction (g) of phosphate that reaches the surface and is removed in particulate form. This will be a fraction of the total input from rivers and upwelling and will be equal to $C_S V_S$. The equation may be expressed:

$$g(C_R V_R + C_L V_M) = C_R V_R + C_L V_M - C_U V_M \qquad (6.10)$$

solving for g:

$$g = \frac{C_R V_R + C_L V_M - C_U V_M}{C_R V_R + C_L V_M} \qquad (6.11)$$

or:

$$g = 1 - \frac{\frac{V_M}{V_R}\frac{C_U}{C_R}}{1 + \frac{V_M}{V_R}\frac{C_L}{C_R}} \qquad (6.12)$$

If the values used in the determination of f are substituted in Eq. 6.12, then g = 0.95, that is 95% of the phosphate reaching the upper layer of the ocean is removed again as particulate matter. This value of g agrees well with its intuitive value, because as phosphate is depleted in the upper layer, g must lie close to unity. Since f is the fraction of particles surviving destruction and g is the fraction of phosphate being removed as particulate matter, their product (fg) must be the fraction of the oceans total phosphate which is removed during each ocean mixing cycle (i.e. the cycle by which all of the water of the upper layer has passed through the lower layer and returned to its original position). The product fg may be independently determined by the equation:

$$fg = \frac{1}{1 + \frac{V_M}{V_R}\,\frac{C_L}{C_R}} \qquad (6.13)$$

For phosphate this value is about 0.01 i.e. only 1% of the total phosphate in the oceans is lost to the sediment each mixing cycle. $^{14}C$ studies (e.g. Broecker, 1963; Broecker and Yuan-Hui, 1970) have demonstrated that, in the present oceans, the time required for one mixing cycle is 1600 years. It is therefore possible to calculate the time necessary to remove an amount of phosphate equal to the total phosphate in the present oceans. The equation may be expressed:

$$t = \frac{T_M}{fg} \qquad (6.14)$$

where $T_M$ is the time required for one mixing cycle. The value of t for phosphate is therefore 160,000 years.

The model emphasises only the major processes controlling the movement of phosphate in the sea. It does not attempt to explain any second-order features of oceanic circulation such as those which result in higher concentrations of phosphate in deep Pacific water than in deep Atlantic water, while inumerable deviations from the norm have been ignored. Nevertheless, it provides an order of magnitude estimate for the behaviour of phosphate in the present oceans, a prerequisite for understanding ancient ocean systems.

The phosphate content of the ocean appears to be in a state of equilibrium, the abundance of phosphate in the sea is equal to that necessary to supply an amount of phosphate to the seafloor which is equal to that added by rivers. If phosphate were removed faster than it is added, the phosphate content of the oceans would fall, and primary productivity would decline, as would the amount of particulate matter surviving destruction. Phosphate would continue to decrease until equilibrium was reestablished.

The amount of phosphate dissolved in the sea is controlled by: (a) the rate of upwelling of deep ocean water, (b) the percentage of particles that survive oxidation, (c) the phosphate content of the Earth's rivers, and (d) the rate of runoff. Ultimately, then, it is dependent on a number of factors

that include global geography, climate and atmospheric $CO_2$ content. Since the residence time for phosphate is less than $2 \times 10^5$ y, the reaction time of its oceanic concentration to environmental changes would be a fraction of a million years, a geologically insignificant period.

## 6.3 Seafloor phosphorites

Present-day seafloor phosphorites are generally found in water depths of < 500 m on offshore banks, continental shelves and marginal plateaux (Fig. 6.8) where sedimentation is slow or negligible. Continental shelf phosphorites are generally pelletal; deeper deposits massive or nodular. The majority of sites are concentrated within $40^\circ$ latitude of the Equator (McKelvey, 1963, 1967; Sheldon, 1964).

The association of known seafloor phosphorites with regions of upwelling currents (Fig. 6.9), particularly those associated with current divergence and related phenomena, has led to suggestions of a cause-effect relationship (Kazakov, 1937; Brongersma-Sanders, 1957; McKelvey, 1963, 1967). Certainly upwelling is a major mechanism for transfer of phosphorus into the photic zone (6.2.5), and supports high concentrations of organisms from dinoflagellates and diatoms to sharks, sea-mammals and seabirds. Plankton blooms, organic discolourations and mass mortalities are not unusual phenomena in these areas (Brongersma-Sanders, 1957). Radiometric data on seafloor phosphorites (Kolodny, 1969; Kolodny and Kaplan, 1970) indicate, however, that most of these deposits are pre-Holocene in age. If the validity of the cause-effect hypothesis is to be ascertained, the nature, age and occurrence of modern seafloor phosphorites must be examined. Furthermore, those deposits which have been shown to be Recent (Baturin et al., 1972; Veeh et al., 1973; Manheim et al., 1975; Burnett and Veeh, 1977) provide the only modern analogues to ancient phosphorites; an examination of their character, distribution and depositional environment is invaluable to the interpretation of ancient deposits and provides important insights into, and constraints on, the phosphatization process.

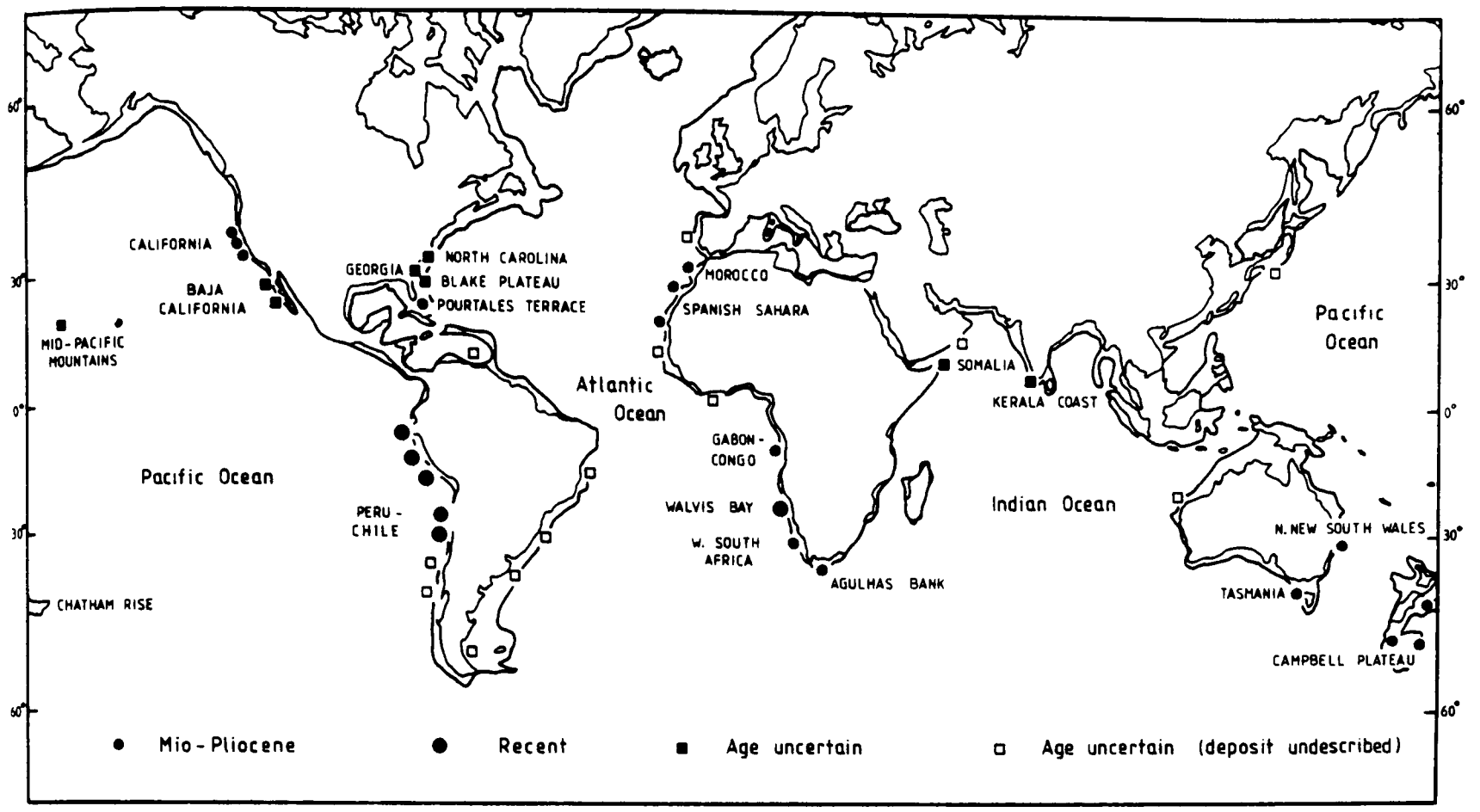


Fig. 6.8 Distribution of seafloor phosphorites.
The locality names are those referred to in the text. The open squares represent sites plotted by other authors (McKelvey, 1963, 1967; Bezrukov et al., 1961) but are undescribed. The 1000 m bathymetric contour (heavy line) delimits the area of the continental shelves; present-day land areas (thin line) are also shown. The map is based on a Mercator projection. (Base map after Smith and Briden, 1977).

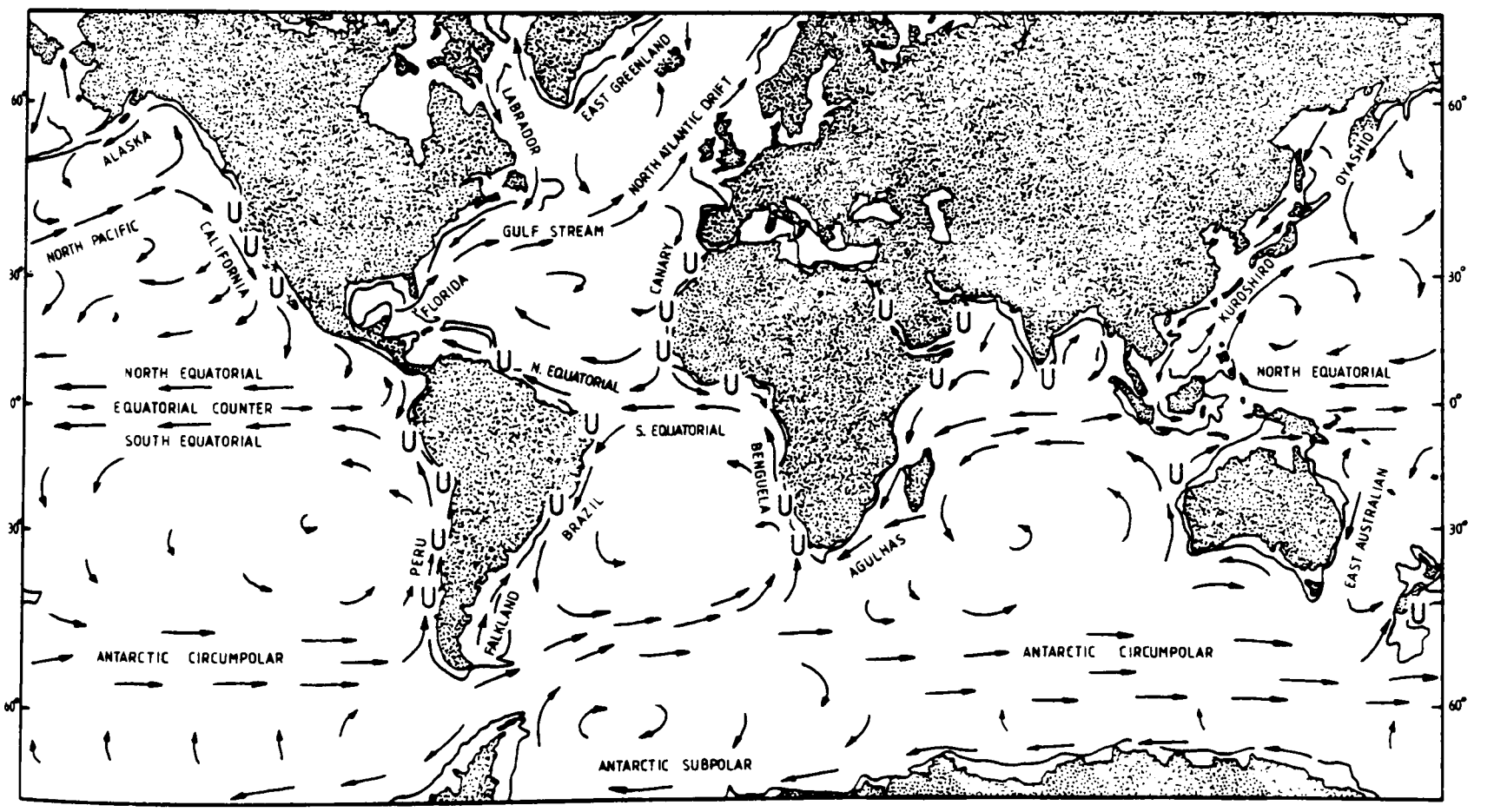


Fig. 6.9 Ocean-surface currents and their relation to upwelling regions. The 1000 m bathymetric contour (heavy line) delimits the area of the continental shelves; land areas are stippled. Ocean currents based on Sverdrup et al. (1942), Mink (1955) and Shepard (1973); upwelling regions after Brongersma-Sanders (1957); base map from Smith and Briden (1977) - Mercator projection.

### 6.3.1 California Shelf, USA

Phosphorite samples were first described from this area by Dietz et al. (1942) and more recently by Emery and Dietz (1950), Emery (1960), Mero (1961) and Pasho (1973). The phosphorite occurs in a variety of forms, and ranges in size from silt-grade particles to 60 cm blocks. Larger examples consist of nodules or slabs, usually with flat bottoms and nodular tops; conglomeratic varieties are common. Finer material occurs as small grains, ovules (probably of faecal origin) and ooliths of sand to gravel grade. All forms are characterised by brown or black glazed surfaces, and those collected from deeper water ( >300 m) are further coated by thin manganese skins (Dietz, 1955). The cores of the nodules are commonly dark and enriched in organic matter (Emery and Dietz, 1950; Kolodny and Kaplan, 1970; Pasho, 1973). Most of the phosphorite, which has a mean $P_2O_5$ content of ~28% (Pasho, 1973), contains substantial proportions of diluents, principally glauconite, calcareous debris, euhedral feldspars and volcanic rock fragments, in a carbonate-fluorapatite matrix. The carbonate (dominantly foraminiferans) included within the phosphorite displays varying degrees of replacement by phosphate.

The majority (~95%) of the phosphorite is located in water depths of 30 - 300 m (Emery, 1960); below 300 m phosphorite becomes increasingly diluted by the deposition of detrital sediments. The phosphorites are generally associated with glauconitic foraminiferal sands, and, in shallower water, are heavily encrusted by bryozoans, brachiopods, tube-worms, sponges and corals. The deposits cover an estimated area of $16 \times 10^3$ sq km, and if they are assumed to be only 3 cm thick then the region contains in excess of $10^9$ tonnes of rock. Nevertheless, at the present time (1980), a combination of water depths and alternative sources make the area commercially unattractive.

Most of the phosphorite contains mid to late Miocene foraminiferans and is therefore considered to be of that age, although some of the lighter brown nodules enclose late Pliocene to Recent forms and are therefore younger (Dietz et al., 1942; Emery and Dietz, 1950). It is noteworthy that these latter forms indicate depths similar to those at the present day, although radiometric dating

(Kolodny, 1969; Kolodny and Kaplan, 1970) demonstrates that the deposits are predominantly pre-Holocene ( $>8 \times 10^5$ y).

The present seafloor is strongly oxidizing and supports a prolific benthonic fauna, despite the area being the site of upwelling caused by the coastal divergence of the California Current.

### 6.3.2 Baja California Shelf, Mexico

The locality has been described in detail by D'Anglejan (1967, 1968a, b) and was also considered by Overall (1968). Phosphate pellets, grains and pebbles occur on an erosional platform cut into the west flank of a synclinal complex (D'Anglejan, 1979). The phosphorites are predominantly well-sorted, sand-grade carbonate-fluorapatite with mean $P_2O_5$ contents of ~30%. D'Anglejan (1967) distinguished two major types of phosphatic particle:

(a) black, fine-sand grade, structureless ovoids and

(b) biogenic material, including reworked phosphatic brachiopod shells.

The deposits are associated with opaline silica and pyrite-bearing reducing muds; opaline silica commonly envelops and infills crevices in the phosphatic component. The phosphorites occur in water depths of 50 - 800 m, but the highest concentrations are in water 50 - 100 m deep, where they are associated with sand-grade sediments. Nodular phosphorites generally occur from 100 - 200 m depth and most of these are clearly formed by the replacement and reworking of the Pliocene(?) limestones that rest on top of the local Miocene unconformity. The age of the bulk of the deposit is uncertain, although D'Anglejan (1967) records 'old' $^{234}U/^{238}U$ ratios, which have been confirmed as pre-Holocene ( $>8 \times 10^5$y) by Kolodny (1969) and Kolodny and Kaplan (1970). D'Anglejan concludes, therefore, that his Recent $^{14}C$ dates are in error due to contamination.

The region has a generally arid climate and is the site of intense divergent upwelling of the California Current from April to June. During this period the oxygen-minimum/phosphate-maximum layer may impinge onto the Banks and increase the phosphate content of the bottom waters. Nevertheless, no Recent phosphorite has been confirmed, although D'Anglejan (1968b, 1979) has postulated Recent

early-diagenetic phosphatization in foraminiferal calcarenites some distance from the former deposit.

### 6.3.3 Blake Plateau, Florida USA

Phosphorite/manganese concretions were first recovered from the Blake Plateau in 1881 (Murray, 1885). The phosphorites range in size from sand-grade to boulders of replaced limestone weighing up to 56 kg. Conglomeratic varieties occur on the shallower portions of the Plateau. The phosphorites are intimately associated with a manganese pavement, which they generally underlie (Pratt and McFarlin, 1966; Pratt and Manheim, 1967; Pratt, 1971), and occur in water depths of 200 - 600 m on the NW side of the Plateau, the remainder of which is dominated by manganese mineralization.

Nearby shelf sediments consist of quartz and shell sands containing minor amounts of phosphorite (Gorsline, 1963) but the sediments of the Plateau are foraminiferal (globogerinid) and pteropod calcarenites; ahermatypic coral mounds are commonly associated with these sediments. Much of the phosphorite/manganese pavement has little sediment cover, however, due to the bottom-current activity associated with the Gulf Stream.

Late Cretaceous to Pliocene fossils have been recorded from within the phosphorite (Pratt and Manheim, 1967; Pratt, 1971) and $^{234}U/^{238}U$ ratios also indicate a pre-Holocene age for the period of phosphatization (Kolodny, 1969; Kolodny and Kaplan, 1970). There is no indication of Recent phosphorite formation (Manheim, 1979), but manganese deposition appears to be a contemporary phenomenon. The change in mineralization was probably due to the increase in depth that accompanied the gradual subsidence of this part of the Atlantic outer continental shelf which has fallen 2,700 m since the Lower Cretaceous (Enos and Freeman, 1979).

### 6.3.4 Straits of Florida, USA

Two extensive (100 x 25 km) submarine terraces are situated in the Straits

of Florida - the Pourtalès Terrace to the south, and the Miami Terrace to the north. The morphology of the terraces has been interpreted (Burnett and Gomberg, 1977) as a palaeokarst phenomenon. The Pourtalès Terrace was originally reported as a seafloor phosphorite site in 1888 (Agassiz, 1888) and the phosphorites have been examined by Bush (1951), Gorsline and Milligan (1963), Gomberg (1976) and Burnett and Gomberg (1977). The Miami Terrace phosphorites are a more recent discovery (Malloy and Hurley, 1970; Neumann and Ball, 1970; Ballard and Uchupi, 1971; Pratt, 1971; Mullins and Neumann, 1979). The phosphorites occur as phosphatized shallow-water limestones which have been replaced in situ on the Pourtalès Terrace (Burnett and Gomberg, 1977) but are found as large, loose slabs and irregular masses on the Miami Terrace (Mullins and Neumann, 1979). The Pourtalès Terrace material is underlain by a discontinuous phosphatic lag deposit consisting of rounded and polished bones and teeth, coprolites and irregularly-shaped phosphatized limestone cobbles. Similar nodular varieties have been recovered from the lower Miami Terrace (600 - 700 m). The phosphatized limestones are brown-black in colour, generally foraminiferal and contain glauconite, echinoid spines, corals and bivalve debris. Nodules and blocks are commonly encrusted by tube-worms and bryozoans, and are frequently bored. The phosphate mineral has been identified as carbonate-fluorapatite.

The phosphorites occur in water depths of 200 - 400 m on the Pourtalès Terrace and the upper Miami Terrace, but nodular varieties have also been recovered from the lower Miami Terrace (600 - 700 m). The phosphorites underlie a zone of strong surface currents. The warm, saline tropical and equatorial waters which sweep the Florida Straits are, at least periodically, of sufficient intensity to prevent the settling of fine material on the terraces. The lack of sediment cover on the limestone outcrop may have led to the removal of considerable thicknesses of lithified material by bioerosion (Mullins and Neumann, 1979) (cf. 3.3.2). The seafloor is strongly oxidizing and has an abundant benthos and although the deep-flowing Florida current is forced up over the shallow marine portion of the Florida Peninsula (Sverdrup et al., 1946), there is no evidence of Recent upwelling in the area.

The phosphatized limestones are of Eocene to Pliocene age (Burnett and

Gomberg, 1977) but most of the phosphorite has been dated as Middle Miocene on foraminiferal evidence (Milligan, 1962; Gorsline and Milligan, 1963; Mullins and Neumann, 1979). Since the phosphorite is clearly replacing pre-existing limestone, the palaeontological data only provide maximum ages for the phosphatization process. Uranium series results on Pourtalès Terrace phosphorites (Burnett and Gomberg, 1977) indicate, however, that phosphatization is not contemporary; the only exception may be the small mount of 'authigenic' phosphatic material which has been deposited within cavities in Quaternary limestones.

### 6.3.5 Georgia and North Carolina Shelf, USA

The phosphatic sediments of this region are estuarine and beach sands in which the largest phosphatic material only reaches 1.5 cm across (Pevear, 1966, 1967; Pevear and Pilkey, 1966; Luternauer and Pilkey, 1967; Pilkey and Luternauer, 1967). The phosphorite constitutes only 1% of the region's shelf, beach and estuarine sediments. It occurs in three forms: (a) black, opaque grains, (b) red-brown to amber, transluscent grains, and (c) mottled grains. All three types are isotropic and have polished surfaces. The colour differences are due to oxidation (Pevear and Pilkey, 1966) which transforms the pyrite and organic matter included in the primary black grains. The amber variety is absent from estuarine facies, and even on shelf and beach is subordinate to black forms. The highest phosphorite concentrations occur in water depths of 20 - 30 m but phosphorite has been recovered from depths of 0 - 50 m.

A detrital origin is implied by the grain-size distribution which is identical to that of coexisting quartz sands. Furthermore, identical grains occur in the Miocene rocks of the coastal plain, and tumble-barrel experiments have shown that the highly-polished nature of the grains may be due to mechanical abrasion. Modern rivers are apparently not contributing any phosphorite from land sources so the material must be either from a Pleistocene input or result from reworking of Miocene(?) phosphatic sediments on the continental shelf.

There is no upwelling in the area at the present day which has led Pevear

(op cit.) to propose an estuarine origin involving the phosphatization of pre-existing limestones. Reexamination of the onshore deposits (Riggs, 1979a, b), however, suggests that upwelling on the shelf during the Miocene caused the deposition of phosphatic muds that were subsequently reworked to form pelletal clasts, which were mixed with grains of biogenic origin. Deposition took place in entrapment basins on the flanks of regional 'highs'.

### 6.3.6 Peru-Chile Shelf

First discovered by Murray in 1898, nothing was published concerning the composition of these deposits until recent Russian work (Baturin, 1971; Baturin and Petelin, 1972). The Chile Shelf phosphorites consist of coprolites, bone fragments and dull-surfaced nodules from 3 mm to 10 cm across. Most nodules, however, are in the 5 - 10 cm range and contain structureless phosphatized ovules with detrital-grain nuclei. These ovules, which are probably of faecal origin, also occur in the surrounding diatomaceous oozes. The phosphate, a carbonate-fluorapatite, occurs as an inorganic(?) precipitate on diatom frustules (Burnett, 1974, 1977) and as localized apatitic replacements of Recent benthonic foraminiferans (Manheim et al., 1975). The nodules display a continuous and progressive mineralization series which can be divided into four stages:

(1) white to light-grey, unconsolidated forms with 15% $P_2O_5$,

(2) light-grey more compact varieties with 20% $P_2O_5$ and a 'hardness' of 2 - 3.

(3) light-grey to grey, consolidated examples, 'hardness' 4 - 6, $P_2O_5$ 25%,

(4) black, consolidated nodules with a 'hardness' of 5 and $P_2O_5$ contents up to 32%.

The $P_2O_5$, CaO, $CO_2$ and F content of the nodules increases with progressive consolidation, although the highest $P_2O_5$ values are generally only associated with recognisable coprolites. Unlike SW African examples (6.3.7), no nodules have been recorded in the initial stages of phosphatization i.e. with $P_2O_5$ values of 5% or less.

The Russian work provides little information concerning the environment of deposition of these phosphorites but more data are available for similar deposits

on the Peruvian Shelf (Veeh et al., 1973; Manheim et al., 1975; Burnett, 1974, 1977; Burnett and Veeh, 1977; Burnett and Soutar, 1979). Again accompanying sediments are dark-green, organic-rich, laminated, diatomaceous oozes. The region is one of intense coastal upwelling where a seasonal eastern boundary current (the Peru Current) maintains a well-developed oxygen-minimum layer which intensifies towards the coast (Wooster and Reid, 1963). Upwelling results in bottom water concentrations of 2 $\mu$g-atom P $l^{-1}$ but pore-water values have been estimated up to 60 $\mu$g-atom P $l^{-1}$ (Manheim, 1975). Current activity is sufficient to allow only a minimal terrigenous and carbonate detrital input. The phosphorites are confined to two narrow bands at depths of 100 and 400 m (Veeh et al., 1973; Burnett, 1974; Soutar and Burnett, 1979) which roughly coincides with the upper and lower boundaries of the oxygen-minimum layer where it impinges on the seafloor.

The Chilean material has been dated as late Quaternary ($55 \pm 35 \times 10^3$ y) by Baturin et al. (1972) while $^{234}U/^{238}U$ ratios for the Peruvian material (Burnett et al., 1973; Veeh et al., 1973; Burnett and Veeh, 1977) yields ages of $3 \times 10^5$ y to Recent. $^{230}Th/^{234}U$ data for the latter deposit indicates an upper limit of $125 \times 10^3$ y and a Recent date is also confirmed by the foraminiferal evidence (Manheim et al., 1975). McArthur (1978), however, has criticised the uranium dating techniques of Burnett (op cit.) and has suggested that the lithified nodules, considered by the latter author to be Recent, are in-fact of Miocene age. McArthur (1978) does not, however, dispute the Recent age of the soft 'authigenic' phosphorites in the area.

It has been suggested (Burnett, 1974; Burnett and Veeh, 1977) that phosphatization is episodic, and that periods of mineralization may be correlated with high stands of sea-level. Certainly during regressive periods, reworking rather than deposition of new phosphorite might be expected. Such reworking has been demonstrated by Baturin and Patelin (1972) and has been suggested as a mechanism for uranium enrichment of the lithified nodules (McArthur, 1978).

### 6.3.7 Walvis Bay, Namibia SW Africa

Previously recognised as a seafloor phosphorite site (McKelvey, 1963, 1967), the suggestion of Baturin (1969) that the area is the site of contemporary phosphorite formation has led to a substantial volume of literature in the last decade (Baturin, 1969, 1971a, b, 1974; Baturin et al., 1970, 1972; Senin, 1970, 1977; Romankevich and Baturin, 1972; Summerhayes et al., 1973; Veeh et al., 1974; Price and Calvert, 1978; Calvert, 1979).

Two distinct environments are found within the region, one is apparently the site of active phosphatization while the other contains only remanié material. The phosphorites in the former region have been studied in the greatest detail and yield the most comprehensive information concerning the phosphatization process. Five forms of phosphorite may be distinguished:

(1) Unconsolidated straw-yellow lenses, clots and laminae 1 - 5 mm thick and clots occasionally up to 10 cm across. This variety has $P_2O_5$ contents of 3 - 11%.

(2) Round, tabular, elongate or irregular phosphatic nodules varying in colour from cream to dark-grey and brown. These nodules are generally up to 2 cm across and are fragmented, anisotropic and contain microfossil 'ghosts' in thin-section, $P_2O_5$ values are from 20 - 30%.

(3) Pelletal phosphorite consisting of black, spherical and ovoid grains which include ovules, ooliths and faecal pellets. These are usually 0.1 - 0.25 mm in diameter.

(4) Fish teeth, scales and bones and sea-mammal remains.

(5) Phosphate-rich diatomaceous sediment containing ~1% $P_2O_5$.

Although the first two varieties form separate categories in the classification, they are end-members in a continuous phosphatization series, similar to that seen in the Peru-Chile material (6.3.6). In shallow water (85 m), bored nodules have also been described (Baturin, 1974), indicating that oxygenating bottom conditions occur at least intermittently in the anoxic region (see below). The area containing examples of progressive mineralization is restricted to water depths of 50 - 130 m (the area of diatomaceous mud deposition), however, phosphorites have been recovered from water depths of up to 2000 m (Summerhayes et al., 1973).

Maximum phosphorite concentrations are associated with the sediments of the outer shelf in water depths of 150 - 320 m (Senin, 1970). The phosphorites are predominantly pelletal, black nodular varieties associated with quartz sands and calcarenites; their greatest concentration occurs in a basinal structure in the shelf profile. Since evidence for progressive phosphatization is lacking in this area, the phosphorites are considered to be the products of Mio-Pliocene reworking and redeposition. Similar reworked Mio-Pliocene phosphorites occur to the north in offshore southern Gabon and northern Congo (Cornen et al., 1973).

There is a clear distinction of sediment type between regions of actively-forming and reworked phosphorites; diatomaceous oozes accompany unconsolidated forms, calcarenites and quartz-sands the pelletal varieties. The transition is reflected by the change from anoxic to oxic bottom conditions, the boundary between which has been regarded (Senin, 1970) as being particularly favourable for phosphatization (cf. Peru-Chile).

The region is effected by intermittent upwelling in association with the Benguela Current. Massive phytoplankton production results in the rapid sinking and incomplete-regeneration of biogenic debris to depths of 50 - 150 m. This process, in combination with the low terrigenous detrital-input, causes the accumulation of diatomaceous oozes in this depth range. These oozes contain 5 - 20% $C_{org}$ and their interstitial waters are highly enriched in carbohydrates and phosphate. Pore-waters have pH ranges of 7.2 - 7.8 and are strongly reducing (Eh = -200 mV).

The validity of this environment to the genesis of phosphorites depends on the associated phosphorite being contenporaneous. Initial uranium isotope investigations (Baturin et al., 1972), which yielded Recent dates ($24 \pm 27 \times 10^3$ y) for soft nodules, have been confirmed by later workers (Veeh et al., 1974), who report $^{234}U/^{238}U$ ratios of $1.16 \pm 0.02$ for unconsolidated material and $0.87 \pm 0.01$ to $1.02 \pm 0.01$ for other types of phosphorite. Only the latter ratios represent pre-Holocene ( $> 7 \times 10^5$ y) ages. Palaeontological evidence, provided by diatom species enclosed in the nodules, confirms these results (Baturin, 1974).

### 6.3.8 North-west African Shelf

Phosphorites in this region were reported by Murray and Chumley (1924) and more recently by Tooms and Summerhayes (1968), Summerhayes (1970a, 1972), Summerhayes et al. (1972), Kharin and Soldatov (1975) and McArthur (1974, 1978). All major varieties of phosphorite, except unconsolidated nodules, have been reported from this locality. Angular fragments and blocks of phosphatized limestone up to 150 cm across and with $P_2O_5$ contents of 5 - 25% occur off Morocco and the Spanish Sahara in water depths of 135 - 460 m (Kharin and Sodatov, 1975) and further south off Liberia (Schlee et al., 1974). Conglomeratic and brecciated phosphorites containing glauconitic sandstones and phosphatized foraminiferal limestones occur in the same region. The majority of the phosphorite, however, is pelletal and associated with relic sands of Pleistocene age (Summerhayes et al., 1972).

Geological and geophysical studies (Summerhayes et al., 1971) have demonstrated that the two phosphorite-bearing Moroccan Basins continue out onto the continental shelf. These basins, which contain Maastrichtian to Eocene phosphorites, are the source of much of the shelf phosphorite, although foraminiferal evidence (Kharin and Soldatov, 1975) suggests that a mid Miocene generation is also present. Mid Miocene to early Pliocene dates have been assigned to the Spanish Sahara and Liberian shelf material, but again, an older component may be admixed. There is no evidence of contemporary phosphatization in the region (Summerhayes et al., 1972), despite it being the site of active upwelling by the Canary Current along the arid coastline.

### 6.3.9 Agulhas Bank, South Africa

The first reported seafloor phosphorites were dredged from the South African continental shelf in 1873 during the cruise of the HMS Challenger (Murray and Renard, 1891). The deposits were described in detail by Cayeux (1905, 1934) and more recently by Parker (1971, 1975), Parker and Siesser (1972), Summerhayes (1972b, 1973), Baturin and Dubinchuk (1974), Birch (1975, 1979a, b), Rogers (1977), Siesser (1978) and Fuller (1979). The phosphorites occur in three main associations:

(1) Conglomeratic phosphorites consisting of phosphatized limestone pebbles and macrofossils set in a glauconite, micrite and phosphatized micrite matrix. The category has average $P_2O_5$ values of 17 - 18% (Parker, 1975).

(2) Non-conglomeratic phosphorites consisting of phosphatized limestones with average $P_2O_5$ contents of 15% (Parker, 1971; Parker and Siesser, 1972).

(3) Disseminated sand-grade phosphorite and phosphatic glauconite (Summerhayes, 1973; Birch 1979a, b, c).

The first two categories are regarded (Parker, 1971, 1975) as representing contrasting inner- and outer-shelf depositional environments. Glauconite, macrofossil debris and terrigenous grains are concentrated near-shore (100 - 200 m), and planktonic foraminiferans, quartz-silt and lime-mud off-shore (200 - 500 m). Changes in sea-level have caused the migration of these facies and reworking of pre-existing phosphorites to form conglomeratic varieties. The third category is ubiquitous to the bank and is associated with shelly and quartzose sands, glauconitic sands and muds.

Cayeux's (1934) suggestion of a pre-Pleistocene age for these deposits was confirmed by Uranium-disequilibrium studies (Kolodny, 1969; Kolodny and Kaplan, 1970) which yielded pre-Holocene ( $> 8 \times 10^5$ y). Recent foraminiferal work (Siesser, 1978; Birch, 1979a) has indicated a mid Miocene to Pliocene age, although it has been suggested (Summerhayes, 1973) that a limited amount of carbonate-fluorapatite may be forming during early diagenesis, in faecal pellets of the organic-rich diatomaceous muds which characterise the western Agulhas Bank at the present day.

Benguela-type upwelling occurs along the south-west African and western South African coasts, but only as far south as Cape Point (Shannon, 1966). Thus it does not influence the broad expanse of the Agulhas Bank which lies to the south and west of the Cape. The westward-flowing Agulhas Current sweeps across the Bank but its surface waters are poor in nutrients and have a low biological productivity; below the thermocline, however, the Agulhas Current waters are enriched in phosphate and their intrusion onto the shelf provides a plausible mechanism for Miocene phosphatization (Siesser, 1978).

### 6.3.10 Gulf of Aden, Somalia East Africa

This locality was reported by Gevork'yan and Chungunnyy (1969, 1970) and independantly by Schott (1970, 1976). Nodules are brown coloured and generally 2 - 3 cm across (occasionally 5 cm). They contain $P_2O_5$ contents of up to 30% and are of uncertain age, although Mesozoic and Caenozoic phosphorite-bearing sediments outcrop on nearby islands and provide a potential detrital source.

The area is a site of regional upwelling in the summer, when surface concentrations of 10 $\mu$g-atom N $l^{-1}$ and 1 $\mu$g-atom P $l^{-1}$ have been recorded (Wyrtki, 1971). It is not known whether the upwelling and phosphorites are directly related.

### 6.3.11 Northern New South Wales, Australia

First reported by Loughnan and Graig (1962), the deposits have been described in more detail by Von der Borch (1970), Marshall (1971) and Kress and Veeh (1980). Three types of phosphorite have been recovered:

(1) Small, dull-grey, irregular and unpolished nodules having an average diameter of 3 cm. These consist of phosphatized micrites rich in planktonic foraminiferans, and are commonly encrusted. They have $P_2O_5$ contents of up to 20%.

(2) Equidimensional, subrounded and glazed particles from coarse-sand grade to 20 cm across. Nodules commonly display external goethitic crusts up to 3 mm thick, and are composed of phosphatized clay-grade components.

(3) Conglomerates of both of the above categories admixed with phosphatized bone, coral and sharks teeth.

The first category occurs at a depth of 385 m while the latter two are recorded from 210 - 290 m. Enclosed foraminiferans have been dated as mid Miocene, and Mio-Pliocene crabs have been recorded from the phosphatized clays. Recent radiometric data (Kress and Veeh, 1980) confirms a Miocene age for the second and third categories but indicates ages of 50,000 - 55,000 y for the dull-surfaced nodules, so limited contemporary phosphatization appears likely. The area is swept by the East Australia Current which keeps the area free of detritus, but no upwelling has been recorded.

Pre-Holocene phosphorites have been recorded off Tasmania and on Seamount NT5, north-east of Australia (Kolodny, 1969; Kolodny and Kaplan, 1970). The latter occur at depths of 521 - 322 m.

6.3.12 Chatham Rise, New Zealand

Phosphorites from the Chatham Rise were reported by Reed and Hornibrook (1952) and have more recently been described by Norris (1964), Pasho (1973, 1976) and Cullen (1979). They have been examined from an economic standpoint by Summerhayes (1967), Watters (1968) and Buckenham et al. (1971). The nodules are generally less than 5 cm although examples of up to 15 cm have been recorded. They usually have smooth, black, glauconitized outer surfaces and are commonly encrusted and bored. Empty burrows often cut the nodules, which consist of well-lithified, incompletely-phosphatized foraminiferal limestones and chalks with ~30% foraminiferans. They contain 16 - 26% $P_2O_5$.

The nodules occur mainly at the base of greenish, glauconitic, sandy muds which overlie soft foraminiferal oozes of Oligocene age above indurated Oligocene chalks. The seafloor is well oxygenated and the majority of nodules are recovered from depths of 370 - 400 m (Cullen, 1979); none have been found shallower than 200 m.

Enclosed foraminiferans are all late Miocene, a pre-Holocene date being confirmed by isotopic data (Kolodny, 1969; Kolodny and Kaplan, 1970; Cullen, 1979). The region displays contemporary upwelling (Brongersma-Sanders, 1957) but this does not result in anoxic bottom conditions.

Comparable deposits of phosphatized Miocene limestones also occur on the Campbell Plateau (Summerhayes, 1967) off south-east New Zealand.

6.3.13 Other localities

Phosphorites have been recovered from the central Pacific, Mid-Pacific Mountains region by Hamilton (1956), Hamilton and Rex (1959) and Bezrukov et al. (1969). They consist of white to brown phosphorites, altered basalts with

phosphate-filled pores, and phosphate-cemented tuff-breccias. Fe-Mn concretions in the area occasionally have phosphatic cores. The age of these deposits is regarded as being Cretaceous - Tertiary.

Fe-Mn phosphorites and phosphatized micrites have been recovered from the slopes of a seamount on the Aves Swell, eastern Caribbean, from water depths of 620 - 730 m (Marlowe, 1971). The foraminiferans contained within these nodules are indicative of a Miocene age. Phosphatized Miocene limestones are also known from Gerda Guyot in the south-east Bahamas (Milliman, 1974 p.291).

Phosphate-rich sediments have been recorded off the Kerala coast of southern India in silty sands and silty clays (Murty et al., 1968) in an upwelling region which displays phosphate-enriched surface waters during the monsoons. No further details are available.

A series of further localities have been marked on the seafloor phosphorite distribution maps of previous authors (Bezrukov et al., 1961; McKelvey, 1963, 1967) but no information is available concerning the nature of these deposits.

### 6.3.14 Classification

An examination of the ages of seafloor phosphorites (Fig. 6.10) demonstrates that they fall into two age groupings: (a) Recent and (b) Mio-Pliocene. Other material, such as the Maastrichtian phosphorite admixed in the north-west African deposits (6.3.8), occurs as a minor constituent in some examples. Age is not, however, the only property that distinguishes the two groups; their associated sediments and depositional environments are also different.

Recent phosphorites are associated with strongly-reducing, organic-rich, diatomaceous muds. They are apparently forming during early diagenesis immediately below the sediment/water interface, particularly beneath regions of the seafloor which show a rapid transition from oxidizing to reducing conditions (such as where the $O_2$ minimum layer impinges on the continental shelves). Both SW Africa and Peru-Chile are flanked by arid hinterlands, the Namibian and Sechura deserts respectively.

Mio-Pliocene phosphorites, on the other hand, are characterised by their

association with oxidizing seafloors and carbonate sediments, particularly foraminiferal sands and muds. Furthermore, most examples are clearly replacive in origin - they contain phosphatized and otherwise mineralized pre-existing limestones and the accompanying pelletal and nodular forms are commonly similarly derived. Continental margins associated with the group have a variety of climates; only Baja California, NW Africa and Somalia are arid at the present-day.

| Site | Type | Depth | Age | Dating | Associated sediment | Environment | Currents |
|---|---|---|---|---|---|---|---|
| California Shelf USA | Pelletal, nodular | 30 - 300m | Middle-Late Miocene & Late Pliocene | Foraminiferal, radiometric | Glauconitic and foraminiferal sands | Oxidizing | Upwelling |
| Baja California Shelf Mexico | Pelletal | 50 - 100 m | Pliocene (?) | Radiometric | Opaline silica - bearing muds | Reducing | Upwelling |
| | Nodular & phosphatized limestone | 100 - 200 m | | | | | |
| Blake Plateau, Florida, USA | Pelletal, nodular, phosphatized limestone | 200 - 600m | Late Cretaceous - Pliocene | Palaeontological, radiometric | Foraminiferal and pteropod calcarenites | Oxidizing (?) | No upwelling |
| Pourtalès Terrace Florida, USA | Phosphatized limestone & nodular | 200 - 400m | Middle Miocene | Foraminiferal, radiometric | Foraminiferal limestones | Oxidizing | No upwelling |
| Georgia and North Carolina Shelf, USA | Pelletal | 0 - 50m | Miocene (?) | Geological | Quartz sands | Oxidizing | No upwelling |
| Peru - Chile Shelf | Nodular, pelletal | 100 - 400m | Recent | Radiometric, foraminiferal | Diatomaceous muds | Reducing | Upwelling |
| Walvis Bay, Namibia, W. Africa | Nodular, pelletal | 50 - 130m | Recent | Radiometric, diatom | Diatomaceous muds | Reducing | Upwelling |
| | | 130 - 320m | pre - Holocene | | Quartz sands & calcarenite | Oxidizing | Upwelling |
| NW African Shelf | Pelletal, nodular, phosphatized limestone | 135 - 460m | Maastrichtian - Eocene & Middle Miocene | Foraminiferal | Glauconitic and foraminiferal sands | Oxidizing | Upwelling |
| Agulhas Bank, South Africa | Pelletal, nodular, phosphatized limestone | 100 - 200m | Middle Miocene - Pliocene | Foraminiferal, radiometric | Glauconitic and detrital snd | Oxidizing | No upwelling |
| | | 200 - 500m | | | Foraminiferal sands and muds | | |
| Somalia, East Africa | Nodular | — | Mesozoic - Cenozoic | Geological | — | Oxidizing (?) | Upwelling |
| N. New South Wales, Australia | Pelletal, nodular | 210 - 290m | Middle Miocene | Foraminiferal, radiometric | Foraminiferal muds | Oxidizing | No upwelling |
| | Nodular | 385m | | | | | |
| Campbell Plateau & Chatham Rise, NZ | Nodular, phosphatized limestone | 400 - 500m | Late Miocene | Foraminiferal, radiometric | Foraminiferal oozes glauconitic silts & muds | Oxidizing | Upwelling |

Fig. 6.10 Summary diagram of major seafloor phosphorite deposits. Environment refers to the seafloor and not conditions below the sediment/water interface.

Despite the different facies associations and mineralization styles, both groups have a common property in their relation with regions of contemporary upwelling (Fig. 6.9). The lack of correspondence of some of the Mio-Pliocene category may be attributed to minor changes in oceanic circulation since the Miocene (cf. Freas and Eckstrom, 1968).

It must be concluded that global changes during the Tertiary have resulted in the restriction of phosphorite deposition to precipitation of phosphate in a diatomaceous mud facies. Possible mechanisms are discussed below.

## 6.4 Genesis of seafloor phosphorites

Observational data provide a sound basis for comparison between modern seafloor phosphorites and ancient deposits. Information available from present-day deposits will always be more comprehensive than that preserved in the geological record. Consequently an examination of phosphatization in modern environments provides a valuable guide to an interpretation of the past.

### 6.4.1 Source of the phosphate

In the discussion of phosphate in the oceans it has been demonstrated that shallow water masses are highly depleted in phosphate as a result of its assimilation by marine organisms, yet seafloor phosphorites are shallow-water deposits. If it is assumed, not unreasonably, that phosphorites form in water of above average phosphate content, then the enigma must be explained by local, higher concentrations of phosphate in shallow water. Above-average concentrations have been postulated from four main sources: (1) volcanic exhalations, (2) estuarine waters, (3) cold surface currents and (4) upwelling currents. It might be considered that organisms provide a further source, but an examination of the phosphate cycle (6.2.4) demonstrates that this is not so; the biota reacts to preexisting high concentrations rather than producing its own.

A number of authors have considered volcanism an important source of both phosphate and fluorine (Salvan, 1952; Bidaut, 1953; Miller, 1964) while others (Mansfield, 1940) believe that fluorine alone, associated with periods of volcanicity, is the controlling factor. However, recent work (Froelich et al., 1977) on phosphate concentrations on the East Pacific Rise, has indicated (on geochemical grounds) that although the region shows high concentrations of phosphate due to sorption onto hydrothermal iron oxides, little or none of this phosphate is hydrothermally or otherwise volcanically derived. There is, furthermore, no fluorine problem since the element is available in excess relative to phosphate of that necessary for the formation of carbonate-fluorapatite (Kazakov, 1950). The occurrence of clinoptilolite in the Miocene phosphorites of

North Carolina coastal plain has led to the suggestion (Rooney and Kerr, 1967) that ash falls associated with volcanicity may cause mass mortalities that in-turn provide the phosphate concentrations necessary for phosphorite formation. Since clinoptilolite is only a minor constituent of the total sediment (Cathcart, 1968) such suggestions appear unlikely.

Rivers contain four times more phosphate than surface waters (6.2.5) and consequently have been put forward as a source for the phosphate in phosphorites (Pevear, 1966, 1967; Bushinskii, 1964, 1969). Postulation of an estuarine source, however, has a major disadvantage; estuaries are generally areas of high sedimentation and any 'proto'-phosphorite would be swamped with detritus and merely form a phosphate enriched sediment. Any viable model, therefore, must embrace a mechanism which accounts for the bulk of river sediment not reaching the estuary (Cook, 1976; Cook and Mayo, 1980). A study of the organic geochemistry of a number of phosphorite deposits, including Miocene material from the Tasmanian shelf, North Carolina and Florida (Powell et al., 1974), revealed evidence of land-derived plant material in the North Carolina deposit alone. The authors conclude that there is little evidence for an estuarine origin for most phosphorites, a conclusion that is consistent with the facies association of most seafloor phosphorites.

Cold surface currents increase the phosphate concentration in large portions of the oceans at the present-day. They presumably occurred in the past, their effectiveness being dependent on the size of the ice caps and palaeogeography. However, the majority of seafloor phosphorites lie within $40^{\circ}$ latitude of the equator (Fig. 6.8) and within this region most cold currents are associated with coastal upwelling, so it is difficult to separate the two mechanisms. Since upwelling water contains twenty times the phosphate concentration of surface water (6.2.5), it provides a strong potential source. Coastal upwelling (Fig. 6.9) occurs by two main processes: divergent upwelling, a response to seaward moving surface waters, and dynamic upwelling or shoaling of a current over a topographic high. Divergent upwelling appears to be the dominant type associated with seafloor phosphorites, although some of the Mio-Pliocene group may have been associated with dynamic upwelling during the Tertiary.

### 6.4.2 Phosphatization mechanisms

Most seafloor phosphorites are composed of phosphatized sediment rather than accumulations of allochthonous phosphate-rich inorganic or biogenic detritus. Consequently, two schools of thought have evolved to explain the origin of phosphatic sediments. The first considers that precipitation is the dominant process, the second, replacement.

#### 6.4.2a Precipitation

The basic premise of the original upwelling theory (Kazakov, 1937) is that the ascent of phosphate-rich waters in regions of upwelling involves a decrease in the partial pressure of $CO_2$ (with a consequent rise in pH) resulting in the supersaturation of seawater relative to carbonate-fluorapatite, and direct inorganic precipitation. This suggestion is supported by observations that seawater is near equilibrium or saturated relative to carbonate-fluorapatite (Kramer, 1964; Roberson, 1966; Pytkowicz and Kester, 1967; Atlas, 1975), however, skeletal material is dissolving in phosphate-enriched deep ocean water at the present-day (Arrhenius, 1963). An answer to this problem is provided by a reexamination of the dissociation constants of phosphoric acid in seawater and a correction used for the complexing phosphate ion (Skopintsev, 1972). Recalculations, which may also be applicable to carbonate-fluorapatite, demonstrate that seawater is undersaturated with respect to calcium phosphate.

Further problems arise with the simple inorganic precipitation model. The conditions which are required for carbonate-fluorapatite precipitation are essentially the same as those which result in the precipitation of calcite (Gulbrandsen, 1969). Since dissolved carbonate species are at several orders of magnitude higher concentration than phosphate species, such a coprecipitation would result in the complete swamping of the apatite fraction. In order for large quantities of apatite to form with only negligible amounts of calcite, the dissolved phosphate content must be high enough so that the calcium ion is being controlled by apatite rather than calcite equilibria. Furthermore, apatitic precipitates, analogous to calcareous 'whiting', have not been proven in areas of

upwelling, although an unidentified milky-white turbidity has been reported in the area of high productivity around the Andaman Islands (Gulbrandsen and Roberson, 1973). In addition, experimental studies (Simpson, 1964; LeGeros, 1965; LeGeros et al., 1967) have shown that any precipitated phosphate would be too fine grained to be deposited in areas of bottom-current activity (Bushinski, 1966), such as those that typify recent seafloor phosphorites.

A final objection is raised by the observation that $Mg^{2+}$ ions inhibit the precipitation of apatite (Bachra et al., 1965; Martens and Harriss, 1970), probably because $Mg^{2+}$ competes with $Ca^{2+}$ for sites in the apatite structure. It is difficult to envisage, therefore, how the Mg : Ca ratio in normal seawater could be sufficiently lowered to allow the precipitation of apatite.

If, as suggested, direct precipitation in normal seawater is unlikely, or indeed impossible, then the 'authigenic' phosphorites observed on the seafloor must be the result of interactions at, or below, the sediment/water interface. It has been shown that Recent phosphorites (6.3.14) are forming in highly reducing sediments. The phosphate concentrations in the pore-waters of oxygenating sediments differ little from the phosphate content of the overlying seawater, but those of anoxic examples contain from ten to one hundred times greater concentrations than in seawater (Sholkovitz, 1973; Cook, 1974, 1976; Burnett, 1974, 1977). Cores from the Peru Shelf (6.3.6) show that maximum phosphate concentrations occur at 15 cm depth in the sediment, and at this point are over two orders of magnitude greater than the saturation value of carbonate-fluorapatite suggested by Roberson (1966). The high organic-matter content of these sediments suggests that the phosphate is supplied from the decay of this material, principally diatoms.

Decomposing organic matter within the sediment produces other changes in the pore-waters. Laboratory experiments have shown (Berner, 1969) that such decomposition causes the formation of $NH_4^+$ and other nitrogenous bases from the breakdown of proteins and other organic compounds, and produces a commensurate rise in pH. Variation of pH in anoxic sediments during early diagenesis is also effected by other processes such as the release of $CO_2$ into pore-waters during the oxidation of organic materials. Since carbonate-fluorapatite is less soluble

at high pH (Roberson, 1966; Pytkowicz and Kester, 1967) such a rise may cause the precipitation of apatite.

X-ray investigation of the sediments associated with Peru-Chile phosphorites (Burnett, 1974, 1977) show that they contain dolomite, chlorite or sepiolite in association with the apatite. The presence of such Mg-bearing authigenic minerals suggests that uptake of Mg during their formation might be sufficient to lower the Mg : Ca ratio so as to allow the precipitation of carbonate-fluor-apatite in the pore-waters. Furthermore, it has been suggested (Drever, 1971) that under anoxic conditions $Mg^{2+}$ may replace $Fe^{3+}$ in clays, later reduction resulting in the formation of iron sulphides.

Interstitial waters have a further property not applicable to normal seawater, that is the presence of numerous nucleation sites. Apatite may form (Stumm and Morgan, 1970), presumably epitaxially, on calcite, the presence of which greatly accelerates the precipitation process (Stumm and Leckie, 1970). This effect is supported by the observation that pore-waters from high-carbonate ( > 95% $CaCO_3$) sediments are in equilibrium with apatite at all depths (Berner, 1974). The diatomaceous oozes associated with Recent phosphorites are devoid of calcite but in this case siliceous matter, feldspar crystals and fish-bone apatite may act as suitable sites for the initiation of authigenic apatite growth (Burnett, 1974, 1977; Baturin and Bezrukov, 1979).

Thus at least four properties of anoxic pore-waters favour the inorganic precipitation of apatite: (1) a high flux of inorganic phosphate, (2) $Mg^{2+}$ depletion during diagenesis, (3) high pH and (4) suitable nucleation sites. However, although inorganic precipitation of phosphate in anoxic sediments is feasible, its validity, in a natural system in which there is such a prolific biota, may be doubted. It has been suggested (see above) that diatoms are a major source of phosphate in Recent phosphorites. This suggestion is supported by the inverse relationship between loss of organic matter and phosphatization during lithification of phosphatic pellets on the SW African Shelf (Romankevich and Baturin, 1972), although this stoichiometry does not determine the role played by organic matter in phosphatization. The report of phosphorite concretions in the kidneys of bivalves (Doyle et al., 1978) provides a novel mechanism for

the biogenic origin of sand-grade phosphorite in some deposits, but is inapplicable in anoxic muds. The high phosphate content of plankton (3,500 ppm P; Bowen, 1966) makes them an attractive source for the incorporation of phosphate into shallow-water sediments. Other organic processes have been proposed that would account for actual precipitation. Bacteria are known to cause phosphate precipitation in soils (Trudinger, 1976) by the formation, under reducing conditions, of hypophosphite ($PO_2^{3+}$) which is more soluble than $PO_4^{2-}$. Later organic oxidation causes the precipitation of phosphate. Reduced forms of phosphate are, however, unknown from the modern marine environment (Gulbrandsen, 1969). The suggestion that organic enzymes, which occur in bacteria and marine algae, may cause apatite precipitation (McConnell, 1965) cannot be proven experimentally (Bachra and Trautz, 1962) and therefore appears unlikely. Identifications of fossil bacteria (Cayeux, 1936; Oppenheimer, 1958; Riggs, 1979a, b) in phosphorites are dubious. It appears, therefore, that although organisms and the decay of organic matter may effectively control pore-water chemistry, it cannot be proven (with the exception of bivalve kidney concretions) that they directly cause the precipitation of phosphate in the marine environment.

6.4.2b Replacement

The phosphatization of skeletal carbonate was first recognised from the seafloor by Murray and Renard (1891) and later by many other workers. Experimental work (Ames, 1959, 1960; Stumm and Leckie, 1970) has demonstrated that $CaCO_3$ is converted to hydroxy- or carbonate-apatite by the partial replacement of $CO_3^{2-}$ groups by $PO_4^{3-}$. These experiments alone do not necessarily reflect the interactions between circulating phosphate-rich seawater and calcareous organic remains. Micro-organisms may influence the extent of these interactions by maintaining a substantial proportion of the phosphate in particulate form or as dissolved organic phosphate, and by controlling environmental factors such as pH, which determine solubility equilibria.

Mio-Pliocene phosphorites are typified by limestone replacement (6.3.14) and there is evidence (D'Anglejan, 1968) of Recent replacive phosphatization of foraminiferan shells in carbonate sediments off California. Similar processes

occur in the diatomaceous sediments off Peru (Manheim et al., 1975).

Faecal pellets, which are initially only slightly phosphatic (3.4.3b), commonly undergo further phosphatization after deposition. They are abundant in the SW African phosphorites (Senin, 1970) and many other seafloor and land examples. Consequently, the phosphatization of faecal pellets has been proposed as a mechanism for pelletal phosphorite formation (Bushinski, 1964, 1966). The occurrence of phosphatic ooliths in many pelletal phosphorites has led to the suggestion (Emigh, 1958, 1967) that such deposits have had calcareous precursors. Ooliths are, however, generally only a minor constituent; the bulk of grains are ovules rather than ooliths and show no indication of calcitic parent material. Skeletal fragments are ubiquitous to Caenozoic phosphorites and also undergo intense post-depositional phosphatization. The frequency with which material of an initially above-average phosphate content becomes further phosphatized suggests a cause-effect relationship. Such material may act as a nucleation site for migrating phosphate-rich pore-fluids within the sediment.

The diagenetic phosphatization observed in Recent phosphorites is not purely a precipitation process. The initial stages of formation may be envisaged as the migration of phosphate into the sediment to produce scattered nodules of gel-like calcium phosphate incorporating a variety of non-phosphatic particles (Baturin, 1969, 1971; Senin, 1970; Romankevich and Baturin, 1972; Baturin and Bezrukov, 1979). Following this primary stage, however, replacement processes must occur since initially-high $SiO_2$, $Al_2O_3$ and $Fe_2O_3$ contents fall with increasing $P_2O_5$, CaO, $CO_2$ and F until the former group of elements is only present in minor amounts.

Seafloor phosphatization is not limited to sediments and pre-existing phosphatic material. Recent phosphatized wood has been reported from a depth of 410 m in the Gulf of Tehuantepec (Goldberg and Parker, 1960) and phosphatized calcic plagioclase phenocrysts are known in association with seamount phosphorites (A.P. Lisitzin in Burnett, 1977). These observations support the suggestion (Cook, 1970) that, under favourable conditions, diagenetic phosphatization, calcification and silicification will occur readily, probably due to changes of pH in the interstitial waters.

6.4.2c Reworking

Both precipitation and replacement have been shown to be viable mechanisms for phosphatization, but do not alone explain the exceptionally high phosphate content of the average phosphorite. Recent phosphorites are currently forming as isolated patches in sediments poor in pre-existing phosphatic material; the sediment as a whole contains considerable less phosphate than most ancient examples. However, several changes of sealevel have occurred during the Quaternary and considerable reworking of the Peruvian and SW African shelf sediments has taken place (Baturin, 1971a). Winnowing of the diatomaceous muds has resulted in the concentration of the phosphatic material as a lag deposit, which, in the case of SW Africa, now lies offshore of the Recent phosphorites (6.3.7). Reworking is a result of increased bottom current activity, which does not necessarily reflect changes in sealevel, although such variations do provide a plausible mechanism for present-day seafloor phosphorites. Subsequent mechanical reworking of sediments, therefore, is an important feature in the upgrading of a phosphatic sediment to a phosphorite, furthermore, it provides a mechanism for the occurrence of many Mio-Pliocene phosphorites in carbonate-sand facies. Much (but not all) of this pre-Holocene material may have originally formed in an environment identical to that of modern phosphorites but was subsequently upgraded and admixed with other sand-grade components by later reworking.

Although precipitation is the dominant mechanism at the present-day this is predominantly due to the absence of carbonate in areas of Recent phosphatization. It has been suggested (Fischer and Arthur, 1977) that an expansion of the oxygen-minimum layer occurred during the Miocene, due to a high diversity of organisms and relatively-sluggish oceanic convection. Regions of anoxic organic-rich bottom sediment (not necessarily diatomaceous oozes), therefore, may have been more widespread at that time. Carbonate contained within these sediments and limestones outcropping on the seafloor would be readily mineralized in such an environment. Quaternary reworking has subsequently removed the associated reducing sediments and produced a coarse-grained phosphorite lag.

6.4.3 Global factors

The question remains as to why phosphatization was more widespread during the Mio-Pliocene than the Holocene. It is generally accepted that temperatures were higher during the Tertiary than they are at the present (Schwarzbach, 1963). Since the solubility of apatite decreases with increasing temperature, it has been suggested (Kolodny, 1969; Kolodny and Kaplan, 1970) that this relative increase in temperature may have been sufficient to cause the precipitation of carbonate-fluorapatite in upwelling regions. It has been shown (6.4.2b) that direct inorganic precipitation of apatite is improbable, but seawater temperatures exert a control on porewaters such that temperature may be an important factor. Support for this hypothesis is provided by the restriction of Recent phosphorites to low latitudes. If temperature was the only control the relatively high temperatures of the Palaeogene would have caused widespread phosphorite deposition at that time; yet pre-Middle Miocene material is rare or absent in seafloor phosphorites.

Significant changes in global nutrient budgets may be required during periods of extensive phosphorite accumulation (Piper and Codispoti, 1975). The close correspondence between observed phosphorus-nitrogen ratios in the oceans and those required by organisms (6.2.1) means that an increase in marine denitrification would cause a lowering of productivity, since nitrogen would become the sole biolimiting element, and would allow the accumulation of excess phosphate in seawater. Increased denitrification might be caused by climatic change but may also result from an increase in the areal extent of the oxygen-minimum layer (Piper and Codispoti, 1975) such as would be expected during a transgression. Widepread transgressions occurred during the early Miocene and early Pliocene (Hallam, 1963) but the degree to which the intermediate period is regressive is considerably confused by the world-wide tectonism that occurred at that time. The proposal (Fischer and Arthur, 1977) that the Miocene was a period of slow oceanic circulation is not supported by the adaptive radiation of whale species at that time, which is indicative of increased circulation and productivity (Lipps and Mitchell, 1976). However, more work on Mio-Pliocene palaeogeography is required before any firm conclusions can be reached concerning the temporal and areal controls on the genesis of these deposits.

## 6.5 Conclusions

(1) Phosphorus (along with nitrogen and silica) is classified as a biolimiting element because it is almost totally depleted by plant growth in the photic zone of the ocean. The P : N ratio of organic tissue and seawater is identical (1P:15N).

(2) Phosphorus occurs in seawater as dissolved inorganic and organic phosphate and in particulate forms. The dominant inorganic phosphate species is $HPO_4^{2-}$ although most phosphate occurs as complexes of $Mg^{2+}$ and $Ca^{2+}$. Details of organic and particulate forms are poorly known, but the phosphorus cycle in the oceans is intimately related to organic processes.

(3) Phosphate concentrations in surface waters are generally <1.0 µg-atom P $l^{-1}$, but most of this is utilised during the spring plankton-bloom in temperate latitudes, and throughout the year in the tropics. Phosphate increases with depth and reaches a maximum at 500 - 2000 m - the region of the oxygen-minimum layer. Here the seawater may contain in excess of 3.0 µg-atom P $l^{-1}$.

(4) The movement of elements in the oceans may be modelled by a simple two-box system. The boxes represent a nutrient-depleted, shallow, warm water-mass and a nutrient-rich, deep, cold water-mass. Nutrients can only be added to the shallow water-mass by upwelling and terrestrial runoff. In the present oceans upwelling provides twenty times the volume of water to the upper layer compared to that provided by runoff, which furthermore contains five times less phosphate. Upwelling is therefore the major mechanism of phosphate replenishment in surface waters. An amount of phosphate equal to the total phosphate in the present ocean is removed every $15 \times 10^4$ y, so the reaction time to oceanographical changes is geologically relatively rapid.

(5) The amount of phosphate dissolved in the sea is controlled by the:

(a) rate of upwelling of deep-ocean water,

(b) percentage of particles that survive oxidation,

(c) phosphate content of the Earth's rivers and

(d) rate of runoff.

(6) Modern seafloor phosphorites fall into two categories:

(a) Recent phosphorites, associated with strongly-reducing, organic-rich, diatomaceous oozes. Phosphatization occurs during early diagenesis below the sediment/water interface, particularly beneath regions of the seafloor that show a rapid transition from oxidizing to reducing conditions.

(b) Mio-Pliocene phosphorites, associated with oxidizing seafloors and predominantly carbonate sediments. Phosphatization occurred by the replacement of pre-existing carbonates but is now inactive.

All of the former and many of the latter group occur at sites of present-day upwelling.

(7) Upwelling currents provide the only viable source of the large quantities of phosphate in seafloor phosphorites.

(8) Phosphatization occurs initially by the precipitation of carbonate-fluorapatite from phosphate-enriched anoxic pore-waters probably under the influence of organic processes. Precipitation is followed by replacement of enclosed diluents; carbonate and components with high initial phosphate contents are particularly favourable nucleation sites and replacement media.

(9) The formation of a phosphorite rather than a phosphate-rich sediment requires reworking and concentration by elevated current activity, which is commonly linked with regressive phases. Mio-Pliocene phosphorites may not be in their original environment because of this process.

(10) Phosphatization was widespread during the Mio-Pliocene because of high temperatures, regression, and possibly an expansion of the oxygen-minimum/phosphate-maximum layer.

## Chapter 7 : Conclusions


| | | |
|---|---|---|
| 7.1 | Lithofacies | 466 |
| 7.2 | Genesis of basal hardgrounds | 466 |
| 7.3 | Origin of the basal lag | 469 |
| 7.4 | Composition of phosphatic chalks | 470 |
| 7.5 | Age of the phosphorite | 472 |
| 7.6 | Environmental interpretation | 473 |
| 7.7 | Palaeoceanography | 476 |
| 7.8 | Late diagenesis | 480 |
| 7.9 | Research priorities | 480 |

## 7.1 Lithofacies

The bulk of the Coniacian to Campanian succession in the Anglo-Paris Basin is composed of friable, white coccolith-biomicrites containing accessory skeletal carbonate (especially foraminiferans and inoceramid prisms) and traces of terrigenous and 'authigenic' minerals. These white chalks are essentially parallel-bedded and subhorizontal, bedding being picked out by marl seams, lines of nodular flint, erosion surfaces and occasional hardgrounds. The homogeneity of the succession is broken by the occurrence of lenticular bodies of poorly-consolidated, chocolate-brown, pelletal phosphorite containing in excess of 5% $P_2O_5$, and commonly overlying an intensely indurated and mineralized hardground. Most of these phosphatic chalks occur in the Picardy region of northern France, but scattered examples are recorded from elsewhere in the Anglo-Paris Basin. They were deposited in elongate, erosional cuvettes up to 1 km in length, 250 m wide and 30 m deep, incised into white chalks of the late Coniacian to Santonian, and floored by basal hardgrounds.

## 7.2 Genesis of basal hardgrounds

The current activity which eroded the cuvettes increased the grain-size of the sediment at their base. The resulting increase in permeability enabled greater movement of pore-water by the flushing action of currents and bioturbation. The pore-fluids precipitated a fine-grained, primary low-Mg calcite cement, probably by the syntaxial overgrowth of pre-existing carbonate. Induration occurred below the sediment/water interface where grain-movement was sufficiently small to allow cementation, but interaction with fresh seawater enabled the precipitation of large volumes of cement. Subsequent scour exposed these hard layers on the seafloor where they were encrusted, bored and mineralized to produce well-developed basal hardgrounds. Cementation was most pronounced in the axial regions of the cuvettes where the strongest current activity produced the coarsest sediments. Coarsening was not solely related to the removal of coccoliths by winnowing, but involved the formation of numerous small white-chalk intraclasts which

were subsequently incorporated into the lithified sediment of the hardground. Restricted mineralization (glauconitization and phosphatization of intraclasts, bioclasts and faecal pellets) also predated the main phase of lithification.

In the axial regions, the intensely-indurated summit of the basal hardground is commonly ~30 cm thick and is underlain by a further 30 cm of progressively less-indurated chalk. Cementation is geochemically discernible up to ~90 cm below the hardground surface because the indurated chalk is enriched in Fe, Mn and Mg but depleted in Sr, reflecting the inorganic low-Mg calcite mineralogy of the cement. The thickness of the basal hardground and the intensity of lithification generally decrease towards the margins of the cuvette, where the hardground passes laterally into an unlithified burrowed junction, and finally homogeneous white chalks. This lateral decline in cementation is associated with a reduction in the erosional hiatus associated with the surface of the hardground.

White chalk substrates were pelletal and thixotropic due to the sedimentation of coccoliths as zooplankton faecal pellets. In contrast, exposed basal hardgrounds produced hard seafloors which were colonised by a distinctive hard-substrate dependent biota. This biota considerably modified the primary morphology of the hardground surface. Mechanical erosion produced well-rounded intraclasts associated with relatively-planar surfaces. Irregularities in the primary hardground surface, therefore, were generally related to the broad, idiomorphic Thalassinoides burrow system which penetrated the hardground and remained open during lithification and exposure. Cementation, however, restricted the activity of the crustaceans which produced the original Thalassinoides system, causing them to produce narrower, stenomorphic burrows, both within the preexisting system (as it filled with sediment), and elsewhere in the hardground during cementation. Boring by sponges, bivalves and worms led to secondary, convolute and commonly concave morphologies, and may have removed a considerable thickness of hardground sediment. Encrustation by bivalves, tube worms, corals and bryozoans commonly followed, or was interspersed with, phases of bioerosion.

A close interaction between biological activity and mineralization is seen in all basal hardgrounds. The walls of burrows and borings are always the most intensely-mineralized portion of the hardground, areas displaying a diverse

endolithic community are invariably better mineralized than unbored lateral equivalents. Phosphatization and glauconitization of granular material occurred during the early stages of lithification, but it was only after the hardground had been strongly-indurated and exposed that there was intense mineralization. Glauconitization generally predated phosphatization, occurring by the replacement of clay minerals within the indurated chalk in the roofs of Thalassinoides burrows and in the surface of the hardground. Phosphatization, on the other hand, took place by the replacement of carbonate (initially only cement, but with continued mineralization, also enclosed carbonate grains) on the floors of burrows and in the hardground surface. Another form of intense phosphatization is shown by the thin ( ~0.5 mm), shiny-phosphate skin complexes that coat the surface (and extend down into the upper portion of burrow systems) of all basal hardgrounds. These skins exhibit a binary structure consisting of alternations of thin (20 - 200 μm) laminated veneers of pure carbonate-fluorapatite and thicker layers of phosphatized organic-matter rich micrite. They are probably of thallophytic origin, being replaced organic mats which coated the exposed surface of the basal hardgrounds.

Secondary iron minerals (particularly goethite) are also common. Some of these were produced by the weathering of glauconite or were derived from overlying iron-rich Tertiary deposits. Others, however, pseudomorph pyrite, indicating high organic-matter contents (the only source of iron in pure carbonate sediments) and subsurface anoxia within the hardground sediment during early diagenesis. Similar conditions were also conducive to glauconitization and phosphatization although the two minerals differ in their source-material requirements.

Thus biological activity was directly responsible for the final morphology of most basal hardgrounds, and indirectly responsible for their mineralization. Decaying organic material initially caused the precipitation of pyrite in the lithifying sediment. Subsequently it produced suitable geochemical conditions for glauconitization of clay minerals and replacement of carbonate by phosphate. Hardgrounds were prefered sites for mineralization because they exposed immobilised fine-grained carbonate sediment at, or near, the sediment/water interface

for extended periods, and because they provided substrates that were conducive to enhanced seafloor biological-activity, and therefore higher concentrations of organic matter during early diagenesis.

Skeletal material associated with basal hardgrounds commonly exhibits microborings which may be attributed to the activity of thallophytes, probably algae. White chalks were deposited at depths of 150 - 300 m but the occurrence of probable algal borings and skins in basal hardgrounds suggests deposition within the photic zone i.e. $<150$ m. Such shallowing may in-part explain the erosion which produced the cuvettes and was certainly important during the deposition of the enclosed phosphorite.

## 7.3 Origin of the basal lag

Phosphatic chalks are composed of a sand-grade phosphatic component surrounded by a coccolith-biomicrite matrix identical to many white chalks. Phosphatized material includes intraclasts, ooliths, faecal pellets and steinkerns, and mineralized bioclasts, particularly foraminiferans, inoceramid prisms, echinoderm and bryozoan debris, sponge spicules, ostracodes, bone fragments, elasmobranch teeth and teleost otoliths. This pelletal phosphate gives the rock its characteristic brown colour and yields whole-rock $P_2O_5$ values of $\geqslant 5\%$ for phosphatic chalks sensu stricto.

The phosphorite is only a few centimetres thick at the margins of the cuvettes but may reach 17 m (e.g. Beauval quarry) in their axial regions. Whatever the thickness of the main phosphatic chalk, however, the basal hardground is generally overlain by an intraclastic pebble-lag of bored and otherwise bioeroded, phosphatized and phosphate.skin coated fragments of chalk. Intraclasts within this basal lag were produced by both biological and physical processes and include fragments of white, hardground and phosphatic chalk, hardground chalk being volumetrically dominant. The lag reflects the changeover from non-deposition to sedimentation and is therefore usually the coarsest and most phosphatic sediment in the succession. It is also the dominant sediment-fill of the Thalassinoides burrows which penetrate the basal hardground.

The basal lags contain a prolific, varied and highly distinctive fauna typified by the worm tube 'Terebella' phosphatica, the ahermatypic scleractinian coral Diblasus arborescens and abundant oysters, particularly Lopha semiplana. These fossils form local patch-reefs on the surface of the basal hardgrounds but are rarely seen in situ being more commonly found reworked into the basal lags. Other fauna includes cirripeds (Scalpellum), infaunal aragonitic bivalves, gastropods, asteroid ossicles (including calcarenite-associated species), cidarid spines, fragments of Micraster tests and vertebrate remains. This mixture of hard- and soft-substrate dependent forms suggests that the basal hardground was not buried by a single event, but was initially covered by migrating waves of calcarenitic sediment similar to those seen on most modern hardgrounds. The variety of potential ecological niches may in-part explain the abundance and variety of the fauna. Preservational processes were similar throughout the period of phosphorite deposition so the restriction of many species to basal lags must be a primary feature.

## 7.4 Composition of phosphatic chalks

In addition to a characteristic basal lag facies, phosphatic chalks show a number of additional trends during their evolution. The occurrence of channel fill cross-bedding at the base of some sequences indicates that the strong current conditions that produced the cuvette and basal hardground continued into the early phases of phosphorite deposition. Bioturbation has destroyed most bedding structures, but the rare occurrence of laminated planar beds in the upper part of some successions indicates phases when the benthos was inactive.

Phosphatic chalks show varying degrees of compositional change throughout the sequence. The proportion of faecal pellets, phosphatic ooliths, cidarid spines, bone fragments and benthonic foraminiferans decline as the phosphatic chalk becomes finer grained and less phosphatic. Coprolitic and oolitic microfacies are characteristic of basal beds, while inoceramid prisms or pelagic foraminiferans are the dominant component of poor phosphatic chalk facies. Calcisponge and echinoderm biocalcarenites occur at the summit of some sequences and in early Campanian

chalks elsewhere.

These trends indicate the interaction of several processes. The general reduction in grain-size away from the basal hardground may be regarded as a result of decreasing current activity during the evolution of the cuvette but this is not the only mechanism. The sudden reduction in grain-size above the basal lag may be attributed to blanketing of the basal hardground with sediment, causing the cessation of in situ intraclast formation, and thereafter requiring all subsequent intraclasts to be laterally derived and therefore finer-grained.

The concentration of phosphatic ooliths on the hardground surface was also probably current controlled, but the large number of faecal pellets may be related to the hardground-tied fauna. This fauna may also have had a more indirect effect on the composition of the phosphorite. The link between organic activity and phosphatization seen in basal hardgrounds is also apparent in the overlying phosphorite. Material with an initially high phosphate content such as faecal pellets and bioclasts is particularly susceptible to phosphatization. In addition, the biota itself provides a mechanism for concentration of phosphate on the seafloor. It is suggested, therefore, that decomposition of organic matter within the sediment released phosphate into the surrounding pore-water and thereby provided the local concentration of dissolved phosphate necessary for phosphatization during early diagenesis. If this biota was essentially hardground-tied, then as the basal hardground became mantled in sediment, the local source of phosphate would disappear and material would have to be derived laterally from the exposed sides of the cuvette. Thus compositional trends were not only dependent on energy levels but also the supply of material suitable for phosphatization and the concentration of dissolved phosphate, factors which are clearly closely related and interdependent.

In addition to changes in microfacies during the evolution of the cuvette, other larger-scale feature have also been observed. During the early history of some cuvettes, erosional oversteepening of the sides produced large intraformational slump-folds in the basal hardground and overlying phosphatic chalk. This folding was accompanied by dislocation and rafting of hardground blocks into the axial region and produced local mélanges in the phosphorite. On a smaller scale,

white chalks intercalated within the phosphorite are commonly broken-up by bioturbation to produce a pseudonodular or burrowed-out structure. Rounding and mineralization of these nodules during subsequent burrowing has formed unexposed pseudoconglomerates. Elsewhere, local hardgrounds occur in the upper part of some successions. Finally, unbioturbated junctions at the top of some phosphatic chalks may be related to scouring followed by deposition of a mass flow of white chalk on top of the erosion surface.

## 7.5 Age of the phosphorite

All the phosphatic chalks of northern France and southern England are Santonian, mid M. coranguinum Zone, to low Campanian, O. pilula Zone, the bulk of the phosphorite being post U. socialis Zone in age. The age of the oldest phosphatic chalk varies considerably from site to site, and although all basal hardgrounds are overlain by post-Coniacian basal lags, only the stratigraphically lowest contain Actinocamax verus, Gonioteuthis granulata and common steinkerns of Micraster coranguinum. Above this, occasional Gonioteuthis and oysters are the only common macrofauna, although the intense bioturbation indicates an active infauna. At the summit of many phosphatic chalks, however, a distinct faunal sequence may be discerned. A bed of Gonioteuthis quadrata quadrata with occasional Belemnitella praecursor occurs just below the highest phosphorite. This Gonioteuthis Bed overlies but is separated from a bed of Offaster pilula with occasional G. q. quadrata. The occurrence of Echinocorys truncata within and immediately below the Offaster Bed at some localities, indicates that it corresponds to the lower belt of O. pilula, 'abundant O. pilula' Subzone of southern England. The presence of rare Echinocorys cincta in the youngest phosphatic chalk demonstrates a correlation with the overlying E. cincta belt of the same subzone. These data correspond well with the foraminiferal zonation which dates the final period of phosphatization as being within Biozone h at most sites. At some localities (e.g. Hardivillers, Faucouzy), a thin phosphorite containing abundant G. q. quadrata overlies a hardground occurring within the upper white chalk, above the level of the main phosphorite. These phosphatic chalks have not been dated exactly but contain

belemnite 'populations' which show trends towards a mid Campanian G. q. gracilis morphology.

Comparisons of zonal thicknesses between phosphatic chalks, white chalks in their immediate vicinity and white chalks elsewhere in the Anglo-Paris Basin, indicate that the attenuation exhibited by the phosphorites is also seen, albeit to a lesser degree, in white chalks from the same area. Furthermore, the degree of attenuation is insufficient for winnowing to be the sole mechanism of phosphate concentration, and requires an abnormally high pelletal phosphate content in the primary sediment.

## 7.6 Environmental interpretation

The petrography of pelletal phosphate indicates that phosphatization is partly dependent on the structure and mineralogy of the grain. The cement of lithified micrite is more prone to replacement than skeletal material, foraminiferan tests and echinoderm shell etc. are only phosphatized in the most extremely mineralized sediment. Nevertheless, phosphatization is commonly related to high organic-matter contents (both primary and linked to microboring) in the original grains, although a dominantly external source of phosphate is indicated by decreasing mineralization from the margins inwards.

A connection between organic matter, anaerobic diagenesis and phosphatization is indicated by a number of lines of evidence. Unweathered phosphatic chalks contain abundant disseminated pyrite, reduced iron and probably high organic matter contents. Similarly, recent seafloor phosphorites are associated with strongly reducing, organic-rich oozes, although they differ in their formation in siliceous rather than carbonate sediments. Carbonate-associated Mio-Pliocene phosphorites, however, are common on the seafloor. In modern environments, phosphatization occurs during early diagenesis below the sediment/water interface; the presence of mineralized but unexposed 'nodules' in phosphatic chalk pseudoconglomerates indicates a similar mechanism here.

The initial formation of modern phosphate nodules is a precipitation process which forms irregular masses of phosphatic sediment within diatomaceous oozes.

Replacement of the enclosed sediment only occurs during a later consolidational phase. In contrast, the textural evidence suggests that phosphatization in chalks was essentially replacive from the onset, and precipitation of apatite was a subordinate process. These differences, however, merely reflect the different physico-chemical characteristics of the host sediment, and its response to mineralization. They do not necessarily reflect any fundamental differences in the diagenetic environment.

The rapidity of phosphatization and its association with organic material is further evidenced by the mineralization of skeletal aragonite (which was dissolved rapidly at or near the sediment/water interface in the Chalk sea), the preservation of faecal pellets (normally destroyed on the seafloor), records of phosphatized animal soft-parts including gastropod intestines and ostracode appendages, and the replacement of organic mucilaginous coatings - the phosphate skins which coat the basal hardgrounds and most components in the overlying phosphorites.

The correlation between anaerobic diagenesis and phosphatization is well-established for Recent phosphorites. Here, decaying organic matter liberates phosphorus and raises the pH within the sediment because of the formation of $NH_4$ and other nitrogenous bases. It is this environment of high pH and high alkalinity that is favourable for phosphate replacement and precipitation. Nevertheless, it must be emphasised that mineralization within this high-phosphate, reducing environment is essentially a pore-water controlled process, and does not necessarily imply an anaerobic seafloor or water column. Indeed in both the Peru-Chile and SW African shelves, phosphatization is concentrated beneath the boundary between oxidizing and reducing seafloors. This may be because under totally anoxic conditions, phosphate is free to diffuse into oceanic bottom-waters and is not retained in the sediment pore-water, while under oxic conditions it is bound to iron and manganese to become insoluble. Thus, an environment of partial, or perhaps intermittent, anoxia is most favourable to the formation of modern phosphorites.

The preservation of organic matter, reduced iron and pyrite in unweathered phosphatic chalks are indicative of anaerobia but the abundance of infauna

(indicated by bioturbation) and the occurrence of epifauna and other benthonic organisms indicate aerobic conditions on the seafloor and within the upper part of the sediment. Certainly in the modern oceans benthonic foraminiferans and some species of worm flourish in and adjacent to the oxygen-minimum layer (indicating that they are facultative anaerobes), but in phosphatic chalks the occurrence of less versatile fauna such as octocorals and echinoderms confirms at least intermittent phases when the seafloor was well-oxygenated. These observations are not necessarily contradictory, however, for it is possible to envisage a seafloor where aerobia and anaerobia alternate beneath the sediment surface but where previous anaerobic phases are destroyed by the bioturbation of the next aerobic phase. The occasional preservation of laminated bedding in phosphatic chalks provides some evidence for this process. In addition, some mineralization was predominantly microenvironmental, occurring within faecal pellets, shells and beneath organic coatings but nevertheless requiring an additional external source of phosphate.

Contradictory data concerning oxygen availability on the seafloor and within the sediment during the formation of phosphatic chalks are paralleled by conflicting indicators of current activity. The erosion of phosphatic chalk cuvettes and the formation of basal hardgrounds indicate strong current conditions, and slump folding of the basal beds has been attributed to erosional oversteepening. Furthermore, basal hardgrounds and lags are characterised by patch-reefs of corals, tube-worms and oysters which were favoured by high current activity. Finally, the coarse-grained, occasionally crossbedded, basal phosphorites commonly contain phosphatized ooliths, time-honoured indicators of sediment mobility. Nevertheless, except where they have been decalcified by weathering, phosphatic chalks are never clean-washed phosphate sands and are generally supported by their micritic matrix. This micrite may have been introduced from overlying chalks into the coarsest basal beds but is certainly a primary feature of most of the succession. It could not have been deposited in a continually-winnowed environment. The taphonomy of fauna from the Gonioteuthis Beds and elsewhere in the phosphorite indicates minimal reworking, while preservation of faecal pellets is generally regarded as being characteristic of low-energy deposits.

As with oxygen availability, these apparent contradictions are not insoluble. Firstly the coarse grain-size of the pelletal phosphate does not necessarily directly reflect the hydrodynamic conditions during its deposition. Much of the intraclastic material within the phosphorite is bioeroded fragments of hardground and not the product of physical reworking. Faecal pellets are an important factor in the observed sediment coarsening near the hardground surface, but their size reflects the physiology of the defecating organism and subsequent mineralization processes, and not current activity. Furthermore, some other potential indicators of high-energy conditions are ambiguous; the well-rounded nature of many grains (e.g. faecal pellets), for instance, is a primary and not secondary feature. The smooth, shiny surfaces exhibited by most components is due to the deposition of iridescent phosphate and not abrasive polishing. Thus, although there must have been a high current-regime during the early phases of erosion and hardground formation, subsequent current were probably substantially weaker and intermittent. Rapid winnowing, perhaps controlled by abnormal storm activity, is suggested by the inhomogeneity of the belemnite 'population' from on top of the Ribemont Gonioteuthis Hardground.

Examination of modern phosphorites has demonstrated that formation of a phosphorite rather than a phosphate-rich sediment requires reworking and concentration by winnowing, and this occurs during discrete periods, linked with regression. A similar cyclic process is proposed for phosphatic chalks and may be linked with the cyclicity exhibited by fluctuating oxygenation during diagenesis. It is suggested, therefore, that oxic phases of colonisation, bioturbation and winnowing alternated with quiescent anoxic phases of mineralization. The short-term glaciation-controlled regressions that produced the cyclicity seen in Quaternary seafloor-phosphorites cannot be invoked for phosphatic chalks, although here the periodicity may be inherent in the current type or have another form of climatic control.

## 7.7 Palaeoceanography

So far the depositional environment has only been considered within indiv-

idual cuvettes. It has been noted, however, that a number of cuvettes may form in the same general area. The well-documented examples near Hallencourt, for instance, consist of three separate and progressively-younger cuvettes of mid Santonian to early Campanian age, yet each has the same axial trend. It is concluded that, of the possible mechanisms, only a permanent ocean current would have sufficient erosive power to produce such large-scale structures, yet operate in the same position and maintain the same trend for such a long period ($\sim 4$ million years). It was also suggested that the restriction of phosphatic chalks to the Santonian to early Campanian may be linked with a regression which enabled the ocean currents to achieve significant erosional effects, and thereby form the cuvettes which were to act as entrapment basins for the phosphorite.

Neither of these mechanisms explains why deposition of phosphatic chalks took place on such a large scale within the Anglo-Paris Basin (including the Mons Basin of Belgium, e.g. Leriche, 1935) during the mid Santonian to early Campanian. Furthermore, conditions appear to have remained favourable for phosphate deposition during the late Campanian to Maastrichtian in the Middle East (Wurzburger, 1968) and Belgium (Cornet, 1886; Cornet and Briart, 1878; Cornet, 1905, 1922) and into the Eocene in North Africa (Salvan, 1960). All these deposits appear to be of the same general type, being composed of thin (rarely $>3$ m) beds of pelletal phosphate. Prior to this, Cretaceous pelletal phosphorites were rare and poorly developed e.g. in the mid Turonian of Lewes (Strahan, 1896) and in Cambrai (Leriche, 1909; Cayeux, 1939). It is suggested, therefore, that a major change in oceanic régime occurred prior to the mid Santonian which resulted in the deposition of the phosphatic chalk lithofacies.

In addition to an association with anoxic environments, Recent phosphorites have two other characteristics which may be comparable to phosphatic chalks. Firstly, they are located in areas where the supply of terrigenous and carbonate detritus is minimal. Little land was available in Europe as a source of detrital sediment during the post-Coniacian portion of the late Cretaceous (Fig. 7.1), so that terrigenous input was negligible in all facies at this time. Similarly, carbonate sedimentation rates were uniformly low, although the attenuation seen in the region of phosphatic chalk cuvettes indicates abnormally-low deposition

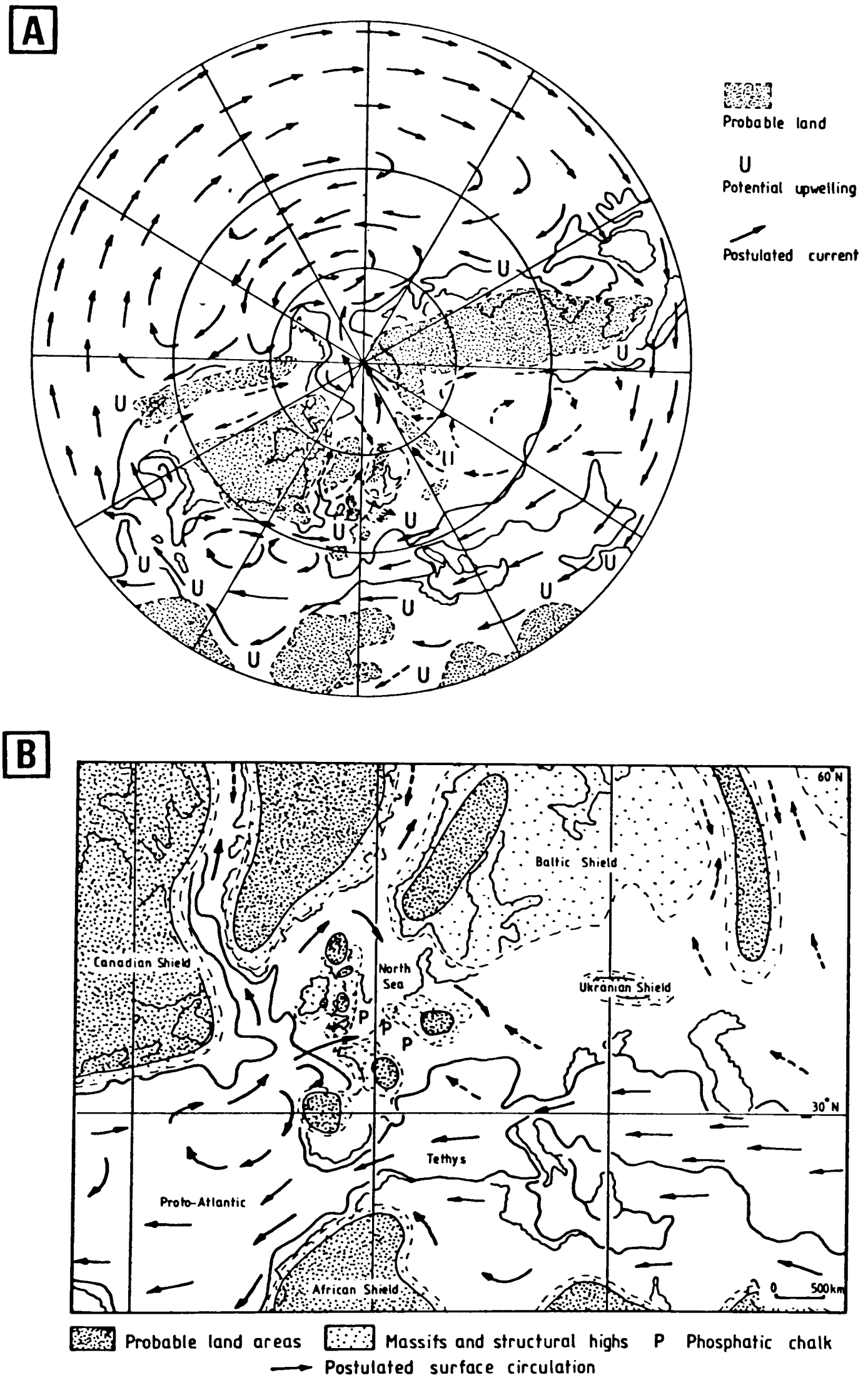


Fig. 7.1 Late Santonian to early Campanian palaeogeography of the Anglo-Paris Basin. The palaeocontinents have been reconstructed by Smith and Briden (1977). Palaeoceanography has been determined by analogy to modern surface-current circulation, and incorporates data from Freas and Eckstrom (1968), Luyendyk et al. (1972) and Gordon (1973). Thick continuous lines are the breaks of slope along the continental shelf areas or pre-collision boundaries (e.g. N. Italy). The fine continuous lines mark present-day land-masses. A. Northern hemisphere, the map is drawn on a north polar stereographic projection, B. Europe, based on a Mercator projection.

rates in these areas.

Modern phosphorites are all associated with areas of strong and persistent upwelling, and it is concluded that this is the only viable source of the large quantities of phosphate in seafloor phosphorites. Both here and in phosphatic chalks, there is strong evidence for a causative relationship between biological activity and phosphatization. Consequently, organic material might be regarded as an additional source of phosphate. This is not so, because phosphorus is a biolimiting element and therefore high biological-productivity is the result, rather than the cause, of high phosphate concentrations in seawater. Pelagic and benthonic organisms do, however, play an important role in introducing phosphate into the sediment by the sedimentation of particulate matter (in the form of faecal material and cadavers). It is the decay of this organic material during early diagenesis which provides the source of phosphorus for replacement and precipitation. Entombment of organic matter, rather than recycling in the water column, is aided by shallow water ( $<150$ m) and poorly-oxygenated bottoms, both characteristics of modern seafloor-phosphorites and phosphatic chalks.

There remains the feasibility of upwelling as a source of the phosphate in phosphatic chalks. Conditions conducive to upwelling have been summarised by Freas and Eckstrom (1968; also in Cook, 1976). The Anglo-Paris Basin lay on the west side of a continent within the belt of the westerlies (approximately between $20^{\circ}$ and $40^{\circ}$), and was surrounded by, albeit much reduced, landmasses (Fig. 7.1) with arid(?) climates. Consequently, the eastern side of the basin was a potential area of oceanic upwelling caused by seaward moving surface water (upwelling by divergence) or shelving of a current over a submarine topographic high (dynamic upwelling). Luyendyk et al. (1972) and Hart (1976) suggest that a primitive 'gyre' developed in the North Atlantic during the late Cenomanian, and that this was an early development of a proto-Gulf Stream. If the Gulf Stream was initiated in the Cenomanian, the continuing opening of the North Atlantic during the Turonian and Coniacian would have led to the development of a strong permanent current by the Santonian. At the present day the Gulf Stream is able to intrude onto the continental shelves (Atkinson, 1977), so the current would have been able to flow into the Chalk sea during the late Cretaceous.

There is no evidence for extensive land during the Campanian in any of the massifs surrounding the area under consideration (Fig. 7.1), and it is possible that Armorica, Cornubia and the Ardennes were trangressed by this time. That these areas provided a seafloor topography seems more likely. 'Marginal' glauconitic chalks of late Campanian age occur in eastern Belgium (Calembert, 1956; Schmid, 1959) and similar facies are recorded from the Santonian to Campanian of Northern Ireland (Hancock, 1961). Thus the permanent current set up in the proto-Atlantic may have been deflected and caused to upwell along a trend which parallels the London-Brabant Massif and western Ardennes.

## 7.8 Late diagenesis

The most prominent manifestation of late diagenesis in phosphatic chalks is the silicification of bioclasts and the formation of flint nodules. Silicification was a multistage process involving the liberation of silica from biogenic opal-A, the formation of opal-CT lepispheres during early diagenesis at sites of organic matter, and a final late-diagenetic migration of silica combined with the transformation of opal-CT to chalcedonic $\alpha$-quartz.

Pressure-solution features are poorly developed when compared with many older chalks, but include the occurrence of flaser structures in primary marl seams and occasional stylolites in basal hardgrounds. Large nodules of late-diagenetic pyrite are common in some beds, and cementation, apparently related to fracture and fault patterns, has also been noted. The latter indicates the migration of appreciable volumes of pore-fluids during deep-burial diagenesis.

## 7.9 Research priorities

The present study has established the distribution, age and stratigraphy, and has formulated a depositional model for the phosphatic chalks of the Anglo-Paris Basin. Nevertheless, our knowledge of the biostratigraphy of phosphatic chalks remains poor. Many successions are inadequately exposed and have yielded little diagnostic macrofauna. The resulting zonations are necessarily imprecise.

Further collecting is required to firmly establish a reliable zonation for these sequences. The nature of the present study has precluded a detailed examination of the palaeoecology of most of the fauna. Basal lags in particular contain prolific and varied assemblages that included a number of aragonitic bivalves, gastropods, corals etc. which are rare or unrecorded from white chalks. This fauna clearly warrants careful taxonomic and palaeoecological study.

Limited exposure means that few data are available concerning lateral facies-variation. An examination of borehole material might provide more detailed information. In addition, it has been demonstrated that the chocolate-brown colour of phosphatic chalks is the result of oxidation during weathering, and that fresh, unweathered material is reduced, containing pyrite and larger amounts of organic matter. Geochemical data considered here have been limited to major and minor element and mineralogical trends across the white-hardground-phosphatic chalk transition. The establishment of these trends is a prerequisite to further study, and examination of trace-element, rare-earth, stable-isotope and organic geochemistry would all be invaluable in eluscidating the nature of the depositional environment and subsequent diagenetic processes. Trace-elements and organic geochemistry should provide better indications of the role played by organic-matter in the phosphatization process. Stable isotopes (oxygen, carbon and sulphur) and rare-earths are required to confirm the hypothesis that the primary hard-ground cement was low-Mg calcite, and should establish Eh/pH conditions during phosphatization. In all of these studies, unoxidised borehole material would be invaluable.

The precise nature of the mineralization process is still moot. Petrographical evidence indicates that phosphatization in phosphatic chalks and hardgrounds primarily occurred by the replacement of carbonate, particularly intraclasts and material with a high primary-phosphate content. SEM data indicates that this is partly due to the preferential replacement of cement, but may also involve the precipitation of phosphate within pore-spaces. An integrated SEM, TEM and micro-probe study would clarify the relative importance of replacement-precipitation reactions in phosphatic chalks.

Interpretation in sedimentary geology relies heavily on modern analogues.

The oceanography and marine geology in areas of modern phosphorites is poorly documented and requires urgent consideration. Detailed examination of Mio-Pliocene seafloor phosphorites, their depositional environment, and associated palaeoceanographical conditions is required to ascertian why phosphatization is now restricted to diatomaceous oozes, but commonly occurred in carbonate sediments during the Tertiary. In the laboratory, an understanding of precipitation and replacement of phosphate minerals is in its infancy. Studies to improve our knowledge of the solution chemistry of marine apatites, particularly the laboratory synthesis of carbonate-fluorapatites of varing composition, the influence of other dissolved species and organic matter, are necessary prerequisites to the formulation of valid geochemical models.

# Appendix 1 : Geochemical methods and results


| | | |
|---|---|---|
| A1.1 | Sample preparation | 484 |
| | A1.1.1 Rocks | 484 |
| | A1.1.2 Soft sediments | 485 |
| A1.2 | Solution preparation | 485 |
| | A1.2.1 Acetic acid dissolution | 485 |
| | A1.2.2 Hydrochloric acid digestion | 486 |
| | A1.2.3 Whole-rock dissolution | 487 |
| A1.3 | XRF discs | 487 |
| A1.4 | Analytical precision and accuracy | 488 |
| A1.5 | Analytical techniques | 489 |
| | A1.5.1 Colourimetric phosphate analysis | 489 |
| | A1.5.2 Atomic absorption spectrophotometry | 491 |
| | A1.5.3 X-ray fluorescence spectrometry | 494 |
| A1.6 | Electron microprobe analysis | 495 |
| A1.7 | Scanning electron microscopy | 495 |
| A1.8 | Results | 497 |

## A1.1 Sample preparation

Thirty-six fresh, unweathered, 10 - 30 cm block specimens were collected in the field specifically for geochemical analysis. Indurated samples were cut in two, and one half faced to display any sedimentological variation. Representative portions of the second half were broken off for powdering or thin sectioning. Soft sediments were split and one half wet-sieved to remove the micritic matrix. Representative portions of the remainder were powdered or impregnated with araldite and thin sectioned.

### A1.1.1 Rocks

All specimans were liberally washed with tap water, dried, placed in heavy-gauge polythene bags and fragmented into 0.5 - 1.0 cm chips by resting the part-filled bag on a concrete surface and striking it with a geological hammer. The bags served to contain the rock fragments and prevent contamination. The contents were emptied into a nylon sieve, washed, and ~300 g of chips removed for powdering. White chalks containing large numbers of discrete phosphatic-chalk filled burrows were separated into their two components; in those with smaller amounts of fill the phosphorite-contaminated portions were discarded. Abnormal lithologies, faces displaying saw-marks, and weathered or otherwise discoloured fractions were avoided in all samples. Soft chips were reduced further in a fresh polythene bag; harder material in a steel percussion mortar. Powders were transfered to an agate planetary ball mill containing three 3 cm agate balls. To minimise salting between samples, all equipment had been previously washed with 50% v/v HCl, deionized water and acetone dried. Samples were ground until no grittyness could be detected between the fingers (difficult specimens being finished by hand in an agate mortar and pestle), then transfered to 3000 ml beakers containing 2500 ml of deionized water. These were placed on stirring hotplates, heated to 60°C and mixed by Teflon-coated magnetic stirrers for one hour. This procedure was designed to remove any salt impregnation; samples from Hardivillers quarry produced needle-like

extrusions of halite during drying and were consequently not analysed due to the possibility of more insidious contamination. The beakers were removed from the hotplates, allowed to cool and the contents filtered through Whatman No. 40 paper washed with deionized water followed by acetone. Paper and filtrate were dried for 1 hr at 60 - 70°C. The final powders were stored in clean, sealed glass jars, subsamples being obtained by hand.

### A1.1.2 Soft sediments

After removal of abnormally-large intraclasts and shells, samples were mixed and powdered in a percussion mortar. The sediments were reduced further in an agate planetary ball mill and the desalination and drying procedure followed as for the rock specimens.

## A1.2 Solution preparation

Three separate solutions were made from each sample, a. an acetic-acid soluble portion to determine the composition of the calcitic fraction, b. a hydrochloric-acid soluble portion which after the subtraction of (a) gives the composition of the phosphate, and c. a whole-rock solution for comparison with published analyses and to estimate the composition of the 'insoluble' residue. Three different solutions were prepared to provide a cross check on the different dissolution methods since the purer samples are almost entirely calcite and these should therefore yield similar results for all three solutions for most elements. The method provides an extra precision check that would not be possible if the different phases were removed from individual subsamples by progressive dissolutions. Analar chemicals were used throughout. To prevent contamination, all apparatus was cleaned with 50% v/v HCl followed by two washes of deionized water.

### A1.2.1 Acetic acid dissolution

Sodium acetate ($CH_3COOHNa \cdot 3H_2O$) was utilized to buffer 18M glacial acetic acid ($CH_3COOH$) to a pH of 5. A 1M buffered solution was prepared by adding 190.5 g of sodium acetate to 36 ml of acetic acid in a 2000 ml volumetric flask and making up to volume with deionized water. The buffering was designed to minimise the dissolution of the non-carbonate fraction. The following procedure was followed:

(1) Place 0.5 g of accurately-weighed powder in a clean 100 ml beaker. Add 75 ml of buffered acetic acid and cover.

(2) Put the covered beaker in a deionized-water filled ultrasonic bath for 1 hr. The bath provides agitation and warmth, ensuring complete dissolution of the soluble portion of the rock.

(3) Allow to cool.

(4) Add 10 ml of buffered acetic acid and place in an ultrasonic bath for a further 1 hr.

(5) Immediately filter twice through two 7 cm Whatman No. 42 papers, rinsing through with deionized water.

(6) Filter second time into a 100 ml volumetric flask. Allow to cool and make up to volume with deionized water. Store in sealed polypropylene bottle.

### A1.2.2 Hydrochloric acid digestion

The dissolution method is modified from Maxwell's (1968 p.487) procedure for the determination of acid insoluble residues in carbonates:

(1) Place 1 g of accurately weighed powder into a clean 250 ml beaker and add 20 ml of cold deionized water.

(2) Cover and, while swirling, add 5 ml of 12M HCl.

(3) Allow effervescence to cease and add 20 ml of hot deionized water.

(4) Digest the covered mixture on a stirring hotplate at near-boiling for 15 min.

(5) Filter at once through a 7 cm Whatman No. 40 paper into a 100 ml volumetric flask, washing powder and residue with 20 ml of hot 5% v/v

HCl.

(6) Allow to cool. Make up to volume with deionized water and store in sealed polypropylene bottle.

(7) Transfer paper and residue to a weighed 25 ml platinum crucible. Cover and heat over a bunsen flame until the paper has charred.

(8) Place in a furnace and ignite at 1000°C for 30 min.

(9) Cool in a dessicator and weigh.

(10) Repeat until a constant weight.

### A1.2.3 Whole-rock dissolution

The procedure is modified from a method suggested by A. Wilson (pers. comm.):

(1) Place 0.5 g of accurately-weighed powder in a platinum dish.

(2) Moisten with 2 ml of cold deionized water.

(3) Slowly add 10 ml of 28M HF followed by 8 ml of 12M perchloric acid ($HClO_4$).

(4) Slowly decompose on sand bath. Take to near dryness but do not dry.

(5) Allow to cool. Add 5 ml of perchloric acid and then 4 ml of saturated boric acid*1 ($H_3BO_3$).

(6) Evapourate slowly on sand bath to near dryness but do not dry.

(7) Add 10 ml of 50% v/v HCl and digest slowly on sand bath.

(8) Allow to cool. Transfer to a 50 ml volumetric flask and make up to volume with deionized water. Store in a polypropylene bottle.

## A1.3 XRF discs

Samples were prepared for X-ray fluorescence (XRF) analysis by grinding

*1 A saturated boric acid solution is 5% by volume. Add 30 g of boric acid to 500 ml of near-boiling deionized water. Heat the mixture until all of the $H_3BO_3$ has dissolved (stir with a magnetic stirrer), allow to cool, and store in a polypropylene bottle.

10 g of powder with 0.6 ml of Moviol PVA and pressing into 4 cm discs with a hydraulic pressure of 10 tonnes. Discs were dried for 1 hr at 60°C prior to labelling and storage. Standards were prepared by the same method.

## A1.4 Analytical precision and accuracy

Duplicate analyses on randomly selected samples were carried out for all three solutions on each element, and a precision calculation performed. Twenty-five duplicate solutions were made from a total of 108 rock solutions. In addition, nine solutions were prepared from three duplicate powders produced from rocks collected from the same horizons as three of the original samples. Lastly, as an additional check, a number of duplicate dilutions were made from the same stock solutions (these were not used in the precision calculations). Precision of the 25 duplicates was estimated by a method described by Khaleelee (1969):

The percentage deviation for each duplicate analysis from the mean of each pair of duplicates is given by:

$$Xp = \left[ \frac{X_1 - X_2}{2} \Big/ \frac{X_1 + X_2}{2} \right] \times 100 \qquad (A1.1)$$

where $X_1$ and $X_2$ represent the two determinations. The mean percentage deviation for all duplicates is given by:

$$\bar{X}p = \frac{Xp}{N} \qquad (A1.2)$$

where N represents the number of duplicate pairs. The standard deviation of the individual percentage deviations (Xp) about the mean percentage deviation ($\bar{X}p$) is given by:

$$\sigma^2 = \frac{\sum (Xp - \bar{X}p)^2}{N - 1} \qquad (A1.3)$$

At the 95% confidence level, if individual percentage deviations are normally distibuted about the mean, the precision may be estimated:

$$p = \pm \bar{X}p \ . (\pm 2\sigma)\% \qquad (A1.4)$$

The results of the precision tests for the various techniques will be considered in Section A1.5.

No standard rocks of comparable composition to either chalks or phosphorites were available to me, so it was not possible to run an internal standard as an independant check of the accuracy of the analyses. Nevertheless, the high precision obtained, and the closely-comparable values of the three different extraction methods for some elements, suggests that the accuracy approaches the precision. In any case, absolute accuracy is of considerably less importance than precision since my conclusions (Chapter 4) are based on relative rather than absolute abundances.

## A1.5 Analytical techniques

Three separate techniques were employed for the analysis of the major and minor elements:

(a) Colourimetry

(b) Atomic Absorption Spectrophotometry

(c) X-ray Fluorescence

### A1.5.1 Colourimetric phosphate analysis

Phosphate was determined as the heteropoly blue complex which results from the selective reduction of molybdophosphoric acid, the intensity of the blue colour being proportional to the phosphate present. Hydrazinium suphate ($NH_2 \cdot NH_2 \cdot H_2SO_4$) was chosen as the reducing agent since the colour may be developed rapidly. The method is as follows:

(1) Prepare 25 ml (10 ml for acetic solutions) volumetric flasks by

soaking in 18M $H_2SO_4$ overnight and washing three times with deionized water.

(2) Make a standard solution by dissolving 0.0959 g of potassium dihydrogen orthophosphate ($KH_2PO_4$) (dried at 110°C before weighing) in 1 litre of deionized water. This solution contains 50 ppm $P_2O_5$.

(3) Prepare reagents:

(a) Ammonium molybdate. Dissolve 5 g of $(NH_4)_6MO_7O_{24}\cdot 4H_2O$ in 200 ml of 5M $H_2SO_4$ (dilute 70 ml of 18M $H_2SO_4$ to 250 ml) and dilute to 250 ml with more 5M $H_2SO_4$.

(b) Hydrazinium sulphate. A 0.15% w/v aqueous solution.

(4) Pipette the required amount of rock solution into a 25 ml volumetric flask (the amount is dependant on the $P_2O_5$ content but the final solution must lie within the range of six standards - 0.5, 1.0, 2.0, 3.0, 4.0 and 5.0 ppm $P_2O_5$. Dilutions ranged from 4 in 10 ml for the acetic solutions from white chalks to 50 µl in 25 ml for the total solutions of phosphorites. Initial dilutions, therefore, require some a priori knowledge of the rock compositions). Add 2.5 ml of (a) and 1 ml of (b). Prepare standard solutions and a blank by the same method. As a safeguard against chemical interferences, equal amounts of buffered acetic acid were added to blanks and standards for the acetic solution runs. Dilute with deionized water to within 2 cm of the graduation mark, stopper and mix.

(5) Immerse unstoppered flasks in boiling water for 10 min. Remove and cool rapidly in running water. Allow to come to room temperature, dilute to volume and mix.

(6) Measure the blue complex at 830 mµ in 1 cm cells (a Pye-Unicam SP30 spectrophotometer was used in the present study).

(7) Draw calibration curve from the six standards, read off unknown values in ppm and calculate the $\%P_2O_5$ in the rock.

Total and HCl solutions gave a precision ($\bar{X}p$) of $\pm$ 1% ($2\sigma$ of 3%) for values 0.15 - 28.75% $P_2O_5$ on 12 duplicates. The precision ($\bar{X}p$) of the acetic solutions was $\pm$ 6% ($2\sigma$ of 8%) on 9 duplicates for the range 150 - 6900 ppm $P_2O_5$.

## A1.5.2 Atomic absorption spectrophotometry

A Perkin-Elmer 306 Atomic Absorption Spectrophotometer was used in conjunction with the Special Burner Control option. Operating conditions were taken from the Perkin-Elmer Analytical Methods book. Perkin-Elmer 'Itensitron' hollow cathode lamps were used throughout, at the recommended source currents. Instrument settings are given in Table A1.1. Acetylene was the fuel used for all analyses, the cylinder pressure being kept above 75 PSI to prevent interference due to acetone release.

| Element | Operating conditions | | | | | | | | |
|---|---|---|---|---|---|---|---|---|---|
| | Wavelength (nm) | Region | Operating lamp current (mA) | Slit width | Oxidant | Flame type | Oxidant flow | Fuel flow | Comments |
| Al | 309 | UV | 25 | 4 | $N_2O$ | Rich Red | 38 | 55 | |
| Ca | 211 x 2 | VIS | 10 | 4 | Air | Lean Blue | 55 | 32 | |
| Fe | 348.3 | UV | 30 | 3 | Air | Lean Blue | 55 | 32 | |
| Mg | 285 | UV | 6 | 4 | Air | Lean Blue | 55 | 32 | |
| Mn | 279 | UV | 20 | 3 | Air | Lean Blue | 55 | 32 | |
| K | 383 x 2 | VIS | 12 | 4 | Air | Lean Blue | 55 | 32 | Filter on |
| Na | 295 x 2 | VIS | 8 | 4 | Air | Lean Blue | 55 | 32 | |
| Sr | 230.5 x 2 | VIS | 20 | 3 | Air | Slightly yellow | 53 | 40 | |

TABLE A1.1 Perkin-Elmer 306 Atomic Absorption Spectrophotometer instrument settings utilised during the present study

The pH of the rock solutions, standards and blanks was controlled by the addition of 2 ml of 50% v/v HCl to each 25 ml flask (4 to 50 ml); the matrices of the acetic solution standards and blanks were standardised by the addition of the required amounts of buffered acetic acid. A solution containing 10% w/v lanthanum (26.6% w/v $LaCl_3 \cdot 7H_2O$) was added to all solutions to give a final lanthanum concentration of 1% w/v. The addition of large excesses of lanthanum provides an important control on chemical interferences in complex solutions, since it acts as an ionization buffer and releasing agent for a number of metals (particularly the higher alkali metals).

Standards were prepared from BDH 1000 ppm standard solutions for atomic absorption spectrophotometry. The working ranges, which depend on the sensitivity of the instrument for that particular element, are shown in Table A1.2. Unfortunately, the degree of variation in concentration of different elements

and the varying sensitivity of the technique required that six dilutions were made for the eight elements analysed (Fig. A1.1), although few solutions had

| Element | Standards (ppm) | | | | | Upper limit of linearity |
|---|---|---|---|---|---|---|
| Al | 5.0 | 10.0 | 15.0 | 20.0 | 25.0 | |
| Ca | 2.0 | 4.0 | 6.0 | 8.0 | 10.0 | 6.0 |
| Fe | 2.0 | 4.0 | 6.0 | 8.0 | 10.0 | 6.0 |
| Mg | 0.2 | 0.4 | 0.6 | 0.8 | 1.0 | 0.6 |
| Mn | 0.5 | 1.0 | 2.0 | 3.0 | 4.0 | 3.0 |
| K | 0.2 | 0.5 | 1.0 | 1.5 | 2.0 | |
| Na | 0.2 | 0.4 | 0.6 | 0.8 | 1.0 | |
| Sr | 1.0 | 2.0 | 3.0 | 4.0 | 5.0 | |

Concentrations chosen to give maximum range of absorbance values while maintaining linearity of the standard curves within the range of most unknowns.

TABLE A1.2 Element concentrations of the standard solutions used for AA spectrophotometry.

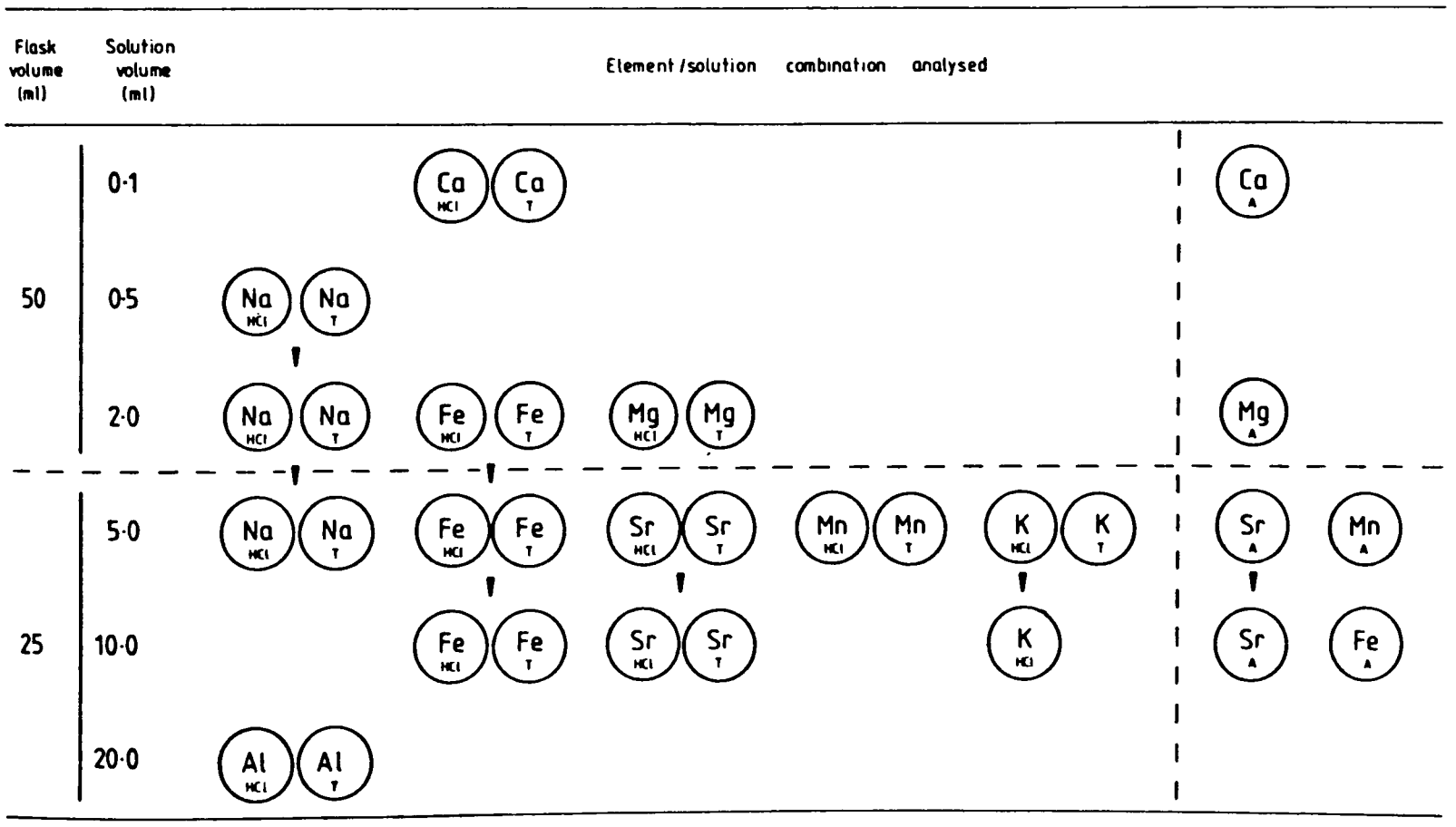


Fig. A1.1 Dilutions necessary to complete analysis of three different dissolutions of a mixed white chalk/phosphorite suite for eight elements. A = acetic solution; HCl = HCl solution; T = whole rock solution (Note: acetic acid solution values should be multiplied by two if prepared as in Section A1.2.1).

to be prepared in the maximum number of dilutions. Standards are interchangable between the HCl soluble and whole-rock solutions (left side of Fig. A1.1) but addition of equivalent amounts of buffered acetic acid to standards made for

low-dilution acetic runs (bottom right in Fig. A1.1) caused considerable enhancement in the absorbance of some elements (Fig. A1.2). The presence of

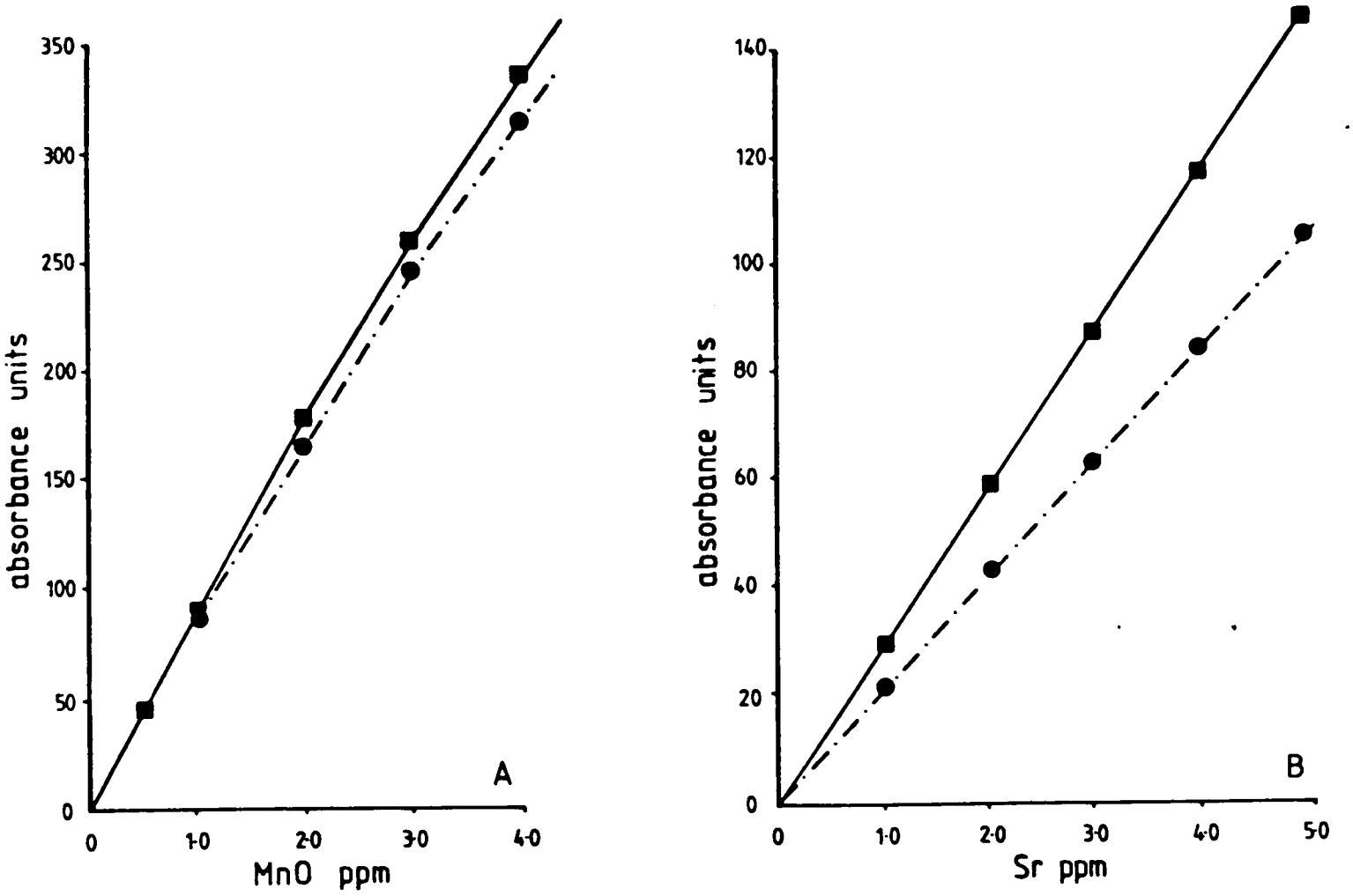


Fig. A1.2 Absorbance enhancement in standard solutions containing 1M buffered acetic acid. A. 20% v/v in five manganese standards. B. 40% v/v in five strontium standards. Solid lines and squares = spiked standard; dashed lines and filled circles = normal standard. Solutions were made from the same BDH standards, contained the same amounts of HCl and lanthanum, and were measured during the same runs under identical instrument conditions.

large excesses of sodium in these solutions produced a bright-yellow discolouration of the acetylene flame, while the drying of solution in the burner slot caused eventual blockage. This was prevented by extended periods of deionized water aspiration between both samples and standards. Small blockages were detected by the loss of absorbance on the standards and could be remedied by washing the burner head in deionized water prior to continuation of the analysis. Enhancement must result from the reduction of an existing depressive interference present in the other solutions. Of the elements run with >20% v/v 1M buffered acetic acid, no enhancement was detected for iron, a slight increase was noted for manganese (Fig. A1.2A), and pronounced enhancement was observed with strontium (Fig. A1.2B). It is unlikely that the acetic is acting as a significant releasing agent since aluminate, silicate, phosphate and other oxyanions, which are likely to form stable oxides, are at very low levels in the

solutions. It is suggested, therefore, that the presence of several percent sodium acts as a more effective ionization buffer than the 1% lanthanum which is also present. Matrix effects due to the altered physico-chemical properties of the solutions may also be a contributary factor.

Triplicate analyses were made of each solution for each element, standards being measured initially and then after each batch of 20 samples. Average values were utilised in the construction of the standard curves and in the determination of the unknowns.

The precision of the method varied with the element, its concentration and the method of dissolution. Precision was generally highest with the whole-rock analyses (Table A1.3) and poorest in the acetic dissolutions. The less-satisfactory reproducibility of the HCl-soluble aluminium and acetic-soluble iron was due to the low concentrations of the elements in these solutions.

| Element | Precision (%) | | | | | | | | |
|---|---|---|---|---|---|---|---|---|---|
| | Acetic | | | HCl | | | Whole rock | | |
| | $\bar{X}_p$ | | $2\sigma$ | $\bar{X}_p$ | | $2\sigma$ | $\bar{X}_p$ | | $2\sigma$ |
| Al | | | | 10 | ± | 15 | 1 | ± | 1 |
| Ca | 1 | ± | 2 | 1 | ± | 1 | 1 | ± | 2 |
| Fe | 12 | ± | 16 | 2 | ± | 4 | 2 | ± | 2 |
| Mg | 3 | ± | 4 | 2 | ± | 1 | 1 | ± | 3 |
| Mn | 2 | ± | 3 | 1 | ± | 1 | 1 | ± | 2 |
| K | | | | 4 | ± | 8 | 1 | ± | 2 |
| Na | | | | 3 | ± | 1 | 1 | ± | 3 |
| Sr | 3 | ± | 3 | 3 | ± | 4 | 2 | ± | 3 |

TABLE A1.3 Estimates of the precision obtained by AA spectrophotometry. Based on the method of Khaleelee (1969; see Section A1.4).

### A1.5.3 X-ray fluorescence spectrometry

Silica analysis was performed on pressed pellets with a Philips 1410 spectrometer. All but one sample contained estimated $SiO_2$ values in the range 0.5 - 5.0% and, since no standard rocks were available within this range, artificial standards were prepared by adding powdered quartz to Analar calcium

carbonate to produce pellets with 0.5, 1.0, 3.0, 5.0, 10.0, 15.0 and 20.0% $SiO_2$. Quartz was used in preference to Specpure silica since the latter gives erroneous results when used for the purpose (A. Wilson pers. comm.); the use of a calcium carbonate matrix enables possible compositional effects to be disregarded. Analyses were run using a PET crystal, coarse collimator, spinner, Cr tube at 60 kV and 24 mA and a flowcounter at 1500 V with a count time of 10 s. Silicon was measured at the Si K$\alpha$ ($2\theta \sim 109.10 \pm 0.10^{\circ}$) and backgrounds at $111.20^{\circ}$ $2\theta$ with a lower level of 1.20 and window of 0.50. Peak and background were measured three times on each side for both samples and standards. A monitor containing 4% $SiO_2$ was measured by the same method after each sample and standard and sample/monitor ratios used rather than absolute values in order to compensate for machine drift. The exact position of the Si K$\alpha$ line was determined hourly.

An assessment of the precision was made by comparing values obtained from either side of the pellets (mean values are used in the computation of the $SiO_2$ percentage) which produced an $\bar{X}p$ of $\pm$ 0.52 ($2\sigma \pm 0.80$).

## A1.6 Electron microprobe analysis

Analyses were performed on a Cambridge Scientific Instruments Microscan 9 electron microprobe. Thin sections of rocks were prepared by fine polishing of 40 μm sections followed by coating with a layer of carbon 200 $\pm$ 50 Å thick. Machine settings are shown in Table A1.4 and the standards in Table A1.5. All elements were analysed on a single run at 20 nanoamps using both spectrometers. Results were processed online using a Cambridge Instruments correction program on a Digital PDP 11 computer.

## A1.7 Scanning electron microscopy

Visual and analytical work was performed utilising a JEM TEMSCAN 100CX with ASID scanning attachment manufactured by JEOL. Specimens were prepared as broken or polished and etched chips mounted on brass clips and coated with

| Element | Crystal | θ (Peak)° | Count time (s) |
|---|---|---|---|
| Al Kα | RAP | 18.61 | 15 |
| Ca Kα | PET | 22.63 | 20 |
| Fe Kα | $LIF_{200}$ | 28.77 | 15 |
| Mg Kα | RAP | 22.25 | 15 |
| P Kα | PET | 44.71 | 10 |
| K Kα | PET | 25.35 | 20 |
| Na Kα | RAP | 27.13 | 60 |
| Si Kα | RAP | 15.82 | 15 |

Accelerating voltage 20kV; Electron beam raster 10 - 15 $\mu m^2$; Collimator slits out; All elements measured at 20 nA.

TABLE A1.4 Instrument settings for elements analysed on the electron microprobe.

| Element | Mineral | Concentration | Source |
|---|---|---|---|
| Al | Corundum | 52.92% | Mt. Davies, USA, OUM3933 |
| Ca | Wollastonite | 24.20% | Willsboro, USA, OUM16148 |
| Fe | Haematite | 69.94% | Elba, Italy, OUM830 |
| Mg | Periclase | 60.31% | Synthetic Mgo, Durham Univ. |
| P | Apatite | 18.34% | St Gotthard, Switz., OUM2663 |
| K | Orthoclase | 13.44% | Synthetic orthoclase, Durham University |
| Na | Jadeite | 10.93% | B.C.M. Butler, Oxford Univ. |
| Si | Wollastonite | 24.20% | Willsboro, USA, OUM16148 |

TABLE A1.5 Standards used for calibrating the electron microprobe.

a 200 ± 50 Å thick layer of carbon. Conductivity was assured by applying a thick carbon dag to the sides of specimens and the top of specimen holders. Optimum definition was obtained with a gun voltage of 40 kV and a beam current of 100 μA. Mineralogical identifications were made from information provided by the X-ray analysis facility equipped with a KEVEX detector and connected on-line to a Nova computer. Computer identification of the element Kα lines on the X-ray spectra enabled rapid semiquantitive determination of crystallite composition from which the mineralogy could usually be inferred. Analysis of unfavourably-oriented crystallites occasionally necessitated increases in gun voltage up to 100 kV.

## A1.8 Results

Brief desriptions of the samples analysed are presented in Table A1.6 and the results in Table A1.7. Three sets of solutions were prepared from rocks that were lateral equivalents of those analysed in the main sampling scheme (A1.4). The analytical results for these powders (Table A1.8) compare favourably with the original samples (Table A1.7), demonstrating that they are indeed representative of the lithology from which they were taken.

Prior to data analysis (Chapter 4) each whole-rock value was compared with its corresponding HCl- and acetic-soluble values to determine whether any elements were being totally extracted in all samples by the preferential leaches. Each data set was compared subjectively to see if they were sufficiently close for differences to be attributed to analytical error. Mean values were t-tested and it was decided that the whole-rock and HCl-soluble solutions were the same for P, Na, Mn and Sr but that other elements were different. The mean values (Table A1.9) were then utilised in all further calculations.

TABLE A1.6 Description of specimens used for bulk geochemical analysis

| Number | Bed | Loc. | Lithology | Mineralization | Comments |
|---|---|---|---|---|---|
| BVL/BG/1 | B1/3 | 600 | white chalk | | scattered limonitic wisps |
| BVL/BG/2 | B1/3 | 200 | white chalk | | occasional grey marl(?) and brown limonite-stained burrow-fills |
| BVL/BG/3 | B1/4 | 100 | hardground chalk | sparse MnO, spar, limonite | calcite spar remains prominent; scattered mineralized intraclasts and bioclasts; grey marl(?) and brown limonite-stained Thalassinoides burrow fills |
| BVL/BG/4 | B1/4 | 90 | hardground chalk | sparse MnO, spar, limonite | discrete phosphatic-chalk filled burrows excluded but some indistinct-bioturbation associated pelletal phosphate |
| BVL/BG/5 | B1/4 | 60 | hardground chalk | limonitic wisps, scattered pelletal phosphate, MnO, spar | phosphatic-chalk filled 5 mm Thalassinoides common; fills excluded |
| BVL/BG/6 | B1/4 | 30 | hardground chalk | limonitic patches, MnO, scattered pelletal phosphate, spar | grey marl(?) and phosphatic-chalk filled 1 cm Thalassinoides prominent; phosphatic fills excluded |
| BVL/BG/7 | B1/4 | 20 | hardground chalk | MnO, very weak glauconite and phosphate, spar, | abundant white chalk intraclasts; phosphatic burrow-fills excluded; sediment finely intraclastic |
| BVL/BG/8 | B1/4 | 10 | hardground chalk | limonite, MnO, weak glauconite and phosphate, spar | phosphatic burrow-fills and mineralized hardground-surface excluded |
| BVL/BG/9 | B1/4 | top | hardground surface | strong glauconite, phosphate, limonite, MnO | sediment includes many mineralized intraclasts; phosphatic-chalk burrow-fills excluded |
| BVL/BG/10 | B1/4 | top | hardground surface | strong phosphate and glauconite, limonite, MnO | collected from an area where the intercalated poorly phospha chalk and Beauval Coral Bed are absent; surface bivalve and worm bored; phosphatic-chalk burrow-fills excluded |
| BVL/BG/11 | B1/4 | top | hardground surface | glauconite, phosphate, limonite, MnO | predominantly consists of cemented 5 cm mineralized intraclasts; lithology only represented on dislocated blocks of basal hardground on top of overfold |

TABLE A1.6 Description of specimens used for bulk geochemical analysis

| Number | Bed | Loc. | Lithology | Mineralization | Comments |
|---|---|---|---|---|---|
| BVL/BG/1 | B1/3 | 600 | white chalk | | scattered limonitic wisps |
| BVL/BG/2 | B1/3 | 200 | white chalk | | occasional grey marl(?) and brown limonite-stained burrow-fills |
| BVL/BG/3 | B1/4 | 100 | hardground chalk | sparse MnO, spar, limonite | calcite spar remains prominent; scattered mineralized intraclasts and bioclasts; grey marl(?) and brown limonite-stained Thalassinoides burrow fills |
| BVL/BG/4 | B1/4 | 90 | hardground chalk | sparse MnO, spar, limonite | discrete phosphatic-chalk filled burrows excluded but some indistinct-bioturbation associated pelletal phosphate |
| BVL/BG/5 | B1/4 | 60 | hardground chalk | limonitic wisps, scattered pelletal phosphate, MnO, spar | phosphatic-chalk filled 5 mm Thalassinoides common; fills excluded |
| BVL/BG/6 | B1/4 | 30 | hardground chalk | limonitic patches, MnO, scattered pelletal phosphate, spar | grey marl(?) and phosphatic-chalk filled 1 cm Thalassinoides prominent; phosphatic fills excluded |
| BVL/BG/7 | B1/4 | 20 | hardground chalk | MnO, very weak glauconite and phosphate, spar, | abundant white chalk intraclasts; phosphatic burrow-fills excluded; sediment finely intraclastic |
| BVL/BG/8 | B1/4 | 10 | hardground chalk | limonite, MnO, weak glauconite and phosphate, spar | phosphatic burrow-fills and mineralized hardground-surface excluded |
| BVL/BG/9 | B1/4 | top | hardground surface | strong glauconite, phosphate, limonite, MnO | sediment includes many mineralized intraclasts; phosphatic-chalk burrow-fills excluded |
| BVL/BG/10 | B1/4 | top | hardground surface | strong phosphate and glauconite, limonite, MnO | collected from an area where the intercalated poorly phosphat chalk and Beauval Coral Bed are absent; surface bivalve and worm bored; phosphatic-chalk burrow-fills excluded |
| BVL/BG/11 | B1/4 | top | hardground surface | glauconite, phosphate, limonite, MnO | predominantly consists of cemented 5 cm mineralized intraclasts; lithology only represented on dislocated blocks of basal hardground on top of overfold |

TABLE A1.6 (cont.)

| | | | | | |
|---|---|---|---|---|---|
| BVL/BG/12 | | | indurated phosphorite | phosphate, MnO | lithified top of 'Terebella' phosphatica encrusted, dislocated block of basal hardground (Fig. 2.22) |
| BVL/BG/13 | B1/5 | | white chalk | pelletal phosphate | poorly-fossiliferous lateral equivalent of the Beauval Coral Bed; weakly lithified; silicified fauna and phosphatic-chalk burrow-fills avoided |
| BVL/BG/14 | B1/5 | | silicified coral | silica, phosphate, MnO | Beauval Coral Bed; silicified fauna only |
| BVL/BG/15 | B1/5 | | poorly-phosphatic chalk | pelletal phosphate | intercalated poorly-phosphatic chalk |
| BVL/BG/16 | B1/6 | base | basal lag | phosphate, pelletal phosphate | phosphatized-intraclast lag in a phosphatic-chalk matrix |
| BVL/BG/17 | B2/1 | 50 | burrowed-out white chalk | limonite | yellow-stained nodules at the summit of the unit |
| BVL/BG/18 | B6/2 | 800 | phosphatic chalk | pelletal phosphate | upper phosphatic chalk |
| NLU/BG/19 | N2/1 | 110 | hardground chalk | limonitic wisps | abundant Chondrites and 5 mm Thalassinoides, the phosphatic-chalk fill of the latter excluded |
| NLU/BG/20 | N2/1 | 90 | phosphatic chalk | pelletal phosphate, limonite | burrow-fill of ≤3 cm Thalassinoides; 1-3 mm phosphatized intraclasts common; several generations of burrowing |
| NLU/BG/21 | N2/1 | 90 | hardground chalk | limonite | intensely bioturbated; phosphatic burrow-fills separated |
| NLU/BG/22 | N2/1 | 75 | phosphatic chalk | pelletal phosphate, limonite | burrow-foll of ≤5 cm Thalassinoides; 5 mm phosphatized intr clasts common; several generations of burrowing |
| NLU/BG/23 | N2/1 | 75 | hardground chalk | limonite | intensely bioturbated; occasional limonite-preserved sponges; phosphatic burrow-fills separated |
| NLU/BG/24 | N2/1 | 60 | hardground chalk | limonite | phosphatic-chalk filled Thalassinoides and white-chalk filled Chondrites common; abundant limonitic clay and phosphatic-chalk filled fractures; fractures and phosphati burrow-fills excluded |
| NLU/BG/25 | N2/1 | 45 | hardground chalk | limonite, MnO, scattered pelletal phosphate | numerous burrows; lithification poor; fracture planes flat and stylolitic; phosphatic-chalk filled burrows excluded |
| NLU/BG/26 | N2/1 | 30 | hardground chalk | limonite, phosphate, MnO | mineralization occurs outwards from numerous phosphatic-chalk filled ≤2 cm Thalassinoides (fills excluded); |

TABLE A1.6 (cont.)

| | | | | | |
|---|---|---|---|---|---|
| NLU/BG/27 | N2/1 | 20 | hardground chalk | limonite, glauconite, MnO phosphate | stenomorphic <1 cm Thalassinoides, filled with phosphatic chalk and glauconitized-chalk filled Chondrites common; pronounced fracturing with injection by phosphatic chalk; phosphatic burrow-fills excluded |
| NLU/BG/28 | N2/1 | 5 | hardground chalk | MnO, limonite, phosphate | phosphatic-chalk filled stenomorphic <1 cm Thalassinoides (fills excluded); sediment finely intraclastic; pronounced fracturing |
| NLU/BG/29 | N2/1 | top | hardground surface | phosphate, glauconite, MnO, limonite | worm bored top with dull-phosphate mineralization from an area where original top has been undermined by burrowing; phosphatic burrow-fills excluded |
| NLU/BG/30 | N2/1 | top | hardground surface | strong phosphate, limonite, goethite, MnO, glauconite | feint black MnO(?) stain just below worm bored, shiny-phosphate veneered surface |
| NLU/BG/31 | N2/2 | base | phosphatized intraclasts | strong phosphate, MnO, goethite, limonite | Type 1 and 2 nodules only (Fig. 2.50); shiny-phosphate skins; worm bored surfaces; goethite flecks at cores |
| NLU/BG/32 | N2/2 | 30 | phosphatic chalk | pelletal phosphate | indistinct white-chalk filled bioturbation intense; large (> 3 mm) intraclasts rare |
| VDLT/BG/33 | V2/2 | | phosphatized intraclasts | phosphate | nodules only |
| OVL/BG/34 | O1/2 | | poorly-phosphatic chalk | pelletal phosphate, phosphate, MnO, silica, glauconite | cemented mineralized lag |
| OBG/BG/35 | | | phosphatic chalk sensu lato | pelletal phosphate, limonite | early Campanian Craie de Trivieres, Ciment d'Obourg quarry, Obourg, Belgium |
| OBG/BG/36 | | | phosphatic chalk sensu lato | pelletal phosphate | as above |

Location of specimens (Loc.) is given in centimetres from the top of the bed. Samples are listed in stratigraphical order for each locality (starting at base with lowest specimen numbers). BVL = Beauval quarry; NLU = Nurlu quarry; VDLT = Villers-devant-le-Thour, Le Tremblot quarry; OVL = Orville quarry (Champs d'Argent); OBG = Obourg (Belgium). Types of mineralization are listed in order of importance.

TABLE A1.7 Results of geochemical analyses

| Element | BVL/BG/1 | | | BVL/BG/2 | | | BVL/BG/3 | | | BVL/BG/4 | | |
|---|---|---|---|---|---|---|---|---|---|---|---|---|
| | a | b | c | a | b | c | a | b | c | a | b | c |
| $SiO_2$ | 1.2000 | | | 1.2800 | | | 1.0400 | | | 0.9100 | | |
| $Al_2O_3$ | 0.2490 | 0.0240 | | 0.2740 | 0.0470 | | 0.2030 | 0.0220 | | 0.1870 | 0.0280 | |
| $Fe_2O_3$ | 0.3700 | 0.1700 | 0.0138 | 0.2640 | 0.1220 | <0.0050 | 0.1930 | 0.0718 | 0.0178 | 0.2200 | 0.1100 | 0.0218 |
| MnO | 0.0342 | 0.0355 | 0.0349 | 0.0381 | 0.0401 | 0.0426 | 0.0387 | 0.0409 | 0.0420 | 0.0611 | 0.0613 | 0.0607 |
| MgO | 0.2330 | 0.1950 | 0.1670 | 0.2090 | 0.1770 | | 0.2170 | 0.1850 | 0.1710 | 0.2480 | 0.2160 | 0.1940 |
| CaO | 54.9000 | 53.9000 | 53.9000 | 55.4000 | 55.0000 | 54.8000 | 55.3000 | 54.6000 | 55.0000 | 55.4000 | 54.3000 | 55.3000 |
| $Na_2O$ | 0.0322 | 0.0292 | | 0.0252 | 0.0220 | | 0.0179 | 0.0173 | | 0.0259 | 0.0354 | |
| $K_2O$ | 0.0470 | 0.0090 | | 0.0497 | 0.0130 | | 0.0425 | 0.0070 | | 0.0396 | 0.0120 | |
| $P_2O_5$ | 0.3000 | 0.3000 | 0.0165 | 0.1800 | 0.1800 | 0.0140 | 0.2100 | 0.2100 | 0.0148 | 0.4300 | 0.4400 | 0.0200 |
| Sr | 0.0586 | 0.0588 | 0.0574 | 0.0572 | 0.0588 | 0.0620 | 0.0551 | 0.0555 | 0.0553 | 0.0491 | 0.0520 | 0.0476 |
| Insoluble residue | 1.1600 | | | 1.2100 | | | 1.0300 | | | 0.8100 | | |
| $P_2O_5$/CaO | 0.0055 | 0.0056 | 0.0003 | 0.0032 | 0.0033 | 0.0003 | 0.0038 | 0.0038 | 0.0003 | 0.0078 | 0.0081 | 0.0004 |

a = whole rock, b = HCl-soluble portion, c = buffered acetic acid soluble; BVL = Beauval quarry.

TABLE A1.7 (cont.)

| Element | BVL/BG/5 | | | BVL/BG/6 | | | BVL/BG/7 | | | BVL/BG/8 | | |
|---|---|---|---|---|---|---|---|---|---|---|---|---|
| | a | b | c | a | b | c | a | b | c | a | b | c |
| $SiO_2$ | 0.8300 | | | 0.7700 | | | 0.6100 | | | 0.7400 | | |
| $Al_2O_3$ | 0.1770 | 0.0050 | | 0.1420 | 0.0140 | | 0.1350 | 0.0240 | | 0.1340 | 0.0430 | |
| $Fe_2O_3$ | 0.3650 | 0.0478 | 0.0244 | 0.2410 | 0.0811 | 0.0189 | 0.2720 | 0.1390 | 0.0218 | 0.5100 | 0.3010 | 0.0190 |
| MnO | 0.0445 | 0.0447 | 0.0452 | 0.0581 | 0.0568 | 0.0568 | 0.1080 | 0.1080 | 0.1080 | 0.1290 | 0.1250 | 0.1210 |
| MgO | 0.2100 | 0.1800 | 0.1640 | 0.2360 | 0.2070 | 0.1870 | 0.2830 | 0.2630 | 0.2470 | 0.3100 | 0.2910 | 0.2530 |
| CaO | 55.4000 | 53.7000 | 54.2000 | 54.6000 | 54.0000 | 53.9000 | 57.1000 | 55.5000 | 53.7000 | 55.3000 | 55.0000 | 51.9000 |
| $Na_2O$ | 0.0217 | 0.0361 | | 0.0364 | 0.0259 | | 0.0273 | 0.0229 | | 0.0420 | 0.0361 | |
| $K_2O$ | 0.0382 | 0.0082 | | 0.0382 | 0.0072 | | 0.0282 | 0.0070 | | 0.0347 | 0.0121 | |
| $P_2O_5$ | 0.3000 | 0.3100 | 0.0163 | 0.4000 | 0.3900 | 0.0170 | 0.5000 | 0.4900 | 0.0175 | 1.1700 | 1.1000 | 0.0280 |
| Sr | 0.0572 | 0.0530 | 0.0527 | 0.0464 | 0.0485 | 0.0504 | 0.0454 | 0.0465 | 0.0430 | 0.0454 | 0.0465 | 0.0418 |
| Insoluble residue | 1.0000 | | | 0.7000 | | | 0.6200 | | | 0.5900 | | |
| $P_2O_5$/CaO | 0.0054 | 0.0058 | 0.0003 | 0.0073 | 0.0072 | 0.0003 | 0.0088 | 0.0088 | 0.0003 | 0.0212 | 0.2000 | 0.0005 |

a = whole rock, b = HCl-soluble portion, c = buffered acetic acid soluble; BVL = Beauval quarry.

TABLE A1.7 (cont.)

| Element | BVL/BG/9 | | | BVL/BG/10 | | | BVL/BG/11 | | | BVL/BG/12 | | |
|---|---|---|---|---|---|---|---|---|---|---|---|---|
| | a | b | c | a | b | c | a | b | c | a | b | c |
| $SiO_2$ | 1.5200 | | | 2.2200 | | | 1.3000 | | | 0.9900 | | |
| $Al_2O_3$ | 0.2760 | 0.1900 | | 0.3850 | 0.3520 | | 0.2760 | 0.2140 | | 0.2130 | 0.2290 | |
| $Fe_2O_3$ | 1.3200 | 1.0600 | <0.0050 | 3.5000 | 3.2500 | 0.0067 | 1.7900 | 1.5700 | <0.0050 | 0.1813 | 0.7720 | <0.0050 |
| MnO | 0.1010 | 0.1010 | 0.0943 | 0.0491 | 0.0532 | 0.0300 | 0.0581 | 0.0578 | 0.0323 | 0.0181 | 0.0222 | 0.0013 |
| MgO | 0.3420 | 0.3320 | 0.2180 | 0.3630 | 0.3580 | 0.0809 | 0.2870 | 0.2740 | 0.0710 | 0.2890 | 0.2850 | 0.0475 |
| CaO | 55.5000 | 53.6000 | 45.9000 | 53.5000 | 51.8000 | 21.3000 | 54.4000 | 50.2000 | 20.2000 | 54.8000 | 51.3000 | 10.9000 |
| $Na_2O$ | 0.1520 | 0.1450 | | 0.5630 | 0.5570 | | 0.6110 | 0.5900 | | 0.7820 | 0.8330 | |
| $K_2O$ | 0.0882 | 0.0696 | | 0.1750 | 0.1640 | | 0.0560 | 0.0512 | | 0.0516 | 0.0476 | |
| $P_2O_5$ | 4.8300 | 4.8300 | 0.0280 | 20.0000 | 19.8000 | 0.2650 | 21.9000 | 21.6000 | 0.2420 | 28.8000 | 28.5000 | 0.6900 |
| Sr | 0.0670 | 0.0638 | 0.0416 | 0.1300 | 0.1390 | 0.0235 | 0.1520 | 0.1460 | 0.0242 | 0.1890 | 0.1880 | 0.0193 |
| Insoluble residue | 0.6300 | | | 0.7100 | | | 0.4600 | | | 0.4000 | | |
| $P_2O_5/CaO$ | 0.0870 | 0.0901 | 0.0006 | 0.3740 | 0.3820 | 0.0124 | 0.4030 | 0.4300 | 0.0120 | 0.5260 | 0.5560 | 0.0633 |

a = whole rock, b = HCl-soluble portion, c = buffered acetic acid soluble; BVL = Beauval quarry.

TABLE A1.7 (cont.)

| Element | BVL/BG/13 | | | BVL/BG/14 | | | BVL/BG/15 | | | BVL/BG/16 | | |
|---|---|---|---|---|---|---|---|---|---|---|---|---|
| | a | b | c | a | b | c | a | b | c | a | b | c |
| $SiO_2$ | 1.3400 | | | 19.1000 | | | 1.1000 | | | 1.7000 | | |
| $Al_2O_3$ | 0.1680 | 0.0660 | | 0.0990 | 0.0710 | | 0.2170 | 0.0990 | | 0.3420 | 0.2420 | |
| $Fe_2O_3$ | 0.5080 | 0.3670 | 0.0276 | 0.6220 | 0.5240 | <0.0050 | 0.7990 | 0.5430 | <0.0050 | 1.0600 | 0.8290 | <0.0050 |
| MnO | 0.1470 | 0.1470 | 0.1382 | 0.0917 | 0.0904 | 0.0814 | 0.0936 | 0.0941 | 0.0814 | 0.0367 | 0.0376 | 0.0162 |
| MgO | 0.3200 | 0.2950 | 0.2430 | 0.2710 | 0.2630 | 0.1840 | 0.2950 | 0.2850 | 0.1720 | 0.2980 | 0.2980 | 0.0846 |
| CaO | 54.6000 | 53.9000 | 50.3000 | 45.6000 | 44.7000 | 35.6000 | 53.5000 | 53.2000 | 39.6000 | 53.0000 | 50.7000 | 22.8000 |
| $Na_2O$ | 0.0752 | 0.0752 | | 0.2280 | 0.2060 | | 0.2790 | 0.2880 | | 0.5550 | 0.5370 | |
| $K_2O$ | 0.0337 | 0.0157 | | 0.0275 | 0.0218 | | 0.0542 | 0.0330 | | 0.0788 | 0.0535 | |
| $P_2O_5$ | 2.1800 | 2.2000 | 0.0363 | 7.0000 | 7.0800 | 0.1000 | 9.5000 | 9.5800 | 0.1200 | 19.5000 | 19.5000 | 0.2270 |
| Sr | 0.0551 | 0.0530 | 0.0458 | 0.0551 | 0.0538 | 0.0220 | 0.0945 | 0.0950 | 0.0412 | 0.1550 | 0.1480 | 0.0269 |
| Insoluble residue | 1.0000 | | | 14.4000 | | | 0.6400 | | | 0.8700 | | |
| $P_2O_5/CaO$ | 0.0399 | 0.0408 | 0.0072 | 0.1540 | 0.1580 | 0.0028 | 0.1780 | 0.1800 | 0.0030 | 0.3680 | 0.3850 | 0.0099 |

a = whole rock, b = HCl-soluble portion, c = buffered acetic acid soluble; BVL = Beauval quarry.

TABLE A1.7 (cont.)

| Element | BVL/BG/17 | | | BVL/BG/18 | | | NLU/BG/19 | | | NLU/BG/20 | | |
|---|---|---|---|---|---|---|---|---|---|---|---|---|
| | a | b | c | a | b | c | a | b | c | a | b | c |
| $SiO_2$ | 1.0700 | | | 0.7400 | | | 2.1400 | | | 4.1800 | | |
| $Al_2O_3$ | 0.2490 | 0.1370 | | 0.1740 | 0.1180 | | 0.4840 | 0.0280 | | 0.7980 | 0.3450 | |
| $Fe_2O_3$ | 1.3300 | 1.0800 | <0.0050 | 0.4130 | 0.3200 | <0.0050 | 0.4220 | 0.1150 | 0.0276 | 1.3900 | 1.0500 | <0.0050 |
| MnO | 0.0359 | 0.0382 | 0.0349 | 0.0288 | 0.0289 | 0.0207 | 0.0507 | 0.0455 | 0.0471 | 0.0342 | 0.0353 | 0.0284 |
| MgO | 0.2750 | 0.2640 | 0.2340 | 0.2550 | 0.2530 | 0.1540 | 0.2340 | 0.1650 | 0.1480 | 0.2940 | 0.2550 | 0.1180 |
| CaO | 54.6000 | 53.2000 | 46.3000 | 53.7000 | 52.6000 | 38.6000 | 54.0000 | 53.6000 | 52.2000 | 51.2000 | 51.1000 | 40.9000 |
| $Na_2O$ | 0.1690 | 0.1670 | | 0.2960 | 0.3160 | | 0.0290 | 0.0234 | | 0.2550 | 0.2580 | |
| $K_2O$ | 0.0551 | 0.0308 | | 0.0449 | 0.0347 | | 0.0861 | 0.0120 | | 0.1570 | 0.0606 | |
| $P_2O_5$ | 5.3800 | 5.5000 | 0.0410 | 10.1000 | 10.2000 | 0.1210 | 0.1500 | 0.1500 | 0.0160 | 6.0000 | 6.4000 | 0.0690 |
| Sr | 0.0788 | 0.0835 | 0.0550 | 0.1160 | 0.1110 | 0.0442 | 0.0840 | 0.0885 | 0.0816 | 0.1160 | 0.1080 | 0.0608 |
| Insoluble residue | 0.6800 | | | 0.3200 | | | 2.5600 | | | 2.6700 | | |
| $P_2O_5/CaO$ | 0.0985 | 0.1030 | 0.0009 | 0.1880 | 0.1940 | 0.0031 | 0.0028 | 0.0028 | 0.0003 | 0.1170 | 0.1250 | 0.0017 |

a = whole rock, b = HCl-soluble portion, c = buffered acetic acid soluble; BVL = Beauval quarry, NLU = Nurlu quarry.

TABLE A1.7 (cont.)

| Element | NLU/BG/21 | | | NLU/BG/22 | | | NLU/BG/23 | | | NLU/BG/24 | | |
|---|---|---|---|---|---|---|---|---|---|---|---|---|
| | a | b | c | a | b | c | a | b | c | a | b | c |
| $SiO_2$ | 1.8800 | | | 4.6400 | | | 1.8000 | | | 1.5600 | | |
| $Al_2O_3$ | 0.3900 | 0.0280 | | 0.8170 | 0.4060 | | 0.3670 | 0.0660 | | 0.3260 | 0.0330 | |
| $Fe_2O_3$ | 0.5170 | 0.2080 | 0.0244 | 1.5400 | 1.2900 | <0.0050 | 0.5730 | 0.3240 | 0.0244 | 0.4610 | 0.2670 | 0.0356 |
| MnO | 0.0549 | 0.0558 | 0.0568 | 0.0329 | 0.0334 | 0.0252 | 0.0604 | 0.0612 | 0.0588 | 0.0730 | 0.0746 | 0.0710 |
| MgO | 0.2250 | 0.1820 | 0.1580 | 0.3060 | 0.2710 | 0.1100 | 0.2450 | 0.2010 | 0.1730 | 0.2450 | 0.2040 | 0.1780 |
| CaO | 54.5000 | 54.0000 | 52.1000 | 52.1000 | 52.1000 | 38.9000 | 54.6000 | 54.1000 | 53.4000 | 54.3000 | 53.9000 | 52.0000 |
| $Na_2O$ | 0.0375 | 0.0377 | | 0.3120 | 0.3000 | | 0.0378 | 0.0341 | | 0.0350 | 0.0256 | |
| $K_2O$ | 0.0764 | 0.0130 | | 0.1700 | 0.0696 | | 0.0698 | 0.0160 | | 0.0569 | 0.0108 | |
| $P_2O_5$ | 0.3000 | 0.3400 | 0.0170 | 7.7500 | 7.9000 | 0.0820 | 0.4000 | 0.4300 | 0.0150 | 0.2900 | 0.3000 | 0.0155 |
| Sr | 0.0799 | 0.0878 | 0.0814 | 0.1180 | 0.1130 | 0.0564 | 0.0839 | 0.0803 | 0.0792 | 0.0775 | 0.0745 | 0.0734 |
| Insoluble residue | 1.9600 | | | 2.8100 | | | 1.6400 | | | 1.5400 | | |
| $P_2O_5$/CaO | 0.0055 | 0.0063 | 0.0003 | 0.1490 | 0.1520 | 0.0021 | 0.0073 | 0.0079 | 0.0003 | 0.0053 | 0.0056 | 0.0003 |

a = whole rock, b = HCl-soluble portion, c = buffered acetic acid soluble; NLU = Nurlu quarry.

TABLE A1.7 (cont.)

| Element | NLU/BG/25 | | | NLU/BG/26 | | | NLU/BG/27 | | | NLU/BG/28 | | |
|---|---|---|---|---|---|---|---|---|---|---|---|---|
| | a | b | c | a | b | c | a | b | c | a | b | c |
| $SiO_2$ | 1.2700 | | | 1.2400 | | | 1.4000 | | | 1.4300 | | |
| $Al_2O_3$ | 0.2600 | 0.0240 | | 0.2570 | 0.0330 | | 0.2720 | 0.0430 | | 0.3000 | 0.0520 | |
| $Fe_2O_3$ | 0.5080 | 0.2080 | 0.0356 | 0.6830 | 0.3810 | 0.0520 | 0.8290 | 0.5030 | 0.0598 | 1.0900 | 0.6890 | 0.0571 |
| MnO | 0.0755 | 0.0795 | 0.0755 | 0.1010 | 0.1020 | 0.0968 | 0.1390 | 0.1420 | 0.1360 | 0.1390 | 0.1350 | 0.1350 |
| MgO | 0.2450 | 0.2010 | 0.1800 | 0.2560 | 0.2150 | 0.1920 | 0.2840 | 0.2410 | 0.2170 | 0.2880 | 0.2450 | 0.2040 |
| CaO | 54.0000 | 53.6000 | 52.2000 | 54.6000 | 54.0000 | 52.2000 | 54.0000 | 53.9000 | 52.1000 | 54.5000 | 53.3000 | 52.1000 |
| $Na_2O$ | 0.0375 | 0.0309 | | 0.0448 | 0.0407 | | 0.0431 | 0.0376 | | 0.0473 | 0.0344 | |
| $K_2O$ | 0.0470 | 0.0084 | | 0.0488 | 0.0096 | | 0.0577 | 0.0140 | | 0.0592 | 0.0148 | |
| $P_2O_5$ | 0.5000 | 0.5400 | 0.0200 | 0.5400 | 0.6000 | 0.0200 | 0.8300 | 0.8900 | 0.0228 | 0.6800 | 0.6800 | 0.0220 |
| Sr | 0.0751 | 0.0785 | 0.0734 | 0.0729 | 0.0703 | 0.0670 | 0.0632 | 0.0638 | 0.0583 | 0.0621 | 0.0638 | 0.0588 |
| Insoluble residue | 1.4100 | | | 1.3500 | | | 1.3500 | | | 1.3600 | | |
| $P_2O_5/CaO$ | 0.0093 | 0.0101 | 0.0004 | 0.0099 | 0.0111 | 0.0004 | 0.0154 | 0.0165 | 0.0004 | 0.0125 | 0.0128 | 0.0004 |

a = whole rock, b = HCl-soluble portion, c = buffered acetic acid soluble; NLU = Nurlu quarry.

TABLE A1.7 (cont.)

| Element | NLU/BG/29 | | | NLU/BG/30 | | | NLU/BG/31 | | | NLU/BG/32 | | |
|---|---|---|---|---|---|---|---|---|---|---|---|---|
| | a | b | c | a | b | c | a | b | c | a | b | c |
| $SiO_2$ | 1.4600 | . | | 1.5200 | | | 1.6500 | | | 1.0000 | | |
| $Al_2O_3$ | 0.2950 | 0.1280 | | 0.3170 | 0.2550 | | 0.3350 | 0.2650 | | 0.2190 | 0.1800 | |
| $Fe_2O_3$ | 1.2500 | 0.9630 | 0.0520 | 3.5700 | 3.1500 | <0.0050 | 3.9900 | 3.4300 | <0.0050 | 1.0400 | 0.9250 | <0.0050 |
| MnO | 0.1600 | 0.1620 | 0.1520 | 0.0507 | 0.0534 | 0.0355 | 0.0445 | 0.0455 | 0.0284 | 0.0329 | 0.0352 | 0.0258 |
| MgO | 0.3010 | 0.2750 | 0.2180 | 0.2950 | 0.2860 | 0.0864 | 0.3180 | 0.3090 | 0.0706 | 0.2710 | 0.2690 | 0.1480 |
| CaO | 55.5000 | 54.2000 | 51.5000 | 51.9000 | 51.4000 | 23.6000 | 50.7000 | 50.4000 | 20.9000 | 53.3000 | 52.2000 | 35.2000 |
| $Na_2O$ | 0.0655 | 0.0539 | | 0.5970 | 0.6040 | | 0.6740 | 0.6800 | | 0.4150 | 0.4000 | |
| $K_2O$ | 0.0719 | 0.0376 | | 0.0764 | 0.0678 | | 0.0889 | 0.0770 | | 0.0479 | 0.0422 | |
| $P_2O_5$ | 1.2500 | 1.3000 | 0.0235 | 18.2000 | 18.2000 | 0.2150 | 19.7000 | 19.2000 | 0.2680 | 10.9000 | 10.8000 | 0.2050 |
| Sr | 0.0653 | 0.0654 | 0.0572 | 0.1360 | 0.1350 | 0.0292 | 0.1500 | 0.1550 | 0.0316 | 0.1290 | 0.1240 | 0.0496 |
| Insoluble residue | 0.8900 | | | 0.5600 | | | 0.4900 | | | 0.2900 | | |
| $P_2O_5$/CaO | 0.0225 | 0.0240 | 0.0005 | 0.3510 | 0.3540 | 0.0091 | 0.3890 | 0.3810 | 0.0128 | 0.2050 | 0.2070 | 0.0058 |

a = whole rock, b = HCl-soluble portion, c = buffered acetic acid soluble; NLU = Nurlu quarry.

TABLE A1.7 (cont.)

| Element | VDLT/BG/33 | | | OVL/BG/34 | | | OBG/BG/35 | | | OBG/BG/36 | | |
|---|---|---|---|---|---|---|---|---|---|---|---|---|
| | a | b | c | a | b | c | a | b | c | a | b | c |
| $SiO_2$ | 1.6400 | | | 0.9600 | | | 3.3900 | | | 3.6100 | | |
| $Al_2O_3$ | 0.4720 | 0.3450 | | 0.1420 | 0.0990 | | 0.4160 | 0.1560 | | 0.4490 | 0.1130 | |
| $Fe_2O_3$ | 1.9900 | 1.6400 | <0.0050 | 1.1800 | 0.8520 | <0.0050 | 1.1800 | 0.9440 | 0.0109 | 1.7700 | 1.1700 | 0.0298 |
| MnO | 0.0314 | 0.0309 | 0.0245 | 0.1170 | 0.1150 | 0.0936 | 0.0148 | 0.0151 | 0.0155 | 0.0161 | 0.0164 | 0.0161 |
| MgO | 0.2520 | 0.2490 | 0.1020 | 0.3300 | 0.3240 | 0.2480 | 0.2780 | 0.2510 | 0.1970 | 0.2940 | 0.2460 | 0.2030 |
| CaO | 52.5000 | 51.6000 | 31.7000 | 55.1000 | 52.6000 | 45.1000 | 53.2000 | 52.8000 | 49.6000 | 53.5000 | 52.4000 | 48.9000 |
| $Na_2O$ | 0.5160 | 0.4110 | | 0.1810 | 0.1770 | | 0.1010 | 0.0899 | | 0.1080 | 0.0937 | |
| $K_2O$ | 0.0853 | 0.0618 | | 0.0347 | 0.0257 | | 0.0988 | 0.0395 | | 0.1020 | 0.0273 | |
| $P_2O_5$ | 13.0000 | 13.3000 | 0.1120 | 6.1300 | 6.2000 | 0.0640 | 1.5000 | 1.5300 | 0.0330 | 1.6900 | 1.7300 | 0.0480 |
| Sr | 0.1360 | 0.1310 | 0.0510 | 0.0540 | 0.0593 | 0.0244 | 0.0853 | 0.0894 | 0.0728 | 0.0864 | 0.0933 | 0.0770 |
| Insoluble residue | 0.6100 | | | 0.5900 | | | 2.3000 | | | 2.8300 | | |
| $P_2O_5$/CaO | 0.2480 | 0.2580 | 0.0035 | 0.1110 | 0.1180 | 0.0014 | 0.0282 | 0.0290 | 0.0007 | 0.0316 | 0.0330 | 0.0098 |

a = whole rock, b = HCl-soluble portion, c = buffered acetic acid soluble; VDLT = Villers-devant-le-Thour, OVL = Orville, OBG = Obourg (Belgium).

| Element | BVL/BG/7R | | | BVL/BG/8R | | | BVL/BG/9R | | |
|---|---|---|---|---|---|---|---|---|---|
| | a | b | c | a | b | c | a | b | c |
| $SiO_2$ | 0.6100 | | | 0.7100 | | | 1.4600 | | |
| $Al_2O_3$ | 0.1300 | 0.0240 | | 0.1300 | 0.0470 | | 0.2620 | 0.1700 | |
| $Fe_2O_3$ | 0.2720 | 0.1110 | 0.0244 | 0.5080 | 0.3190 | 0.0218 | 1.2300 | 0.9440 | <0.0050 |
| MnO | 0.1080 | 0.1080 | 0.1050 | 0.1270 | 0.1250 | 0.1220 | 0.1010 | 0.1020 | 0.0936 |
| MgO | 0.2820 | 0.2640 | 0.2340 | 0.3110 | 0.2950 | 0.2470 | 0.3420 | 0.3230 | 0.2130 |
| CaO | 57.2000 | 55.2000 | 53.5000 | 55.9000 | 55.0000 | 52.0000 | 55.1000 | 53.9000 | 46.1000 |
| $Na_2O$ | 0.0196 | 0.0222 | | 0.0410 | 0.0435 | | 0.1430 | 0.1420 | |
| $K_2O$ | 0.0275 | 0.0078 | | 0.0347 | 0.0157 | | 0.0810 | 0.0600 | |
| $P_2O_5$ | 0.5200 | 0.5000 | 0.0247 | 1.1800 | 1.1800 | 0.0340 | 4.7000 | 4.8300 | 0.0410 |
| Sr | 0.0443 | 0.0428 | 0.0454 | 0.0443 | 0.0448 | 0.0434 | 0.0653 | 0.0633 | 0.0434 |
| Insoluble residue | 0.6400 | | | 0.5300 | | | 0.6000 | | |
| $P_2O_5$/CaO | 0.0091 | 0.0091 | 0.0005 | 0.0211 | 0.0215 | 0.0007 | 0.0853 | 0.0896 | 0.0009 |

TABLE A1.8 Results of geochemical analyses of three replicate rock samples. a = whole rock, b = HCl-soluble portion, c = buffered acetic acid soluble; BVL = Beauval quarry. Sample numbers correspond to those in the main sample batch, R = replicate.

| Sample number | $P_2O_5$ | $Na_2O$ | Sr | MnO |
|---|---|---|---|---|
| | (%) | | (ppm) | |
| BVL/BG/1 | 0.30 | 307 | 587 | 348 |
| BVL/BG/2 | 0.18 | 236 | 580 | 391 |
| BVL/BG/3 | 0.21 | 176 | 553 | 398 |
| BVL/BG/4 | 0.44 | 306 | 506 | 612 |
| BVL/BG/5 | 0.31 | 289 | 551 | 446 |
| BVL/BG/6 | 0.40 | 311 | 475 | 574 |
| BVL/BG/7 | 0.50 | 251 | 459 | 1080 |
| BVL/BG/8 | 1.14 | 390 | 459 | 1270 |
| BVL/BG/9 | 4.83 | 1480 | 654 | 1010 |
| BVL/BG/10 | 19.90 | 5600 | 1350 | 511 |
| BVL/BG/11 | 21.80 | 6010 | 1490 | 579 |
| BVL/BG/12 | 28.60 | 8070 | 1880 | 201 |
| BVL/BG/13 | 2.19 | 752 | 540 | 1470 |
| BVL/BG/14 | 7.04 | 2170 | 544 | 910 |
| BVL/BG/15 | 9.54 | 2840 | 947 | 938 |
| BVL/BG/16 | 19.50 | 5460 | 1520 | 371 |
| BVL/BG/17 | 5.44 | 1682 | 812 | 370 |
| BVL/BG/18 | 10.10 | 3060 | 1130 | 288 |
| NLU/BG/19 | 0.15 | 262 | 863 | 481 |
| NLU/BG/20 | 6.20 | 2560 | 1120 | 347 |
| NLU/BG/21 | 0.32 | 376 | 839 | 553 |
| NLU/BG/22 | 7.83 | 3060 | 1160 | 331 |
| NLU/BG/23 | 0.42 | 359 | 821 | 608 |
| NLU/BG/24 | 0.30 | 303 | 760 | 738 |
| NLU/BG/25 | 0.52 | 342 | 768 | 775 |
| NLU/BG/26 | 0.57 | 427 | 716 | 1010 |
| NLU/BG/27 | 0.86 | 403 | 635 | 1400 |
| NLU/BG/28 | 0.68 | 408 | 629 | 1370 |
| NLU/BG/29 | 1.28 | 597 | 654 | 1610 |
| NLU/BG/30 | 18.20 | 6000 | 1360 | 520 |
| NLU/BG/31 | 19.40 | 6770 | 1520 | 450 |
| NLU/BG/32 | 10.90 | 4060 | 1260 | 340 |
| VDLT/BG/33 | 13.10 | 4640 | 1330 | 311 |
| OVL/BG/34 | 6.17 | 1790 | 566 | 1160 |
| OBG/BG/35 | 1.52 | 955 | 874 | 149 |
| OBG/BG/36 | 1.71 | 1010 | 898 | 162 |

TABLE A1.9 Mean of whole-rock and HCl-soluble values for those elements judged to be totally extracted in all samples by the latter method.

Appendix 2 : Biometric equations


| | | |
|---|---|---|
| A2.1 | Introduction | 513 |
| A2.2 | Regression equation | 513 |
| A2.3 | Slope of the regression line (b) | 513 |
| A2.4 | The y intercept of the regression line (a) | 513 |
| A2.5 | Correlation coefficient (r) | 513 |
| A2.6 | Standard error of the regression line ($SE_{yx}$) | 514 |
| A2.7 | Standard error of the slope ($SE_b$) | 514 |
| A2.8 | Standard error of the y intercept ($SE_a$) | 514 |
| A2.9 | Significance tests (students-t) | 514 |

## A2.1 Introduction

Equations utilised in the biometric analysis of belemnite 'populations' are relatively simple staistical formulae. Nevertheless, statistics books do nor always agree on the most applicable derivation of a particular formula and furthermore some formulae are difficult to obtain. Consequently, there follows a selection of the equations used to calculate the statistical parameters presented in Chapter 5. The equations originate from a number of sources which include Hald (1957), Simpson et al. (1960) and Nie et al. (1975). Standard mathematical symbols are used throughout. Further information may be obtained from the listed references and Sokal and Rohlf (1969).

## A2.2 The regression equation

$$\hat{y} = a + bx \qquad \text{(A2.1)}$$

where values of y, the dependent variable, are estimated from the values of x, the independent variable.

## A2.3 The slope of the regression line (b)

$$b = \frac{\sum(x - \bar{x})\,(y - \bar{y})}{\sum(x - \bar{x})^2} = \frac{SP_{xy}}{SS_x} \qquad \text{(A2.2)}$$

## A2.4 The y intercept of the regression line (a)

$$a = \bar{y} - b\bar{x} \qquad \text{(A2.3)}$$

## A2.5 The correlation coefficient (r)

$$r = \sqrt{\frac{\sum(\hat{y} - \bar{y})^2}{\sum(y - \bar{y})^2}} = \frac{SS_{reg}}{SS_y}$$

where $\sum(y - \bar{y})^2 = \sum(\hat{y} - \bar{y})^2 + \sum(y - \hat{y})^2$

$SS_y = SS_{reg} + SS_{res}$

$$\therefore r = \sqrt{\frac{SS_y - SS_{res}}{SS_y}} \qquad \text{(A2.4)}$$

A2.6 The standard error of the regression line ($SE_{yx}$)

$$SE_{yx} = \sqrt{\frac{\sum(y - \hat{y})^2}{N - 2}} = \sqrt{\frac{SS_{res}}{N - 2}} \qquad \text{(A2.5)}$$

A2.7 The standard error of the slope ($SE_b$)

$$SE_b = \sqrt{\frac{\sum(y - \hat{y})^2 / (N - 2)}{\sum(x - \bar{x})^2}}$$

$$= \sqrt{\frac{SS_{res} / (N - 2)}{SS_x}} \qquad \text{(A2.6)}$$

A2.8 The standard error of the y intercept ($SE_a$)

$$SE_a = \sqrt{SE_{yx}^2 \left(\frac{1}{N} + \frac{\bar{x}^2}{(x - \bar{x})^2}\right)}$$

$$= \sqrt{SE_{yx}^2 \left(\frac{1}{N} + \frac{\bar{x}^2}{SS_x}\right)} \qquad \text{(A2.7)}$$

A2.9 Significance tests (students-t)

$$t = \frac{a - \alpha}{SE_a} \qquad \text{with } N - 2 \text{ degrees of freedom} \qquad \text{(A2.8)}$$

$$t = \frac{b - \beta}{SE_b} \qquad \text{with } N - 2 \text{ degrees of freedom}$$

where $\alpha$ and $\beta$ are predicted values

# Appendix 3 : Phosphatic chalk echinoids

## A3.1 Introduction

In the absence of ammonites, echinoderms and belemnites are the main macro-faunal index fossils of the Upper Cretaceous. Phosphatic chalk belemnites have been examined in detail in Chapter 5. The small number of echinoderms recovered precludes a similarly detailed study of their distribution. Nevertheless, echinoderms in general, and echinoids in particular, are important zonal indicators in phosphatic chalks. Consequently, there is included in this appendix, a series of figures which illustrate the major echinoid morphotypes recovered from contemporary exposures of phosphatic chalk. The stratigraphical range of some of the Echinocorys and other echinoderms is shown in Fig. 1.4.

Fig. A3.1 Phosphatic chalk Micraster.
Nos. 1 - 3. Micraster coranguinum cf. rostratus (Mantell), from the upper phosphatic chalk of Beauval quarry, low Santonian M. testudinarius(?) Zone. 1. left lateral, 2. apical, 3. oral views of KZ6834, all x 1.
Nos. 4 - 6. Micraster coranguinum (Leske). Intermediate white chalk, bed B4/2, Beauval quarry. Middle - high Santonian U. socialis(?) Zone. The specimen has a thin test and is slightly crushed; it shows some similarities to M. coranguinum simpsoni Stokes. 4. left lateral, 5. apical, 6. oral views, KZ6831, x 1.
Nos. 7 - 9. Micraster coranguinum (Leske). Lower phosphatic chalk, bed B3/4 (Mélange unit), Beauval quarry. Low - middle Santonian M. coranguinum Zone. The labrum has been destroyed by echinoid(?) bioerosion, and the test contains numerous pouch-like Rogerella bores. 7. left lateral, 8. apical, 9. oral views, KZ6826, x 1.
Nos. 10 - 12. Micraster coranguinum (Leske). Lower phosphatic chalk, basal lag, Beauval quarry. Low - middle Santonian M. coranguinum Zone. 10. left lateral, 11. apical, 12. oral views of a juvenile with phosphatized test, KZ6818, x 1.5.
All specimens coated with ammonium chloride.

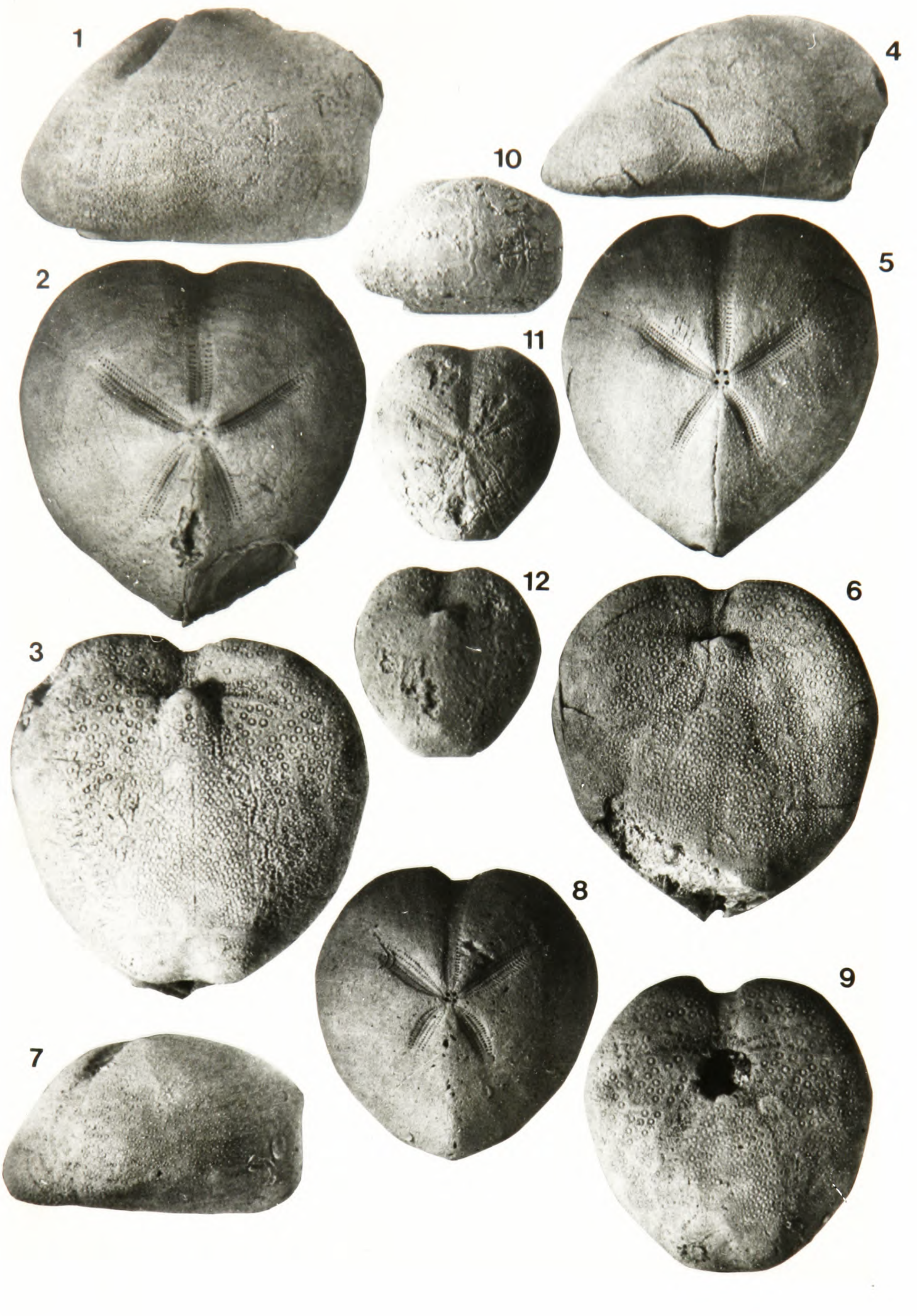
1
4
10
2
5
11
12
6
3
8
9
7

Fig. A3.2 Phosphatic chalk Echinocorys I.
Nos. 1 - 4. Echinocorys sp., from the phosphatic chalk, bed N2/2, of Nurlu quarry. Low - middle Santonian M. coranguinum(?) Zone. A low subconical form occurring in the oldest phosphatic chalk at this locality. 1. left lateral, 2. apical, 3. oral, 4. posterior views, KZ6933, x 1.
Nos. 5 - 8. Echinocorys cf. elevata Brydone. Intermediate white chalk, bed B2/3 (phosphatic chalk lenticle), Beauval quarry. Middle Santonian U. socialis Zone. Morphologically identical to E. elevata but associated with fragments of Uintacrinus socialis and therefore stratigraphically younger than E. elevata sensu Brydone (1912). 5. left lateral, 6. apical, 7. oral, 8. posterior views, KZ6830, x 1.
All specimens coated with ammonium chloride.


1
2
3
4
5
6
7
8

Fig. A3.3 Phosphatic chalk Echinocorys II.
Nos. 1 - 4. Echinocorys elevata Brydone. Specimen from the sediment on top of the Winterbourne Phosphatic Chalk Hardground (base of bed W1/4). High Santonian M. testudinarius Zone. A large percentage of the test has been severely etched by Tertiary weathering which has revealed the underlying plate structure. 1. left lateral, 2. apical, 3. oral, 4. posterior views, K17001, x 1.
Nos. 5 - 8. Echinocorys sp. Basal lag preservation, collected out of situ, Hallencourt pit. High Santonian - low Campanian(?). An undescribed form of Echinocorys with part-phosphatized test, similar to but less elevated than an example from Hardivillers (Fig. A3.5, nos. 1 - 4). 5. left lateral, 6. apical, 7. oral, 8. posterior views, KZ6869, x 1.
All specimens coated with ammonium chloride.

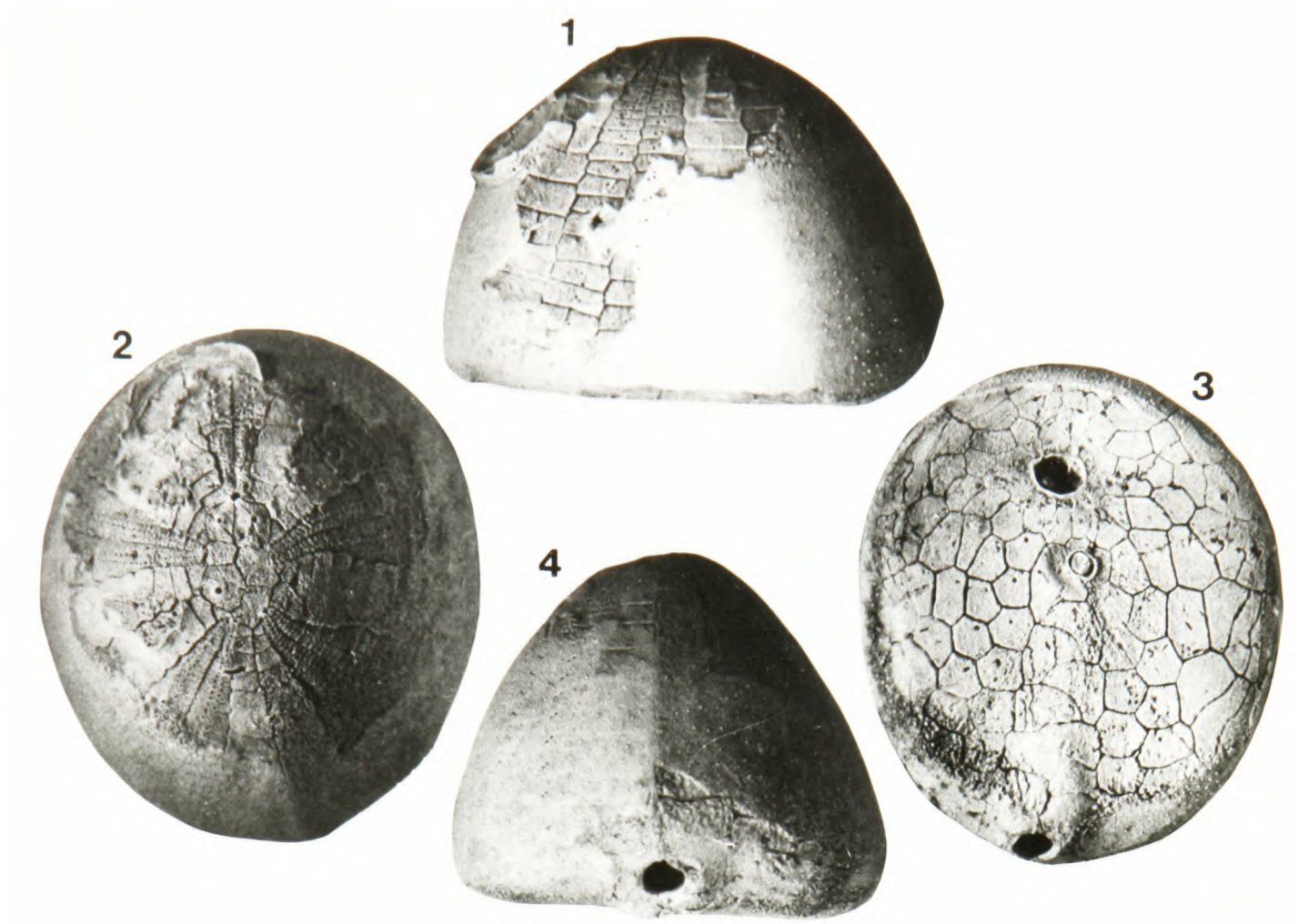
1
2
3
4


5
6
7
8

1



2



3

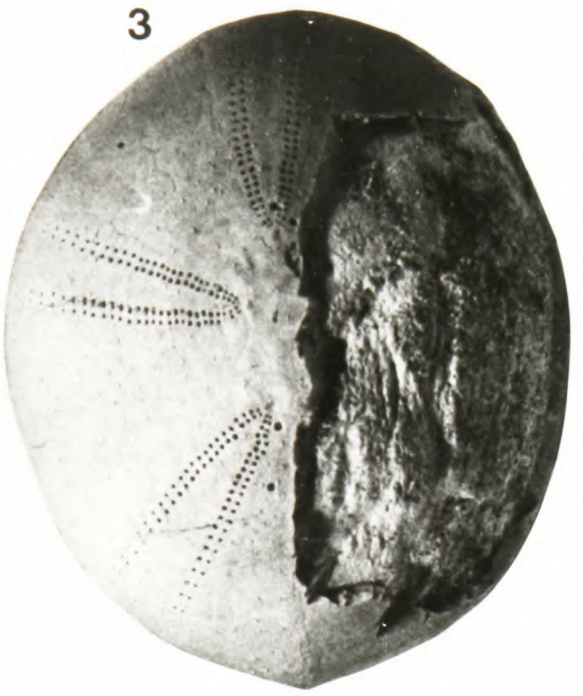

4



5



6

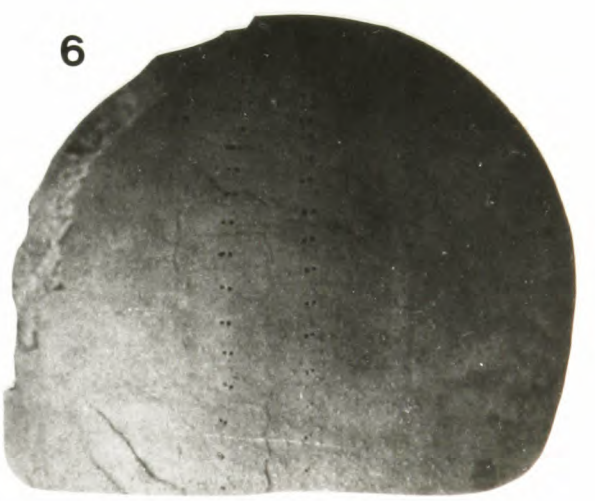

Fig. A3.5 Phosphatic chalk Echinocorys IV.
Nos. 1 - 4. Echinocorys sp. Specimen from on top of the minor hardground within the phosphatic chalk, base of bed H6/2, Hardivillers quarry. High Santonian - low Campanian. 1. right lateral, 2. apical, 3. oral, 4. posterior views, KZ6873, x 1.
Nos. 5 - 8. Echinocorys truncata Griffith and Brydone. Upper phosphatic chalk, base of bed B9/2, from directly on top of the Beauval Echinocorys Hardground. Low Campanian, E. depressula Subzone, O. pilula Zone. The small size is typical of the species. 5. left lateral, 6. apical, 7. oral, 8. posterior views, KZ 6833, x 1.
All specimens coated with ammonium chloride.

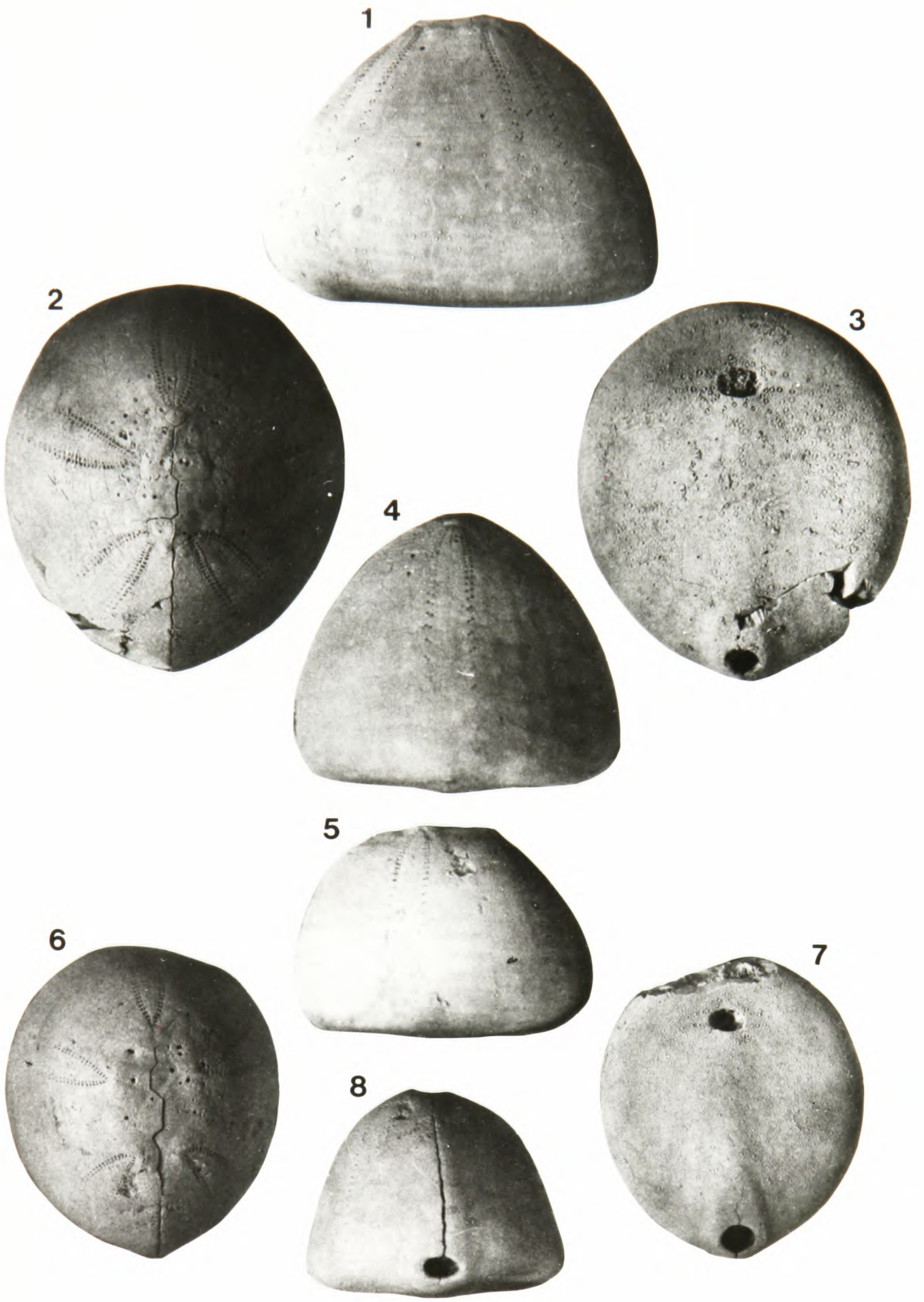
1
2
3
4
5
6
7
8

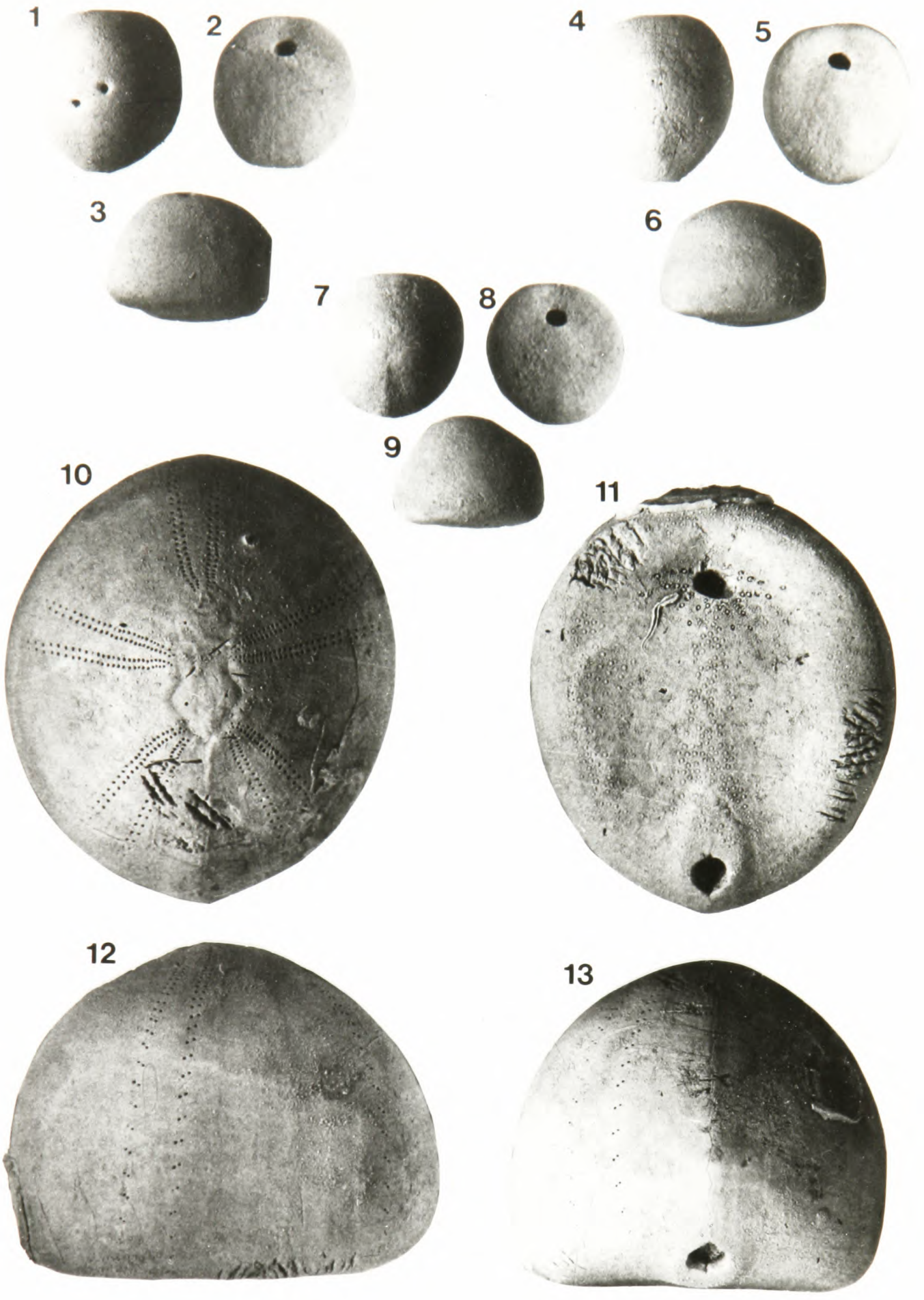
1
2
3
4
5
6
7
8
9
10
11
12
13

## Map 1 : Explanation

Upper Cretaceous stage map of the Picardy region of northern France showing the distribution of Santonian to Campanian phosphatic chalks.

The map displays the distribution of Cretaceous sediments in the region after the removal of the Quaternary and thinner Tertiary cover. All known French sites of phosphatic chalks are shown except for St Martin-du-Tertre (Yonne), which lies 160 km to the south, and a borehole record near Dourges (Pas-de-Calais), which is situated 1 km north of the area covered by the map.

Stage boundaries are based on data provided by French (BRGM) 1 : 80,000 and 1 : 50,000 geological maps and borehole logs included with the latter. Additional information was obtained from fieldwork and Devries et al. (1974). Stage boundaries are chiefly based on the microfaunal zonation of Monciardini (Chapter 1). The Turonian includes Biozone a, which spans the Turonian - Coniacian boundary; Biozone f is included in the Campanian, although it spans the Santonian - Campanian boundary. The large area mapped as Coniacian in the northern portion of the map may include some early Santonian sediments; no microfaunal zonation is available for this area, and although the highest chalk has been tentatively assigned to the Micraster coranguinum Zone, the absence of macrofauna makes the zonal boundaries uncertain.

## References

AGGASSIZ, A., 1888. Three cruises of the USC and GS Steamer Blake. Bull. Mus. Comp. Zool. Harvard, 14: 314p.

AMES, L.L. Jr., 1959. The genesis of carbonate apatites. Econ. Geol., 54: 829 - 841.

AMES, L.L. Jr., 1960. Some cation substitutions during the formation of phosphate from calcite. Econ. Geol., 55: 354 - 362.

ARMSTRONG, F.A.J., 1965. Phosphorus. In: J.P. Riley and C. Skirrow (Eds.), Chemical Oceanography 1 (First Edition), Academic Press, London, New York, 323 - 364.

ARMSTRONG, F.A.J. and HARVEY, H.W., 1950. The cycle of phosphorus in the waters of the English Channel. J. Mar. Biol. Ass. UK, 29: 145 - 162.

ARNAUD, H., 1877. Mémoire sur le terraine Crétacé du Sud-ouest de la France. Mém. Soc. Géol. Fr., (2), 10: 1 - 110.

ARNAUD, H., 1883. Position des Hippurites dilatata et Hippurites bioculatus dans la serie Crétacée. Bull. Soc. Géol. Fr., (3), 12: 138 - 157.

ARNAUD, H., 1897. Divisions naturelles du Crétace Superieur au-dessus du Santonien dans le sud-ouest et dans la region Pyréneéne. Bull. Soc. Géol. Fr., (3), 25: 676 - 681.

ARRHENIUS, G., 1963. Pelagic sediments. In: M.N. Hill (Ed.), The Sea 3, Wiley and Sons, New York, 655 - 727.

ATKINSON, L.P., 1977. Modes of gulf stream intrusion into the South Atlantic Bight shelf waters. Geophys. Res. Lett., 4: 583 - 586.

ATLAS, E.L., 1975. Phosphate equilibria in seawater and interstitial waters. Unpub. PhD dissertation, Corvallis, Oregon State University, 154p.

ATLAS, E., 1979. Solubility controls of carbonate-fluorapatite in seawater (Abs.). In: W.C. Burnett and R.P. Sheldon (Eds.), Report on the marine phosphatic sediments workshop. East-West Center, Honolulu, 19 - 20.

AUBRY, M.P., 1974. Étude de la craie au microscope electronique à balayage. Les

Nannofacies. Travaux Lab. Micropaléont. Univ. Paris, 3: 225 - 295.

BACHRA, B.M. and TRAUTZ, O.R., 1962. Carbonic anhydrase and the precipitation of apatite. Science, 137: 337 - 338.

BACHRA, B.N., TRAUTZ, O.R. and SIMON, S.L., 1965. Precipitation of calcium carbonates and phosphates - III; The effect of magnesium and fluorine ions on the spontaneous precipitation of calcium carbonate and phosphates. Archives Oral Biol., 10: 731 - 738.

BALLARD, R.D. and UCHUPI, E., 1971. Geological observations of the Miami Terrace from the submersible Ben Franklin. Mar. Technol. Soc. J., 5: 43 - 48.

BAILEY, H.W., 1975. A preliminary microfaunal investigation of the lower Senonian at Beer, south-east Devon. Proc. Ussher Soc., 3: 280 - 285.

BAILEY, R.J. and ATHERTON, M.P., 1969. The petrology of a glauconitic sandy chalk. J. Sed. Pet., 39: 1420 - 1431.

BANDY, O.L. and RODOLFO, K.S., 1964. Distribution of Foraminifera and sediments, Peru-Chile Trench area. Deep Sea Res., 11: 817 - 837.

BANERJEE, D.M., 1971. Pre-Cambrian stromatolitic phosphorites of Udaipur, Rajasthan, India. Bull. Geol. Soc. Am., 82: 2319 - 2330.

BARBER, C., 1974. Major and trace element associations in limestones and dolomites. Chem. Geol., 14: 273 - 280.

BARNARD, T. and BANNER, T.F., 1953. Arenaceous foraminifera from the Upper Cretaceous of England. Quart. J. Geol. Soc. London, 109: 207.

BARR, F.T., 1962. Upper Cretaceous planktonic foraminifera from the Isle of Wight, England. Palaeontology, 4: 552 - 580.

BARROIS, C., 1875a. Description géologique de la Craie de l'Ile de Wight. Ann. Sci. Géol., 6: 30 - 60.

BARROIS, C., 1875b. Ondulations de la Craie dans le sud de L'Angleterre. Ann. Soc. Géol. Nord, 2: 85 - 111.

BARROIS, C., 1876. Recherches sur le terrain Crétacé Supérieur de l'Angleterre et de l'Irelande. Mém. Soc. Géol. Nord, Lille, 232p.

BARROIS, C., 1878a. Mémoire sur le terrain Crétacé des Ardennes et des régions voisines. Ann. Soc. Géol. Nord, 5: 227 - 487.

BARROIS, C., 1878b. Exposé de ses recherches sur le terrain Crétacé des Ardennes

et des régions voisines. Bull. Soc. Géol. Fr., (3), 7: 19 - 27.

BARROIS, C., 1878c. Le terrain Crétacé des Ardennes. Ann. Soc. Géol. Nord, 5: 480.

BATE, R.H., 1972. Phosphatized ostracods with appendages from the Lower Cretaceous of Brazil. Palaeontology, 15: 279A - 393.

BATHURST, R.G.C., 1966. Boring algae, micrite envelopes and lithification of molluscan biosparites. Geol. J., 5: 15 - 32.

BATHURST, R.G.C., 1975. Carbonate sediments and their diagenesis (2nd Edition). Developments in Sedimentology 12, Elsevier, Amsterdam, Oxford, New York, 658p.

BATURIN, G.N., 1969. Authigenic phosphate concretions in Recent sediments of the Southwest African Shelf. Dokl. Akad. Nauk.SSSR, Earth Sci. (Am. Geol. Inst. Translation), 189: 227 - 230.

BATURIN, G.N., 1971a. Formation of phosphate sediments and water dynamics. Oceanology (Am. Geophys. Union Translation), 11: 372 - 376.

BATURIN, G.N., 1971b. Stages of phosphorite formation on the ocean floor. Nature Physical Science, 232: 61 - 62.

BATURIN, G.N., 1974. New data on the Upper Quaternary phosphorite nodules on the SW African Shelf. Oceanology (Am. Geophys. Union Translation), 14: 856 - 860.

BATURIN, G.N., KOCHENOV, A.V. and PETELIN, V.P., 1970. Phosphorite formation on the shelf of southwest Africa. Lithol. Min. Res. (Consultants Bureau Translation), 5: 266 - 276.

BATURIN, G.N., MERKULOVA, K.I. and CHALOV, P.I., 1972. Radiometric evidence for Recent formation of phosphatic nodules in marine shelf sediments. Mar. Geol., 13: M37 - M41.

BATURIN, G.N. and PETELIN, V.P., 1972. Phosphorite concretions on the Chilean Shelf. Lithol. Min. Res. (Consultants Bureau Translation), 7: 261 - 267.

BATURIN, G.N. and DUBINCHUK, V.T., 1974. Microstructures of Agulhas Bank phosphorites. Mar. Geol., 16: M63 - M70.

BATURIN, G.N. and BEZRUKOV, P.L., 1979. Phosphorites on the sea floor and their origin. Mar. Geol., 31: 317 - 332.

BAYER, P.S., GUINESS, E.A., LYNCH-BLOSSE, M.A. and STOLZMAN, R.A., 1977. Greensand fecal pellets from New Jersey. J. Sed. Pet., 47: 267 - 280.

BAYLE, E., 1879. Explication de la carte géologique de la France: Atlas I rapartie: Fossiles principaux des terrains.

BERNER, R.A., 1969a. Migration of iron and sulfur within anaerobic sediments during early diagenesis. Am. J. Sci., 267: 19 - 42.

BERNER, R.A., 1969b. Chemical changes affecting dissolved calcium during the bacterial decomposition of fish and clams in sea water. Mar. Geol., 7: 253 - 274.

BERNER, R.A., 1970. Sedimentary pyrite formation. Am. J. Sci., 268: 1 - 23.

BERNER, R.A., 1973. Phosphate removal from sea water by absorption on volcanogenic ferric oxides. Earth Planet. Sci. Lett., 18: 77 - 86.

BERNER, R.A., 1974. Kinetic models for the early diagenesis of nitrogen, sulfur, phosphorus and silicon in anoxic marine sediments. In: E. Goldberg (Ed.), The Sea 5, Wiley and Sons, New York, 427 - 450.

BEZRUKOV, P.L., LISITSYN, A.P., PETELIN, V.P. and SKORNYAKOVA, N.S., 1961. Map of ocean bottom sediments (in Russian). In: N.M. Strakov (Ed.) Recent sediments of Seas and Oceans, Moscow.

BEZRUKOV, P.L., ANDRUSHCHENKO, P.F., MURDMAA, I.O. and SKORNYAKOVA, N.S., 1969. Phosphorite on the ocean floor in the central Pacific. Dokl. Akad. Nauk. SSR, Earth Sci. (Am. Geol. Inst. Translation), 185: 192 - 195.

BIDAULT, H., 1953. Note préliminaires sûr un mode de formation possible des phosphates dinantiens des Pyrenées. Int. Géol. Cong. 19th, Algiers, Compt. Rendu, Sect. 11, Fasc. 11, 185 - 190.

BIGNOT, G. and DEFRETIN, S., 1967. Remarques sur les spongaires siliceux de la craie de la région de Dieppe (Seine-Maritime). Bull. Soc. Géol. Normandie, 57: 9 - 14.

BIGNOT, G. and EBRAHIMZADEH-ASSADIAN, K., 1969. La Craie à Marsupites testudinarius du Cap d'Ailly (près de Dieppe, Seine-Maritime). Bull. Soc. Géol. Normandie, 59: 4 - 15.

BIGNOT, G. and AUBRY, M.P., 1973. Géologie de la Craie dans le Bassin parisien. Bull. Liaison Lab. P. et Ch. Spécial 5: 11 - 22.

BIRCH, G.F., 1975. Sediments on the continental margin off the west coast of South Africa. Joint GSO/UCT Mar. Geosci. Bull. 6, Dept. Geol. Univ. Cape Town, 142p.

BIRCH, G.F., 1979a. Phosphatic rocks on the western margin of South Africa. J. Sed. Pet., 49: 93 - 110.

BIRCH, G.F., 1979b. The nature and origin of mixed apatite/glauconite pellets from the continental shelf off South Africa. Mar. Geol., 29: 313 - 334

BIRCH, G.F., 1979c. Phosphorite pellets and rock from the western continental margin and adjacent coastal terrace of South Africa. Mar. Geol., 33: 91 - 116.

BLACK, M., 1933. The algal sediments of Andros Island, Bahamas. Phil. Trans. Roy. Soc. London, Ser. B., 222: 165 - 192.

BLACK, M., 1953. The constitution of the chalk. Proc. Geol. Soc. London, 1499: 81 - 86.

BLACK, M., 1965. Coccoliths. Endeavour, 24: 131 - 137.

BLACKITH, R.E. and REYMENT, R.A., 1971. Multivariate morphometrics. Academic Press, London, New York, 412p.

BLONDEAU, A., POMEROL, B., POMEROL, C., BÉGON, J.C., GUÉRIN, B. and HARDY, R., 1974. Carte géologique de la France à 1/50,000, 102: Beauvais, et notice explicative. Publ. Bur. Rech. Géol. Min., Orleans.

BLONDEAU, A., FROELICH, F., POMEROL, B. and POMEROL, C., 1978. Carte géologique de la France à 1/50,000, 80: St Just-en-Chaussée, et notice explicative. Publ. Bur. Rech. Géol. Min., Orleans.

BLOOM, W. and FAWCETT, D.W., 1968. A textbook of histology (9th Edition). Saunder, Philidelphia, 858p.

BOLTENHAGEN, C., MENILLET, F. and TERNET, Y., 1968. Carte géologique de la France à 1/50,000, 74: Montivillers-Etretat, et notice explicative. Publ. Bur. Rech. Géol. Min., Orleans.

BONTE, A., BROQUET, P., BELLERY, B., DEZWARTE, J.M. and FENET, B., 1964. La craie phosphatée dans le Nord et le Pas-de-Calais. Ann. Soc. Géol. Nord, 84: 41 - 42.

BOUILLER, R., FLEURY, R., NEAU, G., WEECKSTEEN, M., SCOLARI, G. and VINCENT, P.L., 1971. Carte géologique de la France à 1/50,000, 331: Sens, et notice explicative. Publ. Bur. Rech. Géol. Min., Orleans.

BOWEN, H.J.M., 1966. Trace elements in biochemistry. Academic Press, London, 241p.

BOWEN, R., 1966. Palaeotemperature Analysis. Elsevier, Amsterdam, London, New York, 265p.

BRADLEY, W.H., 1931. Origin and microfossils of the oil shale of the Green River Formation of Colorado and Utah. US Geol. Surv. Prof. Pap., 168: 58p.

BRAITHWAITE, C.J.R., 1968. Diagenesis of phosphatic carbonate rocks on Remire Amrantes, Indian Ocean. J. Sed. Pet., 38: 1198 - 1212.

BRAY, J.T., BRICKER, O.P. and TROUP, B.N., 1973. Phosphate in interstitial waters of anoxic sediments: oxidation effects during sampling procedure. Science, 180: 1362 - 1364.

BRIQUET, A., 1902a. Note sur le gisement de craie phosphatée exploité à Orville. Ann. Soc. Géol. Nord, 31: 79 - 82.

BRIQUET, A., 1902b. Note sur les gisements de craie phosphatée exploités à Beauval. Ann. Soc. Géol. Nord, 31: 83 - 86.

BRISTOW, H.W., REID, C. and STRAHAN, A., 1889. The geology of the Isle of Wight. Mem. Geol. Surv. England Wales, HMSO, London, 349p.

BROECKER, W.S., 1963. Radioisotopes and large-scale oceanic mixing. In: M.N. Hill (Ed.), The Sea 2, The Composition of Sea-Water: Comparative and descriptive Oceanography, Wiley-Interscience, New York, London, 88 - 108.

BROECKER, W.S., 1971. A kinetic model for the chemical composition of seawater. Quat. Res., 1: 188 - 207.

BROECKER, W.S., 1974. Chemical Oceanography. Harcourt Brace Jovanovich, New York, Chicago, San Francisco, Atlanta, 214p.

BROECKER, W.S. and YUAN-HUI, L., 1970. Interchange of water between the major oceans. J. Geophys. Res., 75: 3545 - 3552.

BROMLEY, R.G., 1965. Studies in the lithology and conditions of sedimentation of the Chalk Rock and comparable horizons. Unpub. PhD Thesis, Univ. London, 355p.

BROMLEY, R.G., 1967a. Marine phosphorites as depth indicators. Mar. Geol., 5: 503 - 509.

BROMLEY, R.G., 1967b. Some observations on burrows of thalassidean crustacea in Chalk hardgrounds. Quart. J. Geol. Soc. London, 123: 157 - 182.

BROMLEY, R.G., 1968. Burrows and boring in hardgrounds. Geol. Soc. Denmark Bull., 18: 247 - 250.

BROMLEY, R.G., 1970. Borings as trace fossils and Entobia cretacea Portlock, as

an example. In: T.P. Crimes and J.C. Harper (Eds.), Trace Fossils, Geol. J. Spec. Issue, 3: 49 - 90.

BROMLEY, R.G., 1975a. Trace fossils at omission surfaces. In: R.W. Frey (Ed.), The Study of Trace Fossils, Springer-Verlag, New York, 399 - 428.

BROMLEY, R.G., 1975b. Comparative analysis of fossil and recent echinoid bioerosion. Palaeontology, 18: 725 - 739.

BROMLEY, R.G., 1978. Hardground diagenesis. In: R.W. Fairbridge and J. Bourgeois (Eds.), Encyclopedia of Earth Sciences VI: The Encyclopedia of Sedimentology, Dowden Hutchinson and Ross, Stroudsburg Penn., 397 - 400.

BROMLEY, R.G., 1979. Chalk and bryozoan limestone: facies, sediments and depositional environments. In: T. Birkelund and R.G. Bromley (Eds.) Cretaceous-Tertiary Boundary Events, Univ. Copenhagen, 16 - 35.

BROMLEY, R.G., SCHULZ, M.G. and PEAKE, N.B., 1975. Paramoudras: giant flints, long burrows and the early diagenesis of chalks. Kgl. Danske. Vidensk. Selsk. Biol. Skr., 20: 31 p.

BRONGERSMA-SANDERS, M., 1957. Mass mortalities in the sea. In: J.W. Hedgpleth (Ed.), Treatise on Marine Ecology 1: Ecology, Geol. Soc. Am. Mem., 67: 941 - 1010.

BROQUET, P., 1973. La craie phosphatée en Picardie, perspectives d'avenir de la prospection. Ann. Sci. Univ. Besançon, 20: 143 - 152.

BROWN, G., CATT, J.A., HOLLYER, S.E. and OLLIER, C.D., 1969. Partial silicification of Chalk fossils from the Chilterns. Geol. Mag., 106: 583 - 586.

BRYDONE, R.M., 1912. The Stratigraphy of the Chalk of Hants. Dulau, London, 116p.

BRYDONE, R.M., 1913. The proposed recognition of two stages of the Upper Chalk. Geol. Mag., 50: 56 - 62; 380 - 381.

BRYDONE, R.M., 1914. The Zone of Offaster pilula in the south English Chalk. Geol. Mag., 51: 359 - 369; 405 - 411; 449 - 459; 509 - 513.

BRYDONE, R.M., 1915. The Marsupites Chalk of Brighton. Geol. Mag., 2: 12 - 15.

BRYDONE, R.M., 1917. The base of the Chalk Zone of Holaster planus in the Isle of Wight. Geol. Mag., 4: 245 - 249.

BRYDONE, R.M., 1918. The thickness of the Zone of Belemnitella mucronata on the Isle of Wight. Geol. Mag., 5: 350 - 354.

BRYDONE, R.M., 1932a. The lower beds of the Chalk near Ipswich. J. Ipswich Dist.

Nat. Hist. Soc., 1: 153 - 157.

BRYDONE, R.M., 1932b. Uintacrinus in North Suffolk. J. Ipswich Dist. Nat. Hist. Soc., 1: 158 - 161.

BRYDONE, R.M., 1939. The Chalk Zone of Offaster pilula. Dulau, London.

BUCKENHAM, M.H., ROGERS, J. and ROUSE, J.E., 1971. Assessment of Chatham Rise phosphorites. Proc. Aust. Inst. Min. Metal. Ann. Conf., 8: 1 - 13.

BUKRY, D., 1974. Coccoliths as paleosalinity indicators - evidence from the Black Sea. In: The Black Sea - Geology, Chemistry and Biology, Am. Assoc. Petrol. Geol. Mem., 20: 353 - 363.

BURNABY, T.P., 1962. The palaeoecology of the Foraminifera of the Chalk Marl. Palaeontology, 4: 599 - 608.

BURNETT, W.C., 1977. Geochemistry and origin of phosphorite deposits from off Peru and Chile. Geol. Soc. Am. Bull., 88: 813 - 823.

BURNETT, W.C., VEEH, H.H. and SOUTAR, A., 1973. Geochemistry and radiometric ages of sea-floor phosphorites from the continental margin of Peru and Chile. Geol. Soc. Am. Abs. Progs., 5: 18 - 19.

BURNETT, W.C. and GOMBERG, D.N., 1977. Uranium oxidation and probable subaerial weathering of phosphatized limestone from the Poutalès Terrace. Sedimentology, 24: 291 - 302.

BURNETT, W.C. and VEEH, H.H., 1977. Uranium-series disequilibrium studies on phosphorite nodules from the west coast of South America. Geochim. Cosmochim. Acta, 41: 755 - 764.

BURNETT, W.C. and SHELDON, R.P., 1979. Report on the Marine phosphatic Sediments Workshop. (Eds.), East-West Center, Honolulu, 65p.

BURNETT, W.C.,and SOUTAR, A., 1979. Environment of deposition of phosphorite off Peru. In: W.C. Burnett and R.P. Sheldon (Eds.) Report on the Marine phosphatic Sediments Workshop, East-West Center, Honolulu, 10.

BURST, J.F., 1958a. Glauconite pellets. Their mineral nature and application to stratigraphic interpretations. Bull. Am. Assoc. Petrol. Geol., 42: 310 - 327.

BURST, J.F., 1958b. Mineral heterogeneity in glauconite pellets. Am. Min., 43: 481 - 497.

BUSH, J., 1951. Rock from the Straits of Florida. Bull. Am. Assoc. Petrol. Geol.,

35: 102 - 107.

BUSHINSKI, G.I., 1964. On the shallow-water origin of phosphorite sediments. In: M.L.J.U. van Straaten (Ed.), Deltaic and Shallow Marine Deposits, Elsevier, Amsterdam, 62 - 70.

BUSHINSKI, G.I., 1966. The origin of marine phosphorites. Lithol. Min. Res. (Consultants Bureau Translation), 3: 292 - 311.

BUSHINSKI, G.I., 1969. Phosphoria Formation. Akad. Nauk. SSSR Trans. 210: 103p. (In Russian).

BUTEUX, C.J., 1849. Esquisse géologique du département de la Somme. Mém. Acad. Amiens, Paris, 122p.

BUTEUX, C.J., 1864. Esquisse géologique du département de la Somme (2nd Edition). Abbeville, 136p.

BUTLER, E., CORNER, E.D.S. and MARSHAL, S.M., 1969. On the nutrition and metabolism of zooplankton VI: Feeding efficiency of Calanus in terms of nitrogen and phosphorus. J. Mar. Biol. Ass. UK, 49: 977 - 1001.

BUURMAN, P. and VAN DER PLAS, L., 1971. The genesis of Belgian and Dutch flints and cherts. Geol. Mijnb., 50: 9 - 27.

CALEMBERT, L., 1956. Le Crétacé supérieur de la Hesbaye et du Brabant. Excursion du 19 Sept. 1955. Ann. Soc. Géol. Belg., 80: B129 - B156.

CALVERT, S.E., 1979. Environment of phosphorite deposition off Namibia. In: W.C. Burnett and R.P. Sheldon (Eds.), Report on the Marine Sediments Workshop, East-West Center, Honolulu, 8 - 9.

CALVERT, S.E. and PRICE, N.B., 1970. Minor element contents of Recent organic-rich sediments off south-west Africa. Nature, 227: 593 - 595.

CALVERT, S.E. and PRICE, N.B., 1971. Recent sediments of the south-west African shelf. In: F.M. Delany (Ed.), Geology of the East Atlantic Continental Margin, ICSU/SCOR Working Party, 31 Symp. Camb. 1971, Inst. Geol. Sci. Rep., 70/16: 171 - 185.

CARTER, R.M., 1968. The functional morphology of Arctostrea Pervinquière 1910. Palaeontology, 11: 458 - 485.

CARTER, R.M., 1972. Adaptions of British Chalk Bivalvia. J. Paleont., 46: 325 - 340.

CASEY, R., 1960. A Lower Cretaceous gasropod with fossilized intestines. Palaeont-

ology, 2: 270 - 276.

CATHCART, J.B., 1968. Florida-type phosphorite deposits of the United States: origi and techniques for prospecting. UN Min. Res. Dev. Ser., 32: 178 - 186.

CAYEUX, L., 1890a. Mémoire sur la 'Craie grise' du nord de la France. Ann. Soc. Géol. Nord, 17: 105 - 141.

CAYEUX, L., 1890b. Coup d'oeil sur la composition du Crétacé des environs de Péronne. Ann. Soc. Géol. Nord, 17: 227 - 245.

CAYEUX, L., 1897. Contribution à l'étude micrographique des terrains sédimentaires II: Craie du bassin de Paris. Mém. Soc. Géol. Nord, 4: 207 - 587.

CAYEUX, L., 1905. Les concrétions phosphatée de l'Agulhas Bank, d'apres le docteur L.W. Collet. Genèse des phosphates de chaux sédimentaires. Bull. Soc. Géol. Fr., (4), 5: 750 - 753.

CAYEUX, L., 1929. Les roches sédimentaires de France. Roches siliceuse. Mém. Carte Geol. Fr., 774p.

CAYEUX, L., 1934. The phosphatic nodules of the Agulhas Bank (A study of submarine geology). Ann. South Afr. Mus., 31: 105 - 136.

CAYEUX, L., 1936. Existence de nombreuses bactéries dans les phosphates sédimentaires de tout ages. Conséquences. Compt. Rend. Acad. Sci. Paris, 203: 1198 - 1200.

CAYEUX, L., 1939. Les phosphates de chaux sédimentaires de France I. France metropolitaine. Étude des gîtes mineraux de la France. Impr. Nationale, Paris, 349p.

CAYEUX, L., 1941. Les phosphates de chaux sédimentaires de France II. Egypte, Tunisie, Algérie. Étude des gîtes mineraux de la France. Impr. Nationale, Paris, 660p.

CAYEUX, L., 1950. Les phosphates de chaux sédimentaires de France III. Étude des gîtes mineraux de la France. Impr. Nationale, Paris, 358p.

CAYEUX, L., 1967. Répartition des Echinides du Coniacien du Bec de Caux. Bull. Soc. Géol. Normandie, 57: 21 - 38.

CELET, P., COULOMBEAU, C., MONCIARDININ, C. and AGACHE, R., 1978. Carte géologique de la France à 1/50,000, 48: Péronne, et notice explicative. Publ. Bur. Rech. Géol. Min., Orleans.

CHAPMAN, F., 1892. Microzoa from the phosphatic chalk of Taplow. Quart. J. Geol.

Soc. London, 48: 514 - 518.

CHARLES, G., 1953. Sur l'origine des gisements de phosphates de chaux sédimentaires. Congr. Géol. Int. Compt. Rend., 19th, Algiers 1952, 11: 163 - 184.

CHENEY, T.M., McCLELLAN, G.H. and MONTGOMERY, E.S., 1979. Sechura phosphate deposits, their stratigraphy, origin and composition. Econ. Geol., 74: 232 - 259.

CHRISTENSEN, W.K., 1970. Actinocamax primus Arkhangelsky from Scania, Sweden. Stockh. Contr. Geol., 21: 69 - 76.

CHRISTENSEN, W.K., 1971. Belemnitella propinqua propinqua (Moberg, 1885) from Scandinavia. Bull. Geol. Soc. Denmark, 20: 369 - 384.

CHRISTENSEN, W.K., 1973. The belemnites and their stratigraphical significance. In: J. Bergström, W.K. Christensen, C. Johansen and E. Norling, An extension of Upper Cretaceous rocks to the Swedish west coast at Sardal. Bull. Geol. Soc. Denmark, 22: 113 - 140.

CHRISTENSEN, W.K., 1974. Morphometric analysis of Actinocamax plenus from England. Bull. Geol. Soc. Denmark, 23: 1 - 26.

CHRISTENSEN, W.K., 1975a. Upper Cretaceous belemnites from the Kristianstad area of Scania. Fossils Strata, 7: 1 - 69.

CHRISTENSEN, W.K., 1975b. Designation of lectotypes for Gonioteuthis westfalica-granulata and G. granulataquadrata. Paläont. Z., 49: 126 - 134.

CHRISTENSEN, W.K., 1976a. First record of Belemnellocamax balsvikensis (Brotzen, 1960) from NW Germany. N. Jb. Geol. Paläont. Mh., H9: 522 - 531.

CHRISTENSEN, W.K., 1976b. Palaeobiogeography of Late Cretaceous belemnites of Europe. Paläont. Z., 50: 113 - 129.

CHRISTENSEN, W.K., ERNST, G., SCHMID, F., SCHULZ, M.G. and WOOD, C.J., 1975. Belemnitella mucronata mucronata (Schlottheim, 1813) from the Upper Campanian: Neotype, biometry, comparisons and biostratigraphy. Geol. Jb., A28: 27 - 57.

COOK, P.J., 1970. Repeated diagenetic calcitization, phosphatization and silicification in the Phosphoria Formation. Geol. Soc. Am. Bull., 81: 2107 - 2116.

COOK, P.J., 1972. Petrology and geochemistry of the phosphate deposits of northwest Queensland, Australia. Econ. Geol., 67: 1193 - 1213.

COOK, P.J., 1974. Phosphate content of sediments from Deep-sea sites 259 - 263,

East Indian Ocean. Init. Rep. DSDP Washington, 27: 455 - 461.

COOK, P.J., 1976. Sedimentary phosphate deposits. In: K.H. Wolf (Ed.), Handbook of Stratabound Ore Deposits, Elsevier, Amsterdam, London, New York, 505 - 535.

COOK, P.J. and MAYO, W., 1980. Geochemistry of a tropical estuary (Broad Sound, Queensland). Bull. Bur. Min. Res. Australia, 182: (in press).

COOPER, L.H.N., 1948. Particulate ammonia in sea-water. J. Mar. Biol. Ass. UK, 27: 322 - 325.

COOPER, L.H.N., 1951. Chemical properties of the sea water in the neighbourhood of the Labradie Bank. J. Mar. Biol. Ass. UK, 30: 21 - 26.

COOPER, M.R., 1977. Eustacy during the Cretaceous: its implications and importance. Palaeogeogr. Palaeoclimatol. Palaeoecol., 22: 1 - 60.

COPENHAGEN, W.J., 1953. The periodic mortality of fish in the Walvis region. S. Afr. Dept. Commerce Industry Fisheries Div. Invest. Rept., 14: 1 - 34.

COQUAND, H., 1856. Notice sur la formation crétacée du départment de la Charente. Bull. Soc. Géol. Fr. (2), 14: 55 - 98.

COQUAND, H., 1857. Position des Ostrea columba et biauriculata dans le groupe de la craie inférieure. Bull. Soc. Géol. Fr. (2), 14: 745 - 766.

COQUAND, H., 1858. Description physique, géologique, paléontologique et minéralogique du départment de la Charente. Tome 1: Dodivers, Besancon; Tome 2: Barlatier -Feyssat et Demanchy, Marseille.

CORNEN, G., GIRESSE, P. and ODIN, G.S., 1973. Découverte de dépôts phosphatés négénes sous-marins sur les plateaux continentaux du Sud du Gabon et du Nord du Congo. Bull. Soc. Géol. Fr. (7), 15: Comp. Rend. Somm., 9 - 10.

CORNER, E.D.S. and DAVIES, A.G., 1971. Plankton as a factor in the nitrogen and phosphorus cycles in the Sea. Adv. Mar. Biol., 9: 101 - 204.

CORNET, F.L., 1886. On the Upper Cretaceous series and the phosphatic beds in the neighbourhood of Mons (Belgium). Quart. J. Geol. Soc. London, 42: 325 - 340.

CORNET, F.L. and BRIART, A., 1878. Sur la craie brune phosphatée de Ciply. Ann. Soc. Géol. Belg., 5: 11 - 22.

CORNET, J., 1905. Sur les facies de la Craie phosphatée de Ciply. Ann. Soc. Géol. Belg., 32: M137 - M146.

CORNET, J., 1922. Les formations Crétaciques et Tertiares des environs de Mons.

Congr. Géol. Int. Livret-Guide, 13th, Brussels 1922, Excursion C1, 24p.

CORNET, J., 1925. Sur les bancs de craie phosphatée intercalés dans la craie à Actinocamax quadratus des environs de Mons. Ann. Soc. Géol. Belg., 48: 237 - 241.

CORRELL, D.L., 1965. Pelagic phosphorus metabolism in Antarctic waters. Limnol. Oceanogr., 10: 364 - 370.

COUSTEAU, J. and DIOLÉ, P., 1973. Octopus and Squid: The soft Intelligence. Cassell, London, 304p.

CRAIG, G.Y., 1967. Size-frequency distributions of living and dead populations of Pelecypods from Bimini, Bahamas, BWI. J. Geol., 75: 34 - 45.

CULLEN, D.J., 1979. Distribution, composition and origin of phosphate nodules from the Chatham Rise. In: W.C. Burnett and R.P. Sheldon (Eds.), Report of the Marine Phosphatic Sediments Workshop, East-West Center, Honolulu, 13 - 14.

CURRY, D. and SMITH, A.J., 1975. New discoveries concerning the geology of the central and eastern parts of the English Channel. Phil. Trans. Roy. Soc. London, A279: 155 - 167.

DALBIEZ, M.F., 1959. Corrélations et résolutions. Coll. Crétacé Supér. Franç., Compt. Rend. Congr. Socs. Sav., Dijon, 857 - 867.

D'ANGLEJAN, B.F., 1967. Origin of marine phosphorites off Baja California, Mexico. Mar. Geol., 5: 15 - 44.

D'ANGLEJAN, B.F., 1968a. Origin of marine phosphorites off Baja California, Mexico. UN Min. Res. Dev. Ser., 32: 151 - 152.

D'ANGLEJAN, B.F., 1968b. Phosphate diagenesis of carbonate sediments as a mode of in situ formation of marine phosphorites: Observations on a core from the eastern Pacific. Can. J. Earth Sci., 5: 81 - 87.

D'ANGLEJAN, B.F., 1979. Phosphorite deposits off Baja California. In: W.C. Burnett and R.P. Sheldon (Eds.), Report of the Marine Phosphatic Sediments Workshop, East-West Center, Honolulu, 9.

D'ARCY, D. and ROUX, J.C., 1971. Carte du toit des Dièves en Picardie. Bull. Bur. Rech. Géol. Min., (2), 2-1971: 43 - 46.

DEBRABANT, P. and PAQUET, J., 1975. L'association glauconites-phosphates-carbonates (Albien de la Sierra de Espuña, Espagne Méridionale). Chem. Geol., 15: 61 - 75.

DEER, W.A., HOWIE, R.A. and ZUSSMAN, J., 1962a. Rock Forming Minerals Vol. 3: Sheet Silicates, Longmans, London, 270p.

DEER, W.A., HOWIE, R.A. and ZUSSMAN, J., 1962b. Rock Forming Minerals Vol. 5: Non-Silicates, Longmans, London, 371p.

DE GROSSOUVRE, A., 1889. Sur le terrain crétacé dans le Sud-Ouest du bassin de Paris. Bull. Soc. Géol. Fr. (3), 17: 475 -

DE GROSSOUVRE, A., 1894a. Sur la craie grise. Bull. Soc. Géol. Fr. (3), Compt. Rend. Séances, 22: 57 - 58.

DE GROSSOUVRE, A., 1894b. Sur la discordance de la craie blanche et de la craie grise. Bull. Soc. Géol. Fr. (3), Compt. Rend. Séances, 22: 67 - 68.

DE GROSSOUVRE, A., 1897. Sur la limite du Crétacé et Tertiare. Bull. Soc. Géol. Fr. (3), 25: 57 - 81.

DE GROSSOUVRE, A., 1899. Quelques observations sur les Belemnitelles et en particulier sur celles des Corbières. Bull. Soc. Géol. Fr. (3), 27: 129 - 135.

DE GROSSOUVRE, A., 1901. Recherches sur la craie supérieure I: Stratigraphie generale. Mém. Surv. Carte Géol. Det. Fr., 1013p.

DE GROSSOUVRE, A., 1907. Sur la craie grise à Belemnitelles. Compt. Rend. Assoc. Fr. Avanc. Sci. Congr. Rheims, 36th, Notes Mém., 403 - 406.

DE LAPPARENT, A.A., 1893. Traité de Géologie (3rd Ed.) Savy, Paris, 1645p.

DELATTRE, C., 1969. Carte géologique de la France à 1/50,000, 25: St Pol, et notice explicative. Publ. Bur. Rech. Géol. Min., Orleans.

DELATTRE, C., MÉRIAUX, E., WATERLOT, M. and MARLIÈRE, R., 1973. Région du Nord: Flandre, Artois, Boulonnais, Picardie. Guides Géol. Région., Masson, Paris.

DELATTRE, C., MÉRIAUX, E. and D'ARCY, D., 1974. Carte géologique de la France à 1/50,000, 34: Doullens, et notice explicative. Publ. Bur. Rech. Géol. Min., Orleans.

DE MERCEY, N., 1863. Note sur la craie dans le Nord de la France. Bull. Soc. Géol. Fr. (2), 20: 631 - 644.

DE MERCEY, N., 1876. Note sur la direction adoptée pour le tracé des coupes de la carte géologique du département de la Somme, et sur certains rapports entre la structure du sol de la Picardie et celles du détroit du Pas-de-Calais. Bull. Soc. Géol. Fr. (3), 4: 559 - 567.

DE MERCEY, N., 1880. Remarques sur les systèmes de la Basse-Somme et de la Basse-Oise et sur leurs rapports avec la structure et le relief du sol dans une partie du Nord de la France, à l'occasion des indications de M. Daubrée. Bull. Soc. Géol. Fr. (3), 8: 422 - 439.

DE MERCEY, N., 1887a. Sur la position géologique de la carie phosphatée en Picardie. Compt. Rend. Acad. Sci. Paris, 105: 1083 - 1086.

DE MERCEY, N., 1887b. Sur les recherches pour l'exploitation de la craie phosphatée en Picardie. Compt. Rend. Acad. Sci. Paris, 105: 1135 - 1138.

DE MERCEY, N., 1887c. La Craie phosphatée à B. quadratus dans le Nord de la France. Bull. Soc. Géol. Fr. (3), 15: 719 - 725.

DE MERCEY, N., 1891. Remarques sur les gîtes de phosphates de chaux de la Picardie. Bull. Soc. Géol. Fr. (3), 19: 854 - 876.

DE MERCEY, N., 1896. On the existence of rich phosphate of lime in the London Basin. Geol. Mag., 3: 342 - 343.

DE MERCEY, N., 1901. Lettre à M. J. Gosselet. Ann. Soc. Géol. Nord, 30: 191 - 192.

DE MERCEY, N., 1907. Carte géologique de la France à 1/80,000, 21: Montdidier, et notice explicative, Publ. Bur. Rech. Géol. Min., Orleans.

DESTOMBES, J.P., WATERLOT, M. and MERIAUX, E., 1971. Carte géologique de la France à 1/50,000, 24: Hesdin, et notice explicative. Publ. Bur. Rech. Géol. Min., Orleans.

DEVRIES, A., MATHIEU, C., MONCIARDINI, C., PAJAUD, D. and SORNAY, J., 1974. Données lithologiques et biostratigraphique dans le Turonien et le Sénonien de la Thiérache et du Marlois (Nord-Est du bassin de Paris). Bull. Bur. Rech. Géol. Min., (2), 1-1974: 189 - 208.

DIETZ, R.S., 1955. Manganese deposits on the north east Pacific sea floor. J. Calif. Mines Geol., 51: 209 - 220.

DIETZ, R.S., EMERY, K.O. and SHEPARD, F.P., 1942. Phosphorite deposits on the sea floor off southern California. Geol. Soc. Am. Bull., 53: 815 - 848.

DOLLE, L. and DOLLE, P., 1939. Carte géologique de la France à 1/80,000, 22: Laon, (3rd Ed.), et notice explicative. Publ. Bur. Rech. Géol. Min., Orleans

DOLLFUS, G.F., 1930. Carte géologique de la France à 1/80,000, 31: Rouen, et notice explicative. Publ. Bur. Rech. Géol. Min., Orleans.

D'ORBIGNY, A., 1842. Paléontologie Française, Terrains Crétacés I. Céphalopodes. Masson, Paris.

DOUXAMI, H., 1908. Excursion aux phosphates de Templeux-la-Fosse et aux terrains Tertiares du bois de Rocogne. Ann. Soc. Géol. Nord, 37: 187 - 193.

DOWKER, G., 1870. On the Chalk of Thanet, Kent and its connection with the Chalk of east Kent. Geol. Mag., 7: 466 - 472.

DOYLE, L.J., BLAKE, N.J., WOO, C.C. and YEVICH, P., 1978. Recent biogenic phosporite: concretions in mollusk kidneys. Science, 199: 1431 - 1433.

DREVER, J.I., 1971. Magnesium-ion replacement in clay minerals in anoxic marine sediments. Science, 172: 1334 - 1336.

EBRAHIMZADEH-ASSADIAN, K., 1968. Étude stratigraphique et micropaléontologique du Sénonien de Reims et d'Epernay. Thèse 3$^{e}$cycle, Fac. Sci., Paris, 128p.

EMERY, K.O., 1960. The Sea off Southern California, a modern habitat of petroleum. Wiley, New York, 366p.

EMERY, K.O. and DIETZ, R.S., 1950. Submarine phosphate deposits off California and Mexico. J. Calif. Mines Geol., 46: 7 - 15

EMERY, K.O. and RITTENBERG, S.C., 1952. Early diagenesis of California Basin sediments in relation to the origin of oil. Bull. Am. Ass. Petrol. Geol., 36: 725 - 806.

EMIGH, G.D., 1958. Petrography, mineralogy and origin of phosphate pellets from the Phosphoria Formation. Idaho Bur. Min. Geol. Pamph., 114, 60p.

EMIGH, G.D., 1967. Petrology and origin of phosphorites. In: L.A. Hales (Ed.), Anatomy of the Western Phosphate Field, Intermount. Ass. Geol. 15th Ann. Field Conf., 103 - 114.

ENOS, P. and FREEMAN, T., 1979. Lower Cretaceous peritidal limestones at 2,700 m depth, Blake nose, Atlantic Ocean. Geology, 7: 83 - 87.

ERNST, G., 1963a. Stratigraphische und gesteinchemische Untersuchungen im Santon und Campan von Lägerdorf (SW-Holstein). Mitt. Geol. StInst. Hamburg, 32: 71 - 127.

ERNST, G., 1963b. Zur Feinstratigraphie und Biostratonomie des Obersanton und Campan von Misburg und Höver bei Hannover. Mitt. Geol. StInst. Hamburg, 32: 128 - 147.

ERNST, G., 1964. Ontogenie, Phylogenie und Stratigraphie der Belemnitengattung Gonioteuthis Bayle aus dem nordwestdeutschen Santon/Campan. Fortschr. Geol. Rheinld. Westlf., 7: 113 - 174.

ERNST, G., 1966. Fauna, Ökologie und Stratigraphie der Mittelsantonen Schreibkreide von Lägerdorf (SW-Holstein). Mitt. Geol. StInst. Hamburg, 35: 115 - 145.

ERNST, G., 1968. Die Oberkreide-Aufschlüsse im Raume Braunschweig-Hannover und ihre stratigraphische Gleiderung mit Echinodermen und Belemniten. I. Teil. Die jüngere Oberkreide (Santon-Maastricht). Beih. Ber. Naturh. Ges., 5: 235 - 284.

ERNST, G. and SCHULTZ, M.G., 1974. Stratigraphie und Fauna dus Coniac und Santon im Schreibkreide-Richtprofil von Lägerdorf (Holstein). Mitt. Geol-Palaont. Inst. Univ. Hamburg, 43: 5 - 60.

ERNST, H., 1978. Zu Bathymetrie und Sedimentstrukturen der Schreibkreide von Lägerdorf/Holstein (Coniac-Santon): eine quantitative analyse der Foraminiferen-Fauna. Mitt. Geol-Palaont. Inst. Univ. Hamburg, 48: 53 - 78.

ERNST, W.G. and CALVERT, S.E., 1969. An experimental study of the recrystallization of porcellanite and its bearing on the origin of some bedded cherts. Am. J. Sci. 267A: 114 - 133.

FISCHER, A.G. and ARTHUR, M.A., 1977. Secular variation in the Pelagic Realm. In: H.E. Cook and P. Enos (Eds.), Deep-water Carbonate Environments, Spec. Pub. Soc. Econ. Geol. Paleont., 25: 19 - 50.

FOLK, R.L. and ROBLES, R., 1964. Carbonate sands of Isla Perez, Alacran Reef Complex, Yacatan. J. Geol., 72: 255 - 292.

FRANKENBERG, D. and MENZIES, R.J., 1968. Some quantitative analyses of deep-sea benthos off Peru. Deep Sea Res., 15: 623 - 626.

FROELICH, P.N., BENDER, M.L. and HEATH, G.R., 1977. Phosphorus accumulation rates in metalliferous sediments on the East Pacific Rise. Earth Planet. Sci. Lett., 34: 351 - 359.

FREAS, D.H. and ECKSTROM, C.L., 1968. Areas of potential upwelling and phosphate deposition during Tertiary, Mesozoic and Late Paleozoic time. UN Min. Res. Dev. Ser., 32: 228 - 238.

FULLER, A.O., 1979. Phosphate occurrences on the western and southern coastal areas and continental shelves of southern Africa. Econ. Geol., 74: 221 - 231.

GALE, A.S., 1980. Penecontemporaneous folding, sedimentation and erosion in Campanian Chalk near Portsmouth, England. Sedimentology, 27: 137 - 151.

GARRELS, R.M., MACKENZIE, F.T. and HUNT, C., 1975. Chemical Cycles and the Global Environment. Kaufmann, Los Altos, California, 206p.

GARRISON, R.E. and KENNEDY, W.J., 1977. Origin of solution seams and flaser structures in Upper Cretaceous chalks of southern England. Sed. Geol., 19: 107 - 137.

GASTER, C.T.A., 1924. The Chalk of the Worthing District of Sussex. Proc. Geol. Ass., 35: 89 - 110.

GASTER, C.T.A., 1925. Excursion to the Worthing district, Sussex. Proc. Geol. Ass., 36: 99 - 102.

GASTER, C.T.A., 1929. Chalk zones in the neighbourhood of Shoreham, Brighton and Newhaven, Sussex. Proc. Geol. Ass., 40: 328 - 340.

GASTER, C.T.A., 1932. The zones of the Chalk of the Arun Gap, Sussex. Proc. Geol. Ass., 43: 212 - 222.

GASTER, C.T.A., 1937. The stratigraphy of the Chalk of Sussex. Part 1. West Central Area - Arun Gap to Valley of the Adur, with zonal map. Proc. Geol. Ass., 48: 356 - 373.

GASTER, C.T.A., 1939. The stratigraphy of the Chalk of Sussex. Part II. Eastern Area - Seaford to Cuckmere Valley and Eastbourne, with zonal map. Proc. Geol. Ass., 50: 510 - 526.

GASTER, C.T.A., 1941. The Chalk Zones of Offaster pilula and Actinocamax quadratus. Proc. Geol. Ass., 52: 210 - 215.

GASTER, C.T.A., 1944. The stratigraphy of the Chalk of Sussex. Part III. Western Area - Arun Gap to the Hampshire boundary, with zonal map. Proc. Geol. Ass., 55: 173 - 188.

GASTER, C.T.A., 1951. The stratigraphy of the Chalk of Sussex. Part IV. East Central Area - between the Valley of the Adur and Seaford, with zonal map. Proc. Geol. Ass., 62: 31 - 64.

GEVORK'YAN, V.K. and CHUGUNNYY, Y.G., 1969. A new find of accumualtions of phosphate concretions in the Indian Ocean. Dokl. Akad. Nauk. SSSR, Earth Sci. (Am. Geol. Inst. Translation), 187: 230 - 232.

GEVORK'YAN, V.K. and CHUGUNNYY, Y.G., 1970. Phosphate nodules in the bottom sediments of the Gulf of Aden. Oceanology, (Am. Geophys. Union Translation), 10: 233 - 241.

GIBSON, T.G. and TOWE, K.M., 1971. Eocene volcanism and the origin of horizon A. Science, 172: 152 - 153.

GLIMCHER, M.J. and KRANE, S.M., 1968. The organisation and structure of bone and the mechanism of calcification. In: B.S. Gould (Ed.), Treatise on Collogen 2: Biology of Collogen. Academic Press, London, 69 - 251.

GOGUEL, J., 1964. Carte géologique de la France à 1/80,000, 22: Laon (4th Ed.), et notice explicative. Publ. Bur. Rech. Géol. Min., Orleans.

GOLDBERG, E.D. and PARKER, R.H., 1960. Phosphatized wood from the Pacific sea floor. Geol. Soc. Am. Bull., 71: 631 - 632.

GOLDBERG, E.D., McCAVE, I.N., O'BRIEN, P. and STEELE, J.H., 1977 (Eds.). The Sea 6. Marine Modelling. Wiley, New York, London, Sydney, Toronto, 1048p.

GOLDHABER, M.B. and KAPLAN, I.R., 1974. The sulfur cycle. In: E.D. Goldberg (Ed.), The Sea 5. Marine Chemistry. Wiley, New York, 569 - 655.

GOMBERG, D.N., 1976. Geology of the Pourtalès Terrace, Straits of Florida. Unpub. PhD Thesis, Univ. Miami, Coral Gables Florida, 371p.

GORDON, W.A., 1973. Marine life and ocean surface currents in the Cretaceous. J. Geol., 81: 269 - 284.

GORSLINE, D.S., 1963. Bottom sediments of the Atlantic Shelf and slope of the United States. J. Geol., 71: 422 - 440.

GORSLINE, D.S. and MILLIGAN, D.B., 1963. Phosphatic deposits along the margin of the Pourtalès Terrace, Florida. Deep Sea Res., 10: 259 - 262.

GOSSELET, J., 1889. Leçons sur les gîtes de phosphates de chaux du Nord de la France. Ann. Soc. Géol. Nord, 16: 27 - 47.

GOSSELET, J., 1891. Carte géologique de la France à 1/80,000, 13: Cambrai, et notice explicative. Publ. Bur. Rech. Géol. Min., Orleans.

GOSSELET, J., 1893a. Note sur les gîtes du phosphate de chaux de Templeux-Bellicourt et de Buire. Ann. Soc. Géol. Nord, 21: 2 - 10.

GOSSELET, J., 1893b. Compte-rendu de l'excursion géologique à Frévent et à Buire. Ann. Soc. Géol. Nord, 21: 116 - 118.

GOSSELET, J., 1893c. Note sur les gîtes de phosphate de chaux des environs de Fresnoy-le-Grand. Ann. Soc. Géol. Nord, 21: 149 - 159.

GOSSELET, J., 1896a. Note sur les gîtes de phosphate de chaux d'Hem-Monacu, d' Etaves, du Ponthieu, etc. Ann. Soc. Géol. Nord, 24: 109 - 134.

GOSSELET, J., 1896b. Sur les gisements de phosphate de chaux d'Hem-Monacu. Bull. Soc. Géol. Fr. (3), 24: 878.

GOSSELET, J., 1897. Limites supérieures et latérales des couches de craie phosphatée d'Etaves et de Fresnoy. Ann. Soc. Géol. Nord, 26: 119 - 129.

GOSSELET, J., 1898. Note sur le gîte de phosphate de chaux d'Haravesnes. Ann. Soc. Géol. Nord, 27: 16 - 21.

GOSSELET, J., 1900a. Note sur les gîtes de craie phosphatée des environs de Roisel suivie des considerations générales sur les dépots de craie phosphatée de Picardie. Ann. Soc. Géol. Nord, 29: 65 - 86.

GOSSELET, J., 1900b. Phosphates de chaux de Picardie. Congr. Géol. Int. Livret-Guide, 8th, Paris 1900, 11 - 20.

GOSSELET, J., 1901a. Plis dans la craie du Nord du bassin de Paris révélés par l'exploitation des phosphates. Ann. Soc. Géol. Nord, 30: 7 - 13.

GOSSELET, J., 1901b. Observations géologique faites dans les exploitations de phosphates de chaux en 1901. Ann. Soc. Géol. Nord, 30: 208 - 243.

GOSSELET, J., 1901c. Carte géologique de la France à 1/80,000, 22: Laon, et notice explicative. Publ. Bur. Rech. Géol. Min., Orleans.

GOSSELET, J., 1902a. Observations concernant le gisement de la craie phosphatée. Lettre à M. Lasne. Ann. Soc. Géol. Nord, 31: 59 - 61.

GOSSELET, J., 1902b. Observations sur la sédimentation de la Craie. Réflexions sur la craie conglomeroide et sur les bancs durcis et verdis. Ann. Soc. Géol. Nord, 31: 63 - 79.

GOSSELET, J., 1909a. Aperçu géologique du departement du Nord. Ann. Soc. Géol. Nord, 38: 192 - 248.

GOSSELET, J., 1909b. Carte géologique de la France à 1/80,000, 7: Arras (2nd Ed.), et notice explicative. Publ. Bur. Rech. Géol. Min., Orleans.

GOSSELET, J., CAYEUX, L. and DE MERCEY, N., 1894. Carte géologique de la France à 1/80,000, 12: Amiens (2nd Ed.), et notice explicative. Publ. Bur. Rech. Géol.

Min., Orleans.

GRAVES, L., 1847. Topographie géognostique de l'Oise. Masson, Paris.

GRIFFITH, C. and BRYDONE, R.M., 1911. The Zones of the Chalk of Hants. Dulau, London, 35p.

GUÉRIN, B., MAUCORPS, J., SOLAU, J. and POMEROL, C., 1977. Carte géologique de la France à 1/50,000, 85: Chateau-Porcien, et notice explicative. Publ. Bur. Rech. Géol. Min., Orleans.

GULBRANDSEN, R.A., 1966. Chemical composition of phosphorites from the Phosphoria Formation. Geochim. Cosmochim. Acta, 30: 769 - 778.

GULBRANDSEN, R.A., 1969. Physical and chemical factors in the formation of marine apatite. Econ. Geol., 64: 365 - 382.

GULBRANDSEN, R.A., 1970. Relation of carbon dioxide content of apatite of the Phosphoria Formation to regional facies. US Geol. Surv. Prof. Pap., 700B: B9 - B13.

GULBRANDSEN, R.A. and ROBERSON, C.E., 1973. Inorganic phosphorus in seawater. In: E.J. Griffith et al. (Eds.), Environmental Phosphorus Handbook, Wiley, New York, 117 - 140.

HÅKANSSON, E., BROMLEY, R.G. and PERCH NIELSEN, K., 1974. Maastrichtian chalk of north-west Europe - a pelagic shelf sediment. In: K.J. Hsü and H.C. Jenkyns (Eds.), Pelagic Sediments: On Land and under the Sea, Spec. Publ. Int. Ass. Sedimentol., 1: 211 - 233.

HALD, A., 1957. Statistical theory with engineering applications. Wiley, New York, London, 783p.

HALLAM, A., 1963. Major epeirogenic and eustatic changes since the Cretaceous, and their possible relationship to crustal structure. Am. J. Sci., 261: 397 - 423.

HAMILTON, E.L., 1956. Sunken islands of the Mid-Pacific Mountains. Geol. Soc. Am. Mem., 64: 97p.

HAMILTON, E.L. and REX, R.W., 1959. Lower Eocene phosphatized globigerina ooze from Sylvania Guyot. US Geol. Surv. Prof. Pap., 260W: 785 - 795.

HANCOCK, J.M., 1961. The Cretaceous System of Northern Ireland. Quart. J. Geol. Soc. London, 117: 11 - 36.

HANCOCK, J.M., 1963. The hardness of the Irish Chalk. Irish Nat. J., 14: 157 - 164.

HANCOCK, J.M., 1969. Transgression of the Cretaceous sea in south-west England. Proc. Ussher Soc., 2: 61 - 83.

HANCOCK, J.M., 1972. Crétacé de l'Angleterre, Pays de Galles, Ecosse. (Ed.) Lexique Strat. Int. (3aXI), 1, 162p.

HANCOCK, J.M., 1975a. Petrology of the Chalk. Proc. Geol. Ass., 86: 499 - 535.

HANCOCK, J.M., 1975b. The sequence of facies in the Upper Cretaceous of northern Europe compared with that in the Western Interior. Geol. Ass. Canada Spec. Pap. 13: 83 - 118.

HANCOCK, J.M., 1978. Chalk. In: R.W. Fairbridge and J. Bourgeois (Eds.), Encyclopedia of Earth Sciences VI. The Encyclopedia of Sedimentology, Dowden, Hutchinson and Ross, Stroudsburg, Penn., 115 - 118.

HANCOCK, J.M. and KENNEDY, W.J., 1967. Photographs of hard and soft chalks taken with a scanning electron microscope. Geol. Soc. London Proc., 1643: 249 - 252.

HANCOCK, J.M. and SCHOLLE, P.A., Chalk of the North Sea. In: A.W. Woodland (Ed.), Petroleum and the continental shelf of north-west Europe I., Applied Science, Barking, Essex, 413 - 425.

HANCOCK, J.M. and KAUFFMAN, E.G., 1979. The great transgressions of the Late Cretaceous. J. Geol. Soc. London, 136: 175 - 186.

HART, M.B., 1970. The distribution of Foraminifera in the Albian and Cenomanian of south-west England. Unpub. PhD Thesis Univ. London.

HART, M.B., 1976. The mid-Cretaceous successions of Orphan Knoll (North-west Atlantic): micropalaeontology and palaeoceanographic implications. Can. J. Earth Sci., 13: 1411 - 1421.

HARTMAN, W.D. and GOREAU, T.F., 1970. Jamaican coralline sponges: their morphology, ecology and fossil relatives. Symp. Zool. Soc. London, 25: 205 - 243.

HARVEY, H.W., 1926. Nitrate in the Sea. J. Mar. Biol. Ass. UK, 14: 71 - 88.

HARVEY, H.W., 1955. The Chemistry and Fertility of Sea Waters. Cambridge University Press, London, 224p.

HASEN, J.M., 1977. Dinoflagellate stratigraphy and echinoid distribution in Upper Maastrichtian and Danian deposits from Denmark. Bull. Geol. Soc. Denmark, 26:

1 - 26.

HAUG, E., 1908. Traité de Géologie 2: Les Périodes Géologiques. Chap. 38: Periode Crétacé, Colin, Paris, 1153 - 1396.

HATTIN, D.E., 1975. Petrology and origin of fecal pellets in Upper Cretaceous strata of Kansas and Saskatchewan. J. Sed. Petr., 45: 686 - 696.

HAWKINS, H.L., 1924. Excursion to Newbury and Boxford. Proc. Geol. Ass., 35: 395 - 400.

HAWKINS, H.L., 1942. Some episodes in the geological history of the south of England. Quart. J. Geol. Soc. London, 98: XLIX - LXX.

HAWKINS, H.L., 1948. Investigations of the phosphatic chalk of Taplow, Bucks. Min. Supply Monog., 11.107, 6p.

HAYES, J.D. and PITMAN, W.C. III, 1973. Lithospheric plate motions, sea level changes and climatic and ecological consequences. Nature, 246: 18 - 22.

HAYWARD, J.F., 1940. Variations in a Chalk sea urchin (Echinocorys) in East Anglia. Trans. Norfolk Norwich Nat. Soc., 15: 220 - 244.

HEATH, G.R. and MOBERLY, R., 1971. Cherts from the Western Pacific, Leg 7, Deep Sea Drilling Project. Init. Rept. DSDP Washington, 7: 991 - 1007.

HÉBERT, E., 1863a. Note sur la craie blanche et la craie marneuse dans le bassin de Paris, et sur la division de ce dernier étage en quatre assises. Bull. Soc. Géol. Fr. (2), 20: 605 - 631.

HÉBERT, E., 1863b. Observations géologiques sur quelques points du département de l'Yonne. Bull. Soc. Hist. Nat. Yonne,

HÉBERT, E., 1866. De la craie dans le nord du bassin de Paris. Compt. Rend. Acad. Sci. Paris, 62: 1401 - 1405.

HÉBERT, E., 1872a. Ondulations de la craie dans le bassin de Paris. Bull. Soc. Géol. Fr. (2), 29: 446 - 472.

HÉBERT, E., 1872b. Ondulations de la craie dans le bassin de Paris II. Ondulations et failles indiquées par les coupes. Bull. Soc. Géol. Fr. (2), 29: 583 - 594.

HÉBERT, E., 1874. Comparison de la craie des côtes d'Angleterre avec celles de France. Bull. Soc. Géol. Fr. (3), 2: 416 - 428.

HÉBERT, E., 1875a. Ondulations de la craie dans le bassin de Paris III. Bull. Soc. Géol. Fr. (3), 3: 512 - 546.

HÉBERT, E., 1875b. Classification du terrain Crétacé Supérieur. Bull. Soc. Géol. Fr. (3), 3: 595 - 599.

HEEZEN, B.C. and HOLLISTER, C.D., 1971. The Face of the Deep. Oxford University Press, London, 659p.

HÖLDER, H. and HOLLMANN, R., 1969. Bohrgänge mariner Organismen in jurassischen Hart- und Felsböden. Neues Jb. Geol. Paläont. Abh., 133: 79.

HOLLAND, H.D., 1978. The Chemistry of the Atmosphere and Oceans. Wiley-Interscience, New York, Chichester, Brisbane, Toronto, 351p.

HOWARD, P.F. and HOUGH, M.J., 1979. On the geochemistry and origin of the D-Tree, Wonarah and Sherrin Creek phosphorite deposits of the Georgina Basin, Northern Australia. Econ. Geol., 74: 260 - 284.

HOWER, J., 1961. Some factors concerning the nature and origin of glauconite. Am. Min., 46: 313 - 334.

HUDSON, J.D., 1967. Speculation on the depth relations of calcium carbonate in Recent and ancient seas. Mar. Geol., 5: 473 - 480.

HUME, W.F., 1893. Chemical and Micromineralogical Researches on the Upper Cretaceous Zones of the South of England. Whitehead, Morris, London, 103p.

HURE, A., 1910. Découverte de phosphate de chaux dans la craie des environs de Sens. Bull. Soc. Sci. Hist. Nat. Yonne, 14: 59 - 64.

HURE, A., 1912. A propos du gisement de phosphate de chaux à Saint-Martin-du-Tertre près Sens. Bull. Soc. Sci. Hist. Nat. Yonne, 16: 89 - 96.

JARVIS, I., 1980. The initiation of phosphatic chalk sedimentation - the Senonian (Cretaceous) of the Anglo-Paris Basin. In: Y.K. Bentor (Ed.), Marine Phosphorites, Spec. Publ. Soc. Econ. Paleont. Min., 29, (in press).

JARVIS, I. and WOODROOF, P., 1981. The phosphatic chalks and hardgrounds of Boxford and Winterbourne, Berkshire - two tectonically controlled facies in the late Coniacian to early Campanian (Cretaceous) of southern England. Geol. Mag., 118: (in press).

JEANS, C.V., 1968. The origin of the montmorillonite of the European Chalk with special reference to the Lower Chalk of England. Clay Min., 1: 311 - 329.

JEANS, C.V., 1978. Silicifications and associated clay assemblages in the Cretaceous marine sediments of southern England. Clay Min., 13: 101 - 126.

JEFFERIES, R.P.S., 1962. The palaeoecology of the Actinocamax plenus Subzone (lowest Turonian) in the Anglo-Paris Basin. Palaeontology, 4: 609 - 647.

JEFFERIES, R.P.S., 1963. The stratigraphy of the Actinocamax plenus Subzone (lowest Turonian) in the Anglo-Paris Basin. Proc. Geol. Ass., 74: 1 - 33.

JENKYNS, H.C., 1974. Diagenetic origin of red nodular limestones (Ammonitico Rosso, Knollenkalke) in the Mediterranean Jurassic: a diagenetic model. In: H.J. Hsü and H.C. Jenkyns (Eds.), Pelagic Sediments: On Land and under the Sea, Spec. Publ. Int. Ass. Sedimentol., 1: 249 - 271.

JODOT, P., 1965. Carte geologique de la France à 1/80,000, 81: Sens (4th Ed.), et notice explicative. Publ. Bur. Rech. Géol. Min., Orleans.

JOHANNES, R.E., 1964. Uptake and release of dissolved organic phosphorus by representatives of a coastal marine ecosystem. Limnol. Oceanogr., 9: 224 - 234.

JOHANNES, R.E., 1965. Influence of marine protozoa on nutrient regeneration. Limnol. Oceanogr., 10: 434 - 442.

JOHNSON, H.D., 1978. Shallow silicoclastic seas. In: H.G. Reading (Ed.), Sedimentary Environments and Facies, Blackwell Scientific Publications, Oxford, 207 - 258.

JONES, W.C., 1970. The composition, development, form and orientation of calcareous sponge spicules. Symp. Zool. Soc. London, 25: 91 - 123.

JONES, W.C. and JENKYNS, D.A., 1970. Calcareous sponge spicules: a study of magnesium calcites. Calc. Tiss. Res., 4: 314 - 329.

JØRGENSEN, N.O., 1975. Mg/Sr distribution and diagenesis of Maastrichtian white chalk and Danian bryozoan limestone from Jylland, Denmark. Bull. Geol. Soc. Denmark, 24: 299 - 325.

JUIGNET, P. and KENNEDY, W.J., 1974. Structures sédimentaires et mode d'accumulation de la Craie du Turonien Supérieur et du Sénonien du Pays de Caux. Bull. Bur. Rech. Géol. Min., (2), 1-1974; 19 - 47.

JUKES-BROWNE, A.J., 1908. The geology of the country around Andover. Mem. Geol. Surv. England Wales, 283, 67p.

JUKES-BROWNE, A.J., 1912. The Students Handbook of Stratigraphical Geology (2nd Ed.), Stanford, London, 668p.

JUKES-BROWNE, A.J. and HILL, W., 1903. The Cretaceous rocks of Britain II: The

Lower and Middle Chalk of England. Mem. Geol. Surv. UK, 568p.

JUKES-BROWNE, A.J. and HILL, W., 1904. The Cretaceous rocks of Britain III: The Upper Chalk of England. Mem. Geol. Surv. UK, 566p.

JUKES-BROWNE, A.J. and WHITE, H.J.O., 1908. The geology of the country around Henley-on-Thames and Wallingford. Mem. Geol. Surv. England Wales, 254, 113p.

KASTNER, M. and KEENE, J.B., 1975. Diagenesis of pelagic siliceous oozes. Ninth Int. Congr. Sedimentol. Nice, 7: 89 - 99.

KAUFFMAN, E.G., 1965. The Upper Cretaceous Inoceramus of Puerto Rico. Proc. Fourth Caribbean Geol. Conf. Trinidad 1965, 203 - 218.

KAUFFMAN, E.G., 1966. Notes on Cretaceous Inoceramidae (Bivalvia) of Jamaica. J. Geol. Soc. Jamaica, 8: 32 - 40.

KAZAKOV, A.V., 1937. The phosphorite facies and the genesis of phosphorites. USSR Sci. Inst. Fertilisers Insecticides Trans., 142: 95 - 113. (In Russian).

KAZAKOV, A.V., 1950. The fluorapatite system of equilibrium in the conditions of formation of sedimentary rock. Dokl. Akad. Nauk. SSSR Geol. Ser., 144: 1 - 21. (In Russian).

KEENE, J.B., 1975. Cherts and porcellanites from the North Pacific. Deep Sea Drilling Project Leg 32. Init. Rep. DSDP Washington, 32: 429 - 507.

KENNEDY, W.J., 1967. Burrows and surface traces from the Lower Chalk of southern England. Bull. Brit. Mus. (Nat. Hist.), 15: 127 - 167.

KENNEDY, W.J., 1969. The correlation of the Lower Chalk of south-east England. Proc. Geol. Ass., 80: 459 - 560.

KENNEDY, W.J., 1970a. A correlation of the uppermost Albian and the Cenomanian of south-west England. Proc. Geol. Ass., 81: 613 - 677.

KENNEDY, W.J., 1970b. Trace fossils in the Chalk environment. In: T.P. Crimes and J.C. Harper (Eds.), Trace Fossils, Seel House Press, Liverpool, 263 - 282.

KENNEDY, W.J., 1975. Trace fossils in carbonate rocks. In: R.W. Frey (Ed.), The Study of Trace Fossils, Springer-Verlag, New York, 377 - 398.

KENNEDY, W.J. and HALL, A., 1967. The influence of organic matter on the preservation of aragonite in fossils. Proc. Geol. Soc. London, 1643: 253 - 255.

KENNEDY, W.J. and KLINGER, H.C., 1972. Hiatus concretions and hardground horizons in the Cretaceous of Zululand (South Africa). Palaeontology, 15: 539 - 549.

KENNEDY, W.J. and JUIGNET, P., 1974. Carbonate banks and slump beds in the Upper Cretaceous (Upper Turonian - Santonian) of Haute Normandie, France. Sedimentology, 21: 1 - 42.

KENNEDY, W.J. and GARRISON, R.E., 1975a. Morphology and genesis of nodular phosphates in the Cenomanian Glauconitic Marl of south-east England. Lethaia, 18: 339 - 360.

KENNEDY, W.J. and GARRISON, R.E., 1975b. Morphology and genesis of nodular chalks and hardgrounds in the Upper Cretaceous of southern England. Sedimentology, 22: 311 - 386.

KENNEDY, W.J., LINDHOLM, R.C., HELMOLD, K.P. and HANCOCK, J.M., 1977. Genesis and diagenesis of hiatus- and breccia-concretions from the mid-Cretaceous of Texas and northern Mexico. Sedimentology, 24: 833 - 844.

KERMACK, K.A., 1954. A biometrical study of Micraster coranguinum and M. (Isomicraster) senonensis. Phil. Trans. Roy. Soc. London, B227: 375 - 428.

KESTER, D.R. and PYTKOWICZ, R.M., 1967. Determination of the apparent dissociation constants of phosphoric acid in seawater. Limnol. Oceanogr., 12: 243 - 252.

KETCHAM, B.H., 1939. The absorption of phosphate and nitrate by illuminated cultures of Nitzschia closterium. Am. J. Bot., 26: 399 - 407.

KETCHAM, B.H., CORWIN, N. and KEEN, D.J., 1955. The significance of organic phosphorus determinations in ocean waters. Deep Sea Res., 2: 172 - 181.

KHALEELEE, J., 1969. The application of some data processing techniques to the interpretation of geochemical data. Unpub. PhD Thesis, Univ. London.

KHARIN, G.S. and SOLDATOV, A.V., 1975. Distinctive lithologic features of the phosphorites of the Atlantic Shelf of Africa. Lithol. Min. Res. (Consultants Bureau Translation), 10: 154 - 161.

KIRTLEY, D.W. and TANNER, W.F., 1968. Sabellariid worms: Builders of a major reef type. J. Sed. Pet., 38: 73 - 78.

KOLODNY, Y., 1969. Are marine phosphorites forming today? Nature, 224: 1017 - 1019.

KOLODNY, Y. and KAPLAN, I.R., 1970. Uranium isotopes in sea-floor phosphorites. Geochim. Cosmochim. Acta, 34: 3 - 24.

KRAMER, J.R., 1964. Sea water: Saturation with apatites and carbonates. Science,

146: 637 - 638.

KRESS, A.G. and VEEH, H.H., 1980. Geochemistry and radiometric ages of phosphatic nodules from the continental margin of northern New South Wales, Australia. Mar. Geol., 36: 143 - 157.

KUENZLER, E.J., 1970. Dissolved organic phosphorus excretion by marine phytoplankton. J. Phycol., 6: 7 - 13.

KUENZLER, E.J. and KETCHAM, B.H., 1962. Rate of phosphorus uptake by Phaeodactylum tricornutum. Biol. Bull. Woods Hole, 123: 134 - 145.

KUENZLER, E.J., GUILLARD, R.R.L. and CORWIN, N., 1963. Phosphate-free sea water from reagent blanks in chemical analysis. Deep Sea Res., 10: 749 - 755.

LAMBERT, J., 1878. Notice stratigraphique sur l'étage Sénonien aux environs de Sens. Bull. Soc. Sci. Hist. Nat. Yonne, 32: 129 - 192.

LAMBERT, J., 1879. Note sur la craie dans le département de l'Yonne. Bull. Soc. Géol. Fr. (3), 7: 202 - 207.

LAMBERT, J., 1902. Souvenirs sur la géologie du Sénonais. Bull. Soc. Sci. Hist. Nat. Yonne, 56: 91 - 111.

LASNE, H., 1890. Sur les terrains phosphatés des environs de Doullens. Étage Sénonien et terrains superposés. Bull. Soc. Géol. Fr. (3), 18: 441 - 491.

LASNE, H., 1891. Sur les terrains phosphatés de Picardie. Lettre à M. le Professeur Gosselet. Ann. Soc. Géol. Nord, 19: 52 - 63.

LASNE, H., 1892. Sur les terrains phosphatés des environs de Doullens. Étage Sénonien et terrains superposés (2$^{e}$ note). Bull. Soc. Géol. Fr. (3), 20: 211 - 236.

LASNE, H., 1894. Sur les terrains phosphatés des environs de Doullens. Étage Sénonien et terrains superposés (3$^{e}$ article). Bull. Soc. Géol. Fr., (3), 22: 345 - 354.

LASNE, H., 1902. Observations concernant le gisement de la craie phosphatée. Lettre à M. Gosselet. Ann. Soc. Géol. Nord, 31: 55 - 59.

LEGEROS, R.Z., 1965. Effect of carbonate on the lattice parameters of apatite. Nature, 206: 403 - 404.

LEGEROS, R.Z., TRAUTZ, O.R., LEGEROS, J.P. and KLEIN, E., 1967. Apatite crystallites. Effect of carbonate on morphology. Science, 155: 1409 - 1411.

LEHR, J.R., McCLELLAN, G.H., SMITH, J.P. and FRAZIER, A.W., 1967. Characterization of apatites in commercial phosphate rocks. Coll. Int. Phos. Min. Solids, Toulouse, France.

LEMOINE, P., 1912. Carte géologique de la France à 1/80,000, 20: Neufchatel, et notice explicative. Publ. Bur. Rech. Géol. Min., Orleans.

LERICHE, M., 1908. Sur les fossiles de la craie phosphatée de la Picardie à Actinocamax quadratus. Assoc. Fr. Adv. Sci. Congr. Clermont-Ferrand, 37: 494 - 503.

LERICHE, M., 1909. Sur la limite entre le Turonien et le Sénonien dans le Cambrésis et sur quelques fossiles de la craie grise. Ann. Soc. Géol. Nord, 38: 53 - 73.

LERICHE, M., 1911. Deuxième note sur les fossiles de la craie phosphatée de la Picardie. Bull. Soc. Belge. Géol. Paléont. Hydrol. Mém., 25: 297 - 310.

LERICHE, M., 1935. Sur le Crétacé Supérieur du Hainaut et du Brabant. Ann. Soc. Géol. Belg., 58: 118 - 141.

LERICHE, M. and CELET, P., 1972. Carte géologique de la France à 1/50,000, 49: Bohain-en-Vermandois, et notice explicative. Publ. Bur. Rech. Géol. Min., Orleans.

LERMAN, A., MACKENZIE, F.T. and GARRELS, R.M., 1975. Modelling of geochemical cycles: phosphorus as an example. Geol. Soc. Am. Mem., 142: 205 - 218.

LINDSTROM, M., 1979. Diagenesis of Lower Ordovician hardgrounds in Sweden. Geol. Palaeont., 13: 9 - 24.

LIPPS, J.H. and MITCHELL, E., 1976. Trophic models for the adaptive radiations and extinctions of pelagic marine mammals. Paleobiol., 2: 147 - 155.

LOMBARD, A., 1956. Géologie Sédimentaires. Les Séries Marines. Masson, Paris, 722p.

LOUGHNAN, F.C. and CRAIG, D.C., 1962. A preliminary investigation of the recent sediments off the east coast of Australia. Aust. J. Mar. Freshwater Res., 31: 48 - 56.

LOWENSTAM, H.A. and EPSTEIN, S., 1954. Palaeotemperatures of the post-Aptian Cretaceous as determined by the oxygen isotope method. J. Geol., 62: 207 - 248.

LUTENAUER, J.L. and PILKEY, O.H., 1967. Phosphate grains: Their application to the interpretation of North Carolina Shelf sediments. Mar. Geol., 5: 315 - 320.

LUYENDYK, B.P., FORSYTH, D. and PHILLIPS, J.D., 1972. Experimental approach to the palaeocirculation of the oceanic surface waters. Geol. Soc. Am. Bull., 83: 2649 - 2664.

MACKENZIE, F.T. and WOLLAST, R., 1977. Sedimentary cycling: Models of global processes. In: E.D. Goldberg, I.N. McCave, J.J. O'Brien and J.H. Steele (Eds.), The Sea 6. Marine Modelling. Wiley-Interscience, New York, London, Sydney, Toronto, 739 - 785.

MALLOY, R.J. and HURLEY, R.J., 1970. Geomorphology and geologic structure: Straits of Florida. Geol. Soc. Am. Bull., 81: 1947 - 1972.

MANGOLD-WIRZ, K., 1963. Biologie des Céphalopodes benthiques et nectoniques de la Mer Catalane. 'Vie Milieux', Supp. 13, Hermann, Paris, 285p.

MANHEIM, F.T., 1979. Origin of the Blake Plateau phosphorites. In: W.C. Burnett and R.P. Sheldon (Eds.), Report on the Marine Phosphatic Sediments Workshop, East-West Center, Honolulu, 14.

MANHEIM, F.T., ROWE, G.T. and JIPA, D., 1975. Marine phosphorite formation off Peru. J. Sed. Pet., 45: 243 - 251.

MANSFIELD, G.R., 1940. The role of fluorine in phosphate deposition. Am. J. Sci., 238: 863 - 879.

MARLIÈRE, R., 1954. Le Crétacé. In: P. Fourmarier (Ed.), Prodrome d'une Description Géologique de la Belgique. Soc. Géol. Belge., Liege, 417 - 444.

MARLOWE, J.I., 1971. Dolomite, phosphorite and carbonate diagenesis on a Caribbean seamount. J. Sed. Pet., 41: 809 - 827.

MARSHALL, J.F., 1971. Phosphatic sediments on the eastern Australian upper continental slope. Bur. Min. Res. Aust. Rept. 1971/59 (Unpublished).

MARTENS, C.S. and HARRISS, R.C., 1970. Inhibition of apatite precipitation in the marine environment by magnesium ions. Geochim. Cosmochim. Acta, 34: 621 - 625.

MATHIEU, C., POMEROL, C., JAMAGNE, M., MAUCORPS, J. and SOLAU, J.L., 1971. Carte géologique de la France à 1/50,000, 66: Vervins, et notice explicative. Publ. Bur. Rech. Géol. Min., Orleans.

MATHIEU, C., MAUCORPS, J. and POMEROL, C., 1975. Carte géologique de la France à 1/50,000, 108: Asfeld, et notice explicative. Publ. Bur. Rech. Géol. Min., Orleans.

MATHIEU, G., 1931. Coupe géologique des morts-terrains de la Fosse No. 9 (Siège de Clercq-Crombez) des mines de Dourges. Ann. Soc. Géol. Nord, 56: 130 - 135.

MATTER, A., DOUGLAS, R.G. and PERCH-NIELSEN, K., 1975. Fossil preservation, geochemistry and diagenesis of pelagic carbonates from Shatsky Rise, northwest Pacific. Init. Rept. DSDP, Washington, 32: 891 - 921.

MATTSON, P.H. and PESSAGNO, E.A., 1971. Caribbean Eocene volcanism and the extent of Horizon A. Science, 174: 138 - 139.

MAXWELL, J.A., 1968. Rock and Mineral Analysis. Wiley-Interscience, New York, London, Sydney, Toronto, 583p.

McARTHUR, J.M., 1974. The geochemistry of phosphate concretions from the continental shelf off Morocco. Unpub. PhD Thesis Univ. London, 271p.

McARTHUR, J.M., 1978. Systematic variation in the contents of Na, Sr, $CO_3$ and $SO_4$ in marine carbonate-fluorapatite and their relation to weathering. Chem. Geol., 21: 89 - 112.

McCLELLAN, G.H. and LEHR, J.R., 1969. Crystal chemical investigation of natural apatites. Am. Min., 54: 1374 - 1391.

McCONNELL, D., 1965. Precipitation of phosphates in sea water. Econ. Geol., 60: 1059 - 1062.

McCONNELL, D., 1973. Apatite: its crystal chemistry, mineralogy, utilization geologic and biologic. Springer-Verlag, Berlin, 111p.

McKELVEY, V.E., 1959. Relation of upwelling marine waters to phosphorite and oil. Geol. Soc. Am. Bull., 70: 1783 - 1784.

McKELVEY, V.E., 1963. Successful new techniques in prospecting for phosphate deposits. US Dept. State Nat. Res. UN Conf. App. Sci. Tech. Benefit Less Dev. Areas, Geneva, 2: 164 - 172.

McKELVEY, V.E., 1967. Phosphate deposits. US Geol. Surv. Bull., 1252-D, 21p.

McRAE, S.G., 1972. Glauconite. Earth Sci. Rev., 8: 397 - 440.

MÉNILLET, F., BRETON, J.P., COLLEAU, A. and NEAU, G., 1974. Carte géologique de la France à 1/50,000, 330: Cheroy, et notice explicative. Publ. Bur. Rech. Géol. Min., Orleans.

MENNESSIER, G., AKBAR, R., SKADARI, A., DURZADA, A., BROQUET, G. and MONCIARDINI, C., 1974. Carte geologique de la France à 1/50,000, 45: Hallencourt, et notice

explicative. Publ. Bur. Rech. Géol. Min., Orleans.

MENNESSIER, G., DICKEL, B., MONCIARDINI, C. and AGACHE, R., 1976. Carte géologique de la France à 1/50,000, 47: Albert, et notice explicative. Publ. Bur. Rech. Géol. Min., Orleans.

MENNESSIER, G., MONCIARDINI, C. and AGACHE, R., 1978. Carte géologique de la France à 1/50,000, 63: Roye, et notice explicative. Publ. Bur. Rech. Géol. Min., Orleans.

MERO, J.L., 1961. Sea floor phosphorites. Min. Info. Service State Calif. Div. Mines Geol. 41, No 11.

MEUNIER, S., 1888. Conditions géologiques du gisements phosphate de Beauval. Compt. Rend. Acad. Sci. Paris, 106: 214 - 217.

MEUNIER, S., 1891. Les phosphatières d'Hardivillers, Oise. Le Naturaliste, 1891: 46 - 49; 55 - 56.

MIDDLEMISS, F.A. and BROMLEY, R.G., 1962. Field meeting on the Lower Greensand and Chalk of the Isle of Wight. Proc. Geol. Ass., 73: 449 - 453.

MILLER, J.S., 1829a. Observations on belemnites. Trans. Geol. Soc. London (2), 2: 45 - 62.

MILLER, J.S., 1829b. Observations on the genus Actinocamax. Trans. Geol. Soc. London, (2), 2: 63 - 67.

MILLER, L.J., 1964. The origin of sedimentary phosphate deposits. Econ. Geol., 59: 1619 - 1620.

MILLIGAN, D.B., 1962. Marine geology of the Florida Straits. Unpub. PhD Thesis Florida State Univ., Tallahassee, Florida, 120p.

MILLIMAN, J.D., 1974. Marine Carbonates. Springer-Verlag, Berlin, Heidelberg, New York, 375p.

MILLOT, G., Géologie de Argiles. Masson, Paris, 380p.

MIMRAN, Y., 1975. Fabric deformation in Cretaceous chalks by tectonic stresses. Tectonophysics, 26: 309 - 316.

MIMRAN, Y., 1977. Chalk deformation and large-scale migration of calcium carbonate. Sedimentology, 24: 333 - 360.

MIMRAN, Y., 1978. The induration of Upper Cretaceous Yorkshire and Irish chalks. Sed. Geol., 20: 141 - 164.

MONTY, C., 1965. Recent algal stromatolites in the windward lagoon, Andros Island, Bahamas. Ann. Soc. Géol. Belg., 88: 269 - 276.

MONTY, C., 1967. Distribution and structure of Recent stromalolitic algal mats, eastern Andros Island, Bahamas. Ann. Soc. Géol. Belg., 90: 55 - 100.

MOORE, H.B., 1939. Faecal pellets in relation to marine deposits. In: P.D. Trask (Ed.), Recent Marine Sediments, Am. Assoc. Petrol. Geol. Spec. Publ., 4: 516 - 524.

MOORE, H.B. and KRUSE, P., 1956. A review of present knowledge of faecal pellets. Mar. Lab. Rept. Inst. Mar. Sci. Univ. Miami, 13805, 25p.

MORGAN-JONES, M., 1977. Mineralogy of the non-carbonate material from the Chalk of Berkshire and Oxfordshire, England. Clay Min., 12: 331 - 344.

MÜLLER, A.H., 1956. Die knollenfeuersteine der Schreibkreide, eine frühdiagenetische Bildung. Ber. Geol. Ges., 1: 136 - 146.

MULLINS, H.T. and NEUMANN, A.C., 1979. Geology of the Miami Terrace and its paleoceanographic implications. Mar. Geol., 30: 205 - 232.

MULLINS, H.T., NEUMANN, A.C., WILBER, R.J. and BOARDMAN, M.R., 1980. Nodular carbonate sediment on Bahamian slopes: possible precursors to nodular limestones. J. Sed. Pet., 50: 117 - 131.

MUNK, W.R., 1955. The circulation of the oceans. Scientific American, 193: 96 - 104.

MURATA, K.J. and NAKATA, J.K., 1974. Cristobalitic stage in the diagenesis of diatomaceous shale. Science, 18: 567.

MURATA, K.J. and LARSEN, R.R., 1975. Diagenesis of Miocene siliceous shales, Temblar Range, California. J. Res. US Geol. Surv., 3: 553 - 566.

MURRAY, J., 1885. Report on the results of dredging by the United States Coast Survey Steamer Blake, 27: Report on the specimens of bottom deposits. Bull. Mus. Comp. Zool. Harvard, 12: 37 - 61.

MURRAY, J., 1898. On the annual range of temperature in the surface waters of the ocean and its relation to other oceanographical phenomena. Geographical J., 12: 113 - 137.

MURRAY, J. and RENARD, A.F., 1891. Deep-Sea Deposits. In: C.W. Thompson (Ed.), Report on the Scientific Results of the Voyage of the HMS Challenger, 5, Eyre Spottiswood, London, 391 - 400.

MURRAY, J. and CHUMLEY, J., 1924. The deep-sea deposits of the Atlantic Ocean. Trans. Roy. Soc. Edinburgh, 5: 1 - 252.

MURTY, P.S.N., REDDY, C.V.G. and VAREDACHARI, V.V.R., 1968. Distribution of total phosphorus in the shelf sediments off the west coast of India. Proc. Nat. Inst. Sci. India, 34B: 134 - 141.

NAEF, A., 1922. Die fossilen Tintenfische. Gustav Fisher, Jena, 322p.

NEGRE, G., 1912a. Note sur les gisements de phosphate de Beauval et environs. Ann. Soc. Géol. Nord, 41: 235 - 239.

NEGRE, G., 1912b. Découverte de craie et de sables phosphatés dans le département de l'Yonne. Compt. Rend. Acad. Sci. Paris, 154: 1314 - 1315.

NEGRE, G., 1913. Découverte de craie phosphatée dans l'assise a Belemnitella quadrata à Saint-Martin-du-Tertre près Sens (Yonne). Bull. Soc. Géol. Fr.(4), 13: 212 - 223.

NEGRE, G., 1963. Les craies phosphatées en France: Beauval (1886 - 1963). Ind. Chim., 50: 383 - 386.

NEGRE, G., 1964. Les craies phosphatées en France (II): Saint-Martin-du-Tertre près Sens (1912 - 1934). Ind. Chim., 51: 248 - 249.

NEUGEBAUER, J., 1973. The diagenetic problem of chalk - The role of pressure solution and pore fluid. Neues Jhb. Geol. Palaont. Abh., 143: 223 - 245.

NEUGEBAUER, J., 1974. Some aspects of cementation in chalk. In: K.J. Hsu and H.C. Jenkyns (Eds.), Pelagic Sediments: On Land and under the Sea, Spec. Publ. Int. Assoc. Sedimentol., 1: 149 - 176.

NEUMAN, W.F. and NEUMAN, M.W., 1953. The nature of the mineral phase of bone. Chem. Rev., 53: 1 - 45.

NEUMANN, A.C., 1966. Observations on coastal erosion in Bermuda and measurements of the boring rate of the sponge Cliona lampa. Limnol. Oceanogr., 11: 92 - 108.

NEUMANN, A.C. and BALL, M.M., 1970. Submersible observations in the Straits of Florida, geology and bottom currents. Geol. Soc. Am. Bull., 81: 2861 - 2874.

NEWELL, N.D., PURDY, E.G. and IMBRIE, J., 1960. Bahamian oolitic sand. J. Geol. 68: 481 - 497.

NEWTON, R.S., SEIBOLD, E. and WERNER, F., 1973. Facies distribution patterns on the Spanish Sahara continental shelf mapped with side-scan sonar. 'Meteor'

Forsch-Ergebnisse, 15: 55 - 77.

NORRIS, R.M., 1964. Sediments of Chatham Riase. NZ Dep. Sci. Ind. Res. Bull., 159, 39p.

OPPENHEIMER, C.H., 1958. Evidence of fossil bacteria in phosphate rock. Publ. Inst. Mar. Sci. Univ. Texas, 5: 156 - 159.

PALAEONTOGRAPHICAL SOCIETY, 1954. Directory of British Fossiliferous Localities. Palaeontographical Society, London, 268p.

PALMER, T.P. and FÜRSICH, F., 1974. The ecology of a Middle Jurassic hardground and crevice fauna. Palaeontology, 17: 507 - 524.

PARENT, H., 1896. Note sur les polypiers d'Hem-Monacu. Ann. Soc. Géol. Nord, 24: 135 - 136.

PARKER, R.J., 1971. The petrography and major element geochemistry of phosphorite nodule deposits on the Agulhas Bank, South Africa. S. Afr. Nat. Comm. Oceanogr. Res. Mar. Geol. Prog. Bull., 2, 94p.

PARKER, R.J., 1975. The petrology and origin of some glauconitic and glauco-conglomeratic phosphorites from the South African continental margin. J. Sed. Pet., 45: 230 - 242.

PARKER, R.J. and SIESSER, W.G., 1972. Petrology and origin of some phosphorites from the South African continental margin. J. Sed. Pet., 42: 434 - 440.

PASHO, D.W., 1973. Character and origin of marine phosphorites. Publ. Univ. S. Calif. Geol., 72-5, 188p.

PASHO, D.W., 1976. Distribution and morphology of Chatham Rise phosphorites. NZ Oceanogr. Inst. Mem., 77, Wellington, 28p.

PEAKE, N.B., 1958. The coastal Chalk of north-east Thanet. Geol. Ass. Guide 30, The London Region, 18 - 25.

PEAKE, N.B. and HANCOCK, J.M., 1961. The Upper Cretaceous of Norfolk. Trans. Norfolk Norwich Nat. Soc., 19: 293 - 339.

PEVEAR, D.R., 1966. The estuarine formation of the United States Atlantic Coastal Plain phosphorite. Econ. Geol., 61: 251 - 255.

PEVEAR, D.R., 1967. Shallow water phosphorites. Econ. Geol., 62: 562 - 575.

PEVEAR, D.R. and PILKEY, O.H., 1966. Phosphorite in Georgia Continental Shelf sediments. Geol. Soc. Am. Bull., 77: 849 - 858.

PEYER, B., 1968. Comparative odontology. Univ. Chicago Press, Chicago, 347p.

PILKEY, O.H. and LUTERNAUER, J.L., 1967. A North Carolina Shelf phosphorite deposit of possible commercial interest. Southeastern Geol., 8: 33 - 51.

PIPER, D.Z. and CODISPOTI, L.A., 1975. Marine phosphorite deposits and the nitrogen cycle. Science, 188: 15 - 18.

PLATEL, J.P., 1977. Le Campanien stratotypique dans le synclinal de Saintes (Charente): lithostratigraphie, géomorphologie et biozonation. Bull. Bur. Rech. Géol. Min. (2), 1977-4: 261 - 276.

POMEROL, B. and AUBRY, M.P., 1977. Relation between western European chalks and the opening of the North Atlantic. J. Sed. Pet., 47: 1027 - 1035.

POWELL, T.G., COOK, P.J. and McKIRDY, D., 1974. Organic geochemistry of phosphorites relevence to petroleum genesis. Am. Ass. Petrol. Geol. Bull., 59: 618 - 632.

PRATT, R.M., 1971. Lithology of rocks dredged from the Blake Plateau. Southeastern Geol., 13: 19 - 38.

PRATT, R.M. and McFARLIN, P.F., 1966. Manganese pavements on the Blake Plateau. Science, 151: 1080 - 1082.

PRATT, R.M. and MANHEIM, F.T., 1967. The relation of manganese to phosphorite concretions on the Blake Plateau. Trans. Am. Geophys. Union, 48: 144 - 145.

PRICE, N.B. and CALVERT, S.E., 1978. The geochemistry of phosphorites from the Namibian Shelf. Chem. Geol., 23: 151 - 170.

PRICE, W.J., 1972. Analytical Atomic Absorption Spectrometry. Heyden, London, New York, Rheine, 239p.

PRIEM, F., 1896. Sur les poissons de la craie phosphatée des environs de Péronne. Bull. Soc. Géol. Fr. (3), 24: 9 - 22.

PURDY, E.G., 1963. Recent calcium carbonate facies of the Great Bahama Banks 1. Petrography and reaction groups. 2. Sedimentary facies. J. Geol., 71: 334 - 355; 472 - 497.

PURSER, B., 1978. Early diagenesis and preservation of porosity in Jurassic limestones. J. Petrol. Geol., 1: 83 - 94.

PYTKOWICZ, R.M. and KESTER, D.R., 1967. Relative calcium phosphate saturation in two regions of the North Pacific Ocean. Limnol. Oceanogr., 12: 714 - 718.

RABELLE, M., 1893. Quelques observations géologiques faites aux environs de

Ribemont, rive gauche de l'Oise. Ann. Soc. Géol. Nord, 21: 344 - 349.

RABELLE, M., 1902. Observations géologique aux environs de Ribemont et dans la craie phosphatée d'Etaves et de Fresnoy. Ann. Soc. Géol. Nord, 31: 45 - 49.

RAGUIN, E., 1926. Phosphates de France. In: Les Réserves Mondiale en Phosphates, Int. Géol. Cong. 14th, 197 - 214.

RASMUSSEN, H.W., 1961. A monograph of the Cretaceous Crinoidea. Biol. Skr. Dan. Vid. Selsk., 12: 1 - 428.

RASMUSSEN, H.W., 1971. Echinoid and crustacea burrows and their diagenetic significance in the Maastrichtian - Danian of Stevns Klint, Denmark. Lethaia, 4: 191 - 216.

RAWSON, P.F., CURRY, D., DILLEY, F.C., HANCOCK, J.M., KENNEDY, W.J., NEALE, J.W., WOOD, C.J. and WORSSAM, B.C., 1978. A correlation of Cretaceous rocks in the British Isles. Geol. Soc. London Spec. Rept., 9, 70p.

RECKSIEK, C.W., 1978. California's market squid. Pacific Discovery, 31: 19 - 27.

REED, J.J. and HORNIBROOK, N.D., 1952. Sediments from Chatham Rise. NZ J. Sci., 34: 173 - 189.

REEVES, M.J. and SAADI, T.A.K., 1971. Factors controlling the deposition of some phosphate-bearing strata from Jordon. Econ. Geol., 66: 451 - 165.

REID, R.E.H., 1962a. Sponges of the Chalk Rock. Geol. Mag., 99: 273 - 278.

REID, R.E.H., 1962b. Relationships of faunas and substratum in the palaeoecology of the Chalk and Chalk Rock. Nature, 194: 276 - 277.

REID, R.E.H., 1968. Hexactinellid faunas from the Chalk of England and Ireland. Geol. Mag., 105: 15 - 22.

REID, R.E.H., 1971. The Cretaceous rocks of north-eastern Ireland. Irish Nat. J., 17: 105 - 129.

REID, R.E.H., 1973. The Chalk Sea. Irish Nat. J., 17: 357 - 375.

RENARD, A.F. and CORNET, J., 1891a. De la nature et de l'origine du phosphate de chaux des environs de Mons. Ann. Soc. Géol. Belg., 18: 3 - 13.

RENARD, A.F. and CORNET, J., 1891b. Recherches micrographiques sur la nature et l'origine des roches phosphatées (notice préliminaire). Bull. Acad. Roy. Belg., 21: 126 - 160.

REYMENT, R.A. and NAIDIN, D.P., 1962. Biometric study of Actinocamax verus s.l.

from the Upper Cretaceous of the Russian Platform. Stockh. Contr. Geol., 9: 147 - 206.

RHOADS, D.C., 1967. Biogenic reworking of intertidal and subtidal sediments in Barnstaple Harbour and Buzzards Bay, Massachusetts. J. Geol., 75: 461 - 476.

RHOADS, D.C., 1973. The influence of deposit feeding benthos on water turbidity and nutrient recycling. Am. J. Sci., 273: 1 - 22.

RHOADS, D.C. and YOUNG, D.K., 1970. The influence of deposit feeding organisms on sediment stability and community trophic structure. J. Mar. Res., 28: 150 - 178.

RICHARDS, F.A., 1960. Some chemical and hydrographic observations along the north coast of South America 1. Cabo Tres Puntas to Curaçao, including the Cariaco Trench and the Gulf of Cariaco. Deep Sea Res., 7: 163 - 182.

RICHARDS, F.A. and VACCARO, R.F., 1956. The Cariaco Trench, an anaerobic basin in the Caribbean Sea. Deep Sea Res., 3: 214 - 228.

RIECH, V. and von RAD, U., 1979. Eocene porcellanites and early Cretaceous cherts from the western North Atlantic Basin. Init. Rept. DSDP Washington, 43: 437 - 455.

RIGBY, J.K., 1958. Mass movements in Permian rocks of Trans-Pecos, Texas. J. Sed. Pet., 28: 298 - 315.

RIGGS, S.R., 1979a. Petrology of the Tertiary phosphorite system of Florida. Econ. Geol., 74: 195 - 220.

RIGGS, S.R., 1979b. Phosphorite sedimentation in Florida - a model phosphogenic system. Econ. Geol., 74: 285 - 314.

RIGGS, S.R., 1979c. A petrographic classification of sedimentary phosphorites. In: P.J. Cook and J.H. Shergold (Eds.), Proterozoic - Cambrian Phosphorites, Canberra Pub., Canberra, 63 - 64.

RILEY, J.P., 1971. Micronutrient elements. In: J.P. Riley and R. Chester (Eds.), Introduction to Marine Chemistry, Academic Press, London, New York, 152 - 181.

ROBERSON, C.E., 1966. Solubility implications of apatite in sea water. US Geol. Surv. Prof. Pap., 550D: 178 - 185.

ROBERTSON, A.H.F., 1977. The origin and diagenesis of cherts from Cyprus. Sedimentology, 24: 11 - 30

ROCHFORD, D.J., 1951. Studies in Australian estuarine hydrology 1. Introductory

and comparative features. Aust. J. Mar. Freshwater Res., 2: 1 - 116.

ROGERS, J., 1977. Sedimentation on the continental margin off the Orange River and the Namibian Desert. Joint GSO/UCT Mar. Geosci. Bull., 7, Dept. Geol. Univ. Cape Town, 212p.

ROMANKEVICH, Y.A. and BATURIN, G.N., 1972. Composition of the organic matter in phosphorites from the continental shelf off southwest Africa. Geochem. Int. (Am. Geol. Inst. Translation), 9: 464 - 470.

ROONEY, T.P. and KERR, P.F., 1967. Mineralogic nature and origin of phosphorite, Beaufort County, North Carolina. Geol. Soc. Am. Bull., 78: 731 - 748.

ROTH, P.H., MULLIN, M.M. and BERGER, W.H., 1975. Coccolith sedimentation by faecal pellets: Laboratory experiments and field observations. Geol. Soc. Am. Bull., 86: 1079 - 1084.

ROWE, A.W., 1899. An analysis of the genus Micraster as determined by rigid zonal collecting from the Zone of Rhynchonella cuvieri to that of Micraster coranguinum. Quart. J. Geol. Soc. London, 55: 494 - 547.

ROWE, A.W., 1900. The zones of the white Chalk of the English coast I: Kent and Sussex. Proc. Geol. Ass., 16: 289 - 368.

ROWE, A.W., 1901. The zones of the white Chalk of the English coast II: Dorset. Proc. Geol. Ass., 17: 1 - 76.

ROWE, A.W., 1903. The zones of the white Chalk of the English coast III: Devon. Proc. Geol. Ass., 18: 1 - 51.

ROWE, A.W., 1904. The zones of the white Chalk of the English coast IV: Yorkshire. Proc. Geol. Ass., 18: 193 - 296.

ROWE, A.W., 1908. The zones of the white Chalk of the English coast V: The Isle of Wight. Proc. Geol. Ass., 20: 209 - 352.

RUTOT, M., 1894. Essai de synchronisme des couches Maastrichtian et Sénonienes de Belgique. Bull. Soc. Géol. Belg., 8: 145 - 194.

SALVAN, H., 1952. Phosphates. Int. Géol. Cong. 19th Algiers Monogr. Region., 1 (3rd Ser.), 283 - 321.

SALVAN, H., 1960. Les phosphates de chaux sédimentaires du Maroc, leurs caracteristiques et leurs problèmes (essai de synthèse). Notes Marocaines, 14: 7 - 20.

SANT, V.N., 1979. Precambrian Phosphorite of Rajasthan, India : A Case History. In: P.J. Cook and J.H. Shergold (Eds.), Proterozoic - Cambrian Phosphorites, Canberra Pub., Canberra, 39 - 40.

SARKAR, S., BHATTACHARYYA, A., and CHANDA, S,K., 1980. Recognition of hardgrounds and erosion surfaces: a new criterion. J. Sed. Pet., 50: 83 - 89.

SAYLES, F.L. and MANHEIM,. F.T., 1975. Interstitial solutions and diagenesis in buried marine sediments: results from the Deep Sea Drilling Project. Geochim. Cosmochim. Acta, 39: 103 - 127.

SCHLAGER, W. and JAMES, N.P., 1978. Low-magnesium calcite limestones forming at the deep-sea floor, Tongue of the Ocean, Bahamas. Sedimentology, 25: 675 - 702.

SCHLANGER, S.O. and DOUGLAS, R.G., 1974. Pelagic ooze-chalk-limestone transition and its implications for marine stratigraphy. In: K.J. Hsü and H.C. Jenkyns (Eds.), Pelagic Sediments: On Land and under the Sea, Spec. Publ. Int. Ass. Sedimentol., 1: 211 - 233.

SCHLEE, J., BEHRENDT, J.C. and ROBB, J.M., 1974. Shallow structure and stratigraphy of the Liberian continental margin. Am. Assoc. Petrol. Geol. Bull., 58: 708 - 728.

SCHMID, F., 1953. Schlüsselprofile der Oberen Kreide NW-Deutschlands. Paläont. Z., 27: 234 - 236.

SCHMID, F., 1956. Jetziger Stand der Oberkreide - Biostratigraphie in Nordwestdeutschland: Cephalopoden. Paläont. Z., 30: 7 - 10.

SCHMID, F., 1959a. Biostratigraphie du Campanien - Maastrichtien de NE de la Belgique sur la base des belemnites. Ann. Soc. Géol. Belg., 82B: 235 - 256.

SCHMID, F., 1959b. La définition des limites Santonien - Campanien et Campanien inferieur - superieur en France et dans le nordouest de l'Allemagne. Compt. Rend. Cong. Sav. Dijon, 535 - 546.

SCHMID, F., 1967. Die Oberkreide-Stufen Campan und Maastricht in Limburg (Südniederlande-Nordostbelgien) bei Aachen und in Nordwestdeutschland. Ber. Dt. Ges. Geol. Wiss. A. Geol. Pal., 12: 471 - 478.

SCHOLLE, P.A., 1974. Diagenesis in Upper Cretaceous chalks from England, Northern Ireland and the North Sea. In: K.J. Hsü and H.C. Jenkyns (Eds.) Pelagic Sediments: On Land and under the Sea, Spec. Publ. Int. Ass. Sedimentol., 1: 177 - 210.

SCHOLLE, P.A., 1977a. Chalk diagenesis and its relation to petroleum exploration: oil from chalks a modern miracle? Am. Ass. Petrol. Geol. Bull., 61: 982 - 1009.

SCHOLLE, P.A., 1977b. Current oil and gas production from North American Upper Cretaceous chalks. US Geol. Surv. Circular, 767, 51p.

SCHOLLE, P.A., 1978. A color illustrated guide to carbonate rock constituents, textures, cements and porosities. Am. Ass. Petrol. Geol. Mem., 27, 241p.

SCHOLLE, P.A. and KLING, S.A., 1972. Southern British Honduras: lagoonal coccolith ooze. J. Sed. Pet., 42: 195 - 204.

SCHOLLE, P.A. and KINSMAN, D.J.J., 1973. Diagenesis of Upper Cretaceous chalk from North Sea, England and Northern Ireland. Am. Ass. Petrol. Geol. Bull., 57: 803 - 804 (Abstract).

SCHOLLE, P.A. and KENNEDY, W.J., 1974. Isotopic and petrophysical data on hard-grounds from Upper Cretaceous chalks from western Europe. Geol. Soc. Am. Abs. Progs., 6: 943.

SCHOLLE, P.A. and ARTHUR, M.A., 1980. Carbon isotope fluctuations in Cretaceous pelagic limestones: Potential stratigraphic and petroleum exploration tool. Am. Ass. Petrol. Geol. Bull., 64: 67 - 87.

SCHOTT, W., 1970. "Mogenlichkeiten der Nutzungmineralischer Rohstoffe aus dem Meerestroden und dem Meeresuntergrund. Interocean '70, 1: 23 - 28.

SCHOTT, W., 1976. Mineral (inorganic) resources of the oceans and ocean floors: a general review. In: K.H. Wolf (Ed.), Handbook of Strata-bound and Stratiform Ore Deposits 3. Supergene and Surficial Ore Deposits: Textures and Fabrics, Elsevier, Amsterdam, 245 - 294.

SCWARZBACH, M., 1963. Climates of the Past: An Introduction to Palaeoclimatology. Van Nostrand, London, 328p.

SEILACHER, A., 1971. Preservational history of ceratite shells. Palaeontology, 14: 16 - 21.

SEILACHER, A., 1973. Biostratinomy, the sedimentology of biologically standardized particles. In: R.N. Ginsburg (Ed.), Evolving Concepts in Sedimentology, John Hopkins Univ. Press, Baltimore, London, 159 - 177.

SEIWELL, H.R., 1935. The cycle of phosphorus in the western basin of the North Atlantic I: Phosphate phosphorus. Pap. Phys. Oceanogr. Meteorol., 3: 1 - 56.

SENIN, Y.M., 1970. Phosphorus in bottom sediments of the South-west African Shelf. Lithol. Min. Res. (Consultants Bureau Translation), 5: 8 - 20.

SENIN, Y.M., 1977. Mineral and organic phosphorus in the pore waters of the bottom sediments of the shelf of West Africa. Oceanology (Am. Geophys. Union Translation), 16: 586 - 590.

SÉRONIE-VIVIEN, M., 1956. Étude du Crétacé Supérieur de la vallée de l'Isle. Diplôme Études Sup. Univ. Bordeaux.

SÉRONIE-VIVIEN, M., 1959. Les localités-types du Senonien dans les environs de Cognac et de Barbezieux (Charente). Coll. Crétacé Sup. Franç., Compt. Rend. Congr. Socs. Sav. Dijon, 579 - 589.

SÉRONIE-VIVIEN, M., 1972a. Contribution à l'étude de Sénonien en Aquitaine septentrionale, ses stratotypes: Coniacien, Santonien, Campanien. Les Stratotypes Francaise 2, Édit. Centre Natl. Rech. Sci., 195p.

SÉRONIE-VIVIEN, M., 1972b. Les biozones du Sénonien en Aquitaine septentrionale. Bull. Soc. Linn. Bordeaux, 2: 19 - 24.

SHANNON, L.V., 1966. Hydrology of the south and west coast of South Africa. Invest. Rept. Div. Sea Fish. S. Afr., 58: 1 - 22.

SHAW, A.B., 1956. Quantitative trilobite studies I. The statistical description of trilobites. J. Palaont., 30: 1209 - 1224.

SHELDON, R.P., 1964. Palaeolatitude and paleogeographic distribution of phosphorite. US Geol. Surv. Prof. Pap., 501C: 106 - 113.

SHEPARD, F.P., 1973. Submarine Geology (3rd Ed.). Harper Rowe, New York, Evanston, San Francisco, London, 517p.

SHERLOCK, R.L., NOBLE, A.H. and PRINGLE, J., 1927. The geology of the country around Beaconsfield. Mem. Geol. Surv. England Wales, 255, 59p.

SHINN, E.A., 1969. Submarine lithification of Holocene carbonate sediments in the Persian Gulf. Sedimentology, 12: 109 - 144.

SHINN, E.A., LLOYD, R.M. and GINSBURG, R.N., 1969. Anatomy of a modern carbonate tidal-flat, Andros Island, Bahamas. J. Sed. Pet., 39: 1202 - 1228.

SHINN, E.A., HALLEY, R.B., HUDSON, J.A. and LIDZ, B.H., 1977. Limestone compaction: an enigma. Geology, 5: 21 - 24.

SIESSER, W.G., 1978. Age of phosphorites on the South African continental margin.

Mar. Geol., 26: M17 - M28.

SIEVER, R., 1962. Silica solubility, 0 - 200°, and the diagenesis of siliceous sediments. J. Geol., 70: 127 - 150.

SIEVERTS, H., 1927. Uber die Crinoidengattung Marsupites. Abh. Preuss. Geol. Landesanstadt; N. F. H., 108: 1 - 73.

SILLEN, L.G., 1961. The physical chemistry of seawater. In: M. Sears (Ed.), Oceanography, Am. Ass. Adv. Sci. Publ. 67: 549 - 581.

SIMPSON, D.R., 1964. The nature of alkali carbonate apatites. Am. Min., 49: 363 - 376.

SIMPSON, G.G., ROE, A. and LEWONTIN, R.C., 1960. Quantitative Zoology. Harcourt Brace World Inc., New York, Chicago, San Francisco, Atlanta, 440p.

SKOPINTSEV, B.A., 1972. Saturation of deep Black Sea waters with calcium phosphate. Oceanology (Am. Geophys. Union Translation), 12: 672 - 677.

SMISER, J.S., 1935. A revision of the echinoid genus Echinocorys in the Senonian of Belgium. Mem. Mus. Roy. Hist. Nat. Belg., 67, 51p.

SMITH, A.G. and BRIDEN, J.C., 1977. Mesozoic and Cenozoic Palaeocontinental Maps. Camb. Univ. Press, Cambridge, 63p.

SOKAL, R.R., 1965. Statistical methods in systematics. Biol. Rev., 40: 337 - 391.

SOKAL, R.R. and ROHLF, F.J., 1969. Biometry- The Principles and Practise of Statistics in Biological Research. Freeman, San Francisco, 776p.

SORNAY, J., 1957. Crétacé de la France, Belgique, Pays-Bas, Luxembourg. (Ed.), Lexique Strat. Int., 1 (4aVI), 403p.

SOUTAR, A. and BURNETT, W.C., 1979. Distribution of phosphorite in relation to the oxygen-minimum layer off the west coast of South America. In: W.C. Burnett and R.P. Sheldon (Eds.), Report on the Marine Phosphatic Sediments Workshop, East-West Center, Honoloulu, 24 - 25.

SOUTHGATE, P.N., 1980. Cambrian stromatolitic phosphorites from the Georgina Basin, Australia. Nature, 285: 395 - 397.

SPATH, L.F., 1926. On new ammonites from the English Chalk. Geol. Mag., 63: 77 - 83.

SPEARS, D.A., 1979. Geochemical aspects of the Santonian Chalk of Ramsgate, England and the origin of the chert and clay minerals. Min. Mag., 43: 159 - 164.

SPENCER, C.P., 1975. The micronutrient elements. In: J.P. Riley and G. Skirrow (Eds.), Chemical Oceanography 2 (2nd Ed.), Academic Press, London, New York, San Francisco, 245 - 300.

STANLEY, S.M., 1972. Functional morphology and evolution of byssally attached bivalve mollusks. J. Paleont., 46: 165 - 212.

STEINICH, G., 1965. Die artikulaten Brachiopoden der Rügener Schreibkreide (Unter-Maastricht). Palaeontographica, A2: 220p.

STOKES, R.B., 1975. Royaumes et provinces fauniques du Crétacé établis sur la base d'une étude systematique du genre Micraster. Mém. Mus. Natn. Hist. Nat. Paris, C31: 94p.

STOKES, R.B., 1977. The echinoids Micraster and Epiaster from the Turonian and Senonian of England. Palaeontology, 20: 805 - 821.

STOLLEY, E., 1897. Über die Gliederung des norddeutschen und baltischen Senon sowie die dasselbe characteriserenden Belemniten. Arch. Antrop. Geol. Schlesw-Holst., 2: 216 - 302.

STOLLEY, E., 1916. Neue Beiträge zur kenntnis der norddeutschen oberen Kreide, I - IV. Jber. Niedersachs. Geol. Ver., 9: 95 - 104.

STOLLEY, E., 1930. Einige Bemerkungen über die kreide Südskandinaviens. Geol. Foren. Stockh. Forh., 52: 157 - 190.

STRAHAN, A., 1891. On a phosphatic chalk with Belemnitella quadrata at Taplow. Quart. J. Geol. Soc. London, 47: 356 - 367.

STRAHAN, A., 1892. Phosphatic chalk. Nat. Sci., 1: 284 - 287.

STRAHAN, A., 1895. Phosphatic chalk at Taplow, Berks. Geol. Mag., 2: 336.

STRAHAN, A., 1896. On a phosphatic chalk with Holaster planus at Lewes, with an appendix on Foraminifera and Ostracoda by F. Chapman. Quart. J. Geol. Soc. London, 52: 463 - 473.

STRICKLAND, J.D.H. and SORÓRZANO, L., 1966. Determination of monoesterase hydrolystable phosphate and phosphomonoesterase activity in seawater. In: H. Barnes (Ed.), Some Contemporary Studies in Marine Science, Allen and Unwin, London, 665 - 674.

STUMM, W. and LECKIE, J.O., 1970. Phosphate exchange with sediments; its role in the productivity of surface waters. In: Advances in Water Pollution Research 2,

Pergamon Press, New York, III26/1 - 26/16.

STUMM, W. and MORGAN, J.J., 1970. Aquatic Chemistry. An Introduction Emphasizing Chemical Equilibria in Natural Waters. Wiley-Interscience, New York, 583p.

SUMMERHAYES, C.P., 1967. Marine environments of economic mineral deposition around New Zealand: a review. NZ J. Mar. Freshwater Res., 1: 267 - 282.

SUMMERHAYES, C.P., 1970. Phosphate deposits on the northwest African continental shelf and slope. Unpub. PhD Thesis Univ. London, 282p.

SUMMERHAYES, C.P., 1972a. Geochemistry of continental margin sediments from north-west Africa. Chem. Geol., 10: 137 - 156.

SUMMERHAYES, C.P., 1972b. Aspects of the mineralogy and geochemistry of Agulhas Bank sediments. Tech. Rept. S. Afr. Nat. Comm. Ocean. Res. Mar. Geol. Prog. 4, Dept. Geol. Univ. Cape Town, 64 - 82.

SUMMERHAYES, C.P., 1973. Distribution, origin and economic potential of phosphatic sediments from the Agulhas Bank, South Africa. Trans. Geol. Soc. S. Afr., 73: 271 - 277.

SUMMERHAYES, CP., NUTTER, A.H. and TOOMS, J.S., 1971. The geological structure and development of the continental margin of north-west Africa. Mar. Geol., 11: 1 - 25.

SUMMERHAYES, C.P., NUTTER, A.H. and TOOMS, J.S., 1972. The distribution and origin of phosphate in sediments off NW Africa. Sed. Geol., 8: 3 - 28.

SUMMERHAYES, C.P., BIRCH, G.F., ROGERS, J. and DINGLE, R.V., 1973. Phosphate in sediemnts off southwestern Africa. Nature, 243: 509 - 511.

SURLYK, F., 1972. Morphological adaptions and population structures of Danish Chalk brachiopods (Maastrichtian, Upper Cretaceous). Biol. Skr. Dan. Vid. Selsk., 19: 1 - 57.

SURLYK, F. and BIRKELUND, T., 1977. An integrated study of fossil assemblages from the Maastrichtian white chalk of northwestern Europe. In: E.G. Kauffman and J.E. Hazel (Eds.), Concepts and Methods in Biostratigraphy, Dowden Hutchinson and Ross, Stroudsburg, Penn., 257 - 281.

SVERDRUP, H.U., JOHNSON, M.W. and FLEMING, R.H., 1942. The Oceans. Their Physics, Chemistry and General Biology. Prentice Hall, Englewood Cliffs, NJ, 1087p.

TABATABAÏ, C.M., 1977. La sédimentation phosphatée (ses modialités): Pétrographie

et sédimentologie des Craies phosphatées du Nord du Bassin de Paris. Unpub. Thèse 3e Cycle, Univ. Pierre Marie Curie, Paris, 243p.

TAYLOR, J.D., KENNEDY, W.J. and HALL, A., 1969. The shell structure and mineralogy of the bivalvia. Introduction. Nuculacea - Trigonacea. Bull. Brit. Mus. (Nat. Hist.) Zool. Supp., 3: 125p.

TEHERANI, K.K., 1968. Étude stratigraphique et micropaléontologique du Sénonien de Sens (Yonne). Unpub. Thèse 3e Cycle, Fac. Sci. Paris, 252p.

TEICHERT, C., 1970. Oolite, oolith, ooid: Discussion. Am. Ass. Petrol. Geol. Bull. 54: 1748 - 1749.

TERNET, Y., 1969. Carte géologique de la France à 1/50,000, 57: Fécamp, et notice explicative. Publ. Bur. Rech. Géol. Min., Orleans.

THEVENIN, A., 1896. Mosasauriens de la craie grise de Vaux-Eclusier près Peronne. Bull. Soc. Géol. Fr. (3), 24: 900 - 916.

THOMAS, H., 1914. Carte géologique de la France à 1/80,000, 32: Beauvais, et notice explicative. Publ. Bur. Rech. Géol. Min., Orleans.

THOMPSON, G. and BOWEN, V.T., 1969. Analyses of coccolith ooze from the deep tropical Atlantic. J. Mar. Res., 27: 32 - 38.

TOOMS, J.S. and SUMMERHAYES, C.P., 1968. Phosphatic rocks from the NW African continental shelf. Nature, 218: 1241 - 1242.

TROELSEN, J.C., 1955. Globotruncana contusa in white chalk. Micropalaeontology, 1: 76 - 82.

TRUDINGER, P.A., 1976. Microbiological processes in relation to ore genesis. In: K.H. Wolf (Ed.), Handbook of Strata-Bound and Stratiform Ore Deposits 2: Geochemical Studies, Elsevier, Amsterdam, 135 - 190.

TUCKER, M.E., 1974. Sedimentology of Palaeozoic pelagic limestones: the Devonian Griotte (southern France) and Cephalopodenkalk (Germany). In: K.J. Hsu" and H.C. Jenkyns (Eds.), Pelagic Sediments: On Land and under the Sea, Spec. Publ. Int. Ass. Sedimentol., 1: 71 - 92.

UREY, H.C., LOWENSTAM, H.A., EPSTEIN, S. and McKINNEY, C.R., 1951. Measurements of palaeotemperatures and temperatures of the Upper Cretaceous of England, Denmark and the southeastern United States. Geol. Soc. Am. Bull., 62: 399 - 416.

VACCARRO, R.F., 1963. Available nitrogen and phosphorus and the biochemical cycle in the Atlantic off New England. J. Mar. Res., 21: 284 - 301.

VALYASHKO, V.M., KOGARKO, L.N. and KHODAKOVSKI, I.L., 1968. Stability of fluorapatite, chlorapatite and hydroxyapatite in aqueous solutions at different temperatures. Geochem. Int. (Am. Geol. Inst. Translation), 5: 21 - 30.

VAN GORSEL, J.T., 1973. The type Campanian and the Campanian - Maastrichtian boundary in Europe. Geol. Mijn., 52: 141 - 146.

VAN HINTE, J.E., 1965. The type Campanian and its plaktonic Foraminifera. Proc. K. Ned. Akad. Wet., B68: 8 - 28.

VAN HINTE, J.E., 1976. A Cretaceous time scale. Am. Ass. Petrol. Geol. Bull., 60: 269 - 287.

VEEH, H.H., 1979. Geochemical balance of phosphorus in todays oceans. In: W.C. Burnett and R.P. Sheldon (Eds.), Report on the Marine Phosphatic Sediments Workshop, East-West Center, Honolulu, 30.

VEEH, H.H., BURNETT, W.C. and SOUTAR, A., 1973. Contemporary phosphorites of the continental margin of Peru. Science, 181: 844 - 845.

VEEH, H.H., CALVERT, S.E. and PRICE, N.B., 1974. Accumulation of uranium in sediments and phosphorites on the south west African Shelf. Mar. Chem., 2: 189 - 202.

VEIZER, J., 1974. Chemical diagenesis of belemnite shells and possible consequences for palaeotemperature determinations. N. Jb. Geol. Paläont. Abh., 147: 91 - 111.

VOIGT, E., 1959. Die ökologishe Bedeutung der Hartgründe ('Hardground') in der oberen Kreide. Paläont. Zeitschr., 33: 129 - 147.

VOIGT, E., 1964. Zur Temperatur-Kurve der oberen Kreide in Europa. Geol. Rdsch., 54: 270 - 317.

VOIGT, E. and HÄNTZSCHEL, W., 1956. Die grauen Bänder in der Schreibekreide Nordwestdeutschsland und ihre Deutung als Lebensspuren. Mitt. Geol. StInst. Hamburg, 25: 104 - 122.

VON DER BORCH, C.C., 1970. Phosphorite concretions and nodules from the upper continental slope, northern New South Wales. J. Geol. Soc. Aust., 16: 755 - 759.

VON RAD, U., REICH, V. and RÖSCH, H., 1978. Silica diagenesis in continental margin sediments off northwest Africa. Init. Rept. DSDP, Washington, 41: 879 - 906.

WARME, J.E., 1970. Traces and significance of marine rock borers. In: T.P. Crimes and J.C. Harper (Eds.), Trace Fossils, Seel House Press, Liverpool, 515 - 526.

WARME, J.E., 1975. Borings as trace fossils and the processes of marine bioerosion. In: R.W. Frey (Ed.), The Study of Trace Fossils, Springer-Verlag, New York, 181 - 227.

WARME, J.E. and MARSHALL, N.F., 1969. Marine borers in calcareous terrigenous rocks of the Pacific coast. Am. Zool., 9: 765 - 774.

WARME, J.E., SCANLAND, T.B. and MARSHALL, N.F., 1971. Submarine canyon erosion: Contribution of marine rock burrowers. Science, 173: 1127 - 1129.

WATT, W.D. and HAYES, F.R., 1963. Tracer study of the phosphorus cycle in sea water. Limnol. Oceanogr., 8: 276 - 285.

WATTERS, W.A., 1968. Phosphorite and apatite occurrences and possible resources in New Zealand and outlying islands. NZ Geol. Surv. Rept., 33: 15p. and UN Min. Res. Dev. Ser., 32: 144 - 151.

WEAVER, C.E. and POLLARD, L.D., 1973. The Chemistry of Clay Minerals. Developments in Sedimentology 15, Elsevier, Amsterdam, London, New York, 213p.

WEIR, A.H. and CATT, J.A., 1965. The mineralogy of some Upper Chalk samples from the Arundel area, Sussex. Clay Min., 6: 97 - 110.

WETZEL, O., 1971. Der gemeine Feuerstein als Fundquelle mannigfalter 'Kleinwunder'. Grandboor Hamer., 3: 58 - 77.

WEYL, P.K., 1959. Pressure solution and the force of recrystallization - a phenomenological theory. J. Geophys. Res., 64: 2001 - 2025.

WHITAKER, W., 1865a. On the Chalk of the Isle of Thanet. Quart. J. Geol. Soc. London, 21: 395 - 398.

WHITAKER, W., 1865b. On the Chalk of the Isle of Wight. Quart. J. Geol. Soc. London, 21: 400 - 406.

WHITAKER, W., 1889. The geology of London and of part of the Thames valley I: Descriptive geology. Mem. Geol. Surv. England Wales, HMSO, London, 556p.

WHITE, H.J.O., 1907. The geology of the country around Hungerford and Newbury. Mem. Geol. Surv. England Wales, 267: 150p.

WHITE, H.J.O., 1909. The geology of the country around Basingstoke. Mem. Geol. Surv. England Wales, 284: 119p.

WHITE, H.J.O., 1921. A short account of the geology of the Isle of Wight. Mem. Geol. Surv. Great Britain, HMSO, London, 201p.

WHITE, H.J.O. and TREACHER, L., 1905. On the age and relations of the phosphatic chalk of Taplow. Quart. J. Geol. Soc. London, 61: 461 - 494.

WHITE, H.J.O. and TREACHER, L., 1906. The phosphatic chalks of Winterbourne and Boxford (Berkshire). Quart. J. Geol. Soc. London, 62: 499 - 522.

WILLCOX, N.R., 1953a. The origin of beds of phosphatic chalk with special reference to those at Taplow, England. In: Origine des gisements de phosphate de chaux. Geol. Congr. Int. 19th Algiers Fasc. 11, 119 - 133.

WILLCOX, N.R., 1953b. Some coprolites from phosphatic chalks in SE England. Ann. Mag. Nat. Hist., 6: 369 - 375.

WILLCOX, N.R., 1953c. Zonal variation in selected morphological features of Echinocorys scutata Leske. Geol. Mag., 90: 83 - 96.

WISE, S.W., BUIE, B.F. and WEAVER, F.M., 1972. Chemically precipitated sedimentary cristobalite and the origin of chert. Ecol. Geol. Helv., 65: 157 - 163.

WISE, S.W. and WEAVER, F.M., 1974. Chertification of oceanic sediments. In: K.J. Hsü and H.C. Jenkyns (Eds.), Pelagic Sediments: On Land and under the Sea, Spec. Publ. Int. Ass. Sedimentol., 1: 301 - 326.

WOOLDRIDGE, S.W. and LINTON, D.L., 1955. Structure, Surface and Drainage in South-East England. G. Philip, London, 176p.

WOOSTER, W.S. and REID, S.L.Sr., 1963. Eastern bounadry currents. In: M.N. Hill (Ed.), The Sea 2: Composition of Sea-Water. Comparative and Descriptive Oceanography, Wiley-Interscience, New York, London, 253 - 280.

WORSLEY, T., 1971. Terminal Cretaceous events. Nature, 230: 318 - 320.

WRIGHT, C.W. and WRIGHT, E.V., 1942. The Chalk of the Yorkshire Wolds. Proc. Geol. Ass., 53: 112 - 127.

WRIGHT, C.W. and WRIGHT, E.V., 1951. A survey of the fossil Cephalopoda of the Chalk of Great Britain. Palaeontogr. Soc. Monog., 41p.

WÜRZBURGER, U., 1968. A survey of phosphate deposits in Israel. UN Min. Res. Dev. Ser., 32: 152 - 165.

WYRTKI, K., 1971. Oceanographic Atlas of the International Indian Ocean Expedition. Nat. Sci. Found., Washington DC, 531p.

ZIEGLER, P.A., 1978. North-western Europe - Tectonics and basin development.

Geol. Mijn., 57: 589 - 626.